TECHNISCHE UNIVERSITÄT MÜNCHEN
Lehrstuhl für Elektrische Antriebssysteme und Leistungselektronik

Contributions to high-gain adaptive control in mechatronics

Christoph M. Hackl

Vollständiger Abdruck der von der Fakultät für Elektrotechnik und Informationstechnik der Technischen Universität München zur Erlangung des akademischen Grades eines

Doktor–Ingenieurs

genehmigten Dissertation.

Vorsitzender:		Univ.–Prof. Dr.–Ing. Ralph Kennel
Prüfer der Dissertation:	1.	Univ.–Prof. Dr.–Ing., Dr.–Ing. h.c. Dierk Schröder, i.R.
	2.	Univ.–Prof. Dr. rer. nat. Achim Ilchmann, Technische Universität Ilmenau
	3.	Univ.–Prof. Dr.–Ing. Rolf Findeisen, Otto–von–Guericke–Universität Magdeburg

Die Dissertation wurde am 11.10.2011 bei der Technischen Universität München eingereicht und durch die Fakultät für Elektrotechnik und Informationstechnik am 16.04.2012 angenommen.

This document is typeset with LaTeX/TeX.

Danksagung

Mein ganz besonderer Dank gilt Prof. Dr.–Ing., Dr.–Ing. h.c. Dierk Schröder und Prof. Dr. rer. nat. Achim Ilchmann. Ihr Fordern und Ihr Fördern hat mich außerordentlich geformt, inzwischen auch deutlich geprägt und im (wissenschaftlichen) Arbeiten und Handeln in hohem Maße weitergebracht.

Herrn Prof. Dr.–Ing., Dr.–Ing. h.c. Dierk Schröder möchte ich sehr, sehr herzlich danken für das mir entgegengebrachte Vertrauen und Zutrauen, für die mir zugebilligten Freiheiten bei der Suche und Bearbeitung meines Promotionsthemas, für seine Unterstützung und sein Interesse an meiner Forschung und Tätigkeit als wissenschaftlicher Mitarbeiter und insbesondere für sein Wohlwollen, mich – auch über das zweieinhalbjährige PTS-Industrieprojekt hinaus – weiter am Lehrstuhl zu beschäftigen. So wurde mir überhaupt erst der Weg in wissenschaftliches Arbeiten, in die Wissenschaft und somit zu einer Promotion ermöglicht.

Herrn Prof. Dr. rer. nat. Achim Ilchmann möchte ich aus tiefstem Herzen danken für das besondere Interesse an meiner Forschung, für die intensive Betreuung meiner Promotionsarbeit und vor allem für die in meine Arbeit und in meine Person so bereitwillig investierte Zeit. Ebenso möchte ich nochmals ausdrücklich Danke sagen für die unzähligen, so hilfreichen Anregungen, Verbesserungsvorschläge und Diskussionen, auch wenn all meine bisherigen Dankesworte hierfür stets kommentiert wurden mit dem Hinweis „da nich für“. Über die gesamte Zeitspanne des Zusammenarbeitens durfte ich lernen von einem exzellenten Wissenschaftler, der mir – durch sein kritisches Auge, sein umfassendes Fachwissen und seine nicht enden wollende Bereitschaft, meine anfänglichen „Beweisversuche“ zu verbessern – den Weg zu Wissenschaftlichkeit, Präzision und „ordentlicher“ Mathematik aufgezeigt hat.

Des Weiteren möchte ich Prof. Dr.–Ing. Rolf Findeisen ganz herzlich danken für das meiner Arbeit entgegengebrachte Interesse und für die schnelle Übernahme des Drittgutachtens. Auch möchte ich noch Prof. Dr.–Ing. Ralph Kennel, meinem jetzigen Vorgesetzten und dem Vorsitzenden der Promotionskommission, besonders danken. Ohne seine bereitwillige Zusage, mich als wissenschaftlichen Assistenten an seinem Lehrstuhl zu übernehmen und ohne die mir zugestandenen Freiräume in der Endphase der Promotion, hätte ich diese Arbeit nicht und vor allem nicht so konzentriert abschließen können. Weiterhin gilt mein Dank all meinen (auch ehemaligen) Kollegen und Kolleginnen am Lehrstuhl, insbesondere Dr.–Ing. Christian Endisch (Audi AG) und Dipl.–Ing. Peter Landsmann, für ihre Unterstützung und ihr „Einlassen“ auf mein „exotisches“ Forschungsgebiet.

Mein letzter und tiefster Dank gilt meinen Eltern und ganz besonders meiner lieben Frau. Ihre stützenden Hände, ermutigenden Worte, verständnisvolle Fürsorge, ihre Geduld und ihre Liebe während dieser Promotion waren immer ein unersetzlicher und notwendiger Anker der Kraft für mich.

München, im Oktober 2011 Christoph M. Hackl

Kurzzusammenfassung

Es werden hochverstärkungsbasierte adaptive Regler und deren Anwendung in der Mechatronik diskutiert. Die adaptiven Regler werden für „minimalphasige“ Systeme mit Relativgrad eins oder zwei, bekanntem Vorzeichen der instantanen Verstärkung, beschränkten Störungen und zustandsabhängigen, dynamischen Perturbationen entwickelt. Für die Reglerimplementierung ist keine Systemidentifikation oder Parameterschätzung notwendig. Strukturelle Systemkenntnis ist ausreichend. Die robusten Regler ermöglichen Folgewertregelungen mit vorgegebener asymptotischer oder transienter Genauigkeit und, in Verbindung mit einem proportionalen-integralen Internen Modell, stationäre Genauigkeit. Abschließend werden die Regler zur Geschwindigkeits- und Positionsregelung von starren und elastischen industriellen Servoantrieben eingesetzt und ein erster Ansatz zur hochverstärkungsbasierten adaptiven Positionsregelung von starren Robotern mit Drehgelenken vorgestellt.

Abstract

High-gain adaptive control and its applications in mechatronics are discussed. The high-gain adaptive controllers are presented and developed for “minimum-phase” systems with relative degree one or two, known sign of the high-frequency gain, bounded disturbances and state dependent, functional perturbations. System identification or parameter estimation is not required for controller implementation. Structural system knowledge is sufficient. The robust controllers guarantee tracking with prescribed asymptotic or transient accuracy and, in combination with a proportional-integral internal model, may assure steady state accuracy. Finally, the controllers are applied for speed and position control of stiff and flexible industrial servo-systems and it is shown that high-gain adaptive position control with prescribed transient accuracy of rigid revolute joint robotic manipulators is feasible, if the inertia matrix is known.

"The difficulty lies, not in the new ideas, but in escaping the old ones, which ramify, for those brought up as most of us have been, into every corner of our minds."

John Maynard Keynes (1883–1946)

Contents

Nomenclature

Notation	Meaning
$\mathbb{N}$	$:= \{0, 1, 2, 3, \dots\}$, set of natural numbers
$\mathbb{R}$	$:= (-\infty, \infty)$, set of real numbers
$\mathbb{R}_{\geq 0}$	$:= [0, \infty)$, set of non-negative real numbers
$\mathbb{R}_{>0}$	$:= (0, \infty)$, set of positive real numbers
$\mathbb{C}$	set of complex numbers (for $a, b \in \mathbb{R}$ and imaginary unit j where $\sqrt{j^2} := -1$ [4, p. 111], a complex number is represented by $s = a + jb \in \mathbb{C}$)
$\Re(s)$	$:= a$, real part of $s = a + jb \in \mathbb{C}$
$\Im(s)$	$:= b$, imaginary part of $s = a + jb \in \mathbb{C}$
$\mathbb{C}_{<0}$	$:= \{s \in \mathbb{C} \mid \Re(s) < 0\}$, open left complex half-plane
$\mathbb{C}_{\geq 0}$	$:= \{s \in \mathbb{C} \mid \Re(s) \geq 0\}$, right complex half-plane
$\mathbb{R}[s]$	$:= \left\{ \sum_{k=0}^{n} a_k s^k \,\middle|\, n \in \mathbb{N},\, a_0, \dots, a_n \in \mathbb{R} \right\}$, ring of polynomials with real coefficients
$\mathbb{R}(s)$	$:= \left\{ \frac{p}{q} \,\middle|\, p,\, q \in \mathbb{R}[s],\; q \neq 0 \right\}$, quotient field of real polynomials
$\deg(p)$	degree of polynomial $p \in \mathbb{R}[s]$

In the following, let n, $m \in \mathbb{N}$.

$\boldsymbol{x}$	$:= (x_1, \dots, x_n)^\top \in \mathbb{R}^n$, (column) vector with $x_i \in \mathbb{R}$ for all $i \in \{1, \dots, n\}$
$\|\boldsymbol{x}\|_p$	$:= (\|x_1\|^p + \dots + \|x_n\|^p)^{1/p}$, the p-(vector) norm of $\boldsymbol{x} \in \mathbb{R}^n$ and $p \in [1, \infty)$
$\|\boldsymbol{x}\|$	$:= \|\boldsymbol{x}\|_2 := \sqrt{\boldsymbol{x}^\top \boldsymbol{x}}$, the Euclidean norm (or 2-norm) of $\boldsymbol{x} \in \mathbb{R}^n$
$\|\boldsymbol{x}\|_\infty$	$:= \max\{\|x_1\|, \dots, \|x_n\|\}$, the maximum (or infinity) norm of $\boldsymbol{x} \in \mathbb{R}^n$
$\boldsymbol{A}$	$:= \begin{bmatrix} a_{11} & \dots & a_{1m} \\ \vdots & & \vdots \\ a_{n1} & \dots & a_{nm} \end{bmatrix} \in \mathbb{R}^{n \times m}$, matrix with coefficients $a_{kl} \in \mathbb{R}$ for $k \in \{1, \dots, n\}$ and $l \in \{1, \dots, m\}$
$\mathrm{col}_k(\boldsymbol{A})$	$:= (a_{1k}, \dots, a_{nk})^\top \in \mathbb{R}^n$, the k-th column of $\boldsymbol{A} \in \mathbb{R}^{n \times m}$
$\mathrm{row}_k(\boldsymbol{A})$	$:= (a_{k1}, \dots, a_{km}) \in \mathbb{R}^{1 \times m}$, the k-th row of $\boldsymbol{A} \in \mathbb{R}^{n \times m}$
$\|\boldsymbol{A}\|_p$	$:= \max_{\boldsymbol{x} \in \mathbb{R}^m \setminus \{\boldsymbol{0}\}} \frac{\|\boldsymbol{A}\boldsymbol{x}\|_p}{\|\boldsymbol{x}\|_p}$, the induced (or operator) norm[1] of $\boldsymbol{A} \in \mathbb{R}^{n \times m}$ and $p \in [1, \infty)$
$\mathrm{diag}\{a_1, \dots, a_n\}$	$:= \begin{bmatrix} a_1 & & 0 \\ & \ddots & \\ 0 & & a_n \end{bmatrix} \in \mathbb{R}^{n \times n}$, diagonal matrix with diagonal elements $a_1, \dots, a_n \in \mathbb{R}$

[1] e.g. (i) $p = 1$: $\|\boldsymbol{A}\|_1 = \max_{l \in \{1,\dots,m\}} \sum_{k=1}^{n} |a_{kl}|$ (maximum of the absolute column sum), (ii) $p = 2$: $\|\boldsymbol{A}\| := \|\boldsymbol{A}\|_2 = \max_{\|\boldsymbol{x}\|=1} \|\boldsymbol{A}\boldsymbol{x}\| = \sqrt{\lambda_{\max}(\boldsymbol{A}^\top \boldsymbol{A})}$ (spectral norm) where $\lambda_{\max} \geq 0$ is the largest eigenvalue of $\boldsymbol{A}^\top \boldsymbol{A}$ or (iii) $p = \infty$: $\|\boldsymbol{A}\|_\infty := \max_{k \in \{1,\dots,n\}} \sum_{l=1}^{m} |a_{kl}|$ (maximum of the absolute row sum).

Notation	Meaning
$\boldsymbol{I}_n$	$:= \operatorname{diag}\{1,\dots,1\} \in \mathbb{R}^{n\times n}$, identity (or unit) matrix
$\ker(\boldsymbol{A})$	$:= \{\boldsymbol{x} \in \mathbb{R}^m \mid \boldsymbol{A}\boldsymbol{x} = \boldsymbol{0}\} \subseteq \mathbb{R}^m$, kernel (or null-space) of $\boldsymbol{A} \in \mathbb{R}^{n\times m}$
$\operatorname{im}(\boldsymbol{A})$	$:= \{\boldsymbol{v} \in \mathbb{R}^n \mid \boldsymbol{v} = \boldsymbol{A}\boldsymbol{x}\ \forall\, \boldsymbol{x} \in \mathbb{R}^m\} \subseteq \mathbb{R}^n$, image of $\boldsymbol{A} \in \mathbb{R}^{n\times m}$
$\chi_{\boldsymbol{A}}(s)$	$:= \det(s\,\boldsymbol{I}_n - \boldsymbol{A}) \in \mathbb{R}[s]$, characteristic polynomial of the (quadratic) matrix $\boldsymbol{A} \in \mathbb{R}^{n\times n}$
$\operatorname{spec}(\boldsymbol{A})$	$:= \{s \in \mathbb{C} \mid \det(s\,\boldsymbol{I}_n - \boldsymbol{A}) = 0\}$, spectrum of the (quadratic) matrix $\boldsymbol{A} \in \mathbb{R}^{n\times n}$
$\boldsymbol{A}^k$	$:= \underbrace{\boldsymbol{A}\cdots\boldsymbol{A}}_{k-\text{times}}$, $k \in \mathbb{N}$ and $\boldsymbol{A}^0 = \boldsymbol{I}$
$\boldsymbol{O}_{n\times m}$	$:= \begin{bmatrix} 0 & \dots & 0 \\ \vdots & & \vdots \\ 0 & \dots & 0 \end{bmatrix} \in \mathbb{R}^{n\times m}$, zero matrix
$\boldsymbol{0}_n$	$:= \begin{pmatrix} 0 & \dots & 0 \end{pmatrix}^\top \in \mathbb{R}^n$, zero (column) vector
$GL_n(\mathbb{K})$	general linear group of invertible $n \times n$ matrices with entries in the field $\mathbb{K}$ (e.g. $\mathbb{R}$ or $\mathbb{C}$)
$I \subseteq \mathbb{R}$	an interval[2] on $\mathbb{R}$
$X \subseteq \mathbb{R}^n$	a subset of $\mathbb{R}^n$ (e.g. $X := \{\boldsymbol{x} \in \mathbb{R}^n \mid \|\boldsymbol{x}\| < 4\}$)
∂X	the boundary of X (for example above: $\partial X = \{\boldsymbol{x} \in \mathbb{R}^n \mid \|\boldsymbol{x}\| = 4\}$)
$\overline{X}$	$:= X \cup \partial X$, the closure of X (for example above: $\overline{X} = \{\boldsymbol{x} \in \mathbb{R}^n \mid \|\boldsymbol{x}\| \leq 4\}$)
$\operatorname{dist}(\boldsymbol{x}_0, X)$	$:= \inf_{\boldsymbol{x}\in X} \|\boldsymbol{x}_0 - \boldsymbol{x}\|$, the Euclidean distance between $\boldsymbol{x}_0 \in \mathbb{R}^n$ and a non-empty set $X \subset \mathbb{R}^n$
$\mathbb{B}^n_r(\boldsymbol{x}_0)$	$:= \{\boldsymbol{x} \in \mathbb{R}^n \mid \|\boldsymbol{x}_0 - \boldsymbol{x}\| < r\}$, the open ball of radius $r > 0$ centered at $\boldsymbol{x}_0 \in \mathbb{R}^n$
$\boldsymbol{f}\colon X \to Y$	a function $\boldsymbol{f}(\cdot)$ mapping its domain X to its range Y
$\boldsymbol{f}(\boldsymbol{x})$	the value of $\boldsymbol{f}\colon X \to Y$ evaluated at $\boldsymbol{x} \in X$
$\boldsymbol{f}\|_J$	the restriction of $\boldsymbol{f}\colon X \to Y$ on $J \subset X$
$\mathcal{C}(I;\mathbb{R}^n)$	space of continuous functions $\boldsymbol{f}\colon I \to \mathbb{R}^n$
$\mathcal{C}^k(I;\mathbb{R}^n)$	space of k-times continuously differentiable functions[3] $\boldsymbol{f}\colon I \to \mathbb{R}^n$ and $k \in \mathbb{N} \cup \{\infty\}$
$\mathcal{AC}(I;\mathbb{R}^n)$	space of absolutely[4] continuous functions $\boldsymbol{f}\colon I \to \mathbb{R}^n$
$\mathcal{AC}_{\text{loc}}(I;\mathbb{R}^n)$	space of locally absolutely continuous functions $\boldsymbol{f}\colon I \to \mathbb{R}^n$, i.e. $\boldsymbol{f}\|_J \in \mathcal{AC}(J;\mathbb{R}^n)$ for all compact $J \subseteq I$
$\mathcal{L}^p(I;\mathbb{R}^n)$	space of p-integrable functions $\boldsymbol{f}\colon I \to \mathbb{R}^n$, $p \in [1,\infty)$ with $\int_I \|\boldsymbol{f}(\tau)\|^p \,\mathrm{d}\tau < \infty$ and norm:
$\|\boldsymbol{f}\|_p$	$:= \|\boldsymbol{f}\|_{\mathcal{L}^p} := \left(\int_I \|\boldsymbol{f}(\tau)\|^p \,\mathrm{d}\tau\right)^{1/p}$ ($\mathcal{L}^p$-norm)

[2] An interval $I \subseteq \mathbb{R}$ has following property: if $x, z \in I$ and $x < z$, then, for $x < y < z$, $y \in I$ [4, p. 107]. Let $a, b \in \mathbb{R}$ with $a < b$, then e.g. (a,b), $[a,b)$, $(a,b]$ or $[a,b]$ and $\emptyset$ are intervals.

[3] $\mathcal{C}(I;\mathbb{R}^n) = \mathcal{C}^0(I;\mathbb{R}^n)$ are used synonymously if $k = 0$. If $k = \infty$ then $\mathcal{C}^\infty(I;\mathbb{R}^n)$ is the space of smooth functions.

[4] Let $I \subseteq \mathbb{R}$ be a proper interval (i.e. it is non-empty and consists of more than one element) and $Y \subseteq \mathbb{R}^n$, $n \in \mathbb{N}$. A function $\boldsymbol{f}\colon I \to Y$ is said to be absolutely continuous on I, if for all $\varepsilon > 0$ (arbitrary small!) there exists $\delta := \delta(\varepsilon) > 0$, such that for all $m \in \mathbb{N}$ and every sequence of pairwise disjoint sub-intervals $[a_k, b_k] \subset I$, $k \in \{1,\dots,m\}$, $\sum_{k=1}^m |b_k - a_k| < \delta$ implies $\sum_{k=1}^m \|\boldsymbol{f}(b_k) - \boldsymbol{f}(a_k)\| < \varepsilon$. Moreover, for any compact interval $[x_1, x_2] \subset \mathbb{R}$, a function $\boldsymbol{f}\colon [x_1, x_2] \to Y$ is absolutely continuous if and only if there exists an integrable function $\boldsymbol{g}(\cdot)\colon \mathbb{R} \to \mathbb{R}^n$, such that $\boldsymbol{f}(x) = \boldsymbol{f}(x_1) + \int_{x_1}^x \boldsymbol{g}(s)\,\mathrm{d}s$ for all $x \in [x_1, x_2]$ (see e.g. [172, p. 471]).

Notation	Meaning
$\mathcal{L}^p_{\mathrm{loc}}(I;\mathbb{R}^n)$	space of locally p-integrable functions $\boldsymbol{f}\colon I \to \mathbb{R}^n$, $p \in [1,\infty)$, i.e. $\boldsymbol{f}\vert_J \in \mathcal{L}^p(J;\mathbb{R}^n)$ for all compact $J \subseteq I$
$\mathcal{L}^\infty(I;\mathbb{R}^n)$	space of measurable essentially bounded functions $\boldsymbol{f}\colon I \to \mathbb{R}^n$ with norm:
$\Vert\boldsymbol{f}\Vert_\infty$	$:= \Vert\boldsymbol{f}\Vert_{\mathcal{L}^\infty} := \operatorname{ess-sup}_{t\in I} \Vert\boldsymbol{f}(t)\Vert$ (essential supremum)
$\mathcal{L}^\infty_{\mathrm{loc}}(I;\mathbb{R}^n)$	space of measurable, locally essentially bounded functions $\boldsymbol{f}\colon I \to \mathbb{R}^n$, i.e. $\boldsymbol{f}\vert_J \in \mathcal{L}^\infty(J;\mathbb{R}^n)$ for all compact $J \subseteq I$
$\mathcal{W}^{k,\infty}(I;\mathbb{R}^n)$	space of bounded locally absolutely continuous functions $\boldsymbol{f}\colon I \to \mathbb{R}^n$ with essentially bounded derivatives $\boldsymbol{f}^{(i)} \in \mathcal{L}^\infty(I;\mathbb{R}^n)$ for all $i = 1,\dots,k$, $k \in \mathbb{N}$ and norm:
$\Vert\boldsymbol{f}\Vert_{k,\infty}$	$:= \sum_{i=0}^k \Vert\boldsymbol{f}^{(i)}\Vert_\infty$
$f(s)$	$:= \mathscr{L}\{f(t)\}$ (or $f(s) \bullet\!\!-\!\!\circ f(t)$), Laplace transform of $f\colon \mathbb{R}_{\geq 0} \to \mathbb{R}$ if $f(\cdot) \in \mathcal{L}^1_{\mathrm{loc}}(\mathbb{R}_{\geq 0};\mathbb{R})$ and there exists $\alpha \in \mathbb{R}$ such that $[t \mapsto \exp(-\alpha t) f(t)] \in \mathcal{L}^1(\mathbb{R}_{\geq 0};\mathbb{R})$ [77, p. 742], then the Laplace transform is defined by $$\mathscr{L}\{f(t)\} := (\mathscr{L}f)(s) := \int_0^\infty f(t)\exp(-st)\,\mathrm{d}t\,, \quad \Re(s) \geq \alpha, \tag{N.1}$$
$\operatorname{sign}(x)$	signum (or sign) function defined by $$\operatorname{sign}\colon \mathbb{R} \to \mathbb{R}, \quad x \mapsto \operatorname{sign}(x) := \begin{cases} 1 & ,x > 0 \\ 0 & ,x = 0 \\ -1 & ,x < 0 \end{cases} \tag{N.2}$$
$\operatorname{sat}_{\hat{u}}(x)$	symmetric saturation function, for $\hat{u} > 0$, defined by $$\operatorname{sat}_{\hat{u}}\colon \mathbb{R} \to [-\hat{u},\,\hat{u}], \quad x \mapsto \operatorname{sat}_{\hat{u}}(x) := \begin{cases} \hat{u} & ,x > \hat{u} \\ x & ,-\hat{u} < x < \hat{u} \\ -\hat{u} & ,x < -\hat{u} \end{cases} \tag{N.3}$$
$\operatorname{sat}^{\overline{u}}_{\underline{u}}(x)$	asymmetric saturation function, for $\overline{u} > \underline{u}$, defined by $$\operatorname{sat}^{\overline{u}}_{\underline{u}}\colon \mathbb{R} \to [\underline{u},\,\overline{u}], \quad x \mapsto \operatorname{sat}^{\overline{u}}_{\underline{u}} := \begin{cases} \overline{u} & ,x > \overline{u} \\ x & ,\underline{u} < x < \overline{u} \\ \underline{u} & ,x < \underline{u} \end{cases} \tag{N.4}$$
$d_\lambda(x)$	distance function for adaptive λ-tracking control, for $\lambda > 0$, defined by $$d_\lambda\colon \mathbb{R}_{\geq 0} \to \mathbb{R}_{\geq 0}, \quad x \mapsto d_\lambda(x) := \max\{x - \lambda,\,0\} \tag{N.5}$$
a.a.	stands for *almost all*
a.e.	stands for *almost everywhere*

Chapter 1

Introduction

1.1 Motivation and goal

Many mechatronic applications in industry require motion control (i.e. position or speed control) of work machines such as machine tools or paper coating machines. For instance, high-precision machine tools perform positioning tasks with an accuracy up to $10\,[\mu\text{m}] = 10 \cdot 10^{-6}\,[\text{m}]$ (see [74]). The motion control problem is to find an adequate motion controller which assures that given control objectives (customer specifications) are accomplished. In principle, the control objectives are reference tracking of some suitable reference signal y_{ref} by the system output y (i.e. position or speed) and rejection of disturbances (i.e. unknown loads and friction). The tracking (or control) error, defined by

$$\forall\, t \geq 0\colon \qquad e(t) := y_{\text{ref}}(t) - y(t), \tag{1.1}$$

should be kept "small" for all time $t \geq 0$ [s] even under load. Usually, for given (measured) output $y(\cdot)$, some prescribed set-point $\hat{y}_{\text{ref}} > 0$ and (positive) reference step (see Fig. 1.1)

$$y_{\text{ref}}\colon \mathbb{R} \to \mathbb{R}, \qquad t \mapsto y_{\text{ref}}(t) := \begin{cases} \hat{y}_{\text{ref}} & ,t \geq 0 \\ 0 & ,t < 0 \end{cases}, \tag{1.2}$$

the set-point tracking performance is evaluated by means of (see e.g. [166, p. 5])

- rise time in [s]

$$t^r_{y(\cdot),\tilde{p}} := \inf\left\{ t \geq 0 \;\middle|\; \forall\, \tau \geq t\colon\; y(\tau) \geq \tilde{p}\, \hat{y}_{\text{ref}} \right\}, \qquad \tilde{p} \in (0,1]; \tag{1.3}$$

- (relative) overshoot in [%]

$$\Delta^{os}_{y(\cdot)} := 100 \cdot \max\left\{ 0,\, \frac{\max_{t \geq 0} y(t)}{\hat{y}_{\text{ref}}} - 1 \right\}; \tag{1.4}$$

- and settling time in [s]

$$t^s_{y(\cdot),p} := \inf\left\{ t \geq 0 \;\middle|\; \forall\, \tau \geq t\colon\; |y(\tau) - \hat{y}_{\text{ref}}| \leq p\, \hat{y}_{\text{ref}} \right\}, \qquad p \in (0,1). \tag{1.5}$$

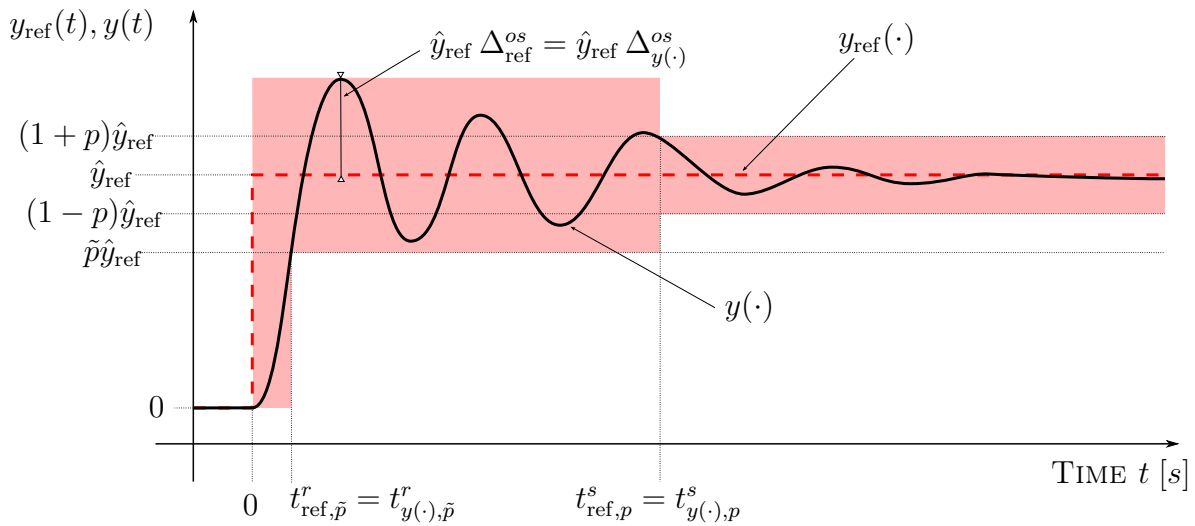

Figure 1.1: *Maximum rise time $t^r_{\text{ref},\tilde{p}}$, maximum overshoot Δ^{os}_{ref} and maximum settling time $t^s_{\text{ref},p}$ for positive reference step (1.2): the exemplary system response $y(\cdot)$ barely satisfies motion control objectives (mco_1)–(mco_3).*

According to these "performance measures" the motion control objectives (mco) are formulated in the "time domain" (see Fig. 1.1) in terms of

(mco_1) maximum rise time $t^r_{\text{ref},\tilde{p}} > 0$ in [s], i.e. $t^r_{y(\cdot),\tilde{p}} \leq t^r_{\text{ref},\tilde{p}}$,

(mco_2) maximum overshoot $\Delta^{os}_{\text{ref}} \geq 0$ in [%], i.e. $\Delta^{os}_{y(\cdot)} \leq \Delta^{os}_{\text{ref}}$, and

(mco_3) maximum settling time $t^s_{\text{ref},p} \geq t^r_{\text{ref},\tilde{p}}$ in [s], i.e. $t^s_{y(\cdot),p} \leq t^s_{\text{ref},p}$.

To avoid deficient work pieces, especially for position control of e.g. machine tools, only very small overshoots are admissible. Maximum rise and settling time depend on application and size of the work machine. To accomplish motion control objectives (mco_1)-(mco_3), the applied motion controller must assure that output $y(\cdot)$ of the closed-loop system evolves within the "red region" in Fig. 1.1. If a non-constant reference $y_{\text{ref}}\colon \mathbb{R}_{\geq 0} \to \mathbb{R}$ is to be tracked, then the motion control objectives are often supplemented or replaced by

(mco_4) minimum tracking accuracy after some prescribed time $\tau_\lambda \geq 0$ [s], i.e., for prescribed accuracy $\lambda > 0$ and suitable reference $y_{\text{ref}}\colon \mathbb{R}_{\geq 0} \to \mathbb{R}$, the following must hold

$$\forall\, t \geq \tau_\lambda \geq 0\colon \qquad |y_{\text{ref}}(t) - y(t)| \leq \lambda.$$

In the majority of cases, the implemented motion controllers are proportional-integral-derivative (PID) controllers (or variants thereof, see e.g. [51, 143]). Since load disturbances and friction may endanger achievement of control objectives (mco_1)–(mco_4), sometimes disturbance observers (see [143]) and/or friction compensation methods (see [28]) are implemented additionally. Usually, controller tuning is done empirically lacking an exact stability analysis. This might endanger operation failures. Analytic controller design relies on good knowledge of the plant and its parameters incorporating system identification and/or estimation. In general, due to system modeling, identification and/or estimation, model-based control system design is time-consuming, involved and expensive (see e.g. [128, 175]).

In this thesis high-gain adaptive[1] control methods—such as adaptive λ-tracking control and funnel control (see [93])—are proposed for speed and position control of a stiff one-mass system (1MS) and an elastic two-mass system (2MS). These methods rely on "structural system knowledge" only and are inherently robust to parameter uncertainties. Precise system identification or parameter estimation is not required. Roughly speaking, high-gain adaptive motion control is motivated by the following three aspects:

Motivation 1: Since the motion control objectives are mainly specified in the time domain (see (mco_1)–(mco_4) and also Fig. 1.1), it is desirable for the commissioning engineer to have a tool at hand, which directly allows to account for these control objectives during implementation. Iterations in controller parameter tuning could be reduced. This desire immediately motivates for the application of funnel control (see Chapter 4) where the tracking error (1.1) is constrained by a prescribed continuous function of time.

Motivation 2: To avoid stick-slip (major problem due to friction), the simplest approach is high gain in the feedback, yielding a "stiff" closed-loop system (see e.g. [10, 50]).

Motivation 3: Due to Newton's Laws or Lagrange's method, mechatronic systems (at least of low order) are "structurally" known, i.e. mathematical models with lumped parameters (see e.g. [77, Section 1.3]) in the form of differential equations can be derived. These models describe the dynamics of the system qualitatively. In contrast, model parameters are (usually) not exactly known. However, by rough estimates, upper and lower bounds on or, by physical means, at least the signs of the model parameters are available. This rough knowledge allows to analyze the system models whether certain "structural properties" are satisfied, e.g. the following facts are known:

- the "direction of influence" of control input on system output (i.e. the sign of the "high-frequency gain" of the system)
- the time derivative (e.g. $\frac{\mathrm{d}^2}{\mathrm{d}t^2}\, y(t)$) of the system output which is directly affected by the control input (i.e. the "relative degree" of the system).
- the "internal dynamics" of the system are "stable" (i.e. stability of the "zero-dynamics"[2] or, for linear systems, the "minimum-phase" property).

Formal definitions of the notions "high-frequency gain", "relative degree" and "minimum-phase" are given in Chapter 2. Many mechatronic systems under motion control are minimum-phase (or have stable zero-dynamics) and their sign of the high-frequency gain is known. Their relative degree depends on setup and application and is, in general, greater than or equal to one. High-gain adaptive control is applicable for minimum-phase systems (or certain nonlinear systems with stable zero-dynamics) with known relative degree and known sign of the high-frequency gain (see [93]).

The proposed high-gain adaptive speed and position controllers are developed, in a general framework, for "minimum-phase systems" with relative degree one *or* two, known sign of the

[1] It is not strictly distinguished between "dynamic tuning" or "time-varying adjustment" of the controller parameters. Both is considered as "high-gain adaptive" control.

[2] For a definition and a detailed discussion see [107, Section 4.3].

high-frequency gain, bounded disturbances and nonlinear, functional state-dependent perturbations. The controllers are "simple" (in the sense of non-complex and of low order), robust to parameter uncertainties and tolerate measurement noise. Unknown friction effects and time-varying disturbances (e.g. load torques) can be rejected and, in addition, the following is guaranteed (if the actuator is sufficiently dimensioned):

- *prescribed asymptotic accuracy*: for given $\lambda > 0$ (e.g. $\lambda = p\,\hat{y}_{\mathrm{ref}}$, see Fig. 1.1) the tracking error (1.1) approaches the interval $[-\lambda, \lambda]$ asymptotically (see "adaptive λ-tracking control" in Chapter 3) or

- *prescribed transient accuracy*: the absolute value $|e(\cdot)|$ of the tracking error (1.1) is bounded by a prescribed positive (possibly non-increasing) function of time (see "funnel control" in Chapter 4).

The *hoped-for goal* of this thesis is to introduce *high-gain adaptive motion control* as a reasonable, simple and quickly to implement (hence cheap) alternative to standard motion control in industry. To ease readability and insight, especially for newcomers not familiar with high-gain adaptive control, theory and applications are treated in great detail and presented in a self-contained manner (see Chapters 2-5). In Chapter 5 the proposed high-gain adaptive controllers are implemented at an industrial servo-system (laboratory setup) for speed and position control of 1MS and 2MS. The measurement results underpin industrial applicability. At the end of Chapter 5 a first result in robotics is established: position funnel control for rigid revolute joint robotic manipulators (with known inertia matrix).

The succeeding Sections 1.2 and 1.3 revisit notion and history of "feedback control", "adaptive control", "mechatronics" and "motion control". Section 1.4 carefully models friction (with dynamic behavior) and the components of the considered mechatronic systems, finally leading to the models of 1MS and 2MS. Based on these two models, Section 1.5 briefly discusses common motion control approaches in industry. The problem formulation is stated in Section 1.6, where Section 1.7 summarizes the contributions of this thesis.

1.2 Feedback control and adaptive control

For engineers "to control" means to alter, drive or direct a process or a plant—i.e. a "dynamical system"—in such a way that its behavior—i.e. its "dynamics"—is improved. The desired improvement is specified by "control objective(s)": e.g. certain characteristics or quantities of the controlled system —i.e. "states" or "outputs"—should be kept close to a prescribed value—i.e. an "operating point" or a "reference"—even if environment is changing, i.e. unknown "disturbances" or "loads" perturb the system (see [138, Section 1.1]). A device controlling a system is called "controller", which generates the "control action" or the "control input" driving the system.

To achieve "automatic control"—i.e. the system is controlled automatically by a controller—negative feedback of system quantities is essential. Therefore these have to be measured (or observed) and "compared" to reference value(s). The resulting "control error" or "tracking error" (for varying references)—the difference between actual measurement and reference—"corrects" the control action in such way that the system is driven towards the reference. The system is

subject to "feedback control". A system with controller and feedback is considered as "closed-loop system". Feedback "is one of the fundamental ideas of engineering" (see [138, Section 1.1]).

The history of feedback control was long time traced back to the "governor" introduced by James Watt (1736–1819) for speed control of steam machines. However, as was shown by Otto Mayr in 1969, control systems were already known around 300 before Christ (BC) (see [132, p. 17-22]). These ancient controllers were used to assure accurate time keeping (by e.g. water clocks). For a chronologically complete overview of the history of control systems from ancient times to 1955 see e.g. [132] (300 B.C.–1800), [21] (1800–1930) and [22] (1930–1955).

Not until 1868, the design of such (mechanical) governors was seemingly performed by trial and error. In March 1868 an article (see [131]) was published by James Clerk Maxwell (1831–1879) in which the dynamics of these "regulators" or "modulators" (as he called the governors) were analyzed concerning stability (in the sense of Linear Control Theory[3]).

In the early years of the 20th century the use of feedback control was limited to special problems in mechanical engineering. Due to the development of electrical amplifiers in 1934 with (negative) "feedback circuits" introduced by Harold Stephen Black (1898–1983) [25], more and more controllers were implemented to control electrical, mechanical and chemical processes in the 1940s [138, Section 1.1]. The fields and the applications were different, but the principle idea of feedback and the mathematical analysis tools were similar. Open-loop frequency response methods introduced by Harry Nyquist (1889–1976) [142] and Hendrik Wade Bode (1905–1982) [26]—known from electronic circuits with feedback amplifiers—formed the basis for controller design and systematic stability analysis of linear time-invariant closed-loop systems.

In 1948, Norbert Wiener (1894–1964) generalized the idea of feedback control to e.g. communication theory, biology, medicine and sociology. His newly founded discipline is called "Cybernetics" (see [185]). Not until 1961 "Control Theory" was considered as separate mathematical discipline (see [138, p. 2]).

In the 1950s desire and need arose to cope with nonlinear control systems exhibiting changing dynamics (depending on the actual operating point) and varying disturbance characteristics (see [16, p. 3]). The control systems should have the capability to "learn", "adjust" or "self-tune" themselves. Inspired by Biology, were the notion of "adaption" is well known as "an advantageous confirmation of an organism to changes in its environment" (see [138, p. 6]), Drenick and Shahbender [47] introduced "adaptive servomechanism[4]" to control theory in 1957. "Adaptive control" was born.

Several definitions of "adaptive control" or "adaptive controllers" can be found in the literature,

[3] J.C. Maxwell analyzed e.g. the roots of polynomials to have negative real parts, however he was not able to formulate a general result. This was achieved by Edward John Routh (1831–1907) in 1877 [154].

[4] The term "servomechanism" was coined in military by the problem of positioning a gun for aiming at the target [183, 184]. Later "servomechanism" became a description for the ability of feedback control systems to simultaneously track reference signals and reject disturbances, known as the servo (mechanism) problem (see e.g. [56]).

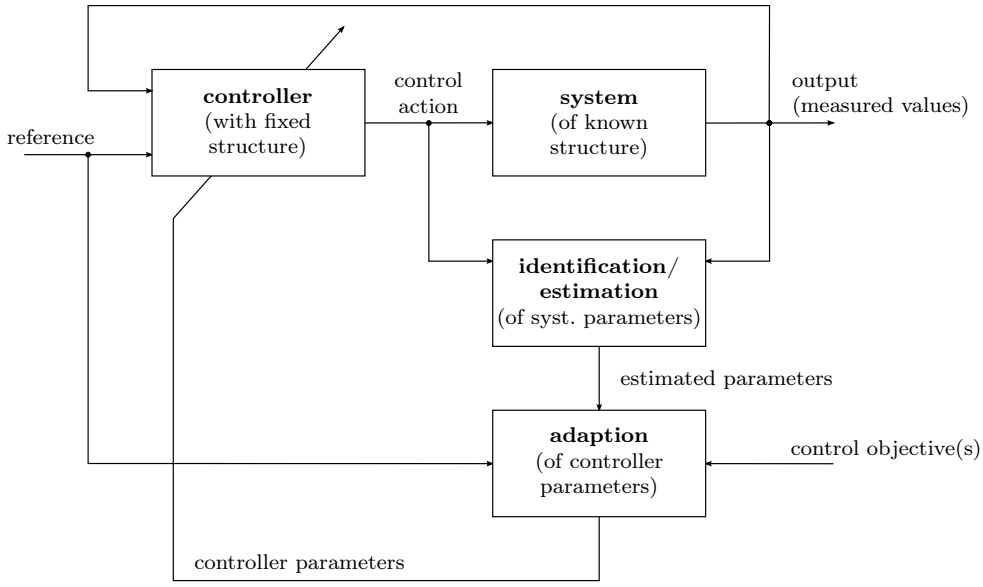

Figure 1.2: *Indirect adaptive control (based on Fig. 1.6 in [106])*

for a collection see e.g. [138, Definitions 1.1.1–2, 1.2–1.4, p. 9-11]. Some authors even questioned the necessity of introducing the term "adaptive" in feedback control considering any feedback as adaptive (see [133]). For this thesis the author follows the informal but pragmatical definition of adaptive controllers given by Karl Johan Åström (1934–) in [16, p. 1]:

> "An adaptive controller is a controller with adjustable parameters and a mechanism for adjusting the parameters."

Note that this definition may also incorporate variable-structure adaptive controllers (see [16, Section 10.4]) with different dynamics for different operating points. In this thesis only adaptive controllers with fixed structure are considered.

First motivating examples for the need of adaptive control were flight control (of e.g. military supersonic aircrafts), process control (e.g. refineries in chemical engineering) or decision making under uncertainty (in e.g. economics). For more details on adaptive control around 1960, the reader is referred to the survey articles [11], [108] and [13].

In the mid 1950s inspired by the problem of designing autopilots for high-performance aircrafts several adaptive schemes were developed, such as gain scheduling[5], self-tuning regulators[6] (STR), model reference adaptive control (MRAC)[7] or dual controllers (see e.g. [16, p. 22-24]). At this time the notions of controllability and observability, state space concepts and tools to analyze stability of nonlinear systems—introduced in the seminal contributions [109–111]

[5]It was severely discussed if gain scheduling is an adaptive controller or not. In view of the informal definition gain scheduling is clearly a adaptive controller [16, p. 19]

[6]In [14] the authors avoided the use of "adaptive" for their controller, since the plant parameters were assumed only constant but unknown (not varying). However, in the notion of the above definition STRs are clearly adaptive controllers.

[7]STR and (indirect) MRAC [106, Section 1.2.4] are nowadays considered as equivalent [16, p. ix].

and [125][8] by Rudolph Emil Kalman (1930–) and Alekandr Mikhailovich Lyapunov (1857–1918), respectively—were still missing or not fully recognized. This "lack of understanding of the properties of the proposed adaptive control schemes" (see [106, Section 1.3]) combined with "a lot of enthusiasm, bad hardware and non-existing theory" (see [12]) lead to severe implementation problems and even worse an accident during flight tests (see [106, p. 23]). As a consequence funding of research on adaptive flight control was cut and the interest in adaptive control rapidly dropped (see e.g. [13] or in great detail [16, p. 2-3] or [106, Section 1.3]). The flight control problem was finally solved by gain scheduling (see e.g. [13] or in more detail [16, p. 414-415]).

A renaissance of adaptive control arose in the years around 1970, when first stability proofs were reported (see e.g. [16, p. 2-3] or [106, p. 24] with lots of references). However, the adaptive schemes were sensitive to small perturbations resulting in potential instability of the closed-loop system. Not before the late 1980s and early 1990s the field revived by breakthroughs in robustness analysis of adaptive control systems (see [106, p. 25]). Since then, research focused more and more on the "transient and steady-state performance" (see [106, p. 25]) of adaptive control systems (mostly with MRAC).

Loosely speaking, feedback control solves the problem of designing a controller with fixed structure and constant parameters for a system with *known structure and (at least roughly known) parameters* to meet given control objective(s) such as stability of the closed-loop system, asymptotic tracking and disturbance rejection, etc.
In contrast, under the assumption that such a controller exists, adaptive control solves the problem of designing a variable controller (in structure and/or parameters) for a plant with *known structure but unknown parameters* (see [106, Section 1.2.3]). Adaptive control may be classified into two categories: "indirect" and "direct" adaptive control (see Fig. 1.2 and 1.3, respectively).

Indirect adaptive control relies on identification algorithms (e.g. recursive least square or gradient methods) to estimate the unknown system parameters. Assuming that these estimates converge to the true values, the controller parameters are adjusted by using the estimated system parameters and an adequate adaption rule (see Fig. 1.2). This approach is nowadays known as the "certainty equivalence principle[9]" (see e.g. [13]). The assumption on convergence is based on "persistent excitation" (see [138, Chapter 6]): to achieve "perfect" identification of a system (i.e. exponential convergence of estimation parameters to real parameters), excitation with a sufficiently large number of amplitudes and frequencies (incorporating all eigenmodes in the case of linear systems) is necessary. The order of the identification problem (number of estimates) at least increases with the order of the system, e.g. for recursive least square methods the number of estimation parameters even grows quadratically with the system order (see [80]). A typical example for indirect adaptive control is model reference adaptive control (MRAC), even though there exist direct model reference adaptive controllers (see [106, p. 14]).

[8] First French translation in 1907: "Problème Géneral de la Stabilité de Mouvement" in Annales de la Faculté des Sciences de l'Université de Toulouse, Vol. 9, pp. 203-474. Reprinted by Princeton University Press in 1949. First English book in 1966 [126], modern translation in [127] with biography and bibliography of A.M. Lyapunov.

[9] The idea of neglecting uncertainties and using estimated values of system parameters as true values (for e.g. controller design) was introduced in [171] as "certainty equivalence method".

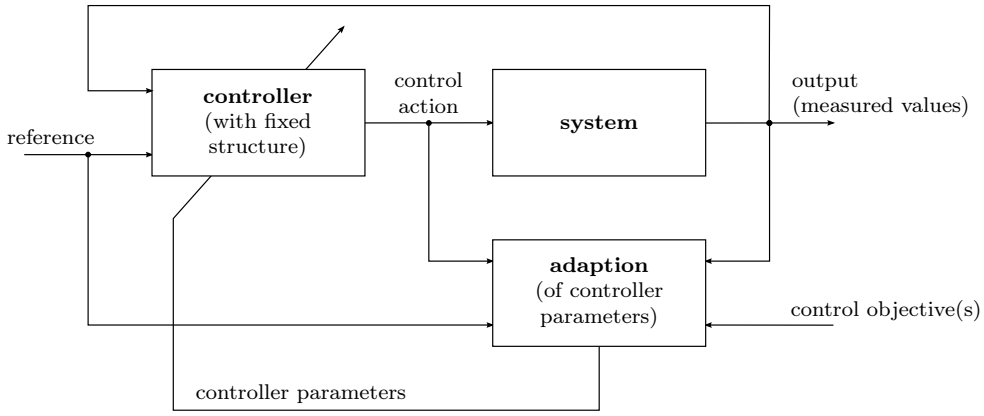

Figure 1.3: *Direct adaptive control (based on Fig. 1.7 in [106])*

For MRAC the control objective is prescribed in terms of a "reference model" which determines how the closed-loop system should behave.

Direct adaptive control does not require system identification or estimation. The adaption of the controller parameters solely depends on measured system output, reference, control action and control objective(s) (see Fig. 1.3). Direct methods are, in general, not applicable to "all" plants but restricted to certain "classes of systems" (e.g. minimum-phase systems, see [106, p. 10]).

A very simple form of direct adaptive control is high-gain adaptive control. High-gain adaptive controllers—also known as "non-identifier based adaptive controllers" (see e.g. the survey [85] or the monograph [86])—exploit the so called "high-gain property" of minimum-phase systems with (strict) relative degree one and known sign of the high-frequency gain[10]: for simple proportional output feedback $u(t) = -k\,y(t)$ and a sufficiently large controller gain $k \geq k^\star > 0$ the closed-loop system is stable (see e.g. [93]). The lower bound $k^\star$ depends on system data and must be known *a priori*. In the adaptive case it is "found online" by (dynamic) adaption. The following high-gain adaptive output feedback controller

$$u(t) = -k(t)y(t), \qquad \dot{k}(t) = y(t)^2,\ k(0) = k_0 > 0 \tag{1.6}$$

"stabilizes" the closed-loop system. The controller gain $k(\cdot)$ is bounded but non-decreasing. If e.g. measurement noise $n_m(\cdot) \in \mathcal{W}^{2,\infty}(\mathbb{R}_{\geq 0};\mathbb{R})$ deteriorates the output, then the adaption in (1.6) becomes $\dot{k}(t) = (y(t) + n_m(t))^2$ and hence the gain $k(\cdot)$ might diverge (see e.g. [93]). In this case or if unknown load disturbances perturb the system, adaptive λ-tracking control should be applied which introduces a dead-zone in gain adaption. Moreover, for reference $y_{\mathrm{ref}}(\cdot) \in \mathcal{W}^{1,\infty}(\mathbb{R}_{\geq 0};\mathbb{R})$, asymptotic accuracy $\lambda > 0$ and tracking error $e(\cdot)$ as in (1.1), the adaptive λ-tracking controller

$$u(t) = k(t)e(t), \qquad \dot{k}(t) = d_\lambda(|e(t) + n_m(t)|),\ k(0) = k_0 > 0,$$

with $d_\lambda(\cdot)$ as in (N.5), assures tracking with prescribed asymptotic accuracy (see e.g. [93]). The

[10] The notions "minimum-phase", "relative degree" and "high-frequency gain" are defined in Definition 2.7, Definition 2.1 and Definition 2.4 for LTI SISO systems, respectively.

gain $k(\cdot)$ albeit bounded is still non-decreasing. In [99] funnel control is introduced. It has a "time-varying" gain

$$k(t) = \frac{1}{\psi(t) - |e(t) - n_m(t)|} \tag{1.7}$$

where $\psi\colon \mathbb{R}_{\geq 0} \to [\lambda, \infty)$, $\lambda > 0$ is a prescribed (possibly non-increasing) continuous "boundary function". If the initial error $e(0)$ "starts" within the boundary, i.e. $\psi(0) > |e(0) - n_m(0)|$, funnel control assures tracking with prescribed transient accuracy. Moreover, the funnel controller gain (1.7) may decrease again.

Since only "structural system knowledge" is required, high-gain adaptive control is inherently robust and makes it attractive for industrial application. For systems with a relative degree higher than one, high-gain adaptive control is still feasible, however the controllers become quite complex (e.g. due to backstepping [103, 190] or due to the use of high-gain observers [34]) or incorporate controller gains with high powers (e.g. $k(t)^7$ for the relative degree two case [103]). Such controllers are not suitable for industrial application. Chapters 3 and 4 present "simple" (in the sense of non-complex and of low order) high-gain adaptive controllers for the relative degree two case which achieve tracking with prescribed asymptotic accuracy and with prescribed transient accuracy, respectively. The controller gains occur with $k(t)^2$ at the most.

Besides the theoretic evolution of adaptive control, it partly became popular in industry. Several applications in industry were published, e.g. chemical reactor control, autopilots for ship steering or speed control of electrical drives (see the surveys [12] or [188] for adaptive control in general and [93] for high-gain adaptive control in particular). However, activities in research on adaptive control theory by far exceed the number of industrial applications: in 1997 the application/theory ratio ranged between 0.02 and 0.1 (see [188]). Adaptive control still lacks widespread industrial acceptance.

1.3 Mechatronics and motion control

The term "Mechatronics" was coined by Ko Kikuchi (see [40])—an electrical engineer of Yaskawa Electric Cooperation—in 1969 (see [119]). The company secured the trademark rights in 1972 (Japan Trademark Registration no. 946594). Since the term "Mechatronics" was soon widely adopted in industry, Yaskawa released its rights in 1982 (see [119]).

In the late 1960s and the early 1970s innovations such as electronic amplification (e.g. operational amplifiers (op-amps) on signal side and power electronics on the actuation side) and micro–processors lead to more and more usage of electronic components in combination with mechanical systems and paved the way for Mechatronics (see [17, 119]). For increasingly complex systems the design process became more and more modularized (see [17]), which helped to develop "mechatronic products" offering enhanced functionality and improved performance (see [17, 119]).

Although the word "Mechatronics" is simply the composition of "mecha" (from mechanism or mechanics) and "tronics" (from electronics, see e.g. [84, 119]), the concept is nowadays

considered in a wider sense. The term is used in numerous ways and its definition changed over the passed 40 years (see e.g. [17, 40, 84, 119, 180]). Some authors even state that a definition is not possible or even desirable (see [76]). A Year 2000 definition of "Mechatronics" was given in [180]:

> "*The synergetic integration of physical systems with information technology [...] and complex-decision making in the design, manufacture and operation of industrial products and processes.*"

Note that the definition above is still not completely accepted in all fields of research or industry. The understanding of "Mechatronics" severely depends on the background of engineers and scientists, which influences the language and the focus on what is "Mechatronics" and even how it is taught (see [29]). Even the most important societies in mechatronics such as the International Federation of Automatic Control (IFAC), the American Society of Mechanical Engineers (ASME), the Institute of Electrical and Electronic Engineers (IEEE) and the Mechatronics Forum often do not use a common language (e.g. session titles of mechatronic conferences differ significantly leading to misunderstanding among the several "Mechatronic dialects", see [29]). For this thesis the Year 2000 definition seems adequate.

By using the notion "physical system" instead of "mechanical system", the Year 2000 definition emphasizes that not only (single) mechanical systems are treated as mechatronic systems but also large-scale distributed systems (e.g. automated highway systems, see [180]). Typical examples of nowadays mechatronic systems are microelectro-mechanical systems (MEMS), computer hard disc drives (HDD, see [180]), car braking systems (see [40]), machine tools with computerized numerical control (CNC), automated teller machines (ATM), automated baggage handling systems at airports (see [17]), manufacturing and process automation systems, automotive and aerospace vehicles, thermal and environmental control systems and vibrational control systems for buildings (see [17]).
The terms "synergetic integration", "information technology" and "complex-decision making" in the definition attribute to the holistic, synergistic and interdisciplinary nature (see [186]) of "Mechatronics" as several science and engineering disciplines—e.g. electronic (electrical), computer, mechanical and software engineering and chemistry, biology and mathematics (systems and control theory)—equally contribute to the design, manufacture and operation of mechatronic products (see [17, 29, 84, 180, 186]).

Mechatronics is well established in many branches of industry such as automotive, manufacturing, aerospace and building/construction industry, electrical drive engineering, robotics and automation, (bio)medical engineering and even consumer electronics (see [84, 180, 186]). Mechatronics is (still) a growing market with increasing revenues, e.g. in 2010 the profit margins of the business segments "Industry Automation" and "Drive Technologies" of SIEMENS were 16.8% and 12.3%, respectively (see SIEMENS financial report 2010, p. 3).

The widespread use of increasingly powerful computers (e.g. micro-processors, digital signal processors (DSP), field programmable gate arrays (FPGA)) with real-time operating systems and software controllers ("software servo-systems", see [119]) made the design process of complex-decision making algorithms "versatile and flexible" (see [186]). Decision making became more and more complex, e.g. neuronal networks, fuzzy logic, optimal and predictive control strate-

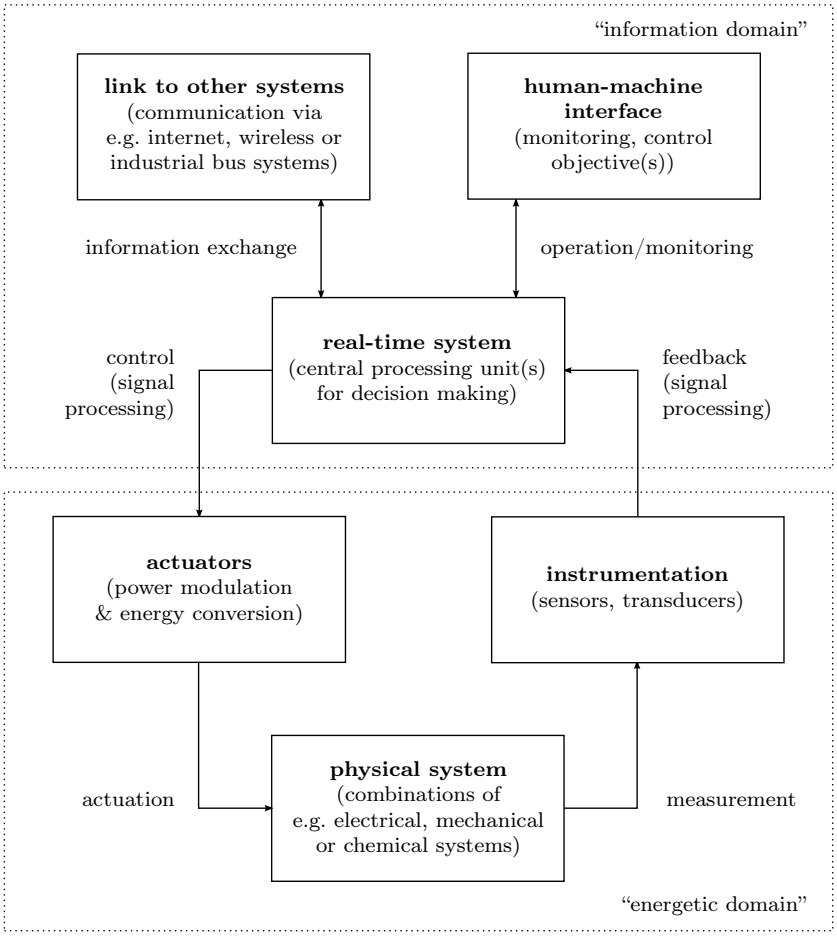

Figure 1.4: *Components of modern mechatronic systems (based on figures in [17, 29, 180])*

gies and high dimensional (nonlinear) controllers could easily be implemented (see e.g. the text book [167, Chapters 5-9,12-14,16-17 and 18]). Mechatronic systems gained "built-in intelligence" (see [186]).

Fig. 1.4 shows the components of a modern mechatronic system, though a clear delimitation among the components is often not possible. At its center there is the real-time system connected to the human-machine interface. It (possibly) exchanges information with other mechatronic systems. The implemented decision algorithms (e.g. controllers) generate the control input(s) to the actuator(s) which provide adequate actuation of the physical system by appropriate energy conversion (e.g. from electrical to mechanical). The installed instrumentation assures measurement of the necessary system states and allows for feedback to the real-time system. Note that a mechatronic system may be split into two domains: the "information" and "energetic domain" (see [29]).

This thesis focuses on motion control of industrial mechatronic systems such as "one-axis servo-systems" (see e.g. [119]). A typical one-axis servo-system is depicted in Fig. 1.5. It consists of electrical drive (power electronics & electrical machine) fed by a power source and linked to a work machine (to be driven). The electrical drive with current controller (torque generation) is considered as actuator, whereas rotor of electrical machine, linkage and work machine repre-

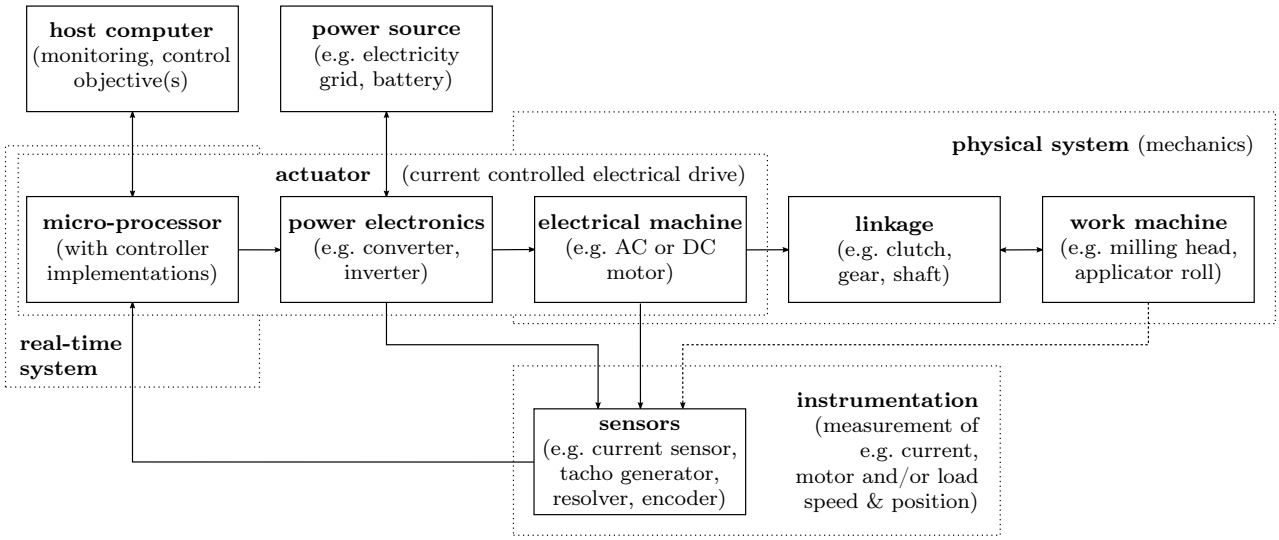

Figure 1.5: *Components of one-axis servo-system in industry*

sent the physical (here: mechanical) system. Note the overlap between actuator and real-time system and physical system, respectively. Several sensors provide measurement signals which allow feedback control. The controllers are implemented on the real-time system with human-machine interface to a host computer for monitoring and/or specifying reference or command signals.

Motion control is considered as the "key technology in mechatronics" (see [143]) with the following—rather vague—control objectives:

- *load position or load speed reference tracking* and
- *disturbance rejection (of e.g. unknown load torques and friction).*

Depending on application, the control objectives are formulated more precisely, e.g. in terms of maximum rise time, maximum overshoot and maximum settling time (see (mco_1)–(mco_4) and Fig. 1.1 on page 2). Motion control may also incorporate a cascaded force control loop (see [143]). Force control is not considered in this thesis.

1.4 Modeling of industrial servo-systems

To give a more formal definition of industrial one-axis servo-systems, the following section will establish mathematical models for a stiff one-mass system (1MS) and an elastic two-mass system (2MS). Although there exist multi-mass systems (see e.g. [166, Section 19.4]), the presented models are fundamental. In industry many one-axis motion control processes may be modeled either as 1MS or 2MS. Both, 1MS and 2MS, are assumed to be driven by an electrical drive (e.g. AC or DC drive) and are subject to friction. The electrical drive provides, by fast torque generation, adequate actuation of the mechanical system. The available torque is, however, constrained due to physical and safety reasons (e.g. the admissible reference torque is saturated). For instrumentation, the setups are equipped with current and position sensors. Sometimes

Translation	**Rotation**
position x [m]	angle ϕ [rad]
velocity v $\left[\frac{\text{m}}{\text{s}}\right]$	angular velocity (speed) ω $\left[\frac{\text{rad}}{\text{s}}\right]$
force f [N]	torque m [Nm]
mass m [kg]	inertia Θ [kg m^2]

Table 1.1: *Notation for translational and rotatory mechanical systems*

also speed sensors are installed. Real-time micro-processors combined with industrial personal computers (as human-machine interface) allow flexible controller design, reference generation and monitoring.

At first models of the components "real-time system", "actuator", "instrumentation" and "physical (mechanical) system" (see Fig. 1.5) are derived or introduced. Then, based on the component's modeling, the models of 1MS and 2MS are presented.

In the following all explanations focus on rotatory systems, hence the relevant quantities are torque in [Nm], angle (position) in [rad] and angular velocity (speed) in [rad/s]. However, in principle, the following also holds for translational systems, simply substitute translational quantities (with corresponding dimensions, e.g. [N], [m] and [m/s])) for rotatory quantities. A comparison of rotatory and translational quantities is listed in Tab. 1.1.

1.4.1 Micro-processor (real-time system)

Modern real-time systems with micro-processors run with very fast execution times ranging from e.g. $50 \cdot 10^{-6}$ [s] to 10^{-3} [s] (see e.g. [79] and SIEMENS SIMATIC S7 System Manual, 04/2011, A5E02486680-03, p. 73). Tasks are executed based on interrupt handling or scheduling. The controllers are implemented with the help of programming languages (e.g. `C/C++`) or graphical user interfaces (e.g. Simulink in Matlab). The compiled code runs in "real-time" on the processing unit(s) and is executed every duty cycle (discrete execution). For this work, it is assumed that the duty cycles are sufficiently short yielding execution in "quasi" continuous time. Inevitable errors due to e.g. sampling, discretization and representation of numbers in binary format (e.g. floating point numbers) are neglected.

1.4.2 Electrical drive (actuator)

An electrical drive—comprising power inverter (or converter) and electrical machine *with* current control loop—is considered as mechatronic actuator generating drive torque m_M [Nm] (see Fig. 1.6). The actuator is a nonlinear dynamical system. Due to physical and safety reasons, its output is constrained by the maximal admissible torque $\hat{u}_A > 0$ [Nm]. The torque in electrical drives is proportional to the product of current i_M [A] and (excitation) flux in the machine (electro-magnetic conversion). Precise modeling of alternating current (AC) or direct current (DC) machines and power inverters can be found in [164, Chapters 3,5,6] and [165, p. 668-671], respectively.

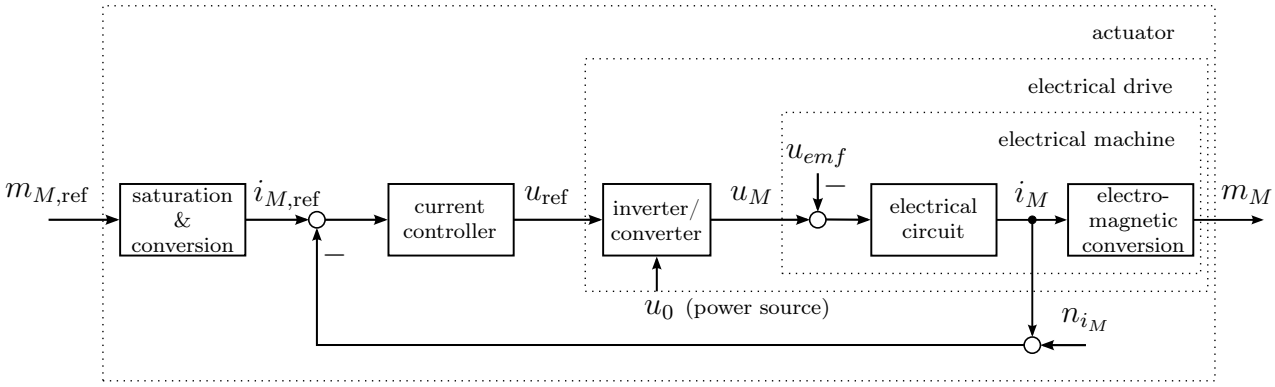

Figure 1.6: *Block diagram of (electrical) actuator with torque (current) control loop*

The basic scheme of a current (or torque) control loop is depicted in Fig. 1.6. The reference torque $m_{M,\text{ref}}$ [Nm]—externally generated by e.g. a motion controller—is applied to the electrical drive, is saturated to protect the machine (from e.g. over-currents) and is converted to the corresponding current reference $i_{M,\text{ref}}$ [A]. This conversion may imply observation/estimation of the machine flux by e.g. the use of a machine model or an observer.

The current controller generates the corresponding reference voltage u_{ref} [V], which is emulated by e.g. pulse width modulation (PWM, for different PWM techniques see [165, Section 8.4]) in the power inverter. The DC intermediate circuit (see e.g. [165, Chapter 7 & 8]) is fed by a power source (e.g. battery or rectifier connected to the power grid) and provides the intermediate circuit voltage $u_0 > 0$ [V] (DC). Due to the high capacity of the DC link capacitor, the voltage u_0 only changes slowly with the load (current drawn by the machine). It is assumed constant, but limits the output voltage u_M [V] of the inverter. The electrical circuit of the machine responds to u_M by current i_M [A], which by electromagnetic conversion results in motor torque m_M. Due to Faraday's Law rotation of the rotor induces a bounded voltage u_{emf} [V] (see Fig. 1.6) counteracting the applied voltage u_M. This induced voltage is called back-emf (electro-motive force) and is proportional to the product of rotor speed and flux. Note that due to saturation of u_M (by u_0) and back-emf u_{emf}, the current gradient $\frac{\mathrm{d}}{\mathrm{d}t} i_M$ is constrained by the quotient of $u_0 - u_{emf}$ and motor inductance. However concerning motion control, it may be assumed that the available voltage $u_0 - u_{emf}$ is sufficiently large compared to the inductance such that sufficiently fast current (and hence torque) changes are feasible.

The current control loop is perturbed by noise $n_{i_M}(\cdot) \in \mathcal{W}^{1,\infty}(\mathbb{R}_{\geq 0}; \mathbb{R})$ from current measurement. Typically, the current controllers are designed such that (ideally) a prescribed maximum overshoot is not exceeded by the current response $i_M(\cdot)$ (e.g. $\Delta^{os}_{i_M(\cdot)} = 4$ [%] for a controller design according to the "Symmetric Optimum", see [166, Section 3.2 & p. 81-82]). Hence, due to saturation of $m_{M,\text{ref}}$ and boundedness of current overshoot and disturbances n_{i_M} and u_{emf}, the generated motor torque m_M is uniformly bounded. For more details on current control and current measurement see e.g. [166, Chapter 15] and [163, Chapter 12], respectively.

Modern power semiconductors—e.g. Metal-Oxide-Semiconductor Field-Effect Transistors (MOSFETs) or Insulated-Gate Bipolar Transistors (IGBTs) (see [160, p. 199] or in great detail [163, Sections 6.6-6.8 and 7.2-7.4])—allow fast switching frequencies f_S $\left[\frac{1}{\text{s}} = \text{Hz}\right]$ ranging

form 7.5 to 16 [kHz]. However, there is delay between reference voltage u_{ref} and applied voltage u_M [V]. A common (linear) approximation of the dynamics of the current control loop of e.g. DC drives is given by the following second-order transfer function

$$\frac{i_M(s)}{i_{M,\text{ref}}(s)} = \frac{1}{1 + 2T_\sigma\, s + 2T_\sigma^2\, s^2}$$

where $T_\sigma > 0$ is inversely proportional to the switching frequency (see [166, p. 231,248]).

Although current control of AC machines is more complex (e.g. requiring space vector modulation [165, Section 8.4.10]), in principle same conclusions also hold for AC drives such as permanent magnetic synchronous machines (PMSM) or induction machines (IM) with power inverters. The torque generation is fast (see e.g. [162, pp. 775-779] for PMSM). Field-oriented torque control (FOC) [166, Section 13.4.4], direct torque control (DTC) [166, Section 15.5.3] and model predictive direct torque control (MPDTC) [62, 148] are most common approaches for AC machines. MPDTC is the fastest control scheme, since e.g. time delays are compensated by using prediction models for inverter and machine.

For modern AC and DC drives, torque and so current references are tracked with a delay ranging from $50 \cdot 10^{-6}$ [s] to $2 \cdot 10^{-3}$ [s] (see e.g. [123] and [143]), whereas the dominating mechanical "time constants" (proportional to mass or inertia) are by multiples larger. Hence, torque generation is fast compared to the dynamics of the actuated mechanical system. It is common to approximate the "dynamics" of the actuator by a simple proportional characteristic (see e.g. [166, p. 249] or the articles [123, 143]). More precisely, for any instant t [s] of time and (possibly unknown) actuator gain $k_A > 0$ [1], it is assumed that the following holds

$$\forall\, t \geq 0\colon \qquad m_M(t) = k_A\, m_{M,\text{ref}}(t). \tag{1.8}$$

Note that torque saturation and deviations in torque generation, due to e.g. actuator dynamics or perturbations (back-emf and measurement noise) in the current control loop, are not considered in (1.8). To account for saturation and (time-varying) perturbations in torque generation, the following "simplified actuator model" (without dynamics) is proposed

$$\forall\, t \geq 0\colon \quad m_M(t) = k_A\, \text{sat}_{\hat{u}_A}\Big(m_{M,\text{ref}}(t) + u_A(t)\Big), \quad \hat{u}_A, k_A > 0,\ u_A(\cdot) \in \mathcal{L}^\infty(\mathbb{R}_{\geq 0}; \mathbb{R}) \tag{1.9}$$

where $\text{sat}_{\hat{u}_A}(\cdot)$ is as in (N.3). The actuator model (1.9) is used throughout this thesis.

1.4.3 Mechanics (physical system)

The components of the mechanical system in Fig. 1.5—e.g. rotor of machine, gears, shafts, clutches and work machines—have dimensions and masses. Depending on the density of the materials, the mass has a (not necessarily homogeneous) distribution over the volume. Accordingly, the center of gravity can be computed by e.g. using computer aided design (CAD). It does not necessarily coincide with the centroid of the volume. For this thesis only "lumped parameter models" (see e.g. [77, p. 14]) are considered, i.e. forces or torques act on the lumped mass or inertia at the center of gravity.

Furthermore, backlash in gears is neglected since it precludes high-precision position and speed control, e.g. limit cycles or steady state errors may occur (see [140]). Gears are regarded as "proportional systems" which yield gear transmission or gear reduction of position, speed and torque proportional to gear ratio $g_r \in \mathbb{R} \setminus \{0\}$ [1]. An overview of mathematical models for gears and gear dynamics is given in [139]. Harmonic drives are a typical example of gears having (almost) no backlash. However, due to flexible splines in the gear, harmonic drives bring elasticity into the mechanical system (see [179, 181]), which additionally motivates the consideration of flexible servo-systems. Two inertias coupled by an harmonic drive can be considered as elastic 2MS (see e.g. [174, Section 6.5]). In addition, friction is significantly increased by harmonic drives (see e.g. [179]) which in turn emphasis precise friction modeling in Section 1.4.5.

1.4.4 Speed and position sensors (instrumentation)

For feedback control, the controlled variable(s) should ideally be available at each instant t [s] of time. For position control actual position $\phi(t)$ [rad] *and* speed $\omega(t) = \dot{\phi}(t)$ $\left[\frac{\text{rad}}{\text{s}}\right]$ are required, whereas for speed control only speed $\omega(t)$ is needed.

Although there exist "sensorless" motion control approaches (without position or speed measurement, see e.g. [166, Chapter 14] for AC drives), their performance concerning closed-loop dynamics and accuracy is very limited. Hence, servo-drives for high-precision motion control are equipped with position and/or speed sensors. Typical sensors in industry are e.g. tacho-generators and resolvers or encoders for speed and position measurement, respectively. For an overview of and more details on position and speed sensors, the reader is referred to [166, Section 8.5] or [48, Chapter A5].
In industry optical encoders are most common, since they are cheap and provide a sufficiently high resolution ranging from $2 - 8 \cdot 10^6$ lines per revolution (with interpolation, see e.g. [166, p. 308]). Nevertheless, encoders are more sensitive to temperature changes, incorrect mounting, mechanical shock and noise than resolvers (see [166, p. 307]).
Although position *and* speed feedback are required for position control, in the majority of cases to reduce costs for instrumentation, solely a encoder (or resolver) is implemented. Then speed $\omega(t) = \dot{\phi}(t)$ is approximated in the capturing device (interface board reading position signals from the sensor) by numeric differentiation (e.g. Euler method)

$$\omega(t) \approx \frac{\phi(t) - \phi(t - T_c)}{T_c} \tag{1.10}$$

where $T_c > 0$ [s] is the cycle time of the capturing device. Due to small cycle times $< 50 \cdot 10^{-6}$ [s] the resulting time-delay is negligible. The approximation works acceptably well, even if measurement noise is present. However, speed feedback ripples (discontinuous speed feedback) may occur. To obtain a "quasi" continuous speed approximation the use of SINCOS encoders is indicated. These encoders allow to interpolate among consecutive lines (see [48, Section A5.3.5]).

Motion sensing is subject to measurement errors. Main causes for deviations in the measured signal are (see e.g. [166, Section 8.2]):

- *the sensor*: due to e.g. limited resolution or bandwidth, manufacturing faults, wear and

aging;

- *the environment*: due to e.g. temperature (changes), contamination, deficient mounting (radial eccentricity, long cabling) and electromagnetic interference (noise);
- and *signal processing*: due to e.g. analogue-to-digital (A/D) and digital-to-analogue (D/A) conversion (sampling, quantization, aliasing errors), signal level matching (OpAmp drift), non-synchronous capturing of analogue signals and time delay.

Most deviations in the measured feedback signal can neither be predicted nor compensated for in the control loop resulting in tracking errors. Hence sensors with sufficient accuracy are necessary. High-precision motion control inherently depends on high-precision motion measurement (see [166, p. 302, Section 8.2]).

In the following it is assumed that the instrumentation of the servo-drive is sufficiently accurate, however small deviations inevitably remain. By subsuming measurement errors in the bounded signal $n_m(\cdot) \in \mathcal{W}^{2,\infty}(\mathbb{R}_{\geq 0};\mathbb{R})$, the following "simplified sensor model" (without dynamics) is proposed

$$\forall\, t \geq 0\colon \qquad y_m(t) = y(t) + n_m(t), \qquad y(\cdot) \in \mathcal{C}(\mathbb{R}_{\geq 0};\mathbb{R}),\ n_m(\cdot) \in \mathcal{W}^{2,\infty}(\mathbb{R}_{\geq 0};\mathbb{R}), \tag{1.11}$$

where $y_m(\cdot)$ represents the deteriorated measurement of some physical quantity $y(\cdot)$ such as position $\phi(\cdot)$ in [rad] (or [m]) or speed $\omega(\cdot)$ in [rad/s] (or [m/s]).

Remark 1.1 (Stochastic noise)**.**
In general, noise is a stochastic process, e.g. "white noise" is a consequence of Brownian motion. Since noise is inevitably induced into the closed-loop system by feedback, the analysis of the differential equation would imply analysis of stochastic differential equations using the theory introduced by Kiyoshi Itō (1915–2008) (see e.g. [144, Chapter 3]). In this thesis only ordinary (or functional) differential equations are considered. It is assumed that the bounded absolutely continuous function $n_m(\cdot)$ "approximates" noise sufficiently well.

1.4.5 Friction

Any contacting bodies in motion with relative velocity are subject to friction counteracting their acceleration. In feedback control systems, friction may cause poor transient performance. Limit cycles, non-vanishing tracking errors, stick-slip or hunting (for controllers with integral action) may occur. Especially, for high-precision position control of e.g. machine tools or robotic manipulators, friction becomes an issue at very low speeds (see e.g. [10, 28, 74, 146]).

1.4.5.1 Contributions from tribology

Tribology is the science of rubbing contacts founded in England in the 1930s (see [10]). It fundamentally contributes to understand friction in more detail and helps to develop friction models required for e.g. analysis of motion control problems. Friction phenomena are examined mainly for translational setups, however the results can be transferred to rotatory systems

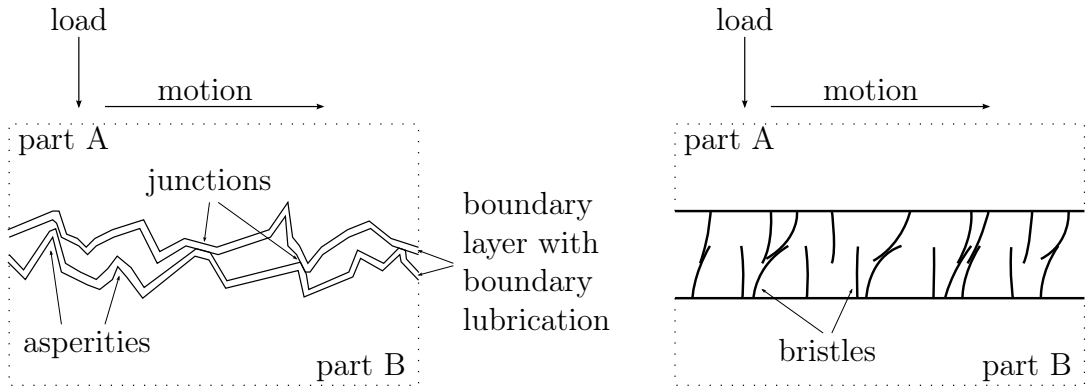

(a) *Microscopic view (based on Fig. 4 in [10]).*

(b) *Simplified view: asperities are modeled as (bending) bristles (based on Fig. 1 in [39]).*

Figure 1.7: *Cross-section of contact surface between mechanical parts A & B.*

(see [10, Section 2.2.2.1]). In the rotatory case, due to ball bearings, friction effects are less serious. Exceptions are e.g. hard disk drives or ball screws (see [10, Section 2.2.2.1]).

In mechatronic systems, fluid lubrication—e.g. oil or grease in ball bearings—is most common for metal-on-metal contacts. The lubricants provide fluid barriers within the intersection (i.e. the microscopical contact area) of the contacting materials to avoid dry friction and hence to reduce mechanical wear. The lubricant is drawn into the intersection by (relative) motion of the contacting parts, if a minimal (relative) velocity is exceeded; i.e. hydrodynamic lubrication for conformal surfaces or elasto-hydrodynamic lubrication for non-conformal surfaces such as ball bearings or gear teeth (see [10]).

The topography of an intersection is rough. The microscopical contact surface was felicitously visualized by R.D. Bowden in 1950 (during a BBC broadcast) with the words "*putting two solids together is rather like turning Switzerland upside down and standing it on Austria — the area of intimate surfaces will be small*" (see [10]). A cross-section of an intersection is depicted in Fig. 1.7(a). The "hills and mountains" are called asperities, which deform due to the total load (e.g. weight) of the parts in contact and build contact areas, i.e. asperity conjunctions with a typical width of $\approx 10^{-5}$ [m] for steel (see Fig. 1.7(a)). Due to e.g. oxidation, a film of boundary lubricant(s) develops within the boundary layer. Boundary lubrication adheres solidly to the metal part and is extremely thin ($\approx 10^{-7}$ [m], see [10]).

For fluid lubricants there exist four regimes of lubrication (see [10]), which directly effect the friction characteristics (see Fig. 1.8):

Regime I: static friction (stiction) and pre-sliding displacement
Experimenting with ball bearings, R.D. Dahl observed in 1977 a linear relation between applied load (e.g. external force or torque) and relative rotation (see [43]). He concluded that the asperities act like springs up to a critical break-away force (after which the parts start to slide). The asperities deform elastically resulting in pre-sliding displacement. Hence, stiction can be modeled as a force proportional to the product of displacement and stiffness of the

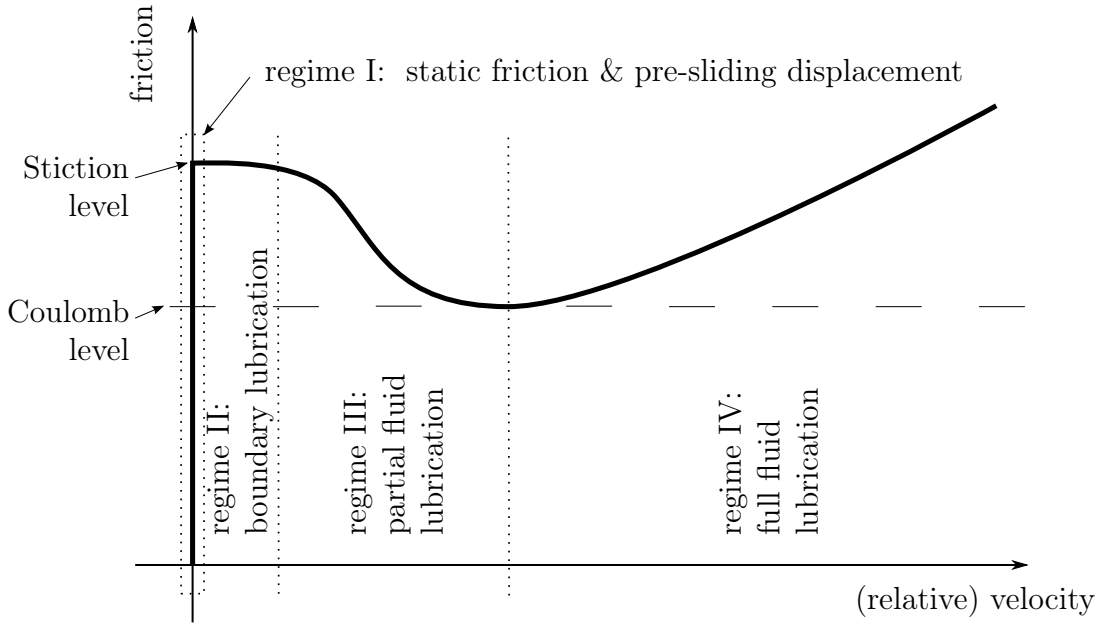

Figure 1.8: *Regimes of lubrication (based on Fig. 5 in [10])*

asperities. For steel materials, pre-sliding displacement ranges from $2 - 5 \cdot 10^{-5}$ [m]. Note that pre-sliding indicates that there "are no discontinuities in friction as a function of time" (see [10]).

Regime II: boundary lubrication
If the break-away force is exceeded, the parts begin to slide. However, for very small (relative) velocities, still a fluid lubrication film cannot develop within the intersection. The materials are in solid-to-solid contact and the boundary layer with boundary lubrication is subject to shear. Note that, friction in this regime is not necessarily higher than in regimes III and IV with partially and full fluid lubrication, e.g. there exist boundary lubricants which reduce stiction level below Coulomb level (see Fig. 1.8). Then stick-slip is eliminated entirely (see [10]).

Regime III: mixed (or partially fluid) lubrication
If velocity exceeds a critical value, fluid lubricants are drawn into the contact area and held there by viscosity. The higher the velocity the thicker the film of the lubricants will be. For a film thickness below the maximal height of the asperities, some few solid-to-solid conjunctions remain. However, due to partial lubrication, friction reduces rapidly allowing for rapid increase in acceleration of the moving parts. This phenomenon is called Stribeck effect (see [10]).
Furthermore, experiments and simulations show that, within regime III, a change in velocity (or load conditions) results in a delayed change in friction level. This time lag is known as frictional memory (or frictional lag, see [39]) with delay times ranging from milliseconds to seconds.

Regime IV: full fluid lubrication
If film thickness of the lubricant(s) exceeds the size of the asperities, full fluid lubrication is reached: the mechanical parts are completely separated and "swim" on the lubricant(s). No more solid-to-solid contacts remain. Hence, material wear is drastically reduced. In this regime friction is governed by hydrodynamics, i.e. viscous friction is proportional to the (sliding) velocity.

In the following the explanations are for the rotatory (or translational) case. Dimensions in parenthesis indicate the translational case, e.g. velocity in [rad/s] (or [m/s]).

1.4.5.2 Static friction modeling

Friction was already observed by Leonardo Da Vinci (1452–1519) [42, Chapter XVIII] as a force proportional to normal force having opposite sign to relative velocity. Later, this friction phenomenon was named after Charles Augustin de Coulomb (1736–1806). In 1779 Coulomb published his memories on his observations on friction (see [41]). Coulomb friction is modeled by

$$\forall u_C > 0\colon \qquad f_C\colon \mathbb{R} \to [-u_C,\, u_C], \qquad \omega \mapsto f_C(\omega) := u_C\, \operatorname{sign}(\omega) \tag{1.12}$$

where u_C is the Coulomb friction level with dimension [Nm] (or [N]) and ω is the velocity in [rad/s] (or [m/s]). Coulomb friction is illustrated in Fig. 1.9(a).

Not until the 19th century, the Coulomb model was extended by static friction (stiction, see [136]) and viscous friction (see [153]). In standstill (i.e. $\omega = 0$) Coulomb level u_C may be exceeded by stiction level u_S (i.e. $u_S \geq u_C$) depending on external load u_L in [Nm] (or [N]). Static friction is given by (see [145, p. 27])

$$\forall u_S > 0\colon \quad f_S\colon \mathbb{R} \to [-u_S,\, u_S], \qquad u_L \mapsto f_S(u_L) := \begin{cases} u_L & ,|u_L| < u_S \ (\wedge\, \omega = 0) \\ u_S \cdot \operatorname{sign}(u_L) & ,|u_L| \geq u_S \ (\wedge\, \omega = 0) \end{cases} \tag{1.13}$$

Viscous friction increases (or decreases) as velocity increases (or decreases). More precisely, for exponent $\delta_V \geq 1$ [1] and viscous friction coefficient ν $\left[\mathrm{Nm/(rad/s)^{\delta_V}}\right]$ (or $\left[\mathrm{N/(m/s)^{\delta_V}}\right]$), viscous friction is modeled by (see [145, p. 26])

$$\forall \nu > 0,\, \delta_V \geq 1\colon \qquad f_V\colon \mathbb{R} \to \mathbb{R}, \qquad \omega \mapsto f_V(\omega) := \nu\, |\omega|^{\delta_V} \operatorname{sign}(\omega). \tag{1.14}$$

A friction model incorporating static, Coulomb and viscous friction is given by (see [145, p. 27])

$$f_{SCV}\colon \mathbb{R} \times \mathbb{R} \to \mathbb{R}, \qquad (\omega, u_L) \mapsto f_{SCV}(\omega, u_L) := \begin{cases} f_V(\omega) & ,\omega \neq 0 \\ f_S(u_L) & ,\omega = 0 \end{cases} \tag{1.15}$$

where $f_V(\cdot)$ and $f_S(\cdot)$ are as in (1.14) and (1.13), respectively. Its graph is qualitatively depicted in Fig. 1.9(b). Note that the definition of stiction in (1.13) requires differential inclusion (see [147]). For systems subject to friction modeled by (1.15), the right hand side of the differential equation (describing the system dynamics) becomes rather a set then an "isolated point".

Although the friction model (1.15) is not correct in general, it was, and still is, common to analyze friction effects in feedback systems. Already in 1902 Richard Stribeck (1861–1950) observed a *"rapid" but continuous decrease* in friction ("negative viscous friction coefficient") in ball bearings for increasing but very low speeds close to standstill (see [176, 177]). This phenomenon is called Stribeck effect nowadays (see Fig. 1.9(c)). For velocities below a threshold velocity, the Stribeck effect may cause (locally) unstable behavior of closed-loop systems with

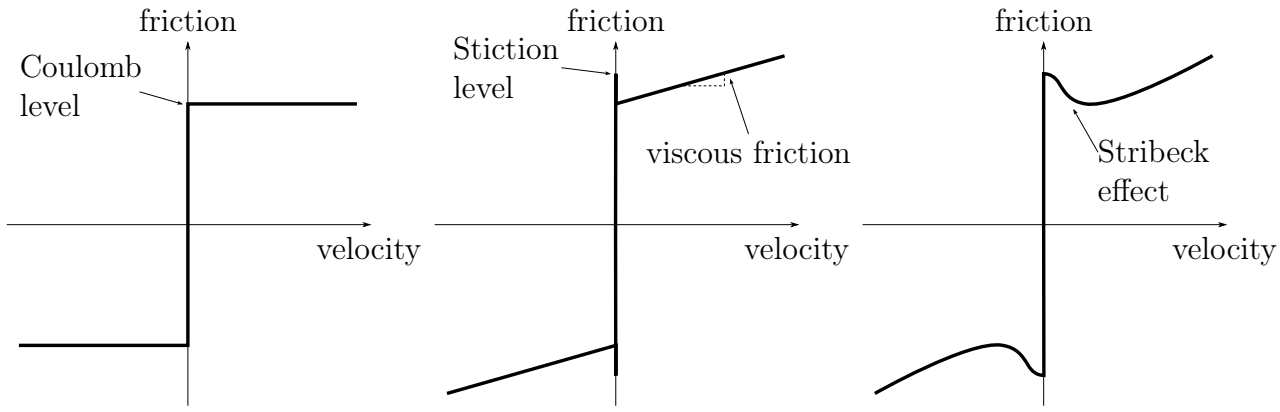

(a) *Coulomb friction* (b) *Static (stiction), Coulumb and (linear) viscous friction* (c) *Static, Coulumb and viscous friction*

Figure 1.9: *Static friction models*

proportional-derivative (PD) controllers, if the derivative gain (weighting velocity) is too small (see [8]).

To model the Stribeck effect, the following Stribeck function is common (see e.g. [10, 147]). For Stribeck velocity ω_S [rad/s] (or [m/s]) and exponent δ_S [1], let the Stribeck function be given by

$$\forall\, u_S \geq u_C > 0\ \forall\, \omega_S > 0\ \forall\, \delta_S \in [1/2,\, 2]\colon$$
$$\beta : \mathbb{R} \to [u_C, u_S], \qquad \omega \mapsto \beta(\omega) := u_C + (u_S - u_C) \exp\left(-\left(\frac{|\omega|}{\omega_S}\right)^{\delta_S}\right). \tag{1.16}$$

A friction model (sometimes called "kinetic friction model", see [3, p. 24-27]) incorporating Coulomb, static, viscous friction *and* Stribeck effect is given by (see [145, p. 28])

$$f_{KFM}\colon \mathbb{R} \times \mathbb{R} \to \mathbb{R}, \qquad (\omega, u_L) \mapsto f_{KFM}(\omega, u_L) := \begin{cases} f_S(u_L) & ,\omega = 0 \\ \beta(\omega)\,\mathrm{sign}(\omega) + f_V(\omega) & ,\omega \neq 0 \end{cases} \tag{1.17}$$

where $f_S(\cdot)$, $\beta(\cdot)$ and $f_V(\cdot)$ are as in (1.13), (1.16) and (1.14), respectively. The qualitative behavior of the friction model (1.17) is shown in Fig. 1.9(c).

Remark 1.2. *The Stribeck function $\beta(\cdot)$ in (1.16) may also be chosen "asymmetric" (see [145, p. 49]) which may reflect reality more precisely (see e.g. [182]). For $u_C^- \leq 0 \leq u_C^+$ and $u_S^- \leq 0 \leq u_S^+$ a possible choice is given by*

$$\beta\colon\ \mathbb{R} \to \mathbb{R}; \quad \omega \mapsto \beta(\omega) := \begin{cases} u_C^+ + (u_S^+ - u_C^+)\exp(-(|\omega|/\omega_S)^{\delta_S}) & ,\omega \geq 0 \\ u_C^- + (u_S^- - u_C^-)\exp(-(|\omega|/\omega_S)^{\delta_S}) & ,\omega < 0 \end{cases}$$

For simplicity, in the following the symmetric Stribeck function (1.18) is used.

1.4.5.3 Dynamic friction modeling

The friction models depicted in Fig. 1.9(a)-(c) are "static" maps from velocity to friction torque (or force). Hence, dynamic friction effects observed in experiments—such as hysteresis, varying break-away forces or pre-sliding displacement (see [39])—cannot be reproduced by the static models (1.12), (1.15) and (1.17), respectively. To model and understand friction effects more precisely, dynamic friction models are required (see e.g. the survey [10] or in great detail [9]). A first motivating idea was presented by Dahl in 1968 (see [44]) describing the dynamics of static friction as spring-like motion. However, his model does not cover the Stribeck effect (see [39]). Based on this first idea and the results of research in tribology, several dynamic friction models have been developed (see e.g. [39], [178], [57] or [49]). This thesis focuses on the popular Lund-Grenoble (LuGre) friction model introduced in [39]. It is nonlinear and dynamic and covers the Stribeck effect. Its generalized form was proposed in [145] and is presented in the following for rotatory (translational) systems.

The LuGre friction model cannot reproduce hysteretic behavior with nonlocal memory (see [178]) and does not account for stochastic distribution of the asperities (see [159]) and nonphysical drift phenomena may occur for small vibrational forces (see [49]). However, it is adequate for the motion control problem considered in this thesis, since most of the friction phenomena observed in "reality" are covered such as sticking (stick-slip), break-away with varying break-away forces, pre-sliding displacement, frictional lag and hysteresis. Moreover, for controllers with integral action, hunting can be reproduced (see e.g. [39, 145]) and it can be rendered passive (see [19]).

For the LuGre friction model the asperity junctions (see Fig. 1.7(a)) are modeled as bending bristles (see Fig. 1.7(b)). The bristles behave like springs with average stiffness $\sigma > 0$ [Nm/rad] (or [N/m]). The deflection of all bristles within the intersection is considered as average bristle deflection $\vartheta(\cdot)$ [rad] (or [m]) of the asperity junctions.
For $\beta(\cdot)$ as in (1.16), average bristle stiffness σ, velocity ω [rad/s] (or [m/s]) and initial average bristle deflection ϑ^0 [rad] (or [m]), the dynamics of the average bristle deflection are modeled by

$$\dot{\vartheta}(t) = \omega(t) - \sigma \frac{|\omega(t)|}{\beta(\omega(t))}\, \vartheta(t), \qquad \vartheta(0) = \vartheta^0 \in \mathbb{R}, \quad \omega(\cdot) \in \mathcal{C}(\mathbb{R}_{\geq 0}; \mathbb{R}). \tag{1.18}$$

Note that, by standard theory of ordinary differential equations (see e.g. Proposition 2.1.19 in [77]), for $\omega(\cdot) \in \mathcal{L}^1_{\mathrm{loc}}(\mathbb{R}_{\geq 0}; \mathbb{R})$ the initial-value problem (1.18) has an unique, global and bounded solution

$$\vartheta_{\omega(\cdot)} \colon \mathbb{R}_{\geq 0} \to \Big[-\max\{u_S/\sigma,\, |\vartheta^0|\},\ \max\{u_S/\sigma,\, |\vartheta^0|\} \Big] \tag{1.19}$$

where boundedness follows from the implications

$$\begin{aligned} &[\![\, |\vartheta_{\omega(\cdot)}(t)| \geq u_S/\sigma \,]\!] \quad \Longrightarrow \\ &\qquad [\![\, \frac{\mathrm{d}}{\mathrm{d}t}\, \vartheta_{\omega(\cdot)}(t)^2 \leq -2|\vartheta_{\omega(\cdot)}(t)\, \omega(t)| \Big(\underbrace{\operatorname{sign}(\vartheta_{\omega(\cdot)}(t)\, \omega(t))}_{\in\{-1,0,1\}} + \sigma \frac{|\vartheta_{\omega(\cdot)}(t)|}{\beta(\omega(t))} \Big) \leq 0. \,]\!] \\ &\qquad\qquad \Longrightarrow \quad [\![\, \forall\, t \geq 0 \colon \qquad |\vartheta_{\omega(\cdot)}(t)| \leq \max\{u_S/\sigma,\, |\vartheta^0|\} \,]\!]\,. \end{aligned}$$

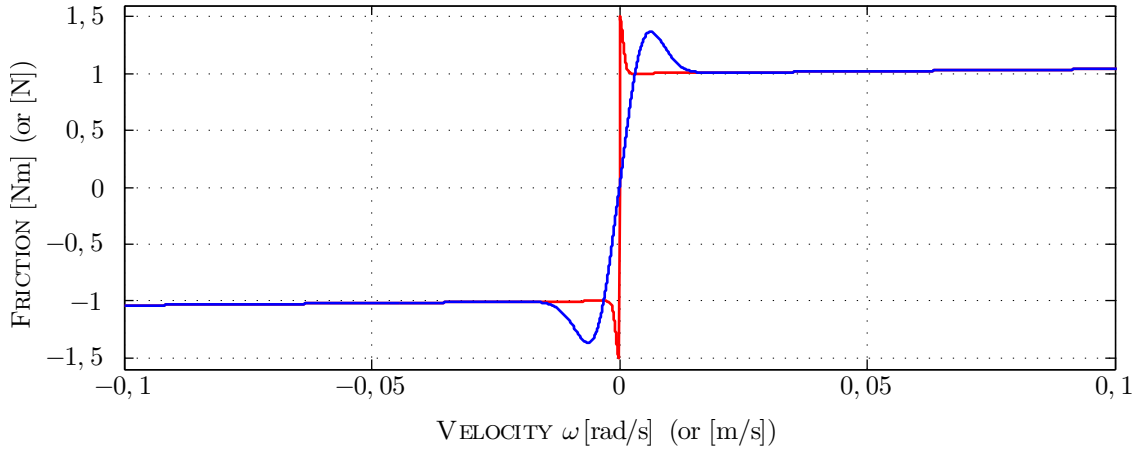

Figure 1.10: *Comparison*[1] *of static friction model* (1.17) *and dynamic LuGre model* (1.21) *with* $\delta_V = 1$*:* — graph$(\beta(\omega)\,\mathrm{sign}(\omega) + f_V(\omega))$ *and* — graph$(\mathfrak{L}_{\vartheta^0}\omega)$ *with the parametrization in Tab. 1.2, respectively.*

To present the LuGre friction model as in [145, Section 3.2-3], for damping coefficient ν_D [Nms/rad] (or [Ns/m]), damping velocity ω_D [rad/s] (or [m/s]) and damping exponent δ_D [1] introduce the damping (of the deflection rate $\dot{\vartheta}(\cdot)$) by

$$\forall\, \nu_D,\, \omega_D > 0\, \forall\, \delta_D \geq 1\colon \qquad f_D : \mathbb{R} \to [0, \nu_D], \quad \omega \mapsto f_D(\omega) := \nu_D \exp\left(-(|\omega|/\omega_D)^{\delta_D}\right) \tag{1.20}$$

and define the "LuGre friction operator" with dimension [Nm] (or [N]) by

$$\left.\begin{aligned} \mathfrak{L}_{\vartheta^0}\colon\ \mathcal{C}(\mathbb{R}_{\geq 0};\mathbb{R}) &\to \mathcal{L}^\infty_{\mathrm{loc}}(\mathbb{R}_{\geq 0};\mathbb{R}) \\ \omega(\cdot) &\mapsto \sigma\,\vartheta_{\omega(\cdot)} + f_D(\omega(\cdot))\left(\omega(\cdot) - \sigma\tfrac{|\omega(\cdot)|}{\beta(\omega(\cdot))}\vartheta_{\omega(\cdot)}\right) + f_V(\omega(\cdot)), \\ \text{where } f_D(\cdot) \text{ as in (1.20)},\ \beta(\cdot) &\text{ as in (1.16)},\ f_V(\cdot) \text{ as in (1.14) and } \vartheta_{\omega(\cdot)} \text{ solves (1.18)}. \end{aligned}\right\} \tag{1.21}$$

The operator $\mathfrak{L}_{\vartheta^0}$ maps speed (or velocity) to friction torque (or force), is parametrized by the initial average bristle deflection ϑ^0 and represents the LuGre friction model introduced in [145, Sections 3.2,3.3] in compact form.

Friction effects covered by the LuGre friction model

At first, the static friction model (1.17) and the dynamic LuGre model (1.21) are compared. Therefore both models are excited by a ramp-like velocity to obtain the "classical plot": friction over velocity. The friction characteristics of both models are illustrated in Fig. 1.10. Note that the dynamic LuGre friction model is not discontinuous at zero velocity and both models include the Stribeck effect.

Next it is shown that the LuGre friction model (1.21) with linear viscous friction (i.e. $\delta_V = 1$) still covers e.g. pre-sliding displacement, frictional lag, hysteresis, stick-slip and limit-cycles (hunting). The following experiments, illustrated in Fig. 1.11, are implemented in Matlab/Simulink using the fixed-step solver `ode4 (Runge-Kutta)` with a step size of 10^{-5} [s]. The simulation

[1] The figure was generated by merging two simulation results with excitation $\dot{\omega}(t) = -2$ $[\mathrm{rad/s^2}]$ and $\dot{\omega}(t) = 2$ $[\mathrm{rad/s^2}]$ for all $t \in [0,\, 0.5]$ [s], respectively. Each run was initialized with $\vartheta^0 = 0$ [rad] and $\omega(0) = 0$ [rad/s].

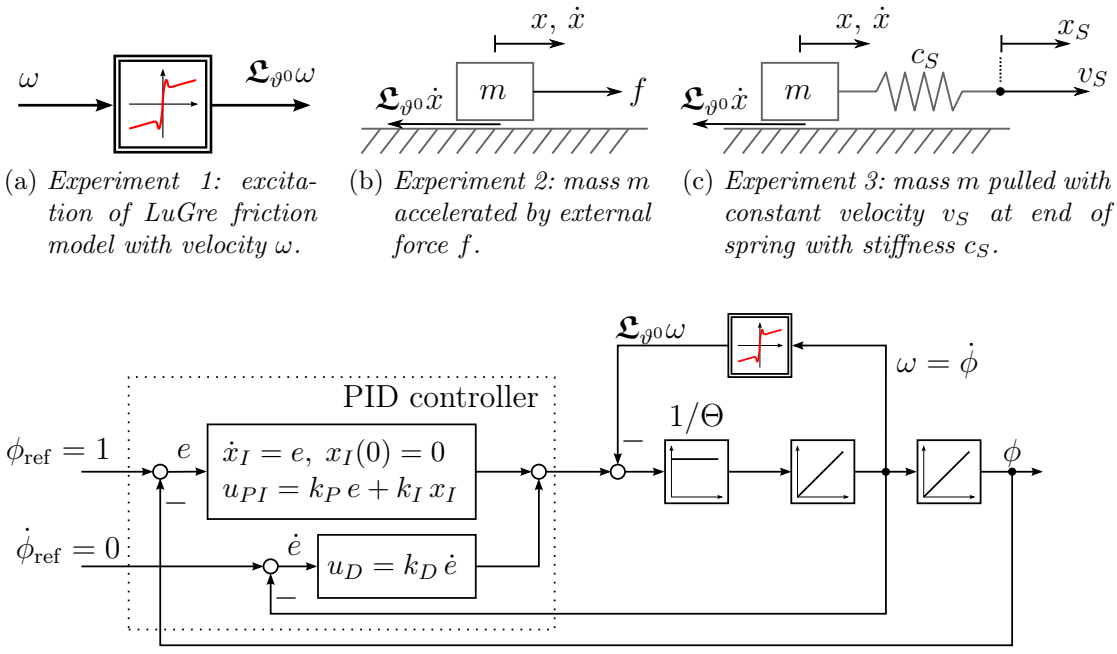

(a) *Experiment 1: excitation of LuGre friction model with velocity ω.*

(b) *Experiment 2: mass m accelerated by external force f.*

(c) *Experiment 3: mass m pulled with constant velocity v_S at end of spring with stiffness c_S.*

(d) *Experiment 4: PID position control of angle ϕ.*

Figure 1.11: *Simulation experiments with LuGre friction model* (1.21)

parameters are collected in Tab. 1.2 and are used for all experiments (with corresponding dimensions). The experiments are similar to those presented in [39]. However, in the present work the damping function (1.20) is implemented additionally for simulations.

Experiment 1: hysteresis and frictional memory
The LuGre friction model (1.21) is excited by a continuous velocity given by

$$\omega\colon \mathbb{R}_{\geq 0} \to \mathbb{R}, \quad t \mapsto \omega(t) = 5 \cdot 10^{-3}(\sin(\omega_0\, t) + 1) \quad \text{where} \quad \omega_0 \in \{1,\, 10,\, 25\}\ [\text{rad/s}]\,.$$

The simulation results are depicted in Fig. 1.12. The LuGre model clearly exhibits hysteresis. For increasing velocities the resulting friction is larger than for corresponding but decreasing velocities (see Fig. 1.12(a)). The hysteresis width is proportional to the velocity change, it is widest for $\omega_0 = 25$ [rad/s].
Furthermore, the LuGre friction model (1.21) reproduces frictional lag as shown in Fig. 1.12(b). For small and decreasing (or increasing, not shown here) velocities the friction increases (or decreases) with time delay.

Experiment 2: pre-sliding displacement
A mass $m > 0$ [kg] is accelerated by the external force f [N] (see Fig. 1.11(c)). Friction as in (1.21) counteracts the acceleration. Position x [m], velocity $\dot{x}$ [m/s], average bristle deflection ϑ [m] and friction force $\mathfrak{L}_{\vartheta^0}\dot{x}$ [N] are observed. The force f is ramped up, held constant for a while and then is ramped up again with less slope (see top of Fig. 1.13(b)). The zoom in Fig. 1.13(a) clearly indicates pre-sliding displacement of position $x(\cdot)$ up to $\approx 0.5 \cdot 10^{-4}$ [m]. The external force is nearly compensated by friction, which is proportional to the deflection of the bristles (see top of Fig. 1.13(b)). As long as the external force $f(\cdot)$ is constant on $[14 - 20]$ [s], velocity $\dot{x}(\cdot)$ drops to zero.

Description	Symbol = Value	[Dimension]
Coulomb friction level	$u_C = 1$	[Nm] or [N]
Stiction friction level	$u_S = 1.5$	[Nm] or [N]
Stiffness	$\sigma = 10^5$	[Nm/rad] or [N/m]
Stribeck velocity	$\omega_S = 0.001$	[rad/s] or [m/s]
Stribeck exponent	$\delta_S = 2$	[1]
Damping friction coefficient	$\nu_D = \sqrt{10^5}$	[Nms/rad] or [Ns/m]
Damping friction velocity	$\omega_D = 0.1$	[rad/s] or [m/s]
Damping friction exponent	$\delta_D = 2$	[1]
Viscous friction coefficient	$\nu = 0.4$	[Nms/rad] or [Ns/m]
Viscous friction exponent	$\delta_V = 1$	[1]
Initial average bristle deflection	$\vartheta_0 = 0$	[rad] or [m]

Table 1.2: *Simulation parameters of LuGre model* (1.21)

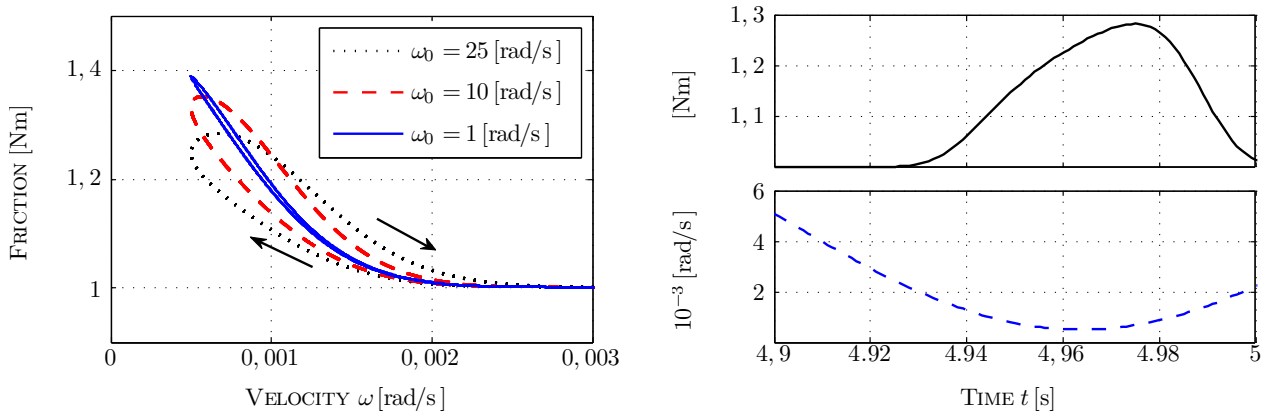

(a) *hysteresis for excitation speeds* $\omega(t) = 5 \cdot 10^{-3}(\sin(\omega_0 t) + 1)$ *where* $\omega_0 \in \{1, 10, 25\}$ [rad/s].

(b) *frictional lag (shown for* $\omega_0 = 25$ [rad/s]*):* — *friction* $(\mathfrak{L}_{\vartheta^0}\omega)(\cdot)$ *(top) and* - - - *speed* $\omega(\cdot)$

Figure 1.12: *Experiment 1—simulation results*

At $t \approx 28$ [s] the break-away force of ≈ 1.5 [N] is reached (see top of Fig. 1.13(b)) and sliding begins (see Fig. 1.13(a)). Friction $(\mathfrak{L}_{\vartheta^0}\dot{x})(\cdot)$ reduces drastically due to relaxation of the bristles (the Stribeck velocity is by far exceeded). The average bristle deflections $\vartheta(\cdot)$ drops to 10^{-5} [m] (see bottom of Fig. 1.13(b)).

Experiment 3: stick-slip

Consider the setup depicted in Fig. 1.11(c). A mass $m > 0$ [kg] is subject to LuGre friction $\mathfrak{L}_{\vartheta^0}\dot{x}$ as in (1.21) parametrized by the values given in Tab. 1.2. The mass is connected to a spring with stiffness $c_S > 0$ [kg/s^2], has position x [m] whereas the position of the spring endpoint is denoted by x_S [m]. The endpoint of the spring is pulled with constant velocity $v_S > 0$ [m/s]. Due to the Stribeck effect (1.16) covered by (1.21), stick-slip occurs: for consecutive time intervals, the mass is at rest and then moving again (see Fig. 1.14(b)). As long as the mass is not moving or moving slower than the spring endpoint, the spring force $c_S(v_S \cdot - x(\cdot))$ is increasing. For spring forces $c_S(v_S \cdot - x(\cdot)) > u_S$ greater than stiction level, the mass accelerates and starts

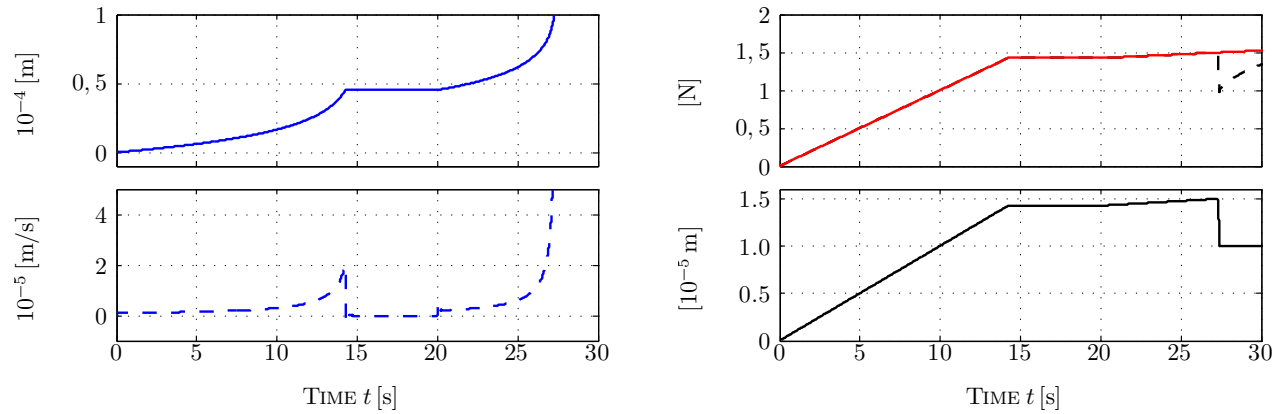

(a) *top:* — *position* $x(\cdot)$ *and bottom:* - - - *velocity* $\dot{x}(\cdot)$ (b) *top:* — *force* $f(\cdot)$ *and* - - - *friction* $(\mathfrak{L}_{\vartheta^0}\dot{x})(\cdot)$*; bottom:* — *average bristle deflection* $\vartheta(\cdot)$

Figure 1.13: *Experiment 2—simulation results: pre-sliding displacement*

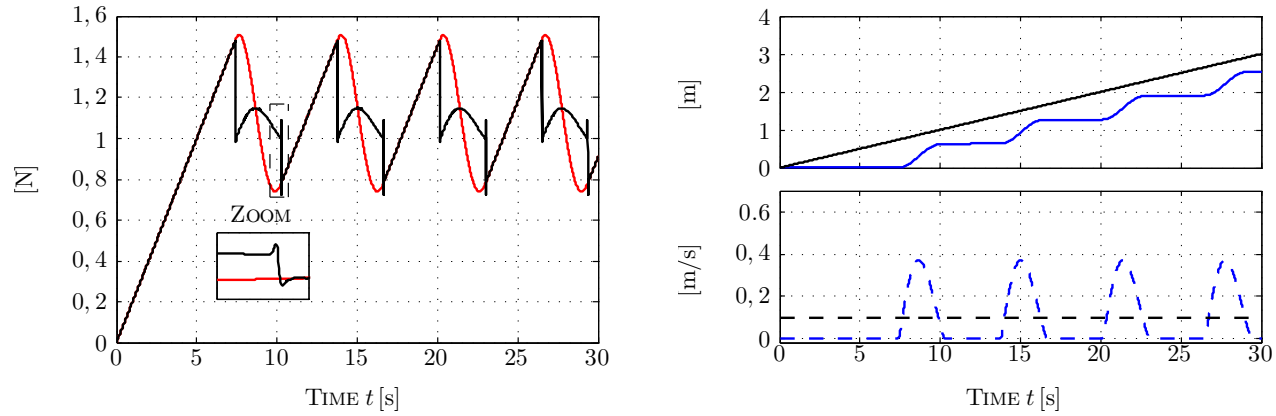

(a) — *friction* $(\mathfrak{L}_{\vartheta^0}\dot{x})(\cdot)$ *and* — *spring force* $c_S(v_S \cdot -x(\cdot))$ (b) *top: positions* — $x(\cdot)$ *and* — $x_S(\cdot)$*; bottom: velocities* - - - $\dot{x}(\cdot)$ *and* - - - $v_S(\cdot)$

Figure 1.14: *Experiment 3—simulation results: stick-slip for simulation parameters* $m = 1$ [kg]*,* $c_S = 2$ [N/m] *and* $v_S = 0.1$ [m/s].

to slide. It "slips". If the Stribeck velocity $\omega_S = 0.001$ [m/s] is exceeded, friction is drastically reduced due to partially fluid lubrication (see regime III) and, in turn, the mass accelerates even more rapidly. For velocities $\dot{x}(\cdot)$ greater than v_S it catches up with the spring endpoint reducing the spring force $c_S(v_S \cdot -x(\cdot))$ (see bottom of Fig. 1.14(b) and Fig. 1.14(a)). For spring forces smaller than friction, the mass decelerates again. Its velocity $\dot{x}(\cdot)$ is decreasing (see bottom of Fig. 1.14(b)). For very low velocities the Stribeck effect results in a rapid but continuous increase of friction (see top of zoom in Fig. 1.14(a)). The remaining spring force cannot accelerate the mass and hence motion is stopped. It "sticks". At standstill the bristles relax completely and friction reduces to a minimum (see bottom of zoom in Fig. 1.14(a)). Now the same phenomenon starts over again. The mass "sticks" and "slips" and follows the spring endpoint $x_S(\cdot)$ in a "staircase-like" manner with time delay (see Fig. 1.14(b)).

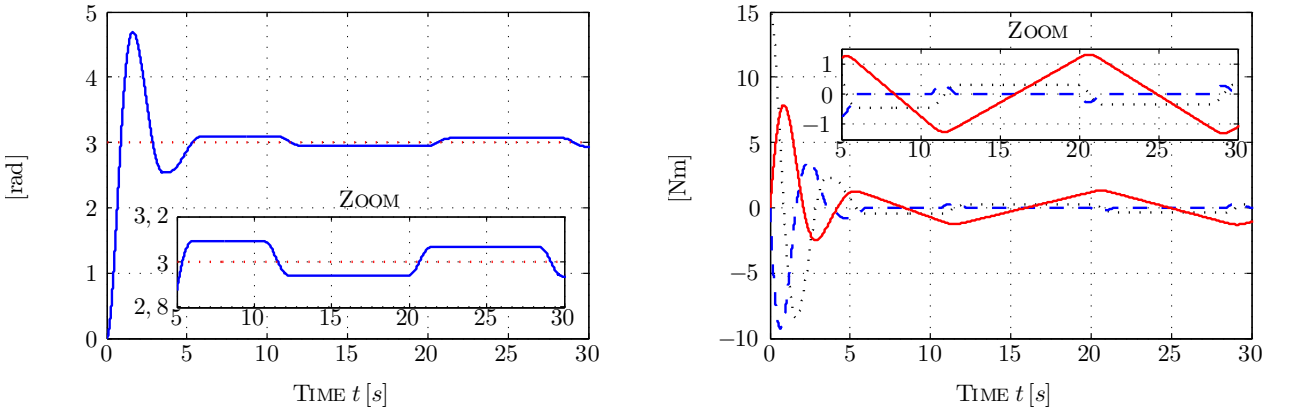

(a) —— *position* $\phi(\cdot)$ *and* ····· *reference* $\phi_{\text{ref}}(\cdot)$

(b) *control action:* ····· $k_P e(\cdot)$ *(proportional),* - - - $k_D \dot{e}(\cdot)$ *(derivative) and* —— $k_I\, x_I(\cdot)$ *(integral)*

Figure 1.15: *Experiment 4—simulation results: hunting (limit cycles) for simulation parameters* $m = 1$ [kg], $\phi_{\text{ref}}(\cdot) = 3$ [rad], $k_P = 5$ [Nm/rad], $k_D = 2$ [Nms/rad] *and* $k_I = 5$ [Nm/(rad s)].

Experiment 4: limit cycles for controllers with integral action (hunting)
Consider the closed-loop system depicted in Fig. 1.11(d). A PID controller—with proportional gain k_P [Nm/rad], integral gain k_I [Nm/(rad s)] and derivative gain k_D [Nms/rad]—governs a rotatory mechanical system with inertia Θ [kg m^2] for position control. The mechanical system is subject to friction modeled by the LuGre friction operator $\mathfrak{L}_{\vartheta^0}$ [Nm] as in (1.21) with parametrization as in Tab. 1.2. The control objective is set-point tracking of the constant reference $\phi_{\text{ref}}(\cdot) = 3$ [rad]. Due to friction the closed-loop system exhibits limit cycles after ≈ 10 [s] (see Fig. 1.15(a), here only shown for $0 - 30$ [s]). Position $\phi(\cdot)$ "oscillates around" the reference $\phi_{\text{ref}}(\cdot)$. Within the (approximate) intervals [12, 20] [s] and [21, 29] [s], the inertia is not moving. Integral control action $k_I\, x_I(\cdot)$ is increasing linearly until the break-away torque of ≈ 1.25 [Nm] is reached (see Fig. 1.15(b)). The inertia is accelerated in the opposite direction until it gets "stuck" again. The proportional $k_P\, e(\cdot)$ and derivative $k_D\, \dot{e}(\cdot)$ control actions are not sufficiently large to stop sticking (see Fig. 1.15(b)). In general, high (proportional) gains obviate hunting by "stiffening" the closed-loop system (see [10]).

Remark 1.3 (Stiff simulation problem)**.**
For numeric simulations, the high stiffness $\sigma \gg 1$ *(e.g.* 10^5 [N] *in Section 1.4.5) in the friction models (1.21) or (1.22) necessitates special solvers (e.g.* `ode23s` *in Matlab) for stiff ordinary differential equations* or *small sampling times to obtain "correct" (numerically stable) solutions (see e.g. [73, Chapter 1,2]). This issue additionally increases the effort of implementation of stiff dynamical friction models for friction compensation (see Section 1.5.3 and [1]).*

Simplified LuGre model with linear viscous friction

As friction identification results show (see e.g. [8, 182] or [151, p. 195] for the laboratory setup), many mechatronic systems in industry exhibit *linear* viscous friction $\omega(\cdot) \mapsto \nu\, \omega(\cdot)$ with viscous friction coefficient $\nu \geq 0$ $\left[\frac{\text{Nms}}{\text{rad}}\right]$ (or $\left[\frac{\text{Ns}}{\text{m}}\right]$), i.e. $\delta_V = 1$ in (1.14).
Therefore (analogue to [96]), friction is split into linear but unbounded viscous friction and bounded nonlinear friction (including e.g. Coulomb friction, stiction and Stribeck effect). More

precisely, the following simplified LuGre friction model will be used in the remainder of this thesis. It is given by

$$\left.\begin{array}{l} \forall\, \omega(\cdot) \in \mathcal{C}(\mathbb{R}_{\geq 0}; \mathbb{R}): \qquad \omega(\cdot) \mapsto \nu\, \omega(\cdot) + (\mathfrak{F}\omega)(\cdot), \\ \text{where } \mathfrak{F}\colon\ \mathcal{C}(\mathbb{R}_{\geq 0}; \mathbb{R}) \to \mathcal{L}^\infty(\mathbb{R}_{\geq 0}; \mathbb{R}),\ \omega(\cdot) \mapsto \sigma\, \vartheta_{\omega(\cdot)} + f_D(\omega(\cdot)) \left(\omega(\cdot) - \sigma \frac{|\omega(\cdot)|}{\beta(\omega(\cdot))} \vartheta_{\omega(\cdot)}\right) \\ \text{and } f_D(\cdot) \text{ as in (1.20)},\ \beta(\cdot) \text{ as in (1.16) and } \vartheta_{\omega(\cdot)} \text{ solves (1.18)}. \end{array}\right\} \tag{1.22}$$

The simplified LuGre friction operator $\mathfrak{F}$ in (1.22) is directly derived from $\mathfrak{L}_{\vartheta^0}$ by neglecting the viscous term (i.e. $f_V(\omega(\cdot)) = 0$) in (1.21). The operator $\mathfrak{F}$ is also parametrized by the initial average bristle deflection ϑ^0, but for notational convenience, the subscript is dropped in the following. Moreover, note that in contrast to the general LuGre operator $\mathfrak{L}_{\vartheta^0}$ the simplified version $\mathfrak{F}$ is uniformly bounded, since for all $\omega(\cdot) \in \mathcal{C}(\mathbb{R}_{\geq 0}; \mathbb{R})$, the following holds

$$\begin{aligned} \forall\, t \geq 0\colon \quad |(\mathfrak{F}\omega)(t)| \leq 2\nu_D \max_{t \geq 0} \left\{ \exp\left(-(|\omega(t)|/\omega_D)^{\delta_D}\right) |\omega(t)| \right\} \left(1 + \frac{\sigma}{u_C} \max\left\{\frac{u_S}{\sigma}, |\vartheta^0|\right\}\right) \\ + \sigma\, \max\left\{\frac{u_S}{\sigma}, |\vartheta^0|\right\} =: M_{\mathfrak{F}} < \infty. \end{aligned} \tag{1.23}$$

1.4.6 Models of stiff and flexible servo-systems

Now, by combining the models (1.9), (1.11) and (1.22) of actuator, sensor and friction, respectively, the models of stiff one-mass system (1MS) and elastic two-mass system (2MS) are introduced. Again, modeling is for the rotatory case. For the translational case substitute the quantities according to Tab. 1.1 (e.g. substitute m [kg] for Θ [kg m^2]).

1.4.6.1 One-mass system (1MS)

The rotatory 1MS consists of inertia Θ [kg m^2] and gear with ratio g_r [1]. The inertia subsumes possibly several stiff coupled masses and the linkage. Backlash is neglected.
The state variable

$$\boldsymbol{x}(t) = (\omega(t),\, \phi(t))^\top$$

represents angular velocity (speed) and angle (position) at time $t \geq 0$ [s] in [rad/s] and [rad], respectively. The mechanical system (see Fig. 1.16) is driven by motor torque m_M [Nm] and is subject to load torque m_L [Nm] and motor and load (gear) side friction. Both friction torques are modeled by the simplified LuGre model (1.22), i.e. $\omega(\cdot) \mapsto \nu_1\omega(\cdot) + (\mathfrak{F}_1\omega)(\cdot)$ and $\omega(\cdot) \mapsto \nu_2\omega(\cdot)/g_r + (\mathfrak{F}_2\omega/g_r)(\cdot)$ for motor and load side friction, respectively. The actuator is modeled as in (1.9). The input of the 1MS is the reference torque $u := m_{M,\text{ref}}$ [Nm].

The mathematical model of the 1MS is given by

$$\left.\begin{array}{rcll} \frac{\mathrm{d}}{\mathrm{d}t}\boldsymbol{x}(t) &=& \boldsymbol{A}\boldsymbol{x}(t) + \boldsymbol{b}\,\mathrm{sat}_{\hat{u}_A}\big(u(t) + u_A(t)\big) + \boldsymbol{B}_L \begin{pmatrix} (\mathfrak{F}_1\omega)(t) \\ m_L(t) + (\mathfrak{F}_2 \frac{\omega}{g_r})(t) \end{pmatrix}, & \\ y(t) &=& \boldsymbol{c}^\top \boldsymbol{x}(t), \qquad & \boldsymbol{x}(0) = \boldsymbol{x}^0 \in \mathbb{R}^2 \end{array}\right\} \tag{1.24}$$

where system matrix $\boldsymbol{A}$ (viscous friction terms are included), input vector $\boldsymbol{b}$, disturbance input matrix $\boldsymbol{B}_L$, output vector $\boldsymbol{c}$, disturbances $u_A(\cdot)$, $m_L(\cdot)$, friction operators $\mathfrak{F}_1$, $\mathfrak{F}_2$ and system

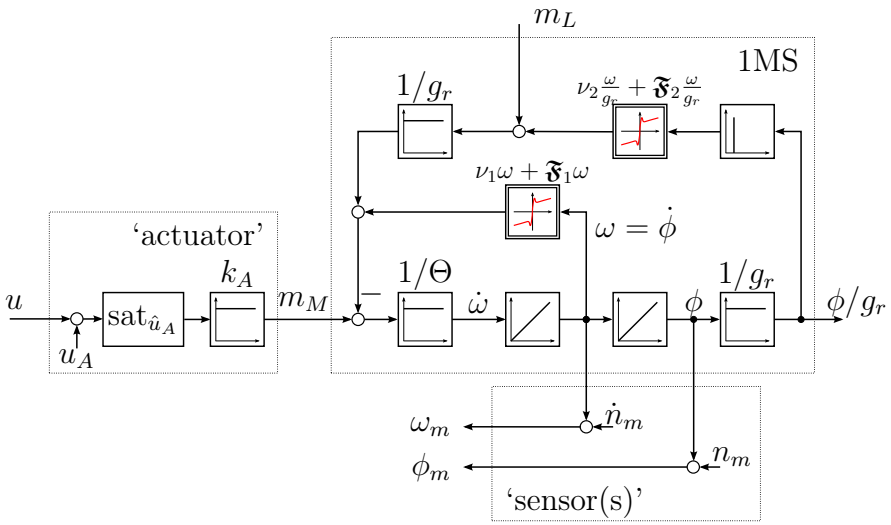

Figure 1.16: *One-mass system (1MS) with 'actuator' and 'sensor(s)' (simplified models), gear and motor & load (gear) side friction.*

parameters are as follow

$$\left.\begin{aligned}&\boldsymbol{A}=\begin{bmatrix}-\frac{\nu_1+\nu_2/g_r^2}{\Theta} & 0\\ 1 & 0\end{bmatrix},\ \boldsymbol{b}=\begin{pmatrix}\frac{k_A}{\Theta}\\ 0\end{pmatrix},\ \boldsymbol{B}_L=\begin{bmatrix}-\frac{1}{\Theta} & -\frac{1}{g_r\Theta}\\ 0 & 0\end{bmatrix},\ \boldsymbol{c}\in\mathbb{R}^2,\ \Theta>0,\\ &g_r\in\mathbb{R}\setminus\{0\},\ \nu_1,\nu_2>0,\ \hat u_A,k_A>0,\ u_A(\cdot),\ m_L(\cdot)\in\mathcal{L}^\infty(\mathbb{R}_{\geq 0};\mathbb{R})\ \text{ and }\ \forall\, i\in\{1,2\}:\\ &\mathfrak{F}_i\ \text{as in (1.22)}\ \text{ with }\ M_{\mathfrak{F}_i}:=\sup\{\,|(\mathfrak{F}_i\zeta)(t)|\mid t\geq 0,\ \zeta(\cdot)\in\mathcal{C}(\mathbb{R}_{\geq 0},\mathbb{R})\,\}<\infty.\end{aligned}\right\}\tag{1.25}$$

Note that due to (1.23), the upper bound $M_{\mathfrak{F}_1}$ and $M_{\mathfrak{F}_2}$ for the friction operators $\mathfrak{F}_1$ and $\mathfrak{F}_2$ exist, respectively. The gear ratio g_r in (1.25) is assumed unknown albeit in many applications, it can be read off on the gear box.

It depends on application and control objective (e.g. position or speed control), which sensors are installed and so which signals are available for feedback. To cover the possible instrumentation configurations (ic) the "general" output vector in (1.25) is chosen. Most common are the following cases:

(1MS-ic$_1$) *speed control:* a tacho-generator provides measurement of motor speed $\omega(\cdot)$ or load speed $\omega(\cdot)/g_r$. If an encoder or a resolver is used, speed is approximated by e.g. numerical differentiation (1.10). The output vector in (1.25) simplifies to $\boldsymbol{c}^\top=\begin{pmatrix}1, & 0\end{pmatrix}$ or $\boldsymbol{c}^\top=\begin{pmatrix}1/g_r, & 0\end{pmatrix}$. The control objective is load speed tracking of reference $\omega_{\mathrm{ref}}(\cdot)/g_r\in\mathcal{W}^{1,\infty}(\mathbb{R}_{\geq 0};\mathbb{R})$ and disturbance rejection of (unknown) load torques and friction. If motor speed $\omega(\cdot)$ is measured, then g_r must be known exactly to compute the load speed error $\omega_{\mathrm{ref}}(\cdot)/g_r-\omega(\cdot)/g_r$.

(1MS-ic$_2$) *position control:* an encoder (or resolver) provides measurement of motor position $\phi(\cdot)$ or load position $\phi(\cdot)/g_r$, whereas $\omega(\cdot)$ is computed by e.g. (1.10). In this case the output vector in (1.25) becomes $\boldsymbol{c}^\top=\begin{pmatrix}0, & 1\end{pmatrix}$ or $\boldsymbol{c}^\top=\begin{pmatrix}=0, & 1/g_r\end{pmatrix}$. The control objective is load position tracking of reference $\phi_{\mathrm{ref}}(\cdot)/g_r\in\mathcal{W}^{2,\infty}(\mathbb{R}_{\geq 0};\mathbb{R})$ and disturbance rejection. Note that (usually) speed reference $\omega_{\mathrm{ref}}(\cdot)=\dot\phi_{\mathrm{ref}}(\cdot)$ is

also available. If $\phi(\cdot)$ and $\omega(\cdot)$ are measured, then ratio g_r is required to compute load position error $\phi_{\text{ref}}(\cdot)/g_r - \phi(\cdot)/g_r$ and load speed error $\omega_{\text{ref}}(\cdot)/g_r - \omega(\cdot)/g_r$.

Similar to (1.11), the measured quantities are deteriorated by $n_m(\cdot) \in \mathcal{W}^{2,\infty}(\mathbb{R}_{\geq 0};\mathbb{R})$ (e.g. noise, see Fig. 1.16) and thus e.g. motor side feedback signals are given by

$$\forall\, t \geq 0\colon \qquad \phi_m(t) = \phi(t) + n_m(t) \qquad \text{and} \qquad \omega_m(t) = \omega(t) + \dot{n}_m(t),$$

respectively. Load side measurements are deteriorated accordingly.

1.4.6.2 Two-mass system (2MS)

Analogue to the 1MS, the 2MS is modeled (see Fig. 1.17). It consists of two masses—motor inertia Θ_1 [kg m^2] and load inertia Θ_2 [kg m^2]—which are coupled by an elastic shaft with stiffness c_S [Nm/rad] and damping d_S [Nms/rad]. The linkage may include a gear with ratio g_r [1]. Again backlash is not considered.
The state variable

$$\boldsymbol{x}(t) = (\omega_1(t),\, \phi_1(t),\, \omega_2(t),\, \phi_2(t))^\top$$

represents speed in [rad/s] and position in [rad] at time $t \geq 0$ [s] of motor and load, respectively. The mechanical system (see Fig. 1.17) is accelerated by drive torque m_M [Nm] and is subject to load torque m_L [Nm] and motor and load side friction, modeled by $\omega_1(\cdot) \mapsto \nu_1\omega_1(\cdot) + (\mathfrak{F}_1\omega_1)(\cdot)$ [Nm] and $\omega_2(\cdot) \mapsto \nu_2\omega_2(\cdot) + (\mathfrak{F}_2\omega_2)(\cdot)$ [Nm], respectively. The actuator is fed by the reference torque $u := m_{M,\text{ref}}$ and is modeled by (1.9).

The mathematical model of the 2MS is given by

$$\left.\begin{aligned} \tfrac{\mathrm{d}}{\mathrm{d}t}\,\boldsymbol{x}(t) &= \boldsymbol{A}\boldsymbol{x}(t) + \boldsymbol{b}\,\mathrm{sat}_{\hat{u}_A}\big(u(t) + u_A(t)\big) + \boldsymbol{B}_L \begin{pmatrix} (\mathfrak{F}_1\omega_1)(t) \\ m_L(t) + (\mathfrak{F}_2\omega_2)(t) \end{pmatrix}, \\ y(t) &= \boldsymbol{c}^\top\boldsymbol{x}(t), \qquad\qquad \boldsymbol{x}(0) = \boldsymbol{x}^0 \in \mathbb{R}^4 \end{aligned}\right\} \tag{1.26}$$

where (viscous friction terms are included in the system matrix again)

$$\left.\begin{aligned} &\boldsymbol{A} = \begin{bmatrix} -\frac{d_S+g_r^2\nu_1}{g_r^2\Theta_1} & -\frac{c_S}{g_r^2\Theta_1} & \frac{d_S}{g_r\Theta_1} & \frac{c_S}{g_r\Theta_1} \\ 1 & 0 & 0 & 0 \\ \frac{d_S}{g_r\Theta_2} & \frac{c_S}{g_r\Theta_2} & -\frac{d_S+\nu_2}{\Theta_2} & -\frac{c_S}{\Theta_2} \\ 0 & 0 & 1 & 0 \end{bmatrix}, \ \boldsymbol{b} = \begin{pmatrix} \frac{k_A}{\Theta_1} \\ 0 \\ 0 \\ 0 \end{pmatrix}, \ \boldsymbol{B}_L = \begin{bmatrix} \frac{-1}{\Theta_1} & 0 \\ 0 & 0 \\ 0 & \frac{-1}{\Theta_2} \\ 0 & 0 \end{bmatrix}, \ \boldsymbol{c} \in \mathbb{R}^4, \\ &\Theta_1,\, \Theta_2 > 0,\ d_S,\, c_S > 0,\ \nu_1, \nu_2 > 0,\ g_r \in \mathbb{R}\backslash\{0\},\ \hat{u}_A, k_A > 0,\ u_A(\cdot) \in \mathcal{L}^\infty(\mathbb{R}_{\geq 0};\mathbb{R}), \\ &m_L(\cdot) \in \mathcal{L}^\infty(\mathbb{R}_{\geq 0};\mathbb{R}) \ \text{ and } \ \forall\, i \in \{1,2\}:\ \mathfrak{F}_i \text{ as in (1.22) with } M_{\mathfrak{F}_i} \text{ as in (1.25)}. \end{aligned}\right\} \tag{1.27}$$

Also for the 2MS, application and control objective(s) determine the feedback signals. To allow for flexibility in modeling, again the "general" output vector in (1.27) is introduced. The most common applications with instrumentation are listed below (see also Fig. 1.17):

(2MS-ic$_1$) *speed control:* the control objective is load speed tracking of reference $\omega_{2,\text{ref}}(\cdot) \in \mathcal{W}^{1,\infty}(\mathbb{R}_{\geq 0};\mathbb{R})$, disturbance rejection (of e.g. unknown load torques and friction) and damping of shaft oscillations. Depending on the installed sensor(s), the following signals are available for feedback:

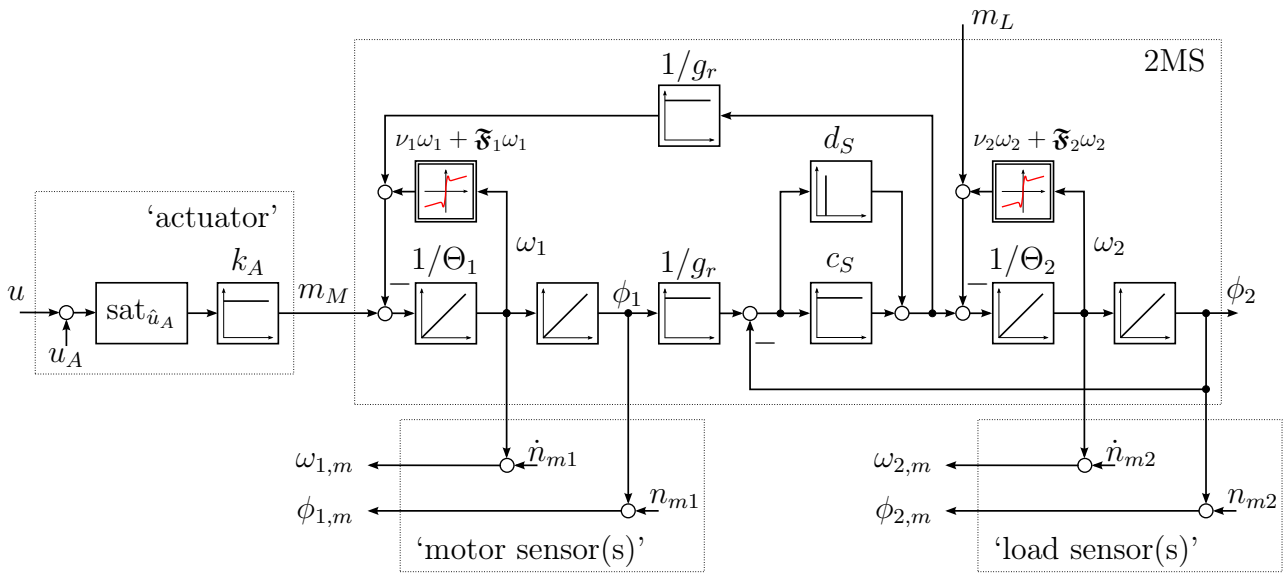

Figure 1.17: *Two-mass system (2MS) with 'actuator' and 'sensors' (simplified models), gear and motor & load side friction*

(a) motor speed $\omega_1(\cdot)$, i.e. $\boldsymbol{c}^\top = \begin{pmatrix}1, & 0, & 0, & 0\end{pmatrix}$ in (1.27).

(b) load speed $\omega_2(\cdot)$, i.e. $\boldsymbol{c}^\top = \begin{pmatrix}0, & 0, & 1, & 0\end{pmatrix}$ in (1.27).

(c) motor speed $\omega_1(\cdot)$ *and* load speed $\omega_2(\cdot)$, i.e. $\boldsymbol{c}^\top = \begin{pmatrix}1, & 0, & 1, & 0\end{pmatrix}$ in (1.27).

(2MS-ic$_2$) *position control:* the control objective is load position tracking of reference $\phi_{2,\mathrm{ref}}(\cdot) \in \mathcal{W}^{2,\infty}(\mathbb{R}_{\geq 0};\mathbb{R})$, disturbance rejection and suppression of shaft oscillations. Depending on instrumentation the following signals are available for feedback:

(a) motor angle $\phi_1(\cdot)$ and its derivative $\dot{\phi}_1(\cdot) = \omega_1(\cdot)$ (motor speed), i.e. $\boldsymbol{c}^\top = \begin{pmatrix}0, & 1, & 0, & 0\end{pmatrix}$ in (1.27).

(b) load position $\phi_2(\cdot)$ and its derivative $\dot{\phi}_2(\cdot) = \omega_2(\cdot)$ (load speed), i.e. $\boldsymbol{c}^\top = \begin{pmatrix}0, & 0, & 0, & 1\end{pmatrix}$ in (1.27).

(c) motor position $\phi_1(\cdot)$, load position $\phi_2(\cdot)$ and, respectively, $\dot{\phi}_1(\cdot) = \omega_1(\cdot)$ and $\dot{\phi}_2(\cdot) = \omega_2(\cdot)$, i.e. $\boldsymbol{c}^\top = \begin{pmatrix}1, & 0, & 1, & 0\end{pmatrix}$ in (1.27).

Due to elasticity in the shaft, the configurations (2MS-ic$_1$) (a) & (b) and (2MS-ic$_2$) (a) & (b) do not allow to suppress shaft oscillations for speed and position control, respectively. To achieve good damping in general, full-state feedback—as in configuration (2MS-ic$_1$) (c) (the torsional angle is obtained by integration, i.e. $\int_0^t \omega_1(\tau)/g_r - \omega_2(\tau)\,\mathrm{d}\tau$) or in configuration (2MS-ic$_2$) (c)—is necessary for speed and position control, respectively (see e.g. [166, Chapter 19] for speed control and [174, Section 6.5] for position control). If full-state feedback is not available, then to achieve adequate damping, full-order observers have to be implemented (which require good system and parameter knowledge) or, for load speed PI control, torque generation must be decelerated such that shaft oscillations are not excited (yielding an increased phase margin to assure stability of the speed control loop, see [166, Section 19.1]).

Similar to the 1MS, also for the 2MS the measured signals are deteriorated (see Fig. 1.17). Invoking the simplified sensor model (1.11), e.g. the feedback signals of load position and load speed are given by

$$\forall\, t \geq 0\colon \qquad \phi_{2,m}(t) = \phi_2(t) + n_{m2}(t) \qquad \text{and} \qquad \omega_{2,m}(t) = \omega_2(t) + \dot{n}_{m2}(t),$$

respectively. Accordingly, motor position $\phi_1(\cdot)$ and speed $\omega_1(\cdot)$ are perturbed by $n_{m1}(\cdot)$ and $\dot{n}_{m1}(\cdot)$, respectively.

Remark 1.4 (Motor and load side friction)**.**
Friction, in general, and as modeled in (1.22)*, in particular, is nonlinear and dynamic. For accurate friction modeling for 1MS and 2MS, the consideration of motor-* and *load-side friction is necessary. A simple conversion from load to motor side friction (or vice-versa) is not admissible in general. Note that, in view of* (1.22)*, the following holds*

$$\forall\, \omega(\cdot) \in \mathcal{C}(\mathbb{R}_{\geq 0}; \mathbb{R})\, \forall c_0 \neq 1\colon \qquad (\mathfrak{F}(c_0\omega))(\cdot) \neq c_0(\mathfrak{F}\omega)(\cdot).$$

Same holds for the general LuGre friction operator (1.21) *(replace* $\mathfrak{F}$ *by* $\mathfrak{L}_{\vartheta^0}$ *above).*

1.5 Motion control in industry

In industry linear proportional-integral-derivative (PID) controllers—or variants thereof such as P, I, PI or PD controllers—are applied in the majority of cases. These controllers are somehow the "standard solution" for industrial control problems. Also for motion control, PI and PID controllers are most common even though supplemented by disturbance observers to improve control performance under load. Besides, there exist special control solutions and friction identification and compensation methods. In general, the control design of these approaches—described in the succeeding sections—strongly depends on good knowledge of system *and* its parameters. The vague system information in (1.25) for the 1MS and in (1.27) for the 2MS may be not sufficient to assure stability of the closed-loop system.

1.5.1 Standard control methods

Integrated real-time systems (in the inverter of electrical drives) or process automation environments (e.g. SIEMENS S7) provide ready-made discrete prototypes of e.g. P, PI or PID controllers, which allow for easy implementation and tuning during e.g. system startup. A prototype of a continuous time PID controller with tuning parameters k_P (proportional gain), k_I (integral gain), k_D (derivative gain) and feedforward control $u_F(\cdot)$ is given by the following ordinary differential equation

$$\left.\begin{aligned} \dot{x}_I(t) &= e(t), \\ u(t) &= k_P\, e(t) + k_I\, x_I(t) + k_D\, \dot{e}(t) + u_F(t), \end{aligned} \qquad \begin{aligned} &x_I(0) = 0, \\ &k_P, k_I, k_D \in \mathbb{R}, \\ &u_F(\cdot) \in \mathcal{L}^\infty(\mathbb{R}_{\geq 0}; \mathbb{R}) \end{aligned} \right\} \tag{1.28}$$

where $e(t)$ and $x_I(t)$ represent tracking error as in (1.1) and state of the integral control action at time $t \geq 0$, respectively. The PID controller (1.28) generates the control action $u(t)$. Therefore, the error derivative $\dot{e}(\cdot)$ is required for feedback which implies that the derivative of

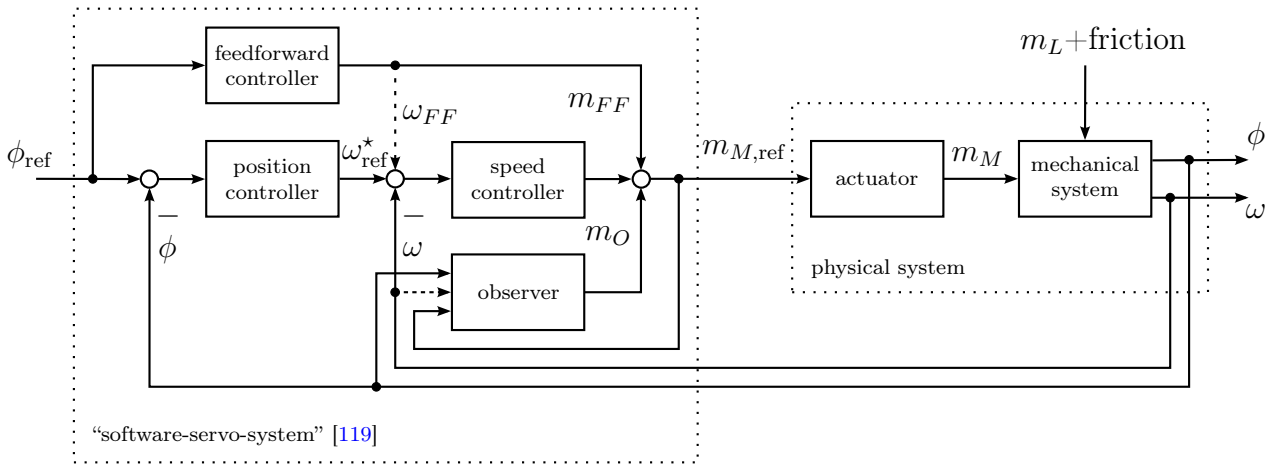

Figure 1.18: *Motion control cascades with feedforward control and disturbance observer in industry (sensors are neglected)*

reference and system output are available (i.e. $\dot{y}_{\text{ref}}(\cdot)$ and $\dot{y}(\cdot)$, respectively). If $\dot{e}(\cdot)$ is *not* available, then to reduce noise sensitivity of derivative control action $k_D\,\dot{e}(\cdot)$, the tracking error $e(\cdot)$ is low-pass filtered and then (numerically) differentiated (see [175] or in great detail [58, Section 7.4]). Although in many applications derivative feedback is not admissible, in the present setup of stiff or elastic servo-systems, or more general in joint position control of robotics it is justified (see e.g. [174, pp. 210-213 and 290-292]). Hence, the "ideal" PID controller in (1.28) is admissible.

P, I, PI and PD controller are derived from (1.28) simply by setting $k_I = k_D = 0$, $k_P = k_D = 0$, $k_D = 0$ and $k_I = 0$, respectively. To cope with actuator saturation—e.g. as in (1.24) or (1.26)—anti-windup strategies should be implemented (see e.g. [166, Section 5.6]).

Although control objectives are mostly formulated in the time domain, controller design and analysis are performed in the frequency domain (see e.g. [175]) by using Laplace transforms and transfer functions. Therefore, in abuse of notation, write e.g. $y(s) := \mathscr{L}\{y(t)\}$ for the Laplace transform of system output $y(\cdot)$ (see notation (N.1)). In the frequency domain, PID controller (1.28) and control action are given by

$$F_{PID}(s) = k_P + \frac{k_I}{s} + k_D\,s \qquad \text{and} \qquad u(s) = F_{PID}(s)\,e(s) + u_F(s) \tag{1.29}$$

where $u(s) = \mathscr{L}\{u(t)\}$, $e(s) = \mathscr{L}\{e(t)\}$ and $u_F(s) = \mathscr{L}\{u_F(t)\}$ represent the Laplace transforms (assuming those exist) of control action $u(\cdot)$, error $e(\cdot)$ and feedforward control $u_F(\cdot)$, respectively.

PI controllers are most common for speed control, whereas PID controllers are usually applied for position control (see e.g. [51, 123, 143, 175]). A wide-spread implementation of PID position control is depicted in Fig. 1.18. It has a cascaded structure, where the inner control loop is governed by a PI speed controller fed by the output $\omega^\star_{\text{ref}}$ of a P position controller and a velocity feedforward term ω_{FF} (see [51, 123]). This structure is similar to the un-cascaded PID position controller (1.29) with position error $e(s) = \phi_{\text{ref}}(s) - \phi(s)$ as "input" (see e.g. [174, Section 6.3.2],

there shown for constant reference).

For high-precision motion control, PI speed controllers and PID position controllers are, in general, not sufficient to assure the control objectives such as rise time, steady-state accuracy or asymptotic disturbance rejection (see [143]). Since modern real-time systems include powerful microprocessors, implementation of more sophisticated control is possible. Typically, in addition to the standard PI or PID controllers, disturbance observers and feedforward controllers are implemented (see Fig. 1.18). The observers are used to estimate load torque m_L and friction deteriorating the control performance of the servo-system (see Fig. 1.18). The estimated torque m_O [Nm]—the output of the disturbance observer—should compensate for disturbances (see [143]). The quality of the compensation depends on observer dynamics, accuracy of system model (see [147]) and actuator dynamics (e.g. "slow" torque generation will corrupt the compensation drastically, see [168]). In general, feedforward control supports feedback control in the sense that available information of the environment (e.g. known disturbance or reference changes) is used to feed the actuator directly. For example, if reference acceleration $\ddot{\phi}_{\text{ref}}$ [rad/s^2] and a good estimate of motor (and/or load) inertia are known a priori, then acceleration feedforward m_{FF} [Nm] is reasonable (see Fig. 1.18 and e.g. [51, 143, 175]).

In industry, stability analysis is mainly based on simplified linear or linearized models (see e.g. [27, 51, 123, 143, 175]). Exceptions, also incorporating nonlinear friction characteristics and backlash, are e.g. the articles [30–32] or in great detail the textbook [167]. Linear stability analysis is performed in the frequency domain either for the open loop system—in terms of gain and phase margin (see [166, Section 2.3]) or Nyquist-criterion (see [166, Section 2.1.1])—or for the closed-loop system in terms of the poles of the transfer function (see [166, Section 2.2]).

Often—lacking a stability analysis at all—the PID controller parameters k_P, k_I and k_D in (1.28) (or (1.29)) are tuned by "trial and error" until the desired control performance is achieved. However, as will be shown below for the 1MS (1.24), (1.25), some care must be exercised when doing so. Already for the low order 1MS position control problem, the integral gain k_I must not exceed an upper bound (depending on the system parameters), otherwise the closed-loop system is unstable. In the following, speed and position control of the linear 1MS are analyzed concerning stability using the Routh-Hurwitz criterion (see e.g. [77, Theorem 3.4.71]) and concerning asymptotic behavior using the final-value theorem (see e.g. [120, p. 20] or [58, p. 601]).

Linear analysis of the 2MS (1.26), (1.27) is neglected. Thorough discussions can be found in [166, Sections 19.1–2] for speed control and in [174, Section 6.5] for position control, respectively. Note that load position PID control of the linear 2MS is unstable for large derivative gains. The upper bound on k_D depends on system parameters Θ_1, Θ_2, c_S and d_S.

1.5.1.1 Speed control of linear 1MS

Consider the 1MS (1.24), (1.25) with viscous friction and load torque. More precisely, assume that the following holds:

(a_1) no actuator disturbance in (1.24), i.e. $u_A(t) = 0$ for all $t \geq 0$;

(a_2) no actuator saturation, i.e. $\hat{u}_A \to \infty$;

(a_3) no measurement errors, i.e. $n_m(t) = 0$ for all $t \geq 0$;

(a_4) no dynamic friction effects, i.e. $\mathfrak{F}_1 = \mathfrak{F}_2 = 0$ (however viscous friction is considered);

(a_5) the initial values are zero, i.e. $(\phi(0), \omega(0)) = (0, 0)$ for the 1MS

Moreover, for $\hat{y}_{\text{ref}}, \hat{m}_L \in \mathbb{R}$, only consider constant references, i.e.

$$y_{\text{ref}} \colon \mathbb{R}_{\geq 0} \to \mathbb{R},\ t \mapsto y_{\text{ref}}(t) := \hat{y}_{\text{ref}} \ \circ\!\!-\!\!\bullet\ y_{\text{ref}}(s) = \mathscr{L}\{y_{\text{ref}}(t)\} = \frac{\hat{y}_{\text{ref}}}{s}, \quad \Re(s) > 0$$

and constant load torques, i.e.

$$m_L \colon \mathbb{R}_{\geq 0} \to \mathbb{R},\ t \mapsto m_L(t) := \hat{m}_L \ \circ\!\!-\!\!\bullet\ m_L(s) = \mathscr{L}\{m_L(t)\} = \frac{\hat{m}_L}{s}, \quad \Re(s) > 0,$$

respectively (see e.g. Table A.3.2 in [77, p. 743] for the Laplace transforms). For load speed control the system output becomes $y(\cdot) = \omega(\cdot)/g_r$, hence $\boldsymbol{c}^\top = (1/g_r,\, 0)$ in (1.25). Then, under the assumptions (a_1)–(a_5) the input-output behavior in the frequency domain is given by

$$\begin{aligned} y(s) &= \boldsymbol{c}^\top (s\boldsymbol{I}_2 - \boldsymbol{A})^{-1}\boldsymbol{b}\, u(s) + \boldsymbol{c}^\top (s\boldsymbol{I}_2 - \boldsymbol{A})^{-1} \operatorname{col}_1(\boldsymbol{B}_L)\, m_L(s) \\ &\overset{(1.24),(1.25)}{=} \underbrace{\frac{k_A}{g_r\,\Theta}\frac{1}{s + \frac{\nu_1+\nu_2/g_r^2}{\Theta}}}_{=:F_{1,speed}^{u,y}(s)} u(s) \underbrace{-\frac{1}{g_r^2\,\Theta}\frac{1}{s + \frac{\nu_1+\nu_2/g_r^2}{\Theta}}}_{=:F_{1,speed}^{m_L,y}(s)} m_L(s). \end{aligned} \tag{1.30}$$

Defining $e(s) := y_{\text{ref}}(s) - y(s)$ and applying a PI controller without feedforward control (i.e. (1.29) with $k_D = 0$ and $u_F = 0$) to (1.30) yields the closed-loop system

$$y(s) = \underbrace{\frac{s\frac{k_P k_A}{g_r\Theta} + \frac{k_I k_A}{g_r\Theta}}{s^2 + s\left(\frac{\nu_1+\nu_2/g_r^2}{\Theta} + \frac{k_P k_A}{g_r\Theta}\right) + \frac{k_I k_A}{g_r\Theta}}}_{=:F_{1,speed}^{y_{\text{ref}},y}(s)} y_{\text{ref}}(s) \underbrace{-\frac{s\frac{1}{g_r^2\Theta}}{s^2 + s\left(\frac{\nu_1+\nu_2/g_r^2}{\Theta} + \frac{k_P k_A}{g_r\Theta}\right) + \frac{k_I k_A}{g_r\Theta}}}_{=:F_{1,speed}^{m_L,y}(s)} m_L(s) \tag{1.31}$$

which, in view of (1.25), is stable for

$$k_P/g_r > 0 \qquad \text{and} \qquad k_D/g_r > 0. \tag{1.32}$$

Furthermore in view of the final-value theorem (see e.g. [120, p. 20]), it holds that

$$\lim_{t\to\infty} y(t) = \lim_{s\to 0}\left\{ s \cdot F_{1,speed}^{y_{\text{ref}},y}(s) \cdot \frac{\hat{y}_{\text{ref}}}{s} \right\} + \lim_{s\to 0}\left\{ s \cdot F_{1,speed}^{m_L,y}(s) \cdot \frac{\hat{m}_L}{s} \right\} \overset{(1.31)}{=} \hat{y}_{\text{ref}}$$

and so constant references $y_{\text{ref}} \colon \mathbb{R}_{\geq 0} \to \hat{y}_{\text{ref}}$ are tracked with zero steady-state error and constant disturbances $m_L \colon \mathbb{R}_{\geq 0} \to \hat{m}_L$ are asymptotically rejected. Usually, the control objectives are formulated in terms of maximum rise time, maximum overshoot and maximum settling time (see Fig. 1.1). Then, since the vague system information in (1.25) does not permit analytic tuning, the controller parameters k_P and k_I have to be found empirically e.g. by "trial and error" or based on the Ziegler-Nichols method (see [120, Section 52.2.2]).

1.5.1.2 Position control of linear 1MS

Now, under identical assumptions as in Section 1.5.1.1, load position control of the linear 1MS is discussed. The output is given by $y(\cdot) = \phi(\cdot)/g_r$, i.e. $\boldsymbol{c}^\top = (0,\ 1/g_r)$ in (1.25) and the following transfer function is obtained

$$\begin{aligned} y(s) &= \boldsymbol{c}^\top (s\boldsymbol{I}_2 - \boldsymbol{A})^{-1}\boldsymbol{b}\, u(s) + \boldsymbol{c}^\top (s\boldsymbol{I}_2 - \boldsymbol{A})^{-1} \operatorname{col}_1(\boldsymbol{B}_L)\, m_L(s) \\ &= \underbrace{\frac{\frac{k_A}{g_r\Theta}}{s\left(s + \frac{\nu_1+\nu_2/g_r^2}{\Theta}\right)}}_{=:F_{1,position}^{u,y}(s)} u(s) - \underbrace{\frac{\frac{1}{g_r^2\Theta}}{s\left(s + \frac{\nu_1+\nu_2/g_r^2}{\Theta}\right)}}_{=:F_{1,position}^{m_L,y}(s)} m_L(s). \end{aligned} \tag{1.33}$$

Using $e(s) := y_{\text{ref}}(s) - y(s)$ and applying the PID controller (1.29) without feedforward control (i.e. $u_F = 0$) to (1.33) yields the closed-loop system

$$\begin{aligned} y(s) = \underbrace{\frac{\frac{k_A}{g_r\Theta}\left(s^2 k_D + s k_P + k_I\right)}{s^3 + s^2\left(\frac{\nu_1+\nu_2/g_r^2}{\Theta} + \frac{k_D k_A}{g_r\Theta}\right) + s\frac{k_P k_A}{g_r\Theta} + \frac{k_I k_A}{g_r\Theta}}}_{=:F_{1,position}^{y_{\text{ref}},y}(s)} y_{\text{ref}}(s) \\ \underbrace{- \frac{s\frac{1}{g_r^2\Theta}}{s^3 + s^2\left(\frac{\nu_1+\nu_2/g_r^2}{\Theta} + \frac{k_D k_A}{g_r\Theta}\right) + s\frac{k_P k_A}{g_r\Theta} + \frac{k_I k_A}{g_r\Theta}}}_{=:F_{1,position}^{m_L,y}(s)} m_L(s) \end{aligned} \tag{1.34}$$

which is stable (Liénard-Chipart criterion, see e.g. [77, Corollary 3.4.73]) for

$$\frac{k_P}{g_r} > 0,\quad \frac{k_D}{g_r} > 0,\quad \frac{k_I}{g_r} > 0 \quad \text{and} \quad \frac{k_I}{g_r} < \frac{k_A}{g_r^2\Theta} k_P k_D \overset{(1.25)}{\leq} \frac{k_P}{g_r}\left(\frac{\nu_1 + \nu_2/g_r^2}{\Theta} + \frac{k_D k_A}{g_r\Theta}\right). \tag{1.35}$$

Moreover, since

$$\lim_{t\to\infty} y(t) = \lim_{s\to 0}\left\{ s \cdot F_{1,position}^{y_{\text{ref}},y}(s) \cdot \frac{\hat{y}_{\text{ref}}}{s} \right\} + \lim_{s\to 0}\left\{ s \cdot F_{1,position}^{m_L,y}(s) \cdot \frac{\hat{m}_L}{s} \right\} \overset{(1.34)}{=} \hat{y}_{\text{ref}},$$

constant references are asymptotically tracked and constant disturbances are rejected. Note that the last condition in (1.35) can be satisfied even if viscous friction is not known (recall $\nu_1, \nu_2 > 0$ in (1.25)), however the sign of gear ratio g_r and bounds on actuator gain k_A and inertia Θ, respectively, must be known a priori to assure stability of the linear closed-loop system (1.34).

1.5.2 Special control methods

Besides, the standard approaches presented above, there exist a variety of special control methods which are particularly of interest for certain applications or fields of research, e.g. H_∞ control of hard disk drives (see [175]), sliding mode control for induction machines (see [149]) or load speed control of the 2MS either by full-state feedback (see [166, Section 19.3]) or by

observer-state feedback (see [27]) to name a few.

H_∞ control is well known for its robust performance (see e.g. [120, Chapter 40]). However, rough knowledge on system and parameters is essential and the controllers—found by μ-synthesis (see e.g. [120, Chapter 42])—have high order which usually implies model reduction to obtain a feasible controller of lower order (see [175]). In addition, to meet the control objective (such as maximum rise time, etc.), iterations in control design are often necessary making H_∞ design time-consuming (see [175]).

The proposed sliding mode controller in [149] for position control of induction machines is robust to parameter uncertainties and uses a variable bandwidth low pass filter to reduce chattering (to avoid torque ripple). However, due to the bang-bang nature of the proposed controller, it seems not adequate for e.g. position control of the 2MS where shaft oscillations are not to be excited.

For the 2MS, if system and its parameters are known acceptably well, full-state feedback or observer-state feedback yields a well damped system response (see e.g. [166, Section 19.3] for speed control and [174, Section 6.6] for position control). Set-point tracking (of constant load references) and disturbance rejection (of constant loads) is achieved. The closed-loop dynamics may be prescribed by pole-placement (see [58, Section 13.3]) or Riccati-design (see [58, Section 13.4] or, equivalently, [120, p. 48] for the design of linear quadratic regulator (LQR)). Maximum rise time, maximum overshoot and maximum settling time can be assured easily (for speed control see e.g. [166, Section 19.3] by pole placement or [70] by LQR design; for position control see e.g. [174, Section 6.6]).

If full-state feedback or observer-state feedback is not feasible, e.g. load side measurements are not available, and shaft oscillations must be suppressed, notch filters to compensate for the elasticity (see [175]) or vibrational suppression control (see [143]) can be used. However, both approaches rely on good knowledge of the 2MS parameters and, in particular, on *exact* knowledge of eigenfrequency $\omega_0^{2MS} = \sqrt{(\Theta_1 + \Theta_2/g_r^2)\, c_s/(\Theta_1\, \Theta_2)}\ \left[\frac{\text{rad}}{\text{s}}\right]$ and damping $D^{2MS} = \omega_0^{2MS} d_S/(2c_S)$ (see [71]), respectively.

1.5.3 Friction identification and compensation

Friction imposes the most severe difficulty for position and speed control. The major problem is to suppress stick-slip in high-precision positioning tasks. There exist three standard approaches to avoid stick-slip (if e.g. disturbance observers are not enough):

- the use of high gain in the feedback (e.g. high-gain PD controllers) to achieve "stiff servo-systems" (see e.g. [10, 39, 50]). For this approach noise sensitivity must be taken into account during implementation.

- the use of dither signals added to control action. Depending on application this approach may not be admissible, since mass or inertia never comes to rest (see e.g. [147]) and

- the use of friction compensation methods (see e.g. [28]).

Ideally friction compensation comprises perfect friction identification and, by adequate feedforward control, perfect compensation of real friction. Friction identification implies good knowledge of the friction characteristic, the choice of an adequate friction model and precise identification/estimation of the model parameters (on- or offline). Similar to disturbance observation and compensation (see above), the quality of friction compensation severely depends on small time delays in the actuator (see e.g. [147, 168]). For a detailed discussion of friction compensation methods see the survey article [28] and the references therein. In the majority of cases, friction compensation is model-based and hence model sensitive (see [147]). Friction model identification is non-trivial, since e.g. recursive least square methods do not work for the LuGre friction model. The dependence on the model parameter is not linear (see e.g. [45, 182]). The LuGre friction model was successfully identified using e.g. particle swarm optimization (see [182]) or genetic algorithms (see [45]). However, friction identification is time-consuming and requires high-resolution instrumentation (see [147]). Depending on the desired accuracy, identification may take 10-100 hours. In particular, stiction level u_S and Stribeck velocity ω_S are hard to identify (see [3, p. 44-45]). Furthermore, sensors with (very) high resolution must be installed to allow for precise friction identification and model verification. Required resolutions are approximately $\leq 10^{-7}$ [m] and $\leq 10^{-4}$ [m/s] for position and velocity measurement, respectively (see e.g. [145, p. 73] for LuGre model identification at a translational setup). There also exist model independent friction compensation methods (see e.g. [159]) using sliding-mode controllers. Here the friction is considered as polynomially bounded disturbance, but still an upper bound on stiction level must be known for controller design.

For speed control, often static friction models are sufficient for adequate friction compensation (see e.g. [161, Section 7.3]). Then an "intelligent observer"—i.e. a Luenberger observers with static neuronal network (e.g. general regression neuronal network (GRNN))—is reasonable. It allows for online identification of e.g. the nonlinear (but static) friction model (1.17). The estimated friction torque (or force) is used for friction compensation by feedforward control (see e.g. [168] or in great detail [167, Chapter 5]).

1.6 Problem formulation

The available motion control concepts in industry (see previous section) work acceptably well. However,

- controller design mainly relies on good system and parameter knowledge (involving system identification or parameter estimation),
- often disturbance observers and/or friction compensation methods are necessary to achieve satisfactory disturbance rejection (increasing controller complexity and implementation effort) and
- controller tuning might be tedious (several tuning iterations are likely to attain desired control performance).

The present work aims at introducing adaptive λ-tracking control and funnel control as simple, robust and easy to tune/implement alternatives to the available motion control concepts in industry.

1.6.1 High-gain adaptive motion control problem

High-gain adaptive controllers are to be developed which are applicable for motion control of industrial servo-systems and, ideally, allow to include motion control objectives (mco_1)–(mco_4) into controller design. The *high-gain adaptive motion control problem* is divided into the following two subproblems:

- the *high-gain adaptive speed control problem*, i.e. to find high-gain adaptive (speed) controllers for 1MS (1.24), (1.25) with instrumentation configuration (1MS-ic_1) and for 2MS (1.26), (1.27) with instrumentation configuration (2MS-ic_1)(c) and
- the *high-gain adaptive position control problem*, i.e. to find high-gain adaptive (position) controllers for 1MS (1.24), (1.25) with instrumentation configuration (1MS-ic_2) and for 2MS (1.26), (1.27) with instrumentation configuration (2MS-ic_2)(c).

For the 2MS, to allow for adequate damping of shaft oscillations, only the instrumentation configurations (2MS-ic_1)(c) and (2MS-ic_2)(c) are considered (see Section 1.4.6.2).

To assure feasibility of motion control objectives (mco_1)–(mco_4), the high-gain adaptive motion control problem is formulated under the following modeling assumptions (ma):

(ma_1) real-time execution is in "quasi-continuous time", i.e. the sampling time is small compared to the dynamics of the servo-system;

(ma_2) instrumentation has sufficiently high resolution and noise has sufficiently small amplitude. More precisely, measurement errors are small compared to the prescribed (asymptotic) accuracy, i.e. $\|n_m\|_\infty \ll \lambda$;

(ma_3) friction behavior of the servo-system is covered by the simplified LuGre model (1.22);

(ma_4) actuation is sufficiently fast and sufficiently dimensioned, i.e. (i) the simplified actuator model (1.9) is justified and (ii) for $M_{\mathfrak{F}_1}$, $M_{\mathfrak{F}_2}$, k_A, $u_A(\cdot)$, $m_L(\cdot)$, g_r and Θ (or Θ_1 and Θ_2) as in (1.25) (or (1.27)) and $\dot{\omega}_{\text{ref}}(\cdot)/g_r \in \mathcal{L}^\infty(\mathbb{R}_{\geq 0};\mathbb{R})$ (or $\dot{\omega}_{2,\text{ref}}(\cdot) \in \mathcal{L}^\infty(\mathbb{R}_{\geq 0};\mathbb{R})$) the following holds

$$\hat{u}_A \gg \max\left\{\frac{M_{\mathfrak{F}_1}}{|g_r|}, \frac{M_{\mathfrak{F}_2}}{|g_r|}, \frac{\|m_L\|_\infty}{|g_r|}, k_A\|u_A\|_\infty, \Theta\|\dot{\omega}_{\text{ref}}\|_\infty \text{ (or } \left(\Theta_1 + \frac{\Theta_2}{g_r^2}\right)\|\dot{\omega}_{2,\text{ref}}\|_\infty\right)\right\};$$

(ma_5) the models (1.24), (1.25) and (1.26), (1.27) of 1MS and 2MS are sufficiently accurate, i.e. un-modeled dynamics are negligible within the specified operation bandwidth.

Furthermore, in view of industrial application and implementation, the developed controllers should have the following properties

(cp_1) *simple and robust*: (i) the controllers have low order and non-complex structure, (ii) parameter uncertainties do not endanger controller applicability and fulfillment of control objectives (mco_1)–(mco_4), (iii) disturbances (e.g. friction and loads) are rejected and (iv) actuator deviation, feedforward control and measurement noise are tolerated;

(cp_2) *easy to implement* (industrial applicability): (i) time-consuming system or friction identification/estimation is not required, i.e. the necessary a priori system knowledge is limited to the qualitative information given in (1.25) or (1.27) and (ii) default building blocks (e.g. for function generation, multiplication, summation, integration, saturation, etc.) of process automation software are sufficient for controller implementation;

(cp_3) *easy to tune*: the controller parameters have distinct and easily to understand influence on the control performance of the closed-loop system.

1.6.2 Generalized high-gain adaptive control problem

The models of 1MS (1.24), (1.25) and 2MS (1.26), (1.27) are quite similar, which motivates for a generalization of the problem formulation to a wider class of systems. In the following two system classes—class $\mathcal{S}_1$ and class $\mathcal{S}_2$—are introduced which subsume "minimum-phase" single-input single-output (SISO) systems with known sign of the high-frequency gain, relative degree one (i.e. class $\mathcal{S}_1$) *or* two (i.e. class $\mathcal{S}_2$) and unknown but bounded disturbances and functional, state-dependent perturbations. The exact definitions of class $\mathcal{S}_1$ and class $\mathcal{S}_2$ follow in Section 1.6.2.2. The notions of relative degree, minimum-phase and high-frequency gain are defined in Chapter 2 (for LTI SISO systems).

The *generalized high-gain adaptive control problem* is now to find high-gain adaptive controllers for system class $\mathcal{S}_1$ and for system class $\mathcal{S}_2$, respectively, which assure achievement of certain generalized control objectives (to be specified in Section 1.6.2.3).

1.6.2.1 Operator class

First, a precise notion of the admissible functional perturbation is required, therefore introduce:

Definition 1.5 (Operator class $\mathcal{T}$)**.**
An operator $\mathfrak{T}$ is element of class $\mathcal{T}$ if, and only if, for some $h \geq 0$ and $n, m \in \mathbb{N}$, the following operator properties hold:

(op_1) $\mathfrak{T}\colon \mathcal{C}([-h,\infty);\mathbb{R}^n) \to \mathcal{L}^\infty_{\mathrm{loc}}(\mathbb{R}_{\geq 0};\mathbb{R}^m)$;

(op_2) *for every $\delta > 0$, there exists $\Delta > 0$, such that, for all $\boldsymbol{\zeta}(\cdot) \in \mathcal{C}([-h,\infty);\mathbb{R}^n)$:*

$$\sup_{t\in[-h,\infty)} \|\boldsymbol{\zeta}(t)\| < \delta \quad \Longrightarrow \quad \|(\mathfrak{T}\boldsymbol{\zeta})(t)\| \leq \Delta \quad \text{for a.a. } t \geq 0,$$

(op_3) *for all $t \geq 0$, the following hold:*

(a) *for all $\boldsymbol{\zeta}(\cdot), \boldsymbol{\xi}(\cdot) \in \mathcal{C}([-h,\infty);\mathbb{R}^n)$:*

$$\boldsymbol{\zeta}(\cdot) \equiv \boldsymbol{\xi}(\cdot) \text{ on } [-h,t] \quad \Longrightarrow \quad (\mathfrak{T}\boldsymbol{\zeta})(s) = (\mathfrak{T}\boldsymbol{\xi})(s) \quad \text{for a.a. } s \in [0,t]$$

(b) *for all $\boldsymbol{\beta}(\cdot) \in \mathcal{C}([-h,t];\mathbb{R}^n)$ there exist $\tau, \delta, c_0 > 0$, such that, for all $\boldsymbol{\zeta}(\cdot), \boldsymbol{\xi}(\cdot) \in \mathcal{C}([-h,\infty),\mathbb{R}^n)$ with $\boldsymbol{\zeta}|_{[-h,t]} = \boldsymbol{\beta} = \boldsymbol{\xi}|_{[-h,t]}$ and $\boldsymbol{\zeta}(s), \boldsymbol{\xi}(s) \in \mathbb{B}^n_\delta(\boldsymbol{\beta}(t))$ for all $s \in [t,t+\tau]$:*

$$\operatorname*{ess\text{-}sup}_{s\in[t,t+\tau]} \|(\mathfrak{T}\boldsymbol{\zeta})(s) - (\mathfrak{T}\boldsymbol{\xi})(s)\| \leq c_0 \sup_{s\in[t,t+\tau]} \|\boldsymbol{\zeta}(s) - \boldsymbol{\xi}(s)\|\,.$$

The constant $h \geq 0$ quantifies the "memory" of an operator $\mathfrak{T} \in \mathcal{T}$. The operator itself maps the space of continuous functions into the space of measurable, locally essentially bounded functions (see Property (op_1)). For any bounded input the operator mapping remains also bounded yielding a kind of "bounded-input bounded-output" property (see Property (op_2)). The mapping only depends on actual and previous inputs and therefore fulfills an assumption of causality (see Property (op_3)(a)). Property (op_3)(b) gives a "locally Lipschitz" like condition, which represents a technical assumption to assure that an appropriate existence theory (see e.g. [99, Theorem 5] or [157, Theorem 7]) is applicable for the analysis of (closed-loop) systems described by functional differential equations.

As will be shown in Chapter 5, the operator class $\mathcal{T}$ covers nonlinear dynamic friction, i.e. LuGre friction operator $\mathfrak{L}_{\vartheta^0}$ as in (1.21) and simplified LuGre friction operator $\mathfrak{F}$ as in (1.22) are both element of class $\mathcal{T}$. Besides nonlinear friction, class $\mathcal{T}$ encompasses e.g. relay, backlash, elasto-plastic & Preisach hysteresis, nonlinear delay systems and infinite-dimensional regular linear systems (see [157, Sec. 2.1] and [158, Sec. 2.1]). In Appendix B two simple operators of class $\mathcal{T}$ are presented.

1.6.2.2 System classes

Now being equipped with operator class $\mathcal{T}$, the system classes $\mathcal{S}_1$ and $\mathcal{S}_2$ may be defined.

Definition 1.6 (System class $\mathcal{S}_1$)**.**
Let $n, m \in \mathbb{N}$, $h \geq 0$, $(\boldsymbol{A}, \boldsymbol{b}, \boldsymbol{c}) \in \mathbb{R}^{n\times n} \times \mathbb{R}^n \times \mathbb{R}^n$ and $\boldsymbol{B}_{\mathfrak{T}} \in \mathbb{R}^{n\times m}$. A system, given by the functional differential equation

$$\left.\begin{aligned} \dot{\boldsymbol{x}}(t) &= \boldsymbol{A}\boldsymbol{x}(t) + \boldsymbol{b}\big(u(t) + u_d(t)\big) + \boldsymbol{B}_{\mathfrak{T}}\big((\mathfrak{T}\boldsymbol{x})(t) + \boldsymbol{d}(t)\big) \\ y(t) &= \boldsymbol{c}^\top \boldsymbol{x}(t), \qquad\qquad \boldsymbol{x}|_{[-h,0]} = \boldsymbol{x}^0(\cdot) \in \mathcal{C}\big([-h,0];\mathbb{R}^n\big) \end{aligned}\right\} \tag{1.36}$$

with disturbances $u_d\colon [-h,\infty) \to \mathbb{R}$ and $\boldsymbol{d}\colon [-h,\infty) \to \mathbb{R}^m$, operator $\mathfrak{T}\colon \mathcal{C}([-h,\infty);\mathbb{R}^n) \to \mathcal{L}^\infty(\mathbb{R}_{\geq 0};\mathbb{R}^m)$, control input $u\colon \mathbb{R}_{\geq 0} \to \mathbb{R}$ and regulated output $y(\cdot)$, is of Class $\mathcal{S}_1$ *if, and only if, the following hold:*

($\mathcal{S}_1$-sp_1) *the relative degree is one and the sign of the high-frequency gain is known, i.e.*

$$\gamma_0 := \boldsymbol{c}^\top \boldsymbol{b} \neq 0 \qquad \textit{and} \qquad \operatorname{sign}(\gamma_0) \textit{ known};$$

($\mathcal{S}_1$-sp_2) *the unperturbed system is minimum-phase, i.e.*

$$\forall\, s \in \mathbb{C}_{\geq 0}\colon \qquad \det \begin{bmatrix} s\boldsymbol{I}_n - \boldsymbol{A} & \boldsymbol{b} \\ \boldsymbol{c}^\top & 0 \end{bmatrix} \neq 0;$$

($\mathcal{S}_1$-sp_3) *the operator is element of class $\mathcal{T}$ and globally bounded, i.e.*

$$\mathfrak{T} \in \mathcal{T} \;\; \textit{and} \;\; M_{\mathfrak{T}} := \sup\left\{\|(\mathfrak{T}\boldsymbol{\xi})(t)\| \;\middle|\; t \geq 0,\; \boldsymbol{\xi}(\cdot) \in \mathcal{C}([-h,\infty),\mathbb{R}^n)\right\} < \infty;$$

($\mathcal{S}_1$-sp_4) *the disturbances are bounded, i.e.*

$$u_d(\cdot) \in \mathcal{L}^\infty([-h,\infty);\mathbb{R}) \;\; \textit{and} \;\; \boldsymbol{d}(\cdot) \in \mathcal{L}^\infty([-h,\infty);\mathbb{R}^m);$$

($\mathcal{S}_1$-sp$_5$) *feedback of the regulated output is admissible, i.e. $y(\cdot)$ is available for feedback.*

Note that, in "real world", the regulated output (i.e. the variable to be controlled) usually differs from the measured output(s) (i.e. the variable(s) available for feedback; recall torque control in Fig. 1.6 or see [77, pp. 74,75]). Condition ($\mathcal{S}_1$-sp$_5$) assures that measured output and regulated output coincide. It is motivated by a practical point of view and is essential for implementation.

Definition 1.7 (System class $\mathcal{S}_2$)**.**
Let $n, m \in \mathbb{N}$, $h \geq 0$, $(\boldsymbol{A}, \boldsymbol{b}, \boldsymbol{c}) \in \mathbb{R}^{n\times n} \times \mathbb{R}^n \times \mathbb{R}^n$ and $\boldsymbol{B}_{\mathfrak{T}} \in \mathbb{R}^{n\times m}$. A system of form (1.36) with disturbances $u_d\colon [-h,\infty) \to \mathbb{R}$ and $\boldsymbol{d}\colon [-h,\infty) \to \mathbb{R}^m$, operator $\mathfrak{T}\colon \mathcal{C}([-h,\infty);\mathbb{R}^n) \to \mathcal{L}^\infty(\mathbb{R}_{\geq 0};\mathbb{R}^m)$, control input $u\colon \mathbb{R}_{\geq 0} \to \mathbb{R}$ and regulated output $y(\cdot)$, is of Class $\mathcal{S}_2$ if, and only if, the following hold:

($\mathcal{S}_2$-sp$_1$) *the relative degree is two and the sign of the high-frequency gain is known, i.e.*

$$\boldsymbol{c}^\top \boldsymbol{b} = 0, \quad \boldsymbol{c}^\top \boldsymbol{B}_{\mathfrak{T}} = \boldsymbol{0}_m^\top, \quad \gamma_0 := \boldsymbol{c}^\top \boldsymbol{A}\boldsymbol{b} \neq 0 \quad \text{and} \quad \operatorname{sign}(\gamma_0) \text{ known};$$

($\mathcal{S}_2$-sp$_2$) *the unperturbed system is minimum-phase (see ($\mathcal{S}_1$-sp$_2$));*

($\mathcal{S}_2$-sp$_3$) *the operator is of class $\mathcal{T}$ and globally bounded (see ($\mathcal{S}_1$-sp$_3$));*

($\mathcal{S}_2$-sp$_4$) *the disturbances are bounded (see ($\mathcal{S}_1$-sp$_4$));*

($\mathcal{S}_2$-sp$_5$) *feedback of the regulated output and its derivative is admissible, i.e. $y(\cdot)$ and $\dot{y}(\cdot)$ are available for feedback.*

The system classes are quite similar and only differ in "system properties" (sp$_1$) and (sp$_5$). Actuator saturation as in (1.24) or (1.26) is neglected in Definition 1.6 and 1.7. Constrained control actions are considered in controller design, e.g. the proposed funnel controllers in Chapter 4 allow for input saturation. In Chapter 5 it will be shown that the *high-gain adaptive speed control problem* and the *high-gain adaptive position control problem* are subproblems of finding adequate high-gain adaptive controllers for system class $\mathcal{S}_1$ and system class $\mathcal{S}_2$, respectively. For speed control output feedback is sufficient, whereas position control additionally requires derivative feedback. Input disturbance $u_d(\cdot)$ in (1.36) may incorporate bounded actuator deviations and/or feedforward commands, whereas disturbance $\boldsymbol{d}(\cdot)$ and functional perturbation $(\mathfrak{T}\boldsymbol{x})(\cdot)$ in (1.36) may account for load torques and nonlinear but bounded friction effects, respectively.

1.6.2.3 Control objectives

For any admissible pair $(y_{\text{ref}}(\cdot), \mathfrak{S})$ of reference $y_{\text{ref}}(\cdot)$ and system $\mathfrak{S}$, i.e.

$$(y_{\text{ref}}(\cdot), \mathfrak{S}) \in (\mathcal{W}^{1,\infty}(\mathbb{R}_{\geq 0};\mathbb{R}),\, \mathcal{S}_1) \qquad \text{or} \qquad (y_{\text{ref}}(\cdot), \mathfrak{S}) \in (\mathcal{W}^{2,\infty}(\mathbb{R}_{\geq 0};\mathbb{R}),\, \mathcal{S}_2),$$

the high-gain adaptive controllers must accomplish (at least the first two of) the following (generalized) control objectives (co):

(co$_1$) *boundedness of system states and control input*, i.e.

$$\boldsymbol{x}(\cdot) \in \mathcal{L}^\infty(\mathbb{R}_{\geq 0};\mathbb{R}^n) \;\text{ and }\; u(\cdot) \in \mathcal{L}^\infty(\mathbb{R}_{\geq 0};\mathbb{R});$$

(co_2) *tracking with prescribed asymptotic accuracy*: for prescribed accuracy $\lambda > 0$ (arbitrary small) the tracking error (1.1) approaches the interval $[-\lambda, \lambda]$ asymptotically, i.e.

$$\forall\, \lambda > 0\colon \qquad \lim_{t\to\infty} \operatorname{dist}\big(|e(t)|, [0, \lambda]\big) = 0;$$

(co_3) *tracking with prescribed transient accuracy*: the absolute value of the tracking error (1.1) is bounded by any prescribed positive (absolutely) continuous function of time, if the initial error is enclosed, i.e.

$$\forall\, \lambda > 0\, \forall\, \psi(\cdot) \in \mathcal{W}^{1,\infty}(\mathbb{R}_{\geq 0}; [\lambda, \infty))\, \forall\, |e(0)| < \psi(0)\, \forall\, t \geq 0\colon \qquad |e(t)| < \psi(t).$$

1.6.2.4 Admissible reference signals

The admissible reference signals $y_{\mathrm{ref}}\colon \mathbb{R}_{\geq 0} \to \mathbb{R}$ emanate from the function space $\mathcal{W}^{k,\infty}(\mathbb{R}_{\geq 0}; \mathbb{R})$ (subspace of the Sobolev space, see e.g. [6, p. 194]) of locally absolutely continuous functions with essentially bounded derivatives up to some order $k \in \mathbb{N}$ equipped with the norm $\|y_{\mathrm{ref}}\|_{k,\infty} := \sum_{i=0}^{k} \|y_{\mathrm{ref}}^{(i)}\|_\infty$. Note that, $y_{\mathrm{ref}}(\cdot) \in \mathcal{W}^{k,\infty}(\mathbb{R}_{\geq 0}; \mathbb{R})$ implies that $y_{\mathrm{ref}}(\cdot)$ is k-times weakly differentiable (i.e. continuously differentiable almost everywhere) and $y_{\mathrm{ref}}(\cdot)^{k-1}$ is (absolutely) continuous. This space covers most of the usually employed reference signals in industry with one important exception: a reference step at some time $t_0 > 0$ [s], i.e.

$$y_{\mathrm{ref}}\colon \mathbb{R}_{\geq 0} \to \mathbb{R}, \qquad y_{\mathrm{ref}}(t) := \begin{cases} \hat{y}_{\mathrm{ref}}, & t \geq t_0 > 0 \\ 0, & t < t_0 \end{cases} \tag{1.37}$$

where $\hat{y}_{\mathrm{ref}} \neq 0$ is its magnitude. Reference steps as in (1.37) (or point-to-point movements, in general) imply sudden, discontinuous changes in the tracking error (1.1) which endangers fulfillment of e.g. motion control objective (mco_4). Hence reference steps of form (1.37) are not admissible and should either be smoothed (e.g. low pass filtered) or approximated by a saturated ramp, given by

$$y_{\mathrm{ref}}\colon\ \mathbb{R}_{\geq 0} \to \mathbb{R}, \qquad t \mapsto y_{\mathrm{ref}}(t) := \mathrm{sat}_0^{\hat{y}_{\mathrm{ref}}}\Big(\alpha(t - t_0)\Big),$$

where $\mathrm{sat}_0^{\hat{y}_{\mathrm{ref}}}(\cdot)$ is as in (N.4) and $\alpha \neq 0$ represents the slope of the ramp. Note that initial reference steps as in (1.2) (i.e. $t_0 = 0$ in (1.37)) are subsumed by the function space $\mathcal{W}^{k,\infty}(\mathbb{R}_{\geq 0}; \mathbb{R})$. For system class $\mathcal{S}_1$ and system class $\mathcal{S}_2$ the corresponding reference $y_{\mathrm{ref}}(\cdot)$ must (at least) be element of $\mathcal{W}^{1,\infty}(\mathbb{R}_{\geq 0}; \mathbb{R})$ and $\mathcal{W}^{2,\infty}(\mathbb{R}_{\geq 0}; \mathbb{R})$, respectively.

Examples of admissible references for class $\mathcal{S}_1$ and for class $\mathcal{S}_2$ are depicted in Fig. 1.19. These exemplary references will qualitatively re-appear throughout this thesis. They challenge the closed-loop system with constant values (initial reference step) and (smoothed) ramp-like signals. Simple speed or position tracking tasks in industry usually employ such "reference trajectories" (see e.g. [66]) comprising initial set-point for production start (see $0-2$ [s] in Fig. 1.19), acceleration to production speed or position (see $2-3$ [s] in Fig. 1.19), production phase (see $3-5$ [s] in Fig. 1.19) and deceleration to standstill (see $5-7$ [s] and $7-8$ [s] in Fig. 1.19). Physical constraints (see Section 1.4) limit maximal acceleration and maximal speed, respectively. Hence, in particular for tracking problems, reference generation must account for these

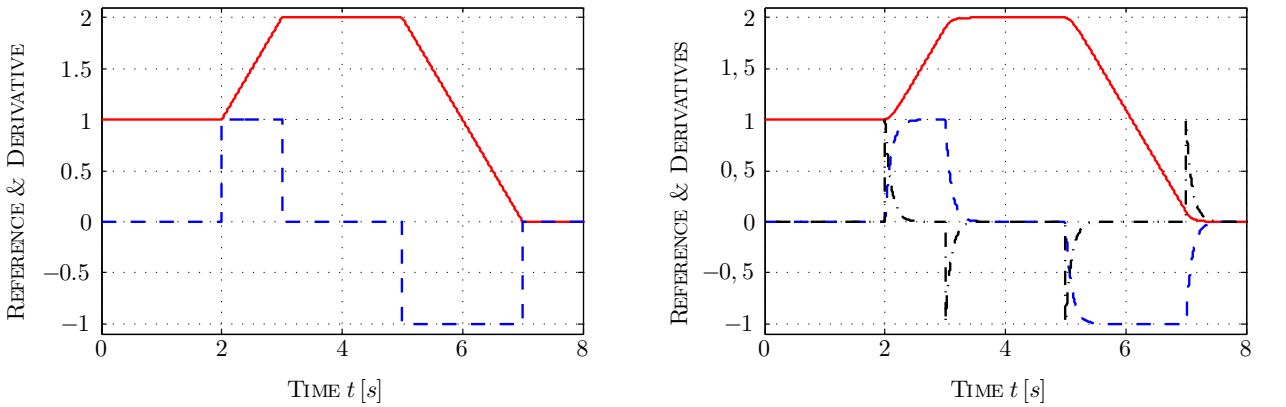

(a) *admissible reference for class* $\mathcal{S}_1$*:* — $y_{\mathrm{ref}}(\cdot)$ *and* - - - $\dot{y}_{\mathrm{ref}}(\cdot)$ *(i.e.* $y_{\mathrm{ref}}(\cdot) \in \mathcal{W}^{1,\infty}(\mathbb{R}_{\geq 0};\mathbb{R})$*)*

(b) *admissible reference for class* $\mathcal{S}_2$*:* — $y_{\mathrm{ref}}(\cdot)$, - - - $\dot{y}_{\mathrm{ref}}(\cdot)$ *and* -·-·- $\ddot{y}_{\mathrm{ref}}(\cdot)/10$ *(i.e.* $y_{\mathrm{ref}}(\cdot) \in \mathcal{W}^{2,\infty}(\mathbb{R}_{\geq 0};\mathbb{R})$*)*

Figure 1.19: *Examples of admissible reference signals for system class* $\mathcal{S}_1$ *and* $\mathcal{S}_2$*, respectively.*

limitations by providing smooth or (at least) continuous reference signals with bounded derivatives.

Remark 1.8 (Reference trajectory generation)**.**
Reference generation and, in general, path planing are non-trivial tasks but essential in motion control (see e.g. [143] or in greater detail [174, Chapter 5]). For this thesis it is assumed that $y_{\mathrm{ref}}(\cdot) \in \mathcal{W}^{1,\infty}(\mathbb{R}_{\geq 0};\mathbb{R})$ *(or* $\mathcal{W}^{2,\infty}(\mathbb{R}_{\geq 0};\mathbb{R})$*) is a reasonable and admissible reference specified by the human operator (via human-machine interface) or provided by an "intelligent" path planing algorithm avoiding collision with obstacles (using e.g. potential fields, gradient descent methods or trajectory planning and polynomial interpolation, see [174, Chapter 5]).*

1.6.2.5 Output disturbances due to measurement errors

Output disturbances are neglected in Definition 1.6 and in Definition 1.7. Such disturbances may be considered as being incorporated into the reference (yielding a deteriorated reference signal). More precisely, if output $y(\cdot)$ in (1.36) is corrupted by measurement errors (e.g. measurement noise, see Section 1.4.4) subsumed in $n_m(\cdot) \in \mathcal{W}^{2,\infty}(\mathbb{R}_{\geq 0},\mathbb{R})$, then the tracking error (1.1) becomes

$$\forall\, t \geq 0\colon \qquad e(t) = y_{\mathrm{ref}}(t) - y(t) - n_m(t) = \Big(y_{\mathrm{ref}}(t) - n_m(t)\Big) - y(t) \tag{1.38}$$

and similarly its derivative. Output disturbance $n_m(\cdot)$ cannot be distinguished from reference $y_{\mathrm{ref}}(\cdot)$ and hence cannot be compensated for by a controller with output feedback. The actual tracking error $y_{\mathrm{ref}}(\cdot) - y(\cdot)$ may evolve outside the prescribed region. Therefore, for perturbed tracking errors as in (1.38), the control objectives (co_2) and (co_3) should be relaxed to

($\widehat{\mathrm{co}}_2$) $\forall\, \lambda > 0\colon \qquad \lim_{t\to\infty} \operatorname{dist}\big(|e(t)|, [0, \lambda + \|n_m\|_\infty]\big) = 0 \qquad$ and

($\widehat{\mathrm{co}}_3$) $\forall\, t \geq 0\colon \qquad |e(t)| < \psi(t) + \|n_m\|_\infty,$

respectively. Note that, in view of modeling assumption (ma_2), the measurement errors are small compared to the prescribed asymptotic accuracy, i.e. $\|n_m\|_\infty \ll \lambda$. Moreover, if $\|n_m\|_\infty$ is known a priori, then substituting $\widehat{\lambda} := \lambda - \|n_m\|_\infty$ for λ in (co_2) and $\widehat{\psi}(\cdot) := \psi(\cdot) - \|n_m\|_\infty$ for $\psi(\cdot)$ in (co_3) assures fulfillment of the primary control objectives, respectively.

1.7 Contributions of this thesis

The *high-gain adaptive speed control problem* was solved in [169] for 1MS and 2MS. However, some issues were not covered, e.g. actuator saturation, gear and motor side friction were neglected. Moreover, dynamic friction effects were solely touched, explicit dynamic friction modeling was not addressed. These issues are covered in the present work and extensions for funnel control such as gain scaling (see [101]) and asymmetric boundary design (see [121]) are considered. The extensions provide more degrees of freedom in controller design and may help to improve tracking performance. Furthermore, high-gain adaptive controllers are proposed which solve the *high-gain adaptive position control problem* for 1MS and 2MS. These high-gain adaptive position controllers with output *and* derivative feedback (i.e. feedback of position and speed) are simple, robust and easy to implement.

The high-gain adaptive (motion) controllers are developed, in a general framework, for systems of class $\mathcal{S}_1$ and for systems of class $\mathcal{S}_2$ (see Definitions 1.6 and 1.7, respectively) to solve the *generalized high-gain adaptive control problem*. The developments are presented in a structured, detailed and self-contained manner to improve readability and ease insight, in particular, for newcomers to high-gain adaptive control: At first "classical" high-gain adaptive control is motivated and introduced for LTI SISO systems with relative degree one and then extended to LTI SISO systems with relative degree two (see Chapter 2). Then adaptive λ-tracking control and funnel control are introduced and discussed for systems of class $\mathcal{S}_1$ and class $\mathcal{S}_2$ (see Chapters 3 & 4). In Chapter 5 it is shown that, depending on application, 1MS (1.24), (1.25) and 2MS (1.26), (1.27) are or can be rendered element of system classes $\mathcal{S}_1$ and $\mathcal{S}_2$. Hence high-gain adaptive motion control is theoretically admissible. That the proposed controllers are indeed applicable in "real world" is shown at the end of Sections 5.2.2 and 5.2.3 by implementation and experimental validation at the laboratory setup of the Institute for Electrical Drive Systems and Power Electronics. Measurement results are presented for high-gain adaptive speed and position control of 1MS and 2MS. Finally, a first result in robotics is established which allows for application of funnel control (with derivative feedback) for position control of rigid revolute joint robotic manipulators if the inertia matrix is known.

This thesis arose from and is based on several publications: most of the results for funnel control with and without extensions (e.g. gain scaling, proportional-integral internal model) for speed control of 1MS and 2MS were already published in [67, 70, 71, 96, 169]. First results for high-gain adaptive position control of 1MS and 2MS (with proportional-integral internal model) have been accepted for publication in "International Journal of Control" (see [65]).

Most of the theoretical results for "classical" high-gain adaptive control, adaptive λ-tracking control and funnel control for systems with relative degree one or two are based on or taken from the monograph [86], the contributions [34, 99, 101, 103, 190] and the joint work [72]. Funnel

control with saturation was introduced in [82] and [83] for LTI multiple-input multiple-output (MIMO) and nonlinear SISO systems with relative degree one, respectively. Funnel control with derivative feedback and saturation for nonlinear SISO systems with relative degree two has been submitted for publication in "SIAM Journal on Control and Optimization" (see the joint work [72]).

Main *theoretical* contributions of this thesis are:

- the detailed modeling of industrial servo-systems (based on a literature research, see Section 1.4, p. 12 ff.) leading to the models of 1MS (1.24), (1.25) and 2MS (1.26), (1.27) with gear, actuator saturation and deviation, load disturbance and dynamic friction on motor *and* load side;
- Theorem 2.36: high-gain adaptive control with derivative feedback for minimum-phase LTI SISO systems with relative degree two and known sign of the high-frequency gain (see p. 79 ff.);
- Theorem 3.13: adaptive λ-tracking control with derivative feedback for systems of class $\mathcal{S}_2$ (see p. 114 ff.);
- Theorem 4.13 and Theorem 4.15 (based on Theorem 2.1 and Theorem 3.3 in [72], resp.): funnel control with derivative feedback and funnel control with derivative feedback & saturation for systems of class $\mathcal{S}_2$, respectively (see p. 156 ff. and p. 165 ff.);
- Lemma 5.3: the LuGre friction operator $\mathfrak{L}_{\vartheta^0}$ as in (1.21) is element of operator class $\mathcal{T}$ (see p. 179 ff.);
- a solution to the *high-gain adaptive position control problem* for 1MS and 2MS, respectively (see Section 5.2.3, p. 202 ff.) and
- Theorem 5.18: (MIMO) funnel control with derivative feedback for position control of rigid revolute joint robotic manipulators (see p. 227 ff.).

Main *experimental* contributions of this thesis are:

- the comparative measurements for the relative degree one case, i.e. application of adaptive λ-tracking control and funnel control with output feedback for speed control of 1MS and 2MS (see Section 5.2.2.3, p. 193 ff.) and
- the comparative measurements for the relative degree two case, i.e. application of adaptive λ-tracking control and funnel control with derivative feedback for position control of 1MS and 2MS (see Section 5.2.3.3, p. 215 ff.).

Chapter 2

High-gain adaptive control

This chapter presents the basic idea(s) of "classical" high-gain adaptive control for linear time-invariant (LTI) single-input single-output (SISO) systems. In Section 2.1 the notions of relative degree, high-frequency gain and minimum-phase property are defined and a "decoupled system description"—the so called Byrnes-Isidori form (BIF)—is presented which is helpful in many proofs. After motivating for high-gain (adaptive) control by the root locus method (see Section 2.2) and presenting a brief historical overview (see Section 2.3.1), in Section 2.3.3 and in Section 2.3.4, high-gain adaptive control is discussed for minimum-phase LTI SISO systems with relative degree one and with relative degree two, respectively. Section 2.4 briefly revisits the notion of high-gain adaptive tracking. Here a so called internal model is connected in series to a high-gain adaptive controller to allow for asymptotic tracking of a reference signal generated by a known linear (homogeneous) differential equation.

2.1 Linear time-invariant single-input single-output systems

There exist two common system descriptions for LTI SISO systems either in state space or in frequency (Laplace) domain. To introduce the state space representation, let $n \in \mathbb{N}$ and $t \geq 0$ [s] and consider the n-th dimensional LTI SISO system, with input $u(t) \in \mathbb{R}$, output $y(t) \in \mathbb{R}$ and state variable

$$\forall\, t \geq 0\colon \qquad \boldsymbol{x}(t) = (x_1(t), \ldots, x_n(t))^\top \in \mathbb{R}^n,$$

given by the ordinary differential equation (ODE)

$$\left.\begin{array}{rcll} \dot{\boldsymbol{x}}(t) & = & \boldsymbol{A}\,\boldsymbol{x}(t) + \boldsymbol{b}\,u(t), & n \in \mathbb{N},\ \boldsymbol{x}(0) = \boldsymbol{x}^0 \in \mathbb{R}^n, \\ y(t) & = & \boldsymbol{c}^\top \boldsymbol{x}(t) + d\,u(t) & (\boldsymbol{A}, \boldsymbol{b}, \boldsymbol{c}, d) \in \mathbb{R}^{n\times n} \times \mathbb{R}^n \times \mathbb{R}^n \times \mathbb{R} \end{array}\right\} \tag{2.1}$$

where $\boldsymbol{A}$, $\boldsymbol{b}$, $\boldsymbol{c}$, d represent system matrix, input and output (coupling) vector and (direct) feedthrough, respectively. The initial-value of the ODE (2.1) is given by $\boldsymbol{x}(0) = \boldsymbol{x}^0$. A system of form (2.1) with $u(\cdot) = 0$ is asymptotically (or, equivalently, exponentially) stable if, and only if, $\operatorname{spec}(\boldsymbol{A}) \subset \mathbb{C}_{<0}$ (see [77, Theorem 3.3.20]). If $\operatorname{spec}(\boldsymbol{A}) \subset \mathbb{C}_{<0}$ and $u(\cdot) \in \mathcal{L}^p(\mathbb{R}_{\geq 0}; \mathbb{R})$, $p \in [1, \infty]$, then a system of form (2.1) is input-output stable or $\mathcal{L}^p$-stable (see [77, p. 132]).

Alternatively, to introduce the system representation in frequency domain, define the coprime

polynomials with real coefficients

$$\begin{aligned} N(s) &:= c_0 + c_1 s + \cdots + c_{m-1} s^{m-1} + c_m s^m \in \mathbb{R}[s] \\ D(s) &:= a_0 + a_1 s + \cdots + a_{n-1} s^{n-1} + s^n \in \mathbb{R}[s] \end{aligned}, \qquad \begin{aligned} &n,\, m \in \mathbb{N},\ n \geq m, \\ &c_m \neq 0 \end{aligned} \tag{2.2}$$

and consider the transfer function

$$F(s) = \frac{y(s)}{u(s)} = \frac{N(s)}{D(s)}, \qquad N,\, D \in \mathbb{R}[s],\ \text{coprime and as in (2.2)} \tag{2.3}$$

from input $u(s) = \mathscr{L}\{u(t)\}$ to output $y(s) = \mathscr{L}\{y(t)\}$ (assuming the Laplace transforms exist). Transfer function (2.3) is said to be proper or strictly proper if $m \leq n$ or $m < n$, respectively. For $n = m = 0$ the transfer function (2.3) simplifies to $F(s) = c_0$. $N(s)$ and $D(s)$ represent numerator and denominator polynomial of transfer function (2.3), respectively. Some $z \in \mathbb{C}$ is called (transmission) zero of (2.3) if $N(z) = 0$ (i.e. a root of the numerator) whereas some $p \in \mathbb{C}$ is called pole of (2.3) if $D(p) = 0$ (i.e. a root of the denominator). A polynomial is called Hurwitz polynomial (or simply Hurwitz) if all its roots have negative real part. A LTI SISO system of form (2.3) is exponentially (or, equivalently, asymptotically) stable if, and only if, the denominator D is a Hurwitz polynomial.

A state space representation (2.1) with $\boldsymbol{x}^0 = \boldsymbol{0}_n$ is called realization of (2.3), if

$$F(s) = \boldsymbol{c}^\top (s\,\boldsymbol{I}_n - \boldsymbol{A})^{-1} \boldsymbol{b} + d, \qquad n \in \mathbb{N},\ (\boldsymbol{A}, \boldsymbol{b}, \boldsymbol{c}, d) \in \mathbb{R}^{n\times n} \times \mathbb{R}^n \times \mathbb{R}^n \times \mathbb{R}. \tag{2.4}$$

Note that n in (2.1) and (2.2) must not necessarily equal. A realization is said to be a minimal realization, if there is no other realization with smaller dimension. (2.1) is a minimal realization of (2.3) if, and only if, $(\boldsymbol{A}, \boldsymbol{b})$ is controllable and $(\boldsymbol{A}, \boldsymbol{c})$ is observable (see [24, Corollary 12.9.15]). The direct feedthrough in (2.4) is uniquely determined by $d = \lim_{s\to\infty} F(s)$ (see [24, p. 799]). Moreover, any strictly proper transfer function has a minimal realization (see [24, Proposition 12.9.3]). Transfer function (2.4) represents the Laplace transform of the impulse response of (2.1) for $\boldsymbol{x}^0 = \boldsymbol{0}_n$ (see [24, pp. 797, 799]). Alternatively, the transfer function (2.4) may be computed as follows (see [24, pp. 799, 832])

$$F(s) = \boldsymbol{c}^\top (s\boldsymbol{I}_n - \boldsymbol{A})^{-1}\boldsymbol{b} + d = \frac{-\det \begin{bmatrix} s\boldsymbol{I}_n - \boldsymbol{A} & \boldsymbol{b} \\ \boldsymbol{c}^\top & -d \end{bmatrix}}{\det(s\boldsymbol{I}_n - \boldsymbol{A})} = d + \sum_{i=1}^{\infty} \frac{\boldsymbol{c}^\top \boldsymbol{A}^{i-1}\boldsymbol{b}}{s^i} \tag{2.5}$$

where, in the last term of (2.5), d and $\boldsymbol{c}^\top \boldsymbol{A}^{i-1}\boldsymbol{b}$ for $i \geq 1$ are called Markov parameters (see [24, p. 799]). For arbitrary $\boldsymbol{x}^0 \neq \boldsymbol{0}_n$, one may write

$$y(s) = \boldsymbol{c}^\top (s\,\boldsymbol{I}_n - \boldsymbol{A})^{-1}\boldsymbol{x}^0 + \left(\boldsymbol{c}^\top (s\,\boldsymbol{I}_n - \boldsymbol{A})^{-1}\boldsymbol{b} + d\right) u(s).$$

2.1.1 Relative degree

The term "relative degree" for nonlinear (or linear) systems in state space was coined by Christopher I. Byrnes (1949–2010) and Alberto Isidori (1942–) (see [36]), whereas the relative degree of transfer functions is also known as pole excess (see [16, p. 93]) or difference degree/order

(dt. Differenzordnung, see [58, Section 13.5.1]). The relative degree is an essential ingredient of several adaptive and nonlinear control concepts, e.g. it must be known for high-gain adaptive control (see e.g. [85]), for model reference adaptive control (see e.g. [138, p. 183-184]) or for exact input/output linearization of nonlinear SISO systems (see e.g. [107, Section 4.2]).

The following definition of the relative degree of LTI SISO systems slightly differs from that given in [107, Remark 4.1.2], also the case of relative degree zero is considered.

Definition 2.1 (Relative degree of LTI SISO systems)**.**
(i) A system of form (2.1) *is said to have* relative degree $r \geq 1$ *if, and only if, the following conditions hold:*

$$d = 0, \qquad \forall\, i \in \{1, \dots, r-2\}\colon \quad \boldsymbol{c}^\top \boldsymbol{A}^i \boldsymbol{b} = 0 \qquad \textit{and} \qquad \boldsymbol{c}^\top \boldsymbol{A}^{r-1} \boldsymbol{b} \neq 0. \tag{2.6}$$

System (2.1) *is said to have* relative degree $r = 0$ *if, and only if,* $d \neq 0$ *in* (2.1)*.*
(ii) A transfer function of form (2.3) *is said to have* relative degree $r = n - m$*.*

Loosely speaking, the relative degree indicates which time derivative of the system output $y(\cdot)$ is directly affected by the control input $u(\cdot)$ and hence how "fast" $y(\cdot)$ is influenced by $u(\cdot)$. The integer r specifies the number of integrators which at least have to "be passed" from input to output. As a consequence, the relative degree cannot exceed the system order, i.e. $r \leq n$. For systems with feedthrough (i.e. $d \neq 0$) the control input directly acts on the system output.

For LTI SISO systems of form (2.1) the relative degree is globally defined, i.e. it holds for any $\boldsymbol{x}^\star \in \mathbb{R}^n$, whereas e.g. for control-affine nonlinear SISO systems of the form

$$\dot{\boldsymbol{x}}(t) = \boldsymbol{f}(\boldsymbol{x}(t)) + \boldsymbol{g}(\boldsymbol{x}(t))\, u(t), \qquad \boldsymbol{x}(0) = \boldsymbol{x}^0 \in \mathbb{R}^n \tag{2.7}$$

with (smooth) functions $\boldsymbol{f}, \boldsymbol{g}\colon \mathbb{R}^n \to \mathbb{R}^n$, it may change over $\mathbb{R}^n$ or may even be undefined for some $\boldsymbol{x}^\star \in \mathbb{R}^n$ (see [107, p. 137 and Example 4.1.1]).

Note that the relative degree of a transfer function (2.3) and its realization (2.1) are related.

Lemma 2.2. *Denote the relative degree of* (2.1) *and* (2.3) *by* $r_{SS} \geq 0$ *and* $r_{TF} \geq 0$*, respectively. If* (2.1) *is a realization of* (2.3)*, then* $r_{SS} = r_{TF}$*.*

Proof. Since (2.1) is a realization of (2.3), (2.4) and (2.5) hold. In view of (2.5) and Definition 2.1, the following holds

$$\forall\, l \geq \max\{1, r_{SS}\}\colon \quad \deg s^l - \deg\left(d\, s^l + \boldsymbol{c}^\top \boldsymbol{b}\, s^{l-1} + \dots + \boldsymbol{c}^\top \boldsymbol{A}^{l-1} \boldsymbol{b}\right) = r_{SS}. \tag{2.8}$$

Hence

$$\begin{aligned} r_{SS} &\overset{(2.8),(2.5)}{=} \deg\left(\det(s\boldsymbol{I}_n - \boldsymbol{A})\right) - \deg\left(\det \begin{bmatrix} s\boldsymbol{I}_n - \boldsymbol{A} & \boldsymbol{b} \\ \boldsymbol{c}^\top & -d \end{bmatrix}\right) \\ &\overset{(2.5),(2.3)}{=} \deg(D) - \deg(N) = n - m = r_{TF}, \end{aligned}$$

which completes the proof. □

The relative degree is invariant to coordinate changes.

Proposition 2.3. *Consider a system of form (2.1) with relative degree r where $0 \leq r \leq n$. The coordinate transformation*

$$\boldsymbol{T}\colon \mathbb{R}^n \to \mathbb{R}^n, \qquad \boldsymbol{x} \mapsto \tilde{\boldsymbol{x}} := \boldsymbol{T}\boldsymbol{x}, \qquad \text{where} \qquad \boldsymbol{T} \in GL_n(\mathbb{R}) \tag{2.9}$$

applied to system (2.1) yields the following system in new coordinates

$$\left.\begin{aligned} \dot{\tilde{\boldsymbol{x}}}(t) &= \underbrace{\boldsymbol{T}\boldsymbol{A}\boldsymbol{T}^{-1}}_{=:\tilde{\boldsymbol{A}}}\,\tilde{\boldsymbol{x}}(t) + \underbrace{\boldsymbol{T}\boldsymbol{b}}_{=:\tilde{\boldsymbol{b}}}\,u(t), && \tilde{\boldsymbol{x}}(0) = \boldsymbol{T}\boldsymbol{x}^0 \\ y(t) &= \underbrace{\boldsymbol{c}^\top\boldsymbol{T}^{-1}}_{=:\tilde{\boldsymbol{c}}^\top}\tilde{\boldsymbol{x}}(t) + d\,u(t). \end{aligned}\right\} \tag{2.10}$$

Denote the relative degree of the transformed system (2.10) by $\tilde{r}$, then $\tilde{r} = r$.

Proof. In view of (2.9) the inverse $\boldsymbol{T}^{-1} \in \mathbb{R}^{n\times n}$ exists and a straightforward calculation gives system (2.10) in new coordinates. First consider the case $d \neq 0$ in (2.1), then $r = 0$ by Definition 2.4. Moreover, in view of (2.10), $\tilde{r} = 0 = r$.
Next consider the case $d = 0$ in (2.1), then $1 \leq r \leq n$ and note that the following holds

$$\forall\, i \in \mathbb{N}\colon \qquad \tilde{\boldsymbol{c}}^\top\tilde{\boldsymbol{A}}^i\tilde{\boldsymbol{b}} = \boldsymbol{c}^\top\boldsymbol{T}^{-1}\underbrace{(\boldsymbol{T}\boldsymbol{A}\boldsymbol{T}^{-1})\cdots(\boldsymbol{T}\boldsymbol{A}\boldsymbol{T}^{-1})}_{i\text{-times}}\boldsymbol{T}\boldsymbol{b} = \boldsymbol{c}^\top\boldsymbol{A}^i\boldsymbol{b}. \tag{2.11}$$

Hence, $\tilde{\boldsymbol{c}}^\top\tilde{\boldsymbol{A}}^{r-1}\tilde{\boldsymbol{b}} = \boldsymbol{c}^\top\boldsymbol{A}^{r-1}\boldsymbol{b} \neq 0$ and $\tilde{\boldsymbol{c}}^\top\tilde{\boldsymbol{A}}^i\tilde{\boldsymbol{b}} = \boldsymbol{c}^\top\boldsymbol{A}^i\boldsymbol{b} = 0$ for all $i \in \{1,\ldots,r-2\}$, which in view of Definition 2.1 yields $r = \tilde{r}$. This completes the proof. □

2.1.2 High-frequency gain

For control system design, it is crucial to determine the "direction of influence" of control action $u(\cdot)$ on system output $y(\cdot)$. The sign of the high-frequency or instantaneous gain[1] (see [15, p. 236]) indicates this influence. That is why the high-frequency gain is sometimes also called control direction (see [150, p. 261,262]). It is defined as follows.

Definition 2.4 (High-frequency gain of LTI SISO systems)**.**
(i) For a system given by (2.1) with relative degree r, the high-frequency gain γ_0 *is defined by*

$$\gamma_0 := \begin{cases} d & , r = 0 \\ \boldsymbol{c}^\top\boldsymbol{A}^{r-1}\boldsymbol{b} & , 1 \leq r \leq n. \end{cases} \tag{2.12}$$

(ii) For a transfer function of form (2.3) with relative degree $0 \leq r \leq n$, the high-frequency gain γ_0 *is defined by*

$$\gamma_0 := \lim_{s\to\infty} s^r F(s) \tag{2.13}$$

[1] Nowadays it is common to use the notion "high-frequency gain" for both system descriptions in time (state space) or in frequency (transfer function) domain. Formerly, "high-frequency gain" denoted the "leading coefficient of the numerator of the transfer function whereas "instantaneous gain" was equivalently used in the time domain (see [37]).

Note that for $F(s)$ as in (2.3) the high-frequency gain is given by $\gamma_0 = c_m$. In general, the high-frequency gain γ_0 corresponds to "the first non-vanishing coefficient of the impulse response" (see [15, p. 334]) and is not to be confused with the steady-state gain (see [24, p. 799])

$$\gamma_\infty := \lim_{s\to 0} F(s) \overset{(2.3)}{=} \frac{c_0}{a_0} \overset{(2.4)}{=} -\boldsymbol{c}^\top \boldsymbol{A}^{-1}\boldsymbol{b} + d,$$

which (for stable LTI SISO systems) quantifies amplification of the control input in steady-state, i.e. $\lim_{t\to\infty} y(t) = \gamma_\infty \lim_{t\to\infty} u(t)$ (if $\lim_{t\to\infty} u(t)$ exists).

Akin to the relative degree, also the high-frequency gain of a transfer function (2.3) and its realization (2.1) are linked.

Lemma 2.5. *Denote the high-frequency gain of (2.1) and (2.3) by γ_0^{SS} and γ_0^{TF}, respectively. If (2.1) is a realization of (2.3), then $\gamma_0^{SS} = \gamma_0^{TF}$.*

Proof. From Lemma 2.2 it follows that realization (2.1) and transfer function (2.3) have identical relative degree r. Consider the case $r = 0$. Then by Definition 2.4 and uniqueness of $d = \lim_{s\to\infty} F(s)$ (see [24, p. 799]) it follows that $\gamma_0^{SS} = d = \lim_{s\to\infty} F(s) = c_m = \gamma_0^{TF}$. Now consider the case $r \geq 1$, then the following holds

$$\begin{aligned}\gamma_0^{TF} = c_m = \lim_{s\to\infty} s^r F(s) &\overset{(2.5)}{=} \lim_{s\to\infty} \left(s^r \sum_{i=1}^{\infty} \frac{\boldsymbol{c}^\top \boldsymbol{A}^{i-1}\boldsymbol{b}}{s^i} \right) \\ &\overset{(2.6)}{=} \lim_{s\to\infty} \left(s^r \sum_{i=r}^{\infty} \frac{\boldsymbol{c}^\top \boldsymbol{A}^{i-1}\boldsymbol{b}}{s^i} \right) = \boldsymbol{c}^\top \boldsymbol{A}^{r-1}\boldsymbol{b} = \gamma_0^{SS}.\end{aligned}$$

This completes the proof. □

Moreover, also the high-frequency gain is invariant to similarity transformations.

Corollary 2.6. *Consider a system of form (2.1) with high-frequency gain γ_0. A coordinate transformation as in (2.9) applied to (2.1) does not change the high-frequency gain, i.e. the high-frequency gain $\tilde{\gamma}_0$ of the transformed system (2.10) equals γ_0.*

Proof. Applying (2.9) to (2.1) yields (2.10). Denote the high-frequency gain of (2.10) and (2.1) by $\tilde{\gamma}_0$ and γ_0, respectively. First consider the case $d \neq 0$. Then $r = 0$ and, in view of (2.10) and Definition 2.4, $\gamma_0 = \tilde{\gamma}_0 = d$. Next consider the case $d = 0$, hence $1 \leq r \leq n$ and, in view of Definition 2.4, $\gamma_0 = \boldsymbol{c}^\top \boldsymbol{A}^{r-1}\boldsymbol{b}$ and $\tilde{\gamma}_0 = \tilde{\boldsymbol{c}}^\top \tilde{\boldsymbol{A}}^{r-1}\tilde{\boldsymbol{b}}$, respectively. Invoking (2.11) yields $\gamma_0 = \tilde{\gamma}_0$. This completes the proof. □

2.1.3 Minimum-phase systems

For this thesis the definition of minimum-phase LTI systems is adopted from [86, p. 10]. Solely, the SISO case is considered.

Definition 2.7 (Minimum-phase LTI SISO system)**.**
(i) A system of form (2.1) is said to be minimum-phase *if, and only if, the following holds*

$$\forall\, s \in \mathbb{C}_{\geq 0}\colon \qquad \det \begin{bmatrix} s\boldsymbol{I}_n - \boldsymbol{A} & \boldsymbol{b} \\ \boldsymbol{c}^\top & -d \end{bmatrix} \neq 0. \tag{2.14}$$

(ii) A transfer function of form (2.3) is said to be minimum-phase *if, and only if, the following holds*

$$\forall\, s \in \mathbb{C}_{\geq 0}\colon \qquad N(s) = c_0 + c_1 s + \cdots + c_{m-1} s^{m-1} + c_m s^m \neq 0. \tag{2.15}$$

Note that in contrast to many (engineering) textbooks on linear control theory (see e.g. [124, p. 294] or [58, p. 194]), minimum-phase systems of form (2.3) (or (2.1))—according to Definition 2.7—are not required to have poles (or eigenvalues) with negative real parts and a positive high-frequency gain. Definition 2.7 allows for minimum-phase systems which are unstable and have high-frequency gains of arbitrary sign.

In view of Definition 2.7, a realization (2.1) of (2.3) is minimum-phase, if it is stabilizable and detectable and the transfer function (2.3) has only zeros in left complex half-plane (see [86, p. 10]). This characterization written more formally gives:

Proposition 2.8. *[86, Proposition 2.1.2]*
Let (2.1) be a realization of (2.3). Then (2.14) holds if, and only if, the following conditions are satisfied

(i) $\forall\, s \in \mathbb{C}_{\geq 0}\colon \quad \operatorname{rank}[s\boldsymbol{I}_n - \boldsymbol{A},\, \boldsymbol{b}] = n$ *(i.e.* $(\boldsymbol{A}, \boldsymbol{b})$ *is stabilizable);*

(ii) $\forall\, s \in \mathbb{C}_{\geq 0}\colon \quad \operatorname{rank}\begin{bmatrix} s\boldsymbol{I}_n - \boldsymbol{A} \\ \boldsymbol{c}^\top \end{bmatrix} = n$ *(i.e.* $(\boldsymbol{A}, \boldsymbol{c}^\top)$ *is detectable);*

(iii) $F(s)$ *as in (2.3) has no (transmission) zeros in* $\mathbb{C}_{\geq 0}$.

Remark 2.9 (Popov-Belevitch-Hautus (PBH) test)**.**
Conditions (i) and (ii) in Proposition 2.8 are also known as the Popov-Belevitch-Hautus (rank) test for stabilizability and detectability, respectively (see [24, Corollaries 12.5.4 and 12.8.4]). Replacing '$\forall\, s \in \mathbb{C}_{\geq 0}$*' by '*$\forall\, s \in \mathbb{C}$*' in conditions (i) and (ii) of Proposition 2.8 gives the Popov-Belevitch-Hautus (rank) test for controllability and observability, respectively (see [24, Corollaries 12.6.19 and 12.3.19]).*

The following proof makes use of the "Kalman decomposition" (see e.g. [24, p. 825]) and differs from the brief proof in [86, p. 10].

Proof of Proposition 2.8.

Step 1: Kalman decomposition of state space realization.
For $D \in \mathbb{R}[s]$ as in (2.3), define $n_1 := \deg(D)$. Since (2.1) is a realization of (2.3), (2.5) holds and, for n as in (2.1), $n \geq n_1$. In view of Proposition 12.9.10 in [24, p. 825], there exists a nonsingular $\boldsymbol{S} \in \mathbb{R}^{n\times n}$ such that

$$\widetilde{\boldsymbol{A}} := \boldsymbol{S}^{-1}\boldsymbol{A}\boldsymbol{S} = \begin{bmatrix} \boldsymbol{A}_1 & \boldsymbol{O} & \boldsymbol{A}_{13} & \boldsymbol{O} \\ \boldsymbol{A}_{21} & \boldsymbol{A}_2 & \boldsymbol{A}_{23} & \boldsymbol{A}_{24} \\ \boldsymbol{O} & \boldsymbol{O} & \boldsymbol{A}_3 & \boldsymbol{O} \\ \boldsymbol{O} & \boldsymbol{O} & \boldsymbol{A}_{43} & \boldsymbol{A}_4 \end{bmatrix},\ \boldsymbol{S}^{-1}\boldsymbol{b} = \begin{pmatrix} \boldsymbol{b}_1 \\ \boldsymbol{b}_2 \\ \boldsymbol{0}_{n_3} \\ \boldsymbol{0}_{n_4} \end{pmatrix} \text{ and } (\boldsymbol{c}^\top\boldsymbol{S})^\top = \begin{pmatrix} \boldsymbol{c}_1 \\ \boldsymbol{0}_{n_2} \\ \boldsymbol{c}_3 \\ \boldsymbol{0}_{n_4} \end{pmatrix} \tag{2.16}$$

where $n_2, \ldots, n_4 \in \mathbb{N}$ such that $\sum_{i=1}^4 n_i = n$, $\boldsymbol{A}_i \in \mathbb{R}^{n_i\times n_i}$ for all $i \in \{1, \ldots, 4\}$, $\boldsymbol{A}_{13} \in \mathbb{R}^{n_1\times n_3}$, $\boldsymbol{A}_{21} \in \mathbb{R}^{n_2\times n_1}$, $\boldsymbol{A}_{23} \in \mathbb{R}^{n_2\times n_3}$, $\boldsymbol{A}_{24} \in \mathbb{R}^{n_2\times n_4}$, $\boldsymbol{A}_{43} \in \mathbb{R}^{n_4\times n_3}$, $\boldsymbol{b}_1 \in \mathbb{R}^{n_1}$, $\boldsymbol{b}_2 \in \mathbb{R}^{n_2}$, $\boldsymbol{c}_1 \in \mathbb{R}^{n_1}$ and

$\boldsymbol{c}_3 \in \mathbb{R}^{n_3}$. Note that, if some $n_i = 0$, $i \in \{2,3,4\}$, then the corresponding entries in (2.16) are empty. Clearly, $F(s) = \boldsymbol{c}^\top (s\boldsymbol{I}_n - \boldsymbol{A})^{-1}\boldsymbol{b} + d = \boldsymbol{c}^\top \boldsymbol{S}(s\boldsymbol{I}_n - \widetilde{\boldsymbol{A}})^{-1}\boldsymbol{S}^{-1}\boldsymbol{b} + d$ and, moreover, the subsystem $(\boldsymbol{A}_1, \boldsymbol{b}_1, \boldsymbol{c}_1, d)$ is a minimal realization of (2.3) (see [24, Proposition 12.9.10]). Hence (see [24, Theorem 12.9.16]) and since $D \in \mathbb{R}[s]$ as in (2.3) is monic, the following holds

$$D(s) = \det(s\boldsymbol{I}_{n_1} - \boldsymbol{A}_1) \quad (= \det(s\boldsymbol{I}_n - \boldsymbol{A}) \text{ if } n_2 = n_3 = n_4 = 0). \tag{2.17}$$

Step 2: It is shown that the following implication holds: ⟦ *(i), (ii) and (iii)* ⟧ $\Longrightarrow$ ⟦ (2.14) ⟧. In view of Step 1, for $\boldsymbol{A}_2$, $\boldsymbol{A}_3$ and $\boldsymbol{A}_4$ as in (2.16), Proposition 12.9.10 in [24, p. 825] gives

$$\text{(i) and (ii)} \quad \Longrightarrow \quad \operatorname{spec}(\boldsymbol{A}_2), \operatorname{spec}(\boldsymbol{A}_3), \operatorname{spec}(\boldsymbol{A}_4) \subset \mathbb{C}_{<0} \quad \text{(if not empty)}. \tag{2.18}$$

Moreover, it is easy to see that (where $\det(s\boldsymbol{I}_{n_i} - \boldsymbol{A}_i) := 1$ if some $n_i = 0$, $i \in \{2,3,4\}$)

$$\det(s\boldsymbol{I}_n - \boldsymbol{A}) = \det(\boldsymbol{S}^{-1}(s\boldsymbol{I}_n - \boldsymbol{A})\boldsymbol{S}) \overset{(2.16)}{=} \det(s\boldsymbol{I}_n - \widetilde{\boldsymbol{A}}) \overset{(2.16)}{=} \prod_{i=1}^{4} \det(s\boldsymbol{I}_{n_i} - \boldsymbol{A}_i). \tag{2.19}$$

Since (2.1) is a realization of (2.3), (2.5) holds and, for $F(s) = \frac{N(s)}{D(s)}$ as in (2.3), rewriting gives

$$\det \begin{bmatrix} s\boldsymbol{I}_n - \boldsymbol{A} & \boldsymbol{b} \\ \boldsymbol{c}^\top & -d \end{bmatrix} \overset{(2.5)}{=} -\frac{N(s)}{D(s)} \det(s\boldsymbol{I}_n - \boldsymbol{A}) \overset{(2.19),(2.17)}{=} -N(s) \prod_{i=2}^{4} \det(s\boldsymbol{I}_{n_i} - \boldsymbol{A}_i). \tag{2.20}$$

Invoking (2.18) and (iii) (i.e. '$N(s) \neq 0$ for all $s \in \mathbb{C}_{\geq 0}$') yields (2.14).

Step 3: It is shown that the following implication holds: ⟦ (2.14) ⟧ $\Longrightarrow$ ⟦ *(i), (ii) and (iii)* ⟧. Note that (2.14) is equivalent to

$$\forall\, s \in \mathbb{C}_{\geq 0}\colon \qquad \operatorname{rank} \begin{bmatrix} s\boldsymbol{I}_n - \boldsymbol{A} & \boldsymbol{b} \\ \boldsymbol{c}^\top & -d \end{bmatrix} = n + 1, \tag{2.21}$$

i.e. the $n+1$ column vectors of $\left[\begin{smallmatrix} s\boldsymbol{I}_n - \boldsymbol{A} & \boldsymbol{b} \\ \boldsymbol{c}^\top & -d \end{smallmatrix}\right]$ are linearly independent for all $s \in \mathbb{C}_{\geq 0}$. Moreover, for any $\boldsymbol{M} \in \mathbb{R}^{k\times l}$, $k, l \in \mathbb{N}$, it holds that $\operatorname{rank}(\boldsymbol{M}) = \operatorname{rank}(\boldsymbol{M}^\top)$ (see [24, Corollary 2.5.3]). As a consequence, (i) and (ii) follow from (2.21). Hence, in view of Step 1, (2.18) holds. Moreover, (2.17), (2.19) and (2.20) also hold. Solving for $N(s)$ in (2.20) and invoking (2.14) and (2.18) yields '$N(s) \neq 0$ for all $s \in \mathbb{C}_{\geq 0}$' which shows (iii). Combining Step 2 and Step 3 completes the proof of Proposition 2.8. □

Example 2.10. *As a consequence of Proposition 2.8 the minimum-phase condition (2.14) implies stabilizability and detectability, whereas there exist stabilizable and detectable systems which are not minimum-phase. For illustration consider the first order system given by*

$$\begin{aligned} \dot{x}(t) &= 2\,x(t) + u(t), \qquad x(0) = x^0 \in \mathbb{R} \\ y(t) &= x(t) + u(t) \end{aligned}$$

which is stabilizable and detectable since

$$\forall\, s \in \mathbb{C}_{\geq 0}\colon \qquad \operatorname{rank} \begin{bmatrix} s-2, & 1 \end{bmatrix} = \operatorname{rank} \begin{bmatrix} s-2 \\ 1 \end{bmatrix} = 1,$$

but $F(s) = (s-2)^{-1} + 1 = (s-1)/(s-2)$ *has the zero* $z = 1$ *in the right complex half-plane.*

To conclude this subsection, note that also the minimum-phase property is invariant to coordinate changes.

Corollary 2.11. *Consider a minimum-phase system of form* (2.1)*. The coordinate transformation* (2.9) *applied to* (2.1) *yields a minimum-phase system of form* (2.10)*.*

Proof. Using the same notation as in (2.10), the result directly follows from

$$\begin{aligned}\det \begin{bmatrix} s\boldsymbol{I}_n - \tilde{\boldsymbol{A}} & \tilde{\boldsymbol{b}} \\ \tilde{\boldsymbol{c}}^\top & -d \end{bmatrix} &= \det \begin{bmatrix} \boldsymbol{T}(s\boldsymbol{I}_n - \boldsymbol{A})\boldsymbol{T}^{-1} & \boldsymbol{T}\boldsymbol{b} \\ \boldsymbol{c}^\top \boldsymbol{T}^{-1} & -d \end{bmatrix} \\ &= \det \left(\begin{bmatrix} \boldsymbol{T} & \boldsymbol{0} \\ \boldsymbol{0} & 1 \end{bmatrix} \begin{bmatrix} s\boldsymbol{I}_n - \boldsymbol{A} & \boldsymbol{b} \\ \boldsymbol{c}^\top & -d \end{bmatrix} \begin{bmatrix} \boldsymbol{T}^{-1} & \boldsymbol{0} \\ \boldsymbol{0} & 1 \end{bmatrix} \right) = \underbrace{\det(\boldsymbol{T}) \det(\boldsymbol{T}^{-1})}_{=1} \det \begin{bmatrix} s\boldsymbol{I}_n - \boldsymbol{A} & \boldsymbol{b} \\ \boldsymbol{c}^\top & -d \end{bmatrix} \neq 0.\end{aligned}$$

This completes the proof. □

2.1.4 Byrnes-Isidori form

In [107, Section 4.1, Proposition 4.1.3] a coordinate transformation is introduced which "decomposes" a n-th order (nonlinear) dynamical system of form (2.7) with (known) relative degree $1 \leq r \leq n$ into a chain of r integrators from control input to system output ("forward dynamics") and a subsystem with reduced order $n - r$ ("internal dynamics"). Since the relative degree of nonlinear systems might only be defined locally around a point $\boldsymbol{x}^\star \in \mathbb{R}^n$ also this coordinate change may only hold locally around $\boldsymbol{x}^\star$. If the "internal dynamics" are decoupled from the control input, then this decomposition is called Byrnes-Isidori form (BIF, see e.g. [72]) which e.g. allows for exact input/output linearization by state feedback (linearization may only hold locally, see [107, Section 4.2]). If the relative degree is defined at $\boldsymbol{x}^\star \in \mathbb{R}^n$, then the BIF does exist at $\boldsymbol{x}^\star$ in general, however the corresponding coordinate transformation may not be found easily (see [107, Remark 4.1.3]).

In contrast, for LTI SISO systems the relative degree is defined globally and hence the decomposition holds globally. Moreover, the coordinate transformation to obtain the BIF can be derived easily. The following lemma gives the explicit transformation matrix for LTI SISO systems of form (2.1) with known relative degree $r \geq 1$. The lemma was found independently of Lemma 3.5 in [103] (there for the MIMO case). The presented proof slightly differs from that given in [103].

Lemma 2.12 (Byrnes-Isidori form of LTI SISO systems with known relative degree)**.** *Consider a system of form* (2.1) *with relative degree* $1 \leq r < n$*, i.e.* (2.6) *holds true. Define*

$$\boldsymbol{C} := \begin{bmatrix} \boldsymbol{c}^\top \\ \boldsymbol{c}^\top \boldsymbol{A} \\ \vdots \\ \boldsymbol{c}^\top \boldsymbol{A}^{r-1} \end{bmatrix} \in \mathbb{R}^{r \times n}, \qquad \boldsymbol{B} := \begin{bmatrix} \boldsymbol{b} & \boldsymbol{A}\boldsymbol{b} & \cdots & \boldsymbol{A}^{r-1}\boldsymbol{b} \end{bmatrix} \in \mathbb{R}^{n \times r} \tag{2.22}$$

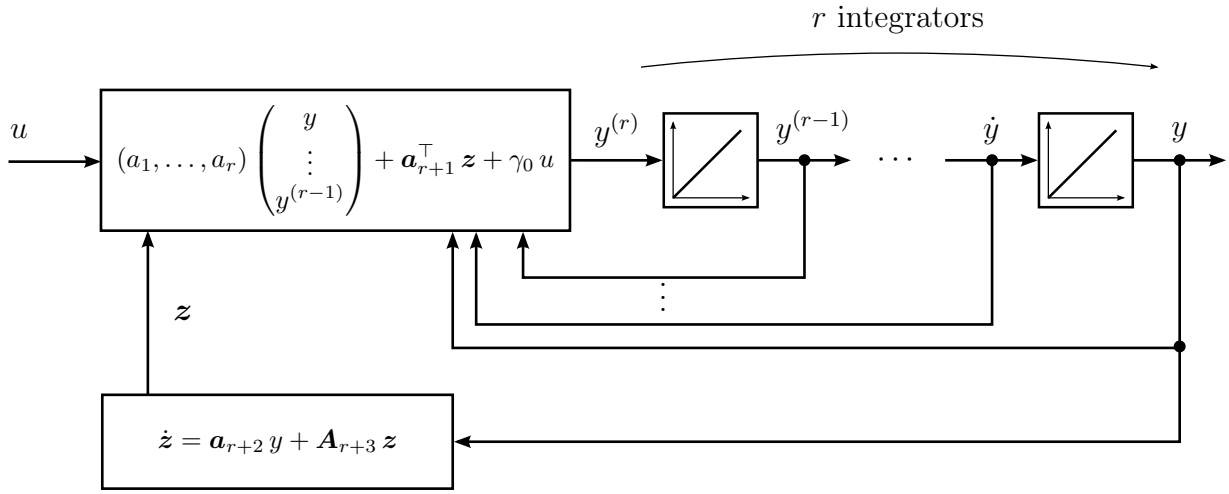

Figure 2.1: *Block diagram of LTI SISO system in BIF with relative degree $r \geq 1$ (initial values are neglected).*

and choose

$$\boldsymbol{V} \in \mathbb{R}^{n\times(n-r)} \qquad \textit{such that} \qquad \operatorname{im} \boldsymbol{V} = \ker \boldsymbol{C}, \quad \textit{i.e.} \quad \boldsymbol{C}\boldsymbol{V} = \boldsymbol{O}_{r\times(n-r)}. \tag{2.23}$$

Then the following hold:

(i) the matrix

$$\begin{aligned} &\boldsymbol{S} = \begin{bmatrix} \boldsymbol{C} \\ \boldsymbol{N} \end{bmatrix} \in \mathbb{R}^{n\times n} \quad \textit{where} \quad \boldsymbol{N} = (\boldsymbol{V}^\top \boldsymbol{V})^{-1} \boldsymbol{V}^\top (\boldsymbol{I}_n - \boldsymbol{B}(\boldsymbol{C}\boldsymbol{B})^{-1}\boldsymbol{C}) \in \mathbb{R}^{(n-r)\times n} \\ &\textit{is invertible with inverse} \quad \boldsymbol{S}^{-1} = \begin{bmatrix} \boldsymbol{B}(\boldsymbol{C}\boldsymbol{B})^{-1}, & \boldsymbol{V} \end{bmatrix}; \end{aligned} \tag{2.24}$$

(ii) the matrix $\boldsymbol{S}$ as in (2.24) with $\boldsymbol{z} \in \mathbb{R}^{n-r}$ allows for a coordinate transformation

$$\boldsymbol{S} \colon \mathbb{R}^n \to \mathbb{R}^n, \qquad \begin{pmatrix} y, & \dot{y}, & \cdots, & y^{(r-1)}, & \boldsymbol{z}^\top \end{pmatrix}^\top := \boldsymbol{S}\boldsymbol{x} \tag{2.25}$$

which gives the Byrnes-Isidori form (BIF) as follows

$$\left.\begin{aligned} \tfrac{d}{dt} \begin{pmatrix} y(t) \\ \dot{y}(t) \\ \vdots \\ y^{(r-1)}(t) \end{pmatrix} &= \underbrace{\begin{bmatrix} 0 & 1 & 0 & \cdots & 0 \\ \vdots & \ddots & \ddots & \ddots & \vdots \\ \vdots & \ddots & \ddots & 1 & 0 \\ 0 & \cdots & \cdots & 0 & 1 \\ a_1 & \cdots & \cdots & a_{r-1} & a_r \end{bmatrix}}_{=:\boldsymbol{A}_r \in \mathbb{R}^{r\times r}} \begin{pmatrix} y(t) \\ \dot{y}(t) \\ \vdots \\ y^{(r-1)}(t) \end{pmatrix} + \begin{bmatrix} \boldsymbol{O}_{(r-1)\times(n-r)} \\ \boldsymbol{a}_{r+1}^\top \end{bmatrix} \boldsymbol{z}(t) + \begin{pmatrix} 0 \\ \vdots \\ 0 \\ 0 \\ \gamma_0 \end{pmatrix} u(t), \\ &\qquad \begin{pmatrix} y(0), & \dot{y}(0), & \cdots, & y^{(r-1)}(0) \end{pmatrix}^\top = \boldsymbol{C}\boldsymbol{x}^0 \\ \dot{\boldsymbol{z}}(t) &= \begin{bmatrix} \boldsymbol{a}_{r+2} & \boldsymbol{O}_{(n-r)\times r} \end{bmatrix} \begin{pmatrix} y(t) \\ \vdots \\ y^{(r-1)}(t) \end{pmatrix} + \boldsymbol{A}_{r+3}\boldsymbol{z}(t), \qquad \boldsymbol{z}(0) = \boldsymbol{N}\boldsymbol{x}^0 \end{aligned}\right\} \tag{2.26}$$

where $\gamma_0 = \boldsymbol{c}^\top \boldsymbol{A}^{r-1}\boldsymbol{b} \in \mathbb{R}$, $\begin{pmatrix} a_1 & a_2 & \cdots & a_r \end{pmatrix} = \boldsymbol{c}^\top \boldsymbol{A}^r \boldsymbol{B}(\boldsymbol{C}\boldsymbol{B})^{-1} \in \mathbb{R}^{1\times r}$, $\boldsymbol{a}_{r+1}^\top = \boldsymbol{c}^\top \boldsymbol{A}^r \boldsymbol{V} \in \mathbb{R}^{1\times(n-r)}$, $\boldsymbol{a}_{r+2} = \frac{1}{\gamma_0}\boldsymbol{N}\boldsymbol{A}^r\boldsymbol{b} \in \mathbb{R}^{(n-r)\times 1}$ and $\boldsymbol{A}_{r+3} = \boldsymbol{N}\boldsymbol{A}\boldsymbol{V} \in \mathbb{R}^{(n-r)\times(n-r)}$;

(iii) if system (2.1) with $d = 0$ is minimum-phase, then for $\boldsymbol{A}_{r+3}$ as in (2.26) the following holds

$$\operatorname{spec}(\boldsymbol{A}_{r+3}) \subset \mathbb{C}_{<0}.$$

In Fig. 2.1 a BIF of a LTI SISO system of form (2.1) with relative degree $r \geq 1$ is depicted. Note that for arbitrary $\alpha \neq 0$ the scaled $\boldsymbol{V}_\alpha := \alpha \boldsymbol{V}$ also satisfies (2.23) and so the BIF is not a unique representation.

Proof of Lemma 2.12.

Step 1: Some essential equalities are shown.
Define $\gamma_0 := \boldsymbol{c}^\top \boldsymbol{A}^{r-1}\boldsymbol{b}$ and note that

$$\boldsymbol{CB} = \begin{bmatrix} \boldsymbol{c}^\top\boldsymbol{b} & \boldsymbol{c}^\top\boldsymbol{A}\boldsymbol{b} & \cdots & \boldsymbol{c}^\top\boldsymbol{A}^{r-2}\boldsymbol{b} & \boldsymbol{c}^\top\boldsymbol{A}^{r-1}\boldsymbol{b} \\ \boldsymbol{c}^\top\boldsymbol{A}\boldsymbol{b} & \boldsymbol{c}^\top\boldsymbol{A}^{2}\boldsymbol{b} & \cdots & \boldsymbol{c}^\top\boldsymbol{A}^{r-1}\boldsymbol{b} & \boldsymbol{c}^\top\boldsymbol{A}^{r}\boldsymbol{b} \\ \vdots & \vdots & \iddots & \vdots & \vdots \\ \boldsymbol{c}^\top\boldsymbol{A}^{r-2}\boldsymbol{b} & \boldsymbol{c}^\top\boldsymbol{A}^{r-1}\boldsymbol{b} & \cdots & \boldsymbol{c}^\top\boldsymbol{A}^{2r-4}\boldsymbol{b} & \boldsymbol{c}^\top\boldsymbol{A}^{2r-3}\boldsymbol{b} \\ \boldsymbol{c}^\top\boldsymbol{A}^{r-1}\boldsymbol{b} & \boldsymbol{c}^\top\boldsymbol{A}^{r}\boldsymbol{b} & \cdots & \boldsymbol{c}^\top\boldsymbol{A}^{2r-3}\boldsymbol{b} & \boldsymbol{c}^\top\boldsymbol{A}^{2(r-1)}\boldsymbol{b} \end{bmatrix} \overset{(2.6)}{=} \begin{bmatrix} 0 & & \gamma_0 \\ & \iddots & \\ \gamma_0 & & \star \end{bmatrix} \in \mathbb{R}^{r\times r}$$

and $\det(\boldsymbol{CB}) = \gamma_0^r \neq 0$. Hence, $\boldsymbol{CB} \in GL_r(\mathbb{R})$ and its inverse has the form

$$(\boldsymbol{CB})^{-1} = \begin{bmatrix} \star & & 1/\gamma_0 \\ & \iddots & \\ 1/\gamma_0 & & 0 \end{bmatrix}. \tag{2.27}$$

Furthermore, it is easy to see that the following hold

$$\boldsymbol{AB} = \begin{bmatrix} \boldsymbol{A}\boldsymbol{b}, & \boldsymbol{A}^2\boldsymbol{b}, & \cdots, & \boldsymbol{A}^r\boldsymbol{b} \end{bmatrix} = \begin{bmatrix} \boldsymbol{B} \begin{bmatrix} \boldsymbol{0}_{r-1}^\top \\ \boldsymbol{I}_{r-1} \end{bmatrix} & \boldsymbol{A}^r\boldsymbol{b} \end{bmatrix}, \tag{2.28}$$

$$\boldsymbol{CA} = \begin{bmatrix} \boldsymbol{c}^\top\boldsymbol{A}, & \boldsymbol{c}^\top\boldsymbol{A}^2, & \cdots, & \boldsymbol{c}^\top\boldsymbol{A}^r \end{bmatrix}^\top = \begin{bmatrix} \begin{bmatrix} \boldsymbol{0}_{r-1} & \boldsymbol{I}_{r-1} \end{bmatrix} \boldsymbol{C} \\ \boldsymbol{c}^\top\boldsymbol{A}^r \end{bmatrix}, \tag{2.29}$$

$$\boldsymbol{NB} = (\boldsymbol{V}^\top\boldsymbol{V})^{-1}\boldsymbol{V}^\top(\boldsymbol{I}_n - \boldsymbol{B}(\boldsymbol{CB})^{-1}\boldsymbol{C})\boldsymbol{B} = \boldsymbol{O}_{(n-r)\times r} \quad \Longrightarrow \quad \boldsymbol{N}\boldsymbol{b} = \boldsymbol{0}_n \tag{2.30}$$

and

$$\boldsymbol{NV} = (\boldsymbol{V}^\top\boldsymbol{V})^{-1}\boldsymbol{V}^\top(\boldsymbol{I}_n - \boldsymbol{B}(\boldsymbol{CB})^{-1}\boldsymbol{C})\boldsymbol{V} \overset{(2.23)}{=} (\boldsymbol{V}^\top\boldsymbol{V})^{-1}\boldsymbol{V}^\top\boldsymbol{V} = \boldsymbol{I}_{n-r}. \tag{2.31}$$

Step 2: It is shown that Assertions (i) and (ii) hold true.
For $\boldsymbol{S}$ as in (2.24) check

$$\boldsymbol{S}\boldsymbol{S}^{-1} = \begin{bmatrix} \boldsymbol{C} \\ \boldsymbol{N} \end{bmatrix} \begin{bmatrix} \boldsymbol{B}(\boldsymbol{CB})^{-1}, & \boldsymbol{V} \end{bmatrix} = \begin{bmatrix} \boldsymbol{I}_r & \boldsymbol{O}_{(n-r)\times(n-r)} \\ \boldsymbol{NB}(\boldsymbol{CB})^{-1} & \boldsymbol{NV} \end{bmatrix} \overset{(2.30),(2.31)}{=} \boldsymbol{I}_n,$$

which shows Assertion (i). Moreover, applying (2.25) to (2.1) with $d = 0$ and defining

$$\boldsymbol{w} := \left(y, \dot{y}, \cdots, \quad y^{(r-1)}\right)^\top \quad \text{and} \quad \begin{pmatrix}\boldsymbol{w}\\ \boldsymbol{z}\end{pmatrix} := \boldsymbol{S}\boldsymbol{x}$$

yields

$$\begin{aligned} \tfrac{\mathrm{d}}{\mathrm{d}t}\begin{pmatrix}\boldsymbol{w}(t)\\ \boldsymbol{z}(t)\end{pmatrix} &= \boldsymbol{S}\boldsymbol{A}\boldsymbol{S}^{-1}\begin{pmatrix}\boldsymbol{w}(t)\\ \boldsymbol{z}(t)\end{pmatrix} + \boldsymbol{S}\boldsymbol{b}\,u(t), \qquad \begin{pmatrix}\boldsymbol{w}(0)\\ \boldsymbol{z}(0)\end{pmatrix} = \boldsymbol{S}\boldsymbol{x}^0 \\ y(t) &= \boldsymbol{c}^\top\boldsymbol{S}^{-1}\left(\boldsymbol{w}(t), \quad \boldsymbol{z}(t)\right)^\top \end{aligned}$$

where

$$\begin{aligned} \boldsymbol{S}\boldsymbol{A}\boldsymbol{S}^{-1} &= \begin{bmatrix}\boldsymbol{C}\boldsymbol{A}\boldsymbol{B}(\boldsymbol{C}\boldsymbol{B})^{-1} & \boldsymbol{C}\boldsymbol{A}\boldsymbol{V}\\ \boldsymbol{N}\boldsymbol{A}\boldsymbol{B}(\boldsymbol{C}\boldsymbol{B})^{-1} & \boldsymbol{N}\boldsymbol{A}\boldsymbol{V}\end{bmatrix}, \\ \boldsymbol{S}\boldsymbol{b} &= \left(\boldsymbol{c}^\top\boldsymbol{b}, \quad \cdots, \quad \boldsymbol{c}^\top\boldsymbol{A}^{r-2}\boldsymbol{b}, \quad \boldsymbol{c}^\top\boldsymbol{A}^{r-1}\boldsymbol{b}, \quad \boldsymbol{N}\boldsymbol{b}\right)^\top \overset{(2.6),(2.30)}{=} \left(\boldsymbol{0}_{r-1}, \quad \gamma_0 \quad , \quad \boldsymbol{0}_{n-r}\right)^\top, \end{aligned}$$

and

$$\begin{aligned} \boldsymbol{c}^\top\boldsymbol{S}^{-1} &= \underbrace{\begin{pmatrix}1 & 0 & \cdots & 0\end{pmatrix}}_{\in\mathbb{R}^{1\times r}}\boldsymbol{C}\boldsymbol{S}^{-1} = \begin{pmatrix}1 & 0 & \cdots & 0\end{pmatrix}\left[\boldsymbol{C}\boldsymbol{B}(\boldsymbol{C}\boldsymbol{B})^{-1}, \boldsymbol{C}\boldsymbol{V}\right] \\ &\overset{(2.23)}{=} \begin{pmatrix}1 & 0 & \cdots & 0\end{pmatrix}\left[\boldsymbol{I}_r, \boldsymbol{O}_{r\times(n-r)}\right] = \begin{pmatrix}1 & 0 & \cdots & 0\end{pmatrix} \in \mathbb{R}^{1\times n}. \end{aligned}$$

Furthermore,

$$\begin{aligned} \boldsymbol{C}\boldsymbol{A}\boldsymbol{B}(\boldsymbol{C}\boldsymbol{B})^{-1} &\overset{(2.29)}{=} \begin{bmatrix}\begin{bmatrix}\boldsymbol{0}_{r-1} & \boldsymbol{I}_{r-1}\end{bmatrix}\boldsymbol{C}\\ \boldsymbol{c}^\top\boldsymbol{A}^r\end{bmatrix}\boldsymbol{B}(\boldsymbol{C}\boldsymbol{B})^{-1} = \begin{bmatrix} 0 & 1 & 0 & \cdots & 0\\ \vdots & \ddots & \ddots & & \vdots\\ 0 & \cdots & 0 & 1 & 0\\ 0 & \cdots & \cdots & 0 & 1\\ \multicolumn{5}{c}{\boldsymbol{c}^\top\boldsymbol{A}^r\boldsymbol{B}(\boldsymbol{C}\boldsymbol{B})^{-1}}\end{bmatrix}, \\ \boldsymbol{C}\boldsymbol{A}\boldsymbol{V} &\overset{(2.29)}{=} \begin{bmatrix}\begin{bmatrix}\boldsymbol{0}_{r-1} & \boldsymbol{I}_{r-1}\end{bmatrix}\boldsymbol{C}\boldsymbol{V}\\ \boldsymbol{c}^\top\boldsymbol{A}^r\boldsymbol{V}\end{bmatrix} \overset{(2.23)}{=} \begin{bmatrix}\boldsymbol{O}_{(r-1)\times(n-r)}\\ \boldsymbol{c}^\top\boldsymbol{A}^r\boldsymbol{V}\end{bmatrix} \end{aligned}$$

and

$$\begin{aligned} \boldsymbol{N}\boldsymbol{A}\boldsymbol{B}(\boldsymbol{C}\boldsymbol{B})^{-1} &\overset{(2.28)}{=} (\boldsymbol{V}^\top\boldsymbol{V})^{-1}\boldsymbol{V}^\top(\boldsymbol{I}_n - \boldsymbol{B}(\boldsymbol{C}\boldsymbol{B})^{-1}\boldsymbol{C})\left[\boldsymbol{B}\begin{bmatrix}\boldsymbol{0}_{r-1}^\top\\ \boldsymbol{I}_{r-1}\end{bmatrix}, \quad \boldsymbol{A}^r\boldsymbol{b}\right](\boldsymbol{C}\boldsymbol{B})^{-1} \\ &= \frac{(\boldsymbol{V}^\top\boldsymbol{V})^{-1}\boldsymbol{V}^\top}{\gamma_0}\left[\boldsymbol{O}_{(n-r)\times(r-1)}, \quad (\boldsymbol{I}_n - \boldsymbol{B}(\boldsymbol{C}\boldsymbol{B})^{-1}\boldsymbol{C})\boldsymbol{A}^r\boldsymbol{b}\right](\boldsymbol{C}\boldsymbol{B})^{-1} \\ &\overset{(2.27)}{=} \frac{(\boldsymbol{V}^\top\boldsymbol{V})^{-1}\boldsymbol{V}^\top}{\gamma_0}\left[(\boldsymbol{I}_n - \boldsymbol{B}(\boldsymbol{C}\boldsymbol{B})^{-1}\boldsymbol{C})\boldsymbol{A}^r\boldsymbol{b}, \quad \boldsymbol{O}_{(n-r)\times(r-1)}\right]. \end{aligned}$$

Combining the results above and defining $\gamma_0 := \boldsymbol{c}^\top\boldsymbol{A}^r\boldsymbol{b}$, $\begin{pmatrix}a_1 & a_2 & \cdots & a_r\end{pmatrix} := \boldsymbol{c}^\top\boldsymbol{A}^r\boldsymbol{B}(\boldsymbol{C}\boldsymbol{B})^{-1}$, $\boldsymbol{a}_{r+1}^\top := \boldsymbol{c}^\top\boldsymbol{A}^r\boldsymbol{V}$, $\boldsymbol{a}_{r+2} := \frac{1}{\gamma_0}\boldsymbol{N}\boldsymbol{A}^r\boldsymbol{b}$ and $\boldsymbol{A}_{r+3} := \boldsymbol{N}\boldsymbol{A}\boldsymbol{V}$ yields the form as in (2.26) which shows Assertion (ii) and completes Step 2.

Step 3: It is shown that Assertion (iii) holds true.
If system (2.1) with $d = 0$ is minimum-phase, then the following holds

$$\forall\, s \in \mathbb{C}_{\geq 0}\colon \quad \det \begin{bmatrix} \boldsymbol{S}(s\boldsymbol{I}_n - \boldsymbol{A})\boldsymbol{S}^{-1} & \boldsymbol{S}\boldsymbol{b} \\ \boldsymbol{c}^\top \boldsymbol{S}^{-1} & 0 \end{bmatrix} = \det \left(\begin{bmatrix} \boldsymbol{S} & \boldsymbol{0}_n \\ \boldsymbol{0}_n^\top & 1 \end{bmatrix} \begin{bmatrix} s\boldsymbol{I}_n - \boldsymbol{A} & \boldsymbol{b} \\ \boldsymbol{c}^\top & 0 \end{bmatrix} \begin{bmatrix} \boldsymbol{S}^{-1} & \boldsymbol{0}_n \\ \boldsymbol{0}_n^\top & 1 \end{bmatrix} \right)$$
$$= \underbrace{\det(\boldsymbol{S}) \det(\boldsymbol{S}^{-1})}_{=1} \det \begin{bmatrix} s\boldsymbol{I}_n - \boldsymbol{A} & \boldsymbol{b} \\ \boldsymbol{c}^\top & 0 \end{bmatrix} \neq 0. \tag{2.32}$$

Moreover, application of the cofactor (or Laplace) expansion [24, p. 114] yields for all $s \in \mathbb{C}_{\geq 0}$

$$\det \begin{bmatrix} \boldsymbol{S}(s\boldsymbol{I}_n - \boldsymbol{A})\boldsymbol{S}^{-1} & \boldsymbol{S}\boldsymbol{b} \\ \boldsymbol{c}^\top \boldsymbol{S}^{-1} & 0 \end{bmatrix} \overset{(2.26)}{=} (-1)^{r+2(n+1)} \gamma_0 \det \begin{bmatrix} \begin{bmatrix} -1 & 0 & \cdots & \cdots & 0 \\ s & -1 & \ddots & \ddots & \vdots \\ 0 & \ddots & \ddots & \ddots & \vdots \\ \vdots & \ddots & \ddots & -1 & 0 \\ 0 & \cdots & 0 & s & -1 \end{bmatrix} & \boldsymbol{O}_{(r-1)\times(n-r)} \\ \boldsymbol{O}_{(n-r)\times(r-1)} & [s\boldsymbol{I}_{n-r} - \boldsymbol{A}_{r+3}] \end{bmatrix}$$
$$= -\gamma_0 \det \left[s\boldsymbol{I}_{n-r} - \boldsymbol{A}_{r+3} \right] \overset{(2.32)}{\neq} 0$$

and hence $\operatorname{spec}(\boldsymbol{A}_{r+3}) \subset \mathbb{C}_{<0}$, which shows Assertion (iii), completes Step 3 and the proof of Lemma 2.12. □

Remark 2.13. *For $\boldsymbol{A}_r$ and $\boldsymbol{A}_{r+3}$ as in (2.26), note that*

$$[\![\ \operatorname{spec}(\boldsymbol{A}_r) \subset \mathbb{C}_{<0} \ \text{ and } \ \operatorname{spec}(\boldsymbol{A}_{r+3}) \subset \mathbb{C}_{<0}\ ]\!] \quad \not\Rightarrow \quad [\![\ \operatorname{spec}(\boldsymbol{A}) \subset \mathbb{C}_{<0}\ ]\!],$$

e.g. let $n = 2$, $r = 1$, $a_1 = A_4 = -1$ and $a_2 = a_3 = 2$ in (2.26) which yields $\chi_{\boldsymbol{A}}(s) = s^2 + 2s - 3$.

Remark 2.14 (BIF of LTI SISO systems with relative degree $r = n$)**.**
Consider a system of form (2.1) with relative degree $r = n$, i.e. (2.6) holds for $r = n$ and $\boldsymbol{C}, \boldsymbol{B} \in \mathbb{R}^{n\times n}$ in (2.22). From (2.27) in the proof of Lemma 2.12 it then follows that $\boldsymbol{C}\boldsymbol{B} \in GL_n(\mathbb{R})$. Hence, by defining $\boldsymbol{S} := \boldsymbol{C}$, it is easy to see that $\boldsymbol{S}^{-1} = \boldsymbol{B}(\boldsymbol{C}\boldsymbol{B})^{-1}$. Then for $r = n$ and $\boldsymbol{A}_r = \boldsymbol{A}_n$ as in (2.26), the coordinate change $\left(y, \ \cdots, \ y^{(n-1)}\right) = \boldsymbol{S}\boldsymbol{x} = \boldsymbol{C}\boldsymbol{x}$ applied to the LTI SISO system (2.1) yields

$$\frac{d}{dt} \begin{pmatrix} y(t) \\ \vdots \\ y^{(n-1)}(t) \end{pmatrix} = \boldsymbol{A}_n \begin{pmatrix} y(t) \\ \vdots \\ y^{(n-1)}(t) \end{pmatrix} + \begin{pmatrix} \boldsymbol{0}_{n-1} \\ \gamma_0 \end{pmatrix} u(t), \qquad \begin{pmatrix} y(0) \\ \vdots \\ y^{(n-1)}(0) \end{pmatrix} = \boldsymbol{C}\boldsymbol{x}(0),$$

where $\gamma_0 = \boldsymbol{c}^\top \boldsymbol{A}^{n-1}\boldsymbol{b}$ and $\begin{pmatrix} a_1 & a_2 & \cdots & a_n \end{pmatrix} = \boldsymbol{c}^\top \boldsymbol{A}^n \boldsymbol{B}(\boldsymbol{C}\boldsymbol{B})^{-1}$. Moreover note that

$$\left| \det \begin{bmatrix} s\boldsymbol{I}_n - \boldsymbol{A} & \boldsymbol{b} \\ \boldsymbol{c}^\top & 0 \end{bmatrix} \right| = \left| \det \begin{bmatrix} \boldsymbol{S}(s\boldsymbol{I}_n - \boldsymbol{A})\boldsymbol{S}^{-1} & \boldsymbol{S}\boldsymbol{b} \\ \boldsymbol{c}^\top \boldsymbol{S}^{-1} & 0 \end{bmatrix} \right| = \left| \det \begin{bmatrix} s\boldsymbol{I}_n - \boldsymbol{A}_n & \begin{pmatrix} \boldsymbol{0}_{n-1} \\ \gamma_0 \end{pmatrix} \\ \begin{pmatrix} 1, & \boldsymbol{0}_{n-1}^\top \end{pmatrix} & 0 \end{bmatrix} \right| = |\gamma_0| \neq 0,$$

whence any LTI SISO system of form (2.1) with relative degree $r = n$ is minimum-phase.

2.2 Motivation for high-gain control: root locus method

In 1948 Walter Richard Evans (1920–1999) developed a graphical tool to analyze LTI SISO systems of form (2.1) (or (2.3)) with $d = 0$ (or $m < n$) and known sign of the high-frequency gain γ_0 under constant "sign-correct" output feedback (and new input $v(s) = \mathscr{L}\{v(t)\}$)

$$\forall\, k \geq 0\colon\ u(t) = -\operatorname{sign}(\gamma_0) k\, y(t) + v(t) \qquad \circ\!\!-\!\!\bullet \qquad u(s) = -\operatorname{sign}(\gamma_0) k\, y(s) + v(s), \tag{2.33}$$

by drawing the "trajectories" of the closed-loop system poles in the complex plane for increasing values of the gain k. His work—based on the ideas of P. Profos (a researcher from Schwitzerland)—was first published in [54] for a second order LTI SISO system. The generalization to higher order LTI SISO systems followed in 1950 (see [55]). In [55] Evans named his graphical analyses tool the "root locus method". His method "helped to usher in a revolution in the practice of servo-mechanism design" (see [52]) and finally lead to the text book [53] in 1954. For a mathematically thorough analysis also incorporating complex gains see e.g. [117]. A nice overview is given in [118].

The root locus method is quite useful to illustrate the motivation for high-gain output feedback control of high-gain stabilizable systems defined as follows.

Definition 2.15 (High-gain stabilizable LTI SISO systems)**.** *[86, p. 19]*
A system given by (2.1) (or (2.3)) is said to be high-gain stabilizable *if there exists $k^\star \geq 0$ such that the closed-loop system (2.1), (2.33) (or (2.3), (2.33)) is exponentially stable for all $k \geq k^\star$, i.e. the system matrix of the closed-loop system (2.1), (2.33) (or the closed-loop transfer function (2.3), (2.33)) has no eigenvalues (or no poles) in $\mathbb{C}_{\geq 0}$.*

As the root locus method was introduced for transfer functions, the following is presented in the frequency domain and is restricted to systems with relative degree greater than or equal to one. Define the monic polynomials $N, D \in \mathbb{R}[s]$ as follows

$$\begin{aligned} N(s) &:= c_0 + c_1 s + \cdots + c_{m-1} s^{m-1} + s^m = \textstyle\prod_{i=1}^{m} (s - z_i(N)) \\ D(s) &:= a_0 + a_1 s + \cdots + a_{n-1} s^{n-1} + s^n = \textstyle\prod_{i=1}^{n} (s - p_i(D)) \end{aligned}, \qquad \begin{aligned} &n,\, m \in \mathbb{N}, \\ &n > m \end{aligned} \tag{2.34}$$

where $z_1(N), \ldots, z_m(N) \in \mathbb{C}$ and $p_1(D), \ldots, p_n(D) \in \mathbb{C}$ are the roots of N and D, respectively (not accounting for multiplicities). Consider a LTI SISO system given by the transfer function

$$F(s) = \frac{y(s)}{u(s)} = \gamma_0 \frac{N(s)}{D(s)}, \qquad \gamma_0 \neq 0,\ N, D \in \mathbb{R}[s] \text{ as in (2.34) and coprime} \tag{2.35}$$

with high-frequency gain γ_0 and relative degree $r = n - m \geq 1$ under proportional output feedback (2.33). The controller gain k is regarded as design parameter and its variation and influence on the closed-loop system (2.35), (2.33), i.e.

$$\frac{y(s)}{v(s)} = \frac{\gamma_0 N(s)}{D(s) + k|\gamma_0| N(s)}, \qquad \gamma_0 \neq 0,\ k \geq 0,\ N, D \in \mathbb{R}[s] \text{ as in (2.34) and coprime} \tag{2.36}$$

is analyzed. The poles of the closed-loop system (2.36), i.e.

$$p_1(k) := p_1(D + k|\gamma_0| N), \ \ldots, \ p_n(k) := p_n(D + k|\gamma_0| N) \in \mathbb{C}, \tag{2.37}$$

alter with increasing (or decreasing) values of k (see [118]). The root locus (see [77, p. 562]) is given by the (infinite) set of complex points

$$\big\{ s \in \mathbb{C} \;\big|\; D(s) + k|\gamma_0| N(s) = 0 \text{ for some } k \geq 0 \big\} \subset \mathbb{C}. \tag{2.38}$$

To obtain an approximation of the root locus successively for any (fixed) $k \geq 0$ the closed-loop poles (2.37) are computed and then plotted in the complex plane. So this (numerical) approximation of the root locus reveals information on e.g. stability, dominant poles and damping of the closed-loop system (2.36). Note that the closed-loop poles (2.37) are continuous functions of the gain k (see [77, Corollary 4.2.4]).

The root locus (2.38) yields a plot in the complex plane which is symmetrical with respect to the real axis and intersects at the root locus center (or root center of gravity, see [118]).

Definition 2.16 (Root locus center of LTI SISO systems)**.**
For $n > m$ consider the monic and co-prime polynomials $N, D \in \mathbb{R}[s]$ as in (2.34). Then

$$\Xi(N, D) := \frac{1}{n-m}\,(c_{m-1} - a_{n-1}) = \frac{1}{n-m}\left(\sum_{i=1}^{n} p_i(D) - \sum_{i=1}^{m} z_i(N) \right) \tag{2.39}$$

is called the root locus center *of (2.35).*

Note that equality in (2.39) directly follows from comparing coefficients of the polynomials and the expanded versions of the products in (2.34) (see Corollary 3 in [117]). Moreover, since poles and zeros with non-zero imaginary part always appear as conjugate-complex pairs, the root locus center is located on the real axis of the complex plane.

Often not the "exact" root locus is required for controller design, primarily the asymptotic behavior of the closed-loop poles (2.37) is of interest which leads to the following definition (see [23]).

Definition 2.17 (Asymptotes of the root locus & angles of departure)**.**
For $n > m$ consider the monic and co-prime polynomials $N, D \in \mathbb{R}[s]$ as in (2.34). For $i \in \{1, \ldots, n-m\}$ define the i-th asymptote of the root locus (2.38) *by*

$$\Upsilon_i \colon \mathbb{R}_{\geq 0} \to \mathbb{C}, \quad k \mapsto \Upsilon_i(k) := \Xi(N, D) + \left(|\gamma_0|\, k\right)^{\frac{1}{n-m}} \exp\left(\frac{(2i-1)\pi j}{n-m} \right). \tag{2.40}$$

The $n-m$ asymptotes intersect at the root locus center $\Xi(N, D)$ as in (2.39) with corresponding angle of departure

$$\forall i \in \{1, \ldots, n-m\} \colon \qquad \alpha_i := \arg(\Upsilon_i) = \frac{(2i-1)\pi}{n-m}. \tag{2.41}$$

Note that the relative degree $r = n - m$ of the transfer function (2.35) indicates how many asymptotes exist. The following theorem describes the asymptotic behavior of the "trajectories" of the closed-loop poles (2.37).

Theorem 2.18 (High-gain root locus of LTI SISO systems)**.**
For $n > m$ and monic and co-prime polynomials $N, D \in \mathbb{R}[s]$ as in (2.34), consider the closed-loop system given by (2.36). Denote the roots of N and $D + k|\gamma_0|N$ by $z_1(N), \dots, z_m(N)$ and $p_1(D + k|\gamma_0|N), \dots, p_n(D + k|\gamma_0|N)$, respectively, then the following hold

(i) There exist m numbers $l_1, \dots, l_m \in \{1, \dots, n\}$ such that for all $i \in \{1, \dots, m\}$:

$$\lim_{k\to\infty} p_{l_i}(D + k\,|\gamma_0|N) = z_i(N) \tag{2.42}$$

(ii) For $\Upsilon_i(k)$ as in (2.40) there exist $n - m$ numbers $l_1, \dots, l_{n-m} \in \{1, \dots, n\}$ such that for all $i \in \{1, \dots, n - m\}$:

$$\lim_{k\to\infty} |p_{l_i}(D + k|\gamma_0|N) - \Upsilon_i(k)| = 0 \tag{2.43}$$

Proof. see the proofs of Theorem 2 and Theorem 3 in [117]. □

Since the limits in (2.42) and (2.43) exist, Theorem 2.18 implies that for $\varepsilon > 0$ (arbitrary small) there exists $k^\star(\varepsilon) \geq 0$ such that for all $k \geq k^\star(\varepsilon)$ the following hold: (i) m of the n closed-loop poles (2.37) remain within the union of the balls $\bigcup_{i=1}^m \mathbb{B}_\varepsilon(z_i(N)) \subset \mathbb{C}$ with radius $\varepsilon > 0$ around the roots of N and (ii) the distance between corresponding asymptote (2.40) and closed-loop pole (2.37) is smaller than ε, i.e. $|p_{l_i}(D + k|\gamma_0|N) - \Upsilon_i(k)| < \varepsilon$ for all $i \in \{1, \dots, n - m\}$. Now two observations may be formulated:

- Observation 1: for minimum-phase systems with relative degree one *or* with relative degree two and negative root locus center there exists $\varepsilon > 0$ and hence $k^\star(\varepsilon) \geq 0$ such that for all $k \geq k^\star(\varepsilon)$ all poles of the closed-loop system (2.36) exhibit negative real parts, i.e. the closed-loop system is exponentially stable (see Fig. 2.2).

- Observation 2: for non-minimum-phase systems (of arbitrary relative degree) or for minimum-phase systems with relative degree greater than two (or equal to two with positive root locus center) there exists $\varepsilon > 0$ and so $k^\star(\varepsilon) \geq 0$ such that for all $k > k^\star(\varepsilon)$ at least one closed-loop pole in (2.37) has non-negative real part and hence the closed-loop system (2.36) is not exponentially stable (see Fig. 2.2).

Observation 1 and Fig. 2.2 illustrate the inherent "high-gain property" of minimum-phase systems (2.35) (or (2.1)) with relative degree one *or* with relative degree two and negative root locus center: these systems are high-gain stabilizable. Observation 2 makes aware of the obstacle of higher relative degrees: (even) minimum-phase systems with relative degree greater than one (and positive root locus center in the relative degree two case) are *not* high-gain stabilizable by simple output feedback of form (2.33).

In general, to allow for high-gain control of minimum-phase systems with higher relative degree, more sophisticated feedback controllers must be used. For $v(s) = \mathscr{L}\{v(t)\}$ and sufficiently large gain k, the following approaches achieve exponential stabilization of minimum-phase systems of form (2.35) with relative degree $r \geq 2$ and known sign of the high-frequency gain γ_0:

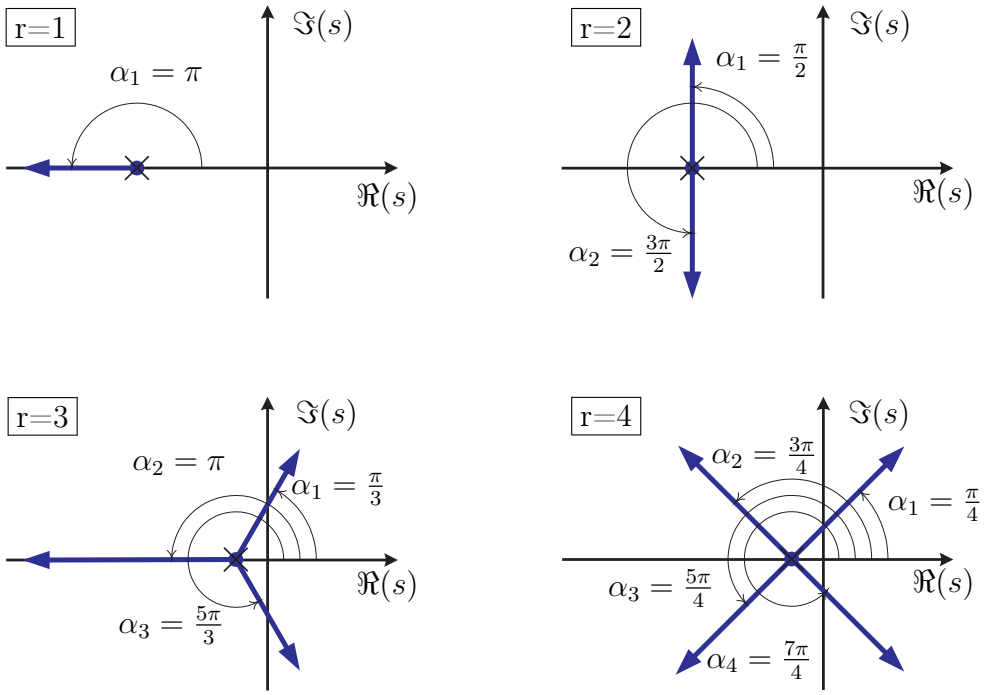

Figure 2.2: *Root locus asymptotes* $\Upsilon_i(\cdot)$ (——) *with angles of departure* α_i, $i = 1, \ldots, 4$, *in the complex plane for systems of form* (2.35) *having relative degree* $r = 1, \ldots, 4$ *and root locus center* ×.

(i) if derivative feedback is admissible up to the order $r-1$, i.e. y, $\dot{y}$ …, $y^{(r-1)}$ are available for feedback, the following simple controller is applicable:

$$u(s) = -\operatorname{sign}(\gamma_0)\, k\, M(s)\, y(s) + v(s), \qquad \begin{array}{l}\text{with } M \in \mathbb{R}[s] \text{ monic and Hurwitz} \\ \text{and } \deg(M) = r-1.\end{array} \tag{2.44}$$

The denominator of the closed-loop system (2.35), (2.44) is given by $D(s)+|\gamma_0|\, k\, M(s)N(s)$ where MN is Hurwitz and $\deg(MN) = n-1$. Hence, for sufficiently large k, exponential stability follows from Observation 1;

(ii) if derivative feedback is not admissible, high-gain observers with high-gain state feedback (see e.g. [33, Section 1.3.3]) or (dynamic) compensators (see e.g. [80]) are applicable which, basically, estimate the $r-1$ output derivatives. For instance, a control law with admissible compensator is given by (see [80, Theorem 5.1])

$$u(s) = -\underbrace{\operatorname{sign}(\gamma_0)\, \frac{k^{r+1}\, M(s)}{s^r + k\, b_r\, s^{r-1} + \cdots + k^{r-1}\, b_2 s + k^r\, b_1}}_{\text{compensator}}\, y(s) + v(s)$$

where $M \in \mathbb{R}[s]$ is monic and Hurwitz with $\deg(M) = r-1$ and, for (known) $b_0 \geq |\gamma_0|$, $b_r, \ldots, b_1 \in \mathbb{R}_{>0}$ such that $s^{r+1} + b_r\, s^r + \cdots + b_2 s^2 + b_1 s + \eta b_0$ is Hurwitz for all $\eta \in (0, 1]$.

In the following, solely systems with relative degree one or two will be considered. Moreover, since derivative feedback is assumed to be admissible in the relative degree two case, the remainder of this thesis will focus on Approach (i) with derivative feedback and its extensions to the adaptive case.

2.3 High-gain adaptive stabilization

Since LTI SISO systems of form (2.1) *with* direct feedthrough (i.e. $d \neq 0$) are of marginal relevance for plant modeling in industry, this section will focus on systems with relative degree greater than zero, i.e.

$$\left.\begin{array}{rcll} \dot{\boldsymbol{x}}(t) & = & \boldsymbol{A}\,\boldsymbol{x}(t) + \boldsymbol{b}\,u(t), & n \in \mathbb{N},\ \boldsymbol{x}(0) = \boldsymbol{x}^0 \in \mathbb{R}^n,\ u(\cdot) \in \mathcal{L}^1_{\mathrm{loc}}(\mathbb{R}_{\geq 0}; \mathbb{R}) \\ y(t) & = & \boldsymbol{c}^\top \boldsymbol{x}(t) & (\boldsymbol{A}, \boldsymbol{b}, \boldsymbol{c}) \in \mathbb{R}^{n\times n} \times \mathbb{R}^n \times \mathbb{R}^n. \end{array}\right\} \tag{2.45}$$

In view of Theorem 2.18 asymptotic stabilization of minimum-phase systems of form (2.45) (or (2.35)) with relative degree one or with relative degree two and negative root locus center is feasible by simple proportional output feedback (2.33), if the controller gain k is chosen larger than or equal to a critical lower bound $k^\star \geq 0$. To fix an admissible value for k in (2.33) the bound $k^\star$ must be known *a priori*. In general it depends (nonlinearly) on the system data, i.e. $k^\star = k^\star(\boldsymbol{A}, \boldsymbol{b}, \boldsymbol{c})$ (or $k^\star = k^\star(\gamma_0, N, D)$ for systems of form (2.35)).

To make this knowledge superfluous and to achieve robust stabilization, the principle idea of high-gain adaptive control is as follows: the controller gain is variable and is (dynamically) adapted such that, loosely speaking, $k^\star$ is found automatically. For the SISO case, a simple high-gain adaptive controller with adequate gain adaption is given by

$$u(t) = -\operatorname{sign}(\gamma_0) k(t)\, y(t) \qquad \text{where} \qquad \dot{k}(t) = y(t)^2, \qquad k(0) = k_0 > 0. \tag{2.46}$$

It assures the following: (i) all states of the closed-loop system (2.45), (2.46) remain bounded and (ii) the equilibrium at the origin is asymptotically reached, i.e.

$$\boldsymbol{x}(\cdot) \in \mathcal{L}^\infty(\mathbb{R}_{\geq 0}; \mathbb{R}^n), \quad \lim_{t\to\infty} k(t) = k_\infty \in \mathbb{R}_{>0} \quad \text{and} \quad \lim_{t\to\infty} \boldsymbol{x}(t) = \boldsymbol{0}_n. \tag{2.47}$$

It will be shown in Sections 2.3.3 and 2.3.4.1 that the controller (2.46) "asymptotically stabilizes" minimum-phase systems with relative degree one or with relative degree two and negative root locus center. In contrast, for relative degree two systems with unknown (or positive) root locus center, additional assumptions on the system or an extended feedback strategy are required (see Sections 2.3.4.2 and 2.3.4.3).

2.3.1 Brief historical overview

A recent overview and "state-of-the-art" (without explicit proofs) of high-gain adaptive control is given in [93]. In compact form high-gain adaptive control, adaptive λ-tracking control and funnel control are introduced, mainly for the relative degree one case. The case of higher relative degree systems is briefly touched. A thorough survey is given in [85] or in the monograph [86].

Whereas adaptive control for the first 20 years focused on indirect methods based on system parameter identification, in the mid-1980s, almost at the same time, three seminal contributions [137] (1983), [129] (February 1984) and [37] (December 1984) were published which introduced the basic idea of high-gain adaptive (or non-identifier based adaptive) control.
The high-gain adaptive controllers proposed in [129] and [37] assure (2.47) for minimum-phase LTI SISO and MIMO systems, respectively, with relative degree one and known sign of the

high-frequency gain. Moreover, in [129], Mareels already tries to generalize his results to systems with *arbitrary-but-known* relative degree if an upper bound on the high-frequency gain is known. The order of his proposed controller depends on the relative degree $r \geq 1$ and is quite high with $(r-1)r/2$ (not counting for the adaption law). Mareels approximates the $r-1$ time derivatives of the system's output by filters of (unnecessarily) increasing order ranging from 1 to $r-1$. Unfortunately, his results do not hold true in general, Hoagg and Bernstein present a counter example for the relative degree five case in 2007 (see [80]). They provide a solution to the problem under same assumptions by introducing a dynamic compensator of r-th order (see [80]).

In 1983 A. Stephen Morse speculated, that a priori knowledge of the sign of the high-frequency gain is necessary for (continuous) adaptive stabilization (see [137]). In the same year Roger D. Nussbaum proved that this conjecture is wrong (see [141]). If the sign of the high-frequency gain is *not* known a priori, then a piecewise right continuous[2] and locally Lipschitz continuous[3] sign-switching function $f_{NB}\colon \mathbb{R} \to \mathbb{R}$ (later on called "Nussbaum function", see e.g. [86, Definition 4.1.1]) with (Nussbaum) properties

$$\sup_{k>k_0} \frac{1}{k-k_0} \int_0^k f_{NB}(x)\,\mathrm{d}x = +\infty \qquad \text{and} \qquad \inf_{k>k_0} \frac{1}{k-k_0} \int_0^k f_{NB}(x)\,\mathrm{d}x = +\infty \tag{2.48}$$

must be incorporated into the controller as follows

$$u(t) = f_{NB}(k(t))\,k(t)y(t) \qquad \text{where} \qquad \dot{k}(t) = y(t)^2, \qquad k(0) = k_0 > 0.$$

to assure on-line detection of sign-correct feedback without probing signals. An example is given by $f_{NB}\colon \mathbb{R} \to \mathbb{R},\ k \mapsto f_{NB}(k) := k^2\cos(k)$, for more examples and a detailed discussion see e.g. [86, Chapter 4]. Controllers which do not require information on the sign of the high-frequency gain are called universal adaptive controllers and were first introduced for high-gain adaptive stabilization in 1983 (see [141], for first order linear systems) and in 1984 (see [187], for LTI SISO systems of arbitrary order). Albeit of theoretical interest universal high-gain adaptive controllers are not reasonable for application in general. They may exhibit a "bursting or peaking phenomena" (see e.g. [38, 75] or [91]) if e.g. noise deteriorates the output measurement. The non-zero input in gain adaption leads to gain drift and possibly to sign switching of the Nussbaum function which results in "short time destabilization" of the closed-loop system with unpredictable bursts in system output (and state). For most plants in industry the sign of high-frequency either can easily be obtained by experiments or is a priori known (due to physical or assembly reasons, see e.g. Sections 5.2.2.1, 5.2.2.2, 5.2.3.1 and 5.2.3.2).

Since 1983 high-gain adaptive control has been successively extended to certain classes of nonlinear SISO and MIMO systems (see e.g. [114] (1987), [156] (1994) or [88] (2002)) and infinite dimensional systems (see [122] (1992)). Universal high-gain adaptive control with internal model is presented e.g. in [75] (1988, for bounded references) or in [135] (1992, for unbounded

[2] Let $n \in \mathbb{N}$, $X \subset \mathbb{R}$, $Y \subseteq \mathbb{R}^n$ and $x^0 \in X$. A function $\boldsymbol{f}\colon X \to Y$ is said to be left [or right] continuous if for every neighborhood $V \subset \mathbb{R}^n$ around $\boldsymbol{f}(x^0)$ there exists a $\delta > 0$ such that $\boldsymbol{f}(X \cap (x^0-\delta, x^0]) \subset V$ [or $\boldsymbol{f}(X \cap [x^0, x^0+\delta)) \subset V$] [4, p. 240]. The function $\boldsymbol{f}\colon X \to Y$ is piecewise left [or right] continuous on X, if it is left [or right] continuous at any point $x^0 \in X$.

[3] see Definition 2.19.

references and disturbances). The internal model assures asymptotic tracking and rejection of suitable reference and disturbance signals (solving a linear ODE), respectively. The same idea (without Nussbaum switching) was already published in 1984 (see [129]) however without thorough proof. Asymptotic tracking without the use of an internal model but a discontinuous high-gain adaptive controller is feasible for nonlinearly perturbed minimum-phase LTI MIMO systems with (strict) relative degree one [155]. In 2006 it was shown that high-gain adaptive control of LTI MIMO systems with relative degree one is robust in the sense of the gap metric (see [59]), i.e. for "small" initial values the controlled systems may even by non-minimum-phase and of higher relative degree. Moreover, high-gain adaptive control retains the properties in (2.47) even if input and output are disturbed by square integrable signals (see [59]).

To the best knowledge of the author, there do not exist (published) results for high-gain adaptive control with derivative feedback.

2.3.2 Mathematical preliminaries

Before discussing the main results of this chapter, some technical preliminaries are introduced to achieve a self-contained presentation.

2.3.2.1 Byrnes-Isidori form of LTI SISO systems with relative degree one and two

In the remainder of this chapter LTI SISO systems with relative degree one and two are of special interest. Moreover, since the Byrnes-Isidori form (BIF) plays an essential role in the upcoming proofs, the BIF of LTI SISO systems with relative degree one and two is derived, respectively.

BIF of LTI SISO systems with relative degree one

Consider a system of form (2.45) with relative degree one, i.e. $r = 1$. Then, from Lemma 2.12, it follows that $\boldsymbol{C} := \boldsymbol{c}^\top \in \mathbb{R}^{1\times n}$, $\boldsymbol{B} := \boldsymbol{b} \in \mathbb{R}^n$ and $\boldsymbol{V} \in \mathbb{R}^{n\times(n-1)}$ such that $\boldsymbol{c}^\top\boldsymbol{V} = \boldsymbol{0}_{n-1}^\top$ which yields the transformation matrix

$$\begin{aligned}&\boldsymbol{S} = \begin{bmatrix}\boldsymbol{c}^\top \\ \boldsymbol{N}\end{bmatrix} \in \mathbb{R}^{n\times n} \quad \text{where} \quad \boldsymbol{N} = (\boldsymbol{V}^\top\boldsymbol{V})^{-1}\boldsymbol{V}^\top(\boldsymbol{I}_n - \tfrac{1}{\gamma_0}\boldsymbol{b}\boldsymbol{c}^\top) \in \mathbb{R}^{(n-1)\times n} \\ &\text{with inverse} \quad \boldsymbol{S}^{-1} = \left[\tfrac{1}{\gamma_0}\boldsymbol{b}\boldsymbol{c}^\top, \quad \boldsymbol{V}\right].\end{aligned} \tag{2.49}$$

The coordinate transformation $\begin{pmatrix} y, & \boldsymbol{z}\end{pmatrix}^\top := \boldsymbol{S}\boldsymbol{x}$ applied to (2.45) yields the BIF of LTI SISO systems with relative degree one, i.e.

$$\left.\begin{aligned}\dot{y}(t) &= a_1 y(t) + \boldsymbol{a}_2^\top \boldsymbol{z}(t) + \gamma_0 u(t), & y(0) &= \boldsymbol{c}^\top\boldsymbol{x}^0 \\ \dot{\boldsymbol{z}}(t) &= \boldsymbol{a}_3 y(t) + \boldsymbol{A}_4 \boldsymbol{z}(t), & \boldsymbol{z}(0) &= \boldsymbol{N}\boldsymbol{x}^0\end{aligned}\right\} \tag{2.50}$$

where

$$\begin{aligned}&\gamma_0 = \boldsymbol{c}^\top\boldsymbol{b} \in \mathbb{R}, \quad a_1 = \boldsymbol{c}^\top\boldsymbol{A}\boldsymbol{b}/\gamma_0 \in \mathbb{R}, \quad \boldsymbol{a}_2^\top = \boldsymbol{c}^\top\boldsymbol{A}\boldsymbol{V} \in \mathbb{R}^{1\times(n-1)}, \\ &\boldsymbol{a}_3 = \tfrac{(\boldsymbol{V}^\top\boldsymbol{V})^{-1}\boldsymbol{V}^\top}{\gamma_0}(\boldsymbol{I}_n - \tfrac{1}{\gamma_0}\boldsymbol{b}\boldsymbol{c}^\top)\boldsymbol{A}\boldsymbol{b} \in \mathbb{R}^{(n-1)\times 1} \quad \text{and} \quad \boldsymbol{A}_4 = \boldsymbol{N}\boldsymbol{A}\boldsymbol{V} \in \mathbb{R}^{(n-1)\times(n-1)}.\end{aligned} \tag{2.51}$$

BIF of LTI SISO systems with relative degree two

For systems of form (2.45) with relative degree two, i.e. $r = 2$, Lemma 2.12 gives

$$\boldsymbol{C} := \begin{bmatrix} \boldsymbol{c}^\top \\ \boldsymbol{c}^\top \boldsymbol{A} \end{bmatrix} \in \mathbb{R}^{2\times n} \qquad \text{and} \qquad \boldsymbol{B} := \begin{bmatrix} \boldsymbol{b} & \boldsymbol{A}\boldsymbol{b} \end{bmatrix} \in \mathbb{R}^{n\times 2} \tag{2.52}$$

and hence

$$\boldsymbol{C}\boldsymbol{B} = \begin{bmatrix} 0 & \gamma_0 \\ \gamma_0 & \boldsymbol{c}^\top \boldsymbol{A}^2 \boldsymbol{b} \end{bmatrix} \in \mathbb{R}^{2\times 2} \qquad \text{and} \qquad \boldsymbol{C}\boldsymbol{B}^{-1} = \begin{bmatrix} -\frac{1}{\gamma_0}\boldsymbol{c}^\top \boldsymbol{A}^2 \boldsymbol{b} & \frac{1}{\gamma_0} \\ \frac{1}{\gamma_0} & 0 \end{bmatrix}. \tag{2.53}$$

Now choose $\boldsymbol{V} \in \mathbb{R}^{n\times(n-2)}$ such that $\boldsymbol{C}\boldsymbol{V} = \boldsymbol{O}_{2\times(n-2)}$ and, moreover, $\boldsymbol{S} \in \mathbb{R}^{n\times n}$ and $\boldsymbol{N} \in \mathbb{R}^{(n-2)\times n}$ as in (2.24), then application of the coordinate transformation $\begin{pmatrix} y, & \dot{y}, & \boldsymbol{z} \end{pmatrix}^\top := \boldsymbol{S}\boldsymbol{x}$ to (2.1) yields the BIF of LTI SISO system with relative degree two, i.e.

$$\left.\begin{aligned} \tfrac{\mathrm{d}}{\mathrm{d}t}\begin{pmatrix} y(t) \\ \dot{y}(t) \end{pmatrix} &= \begin{bmatrix} 0 & 1 \\ a_1 & a_2 \end{bmatrix}\begin{pmatrix} y(t) \\ \dot{y}(t) \end{pmatrix} + \begin{bmatrix} \boldsymbol{0}_{n-2}^\top \\ \boldsymbol{a}_3^\top \end{bmatrix}\boldsymbol{z}(t) + \begin{pmatrix} 0 \\ \gamma_0 \end{pmatrix} u(t), & \begin{pmatrix} y(0) \\ \dot{y}(0) \end{pmatrix} &= \boldsymbol{C}\boldsymbol{x}^0 \\ \dot{\boldsymbol{z}}(t) &= \begin{bmatrix} \boldsymbol{a}_4 & \boldsymbol{0}_{n-2} \end{bmatrix}\begin{pmatrix} y(t) \\ \dot{y}(t) \end{pmatrix} + \boldsymbol{A}_5 \boldsymbol{z}(t), & \boldsymbol{z}(0) &= \boldsymbol{N}\boldsymbol{x}^0 \end{aligned}\right\} \tag{2.54}$$

where

$$\begin{aligned} &\gamma_0 = \boldsymbol{c}^\top \boldsymbol{A}\boldsymbol{b} \in \mathbb{R}, \quad \begin{pmatrix} a_1, & a_2 \end{pmatrix} = \boldsymbol{c}^\top \boldsymbol{A}^2 \boldsymbol{B}(\boldsymbol{C}\boldsymbol{B})^{-1} \in \mathbb{R}^{1\times 2}, \quad \boldsymbol{a}_3^\top = \boldsymbol{c}^\top \boldsymbol{A}^2 \boldsymbol{V} \in \mathbb{R}^{1\times(n-2)}, \\ &\boldsymbol{a}_4 = \tfrac{(\boldsymbol{V}^\top \boldsymbol{V})^{-1}\boldsymbol{V}^\top}{\gamma_0}(\boldsymbol{I}_n - \boldsymbol{B}(\boldsymbol{C}\boldsymbol{B})^{-1}\boldsymbol{C})\boldsymbol{A}^2\boldsymbol{b} \in \mathbb{R}^{(n-2)\times 1} \text{ and } \boldsymbol{A}_5 = \boldsymbol{N}\boldsymbol{A}\boldsymbol{V} \in \mathbb{R}^{(n-2)\times(n-2)}. \end{aligned} \tag{2.55}$$

2.3.2.2 Solution of ordinary differential equation

In this chapter, closed-loop systems (e.g. (2.45), (2.46)) will be considered, which yield initial-value problems given by (nonlinear) ordinary differential equations of the form

$$\dot{\boldsymbol{x}}(t) = \boldsymbol{f}(t, \boldsymbol{x}(t)), \qquad \boldsymbol{x}(t_0) = \boldsymbol{x}^0 \tag{2.56}$$

where $t_0 \in \mathbb{R}$ is the initial time, $\boldsymbol{x}^0 \in \mathbb{R}^n$, $n \in \mathbb{N}$, is the initial state and $\boldsymbol{f}\colon \mathbb{R}\times\mathbb{R}^n \to \mathbb{R}^n$ is called the right-hand side of (2.56). For $T \in (t_0, \infty]$ and $T_- \in [-\infty, t_0)$, a continuously differentiable function $\boldsymbol{x}\colon (T_-, T) \to \mathbb{R}^n$ is called solution of the initial-value problem (2.56) if it satisfies (2.56) for all $t \in (T_-, T)$ and $\boldsymbol{x}(t_0) = \boldsymbol{x}^0$. Such a solution exists and it is unique if the right-hand side of (2.56) satisfies two presuppositions. Before the existence and uniqueness result can be restated, the notion of a "locally Lipschitz continuous" function must be introduced.

Definition 2.19 (see e.g. p. 242 in [5])**.** *Let $n \in \mathbb{N}$, $I \subseteq \mathbb{R}$ and $X \subseteq \mathbb{R}^n$. A continuous function $\boldsymbol{f}\colon I \times X \to \mathbb{R}^n$ is said to be* locally Lipschitz continuous *(with respect to its second argument $\boldsymbol{x} \in X$) if, and only if, for every point $(t_0, \boldsymbol{x}^0) \in I \times X$ there exists a (Lipschitz) constant $L \geq 0$ and a neighborhood[4] $J \times U \subset I \times X$ of $(t_0, \boldsymbol{x}^0)$ such that*

$$\forall\, t \in J\ \forall\, \boldsymbol{x}_1, \boldsymbol{x}_2 \in U\colon \qquad \|\boldsymbol{f}(\boldsymbol{x}_1) - \boldsymbol{f}(\boldsymbol{x}_2)\| \leq L\, \|\boldsymbol{x}_1 - \boldsymbol{x}_2\|.$$

[4] A set $U \subset \mathbb{R}^n$, $n \in \mathbb{N}$, is said to be a *neighborhood* of $\boldsymbol{x}^0 \in \mathbb{R}^n$ if, and only if, there exists $\delta > 0$ such that $\mathbb{B}_\delta^n(\boldsymbol{x}^0) \subset U$ (see [4, p. 144]). Clearly, for $\boldsymbol{x}^0 \in \mathbb{R}^n$ and $\delta > 0$, $\overline{\mathbb{B}}_\delta^n(\boldsymbol{x}^0)$ is a neighborhood of $\boldsymbol{x}^0$.

Note that, in general, the Lipschitz constant L depends on $(t_0, \boldsymbol{x}^0)$ and different neighborhoods yield different Lipschitz constants.

Theorem 2.20 (Existence and uniqueness theorem (see e.g. Theorem 8.16 in [5]))**.**
Let $n \in \mathbb{N}$, $\mathcal{I} \subseteq \mathbb{R}$ an open interval and $\mathcal{D} \subseteq \mathbb{R}^n$ an open, non-empty set. If $\boldsymbol{f}\colon \mathcal{I} \times \mathcal{D} \to \mathbb{R}^n$ is (i) continuous in $\mathcal{I} \times \mathcal{D}$ and (ii) locally Lipschitz continuous (with respect to its second argument) then, for each $(t_0, \boldsymbol{x}^0) \in \mathcal{I} \times \mathcal{D}$, the initial-value problem (2.56) has a unique solution $\boldsymbol{x}\colon (T_-, T) \to \mathbb{R}^n$ with maximal $T \in (t_0, \infty]$, minimal $T_- \in [-\infty, t_0)$, $\boldsymbol{x}(t) \in \mathcal{D}$ for all $t \in (T_-, T)$ and $\boldsymbol{x}(t_0) = \boldsymbol{x}^0$.

Proof. see [5, p. 246]. □

In the remainder of this chapter, only solutions on $\mathbb{R}_{\geq 0}$ with initial time $t_0 = 0$ are considered. Therefore, the (maximal) interval of existence (T_-, T) is restricted to $[0, T)$, $T \in (0, \infty]$. For linear initial-value problems of form (2.45), the solution is given by (see e.g. [5, p. 237])

$$\forall t \geq 0\colon \qquad \boldsymbol{x}(t) = \exp(\boldsymbol{A}t)\,\boldsymbol{x}^0 + \int_0^t \exp\big(\boldsymbol{A}(t-\tau)\big)\boldsymbol{b}\,u(\tau)\,\mathrm{d}\tau\,.$$

It is unique and holds globally, i.e. $T = \infty$. In contrast, the solution of a nonlinear initial-value problem of form (2.56) may blow up in finite time, i.e. $T < \infty$ and $\|\boldsymbol{x}(t)\| \to \infty$ as $t \to T$. Such systems have finite escape time and an exploding solution, as illustrated in the following example.

Example 2.21 (Finite escape time and exploding solution)**.** *Consider the first order nonlinear system given by*

$$\dot{x}(t) = x(t)^2, \qquad x(0) = 1. \tag{2.57}$$

Clearly, the right hand-side of (2.57) is locally Lipschitz continuous, hence there exists a unique solution $x\colon [0, T) \to \mathbb{R}$. It is easy to see that $x(t) = 1/(1-t)$ solves (2.57) for all $t \in [0, 1)$ (i.e. $T = 1$) and, moreover, the solution cannot be extended any further, it "explodes" as $t \to 1$.

2.3.3 Relative degree one systems

Before the well known result of high-gain adaptive stabilization of minimum-phase LTI SISO systems with relative degree one is revisited, the following linear system class is introduced.

Definition 2.22 (System class $\mathcal{S}_1^{\mathrm{lin}}$)**.**
A system of form (2.45) is of Class $\mathcal{S}_1^{\mathrm{lin}}$ if, and only if, the following hold:

($\mathcal{S}_1^{\mathrm{lin}}$-sp$_1$) *the relative degree is one and the sign of the high-frequency gain is known, i.e.*

$$\gamma_0 := \boldsymbol{c}^\top \boldsymbol{b} \neq 0 \qquad \textit{and} \qquad \operatorname{sign}(\gamma_0) \textit{ is known;}$$

($\mathcal{S}_1^{\mathrm{lin}}$-sp$_2$) *it is minimum-phase, i.e. (2.14) holds, and*

($\mathcal{S}_1^{\mathrm{lin}}$-sp$_3$) *the (regulated) output $y(\cdot)$ is available for feedback.*

System class $\mathcal{S}_1^{\text{lin}}$ represents the linear equivalent of system class $\mathcal{S}_1$. Conform to system class $\mathcal{S}_1$, in (2.45), $y(\cdot)$ is considered as regulated output and, to be available for feedback, must coincide with the measured output. Clearly, all systems of class $\mathcal{S}_1^{\text{lin}}$ are high-gain stabilizable.

Note that "system properties" ($\mathcal{S}_1^{\text{lin}}$-sp$_1$) and ($\mathcal{S}_1^{\text{lin}}$-sp$_2$) are sufficient, but not necessary, for high-gain stabilization as illustrated in the following example.

Example 2.23. *Consider the second order system given by*

$$\begin{aligned} \dot{\boldsymbol{x}}(t) &= \begin{bmatrix} 0 & 1 \\ a_0 & a_1 \end{bmatrix} \boldsymbol{x}(t) + \begin{pmatrix} 0 \\ \gamma_0 \end{pmatrix} u(t), \qquad && \boldsymbol{x}(0) = \boldsymbol{x}^0 \in \mathbb{R}^2, \\ y(t) &= \begin{pmatrix} 0 & 1 \end{pmatrix} \boldsymbol{x}(t) && a_0,\, a_1 \in \mathbb{R},\, \gamma_0 > 0 \end{aligned} \tag{2.58}$$

which has relative degree one and a positive high-frequency gain, since $\left(\begin{smallmatrix} 0 & 1 \end{smallmatrix}\right) \left(\begin{smallmatrix} 0 \\ \gamma_0 \end{smallmatrix}\right) = \gamma_0 > 0$. *Moreover, simple calculations show that*

$$\det \begin{bmatrix} s & -1 & 0 \\ -a_0 & s - a_1 & \gamma_0 \\ 0 & 1 & 0 \end{bmatrix} = (-1)^{3+2} \det \begin{bmatrix} s & 0 \\ -a_0 & \gamma_0 \end{bmatrix} = -\gamma_0\, s|_{s=0} = 0,$$

and thus system property ($\mathcal{S}_1^{\text{lin}}$-sp$_2$) is violated. System (2.58) is not minimum-phase. Now switch to the frequency domain; the transfer function of (2.58) is given by

$$F(s) = \frac{y(s)}{u(s)} = \begin{pmatrix} 0 & 1 \end{pmatrix} \left(s\, \boldsymbol{I}_2 - \begin{bmatrix} 0 & 1 \\ a_0 & a_1 \end{bmatrix} \right)^{-1} \begin{pmatrix} 0 \\ \gamma_0 \end{pmatrix} = \frac{\gamma_0\, s}{s^2 - a_1\, s - a_0},$$

which, for $a_0 = 0$, *simplifies to*

$$F(s)|_{a_0=0} = \gamma_0 \frac{\cancel{s}}{\cancel{s}(s - a_1)} = \frac{\gamma_0}{s - a_1}.$$

That is a first order system with relative degree one and positive high-frequency gain $\lim_{s\to\infty} s\, F(s)|_{a_0=0} = \gamma_0 > 0$. *Application of feedback (2.33) yields the closed-loop system with transfer function*

$$\frac{y(s)}{v(s)} = \frac{k\, F(s)|_{a_0=0}}{1 + k\, F(s)|_{a_0=0}} = \frac{\gamma_0\, k}{s - a_1 + \gamma_0\, k},$$

which clearly is stable for all $k > |a_1|/\gamma_0$, *since the denominator is Hurwitz for all* $k > |a_1|/\gamma_0$. *Concluding, for* $a_0 = 0$, *system (2.58) is high-gain stabilizable, but it is neither a minimal realization of* $F(s)|_{a_0=0} = \gamma_0/(s - a_1)$ *nor element of* $\mathcal{S}_1^{\text{lin}}$.

The main result of this section is recorded in the following theorem.

Theorem 2.24 (High-gain adaptive control for systems of class $\mathcal{S}_1^{\text{lin}}$)**.**
Consider a system of class $\mathcal{S}_1^{\text{lin}}$ *given by (2.45). The high-gain adaptive controller*

$$u(t) = -\operatorname{sign}(\boldsymbol{c}^\top \boldsymbol{b})\, k(t) y(t) \quad \textit{where} \quad \dot{k}(t) = q_1\, |y(t)|^{q_2}, \quad k(0) = k_0 \tag{2.59}$$

with design parameters $q_1 > 0$, $q_2 \geq 1$ and $k_0 > 0$ applied to (2.45) yields a closed-loop initial-value problem with the following properties:

(i) there exists a unique and maximal solution $(\boldsymbol{x}, k) : [0, T) \to \mathbb{R}^n \times \mathbb{R}_{>0}$, $T \in (0, \infty]$;

(ii) the solution is global, i.e. $T = \infty$;

(iii) all signals are bounded, i.e. $\boldsymbol{x}(\cdot) \in \mathcal{L}^\infty(\mathbb{R}_{\geq 0}; \mathbb{R}^n)$ and $k(\cdot) \in \mathcal{L}^\infty(\mathbb{R}_{\geq 0}; \mathbb{R}_{>0})$;

(iv) $\lim_{t\to\infty} \dot{k}(t) = 0$ and $\lim_{t\to\infty} \boldsymbol{x}(t) = \boldsymbol{0}_n$.

Remark 2.25 (σ-modification)**.**
Note that the gain adaption in (2.59) yields a non-decreasing gain $k(\cdot)$. σ-modification tries to bypass this undesirable effect (see [105]): for some (small) $\sigma > 0$, the gain adaption in (2.59) is replaced e.g. by

$$\dot{k}(t) = -\sigma\, k(t) + y(t)^2, \qquad k(0) = k_0 > 0,$$

which, clearly, allows for gain decrease. However, high-gain adaptive controllers with σ-modification may yield limit cycles and chaos (see [130]) and, hence, should be "handled with care".

Although the result in Theorem 2.24 is well known (see e.g. [85, Theorem 3.6], there for $q_1 = 1$ and $q_2 = p$) an explicit proof is presented. It differs from that given in [85, Theorem 3.6] and illustrates the basic steps of argumentation as basis for the upcoming proofs.

Proof of Theorem 2.24.

Step 1: It is shown that Assertion (i) holds true, i.e. existence of a unique solution maximally extended on $[0, T)$, $T \in (0, \infty]$.
It suffices to consider system (2.45) in the Byrnes-Isidori form (2.50). Define

$$\mathcal{D} := \mathbb{R} \times \mathbb{R}^{n-1} \times \mathbb{R}_{>0} \qquad \text{and} \qquad \mathcal{I} := \mathbb{R}$$

and the function

$$\boldsymbol{f} \colon \mathcal{I} \times \mathcal{D} \to \mathcal{D}, \qquad (t, (\mu, \boldsymbol{\xi}, \kappa)) \mapsto \begin{pmatrix} a_1\mu + \boldsymbol{a}_2^\top \boldsymbol{\xi} - |\gamma_0|\kappa\,\mu \\ \boldsymbol{a}_3\mu + \boldsymbol{A}_4\boldsymbol{\xi} \\ q_1|\mu|^{q_2} \end{pmatrix}.$$

Then, for $\boldsymbol{S}$ as in (2.49) and $\hat{\boldsymbol{x}} := (y, \boldsymbol{z}, k)^\top$, the closed-loop initial-value problem (2.50), (2.59) can be written as

$$\frac{\mathrm{d}}{\mathrm{d}t}\hat{\boldsymbol{x}}(t) = \boldsymbol{f}(t, \hat{\boldsymbol{x}}(t)), \qquad \hat{\boldsymbol{x}}(0) = \big((\boldsymbol{S}\boldsymbol{x}^0)^\top, \;\; k_0\big)^\top. \tag{2.60}$$

Clearly, the function $\boldsymbol{f}(\cdot,\cdot)$ is continuous for all $(t, (\mu, \boldsymbol{\xi}, \kappa)) \in \mathcal{I} \times \mathcal{D}$ and, for every compact $\mathfrak{C} \subset \mathcal{I} \times \mathcal{D}$, there exists $M_{\mathfrak{C}} > 0$ such that $\big\|(t, (\mu, \boldsymbol{\xi}^\top, \kappa))^\top\big\| \leq M_{\mathfrak{C}}$ for all $(t, (\mu, \boldsymbol{\xi}, \kappa)) \in \mathfrak{C}$. Moreover, for all $(t, (\mu, \boldsymbol{\xi}, \kappa))$, $(t, (\tilde{\mu}, \tilde{\boldsymbol{\xi}}, \tilde{\kappa})) \in \mathfrak{C}$, it follows that

$$\begin{aligned} |\kappa\mu - \tilde{\kappa}\tilde{\mu}| &= |(\kappa - \tilde{\kappa})\mu + \tilde{\kappa}\mu - \tilde{\kappa}\tilde{\mu}| \leq |\mu||\kappa - \tilde{\kappa}| + |\tilde{\kappa}||\mu - \tilde{\mu}| \\ &\leq M_{\mathfrak{C}}(|\kappa - \tilde{\kappa}| + |\mu - \tilde{\mu}|), \\ \big||\mu|^{q_2} - |\tilde{\mu}|^{q_2}\big| &\leq q_2 M_{\mathfrak{C}}^{q_2 - 1}|\mu - \tilde{\mu}| \end{aligned} \tag{2.61}$$

and

$$\begin{aligned}\left\|\boldsymbol{f}(t,(\mu,\boldsymbol{\xi},\kappa))-\boldsymbol{f}(t,(\tilde{\mu},\tilde{\boldsymbol{\xi}},\tilde{\kappa}))\right\| \quad &\leq \quad |a_1||\mu-\tilde{\mu}|+\|\boldsymbol{a}_2\|\left\|\boldsymbol{\xi}-\tilde{\boldsymbol{\xi}}\right\|+|\gamma_0||\kappa\mu-\tilde{\kappa}\tilde{\mu}| \\ &\quad +\|\boldsymbol{a}_3\|\,|\mu-\tilde{\mu}|+\|\boldsymbol{A_4}\|\left\|\boldsymbol{\xi}-\tilde{\boldsymbol{\xi}}\right\|+\left||\mu|^{q_2}-|\tilde{\mu}|^{q_2}\right| \\ &\overset{(2.61)}{\leq} \quad \left(|a_1|+\|\boldsymbol{a}_3\|+q_2M_{\mathfrak{C}}^{q_2-1}+|\gamma_0|M_{\mathfrak{C}}\right)|\mu-\tilde{\mu}| \\ &\quad +(\|\boldsymbol{a}_2\|+\|\boldsymbol{A_4}\|)\left\|\boldsymbol{\xi}-\tilde{\boldsymbol{\xi}}\right\|+|\gamma_0|M_{\mathfrak{C}}|\kappa-\tilde{\kappa}|,\end{aligned}$$

which shows that $\boldsymbol{f}(\cdot,\cdot)$ is locally Lipschitz continuous (with respect to $(\mu,\boldsymbol{\xi},\kappa)\in\mathcal{D}$). Hence, in view of Theorem 2.20, there exists a unique solution $\hat{\boldsymbol{x}}=(y,\boldsymbol{z},k)\colon\ [0,T)\to\mathbb{R}\times\mathbb{R}^{n-1}\times\mathbb{R}_{>0}$ of the initial-value problem (2.60) with maximal $T\in(0,\infty]$ (the interval $(T_-,0)$ is neglected) and $(\boldsymbol{x},k)=(\boldsymbol{S}^{-1}(y,\,\boldsymbol{z}),k)\colon\ [0,T)\to\mathbb{R}^n\times\mathbb{R}_{>0}$ solves closed-loop initial-value problem (2.45), (2.59). This shows Assertion (i) and completes Step 1.

Step 2: Some technical inequalities are shown.
First note that the binomial theorem gives

$$\forall\, m>0\ \forall\, a,b\in\mathbb{R}\colon\qquad \pm\,2\,a\,b=-\left(\frac{a}{\sqrt{m}}\mp\sqrt{m}b\right)^2+\frac{a^2}{m}+mb^2\leq\frac{a^2}{m}+mb^2. \tag{2.62}$$

and by property ($\mathcal{S}_1^{\text{lin}}$-sp$_2$) and Lemma 2.12 the matrix $\boldsymbol{A}_4$ is Hurwitz, i.e. $\operatorname{spec}(\boldsymbol{A}_4)\subset\mathbb{C}_{<0}$ and hence (see e.g. Corollary 3.3.47 in [77, p. 284])

$$\exists\,\text{a unique}\ \ 0<\boldsymbol{P}_4^\top=\boldsymbol{P}_4\in\mathbb{R}^{(n-1)\times(n-1)}\colon\qquad \boldsymbol{A}_4^\top\boldsymbol{P}_4+\boldsymbol{P}_4\boldsymbol{A}_4=-\boldsymbol{I}_{n-1}. \tag{2.63}$$

For $\boldsymbol{P}_4$ as in (2.63) introduce the Lyapunov-like function

$$V\colon\mathbb{R}\times\mathbb{R}^{n-1}\to\mathbb{R}_{\geq 0},\qquad (y,\boldsymbol{z})\mapsto V(y,\boldsymbol{z}):=y^2+\boldsymbol{z}^\top\boldsymbol{P}_4\boldsymbol{z}\geq 0 \tag{2.64}$$

and observe that the following holds (see e.g. [24, Corollary 4.8.2, p.487])

$$\forall\begin{pmatrix}y\\ \boldsymbol{z}\end{pmatrix}\in\mathbb{R}^n\colon\quad \underbrace{\min\left\{1,\,1/\left\|\boldsymbol{P}_4^{-1}\right\|\right\}}_{=:\underline{\mu}_V>0}\left\|\begin{pmatrix}y\\ \boldsymbol{z}\end{pmatrix}\right\|^2\leq V(y,\boldsymbol{z})\leq\underbrace{\max\left\{1,\,\|\boldsymbol{P}_4\|\right\}}_{=:\overline{\mu}_V>0}\left\|\begin{pmatrix}y\\ \boldsymbol{z}\end{pmatrix}\right\|^2 \tag{2.65}$$

By equivalence of norms in $\mathbb{R}^n$ (see [24, Theorem 9.1.8, p. 600]), note that

$$\forall\, p,q\in[1,\,\infty]\ \exists\,\alpha>0,\beta\geq 1\ \forall\,\boldsymbol{\xi}\in\mathbb{R}^n\colon\qquad \alpha\,\|\boldsymbol{\xi}\|_p\leq\|\boldsymbol{\xi}\|_q\leq\beta\,\|\boldsymbol{\xi}\|_p \tag{2.66}$$

and hence (for $q=q_2$ and $p=2$ in (2.66)) it follows that

$$\forall\, t\in[0,T)\colon\quad \dot{k}(t)/q_1=|y(t)|^{q_2}\leq\left\|\begin{pmatrix}y(t)\\ \boldsymbol{z}(t)\end{pmatrix}\right\|_{q_2}^{q_2}\overset{(2.66)}{\leq}\beta^{q_2}\left\|\begin{pmatrix}y(t)\\ \boldsymbol{z}(t)\end{pmatrix}\right\|^{q_2}. \tag{2.67}$$

To conclude Step 2, the time derivative $\frac{\mathrm{d}}{\mathrm{d}t} V(\cdot)$ along the solution of the closed-loop system (2.50), (2.63) is given as follows

$$\begin{aligned}
\forall\, t \in [0,T)\colon \quad \frac{\mathrm{d}}{\mathrm{d}t} V(y(t), \boldsymbol{z}(t)) &= 2\, y(t)\dot{y}(t) + \dot{\boldsymbol{z}}(t)^\top \boldsymbol{P}_4 \boldsymbol{z}(t) + \boldsymbol{z}(t)^\top \boldsymbol{P}_4 \dot{\boldsymbol{z}}(t) \\
&= 2\,(a_1 - |\gamma_0| k(t)) y(t)^2 + 2 y(t) \boldsymbol{a}_2^\top \boldsymbol{z}(t) \\
&\quad + \boldsymbol{z}(t)^\top \left(\boldsymbol{A}_6^\top \boldsymbol{P}_6 + \boldsymbol{P}_6 \boldsymbol{A}_6 \right) \boldsymbol{z}(t) + 2 \boldsymbol{z}(t)^\top \boldsymbol{P}_4 \boldsymbol{a}_3 y(t) \\
&\overset{(2.63)}{\leq} -2\,(|\gamma_0| k(t) - |a_1|) y(t)^2 + 2|y(t)|\, \|\boldsymbol{a}_2\|\, \|\boldsymbol{z}(t)\| \\
&\quad - \|\boldsymbol{z}(t)\|^2 + 2\, \|\boldsymbol{z}(t)\|\, \|\boldsymbol{P}_4\|\, \|\boldsymbol{a}_3\|\, |y(t)| \\
&\overset{(2.62)}{\leq} -2\,(|\gamma_0| k(t) - |a_1| - 4\, \|\boldsymbol{a}_2\|^2 - 4\, \|\boldsymbol{P}_4\|^2\, \|\boldsymbol{a}_3\|^2) y(t)^2 \\
&\quad - \frac{1}{2}\, \|\boldsymbol{z}(t)\|^2 . \qquad (2.68)
\end{aligned}$$

Step 3: It is shown that $k(\cdot)$ is bounded on $[0,T)$.
Seeking a contradiction, assume that $k(\cdot)$ is unbounded on $[0,T)$. In view of (2.59), $k(\cdot)$ is non-decreasing on $[0,T)$, therefore

$$\exists\, t^\star \geq 0\ \forall\, t \in [t^\star, T)\colon \qquad k(t) \geq \frac{1}{|\gamma_0|} \left(|a_1| - 4\, \|\boldsymbol{a}_2\|^2 - 4\, \|\boldsymbol{P}_4\|^2\, \|\boldsymbol{a}_3\|^2 + \frac{1}{4} \right).$$

Defining

$$\mu_V := \frac{1}{2} \min\{1,\, 1/\, \|\boldsymbol{P}_4\|\}$$

and using $-\|\boldsymbol{z}(t)\|^2 \leq -\boldsymbol{z}(t)^\top \boldsymbol{P}_4 \boldsymbol{z}(t)/\, \|\boldsymbol{P}_4\|$ in (2.68) yields

$$\forall\, t \in [t^\star, T)\colon \quad \tfrac{\mathrm{d}}{\mathrm{d}t} V(y(t), \boldsymbol{z}(t)) \ \leq\ -\tfrac{1}{2} y(t)^2 - \tfrac{1}{2}\, \|\boldsymbol{z}(t)\|^2 \leq -\mu_V\, V(y(t), \boldsymbol{z}(t)).$$

Application of the Bellman-Gronwall Lemma (in its differential form [18, Lemma 1.1, p. 2]) gives

$$\forall\, t \in [t^\star, T)\colon \quad V(y(t), \boldsymbol{z}(t)) \leq V(y(t^\star), \boldsymbol{z}(t^\star))\, \exp(-\mu_V (t - t^\star)) \qquad (2.69)$$

and in view of (2.65) it follows that

$$\forall\, t \in [t^\star, T)\colon \quad \left\| \begin{pmatrix} y(t) \\ \boldsymbol{z}(t) \end{pmatrix} \right\| \overset{(2.65),(2.69)}{\leq} \sqrt{\frac{\overline{\mu}_V}{\underline{\mu}_V}}\, \left\| \begin{pmatrix} y(t^\star) \\ \boldsymbol{z}(t^\star) \end{pmatrix} \right\| \exp\left(-\frac{\mu_V}{2} (t - t^\star) \right). \qquad (2.70)$$

Hence for all $t \in [0, T)$

$$\begin{aligned} k(t) &= k(t^\star) + \int_{t^\star}^{t} \dot{k}(\tau)\,\mathrm{d}\tau \\ &\overset{(2.67),(2.70)}{\leq} k(t^\star) + q_1\,\beta^{q_2} \left(\frac{\overline{\mu}_V}{\underline{\mu}_V}\right)^{\frac{q_2}{2}} \left\| \begin{pmatrix} y(t^\star) \\ \boldsymbol{z}(t^\star) \end{pmatrix} \right\|^{q_2} \int_{t^\star}^{t} \exp\left(-\frac{q_2\,\mu_V}{2}(\tau - t^\star)\right) \mathrm{d}\tau \\ &\leq k(t^\star) + \frac{2q_1\,\beta^{q_2}}{q_2\,\mu_V} \left(\frac{\overline{\mu}_V}{\underline{\mu}_V}\right)^{\frac{q_2}{2}} \left\| \begin{pmatrix} y(t^\star) \\ \boldsymbol{z}(t^\star) \end{pmatrix} \right\|^{q_2} < \infty, \end{aligned}$$

which, with continuity of $y(\cdot)$, $\boldsymbol{z}(\cdot)$ and $k(\cdot)$ on $[0, T)$ and compactness of $[0,\, t^\star]$, contradicts unboundedness of $k(\cdot)$ on $[0, T)$.

Step 4: It is shown that Assertion (ii) holds true, i.e. $T = \infty$.
From Step 3 it follows that $k(\cdot)$ is bounded on $[0, T)$. Since $k(\cdot)$ is continuous and non-decreasing on $[0, T)$, the limit $\lim_{t\to T} k(t) =: k_\infty$ exists. Define

$$\sigma := |a_1| + |\gamma_0| k_\infty + \|\boldsymbol{a}_2\| + \|\boldsymbol{a}_3\| + \|\boldsymbol{A}_4\| \geq 0.$$

and observe that for the closed-loop initial-value problem (2.50), (2.59) (neglecting the adaption of $k(\cdot)$ in (2.59)) the following holds

$$\forall\, t \in [0, T)\colon \qquad \left\| \frac{\mathrm{d}}{\mathrm{d}t} \begin{pmatrix} y(t) \\ \boldsymbol{z}(t) \end{pmatrix} \right\| \leq \sigma \left\| \begin{pmatrix} y(t) \\ \boldsymbol{z}(t) \end{pmatrix} \right\|.$$

Hence, for all $T < \infty$, Hilfssatz 3.1 in [116, p. 120] gives

$$\forall\, t \in [0, T)\colon \quad \left\| \begin{pmatrix} y(t) \\ \boldsymbol{z}(t) \end{pmatrix} \right\| \leq \exp(\sigma\, t) \left\| \begin{pmatrix} y(0) \\ \boldsymbol{z}(0) \end{pmatrix} \right\| < \exp(\sigma T) \left\| \begin{pmatrix} y(0) \\ \boldsymbol{z}(0) \end{pmatrix} \right\| < \infty.$$

which, by maximality of T, implies $T = \infty$ and Assertion (ii) is shown. This completes Step 4.

Step 5: It is shown that Assertions (iii) and (iv) hold true, i.e. $k(\cdot) \in \mathcal{L}^\infty(\mathbb{R}_{\geq 0}; \mathbb{R}_{>0})$, $\boldsymbol{x}(\cdot) \in \mathcal{L}^\infty(\mathbb{R}_{\geq 0}; \mathbb{R}^n)$, $\lim_{t\to\infty} \dot{k}(t) = 0$ and $\lim_{t\to\infty} \boldsymbol{x}(t) = \boldsymbol{0}_n$.
Note that $k(\cdot) \in \mathcal{L}^\infty(\mathbb{R}_{\geq 0}; \mathbb{R}_{>0})$ is a direct consequence of Step 3 and 4. Boundedness of $k(\cdot)$ on $\mathbb{R}_{\geq 0}$ combined with (2.59) implies $y(\cdot) \in \mathcal{L}^{q_2}(\mathbb{R}_{\geq 0}; \mathbb{R})$. From system property ($\mathcal{S}_1^{\mathrm{lin}}$-sp$_2$) and Lemma 2.12 it follows that $\mathrm{spec}(\boldsymbol{A}_4) \subset \mathbb{C}_{<0}$ and, in view of the second equation in (2.50), this combined with $y(\cdot) \in \mathcal{L}^{q_2}(\mathbb{R}_{\geq 0}; \mathbb{R})$ implies (see e.g. [46, Theorem C.2.14])

$$\boldsymbol{z}(\cdot) \in \mathcal{L}^{q_2}(\mathbb{R}_{\geq 0}; \mathbb{R}^{n-1}) \qquad \text{and} \qquad \dot{\boldsymbol{z}}(\cdot) \in \mathcal{L}^{q_2}(\mathbb{R}_{\geq 0}; \mathbb{R}^{n-1}).$$

Moreover, in view of the first equation in (2.50), this with $y(\cdot) \in \mathcal{L}^{q_2}(\mathbb{R}_{\geq 0}; \mathbb{R})$ implies $\dot{y}(\cdot) \in \mathcal{L}^{q_2}(\mathbb{R}_{\geq 0}; \mathbb{R})$. Invoking Lemma 2.1.7 in [86, p. 17] then gives

$$(y(\cdot),\, \boldsymbol{z}(\cdot)) \in \mathcal{L}^\infty(\mathbb{R}_{\geq 0}; \mathbb{R}^n) \qquad \text{and} \qquad \lim_{t\to\infty} (y(t),\, \boldsymbol{z}(t)) = \boldsymbol{0}_n,$$

which with $\boldsymbol{S}^{-1}$ as in (2.49) implies

$$\boldsymbol{x}(\cdot) = \boldsymbol{S}^{-1}(y(\cdot),\, \boldsymbol{z}(\cdot)^\top)^\top \in \mathcal{L}^\infty(\mathbb{R}_{\geq 0}; \mathbb{R}^n) \quad \text{and} \quad \lim_{t\to\infty} \boldsymbol{x}(t) = \lim_{t\to\infty} \boldsymbol{S}^{-1}(y(t),\, \boldsymbol{z}(t)^\top)^\top = \mathbf{0}_n.$$

Furthermore

$$\lim_{t\to\infty} \dot{k}(t) = \lim_{t\to\infty} q_1\, |y(t)|^{q_2} = \lim_{t\to\infty} q_1\, |\boldsymbol{c}^\top \boldsymbol{x}(t)|^{q_2} = 0.$$

Hence Assertions (iii) and (iv) are shown, which completes the proof. □

The simple high-gain adaptive controller (2.59) is an "asymptotic stabilizer" of all systems of form (2.45) and element of class $\mathcal{S}_1^{\text{lin}}$. For simplicity the initial controller gain k_0 is restricted to be positive. Clearly, since $k(\cdot)$ is non-decreasing, any negative value is also admissible but not reasonable: $k_0 < 0$ reverses the sign of control action in (2.59) and might initially destabilize the closed-loop system (2.45), (2.59).

Remark 2.26 (Asymptotic stabilization versus asymptotic stability)**.**
Note that, in general, the closed-loop system (2.45), (2.59) *is* not *asymptotically stable in the sense of Lyapunov (see e.g. [77, p. 199-202]). The controller* (2.59) *"solely renders" the origin attractive, i.e.* $\lim_{t\to\infty} \boldsymbol{x}(t) = \mathbf{0}_n$ *(not accounting for the gain* $k(\cdot)$*) and so achieves "asymptotic stabilization" of systems of class* $\mathcal{S}_1^{\text{lin}}$*. For illustration consider the first order system*

$$\dot{y}(t) = a_1\, y(t) + \gamma_0\, u(t), \qquad y(0) = y_0 \in \mathbb{R}, \quad a_1 \in \mathbb{R},\ \gamma_0 \neq 0. \tag{2.71}$$

Clearly, for known $\operatorname{sign}(\gamma_0)$ *system* (2.71) *is element of class* $\mathcal{S}_1^{\text{lin}}$ *and therefore application of high-gain adaptive controller* (2.59) *is admissible. Moreover, for* $a_1 > 0$ *system* (2.71) *is unstable. If, for* $0 < k_0 < a_1$*, controller* (2.59) *is applied to* (2.71)*, then for arbitrary* $\varepsilon > 0$ *there does not exist* $\delta = \delta(\varepsilon) > 0$ *such that* $|y(0)| < \delta$ *implies* $|y(t)| < \varepsilon$ *for all* $t \geq 0$*. The closed-loop system blows up until for some* $t^\star > 0$ *a sufficiently large "stabilizing" gain* $k(t^\star) > a_1$ *is reached.*

Simulations

To analyze the influence of the design parameters q_1 and q_2 in (2.59) on the control performance, consider the closed-loop system (2.71), (2.59). For different choices of q_1 and q_2 the simulation results are depicted in Fig. 2.3. For all simulations the initial gain $k_0 = 1$, the initial value $y_0 = 0.1$ and the parameters $\gamma_0 = 1$ and $a_1 = 10$ are fixed. It is easy to imagine that larger initial gains will result in "faster stabilization" with "smaller peaks" in the output and so such simulations are not shown. For a comprehensive performance analysis the reader is referred to [86, Chapter 7]. The influence of the design parameters on the control performance is summarized in the following remark.

Remark 2.27 (Design parameters q_1, q_2 and k_0)**.**
The factor $q_1 > 0$ *scales gain adaption in* (2.59)*, which allows to accelerate or decelerate adaption speed in particular for small initial values* $|y(0)| \ll 1$*. The exponent* $q_2 \geq 1$ *increases adaption speed for large values of* $|y(\cdot)|$*. Increased adaption speed in turn reduces peaking. The "stabilizing gain" is found more rapidly (see also [91]). A very common choice for the exponent is* $q_2 = 2$ *(then also the proof simplifies). With* $k_0 > 0$ *the control designer is able to fix a first guess for the initial gain, e.g. for system* (2.71) *the choice* $k_0 > a_1$ *yields a closed-loop system* (2.71), (2.59) *which is exponentially stable "right away".*

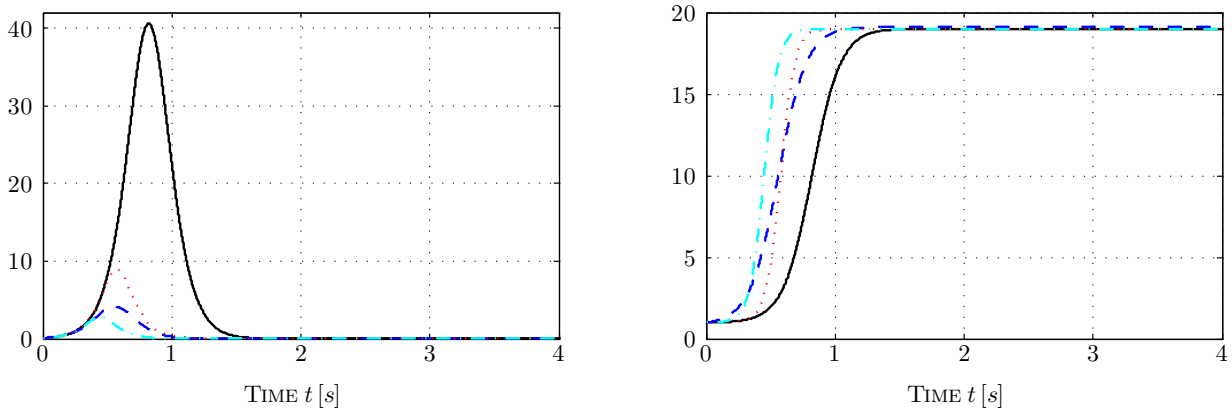

(a) *output* $y(\cdot)$ *for different designs.* (b) *gain* $k(\cdot)$ *for different designs.*

Figure 2.3: *Simulation results for closed-loop system* (2.71), (2.59) *with* $a_1 = 10$, $y_0 = 0.1$ *and* $\gamma_0 = k_0 = 1$ *and different design parameters* $(q_1, q_2) \in \{$—— $(1,1)$, - - - $(10,1)$, ····· $(1,2)$, -·-·- $(10,2)\}$.

2.3.4 Relative degree two systems

In general the simple controller structure in (2.59) cannot be retained for relative degree two systems of form (2.45). Either additional assumptions (e.g. negative root locus center) must be imposed on the system or an extended controller structure must be applied (e.g. incorporating a dynamic compensator or derivative feedback). In this section the following system class is considered.

Definition 2.28 (System class $\mathcal{S}_2^{\text{lin}}$)**.**
A system of form (2.45) *is of Class* $\mathcal{S}_2^{\text{lin}}$ *if, and only if, the following hold:*

($\mathcal{S}_2^{\text{lin}}$-sp$_1$) *the relative degree is two and the sign of the high-frequency gain is known, i.e.*

$$\boldsymbol{c}^\top \boldsymbol{b} = 0, \quad \gamma_0 := \boldsymbol{c}^\top \boldsymbol{A}\boldsymbol{b} \neq 0 \quad \text{and} \quad \operatorname{sign}(\gamma_0) \text{ is known;}$$

($\mathcal{S}_2^{\text{lin}}$-sp$_2$) *it is minimum-phase, i.e.* (2.14) *holds, and*

($\mathcal{S}_2^{\text{lin}}$-sp$_3$) *the (regulated) output* $y(\cdot)$ *and its derivative* $\dot{y}(\cdot)$ *are available for feedback.*

System class $\mathcal{S}_2^{\text{lin}}$ is the linear counterpart to system class $\mathcal{S}_2$ and the following discussion can be regarded as precursor of the generalization(s) to class $\mathcal{S}_2$ presented in Chapter 3 and 4.

2.3.4.1 High-gain adaptive controller if root locus center is negative

The root locus center of systems of form (2.45) with relative degree two is given by

$$\Xi(\boldsymbol{A}, \boldsymbol{b}, \boldsymbol{c}) = \frac{1}{2}\frac{\boldsymbol{c}^\top \boldsymbol{A}^2 \boldsymbol{b}}{\boldsymbol{c}^\top \boldsymbol{A}\boldsymbol{b}} = \frac{1}{2\gamma_0}\boldsymbol{c}^\top \boldsymbol{A}^2 \boldsymbol{b}. \qquad \text{(see Appendix C)} \tag{2.72}$$

As was already noted in Section 2.2, systems of class $\mathcal{S}_2^{\text{lin}}$ with negative root locus center are high-gain stabilizable. Moreover, high-gain adaptive stabilization is feasible by retaining the

simple structure of the high-gain adaptive controller (2.59). Solely the (altered) high-frequency gain is to be incorporated into the controller appropriately.

Theorem 2.29. *Consider a system of class $\mathcal{S}_2^{\mathrm{lin}}$ described by (2.45) with root locus center $\Xi(\boldsymbol{A},\boldsymbol{b},\boldsymbol{c})$ as in (2.72). If $\Xi(\boldsymbol{A},\boldsymbol{b},\boldsymbol{c})<0$, then the high-gain adaptive controller*

$$u(t) = -\operatorname{sign}(\boldsymbol{c}^\top\boldsymbol{A}\boldsymbol{b})\, k(t)\, y(t) \qquad \text{where} \qquad \dot{k}(t) = y(t)^2, \quad k(0) = k_0 > 0 \tag{2.73}$$

applied to (2.45) yields a closed-loop initial-value problem with the properties (i)-(iv) of Theorem 2.24.

Proof. see [86, p. 63-66]. □

Note that, depending on the location of the root locus center $\Xi(\boldsymbol{A},\boldsymbol{b},\boldsymbol{c})<0$ in the left complex half-plane and the initial gain k_0, the closed-loop system (2.45), (2.73) is possibly not well-damped (in the sense of Example 11.3.7 in [24]): there might occur (undesired) oscillations which cannot be damped actively.

Example 2.30. *For illustration consider the second order system given by*

$$\ddot{y}(t) = a_1\, y(t) + a_2\, \dot{y}(t) + \gamma_0\, u(t), \qquad \begin{pmatrix} y(0) \\ \dot{y}(0) \end{pmatrix} = \begin{pmatrix} y_0 \\ y_1 \end{pmatrix} \in \mathbb{R}^2, \quad a_1,\, a_2 \in \mathbb{R},\ \gamma_0 \neq 0. \tag{2.74}$$

Its relative degree is two and, for $a_2<0$, it has a negative root locus center

$$\Xi = \frac{1}{2\gamma_0}\begin{pmatrix} 0, & 1 \end{pmatrix}\begin{pmatrix} \gamma_0 \\ a_2\gamma_0 \end{pmatrix} = a_2/2 < 0.$$

Applying (2.73) to (2.74) yields the simulation results depicted in Fig. 2.4. For the (larger) initial gain $k_0=10$ the closed-loop system (2.74), (2.73) exhibits oscillations with greater amplitude and higher frequency than for the (smaller) initial gain $k_0=1$. This observation holds for both choices of $a_2=-1$ and $a_2=-2$ (see Fig. 2.4(a), (b)). In contrast, the closed-loop system (2.74), (2.73) with root locus center $\Xi=-1$ (i.e. $a_2=-2$) is better damped for $k_0=1$ and $k_0=10$ than that with $\Xi=-0.5$ (i.e. $a_2=-1$), respectively.

The controller (2.73) will not work for systems with positive root locus center $\Xi(\boldsymbol{A},\boldsymbol{b},\boldsymbol{c})>0$. However, if derivative feedback is admissible (as claimed in class $\mathcal{S}_2^{\mathrm{lin}}$), then $\Xi(\boldsymbol{A},\boldsymbol{b},\boldsymbol{c})$ can be shifted arbitrarily.

Corollary 2.31. *Consider a system of class $\mathcal{S}_2^{\mathrm{lin}}$ described by (2.45) with high-frequency gain $\gamma_0=\boldsymbol{c}^\top\boldsymbol{A}\boldsymbol{b}$ and root locus center $\Xi(\boldsymbol{A},\boldsymbol{b},\boldsymbol{c})$ as in (2.72). Then, for continuous $v(\cdot)\colon \mathbb{R}_{\geq 0}\to\mathbb{R}$, application of derivative feedback of the form*

$$u(t) = -\operatorname{sign}(\boldsymbol{c}^\top\boldsymbol{A}\boldsymbol{b})\, k_S\, \dot{y}(t) + v(t), \qquad k_S \neq 0. \tag{2.75}$$

yields a shift of the root locus center, i.e.

$$\Xi_S := \Xi(\boldsymbol{A},\boldsymbol{b},\boldsymbol{c}) - \frac{1}{2}|\gamma_0| k_S. \tag{2.76}$$

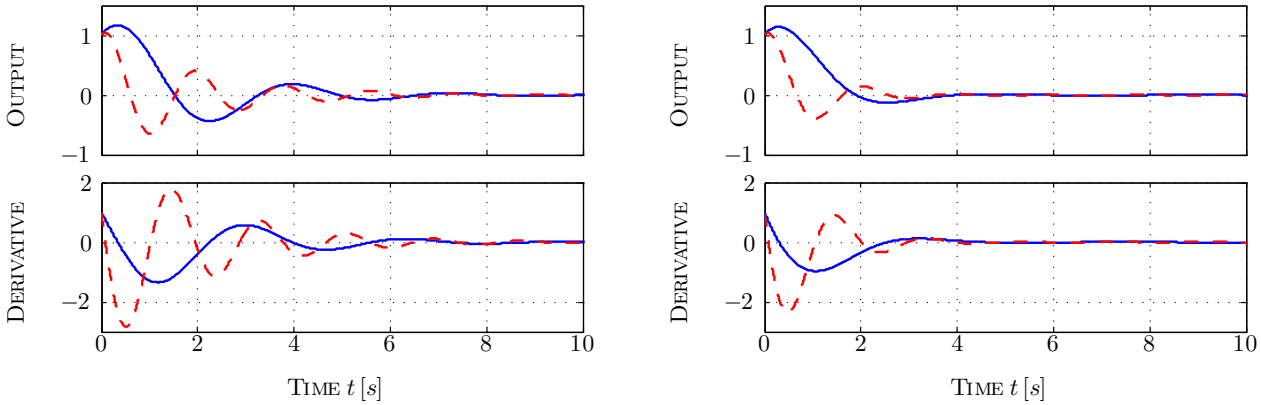

(a) *simulation results for* $\Xi = -0.5$ *(i.e.* $a_2 = -1$*):*
top: —— $y(\cdot)$ *for* $k_0 = 1$, - - - $y(\cdot)$ *for* $k_0 = 10$*;*
bottom: —— $\dot{y}(\cdot)$ *for* $k_0 = 1$, - - - $\dot{y}(\cdot)$ *for* $k_0 = 10$.

(b) *simulation results for* $\Xi = -1$ *(i.e.* $a_2 = -2$*):*
top: —— $y(\cdot)$ *for* $k_0 = 1$, - - - $y(\cdot)$ *for* $k_0 = 10$*;*
bottom: —— $\dot{y}(\cdot)$ *for* $k_0 = 1$, - - - $\dot{y}(\cdot)$ *for* $k_0 = 10$.

Figure 2.4: *Simulation results for closed-loop system* (2.74), (2.73) *with* $(y_0, y_1) = (1, 1)$, $a_1 = -1$, $\gamma_0 = 1$ *and* $k_0 \in \{1, 10\}$ *and* $a_2 \in \{-1, -2\}$.

Proof. Without loss of generality, consider system (2.45) in BIF (2.54). For $\boldsymbol{B}$ as in (2.52) and $(\boldsymbol{CB})^{-1}$ as in (2.53) observe that the following holds

$$\begin{pmatrix} a_1, & a_2 \end{pmatrix} = \boldsymbol{c}^\top \boldsymbol{A}^2 \boldsymbol{B} (\boldsymbol{CB})^{-1} = \begin{pmatrix} \star, & \frac{1}{\gamma_0} \boldsymbol{c}^\top \boldsymbol{A}^2 \boldsymbol{b} \end{pmatrix} \in \mathbb{R}^{1\times 2} \quad \Rightarrow \quad a_2 = \frac{\boldsymbol{c}^\top \boldsymbol{A}^2 \boldsymbol{b}}{\gamma_0} \overset{(2.72)}{=} 2\,\Xi(\boldsymbol{A}, \boldsymbol{b}, \boldsymbol{c}).$$

Moreover, it is easy to see that the closed-loop system (2.54), (2.75) is similar to (2.54): substitute $v(t)$ and $a_2 - |\gamma_0|\, k_S$ for $u(t)$ and a_2, respectively. Hence $a_2 - |\gamma_0|\, k_S =: 2\Xi_S$ which gives (2.76). □

Clearly, Corollary 2.31 allows for a left shift of the root locus center, if e.g. $\rho > 0$, $\Xi(\boldsymbol{A}, \boldsymbol{b}, \boldsymbol{c}) > \rho$ and a lower bound $\underline{\gamma_0} > 0$ on the high-frequency gain (i.e. $\underline{\gamma_0} \leq \gamma_0$) are known, then any $k_S > 2\rho/\underline{\gamma_0}$ in (2.75) gives $\Xi_S < 0$ and Theorem 2.29 assures asymptotic stabilization of the shifted system (2.54), (2.75) with "new" control input $v(\cdot)$. Drawback of this shift is that two parameters must be known roughly. Later it will be shown that a "time-varying shift" of the root locus center—obviating rough parameter knowledge—is feasible.

Remark 2.32. *Consider a system in the frequency domain given by* $F(s)$ *as in* (2.35) *with relative degree* $r \geq 1$ *and root locus center* $\Xi(N, D)$ *as in* (2.39) *and introduce the following input (or output) filter*

$$\begin{aligned} F_F(s) \;&:= \tfrac{u(s)}{u_F(s)} \left(:= \tfrac{y_F(s)}{y(s)} \right) \\ &:= \gamma_F \tfrac{N_F(s)}{D_F(s)} := \gamma_F \textstyle\prod_{i=1}^{n_F} \dfrac{(s - z_i(N_F))}{(s - p_i(N_F))}, \end{aligned} \qquad \begin{aligned} &\gamma_F > 0,\ n_F \in \mathbb{N}, \\ &N_F,\ D_F \in \mathbb{R}[s],\ \textit{monic and coprime}, \\ &\Re(z_i),\ \Re(p_i) < 0 \,\forall\, i \in \{1, \ldots, n_F\}. \end{aligned} \tag{2.77}$$

with relative degree zero. In view of Definition 2.16 the root locus center of the serial intercon-

nection $F_F(s)F(s)$ (or $F(s)F_F(s)$) is given by

$$\frac{1}{r}\left(\sum_{i=1}^{n} p_i(D) - \sum_{i=1}^{m} z_i(N) + \sum_{i=1}^{n_F}(p_i(D_F) - z_i(N_F))\right) = \Xi(N,D) + \frac{1}{r}\sum_{i=1}^{n_F}(p_i(D_F) - z_i(N_F))\,,$$

hence an adequate choice of the zeros $z_1(N_F),\dots,z_{n_F}(N_F)$ and poles $p_1(D_F),\dots,p_{n_F}(D_F)$ of the filter in (2.77) yields an arbitrarily shift of the root locus center of the serial interconnection $F_F(s)F(s)$ (or $F(s)F_F(s)$). Again rough knowledge of the location of $\Xi(N,D)$ is required to achieve e.g. a shift into the left complex half plane.

2.3.4.2 High-gain adaptive controller with dynamic compensator

In 2007, motivated by finding an error in [129] (see Section 2.3.1), Hoagg and Bernstein present "*parameter-monotonic direct adaptive control*" of minimum-phase LTI SISO systems with known sign of and known upper bound on the high-frequency gain if only output feedback is admissible (see [80]). The proposed high-gain adaptive controllers incorporate dynamic compensators (similar to that presented in Section 2.2 but with time-varying gain) and (under the assumptions above) are capable to stabilize systems *either* with unknown but bounded relative degree r if an upper bound $\overline{r}$ on r is known (see [80, Theorem 8.1]) *or* with exactly known relative degree r (see [80, Theorem 8.2]). The more general first controller (see [80, Theorem 8.1]) is robust to uncertainties in the relative degree by the use of Fibanocci series in the gain exponents and is of order $\overline{r}$. The second controller is of order r (not accounting for gain adaption).

Since the relative degree of systems of class $\mathcal{S}_2^{\text{lin}}$ is exactly known and two, in the present work only a simplified version of Theorem 8.2 in [80] is presented. Notation is adopted from [80].

Theorem 2.33. *Consider a system of class $\mathcal{S}_2^{\text{lin}}$ described by (2.45). Let $b_0 \geq |\boldsymbol{c}^\top \boldsymbol{A}\boldsymbol{b}| > 0$ be known and choose $b_1, b_2 > 0$ such that*

$$s^3 + b_2\, s^2 + b_1\, s + \eta\, b_0 \in \mathbb{R}[s]$$

is Hurwitz for all $\eta \in (0,1]$, i.e. $b_1\, b_2 > b_0$. Then the dynamic compensator[5] with high-gain adaptive controller

$$\left.\begin{aligned} \dot{\hat{\boldsymbol{x}}}(t) &= \begin{bmatrix} -k(t)b_2 & 1 \\ -k(t)^2 b_1 & 0 \end{bmatrix}\hat{\boldsymbol{x}}(t) + \begin{bmatrix} 1 \\ \hat{z}_0 \end{bmatrix} y(t), && \hat{\boldsymbol{x}}(0) = \hat{\boldsymbol{x}}^0 \in \mathbb{R}^2 \\ u(t) &= -\operatorname{sign}(\boldsymbol{c}^\top \boldsymbol{A}\boldsymbol{b})\begin{pmatrix} k(t)^3, & 0 \end{pmatrix}\hat{\boldsymbol{x}}(t) && \text{where} \\ \dot{k}(t) &= \gamma \exp\big(-\alpha\, k(t)\big)\, y(t)^2, && k(0) = k_0 \end{aligned}\right\} \tag{2.78}$$

with design parameters $b_1, b_2 > 0$, $\hat{z}_0 > 0$, $\gamma, \alpha > 0$ and $k_0 > 0$ applied to (2.45) yields a closed-loop initial-value problem with the properties:

(i) there exists a unique and maximal solution $(\boldsymbol{x}, \hat{\boldsymbol{x}}, k) : [0, T) \to \mathbb{R}^n \times \mathbb{R}^2 \times \mathbb{R}_{\geq 0}$, $T \in (0, \infty]$;

(ii) the solution is global, i.e. $T = \infty$;

[5] Theorem 8.2 in [80] contained typing errors for the exponents of k in the compensator matrix. The errors are corrected here.

(iii) all signals are bounded, i.e. $(\boldsymbol{x}(\cdot),\, \hat{\boldsymbol{x}}(\cdot)) \in \mathcal{L}^\infty(\mathbb{R}_{\geq 0}; \mathbb{R}^n \times \mathbb{R}^2)$ *and* $k(\cdot) \in \mathcal{L}^\infty(\mathbb{R}_{\geq 0}; \mathbb{R}_{>0})$*;*

(iv) $\lim_{t\to\infty} \dot{k}(t) = 0$ *and* $\lim_{t\to\infty}(\boldsymbol{x}(t),\, \hat{\boldsymbol{x}}(t)) = (\mathbf{0}_n,\, \mathbf{0}_2)$*.*

Proof. see proof of Theorem 8.2 in [80]. □

Gain adaption in (2.78) exponentially decreases for large gains. Interesting to note that already in [129] the proposed gain adaption is proportional to $k(t)^{-(r-1)}$ for systems with relative degree $r \geq 2$. Deceleration of the gain adaption for large gains is essential for the proofs (see e.g. Lemma A.2 in [80] or (2.95) in the proof of Theorem 2.36).

Remark 2.34 (Design parameters γ, α, k_0, b_1, b_2 and $\hat{z}_0$.)**.**
The parameters γ *and* α *directly influence gain adaption, e.g.* $\gamma \gg 1$ *and* $\alpha \ll 1$ *accelerate whereas* $\gamma \ll 1$ *and* $\alpha \gg 1$ *decelerate gain adaption. A large initial gain* $k_0 \gg 1$ *probably yields "faster stabilization" than a small initial value* $k_0 \ll 1$ *(if the controlled system is unstable). The parameters* b_1, b_2 *(under restriction that* $b_1\, b_2 > b_0$*) and* $\hat{z}_0 > 0$ *permit tuning of the dynamic compensator in (2.78). However their influence on the response of the closed-loop system (2.78), (2.45) is not intuitive and hard to guess (see simulations in Section 2.3.4.4). A severe drawback for implementation.*

2.3.4.3 High-gain adaptive controller with derivative feedback

It was already shown in Section 2.3.4.1 that high-gain adaptive stabilization by simple output feedback (2.73) is feasible for systems with relative degree two if either the root locus center is located in or is shifted into the left complex half-plane. For the shift certain system parameters need to be known roughly. What about a "time-varying shift of the root locus center" by replacing the constant gain k_S in (2.73) by the time-varying (adapted) gain $k(t)$? Loosely speaking, this question can be answered affirmatively as will be shown in the following.

First a simple result is presented which reduces the problem of high-gain adaptive stabilization of systems of class $\mathcal{S}_2^{\text{lin}}$ to the problem of high-gain adaptive stabilization of systems of class $\mathcal{S}_1^{\text{lin}}$. The relative degree is reduced by introducing an augmented (auxiliary) output of the form

$$\hat{y}(t) := y(t) + q_1 \dot{y}(t) \quad \text{where} \quad q_1 > 0. \tag{2.79}$$

Moreover, if the original system (2.45) is minimum-phase, then the choice of $q_1 > 0$ in (2.79) retains the minimum-phase condition for the augmented system (2.45), (2.79). This approach is similar to that presented in [96] to allow for high-gain adaptive speed control of elastically coupled electrical drives.

Theorem 2.35. *Consider a system of class* $\mathcal{S}_2^{\text{lin}}$ *described by (2.45) and, for* $q_1 > 0$*, introduce the augmented output as in (2.79). Then the high-gain adaptive controller*

$$u(t) = -\operatorname{sign}(\boldsymbol{c}^\top \boldsymbol{A}\boldsymbol{b})\, k(t)\, \hat{y}(t) \quad \textit{where} \quad \dot{k}(t) = q_2\, |\hat{y}(t)|^{q_3}, \quad k(0) = k_0 \tag{2.80}$$

with design parameters $q_2 > 0$*,* $q_3 \geq 1$ *and* $k_0 > 0$ *applied to (2.45) yields a closed-loop initial-value problem with the properties (i)-(iv) as in Theorem 2.24.*

Proof of Theorem 2.35.
Without loss of generality, consider system (2.45) in BIF (2.54). Define $\hat{\boldsymbol{x}} := (y, \dot{y}, \boldsymbol{z}^\top)^\top$ and observe that (2.45) with output (2.79) can be written as

$$\begin{aligned} \tfrac{\mathrm{d}}{\mathrm{d}t}\,\hat{\boldsymbol{x}}(t) &= \underbrace{\begin{bmatrix} 0 & 1 & \boldsymbol{0}_{n-2}^\top \\ a_1 & a_2 & \boldsymbol{a}_3^\top \\ \boldsymbol{a}_4 & \boldsymbol{0}_{n-2} & \boldsymbol{A}_5 \end{bmatrix}}_{=:\hat{\boldsymbol{A}}} \hat{\boldsymbol{x}}(t) + \underbrace{\begin{pmatrix} 0 \\ \gamma_0 \\ \boldsymbol{0}_{n-2} \end{pmatrix}}_{=:\hat{\boldsymbol{b}}} u(t), \qquad \hat{\boldsymbol{x}}(0) = \boldsymbol{S}\boldsymbol{x}^0 \\ \hat{y}(t) &= \underbrace{\begin{pmatrix} 1 & q_1 & \boldsymbol{0}_{n-2}^\top \end{pmatrix}}_{=:\hat{\boldsymbol{c}}^\top} \hat{\boldsymbol{x}}(t) \end{aligned}$$

Moreover, it is easy to see that the following hold: (i) $\hat{\boldsymbol{c}}^\top \hat{\boldsymbol{b}} = q_1\,\gamma_0 \neq 0$ and $\operatorname{sign}(q_1\gamma_0) = \operatorname{sign}(\gamma_0)$ known, (ii) $\hat{y}$ is available for feedback and (iii)

$$\det \begin{bmatrix} s\boldsymbol{I}_n - \hat{\boldsymbol{A}} & \hat{\boldsymbol{b}} \\ \hat{\boldsymbol{c}}^\top & 0 \end{bmatrix} = |\gamma_0|(s\,q_1 + 1) \det\left(s\boldsymbol{I}_{n-2} - \boldsymbol{A}_5\right) \overset{(\mathcal{S}_2^{\mathrm{lin}}\text{-}sp_2)}{\neq} 0 \quad \forall\, s \in \mathbb{C}_{\geq 0}.$$

Hence system properties ($\mathcal{S}_1^{\mathrm{lin}}$-sp$_1$)-($\mathcal{S}_1^{\mathrm{lin}}$-sp$_3$) of class $\mathcal{S}_1^{\mathrm{lin}}$ are satisfied and Assertions (i)-(iv) follow from Theorem 2.24. This completes the proof. □

Theorem 2.35 guarantees asymptotic stabilization of systems of class $\mathcal{S}_2^{\mathrm{lin}}$ without additional assumptions. Moreover, this result can easily be generalized to adaptive λ-tracking (see Section 3.4) such that control objective (co$_2$) holds for $e(t)$ replaced by $\hat{y}_{\mathrm{ref}}(t) - \hat{y}(t)$, i.e.

$$\forall\, \lambda > 0\colon \qquad \lim_{t\to\infty} \operatorname{dist}\left(|\hat{y}_{\mathrm{ref}}(t) - \hat{y}(t)|, [0, \lambda]\right) = 0.$$

where $\hat{y}_{\mathrm{ref}}(\cdot) \in \mathcal{W}^{1,\infty}(\mathbb{R}_{\geq 0}; \mathbb{R})$ is some feasible reference. Nevertheless, the introduction of the augmented output (2.79) is unattractive, since in general no statements can be made on the asymptotic tracking accuracy of the "original error" $e(\cdot) = y_{\mathrm{ref}}(\cdot) - y(\cdot)$.

Motivated by the approach of Hoagg and Bernstein (see Section 2.3.4.2), the following result was found incorporating derivative feedback (admissible for systems of class $\mathcal{S}_2^{\mathrm{lin}}$) instead of a dynamic compensator. It will allow for a generalization to adaptive λ-tracking control and, in addition, will ensure control objective (co$_2$) (see Section 3.5.3).

Theorem 2.36 (High-gain adaptive control with derivative feedback for systems of class $\mathcal{S}_2^{\mathrm{lin}}$)**.**
Consider a system of class $\mathcal{S}_2^{\mathrm{lin}}$ described by (2.45). The high-gain adaptive controller

$$\left.\begin{aligned} u(t) &= -\operatorname{sign}(\boldsymbol{c}^\top \boldsymbol{A}\boldsymbol{b}) \left(k(t)^2\, y(t) + q_1\, k(t)\, \dot{y}(t)\right) && \text{where} \\ \dot{k}(t) &= q_2 \exp(-q_3\, k(t)) \left\|(y(t),\, \dot{y}(t))^\top\right\|^2, && k(0) = k_0 \end{aligned}\right\} \tag{2.81}$$

with design parameters $q_1, q_2, q_3 > 0$ and $k_0 > 0$ applied to (2.45) yields a closed-loop initial-value problem with the properties (i)-(iv) as in Theorem 2.24.

Remark 2.37 (Design parameters q_1, q_2, q_3 and k_0)**.**
The factor $q_1 > 0$ in (2.81) allows for active damping of the closed-loop system (2.45), (2.81).

Simulations (see Section 2.3.4.4) show that, if a lower bound $\underline{\gamma_0} > 0$ on the high-frequency gain $\gamma_0 = \boldsymbol{c}^\top \boldsymbol{A}\boldsymbol{b}$ is known such that $|\gamma_0| \geq \underline{\gamma_0}$, then (at least) for a second order system the choice $q_1 \geq 2/\sqrt{\underline{\gamma_0}}$ yields an "overdamped" (or a "critically damped") closed-loop system (in the sense of Example 11.3.7 in [24, p. 717-718]). This observation will be important in view of application in real world (see Chapter 5). The parameters $q_2 > 0$ and $q_3 > 0$ directly affect gain adaption and allow for acceleration or deceleration of adaption speed. The parameter $k_0 > 0$ allows to fix a first guess for the initial gain.

Proof of Theorem 2.36.

Step 1: It is shown that Assertion (i) holds true, i.e. existence of a unique solution maximally extended on $[0, T)$, $T \in (0, \infty]$.
It suffices to consider system (2.45) in the form (2.54). Define

$$\mathcal{D} := \mathbb{R}^2 \times \mathbb{R}^{n-2} \times \mathbb{R}_{>0} \qquad \text{and} \qquad \mathcal{I} := \mathbb{R}$$

and the function

$$\boldsymbol{f}\colon\ \mathcal{I} \times \mathcal{D} \to \mathcal{D}, \quad (t, (\boldsymbol{\mu}, \boldsymbol{\xi}, \kappa)) \mapsto \begin{pmatrix} \begin{bmatrix} 0 & 1 \\ a_1 - |\gamma_0|\kappa^2 & a_2 - q_1|\gamma_0|\kappa \end{bmatrix} \boldsymbol{\mu} + \begin{bmatrix} \boldsymbol{0}^\top \\ \boldsymbol{a}_3^\top \end{bmatrix} \boldsymbol{\xi} \\ \begin{bmatrix} \boldsymbol{a}_4 & \boldsymbol{0} \end{bmatrix} \boldsymbol{\mu} + \boldsymbol{A}_5 \boldsymbol{\xi} \\ q_2 \exp(-q_3\,\kappa)\, \|\boldsymbol{\mu}\|^2 \end{pmatrix}.$$

Then, for $\boldsymbol{S}$ as in (2.24) (with $r = 2$) and $\hat{\boldsymbol{x}} := ((y, \dot{y})^\top, \boldsymbol{z}^\top, k)^\top$, the closed-loop initial-value problem (2.54), (2.81) can be expressed in the form (2.60). Note that the function $\boldsymbol{f}(\cdot, \cdot)$ is continuous for all $(t, (\boldsymbol{\mu}, \boldsymbol{\xi}, \kappa)) \in \mathcal{I} \times \mathcal{D}$ and for every compact $\mathfrak{C} \subset \mathcal{I} \times \mathcal{D}$ there exists $M_{\mathfrak{C}} > 0$ such that $\left\|(t, (\boldsymbol{\mu}^\top, \boldsymbol{\xi}^\top, \kappa)^\top)\right\| \leq M_{\mathfrak{C}}$ for all $(t, (\boldsymbol{\mu}, \boldsymbol{\xi}, \kappa)) \in \mathfrak{C}$. Furthermore, for all $(t, (\boldsymbol{\mu}, \boldsymbol{\xi}, \kappa))$, $(t, (\tilde{\boldsymbol{\mu}}, \tilde{\boldsymbol{\xi}}, \tilde{\kappa})) \in \mathfrak{C}$, the following holds

$$\begin{aligned} \left\|\boldsymbol{f}(t, (\boldsymbol{\mu}, \boldsymbol{\xi}, \kappa)) - \boldsymbol{f}(t, (\tilde{\boldsymbol{\mu}}, \tilde{\boldsymbol{\xi}}, \tilde{\kappa})\right\| \ \leq\ & \Big(\left\| \left[\begin{smallmatrix} 0 & 1 \\ a_1 & a_2 \end{smallmatrix}\right] \right\| + \|\boldsymbol{a}_4\| + \\ & M_{\mathfrak{C}} \left(2q_2 \exp(-q_3 k_0) + |\gamma_0|(M_{\mathfrak{C}} + q_1)\right) \Big) \|\boldsymbol{\mu} - \tilde{\boldsymbol{\mu}}\| + \\ & (\|\boldsymbol{a}_3\| + \|\boldsymbol{A}_5\|) \left\|\boldsymbol{\xi} - \tilde{\boldsymbol{\xi}}\right\| + |\gamma_0| M_{\mathfrak{C}} (q_1 + 2M_{\mathfrak{C}}) |\kappa - \tilde{\kappa}|, \end{aligned}$$

which shows that $\boldsymbol{f}(\cdot, \cdot)$ is locally Lipschitz continuous (with respect to $(\boldsymbol{\mu}, \boldsymbol{\xi}, \kappa) \in \mathcal{D}$). Hence Theorem 2.20 yields existence and uniqueness of a solution $\hat{\boldsymbol{x}} = ((y, \dot{y})^\top, \boldsymbol{z}^\top, k)^\top\colon\ [0, T) \to \mathbb{R}^2 \times \mathbb{R}^{n-2} \times \mathbb{R}_{>0}$ of the initial-value problem (2.60) with maximal $T \in (0, \infty]$ (the interval $(T_-, 0)$ is neglected). Clearly, $(\boldsymbol{x}, k) = (\boldsymbol{S}^{-1}(y, \dot{y}, \boldsymbol{z}), k)\colon [0, T) \to \mathbb{R}^n \times \mathbb{R}_{>0}$ solves the closed-loop initial-value problem (2.45), (2.81), which shows Assertion (i) and completes Step 1.

Step 2: Some technical inequalities are shown.
Introduce

$$\boldsymbol{A}_1\colon\ [k_0, \infty) \to \mathbb{R}^{2\times 2}, \quad k \mapsto \boldsymbol{A}_1(k) := \begin{bmatrix} 0 & 1 \\ -|\gamma_0|k^2 & -q_1|\gamma_0|k \end{bmatrix}$$

and

$$\boldsymbol{P}_1\colon\ [k_0,\infty)\to\mathbb{R}^{2\times 2},\quad k\mapsto \boldsymbol{P}_1(k):=\frac{1}{2|\gamma_0|}\begin{bmatrix}\frac{1}{q_1}+\frac{|\gamma_0|k^2}{q_1}+q_1|\gamma_0| & \frac{1}{k}\\ \frac{1}{k} & \frac{1}{|\gamma_0|k^2q_1}+\frac{1}{q_1}\end{bmatrix}.$$

For

$$p_{11}(k):=\frac{\left(\frac{1}{q_1}+\frac{|\gamma_0|k^2}{q_1}+q_1|\gamma_0|\right)}{2|\gamma_0|}>0,\ p_{12}(k):=\frac{1}{2|\gamma_0|k}>0\ \text{ and }\ p_{22}(k):=\frac{\left(\frac{1}{|\gamma_0|k^2}+1\right)}{2q_1|\gamma_0|}>0 \tag{2.82}$$

note that

$$\forall\, k\geq k_1:=\max\{q_1/2,\,1/\sqrt{|\gamma_0|}\}>0\colon\qquad 0<p_{12}(k)+p_{22}(k)\leq 2/(q_1|\gamma_0|). \tag{2.83}$$

In view of (2.82) observe that $p_{11}(k)\,p_{22}(k)-p_{12}(k)^2>0$ for all $k\geq k_0$ and hence it is easy to see that

$$\forall\, k\geq k_0>0\colon\quad \boldsymbol{P}_1(k)=\boldsymbol{P}_1(k)^\top>0\quad\text{ and }\quad \boldsymbol{A}_1(k)^\top\boldsymbol{P}_1(k)+\boldsymbol{P}_1(k)\boldsymbol{A}_1(k)=-k\boldsymbol{I}_2. \tag{2.84}$$

Moreover, since $\boldsymbol{P}_1(\cdot)\in\mathcal{C}^\infty([k_0,\infty);\mathbb{R}^{2\times 2})$, it follows that

$$\forall\, k\geq k_0>0\colon\quad \frac{\partial \boldsymbol{P}_1(k)}{\partial k}=\frac{1}{2|\gamma_0|}\begin{bmatrix}\frac{2|\gamma_0|k}{q_1} & -\frac{1}{k^2}\\ -\frac{1}{k^2} & -\frac{2}{|\gamma_0|k^3q_1}\end{bmatrix}.$$

For any $q_3>0$, simple calculations show that the following holds

$$\begin{aligned}&\forall k\geq k_2:=2\max\{1/q_3,\,1/q_2\}+1>0\colon\\ &q_3\left(\frac{1}{q_1}+\frac{|\gamma_0|k^2}{q_1}+q_1|\gamma_0|\right)-\frac{2|\gamma_0|k}{q_1}>0\quad\text{ and}\\ &\left(q_3\left(\frac{1}{q_1}+\frac{|\gamma_0|k^2}{q_1}+q_1|\gamma_0|\right)-\frac{2|\gamma_0|k}{q_1}\right)\left(q_3\left(\frac{1}{|\gamma_0|k^2q_1}+\frac{1}{q_1}\right)+\frac{2}{|\gamma_0|k^3q_1}\right)-\left(\frac{q_3}{k}+\frac{1}{k^2}\right)^2>0\end{aligned} \tag{2.85}$$

and hence

$$\forall k\geq k_2\colon\qquad q_3\boldsymbol{P}_1(k)-\frac{\partial \boldsymbol{P}_1(k)}{\partial k}>0. \tag{2.86}$$

Due to ($\mathcal{S}_2^{\text{lin}}$-sp$_2$) and Lemma 2.12, the matrix $\boldsymbol{A}_5$ is a Hurwitz matrix, i.e. $\operatorname{spec}(\boldsymbol{A}_5)\subset\mathbb{C}_{<0}$, and therefore

$$\exists\,\text{a unique}\ \ 0<\boldsymbol{P}_5^\top=\boldsymbol{P}_5\in\mathbb{R}^{(n-2)\times(n-2)}\colon\qquad \boldsymbol{A}_5^\top\boldsymbol{P}_5+\boldsymbol{P}_5\boldsymbol{A}_5=-\boldsymbol{I}_{n-2}. \tag{2.87}$$

For notational brevity, define

$$\forall\, t\geq 0\colon\qquad \boldsymbol{w}(t):=(y(t),\dot{y}(t))^\top$$

and, for $\boldsymbol{P}_1(k(t))$ as in (2.84) and $\boldsymbol{P}_5$ as in (2.87), introduce the Lyapunov-like function

$$\begin{aligned} V\colon \mathbb{R}^2 \times \mathbb{R}^{n-2} \times [k_0, \infty) &\to \mathbb{R}_{\geq 0}, \\ (\boldsymbol{w}, \boldsymbol{z}, k) &\mapsto V(\boldsymbol{w}, \boldsymbol{z}, k) := \exp(-q_3\, k) \left(\boldsymbol{w}^\top \boldsymbol{P}_1(k) \boldsymbol{w} + \boldsymbol{z}^\top \boldsymbol{P}_5 \boldsymbol{z} \right) \geq 0. \end{aligned} \tag{2.88}$$

The time derivative $\frac{\mathrm{d}}{\mathrm{d}t} V(\cdot)$ along the solution of the closed-loop (2.54), (2.81) is given as follows

$$\begin{aligned} \forall\, t \in [0, T)\colon \ \frac{\mathrm{d}}{\mathrm{d}t} V(\boldsymbol{w}(t), \boldsymbol{z}(t), k(t)) \ = \ & \exp(-q_3\, k(t)) \Big\{ 2\boldsymbol{w}(t)^\top \boldsymbol{P}_1(k(t)) \dot{\boldsymbol{w}}(t) + 2\boldsymbol{z}(t)^\top \boldsymbol{P}_5 \dot{\boldsymbol{z}}(t) \\ & - \dot{k}(t) \boldsymbol{w}(t)^\top \left(q_3 \boldsymbol{P}_1(k(t)) - \frac{\partial \boldsymbol{P}_1(k(t))}{\partial k} \right) \boldsymbol{w}(t) \\ & - q_3 \dot{k}(t) \boldsymbol{z}(t)^\top \boldsymbol{P}_5 \boldsymbol{z}(t) \Big\}. \end{aligned} \tag{2.89}$$

Furthermore note that, for $l \in \mathbb{N}$ and for $p_{12}(k)$ and $p_{22}(k)$ as in (2.82), the following holds

$$\forall\, \boldsymbol{\alpha},\, \boldsymbol{\beta} \in \mathbb{R}^l\colon \ \left\| \boldsymbol{P}_1(k) \begin{bmatrix} \boldsymbol{0}_l^\top \\ \boldsymbol{\alpha}^\top \end{bmatrix} \boldsymbol{\beta} \right\| = \left\| \begin{bmatrix} p_{12}(k)\, \boldsymbol{\alpha}^\top \\ p_{22}(k)\, \boldsymbol{\alpha}^\top \end{bmatrix} \boldsymbol{\beta} \right\| \leq (p_{12}(k) + p_{22}(k)) \, \|\boldsymbol{\alpha}\| \, \|\boldsymbol{\beta}\| \,. \tag{2.90}$$

Invoking (2.54), (2.81) yields

$$\begin{aligned} \forall\, t \in [0, T)\colon \ 2\boldsymbol{w}(t)^\top \boldsymbol{P}_1(k(t)) \dot{\boldsymbol{w}}(t) \ & \overset{(2.84)}{\leq} \ -k(t) \, \|\boldsymbol{w}(t)\|^2 + 2 \, \|\boldsymbol{w}(t)\| \left\| \boldsymbol{P}_1(k(t)) \begin{bmatrix} 0 & 0 \\ a_1 & a_2 \end{bmatrix} \boldsymbol{w}(t) \right\| \\ & \quad + 2 \, \|\boldsymbol{w}(t)\| \left\| \boldsymbol{P}_1(k(t)) \begin{bmatrix} \boldsymbol{0}^\top \\ \boldsymbol{a}_3^\top \end{bmatrix} \boldsymbol{z}(t) \right\| \\ & \overset{(2.90)}{\leq} \ -k(t) \, \|\boldsymbol{w}(t)\|^2 + 2 \, \|\boldsymbol{w}(t)\| \left(p_{12}(k(t)) + p_{22}(k(t)) \right) \\ & \quad \cdot \left(\left\| (a_1, a_2)^\top \right\| \, \|\boldsymbol{w}(t)\| + \|\boldsymbol{a}_3\| \, \|\boldsymbol{z}(t)\| \right) \\ & \overset{(2.62)}{\leq} \ -\Big(k(t) - 2\big(p_{12}(k(t)) + p_{22}(k(t)) \big) \left\| (a_1, a_2)^\top \right\| \\ & \quad - 4 \big(p_{12}(k(t)) + p_{22}(k(t)) \big)^2 \, \|\boldsymbol{a}_3\|^2 \Big) \, \|\boldsymbol{w}(t)\|^2 - \frac{1}{4} \, \|\boldsymbol{z}(t)\|^2 \end{aligned} \tag{2.91}$$

and

$$\begin{aligned} \forall\, t \in [0, T)\colon \qquad 2\boldsymbol{z}(t)^\top \boldsymbol{P}_5 \dot{\boldsymbol{z}}(t) \ & \overset{(2.87)}{\leq} \ - \|\boldsymbol{z}(t)\|^2 + 2 \, \|\boldsymbol{z}(t)\| \, \|\boldsymbol{P}_5\| \, \|\boldsymbol{a}_4\| \, \|\boldsymbol{w}(t)\| \\ & \overset{(2.62)}{\leq} \ -\frac{3}{4} \, \|\boldsymbol{z}(t)\|^2 + 4 \, \|\boldsymbol{P}_5\|^2 \, \|\boldsymbol{a}_4\|^2 \, \|\boldsymbol{w}(t)\|^2 \,, \end{aligned} \tag{2.92}$$

respectively.

Step 3: It is shown that $k(\cdot)$ is bounded on $[0,T)$.
Seeking a contradiction, assume that $k(\cdot)$ is unbounded on $[0,T)$. In view of (2.81), $k(\cdot)$ is non-decreasing on $[0,T)$, therefore with k_1 as in (2.83) and k_2 as in (2.85)

$$\exists\, t^\star \geq 0\, \forall\, t \in [t^\star, T):\ k(t) \geq \max\left\{k_1,\, k_2,\, q_2 + \frac{4\left\|(a_1,a_2)^\top\right\|}{q_1|\gamma_0|} + \frac{16\left\|\boldsymbol{a}_3\right\|^2}{q_1^2|\gamma_0|^2} + 4\left\|\boldsymbol{P}_5\right\|^2\left\|\boldsymbol{a}_4\right\|^2\right\}. \tag{2.93}$$

Moreover, in view of (2.89), it follows that for all $t \in [t^\star, T)$

$$\begin{aligned}
\frac{\mathrm{d}}{\mathrm{d}t} V(\boldsymbol{w}(t), \boldsymbol{z}(t), k(t)) &\overset{(2.86),(2.81)}{\leq} \exp(-q_3\, k(t))\Big\{2\boldsymbol{w}(t)^\top \boldsymbol{P}_1(k(t))\dot{\boldsymbol{w}}(t) + 2\boldsymbol{z}(t)^\top \boldsymbol{P}_5 \dot{\boldsymbol{z}}(t)\Big\} \qquad (2.94)\\
&\overset{(2.91),(2.92)}{\leq} \exp(-q_3\, k(t))\Bigg\{ -\Big(k(t) - 2\big(p_{12}(k(t)) + p_{22}(k(t))\big)\left\|(a_1,a_2)^\top\right\|\\
&\quad -4\big(p_{12}(k(t)) + p_{22}(k(t))\big)^2\left\|\boldsymbol{a}_3\right\|^2 - 4\left\|\boldsymbol{P}_5\right\|^2\left\|\boldsymbol{a}_4\right\|^2\Big)\left\|\boldsymbol{w}(t)\right\|^2\\
&\quad -\frac{1}{2}\left\|\boldsymbol{z}(t)\right\|^2\Bigg\}\\
&\overset{(2.83)}{\leq} \exp(-q_3\, k(t))\Bigg\{ -\Big(k(t) - q_2 - \frac{4}{q_1|\gamma_0|}\left\|(a_1,a_2)^\top\right\|\\
&\quad -\frac{16}{q_1^2|\gamma_0|^2}\left\|\boldsymbol{a}_3\right\|^2 - 4\left\|\boldsymbol{P}_5\right\|^2\left\|\boldsymbol{a}_4\right\|^2\Big)\left\|\boldsymbol{w}(t)\right\|^2\\
&\quad -\frac{1}{2}\left\|\boldsymbol{z}(t)\right\|^2 - q_2\left\|\boldsymbol{w}(t)\right\|^2\Bigg\}\\
&\overset{(2.93)}{\leq} -q_2\exp(-q_3\, k(t))\left\|\boldsymbol{w}(t)\right\|^2 \overset{(2.81)}{=} -\dot{k}(t). \qquad (2.95)
\end{aligned}$$

Integration from $t^\star$ to $t < T$ and solving for $k(t)$ yields

$$\forall\, t \in [t^\star, T):\qquad k(t) \leq V(\boldsymbol{w}(t^\star), \boldsymbol{z}(t^\star), k(t^\star)) + k(t^\star)$$

and since $[0, t^\star]$ is compact and $\boldsymbol{w}(\cdot)$, $\boldsymbol{z}(\cdot)$ and $k(\cdot)$ are continuous on $[0,T)$ the contradiction follows.

Step 4: It is shown that Assertions (ii) holds true, i.e. $T = \infty$.
From Step 1 & 3 and (2.81) it follows that $k(\cdot)$ is continuous, non-deacreasing and bounded on $[0,T)$. Hence the limit

$$k_\infty := \lim_{t\to T} k(t) \geq k_0 > 0 \tag{2.96}$$

exists and observe that for the closed-loop initial-value problem (2.54), (2.81) (neglecting the

adaption in (2.81)) the following holds

$$\forall\, t \in [0,T)\colon\ \left\| \frac{\mathrm{d}}{\mathrm{d}t} \begin{pmatrix} \boldsymbol{w}(t) \\ \boldsymbol{z}(t) \end{pmatrix} \right\| \leq \left(\left\| \begin{bmatrix} 0 & 1 \\ a_1 & a_2 \end{bmatrix} \right\| + |\gamma_0| k_\infty \big(k_\infty + q_1\big) + \|\boldsymbol{a}_3\| + \|\boldsymbol{a}_4\| + \|\boldsymbol{A}_5\| \right) \left\| \begin{pmatrix} \boldsymbol{w}(t) \\ \boldsymbol{z}(t) \end{pmatrix} \right\|,$$

which with Proposition 2.1.19 in [77, p. 86] implies, by maximality of T, that $T = \infty$. This shows Assertion (ii) and completes Step 4.

Step 5: It is shown that Assertions (iii) and (iv) hold true, i.e. $k(\cdot) \in \mathcal{L}^\infty(\mathbb{R}_{\geq 0}; \mathbb{R}_{>0})$, $\boldsymbol{x}(\cdot) \in \mathcal{L}^\infty(\mathbb{R}_{\geq 0}; \mathbb{R}^n)$, $\lim_{t\to\infty} \dot{k}(t) = 0$ *and* $\lim_{t\to\infty} \boldsymbol{x}(t) = \boldsymbol{0}_n$.
From Step 3 and 4 it directly follows that $k(\cdot) \in \mathcal{L}^\infty(\mathbb{R}_{\geq 0}; \mathbb{R}_{>0})$. Moreover, for k_∞ as in (2.96) the following holds

$$\forall\, t \geq 0\colon\ q_2 \exp(-q_3 k_\infty) \int_0^t \left\| (y(\tau), \dot{y}(\tau))^\top \right\|^2 \mathrm{d}\tau \overset{(2.81)}{\leq} \int_0^t \dot{k}(\tau)\, \mathrm{d}\tau = k(t) - k(0) < k_\infty < \infty,$$

which implies $(y(\cdot), \dot{y}(\cdot))^\top \in \mathcal{L}^2(\mathbb{R}_{\geq 0}; \mathbb{R}^2)$. Hence, in view of the second equation in (2.54) and due to $\operatorname{spec}(\boldsymbol{A}_5) \subset \mathbb{C}_{<0}$, it also follows that $\boldsymbol{z}(\cdot) \in \mathcal{L}^2(\mathbb{R}_{\geq 0}; \mathbb{R}^{n-2})$. Invoking (2.54) again yields

$$\frac{\mathrm{d}}{\mathrm{d}t} (y(\cdot), \dot{y}(\cdot))^\top \in \mathcal{L}^2(\mathbb{R}_{\geq 0}; \mathbb{R}^2) \qquad \text{and} \qquad \dot{\boldsymbol{z}}(\cdot) \in \mathcal{L}^2(\mathbb{R}_{\geq 0}; \mathbb{R}^{n-2}),$$

respectively. Combining the results above and applying Lemma 2.1.7 in [86, p. 17] yields $(y(\cdot), \dot{y}(\cdot))^\top \in \mathcal{L}^\infty(\mathbb{R}_{\geq 0}; \mathbb{R}^2)$ and $\boldsymbol{z}(\cdot) \in \mathcal{L}^\infty(\mathbb{R}_{\geq 0}; \mathbb{R}^{n-2})$, which with $\boldsymbol{S}^{-1}$ as in (2.24) gives

$$\boldsymbol{x}(\cdot) = \boldsymbol{S}^{-1}((y(\cdot), \dot{y}(\cdot))^\top, \boldsymbol{z}(\cdot)^\top)^\top \in \mathcal{L}^\infty(\mathbb{R}_{\geq 0}; \mathbb{R}^n)$$

and hence Assertion (iii) is shown. Furthermore, Lemma 2.1.7 in [86, p. 17] also gives

$$\lim_{t\to\infty} (y(t), \dot{y}(t))^\top = \boldsymbol{0}_2 \qquad \text{and} \qquad \lim_{t\to\infty} \boldsymbol{z}(t) = \boldsymbol{0}_{n-2}$$

which implies

$$\lim_{t\to\infty} \dot{k}(t) \leq q_2 \exp(-q_3\, k_0) \lim_{t\to\infty} \left\| \begin{pmatrix} y(t) \\ \dot{y}(t) \end{pmatrix} \right\|^2 = 0 \qquad \text{and}$$
$$\lim_{t\to\infty} \boldsymbol{x}(t) = \lim_{t\to\infty} \boldsymbol{S}^{-1}((y(t), \dot{y}(t))^\top, \boldsymbol{z}(t)^\top)^\top = \boldsymbol{0}_n.$$

Hence Assertion (iv) is shown. This completes the proof of Theorem 2.36. □

Remark 2.38. *There exists an alternative to controller* (2.80) *which also achieves high-gain adaptive stabilization of systems of class* $\mathcal{S}_2^{\mathrm{lin}}$. *If* (2.81) *is replaced by*

$$\begin{aligned} u(t) &= -\operatorname{sign}(\boldsymbol{c}^\top \boldsymbol{A}\boldsymbol{b}) \big(k(t)\, y(t) + \tfrac{d}{dt} (k(t) y(t)) \big) \qquad \textit{where} \\ \dot{k}(t) &= |y(t)|^p,\ p \geq 1 \quad k(0) = k_0 > 0, \end{aligned} \tag{2.97}$$

then Assertions (i)-(vi) of Theorem 2.24 also hold true (see [85, Proposition 4.1]). The slightly more complex controller (2.81) *has been introduced since it paved the way for and lead to the adaptive* λ*-tracking controller* (3.46) *proposed in Section 3.5.3. It was not possible to general-*

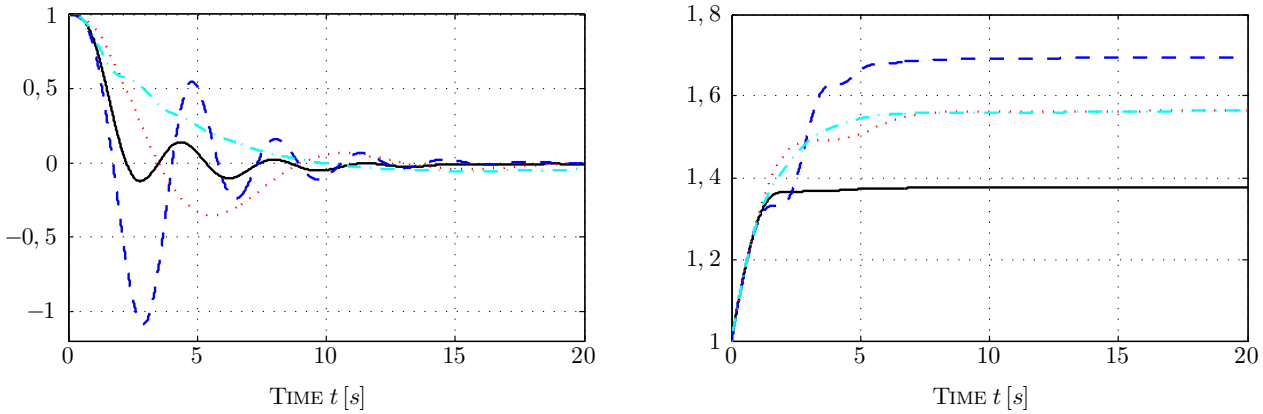

(a) *output* $y(\cdot)$ *for different designs.* (b) *gain* $k(\cdot)$ *for different designs.*

Figure 2.5: *Simulation results for closed-loop system* (2.74), (2.78) *with* $(y_0, y_1) = (1, 0)$, $a_1 = a_2 = 0$, $\gamma_0 = k_0 = b_0 = \gamma = \alpha = 1$ *and* $(b_1, b_2, \hat{z}_0) \in \{$ —— $(2, 1, 0.1)$, - - - - $(2, 1, 1)$, ····· $(2, 5, 0.1)$, -·-·- $(5, 1, 0.1)\}$.

ize (2.97) *to the adaptive* λ*-tracking problem.*

2.3.4.4 Simulations

To investigate the influence of the design parameters of controller (2.78) and (2.81) on the closed-loop system response, both controllers are applied to the exemplary system (2.74) with initial value $(y_0, y_1) = (1, 0)$ and system parameters $a_1 = a_2 = 0$ and $\gamma_0 = 1$. Both closed-loop systems (2.74), (2.78) and (2.74), (2.81) are implemented in Matlab/Simulink.

For the upcoming simulations, only the design parameters $(b_1, b_2, \hat{z}_0)$ of (2.78) and q_1 of (2.81) are modified (see caption of Fig. 2.5 and 2.6). Clearly, the remaining design parameters—i.e. γ, α, k_0 for (2.78) and q_2, q_3, k_0 for (2.81)—only affect gain adaption (adaption speed) and initial gain and so only change the transient response quantitatively (in the sense of a time-scaling in Fig. 2.5 and 2.6, resp.). For simplicity, these tuning parameters are set to one (see captions of Fig. 2.5 and 2.6). The simulation results of the closed-loop system (2.74), (2.78) and (2.74), (2.81) are shown in Fig. 2.5 and Fig. 2.6, respectively.

Discussion for high-gain adaptive controller with dynamic compensator (2.78)*:* Simulation studies reveal (see Fig. 2.5) the following influence of the design parameters $(b_1, b_2, \hat{z}_0)$ on the closed-loop performance (identical behavior was also observed for different values of $\gamma_0 \neq 1$): (i) $b_1 > \max\{b_2, \hat{z}_0\}\gamma_0$ yields a response with nearly no overshoot and small oscillations but "slow" convergence (see -·-·-), (ii) $10\gamma_0 > b_2 \geq \max\{b_1, \hat{z}_0\}\gamma_0$ leads to oscillations with overshoot (see ·····), (iii) $b_2 \gg \max\{b_1, \hat{z}_0\}\gamma_0$ and $\hat{z}_0 \gg \max\{b_1, b_2\}\gamma_0$ result in "brief destabilization" and turbulent but decaying oscillations with large amplitudes ($\gg 10$) and high frequency (not shown due to scaling), (iv) $\hat{z}_0 \approx \max\{b_1, b_2\}\gamma_0$ gives - - - - with large overshoot and (v) $\hat{z}_0 \ll \max\{b_1, b_2\}\gamma_0$ yields —— with small overshoot and fast decay. To conclude, control design of (2.78) is not intuitive and must be performed by trial and error. Moreover, design parameters do not have a distinct influence on the control performance.

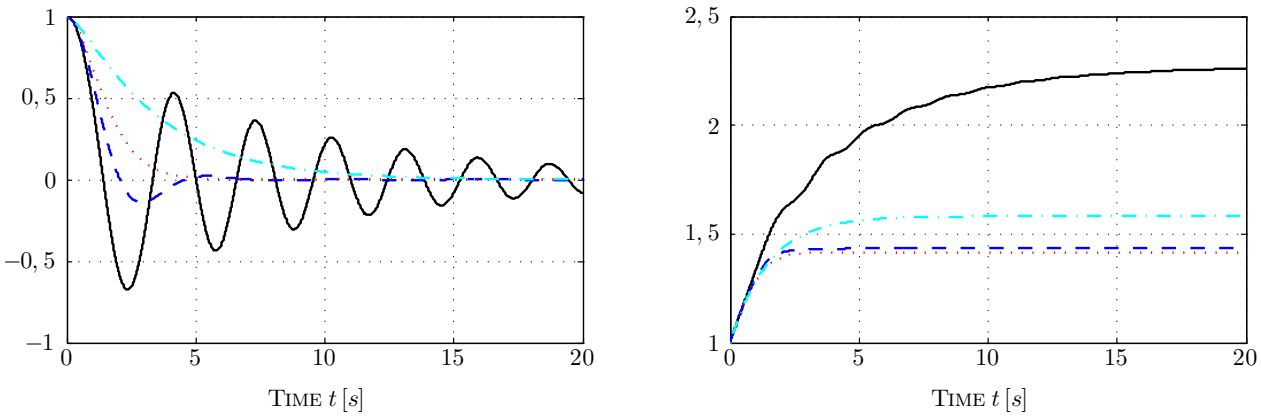

(a) *output* $y(\cdot)$ *for different designs.* (b) *gain* $k(\cdot)$ *for different designs.*

Figure 2.6: *Simulation results for closed-loop system* (2.74), (2.81) *with* $(y_0, y_1) = (1, 0)$, $a_1 = a_2 = 0$, $\gamma_0 = k_0 = q_2 = q_3 = 1$ *and* $q_1 \in \{$ —— 0.1, - - - 1, ····· 2, -·-· 5$\}$.

Discussion for high-gain adaptive controller with derivative feedback (2.81)*:* The damping of the closed-loop system (2.74), (2.81) is easily tuned by variation of q_1 (see Fig. 2.6). It is well known that (weighted) feedback of the output derivative increases damping (see e.g. [174, p. 212-213]). The following observations also hold for $\gamma_0 \neq 1$ and $y_0 \neq 1$ (even though no simulation results are shown). For $q_1 < 2\sqrt{\gamma_0}$, the closed-loop system response exhibits oscillations with increasing amplitude and frequency for decreasing values of q_1. For $q_1 \geq 2\sqrt{\gamma_0}$, the system response is "overdamped", i.e. no overshoot occurs. However, the larger q_1 is chosen, the slower is the closed-loop system response (2.74), (2.81) (see Fig. 2.6).

The influence of q_1 on the closed-loop system (2.74), (2.81) may be explained by the following linear analysis. Application of $u(t) = k^2 y(t) + q_1 k \dot{y}(t)$ with *constant* $k > 0$ to (2.74) with $a_1 = a_2 = 0$ and $\gamma_0 > 0$ yields the harmonic oscillator

$$\ddot{y}(t) + \gamma_0 q_1 k \dot{y}(t) + \gamma_0 k^2 y(t) = 0. \tag{2.98}$$

To obtain an "overdamped" (or a "critically damped") oscillator (2.98) (in the sense of Example 11.3.7 in [24, p. 717-718]) the eigenvalues must satisfy

$$p_{1,2} = -\frac{\gamma_0 q_1 k}{2}\left(1 \pm \sqrt{1 - 4/(\gamma_0 q_1^2)}\right) < 0.$$

If $\gamma_0 \geq \underline{\gamma_0} > 0$ and $\underline{\gamma_0}$ is known, the choice $k > 0$ and $q_1 \geq 2/\sqrt{\underline{\gamma_0}}$ implies $0 \leq 1 - 4/(\gamma_0 q_1^2) < 1$. Clearly, the argumentation above only holds for linear time-invariant systems, nevertheless simulation studies (e.g. in Fig. 2.6) indicate a similar behavior for the time-varying controller (2.81).

2.4 High-gain adaptive tracking with internal model

This far only stabilization of systems of form (2.45) either element of class $\mathcal{S}_1^{\text{lin}}$ or class $\mathcal{S}_2^{\text{lin}}$ was discussed. What happens if reference signals $y_{\text{ref}} \colon \mathbb{R}_{\geq 0} \to \mathbb{R}$ are to be tracked by the system output $y(\cdot)$? Are the presented high-gain adaptive controllers capable to guarantee asymptotic

tracking, i.e.

$$\lim_{t\to\infty} e(t) = \lim_{t\to\infty} \big(y_{\text{ref}}(t) - y(t)\big) = 0\ ? \tag{2.99}$$

The answer is affirmative if reference $y_{\text{ref}}(\cdot)$ is the solution of a known linear differential equation. Then the use of an "internal model" connected in series with the high-gain adaptive controllers (2.59) or (2.81) assures asymptotic tracking as in (2.99) (see e.g. [86, Section 5.1]). The "Internal Model Principle" postulates that "*every good regulator must incorporate a model of the outside world*" being capable to reduplicate "*the dynamic structure of the exogenous signals which the regulator is required to process*" (see [189, p. 210]). Outside world does not only cover known reference but also known disturbance signals. The disturbance dynamics of processes in industry are mostly not structurally known, hence application of internal models for disturbance rejection is often not feasible. In the following disturbance rejection by internal models is neglected, for more information on asymptotic disturbance rejection see e.g. [135]. The internal model principle was extended to a nonlinear framework in [173].

In the remainder of this section, only "non-vanishing" reference signals are considered. For this purpose, introduce the monic polynomial $D_{IM} \in \mathbb{R}[s]$ with associated root set

$$\mathcal{R}(D_{IM}) := \left\{\ s_0 \in \mathbb{C} \;\middle|\; D_{IM}(s_0) = 0\ \right\}$$

and reference class

$$\mathcal{Y}_{\text{ref}} := \left\{ y_{\text{ref}}(\cdot) \in \mathcal{C}^\infty(\mathbb{R}_{\geq 0}; \mathbb{R}) \;\middle|\; D_{IM}\left(\frac{\mathrm{d}}{\mathrm{d}t}\right) y_{\text{ref}}(\cdot) = 0, \quad \begin{array}{l} D_{IM} \in \mathbb{R}[s],\ \text{monic} \\ \text{with } \mathcal{R}(D_{IM}) \subset \mathbb{C}_{\geq 0} \end{array} \right\}. \tag{2.100}$$

Admissible references $y_{\text{ref}}(\cdot) \in \mathcal{Y}_{\text{ref}}$ are e.g. constant, ramp-like, exponential and sinusoidal functions and/or linear combinations thereof. Clearly, since D_{IM} in (2.100) is *not* a Hurwitz polynomial (more precisely, each root has non-negative real part, i.e. $\Re\{s_0\} \geq 0$ for all $s_0 \in \mathcal{R}(D_{IM})$), the admissible reference signals may also tend to $+\infty$ (or $-\infty$) as $t \to \infty$.

Note that, for monic and Hurwitz polynomial $D_{IM} \in \mathbb{R}[s]$, $D_{IM}\left(\frac{\mathrm{d}}{\mathrm{d}t}\right) y_{\text{ref}}(\cdot) = 0$ implies that reference $y_{\text{ref}}(\cdot)$ asymptotically (exponentially) vanishes, i.e. $\lim_{t\to\infty} y_{\text{ref}}(t) = 0$. Hence, for this case, asymptotic tracking as in (2.99) is already accomplished by the stabilization results in Section 2.3 (see also [86, p. 112]).

The principle idea of high-gain adaptive tracking with internal model is as follows: consider a high-gain stabilizable albeit unknown LTI SISO system with transfer function $F(s)$ as in (2.35) and for $y_{\text{ref}}(\cdot) \in \mathcal{Y}_{\text{ref}}$ introduce the internal model described by the following transfer function

$$F_{IM}(s) := \frac{u(s)}{v(s)} := \frac{N_{IM}(s)}{D_{IM}(s)}, \qquad \begin{array}{l} \text{coprime } N_{IM},\ D_{IM} \in \mathbb{R}[s],\ D_{IM} \text{ as in (2.100)}, \\ N_{IM} \text{ monic and Hurwitz}, \\ \deg(N_{IM}) = \deg(D_{IM}) \text{ and } \lim\limits_{s\to\infty} F_{IM}(s) > 0. \end{array} \tag{2.101}$$

from "new" input $v(s)$ to control input $u(s)$. Clearly the internal model in (2.101) is minimum-

phase, has relative degree zero and positive high-frequency gain, i.e.

$$r_{IM} = \deg(N_{IM}) - \deg(D_{IM}) = 0 \qquad \text{and} \qquad \widehat{\gamma}_0 := \lim_{s\to\infty} F_{IM}(s) > 0. \tag{2.102}$$

Hence the serial interconnection

$$F_S(s) := \frac{y(s)}{v(s)} := F_{IM}(s)\, F(s)$$

again is high-gain stabilizable and, moreover, the internal model in (2.101) allows to reduplicate the reference signal $y_{\text{ref}}(\cdot) \in \mathcal{Y}_{\text{ref}}$ (see Lemma 5.1.2 in [86]). Concluding, the problem of high-gain adaptive tracking (with internal model) simplifies to that of high-gain adaptive stabilization (see [86, Section 5.1]).

To formulate the results in the time domain, introduce a minimal realization of the internal model (2.101) as follows

$$\begin{aligned} \dot{\widehat{\boldsymbol{x}}}(t) &= \widehat{\boldsymbol{A}}\widehat{\boldsymbol{x}}(t) + \widehat{\boldsymbol{b}}\, v(t) \\ u(t) &= \widehat{\boldsymbol{c}}^{\top}\widehat{\boldsymbol{x}}(t) + \widehat{\gamma}_0 v(t) \end{aligned}, \qquad \begin{aligned} &\deg(D_{IM}) =: p \in \mathbb{N},\ \widehat{\boldsymbol{x}}(0) = \widehat{\boldsymbol{x}}_0 \in \mathbb{R}^p, \\ &(\widehat{\boldsymbol{A}}, \widehat{\boldsymbol{b}}, \widehat{\boldsymbol{c}}) \in \mathbb{R}^{p\times p} \times \mathbb{R}^p \times \mathbb{R}^p,\ \widehat{\gamma}_0 \text{ as in (2.102)}, \end{aligned} \tag{2.103}$$

where $v(\cdot)$ represents the "new" control input of the serial interconnection of minimal realization (2.103) and LTI SISO system of form (2.45). Furthermore, a technical lemma is required which shows that interconnected system (2.103), (2.45) inherits the system properties of (2.45) such as relative degree, sign of the high-frequency gain and minimum-phase property. The following lemma covers LTI SISO systems with arbitrary relative degree greater than zero. It is similar to Lemma 3.5 in [94] (there for LTI MIMO systems with relative degree one).

Lemma 2.39 (Serial interconnection of internal model and LTI SISO system)**.**
Consider a system of form (2.45) with (known) relative degree $1 \le r \le n$. If (2.103) is a minimal realization of (2.101), then the serial interconnection (2.103), (2.45), given by

$$\left.\begin{aligned} \tfrac{d}{dt}\underbrace{\begin{pmatrix}\boldsymbol{x}(t)\\ \widehat{\boldsymbol{x}}(t)\end{pmatrix}}_{=:\boldsymbol{x}_S(t)} &= \underbrace{\begin{bmatrix}\boldsymbol{A} & \boldsymbol{b}\widehat{\boldsymbol{c}}^{\top}\\ \boldsymbol{O}_{p\times n} & \widehat{\boldsymbol{A}}\end{bmatrix}}_{=:\boldsymbol{A}_S\in\mathbb{R}^{(n+p)\times(n+p)}} \begin{pmatrix}\boldsymbol{x}(t)\\ \widehat{\boldsymbol{x}}(t)\end{pmatrix} + \underbrace{\begin{pmatrix}\widehat{\gamma}_0\boldsymbol{b}\\ \widehat{\boldsymbol{b}}\end{pmatrix}}_{=:\boldsymbol{b}_S\in\mathbb{R}^{n+p}} v(t), \qquad \begin{pmatrix}\boldsymbol{x}(0)\\ \widehat{\boldsymbol{x}}(0)\end{pmatrix} = \underbrace{\begin{pmatrix}\boldsymbol{x}^0\\ \widehat{\boldsymbol{x}}^0\end{pmatrix}}_{=:\boldsymbol{x}_S^0} \in \mathbb{R}^{n\times p} \\ y(t) &= \underbrace{\begin{pmatrix}\boldsymbol{c}^{\top}, & \boldsymbol{0}_p^{\top}\end{pmatrix}}_{=:\boldsymbol{c}_S^{\top}\in\mathbb{R}^{1\times(n+p)}} \begin{pmatrix}\boldsymbol{x}(t)\\ \widehat{\boldsymbol{x}}(t)\end{pmatrix}, \end{aligned}\right\} \tag{2.104}$$

has the following system properties:

(i) its relative degree equals r;

(ii) its high-frequency gain is given by $\boldsymbol{c}_S^{\top}\boldsymbol{A}_S^{r-1}\boldsymbol{b}_S = \widehat{\gamma}_0\, \boldsymbol{c}^{\top}\boldsymbol{A}^{r-1}\boldsymbol{b}$;

(iii) if (2.45) is minimum-phase, then so the serial interconnection (2.104), i.e.

$$\forall\, s \in \mathbb{C}_{\ge 0}\colon \qquad \det\begin{bmatrix} s\boldsymbol{I}_{n+p} - \boldsymbol{A}_S & \boldsymbol{b}_S \\ \boldsymbol{c}_S^{\top} & 0 \end{bmatrix} \neq 0.$$

Proof of Lemma 2.39.
Step1: It is shown that Assertions (i) and (ii) hold true.
Note that

$$\forall\, l \in \mathbb{N}\colon \qquad \boldsymbol{A}_S^l = \begin{bmatrix} \boldsymbol{A} & \boldsymbol{b}\widehat{\boldsymbol{c}}^\top \\ \boldsymbol{O}_{p\times n} & \widehat{\boldsymbol{A}} \end{bmatrix}^l = \begin{bmatrix} \boldsymbol{A}^l & \sum_{i=1}^l \boldsymbol{A}^{l-i}\boldsymbol{b}\widehat{\boldsymbol{c}}^\top \widehat{\boldsymbol{A}}^{i-1} \\ \boldsymbol{O}_{p\times n} & \widehat{\boldsymbol{A}}^l \end{bmatrix} \tag{2.105}$$

where $\boldsymbol{A}^0 = \boldsymbol{I}_n$ and $\widehat{\boldsymbol{A}}^0 = \boldsymbol{I}_p$ and so the following holds

$$\begin{aligned} \forall\, l \in \mathbb{N}\colon \qquad \boldsymbol{c}_S^\top \boldsymbol{A}_S^l \boldsymbol{b}_S &\overset{(2.105)}{=} \begin{pmatrix} \boldsymbol{c}^\top & \boldsymbol{0}_p^\top \end{pmatrix} \begin{bmatrix} \boldsymbol{A}^l & \sum_{i=1}^l \boldsymbol{A}^{l-i}\boldsymbol{b}\widehat{\boldsymbol{c}}^\top \widehat{\boldsymbol{A}}^{i-1} \\ \boldsymbol{O}_{p\times n} & \widehat{\boldsymbol{A}}^l \end{bmatrix} \begin{pmatrix} \widehat{\gamma}_0 \boldsymbol{b} \\ \widehat{\boldsymbol{b}} \end{pmatrix} \\ &= \begin{pmatrix} \boldsymbol{c}^\top \boldsymbol{A}^l, & \sum_{i=1}^l \boldsymbol{c}^\top \boldsymbol{A}^{l-i}\boldsymbol{b}\widehat{\boldsymbol{c}}^\top \widehat{\boldsymbol{A}}^{i-1} \end{pmatrix} \begin{pmatrix} \widehat{\gamma}_0 \boldsymbol{b} \\ \widehat{\boldsymbol{b}} \end{pmatrix} \\ &= \widehat{\gamma}_0 \boldsymbol{c}^\top \boldsymbol{A}^l \boldsymbol{b} + \sum_{i=1}^l \boldsymbol{c}^\top \boldsymbol{A}^{l-i}\boldsymbol{b}\widehat{\boldsymbol{c}}^\top \widehat{\boldsymbol{A}}^{i-1}\widehat{\boldsymbol{b}}. \end{aligned} \tag{2.106}$$

Now, either $r = 1$ then $\boldsymbol{c}_S^\top \boldsymbol{b}_S = \widehat{\gamma}_0 \boldsymbol{c}^\top \boldsymbol{b}$ or $1 < r \leq n$ then $\boldsymbol{c}_S^\top \boldsymbol{b}_S = \boldsymbol{c}^\top \boldsymbol{b} = 0$ and in view of (2.106), $\boldsymbol{c}_S^\top \boldsymbol{A}_S^l \boldsymbol{b}_S = 0$ for all $l \in \{1, \ldots, r-2\}$ and $\boldsymbol{c}_S^\top \boldsymbol{A}_S^{r-1} \boldsymbol{b}_S = \widehat{\gamma}_0 \boldsymbol{c}^\top \boldsymbol{A}^{r-1} \boldsymbol{b} \neq 0$. This completes Step 1.

Step 2: It is shown that Assertion (iii) holds true.
If (2.45) is minimum-phase, then this implies stabilizability and detectability (see Proposition 2.8), i.e.

$$\forall\, s \in \mathbb{C}_{\geq 0}\colon \qquad \operatorname{rank} \begin{bmatrix} s\boldsymbol{I}_n - \boldsymbol{A} & \boldsymbol{b} \\ \boldsymbol{c}^\top & 0 \end{bmatrix} = n + 1.$$

By assumption, (2.103) is a minimal realization of (2.101) and hence the pair $(\widehat{\boldsymbol{A}}, \widehat{\boldsymbol{b}})$ is controllable (and $(\widehat{\boldsymbol{c}}^\top, \widehat{\boldsymbol{A}})$ is observable). Hence the Popov-Belevitch-Hautus condition (see Remark 2.9) implies

$$\forall\, s \in \mathbb{C}\colon \qquad \operatorname{rank} \begin{bmatrix} s\boldsymbol{I}_p - \widehat{\boldsymbol{A}}, & \widehat{\boldsymbol{b}} \end{bmatrix} = p.$$

Combining this yields

$$\forall\, s \in \mathbb{C}_{\geq 0}\colon \ \operatorname{rank} \begin{bmatrix} s\boldsymbol{I}_{n+p} - \boldsymbol{A}_S & \boldsymbol{b}_S \\ \boldsymbol{c}_S^\top & 0 \end{bmatrix} = \operatorname{rank} \begin{bmatrix} s\boldsymbol{I}_n - \boldsymbol{A} & -\boldsymbol{b}\widehat{\boldsymbol{c}}^\top & \widehat{\gamma}_0 \boldsymbol{b} \\ \boldsymbol{O}_{p\times n} & s\boldsymbol{I}_p - \widehat{\boldsymbol{A}} & \widehat{\boldsymbol{b}} \\ \boldsymbol{c}^\top & \boldsymbol{0}_p^\top & 0 \end{bmatrix} = n + p + 1,$$

which shows Assertion (iii) and completes the proof of Lemma 2.39. □

2.4.1 Relative degree one systems

Now high-gain adaptive tracking for systems of class $\mathcal{S}_1^{\text{lin}}$ is presented. From Lemma 2.39 it follows that the serial interconnection of system (2.45) and internal model (2.103) is again element of class $\mathcal{S}_1^{\text{lin}}$ and hence, loosely speaking, a slight modification of the high-gain adaptive

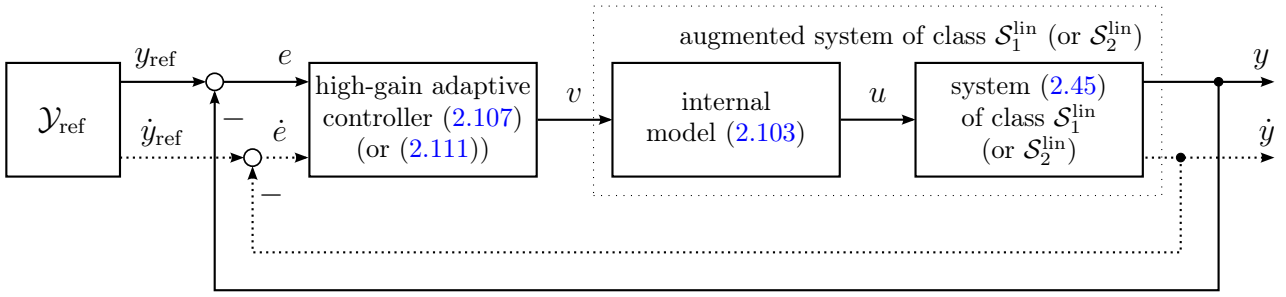

Figure 2.7: *High-gain adaptive (tracking) control of systems of class $\mathcal{S}_1^{\text{lin}}$ (or $\mathcal{S}_2^{\text{lin}}$) with internal model.*

controller (2.59) establishes asymptotic tracking.

Theorem 2.40 (High-gain adaptive tracking control of systems of class $\mathcal{S}_1^{\text{lin}}$)**.**
Consider a system of class $\mathcal{S}_1^{\text{lin}}$ given by (2.45) and some arbitrary $y_{\text{ref}}(\cdot) \in \mathcal{Y}_{\text{ref}}$ with known $D_{IM} \in \mathbb{R}[s]$ as in (2.100). Choose a Hurwitz polynomial $N_{IM} \in \mathbb{R}[s]$ with $\deg(N_{IM}) = \deg(D_{IM})$ such that $\lim_{s\to\infty} \frac{N_{IM}(s)}{D_{IM}(s)} > 0$. If (2.103) is a minimal realization of $\frac{N_{IM}(s)}{D_{IM}(s)}$, then application of the high-gain adaptive (tracking) controller

$$\left.\begin{aligned} v(t) &= \operatorname{sign}(\boldsymbol{c}^\top \boldsymbol{b})\, k(t) e(t), && \text{where} \quad e(t) = y_{\text{ref}}(t) - y(t) \\ \dot{k}(t) &= q_1 \,|e(t)|^{q_2}, && k(0) = k_0 \end{aligned}\right\} \tag{2.107}$$

with design parameters $q_1 > 0$, $q_2 \geq 1$ and $k_0 > 0$ to the serial interconnection (2.104) yields, for arbitrary initial-value $\boldsymbol{x}_S^0 \in \mathbb{R}^{n\times p}$, a closed-loop initial-value problem (2.107), (2.104) with the following properties

(i) there exists a unique and maximal solution $(\boldsymbol{x}_S,\, k) : [0, T) \to \mathbb{R}^{n+p} \times \mathbb{R}_{\geq 0}$, $T \in (0, \infty]$;

(ii) the solution is global, i.e. $T = \infty$;

(iii) the gain is bounded, i.e. $k(\cdot) \in \mathcal{L}^\infty(\mathbb{R}_{\geq 0}; \mathbb{R}_{>0})$;

(iv) the tracking error vanishes asymptotically, i.e. $\lim_{t\to\infty} |e(t)| = \lim_{t\to\infty} |y_{\text{ref}}(t) - y(t)| = 0$;

(v) the state does not grow faster than the reference, i.e.

$$\exists\, M > 0 \,\forall\, t \geq 0 : \qquad \|\boldsymbol{x}_S(t)\| \leq M(1 + \max_{s\in[0,t]} |y_{\text{ref}}(t)|).$$

Clearly, unbounded reference signals $y_{\text{ref}}(\cdot)$ might necessitate unbounded control actions $u(\cdot)$ reduplicated by the internal model (2.103). If so, then in real world such references are not admissible. In contrast, due to Assertions (iii) and (iv), the controller output $v(\cdot)$ as in (2.107) is always bounded. The closed-loop system is depicted in Fig. 2.7.

Proof of Theorem 2.40.
Let $\boldsymbol{w}(\cdot)$ be the unique solution of $\dot{\boldsymbol{w}}(t) = \boldsymbol{A}_S \boldsymbol{w}(t), \boldsymbol{w}(0) = \boldsymbol{w}_0 \in \mathbb{R}^{n+p}$ where $\boldsymbol{A}_S$ as in (2.104). Clearly, such a solution exists on $\mathbb{R}_{\geq 0}$ and $\boldsymbol{w}(\cdot) \in \mathcal{C}^\infty(\mathbb{R}_{\geq 0}; \mathbb{R}^{n+p})$. In view of Lemma 5.1.2 in [86], there exists $\boldsymbol{w}_0^{\text{ref}} \in \mathbb{R}^{n+p}$ such that

$$\begin{aligned} \dot{\boldsymbol{w}}(t) &= \boldsymbol{A}_S \boldsymbol{w}(t), && \boldsymbol{w}(0) = \boldsymbol{w}_0^{\text{ref}} \in \mathbb{R}^{n+p} \\ y_{\text{ref}}(t) &= \boldsymbol{c}_S^\top \boldsymbol{w}(t). \end{aligned} \tag{2.108}$$

Hence, for $\boldsymbol{x}_S(\cdot)$ as in (2.104), $\boldsymbol{w}(\cdot)$ as in (2.108) and

$$\forall\, t \geq 0\colon \qquad \boldsymbol{x}_e(t) := \boldsymbol{w}(t) - \boldsymbol{x}_S(t).$$

the tracking error can be written as follows

$$\forall\, t \geq 0\colon \qquad e(t) = y_{\mathrm{ref}}(t) - y(t) = \boldsymbol{c}_S^\top\big(\boldsymbol{w}(t) - \boldsymbol{x}_S(t)\big) = \boldsymbol{c}_S^\top \boldsymbol{x}_e(t). \tag{2.109}$$

Moreover, in view of (2.104) and (2.108), $\boldsymbol{x}_e(\cdot)$ is the unique solution of

$$\begin{array}{rcll} \dot{\boldsymbol{x}}_e(t) & = & \boldsymbol{A}_S \boldsymbol{x}_e(t) - \boldsymbol{b}_S\, v(t), & \boldsymbol{x}_e(0) = \boldsymbol{w}_0^{\mathrm{ref}} - \boldsymbol{x}_S^0 \in \mathbb{R}^{n+p} \\ e(t) & = & \boldsymbol{c}_S^\top \boldsymbol{x}_e(t). & \end{array} \tag{2.110}$$

In view of Lemma 2.39, system (2.110) is element of class $\mathcal{S}_1^{\mathrm{lin}}$, hence Theorem 2.24 allows for application of (2.59) substituting $v(t)$ and $-e(t)$ for $u(t)$ and $y(t)$, respectively, i.e. (2.107). Furthermore, it follows from Theorem 2.24 that Assertions (i) and (ii) holds true and moreover

$$\boldsymbol{x}_e(\cdot) \in \mathcal{L}^\infty(\mathbb{R}_{\geq 0}; \mathbb{R}^{n+p}), \quad k(\cdot) \in \mathcal{L}^\infty(\mathbb{R}_{\geq 0}; \mathbb{R}_{>0}) \quad \text{and} \quad \lim_{t\to\infty} \boldsymbol{x}_e(t) = \boldsymbol{0}_{n+p}.$$

The last statement implies

$$\lim_{t\to\infty} e(t) = \lim_{t\to\infty} \boldsymbol{c}_S^\top \boldsymbol{x}_e(t) = 0$$

and therefore Assertions (iii) and (iv) hold true. Invoking Lemma 5.1.2 in [86] again gives

$$\exists\, M_1 > 0\ \forall\, t \geq 0\colon \qquad \|\boldsymbol{w}(t)\| \leq M_1\big(1 + \max_{s\in[0,t]} |y_{\mathrm{ref}}(t)|\big).$$

Combining this with $\boldsymbol{x}_e(\cdot) \in \mathcal{L}^\infty(\mathbb{R}_{\geq 0}; \mathbb{R}^{n+p})$ yields

$$\begin{aligned} \forall\, t \geq 0\colon \qquad \|\boldsymbol{x}_S(t)\| = \|\boldsymbol{w}(t) - \boldsymbol{x}_e(t)\| &\leq \|\boldsymbol{w}(t)\| + \|\boldsymbol{x}_e(t)\| \leq \|\boldsymbol{x}_e\|_\infty + M_1\big(1 + \max_{s\in[0,t]} |y_{\mathrm{ref}}(t)|\big) \\ &\leq \underbrace{\max\{\|\boldsymbol{x}_e\|_\infty,\, M_1\}}_{=:M>0} \big(1 + \max_{s\in[0,t]} |y_{\mathrm{ref}}(t)|\big) \end{aligned}$$

which shows Assertion (v) and completes the proof of Theorem 2.40. □

2.4.2 Relative degree two systems

The following result is a direct consequence of Theorem 2.36 and Theorem 2.40. It assures asymptotic tracking of systems element of class $\mathcal{S}_2^{\mathrm{lin}}$.

Corollary 2.41 (High-gain adaptive tracking control of systems of class $\mathcal{S}_2^{\mathrm{lin}}$)**.**
Consider a system of class $\mathcal{S}_2^{\mathrm{lin}}$ given by (2.45) and some arbitrary $y_{\mathrm{ref}}(\cdot) \in \mathcal{Y}_{\mathrm{ref}}$ with known $D_{IM} \in \mathbb{R}[s]$ as in (2.100). Under identical presuppositions as in Theorem 2.40, the high-gain adaptive (tracking) controller

$$\left.\begin{array}{rcll} v(t) & = & \mathrm{sign}(\boldsymbol{c}^\top \boldsymbol{A}\boldsymbol{b})\Big(k(t)^2\, e(t) + q_1\, k(t)\, \dot{e}(t)\Big) & \text{where} \quad e(t) = y_{\mathrm{ref}}(t) - y(t) \\ \dot{k}(t) & = & q_2\, \exp(-q_3\, k(t))\, \big\|(e(t),\, \dot{e}(t))^\top\big\|^2, & k(0) = k_0 \end{array}\right\} \tag{2.111}$$

with design parameters $q_1, q_2, q_3, k_0 > 0$ applied to the serial interconnection (2.104) yields, for arbitrary initial-value $\boldsymbol{x}_S^0 \in \mathbb{R}^{n\times p}$, a closed-loop initial-value problem (2.111), (2.104) with the properties (i)-(v) from Theorem 2.40 and (vi) $\lim_{t\to\infty} |\dot{e}(t)| = \lim_{t\to\infty} |\dot{y}_{\mathrm{ref}}(t) - \dot{y}(t)| = 0$.

Proof of Corollary 2.41.
Similar arguments as in the proof of Theorem 2.40 show that Assertions (i)-(v) hold true. From Lemma 2.39, it follows for the relative degree two case that the serial interconnection (2.104) is element of $\mathcal{S}_2^{\mathrm{lin}}$. Hence, in view of Theorem 2.36, application of (2.81) is feasible substituting $v(t)$, $-e(t)$ and $-\dot{e}(t)$ for $u(t)$, $y(t)$ and $\dot{y}(t)$, respectively. Note that this substitution yields the controller in (2.111). Moreover, Theorem 2.36 gives $\lim_{t\to\infty} e(t) = 0$ and $\lim_{t\to\infty} \boldsymbol{x}_e(t) = \boldsymbol{0}_{n+p}$. Note that this with $\boldsymbol{c}_S^\top \boldsymbol{b}_S = 0$ implies $\lim_{t\to\infty} \dot{e}(t) = \lim_{t\to\infty} \boldsymbol{c}_S^\top \boldsymbol{A}_S \boldsymbol{x}_e(t) = 0$ and therefore Assertion (vi) also holds. □

2.4.3 Simulations

In this section, the application of internal models is illustrated. Simulation results are shown for system (2.71) (with relative degree one) and for system (2.74) (with relative degree two). The control objective is asymptotic tracking of an unbounded reference, given by

$$y_{\mathrm{ref}} \colon \mathbb{R}_{\geq 0} \to \mathbb{R}, \quad t \mapsto y_{\mathrm{ref}}(t) := t + \sin(t) \qquad \circ\!\!-\!\!\bullet \qquad y_{\mathrm{ref}}(s) = \frac{1}{s^2} + \frac{1}{s^2+1}. \tag{2.112}$$

Clearly, $y_{\mathrm{ref}}(\cdot) \in \mathcal{C}^\infty(\mathbb{R}_{\geq 0}; \mathbb{R})$ in (2.112) and, by inspection, one obtains the denominator $D_{IM}(s) = s^4 + s^2$ of the internal model with (unstable) poles $p_{1,2}(D_{IM}) = 0$ and $p_{3,4}(D_{IM}) = \pm j$. For the simulations $N_{IM}(s) = (s+1)^4$ is chosen. Observe that $\deg(N_{IM}) = \deg(D_{IM}) = 4$ and $\lim_{s\to\infty} N_{IM}(s)/D_{IM}(s) = 1 > 0$. Hence an appropriate internal model in the frequency domain is given by

$$F_{IM}(s) = \frac{u(s)}{v(s)} = \frac{N_{IM}(s)}{D_{IM}(s)} = \frac{(s+1)^4}{s^4+s^2} = \frac{4s^3+5s^2+4s+1}{s^4+s^2} + 1. \tag{2.113}$$

For $F_{IM}(s)$ as in (2.113), fix $\widehat{\gamma}_0 = \lim_{s\to\infty} F_{IM}(s) = 1$ and choose the minimal realization

$$\begin{aligned} \dot{\widehat{\boldsymbol{x}}}(t) &= \begin{bmatrix} 0 & 1 & 0 & 0 \\ 0 & 0 & 1 & 0 \\ 0 & 0 & 0 & 1 \\ 0 & -1 & 0 & 0 \end{bmatrix} \widehat{\boldsymbol{x}}(t) + \begin{pmatrix} 0 \\ 0 \\ 0 \\ 1 \end{pmatrix} v(t), \qquad \widehat{\boldsymbol{x}}(0) = \boldsymbol{0}_4 \in \mathbb{R}^4 \\ u(t) &= \begin{pmatrix} 1, & 4, & 5, & 4 \end{pmatrix} \widehat{\boldsymbol{x}}(t) + \widehat{\gamma}_0\, v(t). \end{aligned} \tag{2.114}$$

At first consider the high-gain adaptive tracking problem for system (2.71) with $a_1 = 10$ and $\gamma_0 = y_0 = 1$: the high-gain adaptive (tracking) controller (2.107) with parametrization $q_1 = k_0 = 1$ and $q_2 = 2$ applied to the serial interconnection (2.114), (2.71) assures high-gain adaptive tracking. Simulation results for the closed-loop system (2.107), (2.114), (2.71) are depicted in Fig. 2.8. Note that the serial interconnection (2.114), (2.71) is unstable, hence it takes ≈ 2 [s] until a sufficiently large gain $k(\cdot)$ is found to "stabilize" the closed-loop system (2.107), (2.113), (2.71). After ≈ 2 [s], output $y(\cdot)$ begins to track reference $y_{\mathrm{ref}}(\cdot)$ with errors $|e(\cdot)| \ll 1$ (see Fig. 2.8(a)). Controller output $v(\cdot)$ and controller gain $k(\cdot)$ asymptotically converge to zero and a value smaller than 20, respectively (see Fig. 2.8 (b)), whereas

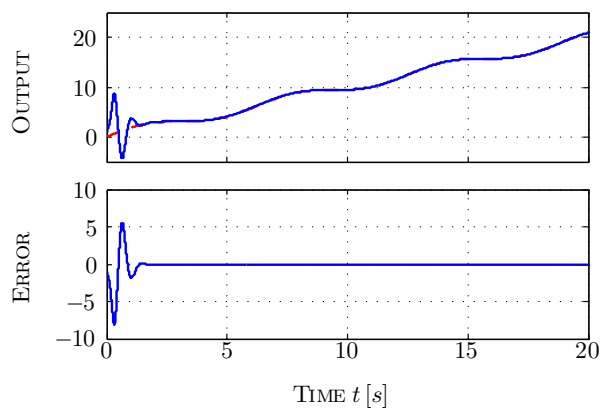

(a) *top:* — *output* $y(\cdot)$ *and* - - - *reference* $y_{\mathrm{ref}}(\cdot)$*; bottom:* — *error* $e(\cdot)$

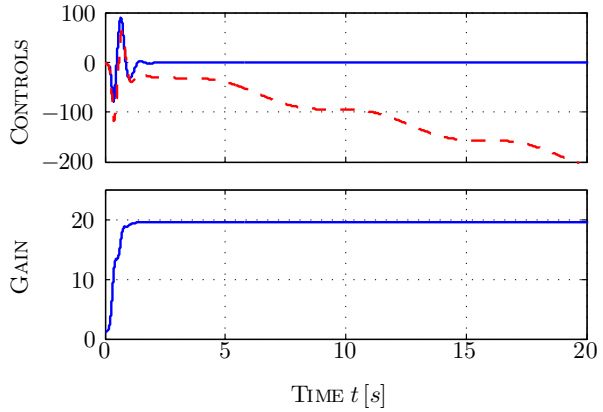

(b) *top:* — *controller output* $v(\cdot)$ *and* - - - *control action* $u(\cdot)$*; bottom:* — *gain* $k(\cdot)$

Figure 2.8: *Simulation results for closed-loop system* (2.107), (2.114), (2.71) *and reference* (2.112) *with parametrization* $y_0 = \gamma_0 = 1$, $a_1 = 10$ *and* $q_1 = k_0 = 1$ *and* $q_2 = 2$.

control action $u(\cdot)$ decreases (without bound) compensating for the scaled reference $y_{\mathrm{ref}}(\cdot)$. The scaling is due to the negative steady-state gain $\gamma_\infty = -1/10$.

Next consider the high-gain adaptive tracking problem for system (2.74) with $(y_0, y_1) = (1, 1)$ and $a_1 = a_2 = \gamma_0 = 1$: here application of (2.111) with parametrization $q_1 = q_2 = q_3 = k_0 = 1$ assures high-gain adaptive tracking. The simulation results for the closed-loop system (2.111), (2.114), (2.71) are shown in Fig. 2.9. The system response is similar to that in Fig. 2.8. Due to the choice $q_3 = k_0 = 1$ in (2.111) gain adaption is decelerated and therefore the "stabilization phase" is longer (≈ 10 [s]). Clearly, also the error derivative converges to zero (see Fig. 2.9(a)). Controller output $v(\cdot)$ and control action $u(\cdot)$ must compensate for large system states (during stabilization phase) and for the (unbounded) reference $y_{\mathrm{ref}}(\cdot)$, respectively (see Fig. 2.9(b)).

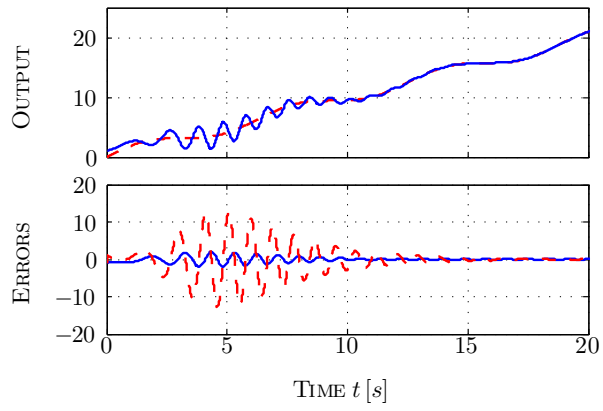

(a) *top:* — *output* $y(\cdot)$ *and* - - - *reference* $y_{\mathrm{ref}}(\cdot)$*; bottom:* — *error* $e(\cdot)$ *and* - - - *derivative* $\dot{e}(\cdot)$

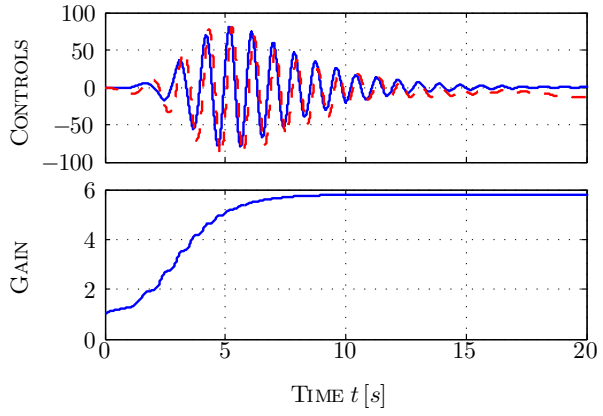

(b) *top:* — *controller output* $v(\cdot)$ *and* - - - *control action* $u(\cdot)$*; bottom:* — *gain* $k(\cdot)$

Figure 2.9: *Simulation results for closed-loop system* (2.111), (2.114), (2.74) *and reference* (2.112) *with parametrization* $(y_0, y_1) = (1, 1)$, $a_1 = a_2 = \gamma_0 = 1$ *and* $q_1 = q_2 = q_3 = k_0 = 1$.

Chapter 3

Adaptive λ-tracking control

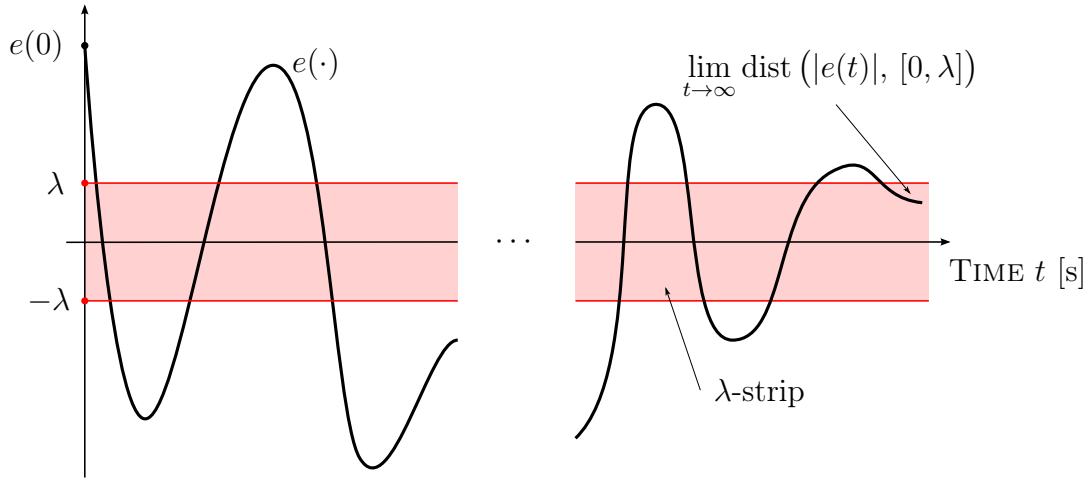

Figure 3.1: *Illustration of λ-strip and control objective (co_2).*

This chapter introduces adaptive λ-tracking control for systems of class $\mathcal{S}_1$ and for systems of class $\mathcal{S}_2$. For suitable reference $y_{\text{ref}}(\cdot) \in \mathcal{W}^{1,\infty}(\mathbb{R}_{\geq 0};\mathbb{R})$ (or $\mathcal{W}^{2,\infty}(\mathbb{R}_{\geq 0};\mathbb{R})$), regulated output $y(\cdot)$ and prescribed asymptotic accuracy $\lambda > 0$, the adaptive λ-tracking controllers assure that the tracking error

$$\forall\, t \geq 0\colon \qquad e(t) = y_{\text{ref}}(t) - y(t)$$

asymptotically converges into the "λ-strip" (see Fig. 3.1), given by

$$\{\ (t,e) \in \mathbb{R}_{\geq 0} \times \mathbb{R} \quad | \quad |e| \leq \lambda\ \}.$$

It will be shown that, for both system classes $\mathcal{S}_1$ and $\mathcal{S}_2$, the developed adaptive λ-tracking controllers accomplish control objectives (co_1) and (co_2), i.e.

$$\boldsymbol{x}(\cdot) \in \mathcal{L}^\infty(\mathbb{R}_{\geq 0};\mathbb{R}^n),\ u(\cdot) \in \mathcal{L}^\infty(\mathbb{R}_{\geq 0};\mathbb{R}) \ \text{ and } \ \forall\, \lambda > 0\colon \ \lim_{t\to\infty} \text{dist}\big(|e(t)|, [0,\lambda] = 0\big). \tag{3.1}$$

3.1 Motivation

Although the high-gain adaptive controllers presented in Chapter 2 work well for minimum-phase LTI SISO systems with known sign of the high-frequency gain and either relative degree

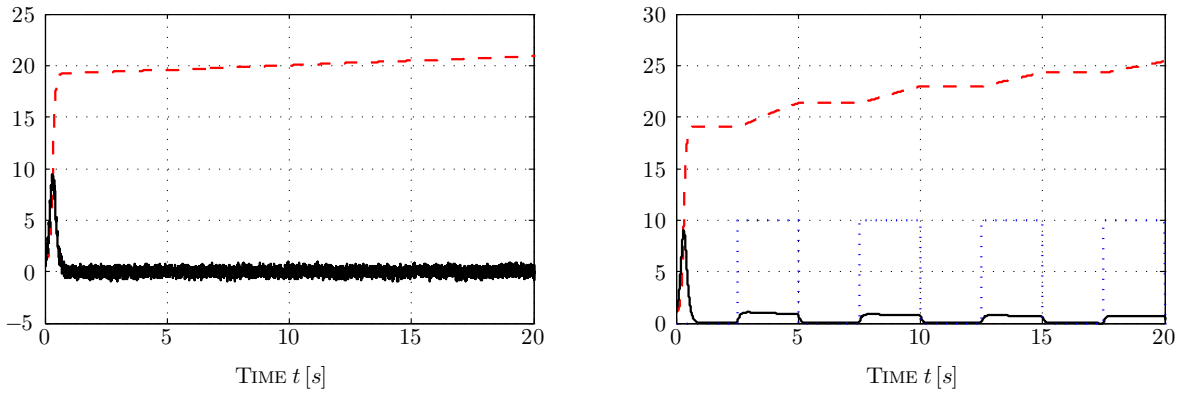

(a) *gain drift due to noise* $n_m(\cdot) \in \mathcal{W}^{2,\infty}(\mathbb{R}_{\geq 0};\mathbb{R})$ *(*$u_d(\cdot) = 0$*):* - - - *gain* $k(\cdot)$, ——*(noisy) output* $y(\cdot)$.

(b) *gain drift due to* ·····*disturbance* $u_d(\cdot) \in \mathcal{L}^\infty(\mathbb{R}_{\geq 0};\mathbb{R})$ *(*$n_m(\cdot) = 0$*):* - - - *gain* $k(\cdot)$ *and* ——*output* $y(\cdot)$.

Figure 3.2: *Simulation results for closed-loop system* (3.2), (3.3) *(only shown for the first* 20 [s]*).*

one or relative degree two (e.g. if derivative feedback is admissible), they are mainly of theoretical interest. High-gain adaptive control as in Chapter 2 has (severe) limitations which motivate for the introduction of adaptive λ-tracking control:

Motivation 1: The models considered in Chapter 2 are linear and do not account for (external) disturbances or nonlinear (functional) perturbations as required for system class $\mathcal{S}_1$ or system class $\mathcal{S}_2$ (see Section 1.6.2.2). Although there exist high-gain adaptive controllers for nonlinear systems, such controllers only work if the system has an equilibrium at the origin (see [114]) or the non-zero equilibrium is a priori known (see [2, Remark 3.4(ii)]). Both are strict presuppositions and do not hold in general.

Motivation 2: The application of internal models allows for asymptotic tracking of reference signals element of the class $\mathcal{Y}_{\text{ref}}$ as in (2.100). However, the reference class $\mathcal{Y}_{\text{ref}}$ is limited, e.g. the exemplary reference signals introduced in Section 1.6.2.4 (see Fig. 1.19) are not covered.

Motivation 3: Noise (in output measurement) or disturbances might cause gain drift in high-gain adaptive control, i.e. the gain diverges as time tends to infinity. To illustrate this phenomenon, consider the following closed-loop system consisting of the first order system

$$\begin{aligned} \dot{x}(t) &= 10\,x(t) + \big(u(t) + u_d(t)\big) \\ y(t) &= x(t) + n_m(t) \end{aligned}, \qquad \begin{aligned} &x(0) = 1,\ u_d(\cdot) \in \mathcal{L}^\infty(\mathbb{R}_{\geq 0};\mathbb{R}), \\ &n_m(\cdot) \in \mathcal{W}^{2,\infty}(\mathbb{R}_{\geq 0};\mathbb{R}) \end{aligned} \tag{3.2}$$

and the high-gain adaptive controller

$$u(t) = -k(t)y(t) \quad \text{where} \quad \dot{k}(t) = y(t)^2,\ k(0) = 1. \tag{3.3}$$

System (3.2) is subject to input disturbance $u_d(\cdot)$ and sensor deviation $n_m(\cdot)$ (e.g. measurement noise). The simulation results are depicted in Fig. 1.19. Albeit bounded both disturbances cause a monotone increase of gain $k(\cdot)$ (see Fig. 3.2 (a) and (b), respectively) which will eventually result in $k(t) \to \infty$ as $t \to \infty$.

By sacrificing asymptotic stabilization (or asymptotic tracking and disturbance rejection) and by introducing a dead-zone in gain adaption, e.g. of the following form

$$\dot{k}(t) = d_\lambda(|e(t)|)^2, \qquad k(0) = k_0 > 0 \;\text{ with }\; d_\lambda(\cdot) \text{ as in (N.5)},$$

adaptive λ-tracking control is applicable to a wider class of (nonlinear) systems with bounded disturbances. Moreover, measurement noise is tolerated, gain $k(\cdot)$ will not diverge and tracking with prescribed asymptotic accuracy in the sense of (3.1) is achieved. Hence, in contrast to high-gain adaptive control, adaptive λ-tracking control is applicable in real world.

3.2 Brief historical overview

For a comprehensive overview of the development of adaptive λ-tracking or "approximate tracking" control see the surveys [85], [93] and the dissertation [33, Chapter 1].

The problem of gain drift due to noise was already mentioned in [129, Remark 4] (1984) and a "more appropriate" gain adaption with dead zone was proposed. The term "[adaptive] λ-tracking [control]" was coined by Ilchmann and Ryan (see [86, Section 5.2] (1993), [95] and [155] (1994)). For constant references Ryan introduces the notion of λ-stabilization (see [156]). For unknown sign of the high-frequency gain the use of Nussbaum functions is feasible and yields universal adaptive λ-tracking (see e.g. [86, Chapter 5] (1993) or [95, 156] (1994)).

The problem of approximate tracking was implicitly solved in [134] (1991) for minimum-phase LTI SISO systems with arbitrary relative degree and (exogenous) disturbances acting on state derivative and output. The proposed controller invokes a non-decreasing gain switching strategy and guarantees prescribed bounded overshoot and, moreover, invariance of the λ-strip after some prescribed time. Gain switching yields discontinuous control action and is undesirable for implementation in "real world" (in particular for motion control).

In 1994 (universal) adaptive λ-tracking control was introduced for nonlinearly perturbed minimum-phase systems with relative degree one (see [95] and [156]) for reference signals $y_{\mathrm{ref}}(\cdot) \in \mathcal{W}^{1,\infty}(\mathbb{R}_{\geq 0};\mathbb{R})$. In [95] the MIMO case is considered whereas [156] focuses on the SISO case but, in addition, allows for actuators with hysteresis and dead-zone (incorporating differential inclusion). The control strategies are similar, require knowledge of an upper bound on the nonlinear perturbation in terms of some continuous function $g\colon \mathbb{R} \to \mathbb{R}_{\geq 0}$ (in the SISO case) and use the following gain adaption

$$\dot{k}(t) = d_\lambda(|e(t)|)\,\big(|e(t)| + g(e(t) - y_{\mathrm{ref}}(t))\big), \qquad k(0) = k_0 > 0. \tag{3.4}$$

In [87] (1998) adaptive λ-tracking control for nonlinear MIMO systems with polynomially bounded nonlinearity is introduced. For controller design an upper bound $s \geq 1$ on the maximal polynomial degree is required and it is shown that gain adaption (3.4) could be replaced by the following simpler variant

$$\dot{k}(t) = d_\lambda(|e(t)|)^s, \qquad k(0) = k_0 > 0. \tag{3.5}$$

Universal adaptive λ-tracking for nonlinear SISO systems with relative degree one described

by functional differential equations is presented in [158] (2002) within a framework of differential inclusion. In [89] (2008) it was shown that adaptive λ-tracking control is robust in terms of the gap metric. Loosely speaking, by defining a measure for the "gap" between a nominal minimum-phase LTI MIMO system $\mathfrak{S}_0$ with relative degree one and a system $\mathfrak{S}$ (possibly not minimum-phase and/or with higher relative degree), it can be shown that for "small" initial values and if the measure is sufficiently small (yielding a "small gap") then adaptive λ-tracking control of system $\mathfrak{S}$ is still feasible.

There are few results for systems with higher relative degree. The most important are [190] (1999) and [34] (2005). In [190] Ye proposes an universal adaptive λ-tracking controller for nonlinear SISO systems with arbitrary-but-known relative degree, unknown high-frequency gain and polynomially bounded nonlinearity (again an upper bound on the maximum polynomial degree is assumed to be known). His control method incorporates a compensator (filter) and is based on a backstepping procedure (resulting in a complex structure, see Section 3.5.1). In contrast, in [34] Bullinger and Allgöwer introduce adaptive λ-tracking control in combination with a high-gain observer for nonlinear SISO systems with arbitrary-but-known relative degree with sector bounded nonlinearity (see Section 3.5.2). Adaptive λ-tracking with derivative feedback for LTI MIMO systems with arbitrary-but-known (and unknown-but-bounded) relative degree is introduced in [81, Section 2.3.3] (2010). However, the proposed controllers require derivative feedback up to the r-th order. System class $\mathcal{S}_2$ has relative degree two (i.e. $r = 2$), but only permits feedback of $y(\cdot)$ and $\dot{y}(\cdot)$.

Adaptive λ-tracking control is applicable in real world. Several applications are mentioned in literature. Most application are found in process automation of chemical reactions (chemical engineering): substrate concentration control of continuous aerobic continuous stirred tank reactors with input constraints (see [61]), set-point temperature control of chemical reactors without and with input constraints (see [2] and [100], resp.), biomass concentration control in activated sludge processes (see [60]) or pH regulation of biogas tower reactors (see [92]). Besides adaptive λ-tracking control was successfully implemented in anesthesia depth control (see [33, Chapter 4] or [35]) or applied to bio-inspired sensors with relative degree two and negative root locus center (see [20], however the proofs are incomplete).

To the best knowledge of the author, theoretical results for adaptive λ-tracking control with derivative feedback for systems of class $\mathcal{S}_2$ (or similar systems which only allow for derivative feedback up to the first order) have not yet been published and, moreover, adaptive λ-tracking control has not yet been applied for speed and position control of industrial servo-systems.

3.3 Mathematical preliminaries

For Chapter 3 and Chapter 4, some more mathematical preliminaries will be required. These are presented in this section. At first "Byrnes-Isidori like forms" of systems of class $\mathcal{S}_1$ and class $\mathcal{S}_2$ are derived. These forms are similar to the Byrnes-Isidori forms presented in Section 2.3.2.1 and facilitate system analysis in the upcoming proofs. Since reference tracking is the control objective, in particular, the rewritten "error Byrnes-Isidori like form" is of interest. At the end of this section, existence theory of functional differential equations is briefly revisited.

3.3.1 Byrnes-Isidori like form of systems of class $\mathcal{S}_1$

System class $\mathcal{S}_1$ comprises systems of form (1.36) with relative degree one (see Definition 1.6). Application of the coordinate transformation $(y,\, \boldsymbol{z}) := \boldsymbol{S}\boldsymbol{x}$ with $\boldsymbol{S}$ as in (2.49) (see Section 2.3.2.1) to (1.36) gives the following Byrnes-Isidori like form of systems of class $\mathcal{S}_1$

$$\left.\begin{aligned} \dot{y}(t) &= a_1 y(t) + \boldsymbol{a}_2^\top \boldsymbol{z}(t) + \gamma_0(u(t)+u_d(t)) + \boldsymbol{c}^\top \boldsymbol{B}_{\mathfrak{T}}\big((\mathfrak{T}(\boldsymbol{S}^{-1}\left(\begin{smallmatrix} y \\ \boldsymbol{z}\end{smallmatrix}\right)))(t) + \boldsymbol{d}(t)\big), \quad && y|_{[-h,0]} = \boldsymbol{c}^\top \boldsymbol{x}^0 \\ \dot{\boldsymbol{z}}(t) &= \boldsymbol{a}_3 y(t) + \boldsymbol{A}_4 \boldsymbol{z}(t) + \boldsymbol{N}\boldsymbol{B}_{\mathfrak{T}}\big((\mathfrak{T}(\boldsymbol{S}^{-1}\left(\begin{smallmatrix} y \\ \boldsymbol{z}\end{smallmatrix}\right)))(t) + \boldsymbol{d}(t)\big), && \boldsymbol{z}|_{[-h,0]} = \boldsymbol{N}\boldsymbol{x}^0 \end{aligned}\right\} \tag{3.6}$$

where γ_0, a_1, $\boldsymbol{a}_2$, $\boldsymbol{a}_3$ and $\boldsymbol{A}_4$ are as in (2.51), respectively. Note the similarity to the BIF (2.50) of LTI SISO systems with relative degree one. Let $y_{\mathrm{ref}}(\cdot) \in \mathcal{W}^{1,\infty}([-h,\infty);\mathbb{R})$ (i.e. extend $y_{\mathrm{ref}}(\cdot) \in \mathcal{W}^{1,\infty}(\mathbb{R}_{\geq 0};\mathbb{R})$ to the interval $[-h,0]$), then substituting $y_{\mathrm{ref}}(t) - e(t)$ for $y(t)$ in (3.6) and solving for $\dot{e}(t)$ gives the "error Byrnes-Isidori like form" as follows

$$\left.\begin{aligned} \dot{e}(t) &= a_1(e(t) - y_{\mathrm{ref}}(t)) + \dot{y}_{\mathrm{ref}}(t) - \boldsymbol{a}_2^\top \boldsymbol{z}(t) - \gamma_0(u(t)+u_d(t)) \\ &\quad -\boldsymbol{c}^\top \boldsymbol{B}_{\mathfrak{T}}\big((\mathfrak{T}(\boldsymbol{S}^{-1}\left(\begin{smallmatrix} y_{\mathrm{ref}} - e \\ \boldsymbol{z}\end{smallmatrix}\right)))(t) + \boldsymbol{d}(t)\big), \qquad e|_{[-h,0]} = (y_{\mathrm{ref}}|_{[-h,0]} - \boldsymbol{c}^\top \boldsymbol{x}^0) \\ \dot{\boldsymbol{z}}(t) &= \boldsymbol{a}_3(y_{\mathrm{ref}}(t) - e(t)) + \boldsymbol{A}_4 \boldsymbol{z}(t) + \boldsymbol{N}\boldsymbol{B}_{\mathfrak{T}}\big((\mathfrak{T}(\boldsymbol{S}^{-1}\left(\begin{smallmatrix} y_{\mathrm{ref}} - e \\ \boldsymbol{z}\end{smallmatrix}\right)))(t) + \boldsymbol{d}(t)\big), \ \boldsymbol{z}|_{[-h,0]} = \boldsymbol{N}\boldsymbol{x}^0 \end{aligned}\right\} \tag{3.7}$$

3.3.2 Byrnes-Isidori like form of systems of class $\mathcal{S}_2$

Systems of class $\mathcal{S}_2$ have relative degree two (see Definition 1.7). For $r = 2$, the coordinate change $(y,\, \dot{y},\, \boldsymbol{z}) := \boldsymbol{S}\boldsymbol{x}$ with $\boldsymbol{S}$ as in (2.24) applied to system (1.36), yields

$$\left.\begin{aligned} \tfrac{\mathrm{d}}{\mathrm{d}t}\begin{pmatrix} y(t) \\ \dot{y}(t)\end{pmatrix} &= \begin{bmatrix} 0 & 1 \\ a_1 & a_2\end{bmatrix}\begin{pmatrix} y(t) \\ \dot{y}(t)\end{pmatrix} + \begin{bmatrix} \boldsymbol{0}_m^\top \\ \boldsymbol{a}_3^\top\end{bmatrix}\boldsymbol{z}(t) + \begin{pmatrix} 0 \\ \gamma\end{pmatrix}(u(t)+u_d(t)) \\ &\quad + \begin{bmatrix} \boldsymbol{0}_m^\top \\ \boldsymbol{c}^\top \boldsymbol{A}\boldsymbol{B}_{\mathfrak{T}}\end{bmatrix}\left((\mathfrak{T}(\boldsymbol{S}^{-1}\begin{pmatrix} y \\ \dot{y} \\ \boldsymbol{z}\end{pmatrix}))(t) + \boldsymbol{d}(t)\right), \ \begin{pmatrix} y \\ \dot{y}\end{pmatrix}\Big|_{[-h,0]} = \boldsymbol{C}\boldsymbol{x}^0 \\ \dot{\boldsymbol{z}}(t) &= \begin{bmatrix} \boldsymbol{a}_4 & \boldsymbol{0}_{n-2}\end{bmatrix}\begin{pmatrix} y(t) \\ \dot{y}(t)\end{pmatrix} + \boldsymbol{A}_5\boldsymbol{z}(t) + \boldsymbol{N}\boldsymbol{B}_{\mathfrak{T}}\left((\mathfrak{T}(\boldsymbol{S}^{-1}\begin{pmatrix} y \\ \dot{y} \\ \boldsymbol{z}\end{pmatrix}))(t) + \boldsymbol{d}(t)\right), \ \boldsymbol{z}|_{[-h,0]} = \boldsymbol{N}\boldsymbol{x}^0, \end{aligned}\right\} \tag{3.8}$$

where γ_0, $(a_1,\, a_2)$, $\boldsymbol{a}_3$, $\boldsymbol{a}_4$ and $\boldsymbol{A}_5$ are as in (2.55), respectively. Note that $\boldsymbol{c}^\top \boldsymbol{B}_{\mathfrak{T}} = \boldsymbol{0}_m^\top$ in ($\mathcal{S}_2$-sp$_1$) is essential for this transformation. For extended reference $y_{\mathrm{ref}}(\cdot) \in \mathcal{W}^{2,\infty}([-h,\infty);\mathbb{R})$, substitute $y_{\mathrm{ref}}(t) - e(t)$ and $\dot{y}_{\mathrm{ref}}(t) - \dot{e}(t)$ for $y(t)$ and $\dot{y}(t)$ in (3.8), respectively, and solve for $(e(t), \dot{e}(t))^\top$ which yields the "error Byrnes-Isidori like form" as follows

$$\left.\begin{aligned} \tfrac{\mathrm{d}}{\mathrm{d}t}\begin{pmatrix} e(t) \\ \dot{e}(t)\end{pmatrix} &= \begin{bmatrix} 0 & 1 \\ a_1 & a_2\end{bmatrix}\begin{pmatrix} e(t) - y_{\mathrm{ref}}(t) \\ \dot{e}(t) - \dot{y}_{\mathrm{ref}}(t)\end{pmatrix} + \begin{pmatrix} \dot{y}_{\mathrm{ref}}(t) \\ \ddot{y}_{\mathrm{ref}}(t)\end{pmatrix} - \begin{bmatrix} \boldsymbol{0}_m^\top \\ \boldsymbol{a}_3^\top\end{bmatrix}\boldsymbol{z}(t) - \begin{pmatrix} 0 \\ \gamma\end{pmatrix}(u(t)+u_d(t)) \\ &\quad - \begin{bmatrix} \boldsymbol{0}_m^\top \\ \boldsymbol{c}^\top \boldsymbol{A}\boldsymbol{B}_{\mathfrak{T}}\end{bmatrix}\left((\mathfrak{T}(\boldsymbol{S}^{-1}\begin{pmatrix} y_{\mathrm{ref}} - e \\ \dot{y}_{\mathrm{ref}} - \dot{e} \\ \boldsymbol{z}\end{pmatrix}))(t) + \boldsymbol{d}(t)\right), \ \begin{pmatrix} e \\ \dot{e}\end{pmatrix}\Big|_{[-h,0]} = \left(\begin{pmatrix} y_{\mathrm{ref}}|_{[-h,0]} \\ \dot{y}_{\mathrm{ref}}|_{[-h,0]}\end{pmatrix} - \boldsymbol{C}\boldsymbol{x}^0\right) \\ \dot{\boldsymbol{z}}(t) &= \begin{bmatrix} \boldsymbol{a}_4 & \boldsymbol{0}_{n-2}\end{bmatrix}\begin{pmatrix} y_{\mathrm{ref}}(t) - e(t) \\ \dot{y}_{\mathrm{ref}}(t) - \dot{e}(t)\end{pmatrix} + \boldsymbol{A}_5\boldsymbol{z}(t) + \boldsymbol{N}\boldsymbol{B}_{\mathfrak{T}}\left((\mathfrak{T}(\boldsymbol{S}^{-1}\begin{pmatrix} y_{\mathrm{ref}} - e \\ \dot{y}_{\mathrm{ref}} - \dot{e} \\ \boldsymbol{z}\end{pmatrix}))(t) + \boldsymbol{d}(t)\right), \\ &\quad \boldsymbol{z}|_{[-h,0]} = \boldsymbol{N}\boldsymbol{x}^0. \end{aligned}\right\} \tag{3.9}$$

3.3.3 Solution of functional differential equation

Systems of class $\mathcal{S}_1$ and $\mathcal{S}_2$ are described by a functional differential equation of form (1.36). More precisely, for $h \geq 0$, a non-empty open set $\mathcal{D} \subset \mathbb{R}^n$, a causal operator $\mathfrak{T}$ element of class $\mathcal{T}$ (see Definition 1.5, p. 40) and a function $\boldsymbol{f}\colon [-h,\infty) \times \mathcal{D} \times \mathbb{R}^m \to \mathbb{R}^n$, initial-value problems of the form

$$\dot{\boldsymbol{x}}(t) = \boldsymbol{f}(t, \boldsymbol{x}(t), (\mathfrak{T}\boldsymbol{x})(t)), \quad \boldsymbol{x}|_{[-h,0]} = \boldsymbol{x}^0 \in \mathcal{C}([-h,0]) \quad \text{with} \quad \boldsymbol{x}^0(0) \in \mathcal{D} \tag{3.10}$$

will be considered. For the upcoming proofs one is interested in a solution of the initial-value problem (3.10). By a solution of the initial-value problem (3.10) one means an absolutely continuous function $\boldsymbol{x}(\cdot)\colon [-h,T) \to \mathbb{R}^n$, $T \in (0,\infty]$ with $\boldsymbol{x} = \boldsymbol{x}|_{[-h,0]}$ which satisfies (3.10) for almost all $t \in [0,T)$ and $\boldsymbol{x}(t) \in \mathcal{D}$ for all $t \in [0,T)$. Such a solution does exist if the function $\boldsymbol{f}(\cdot,\cdot,\cdot)$ in (3.10) satisfies so called "Carathéodory conditions", or in other words, if $\boldsymbol{f}(\cdot,\cdot,\cdot)$ is a "Carathéodory function" defined as follows:

Definition 3.1 (Carathéodory function (in the sense of Footnote 4 in [99]))**.**
Let $n, m \in \mathbb{N}$ and $h \geq 0$. For open and non-empty $\mathcal{D} \subset \mathbb{R}^n$, a function $\boldsymbol{f}\colon [-h,\infty) \times \mathcal{D} \times \mathbb{R}^m \to \mathbb{R}^n$ is said to be a Carathéodory function *if, and only if, the following hold:*

(i) $\boldsymbol{f}(t,\cdot,\cdot)$ is continuous for almost all $t \geq 0$;

(ii) $\boldsymbol{f}(\cdot,\boldsymbol{x},\boldsymbol{w})$ is measurable for each fixed $(\boldsymbol{x},\boldsymbol{w}) \in \mathcal{D} \times \mathbb{R}^m$;

(iii) for each compact $\mathfrak{C} \subset \mathcal{D} \times \mathbb{R}^m$, there exists $l_{\mathfrak{C}}(\cdot) \in \mathcal{L}^1_{\mathrm{loc}}([-h,\infty);\mathbb{R}_{\geq 0})$ such that $\|\boldsymbol{f}(t,\boldsymbol{x},\boldsymbol{w})\| \leq l_{\mathfrak{C}}(t)$ for almost all $t \in [-h,\infty)$ and all $(\boldsymbol{x},\boldsymbol{w}) \in \mathfrak{C}$.

And so an existence theorem can be restated which gives sufficient conditions to conclude on existence of a solution of the initial-value problem (3.10).

Theorem 3.2 (Existence theorem for functional differential equation (see Theorem 5 in [99]))**.**
Let $n, m \in \mathbb{N}$ and $h \geq 0$. Consider an open and non-empty set $\mathcal{D} \subset \mathbb{R}^n$, an operator $\mathfrak{T}$ of class $\mathcal{T}$ and $\boldsymbol{x}^0(\cdot) \in \mathcal{C}([-h,0];\mathbb{R})$ such that $\boldsymbol{x}^0(0) \in \mathcal{D}$. Now, if $\boldsymbol{f}\colon [-h,\infty) \times \mathcal{D} \times \mathbb{R}^m \to \mathbb{R}^n$ is a Carathéodory function, then there exists a solution $\boldsymbol{x}\colon [-h,T) \to \mathbb{R}^n$, $T \in (0,\infty]$ of the initial-value problem (3.10) with $\boldsymbol{x}([0,T)) \subset \mathcal{D}$ and every solution can be extended to a maximal solution. Moreover, if in addition $\boldsymbol{f}(\cdot,\cdot,\cdot)$ is locally essentially bounded and $\boldsymbol{x}\colon [-h,T) \to \mathbb{R}^n$, $\boldsymbol{x}([0,T)) \subset \mathcal{D}$, is a maximal solution with $T < \infty$, then, for every compact $\widetilde{\mathfrak{C}} \subset \mathcal{D}$, there exists $\tilde{t} \in [0,T)$ such that $\boldsymbol{x}(\tilde{t}) \notin \widetilde{\mathfrak{C}}$.

Proof. see [99, p. 10,11]. □

Note that Theorem 3.2 does not guarantee existence of a *unique* solution in contrast to the classical theory of Carathéodory (see e.g. Theorem 2.1.14 in [77]). In contrast to the Carathéodory conditions stated in [77, p. 84], in Definition 3.1, the function $\boldsymbol{f}\colon [-h,\infty) \times \mathcal{D} \times \mathbb{R}^m \to \mathbb{R}^n$ is *not* required to satisfy a locally Lipschitz-like condition.
The last statement in Theorem 3.2 implies that, for any maximal solution $\boldsymbol{x}\colon [-h,T) \to \mathbb{R}^n$ with $T < \infty$, either $\|\boldsymbol{x}(t)\| \to \infty$ as $t \to T$ or the boundary $\partial\mathcal{D}$ of $\mathcal{D}$ is not empty and $\lim_{t\to T} \operatorname{dist}(\boldsymbol{x}(t), \partial\mathcal{D}) = 0$.

3.4 Relative degree one systems

The well known result of adaptive λ-tracking is presented for systems of class $\mathcal{S}_1$. In contrast to the results in [87] or [158] the following theorem allows for nonlinear state-dependent functional perturbations. However, the admissible operators must be globally bounded.

Theorem 3.3 (Adaptive λ-tracking control for systems of class $\mathcal{S}_1$)**.**
Consider a system of class $\mathcal{S}_1$ described by (1.36). Then, for arbitrary initial trajectories $\boldsymbol{x}^0(\cdot) \in \mathcal{C}([-h,0];\mathbb{R}^n)$ and $k^0(\cdot) \in \mathcal{C}([-h,0];\mathbb{R}_{>0})$ and reference signal $y_{\mathrm{ref}}(\cdot) \in \mathcal{W}^{1,\infty}(\mathbb{R}_{\geq 0};\mathbb{R})$, the adaptive λ-tracking controller

$$\left.\begin{aligned} u(t) &= \operatorname{sign}(\boldsymbol{c}^\top \boldsymbol{b})\, k(t) e(t), && \text{where} \quad e(t) = y_{\mathrm{ref}}(t) - y(t) \\ \dot{k}(t) &= q_1\, d_\lambda(|e(t)|)^{q_2}, && k(0) = k^0(0) \end{aligned}\right\} \tag{3.11}$$

with design parameters $q_1 > 0$, $q_2 \geq 2$, $k^0(0) > 0$ and $\lambda > 0$ applied to (1.36) yields a closed-loop initial-value problem with the properties:

(i) there exists a solution $(\boldsymbol{x}, k) : [-h, T) \to \mathbb{R}^n \times \mathbb{R}_{>0}$ which can be maximally extended and $T \in (0, \infty]$;

(ii) the solution is global, i.e. $T = \infty$;

(iii) all signals are bounded, i.e. $\boldsymbol{x}(\cdot) \in \mathcal{L}^\infty(\mathbb{R}_{\geq 0};\mathbb{R}^n)$ and $k(\cdot) \in \mathcal{L}^\infty(\mathbb{R}_{\geq 0};\mathbb{R}_{>0})$;

(iv) the λ-strip is asymptotically reached, i.e. $\lim_{t\to\infty} \operatorname{dist}\Big(|e(t)|, [0,\lambda]\Big) = 0$.

Note that Assertion (iii) combined with the choice of $u(\cdot)$ in (3.11) and boundedness of the reference $y_{\mathrm{ref}}(\cdot)$ establish boundedness of $u(\cdot)$. Hence Theorem 3.3 implies that control objectives (co_1) and (co_2) are accomplished for all systems of class $\mathcal{S}_1$. Simulations are omitted. The adaptive λ-tracking controller (3.11) will be applied for speed control of electrical drives in Section 5.2.2.

Remark 3.4 (Design parameters q_1, q_2, λ and $k^0(0)$.)**.** *Clearly, for arbitrary initial gain trajectory $k^0(\cdot) \in \mathcal{C}([-h,0];\mathbb{R}_{>0})$ the initial gain $k(0) = k^0(0)$ can be specified. The design parameters q_1, q_2 and $k^0(0)$ have identical influence on the control performance of the closed-loop system (1.36), (3.11) as the design parameters q_1, q_2 and k_0 of the high-gain adaptive controller (2.81) (see Remark 2.27). The value of $\lambda > 0$ fixes the desired asymptotic accuracy.*

The following proof differs from that given in [87], nonlinear functional perturbations are included. The proof illustrates the principle idea of argumentation and helps to understand the more technical result for adaptive λ-tracking control with derivative feedback of systems of class $\mathcal{S}_2$ (see Section 3.5.3). Without loss of generality, in the proof (and all other proofs in the remainder of this thesis) measurement noise (or sensor error) $n_m(\cdot) \in \mathcal{W}^{2,\infty}(\mathbb{R}_{\geq 0};\mathbb{R}) \subset \mathcal{W}^{1,\infty}(\mathbb{R}_{\geq 0};\mathbb{R})$ is neglected. A simple substitution of $y_{\mathrm{ref}}(\cdot) - n_m(\cdot)$ for reference $y_{\mathrm{ref}}(\cdot)$ yields the result considering noise. If $n_m(\cdot) \in \mathcal{W}^{2,\infty}(\mathbb{R}_{\geq 0};\mathbb{R})$ corrupts output $y(\cdot)$, then the tracking error $e(\cdot)$ in (3.11) becomes $e(\cdot) = (y_{\mathrm{ref}}(\cdot) - n_m(\cdot)) - y(\cdot)$ and, clearly, the "corrupted reference" $y_{\mathrm{ref}}(\cdot) - n_m(\cdot)$ is (asymptotically) tracked instead of $y_{\mathrm{ref}}(\cdot)$ (recall also the discussion in Section 1.6.2.5).

Proof of Theorem 3.3.

Step 1: It is shown that Assertion (i) holds true, i.e. existence of a maximally extended solution. It suffices to consider system (1.36) of class $\mathcal{S}_1$ in the Byrnes-Isidori like form (3.7). Extend $y_{\mathrm{ref}}(\cdot)$ to $[-h,0)$ such that $y_{\mathrm{ref}}(\cdot) \in \mathcal{W}^{1,\infty}([-h,\infty);\mathbb{R})$. Define the open set

$$\mathcal{D} := \mathbb{R} \times \mathbb{R}^{n-1} \times \mathbb{R}_{>0},$$

the function

$$\begin{aligned} \boldsymbol{f}\colon [-h,\infty) \times \mathcal{D} \times \mathbb{R}^m &\to \mathcal{D}, \\ (t,(\mu,\boldsymbol{\xi},\kappa),\boldsymbol{w}) &\mapsto \begin{pmatrix} a_1(\mu - y_{\mathrm{ref}}(t)) + \dot{y}_{\mathrm{ref}}(t) - \boldsymbol{a}_2^\top \boldsymbol{\xi} - |\gamma_0|\,\kappa\,\mu \\ -\gamma_0\, u_d(t) - \boldsymbol{c}^\top \boldsymbol{B}_{\mathfrak{T}}(\boldsymbol{w} + \boldsymbol{d}(t)) \\ \boldsymbol{a}_3(y_{\mathrm{ref}}(t) - \mu) + \boldsymbol{A}_4\boldsymbol{\xi} + \boldsymbol{N}\boldsymbol{B}_{\mathfrak{T}}(\boldsymbol{w} + \boldsymbol{d}(t)) \\ q_1\, d_\lambda(|\mu|)^{q_2} \end{pmatrix} \end{aligned}$$

and the operator

$$\hat{\mathfrak{T}}\colon \mathcal{C}([-h,\infty);\mathbb{R}^{n+1}) \to \mathcal{L}^\infty_{\mathrm{loc}}(\mathbb{R}_{\geq 0};\mathbb{R}^m), \qquad (\hat{\mathfrak{T}}(\mu,\boldsymbol{\xi},\kappa))(t) := (\mathfrak{T}(\boldsymbol{S}^{-1}\left(\begin{smallmatrix} y_{\mathrm{ref}} - \mu \\ \boldsymbol{\xi} \end{smallmatrix}\right)))(t).$$

Then, for $\hat{\boldsymbol{x}} := (e,\, \boldsymbol{z},\, k)$, the initial-value problem (3.7), (3.11) may be written in the following form

$$\frac{\mathrm{d}}{\mathrm{d}t}\,\hat{\boldsymbol{x}}(t) = \boldsymbol{f}(t,\hat{\boldsymbol{x}}(t),(\hat{\mathfrak{T}}\hat{\boldsymbol{x}})(t)), \qquad \hat{\boldsymbol{x}}|_{[-h,0]} = \left(y_{\mathrm{ref}}|_{[-h,0]} - \boldsymbol{c}^\top \boldsymbol{x}^0,\quad (\boldsymbol{N}\boldsymbol{x}^0)^\top,\quad k^0\right)^\top \tag{3.12}$$

and note that, for any non-empty compact set $\mathfrak{C} \subset \mathcal{D} \times \mathbb{R}^m$, the following holds

$$\exists\, M_{\mathfrak{C}} > 0\ \forall\, ((\mu,\boldsymbol{\xi},\kappa),\boldsymbol{w}) \in \mathfrak{C}\colon \quad \|((\mu,\boldsymbol{\xi},\kappa),\boldsymbol{w})\| \leq M_{\mathfrak{C}}. \tag{3.13}$$

It is easy to see that for $u_d(\cdot) \in \mathcal{L}^\infty([-h,\infty);\mathbb{R})$, $\boldsymbol{d}(\cdot) \in \mathcal{L}^\infty([-h,\infty);\mathbb{R}^m)$ and $y_{\mathrm{ref}}(\cdot) \in \mathcal{W}^{1,\infty}([-h,\infty);\mathbb{R})$, the function $\boldsymbol{f}(\cdot,\cdot,\cdot)$ has the following properties: (i) $\boldsymbol{f}(t,\cdot,\cdot)$ is continuous for each fixed $t \in [-h,\infty)$; (ii) for each fixed $((\mu,\boldsymbol{\xi},\kappa),\boldsymbol{w}) \in \mathcal{D} \times \mathbb{R}^m$ the function $\boldsymbol{f}(\cdot,(\mu,\boldsymbol{\xi},\kappa),\boldsymbol{w})$ is measurable and (iii) for almost all $t \in [-h,\infty)$ and for all $((\mu,\boldsymbol{\xi},\kappa),\boldsymbol{w}) \in \mathfrak{C}$ the following holds

$$\begin{aligned} \|\boldsymbol{f}(t,(\mu,\boldsymbol{\xi},\kappa),\boldsymbol{w})\| \overset{(3.13)}{\leq}\ & M_{\mathfrak{C}}\Big(|a_1| + \|\boldsymbol{a}_2\| + |\gamma_0|\,M_{\mathfrak{C}} + \|\boldsymbol{c}\|\,\|\boldsymbol{B}_{\mathfrak{T}}\| + \|\boldsymbol{a}_3\| \\ & + \|\boldsymbol{A}_4\| + \|\boldsymbol{N}\|\,\|\boldsymbol{B}_{\mathfrak{T}}\| + q_1\,(M_{\mathfrak{C}} + \lambda)^{q_2}\Big) + (\|\boldsymbol{c}\| + \|\boldsymbol{N}\|)\,\|\boldsymbol{B}_{\mathfrak{T}}\|\,\|\boldsymbol{d}\|_\infty \\ & + (|a_1| + \|\boldsymbol{a}_3\|)\|y_{\mathrm{ref}}\|_\infty + \|\dot{y}_{\mathrm{ref}}\|_\infty + |\gamma_0|\,\|u_d\|_\infty =: l_{\mathfrak{C}}. \end{aligned}$$

Hence, in view of Definition 3.1, $\boldsymbol{f}(\cdot,\cdot,\cdot)$ is a Carathéodory function which, in view of Theorem 3.2, implies existence of a solution $\hat{\boldsymbol{x}} : [-h,T) \to \mathbb{R} \times \mathbb{R}^{n-1} \times \mathbb{R}_{>0}$ of the initial-value problem (3.12) with $\hat{\boldsymbol{x}}([0,T)) \in \mathcal{D}$, $T \in (0,\infty]$. Moreover, every solution can be extended to a maximal solution. In the following, let $\hat{\boldsymbol{x}} := (e,\boldsymbol{z},k)\colon [-h,T) \to \mathbb{R}\times\mathbb{R}^{n-1}\times\mathbb{R}_{>0}$ be a fixed and maximally extended solution of the initial-value problem (3.12), where $(e,\boldsymbol{z},k) : [-h,T) \to \mathbb{R}\times\mathbb{R}^{n-1}\times\mathbb{R}_{>0}$ solves the closed-loop initial-value problem (3.7), (3.11) for almost all $t \in [0,T)$ which shows Assertion (i).

Step 2: Some technical preliminaries are introduced.
Introduce the sub-coordinate change

$$\forall\, \nu \in (0,\, 1/2)\colon \qquad \boldsymbol{v}(t) := k(t)^{-\nu}\boldsymbol{z}(t). \tag{3.14}$$

and rewrite the closed-loop system (3.7), (3.11) as follows

$$\left.\begin{aligned} \dot e(t) &= \big(a_1 - |\gamma_0|\,k(t)\big)e(t) - a_1 y_{\mathrm{ref}}(t) + \dot y_{\mathrm{ref}}(t) - \boldsymbol{a}_2^\top k(t)^\nu \boldsymbol{v}(t) - \gamma_0 u_d(t) \\ &\quad -\boldsymbol{c}^\top \boldsymbol{B}_{\mathfrak{T}}\big((\mathfrak{T}(\boldsymbol{S}^{-1}\left(\begin{smallmatrix} y_{\mathrm{ref}} \\ k^\nu \boldsymbol{v}\end{smallmatrix}\right)))(t) + \boldsymbol{d}(t)\big), \qquad e|_{[-h,0]} = (y_{\mathrm{ref}}|_{[-h,0]} - \boldsymbol{c}^\top \boldsymbol{x}^0) \\ \dot{\boldsymbol{v}}(t) &= -\tfrac{\dot k(t)}{k(t)}\boldsymbol{v}(t) + k(t)^{-\nu}\boldsymbol{a}_3(y_{\mathrm{ref}}(t) - e(t)) + \boldsymbol{A}_4\boldsymbol{v}(t) \\ &\quad +k(t)^{-\nu}\boldsymbol{N}\boldsymbol{B}_{\mathfrak{T}}\big((\mathfrak{T}(\boldsymbol{S}^{-1}\left(\begin{smallmatrix} y_{\mathrm{ref}} \\ k^\nu \boldsymbol{v}\end{smallmatrix}\right)))(t) + \boldsymbol{d}(t)\big), \quad \boldsymbol{v}|_{[-h,0]} = (k^0)^{-\nu}\boldsymbol{N}\boldsymbol{x}^0 \end{aligned}\right\} \tag{3.15}$$

Due to system property ($\mathcal{S}_1$-sp$_2$) and Lemma 2.12, the matrix $\boldsymbol{A}_4$ is Hurwitz, i.e. spec$(\boldsymbol{A}_4) \subset \mathbb{C}_{<0}$ and hence (2.63) holds. For $\boldsymbol{P}_4$ as in (2.63) introduce the Lyapunov-like function

$$V_1\colon \mathbb{R}\times\mathbb{R}^{n-1} \to \mathbb{R}_{\geq 0}, \qquad (e,\boldsymbol{v}) \mapsto V_1(e,\boldsymbol{v}) := e^2 + \boldsymbol{v}^\top \boldsymbol{P}_4 \boldsymbol{v} \geq 0.$$

and define the constants

$$\begin{aligned} M_e &:= |a_1|\|y_{\mathrm{ref}}\|_\infty + \|\dot y_{\mathrm{ref}}\|_\infty + |\gamma_0|\|u_d\|_\infty + \|\boldsymbol{c}\|\,\|\boldsymbol{B}_{\mathfrak{T}}\|\,\big(M_{\mathfrak{T}} + \|\boldsymbol{d}\|_\infty\big), \\ M_{\boldsymbol{v}} &:= \|\boldsymbol{P}_4\|\,\Big(\,\|\boldsymbol{a}_3\|\,\|y_{\mathrm{ref}}\|_\infty + \|\boldsymbol{N}\|\,\|\boldsymbol{B}_{\mathfrak{T}}\|\,\big(M_{\mathfrak{T}} + \|\boldsymbol{d}\|_\infty\big)\Big) \qquad \text{and} \\ \mu_V &:= \tfrac{1}{2}\min\{1,\, \tfrac{1}{\|\boldsymbol{P}_4\|}\}. \end{aligned}$$

For notational brevity, write

$$\begin{aligned} &\forall\, t\in[0,T)\colon && V_1(t) &&:=\ V_1(e(t),\boldsymbol{v}(t)) \quad \text{with derivative along (3.15):} \\ &\forall\, t\in[0,T)\colon && \tfrac{\mathrm{d}}{\mathrm{d}t}V_1(t) &&=\ 2\,e(t)\dot e(t) + 2\boldsymbol{v}(t)^\top \boldsymbol{P}_4 \dot{\boldsymbol{v}}(t). \end{aligned} \tag{3.16}$$

In view of (3.15), the following hold for almost all $t\in[0,T)$

$$\begin{aligned} 2\,e(t)\dot e(t) &\overset{(3.15)}{\leq} -\big(2|\gamma_0|k(t) - 2|a_1|\big)e(t)^2 + 2|e(t)|\Big(|a_1|\|y_{\mathrm{ref}}\|_\infty + \|\dot y_{\mathrm{ref}}\|_\infty \\ &\qquad +|\gamma_0|\|u_d\|_\infty + \|\boldsymbol{c}\|\,\|\boldsymbol{B}_{\mathfrak{T}}\|\,\big(M_{\mathfrak{T}} + \|\boldsymbol{d}\|_\infty\big) + \|\boldsymbol{a}_2\|\,k(t)^\nu\,\|\boldsymbol{v}(t)\|\,\Big) \\ &\overset{(3.16),(2.62)}{\leq} -\Big(2|\gamma_0|k(t) - 2|a_1| - \frac{2\,M_e^2}{\mu_V\,\lambda^2} - 8\,\|\boldsymbol{a}_2\|^2\,k(t)^{2\nu}\Big)e(t)^2 + \frac{\mu_V\,\lambda^2}{2} + \frac{\|\boldsymbol{v}(t)\|^2}{8} \end{aligned} \tag{3.17}$$

and

$$\begin{aligned} 2\boldsymbol{v}(t)^\top \boldsymbol{P}_4\dot{\boldsymbol{v}}(t) &\overset{(3.15)}{\leq} -\|\boldsymbol{v}(t)\|^2 \overbrace{-2\frac{\dot k(t)}{k(t)}\boldsymbol{v}(t)^\top \boldsymbol{P}_4\boldsymbol{v}(t)}^{\leq 0} + 2\,k(t)^{-\nu}\,\|\boldsymbol{v}(t)\|\,\|\boldsymbol{P}_4\|\cdot \\ &\qquad \cdot\Big(\,\|\boldsymbol{a}_3\|\,\big(\|y_{\mathrm{ref}}\|_\infty + |e(t)|\big) + \|\boldsymbol{N}\|\,\|\boldsymbol{B}_{\mathfrak{T}}\|\,\big(M_{\mathfrak{T}} + \|\boldsymbol{d}\|_\infty\big)\Big) \\ &\overset{(3.16),(2.62)}{\leq} -\frac{3}{4}\,\|\boldsymbol{v}(t)\|^2 + 8\,k(t)^{-2\nu}\Big(M_{\boldsymbol{v}}^2 + \|\boldsymbol{P}_4\|^2\,\|\boldsymbol{a}_3\|^2\,|e(t)|^2\Big). \end{aligned} \tag{3.18}$$

Inserting (3.17) and (3.18) into (3.16) gives for almost all $t \in [0,T)$

$$\begin{aligned}\frac{\mathrm{d}}{\mathrm{d}t} V_1(t) \;\leq\; & -\Big(2|\gamma_0|k(t) - 2|a_1| - M_e^2 \frac{2}{\mu_V\,\lambda^2} - 8\,\|\boldsymbol{a}_2\|^2\,k(t)^{2\nu} - 8\,k(t)^{-2\nu}\,\|\boldsymbol{P}_4\|^2\,\|\boldsymbol{a}_3\|^2\Big)e(t)^2 \\ & -\frac{1}{2}\,\|\boldsymbol{v}(t)\|^2 + \mu_V\frac{\lambda^2}{2} + 8\,k(t)^{-2\nu}M_{\boldsymbol{v}}^2. \end{aligned} \tag{3.19}$$

Step 3: It is shown that $k(\cdot)$ is bounded on $[0,T)$.
Seeking a contradiction, assume that $k(\cdot)$ is unbounded on $[0,T)$. In view of (3.11), $k(\cdot)$ is non-decreasing on $[0,T)$, whence

$$\begin{aligned}\exists\, t^\star \geq 0\;\forall\, t \in [t^\star,T):\; 2|\gamma_0|k(t) - 2|a_1| - \frac{2M_e^2}{\mu_V\,\lambda^2} - 8\,\|\boldsymbol{a}_2\|^2\,k(t)^{2\nu} - \frac{8\,\|\boldsymbol{P}_4\|^2\,\|\boldsymbol{a}_3\|^2}{k(t)^{2\nu}} \geq 1/2 \\ \text{and} \quad k(t)^{2\nu} \geq \frac{16\,M_{\boldsymbol{v}}^2}{\mu_V\,\lambda^2}. \end{aligned} \tag{3.20}$$

Moreover, using $-\|\boldsymbol{v}(t)\|^2 \leq -\boldsymbol{v}(t)^\top \boldsymbol{P}_4 \boldsymbol{v}(t)/\,\|\boldsymbol{P}_4\|$ in (3.19), it follows that

$$\text{for a.a. } t \in [t^\star,T): \quad \tfrac{\mathrm{d}}{\mathrm{d}t} V_1(t) \overset{(3.20)}{\leq} -\mu_V\,V_1(t) + \mu_V\tfrac{\lambda^2}{2} + 8\,k(t)^{-2\nu}M_{\boldsymbol{v}}^2.$$

Since $|e(t)| \leq \sqrt{V_1(t)}$ for all $t \in [0,T)$ it follows that

$$\forall\, t \in [0,T): \quad \dot{k}(t) \overset{(3.11)}{=} q_1\,d_\lambda(|e(t)|)^{q_2} \leq q_1\,d_\lambda\Big(\sqrt{V_1(t)}\Big)^{q_2}. \tag{3.21}$$

Furthermore, observe that

$$\text{for a.a. } t \in [t^\star,T): \qquad \mu_V\frac{\lambda^2}{2} + 8\,k(t)^{-2\nu}M_{\boldsymbol{v}}^2 \overset{(3.20)}{\leq} \mu_V\lambda^2 \tag{3.22}$$

and, for any $t \in [0,T)$, the following implication holds

$$\Big[\!\Big[\; \sqrt{V_1(t)} \leq \lambda \;\Big]\!\Big] \overset{(N.5)}{\Longrightarrow} \Big[\!\Big[\; d_\lambda\big(\sqrt{V_1(t)}\big) = 0 \;\Big]\!\Big] \tag{3.23}$$

For $d_\lambda(\cdot)$ as in (N.5) consider the non-negative function $d_\lambda(\cdot)^2$ with derivative

$$\frac{\mathrm{d}}{\mathrm{d}s}\,d_\lambda(s)^2 = \begin{cases} 0 & ,\, s < \lambda \\ \lim_{h\to 0}\frac{d_\lambda(s+h)^2 - d_\lambda(s)^2}{h} = 2(s-\lambda) & ,\, s \geq \lambda. \end{cases} \tag{3.24}$$

Clearly, $d_\lambda(\cdot)^2$ is continuously differentiable. Then, the time derivative $\frac{1}{2}\frac{\mathrm{d}}{\mathrm{d}t}\,d_\lambda(\sqrt{V_1(t)})^2$ along

the solution of the closed-loop initial-value problem (3.15) is, for almost all $t \in [t^\star, T)$, given by

$$\begin{aligned}
\tfrac{1}{2}\tfrac{\mathrm{d}}{\mathrm{d}t}\, d_\lambda\Big(\sqrt{V_1(t)}\Big)^2 &= \tfrac{1}{2}\tfrac{\mathrm{d}}{\mathrm{d}s}\, d_\lambda(s)^2\Big|_{\sqrt{V_1(t)}} \tfrac{\mathrm{d}}{\mathrm{d}t}\sqrt{V_1(t)} \overset{(3.24),(N.5)}{=} \tfrac{d_\lambda\left(\sqrt{V_1(t)}\right)}{2\sqrt{V_1(t)}}\tfrac{\mathrm{d}}{\mathrm{d}t}\, V_1(t) \\
&\overset{(3.19)}{\leq} \tfrac{d_\lambda\left(\sqrt{V_1(t)}\right)}{2\sqrt{V_1(t)}}\Big(-\mu_V\, V_1(t) + \mu_V \tfrac{\lambda^2}{2} + 8\, k(t)^{-2\nu} M_{\boldsymbol{v}}^2\Big) \\
&\overset{(3.22)}{\leq} -\tfrac{d_\lambda\left(\sqrt{V_1(t)}\right)}{2\sqrt{V_1(t)}}\left(\mu_V\, V_1(t) - \mu_V \lambda^2\right) \\
&= -\tfrac{\mu_V}{2} d_\lambda\Big(\sqrt{V_1(t)}\Big)^2 \Big(\sqrt{V_1(t)} - \lambda\Big)\Big(1 + \tfrac{\lambda}{\sqrt{V_1(t)}}\Big) \\
&\overset{(3.23)}{\leq} -\tfrac{\mu_V}{2} d_\lambda\Big(\sqrt{V_1(t)}\Big)^2.
\end{aligned}$$

Hence integration yields

$$\forall\, t \in [t^\star, T)\colon \qquad d_\lambda\Big(\sqrt{V_1(t)}\Big)^2 \leq \exp\big(-\mu_V\,(t - t^\star)\big) \max\left\{ d_\lambda\Big(\sqrt{V_1(t^\star)}\Big)^2,\, \lambda^2 \right\}. \tag{3.25}$$

By compactness of $[0, t^\star]$, continuity of $(e(\cdot), \boldsymbol{v}(\cdot))$, $V_1(\cdot) = V_1(e(\cdot), \boldsymbol{v}(\cdot))$ and $d_\lambda\Big(\sqrt{V_1(\cdot)}\Big)$ on $[0, T)$, the contradiction follows

$$\begin{aligned}
\forall\, t \in [t^\star, T)\colon \quad k(t) - k(t^\star) &= \int_{t^\star}^{t} \dot{k}(\tau)\,\mathrm{d}\tau \overset{(3.21)}{\leq} q_1 \int_{t^\star}^{t} d_\lambda\Big(\sqrt{V_1(\tau)}\Big)^{q_2}\,\mathrm{d}\tau \\
&\overset{(3.25)}{\leq} q_1\, \max\left\{ d_\lambda\Big(\sqrt{V_1(t^\star)}\Big)^{q_2},\, \lambda^{q_2} \right\} \int_{t^\star}^{t} \exp\Big(-\frac{q_2 \mu_V}{2}\,(\tau - t^\star)\Big)\,\mathrm{d}\tau \\
&\leq \frac{2 q_1}{q_2 \mu_V}\, \max\left\{ d_\lambda\Big(\sqrt{V_1(t^\star)}\Big)^{q_2},\, \lambda^{q_2} \right\} < \infty.
\end{aligned}$$

Step 4: It is shown that Assertions (ii) holds true, i.e. $T = \infty$.
From Step 3 and (3.46) it follows that $k(\cdot)$ is continuous, non-increasing and bounded on $[0, T)$. Hence the limit

$$k_\infty := \lim_{t \to T} k(t) \geq k(0) > 0$$

exists and in view of the closed-loop system (3.7), (3.11) the following holds for almost all $t \in [0, T)$

$$\begin{aligned}
\left\| \frac{\mathrm{d}}{\mathrm{d}t} \begin{pmatrix} e(t) \\ \boldsymbol{z}(t) \end{pmatrix} \right\| \leq\ & \Big(|a_1| + |\gamma_0|\, k_\infty + \|\boldsymbol{a}_2\| + \|\boldsymbol{a}_3\| + \|\boldsymbol{A}_4\| \Big) \left\| \begin{pmatrix} e(t) \\ \boldsymbol{z}(t) \end{pmatrix} \right\| + |a_1| \|y_{\mathrm{ref}}\|_\infty + \|\dot{y}_{\mathrm{ref}}\|_\infty \\
& + |\gamma_0| \|u_d\|_\infty + \|\boldsymbol{a}_3\|\, \|y_{\mathrm{ref}}\|_\infty + (\|\boldsymbol{c}\| + \|\boldsymbol{N}\|)\, \|\boldsymbol{B}_{\mathfrak{T}}\|\, (M_{\mathfrak{T}} + \|\boldsymbol{d}\|_\infty),
\end{aligned}$$

which with Proposition 2.1.19 in [77, p. 86] implies, by maximality of T, that $T = \infty$. This shows Assertion (ii) and completes Step 4.

Step 5: It is shown that Assertion (iii) holds true, i.e. $k(\cdot) \in \mathcal{L}^\infty(\mathbb{R}_{\geq 0}; \mathbb{R}_{>0})$ and $\boldsymbol{x}(\cdot) \in \mathcal{L}^\infty(\mathbb{R}_{\geq 0}; \mathbb{R}^n)$.
Note that $k(\cdot) \in \mathcal{L}^\infty(\mathbb{R}_{\geq 0}; \mathbb{R}_{>0})$ follows from Step 3 and 4. It remains to show that $\boldsymbol{x}(\cdot) \in \mathcal{L}^\infty(\mathbb{R}_{\geq 0}; \mathbb{R}^n)$.

Step 5a: It is shown that $\boldsymbol{z}(\cdot)$ is bounded on $\mathbb{R}_{\geq 0}$.
For k_∞ as in Step 4 note that the following holds

$$\forall\, t \geq 0\colon \qquad \int_0^t d_\lambda(|e(\tau)|)^{q_2}\,\mathrm{d}\tau \overset{(3.11)}{=} \frac{1}{q_1}\int_0^t \dot{k}(\tau)\,\mathrm{d}\tau \leq \frac{1}{q_1}(k_\infty - k^0(0)) < \infty$$

which implies

$$\dot{k}(\cdot) \in \mathcal{L}^1(\mathbb{R}_{\geq 0};\mathbb{R}_{\geq 0}) \qquad \text{and} \qquad d_\lambda(|e(\cdot)|) \in \mathcal{L}^{q_2}(\mathbb{R}_{\geq 0};\mathbb{R}_{\geq 0}). \tag{3.26}$$

Define

$$\begin{aligned} \delta_2\colon\ \mathbb{R}\to\mathbb{R},\quad e\mapsto \delta_2(e) &:= \begin{cases} d_\lambda(|e|)\frac{e}{|e|} & ,|e|>\lambda \\ 0 & ,|e|\leq\lambda \end{cases} \qquad \text{and} \\ \delta_\infty\colon\ \mathbb{R}\to\mathbb{R},\quad e\mapsto \delta_\infty(e) &:= \begin{cases} \left(1-\frac{d_\lambda(|e|)}{|e|}\right)e & ,|e|>\lambda \\ e & ,|e|\leq\lambda \end{cases} \end{aligned} \tag{3.27}$$

and observe that, in view of (3.26) and (3.27), the following holds

$$\forall\, t\geq 0\colon\ e(t) = \delta_2(e(t)) + \delta_\infty(e(t)) \ \wedge\ |\delta_\infty(e(t))| \leq \lambda \ \text{ and } \ \delta_2(e(\cdot)) \in \mathcal{L}^{q_2}(\mathbb{R}_{\geq 0};\mathbb{R}). \tag{3.28}$$

For $\boldsymbol{P}_4$ as in (2.63) introduce the Lyapunov candidate

$$V_2\colon \mathbb{R}^{n-1}\to\mathbb{R}_{\geq 0},\quad \boldsymbol{v}\mapsto V_2(\boldsymbol{v}) := \boldsymbol{v}^\top \boldsymbol{P}_4 \boldsymbol{v}.$$

For $M_{\boldsymbol{v}}$ as in (3.16),

$$M_1 := 8\,k^0(0)^{-2\nu}\Big(\|\boldsymbol{P}_4\|^2\,\|\boldsymbol{a}_3\|^2\,\lambda^2 + M_{\boldsymbol{v}}^2\Big) \ \text{ and } \ M_2 := 8\,k^0(0)^{-2\nu}\,\|\boldsymbol{P}_4\|^2\,\|\boldsymbol{a}_3\|^2,$$

the time derivative $\frac{\mathrm{d}}{\mathrm{d}t}V_2(\boldsymbol{v}(t))$ along the solution of the (second equation of) closed-loop system (3.15) is, for almost all $t\geq 0$, bounded from above as follows

$$\begin{aligned} \frac{\mathrm{d}}{\mathrm{d}t}V_2(\boldsymbol{v}(t)) &\leq -\|\boldsymbol{v}(t)\|^2 + 2\,k^0(0)^{-\nu}\,\|\boldsymbol{v}(t)\|\,(\|\boldsymbol{P}_4\|\,\|\boldsymbol{a}_3\|\,|e(t)| + M_{\boldsymbol{v}}) \\ &\overset{(3.28)}{\leq} -\|\boldsymbol{v}(t)\|^2 + 2\,k^0(0)^{-\nu}\,\|\boldsymbol{v}(t)\|\Big(\|\boldsymbol{P}_4\|\,\|\boldsymbol{a}_3\|\,(|\delta_2(e(t))|+\lambda) + M_{\boldsymbol{v}}\Big) \\ &\overset{(2.62)}{\leq} -\frac{1}{2}\|\boldsymbol{v}(t)\|^2 + 8\,k^0(0)^{-2\nu}\Big(\|\boldsymbol{P}_4\|^2\,\|\boldsymbol{a}_3\|^2\,(|\delta_2(e(t))|^2+\lambda^2) + M_{\boldsymbol{v}}^2\Big) \\ &\overset{(3.16)}{\leq} -\mu_V V_2(\boldsymbol{v}(t)) + M_1 + M_2\,|\delta_2(e(t))|^2 \leq -\mu_V V_2(\boldsymbol{v}(t)) + M_1 + M_2\big(1+|\delta_2(e(t))|^{q_2}\big) \end{aligned}$$

where Fact 1.12.31 in [24, p. 39] was used in the last step. Application of the Bellman-Gronwall Lemma (in its differential form [18, Lemma 1.1, p. 2]) yields

$$\forall\, t\ \geq\ 0\colon\quad V_2(\boldsymbol{v}(t)) \overset{(3.74)}{\leq} V_2(\boldsymbol{v}(0)) + \frac{M_1+M_2}{\mu_V} + M_2 \underbrace{\int_0^t \overbrace{\exp\left(-\mu_V(t-\tau)\right)}^{\leq 1}|\delta_2(e(\tau))|^{q_2}\,\mathrm{d}\tau}_{\leq \|\delta_2(e)\|_{\mathcal{L}^{q_2}}^{q_2} < \infty}.$$

and therefore $V_2(\boldsymbol{v}(\cdot))$ is bounded on $\mathbb{R}_{\geq 0}$, which implies $\boldsymbol{v}(\cdot) \in \mathcal{L}^\infty(\mathbb{R}_{\geq 0}; \mathbb{R}^{n-2})$. From this, combined with $k(\cdot) \in \mathcal{L}^\infty(\mathbb{R}_{\geq 0}; \mathbb{R}_{>0})$ and (3.14), it follows that $\boldsymbol{z}(\cdot) = k(\cdot)^\nu \boldsymbol{v}(\cdot) \in \mathcal{L}^\infty(\mathbb{R}_{\geq 0}; \mathbb{R}^{n-1})$. This completes Step 5a.

Step 5b: It is shown that $e(\cdot)$ is bounded on $\mathbb{R}_{\geq 0}$.
Define

$$\forall\, t \geq 0\colon\ g(t) := a_1\, y_{\mathrm{ref}}(t) + \dot{y}_{\mathrm{ref}}(t) - \boldsymbol{a}_2^\top \boldsymbol{z}(t) - \gamma_0 u_d(t) - \boldsymbol{c}^\top \boldsymbol{B}_{\mathfrak{T}} \left((\mathfrak{T}(\boldsymbol{S}^{-1}\left(\begin{smallmatrix} y_{\mathrm{ref}} - e \\ \boldsymbol{z} \end{smallmatrix}\right)))(t) + \boldsymbol{d}(t) \right).$$

For $\delta_2(\cdot)$ and $\delta_\infty(\cdot)$ as in (3.27), $k_\infty > 0$ as in Step 4 and $l = \big(1 + a_1\big)/\gamma_0 - \mathrm{sign}(\gamma_0) k_\infty$ rewrite the first equation of the closed-loop system (3.7), (3.11) as follows

$$\tfrac{\mathrm{d}}{\mathrm{d}t}\, e(t) \;=\; -\big(1 - |\gamma_0|(k_\infty - k(t))\big) e(t) + \gamma_0\, l\big(\underbrace{\delta_2(e(t)) + \delta_\infty(e(t))}_{=e(t)} \big) + g(t). \tag{3.29}$$

For M_e as in (3.16) note that the following holds

$$\begin{aligned} &\forall\, t \geq 0\colon\ |g(t)| \leq M_e + \|\boldsymbol{a}_2\|\, \|\boldsymbol{z}\|_\infty =: M_g \qquad \text{and} \\ &[\![\, \lim\nolimits_{t\to\infty}(k_\infty - k(t))(t) = 0 \,]\!] \quad \Longrightarrow \quad \Big[\!\!\Big[\, \exists\, \tilde{t}_1 \geq 0\, \forall t \geq \tilde{t}_1\colon \quad |\gamma_0|(k_\infty - k(t)) \leq \tfrac{1}{4} \Big]\!\!\Big] \end{aligned} \tag{3.30}$$

and observe that the time derivative $\frac{\mathrm{d}}{\mathrm{d}t}\, e(t)^2$ along the solution of (3.29) is, for almost all $t \geq \tilde{t}_1$, bounded from above as follows

$$\begin{aligned} \frac{\mathrm{d}}{\mathrm{d}t}\, e(t)^2 \;&\overset{(3.28),(3.30)}{\leq}\; -2\big(1 - |\gamma_0|(k_\infty - k(t))\big) e(t)^2 + 2|e(t)| \Big(M_g + |\gamma_0| l (\lambda + \delta_2(e(t))) \Big) \\ &\overset{(2.62)}{\leq}\; -e(t)^2 + 4\Big(M_g^2 + |\gamma_0|^2 l^2 \big(\lambda^2 + \delta_2(e(t))^2\big) \Big) \\ &\leq\; -e(t)^2 + 4\Big(M_g^2 + |\gamma_0|^2 l^2 \big(\lambda^2 + 1 + |\delta_2(e(t))|^{q_2}\big) \Big). \end{aligned}$$

Applying the Bellman-Gronwall Lemma and invoking Theorem C.2.14 in [46, p. 241] again yields

$$\forall\, t \geq \tilde{t}_1\colon\ e(t)^2 \overset{(3.28)}{\leq} e(\tilde{t}_1)^2 + 4\Big(M_g^2 + |\gamma_0|^2 l^2 \big(\lambda^2 + 1 + \|\delta_2(e)\|_{\mathcal{L}^{q_2}}^{q_2}\big) \Big) < \infty,$$

which by continuity of $e(\cdot)$ on $\mathbb{R}_{\geq 0}$ and by compactness of $[0, \tilde{t}_1]$ implies $e(\cdot) \in \mathcal{L}^\infty(\mathbb{R}_{\geq 0}; \mathbb{R})$.

Step 5c: It is shown that $\boldsymbol{x}(\cdot) \in \mathcal{L}^\infty(\mathbb{R}_{\geq 0}; \mathbb{R}^n)$.
From Step 3 and 4 it follows that $k(\cdot) \in \mathcal{L}^\infty(\mathbb{R}_{\geq 0}; \mathbb{R}_{>0})$. From Step 5b & 5a it follows that $e(\cdot) \in \mathcal{L}^\infty(\mathbb{R}_{\geq 0}; \mathbb{R})$ and $\boldsymbol{z}(\cdot) \in \mathcal{L}^\infty(\mathbb{R}_{\geq 0}; \mathbb{R}^{n-1})$, resp. This combined with $y_{\mathrm{ref}}(\cdot) \in \mathcal{W}^{1,\infty}(\mathbb{R}_{\geq 0}; \mathbb{R})$ and $\boldsymbol{S}^{-1}$ as in (2.24) yields

$$\boldsymbol{x}(\cdot) = \boldsymbol{S}^{-1}(e(\cdot) - y_{\mathrm{ref}}(\cdot), \boldsymbol{z}(\cdot)^\top)^\top \in \mathcal{L}^\infty(\mathbb{R}_{\geq 0}; \mathbb{R}^n).$$

This shows Assertion (iii) and completes Step 5.

Step 6: It is shown that Assertion (iv) holds true, i.e. $\lim_{t\to\infty} \mathrm{dist}\, \Big(|e(t)|, [0, \lambda] \Big) = 0$.
First note that $e(\cdot) \in \mathcal{L}^\infty(\mathbb{R}_{\geq 0}; \mathbb{R})$, in view of (3.11), implies $\dot{k}(\cdot) \in \mathcal{L}^\infty(\mathbb{R}_{\geq 0}; \mathbb{R}_{>0})$. From

Step 5a recall that $\boldsymbol{v}(\cdot) \in \mathcal{L}^\infty(\mathbb{R}_{\geq 0}; \mathbb{R}^{n-1})$. Combining this with $\boldsymbol{d}(\cdot) \in \mathcal{L}^\infty(\mathbb{R}_{\geq 0}; \mathbb{R}^m)$, $y_{\mathrm{ref}}(\cdot) \in \mathcal{W}^{2,\infty}(\mathbb{R}_{\geq 0}; \mathbb{R})$, $u_d(\cdot) \in \mathcal{L}^\infty(\mathbb{R}_{\geq 0}; \mathbb{R})$ and global boundedness of the operator $\mathfrak{T}$ (see system property ($\mathcal{S}_2$-sp$_3$)) gives, in view of (3.15), $\dot{e}(\cdot) \in \mathcal{L}^\infty(\mathbb{R}_{\geq 0}; \mathbb{R})$. Furthermore it holds that

$$\forall\, t \geq 0\colon \quad \ddot{k}(t) = \frac{\mathrm{d}}{\mathrm{d}t}\left(q_1\, d_\lambda\big(|e(t)|\big)^{q_2}\right) = \begin{cases} 0 & , |e(t)| < \lambda \\ q_1 q_2 d_\lambda \left(|e(t)|\right)^{q_2 - 1} \operatorname{sign}(e(t)) \dot{e}(t) & , |e(t)| \geq \lambda. \end{cases}$$

Hence, $\ddot{k}(\cdot) \in \mathcal{L}^\infty(\mathbb{R}_{\geq 0}; \mathbb{R})$. This with (3.26) allows for application of Lemma 2.1.7 in [86, p. 17] (or Barbălat's Lemma [106, Lemma 3.2.6. p. 76]) which gives $\lim_{t\to\infty} \dot{k}(t) = 0$ and therefore $\lim_{t\to\infty} d_\lambda(|e(t)|) = 0$, which shows Assertion (iv). This completes Step 6 and the proof of Theorem 3.3. □

Remark 3.5. *It can be shown that Assertions (i)-(iv) of Theorem 3.3 also hold for $q_2 \geq 1$. Then, for $0 < \boldsymbol{P}_4 = \boldsymbol{P}_4^\top \in \mathbb{R}^{(n-1)\times(n-1)}$, choose $V_2\colon \mathbb{R}^{n-1} \to \mathbb{R}_{\geq 0}$, $\boldsymbol{v} \mapsto V_2(\boldsymbol{v}) := \sqrt{\boldsymbol{v}^\top \boldsymbol{P}_4 \boldsymbol{v}}$ instead of $V_2(\boldsymbol{v}) := \boldsymbol{v}^\top \boldsymbol{P}_4 \boldsymbol{v}$ in Step 5a and $|e|$ instead of e^2 in Step 5b of the proof of Theorem 3.3. Note that these choices are* not *continuously differentiable at $\boldsymbol{v} = \boldsymbol{0}_{n-1}$ and $e = 0$, respectively, and imply the use of upper right-hand derivatives (see [115, p. 659]) which are not considered in the present work.*

3.5 Relative degree two systems

In this section, adaptive λ-tracking control for systems of class $\mathcal{S}_2$ is discussed. At first the results of Ye [190] and Bullinger & Allgöwer [34] for systems with arbitrary-but-known relative degree are revisited which incorporate dynamic compensators (and backstepping) and high-gain observers, respectively. Both approaches do not require derivative feedback, but the controller structures are complex and do not allow for intuitive tuning. Moreover, both controllers achieve unsatisfactory control performance (see simulations in Section 3.5.4) and so no attempts are made to transfer the results to system class $\mathcal{S}_2$. Both controllers are presented for their respective system class as they were originally introduced (see [34, 190]) but, conform to system class $\mathcal{S}_2$, with restriction to the relative degree two case. Finally, the adaptive λ-tracking controller with derivative feedback is introduced and comparative simulations are presented.

3.5.1 Adaptive λ-tracking controller with backstepping

In 1999 Ye proposes an universal adaptive λ-tracking controller for minimum-phase LTI SISO systems with arbitrary-but-known relative degree, unknown sign of the high-frequency gain and polynomially bounded perturbation. Ye considers systems of the following form

$$\begin{aligned} \dot{\boldsymbol{x}}(t) &= \boldsymbol{A}\boldsymbol{x}(t) + \boldsymbol{b}\, u(t) + \boldsymbol{f}(t, \boldsymbol{x}(t)), & & n \in \mathbb{N},\ \boldsymbol{f}\colon \mathbb{R}_{\geq 0} \times \mathbb{R}^n \to \mathbb{R}^n,\ \boldsymbol{x}(0) = \boldsymbol{x}^0 \in \mathbb{R}^n, \\ y(t) &= \boldsymbol{c}^\top \boldsymbol{x}(t) & & (\boldsymbol{A}, \boldsymbol{b}, \boldsymbol{c}) \in \mathbb{R}^{n\times n} \times \mathbb{R}^n \times \mathbb{R}^n. \end{aligned} \tag{3.31}$$

and imposes three assumptions: (A1) known relative degree r of the unperturbed system, i.e. $\boldsymbol{f} = \boldsymbol{0}_n$ in (3.31) and (2.6), (A2) the unperturbed system is minimum-phase, i.e. $\boldsymbol{f} = \boldsymbol{0}_n$ in (3.31) and (2.14) and (A3) $\boldsymbol{f}\colon \mathbb{R}_{\geq 0} \times \mathbb{R}^n \to \mathbb{R}^n$ is a Carathéodory function and polynomially

bounded, i.e.

$$\forall\, \boldsymbol{x} \in \mathbb{R}^n \text{ for a.a. } t \geq 0\colon \qquad \|\boldsymbol{f}(t,\boldsymbol{x})\| \leq \alpha(1 + |\boldsymbol{c}^\top \boldsymbol{x}|^q) \tag{3.32}$$

where $\alpha > 0$ is *unknown* and $q \in \mathbb{N}$ *known*. For controller design the values r and q are necessary. Note the similarity of systems of form (3.31) and of form (1.36) being element of class $\mathcal{S}_2$. For $q = 0$ class $\mathcal{S}_2$ comprises systems of form (3.31).

Remark 3.6. *Note that the nonlinear perturbation term $\boldsymbol{f}(t,\boldsymbol{x})$ may change the relative degree r of the* unperturbed *linear system. Consider e.g. the case $r = 3$, then $\boldsymbol{c}^\top \boldsymbol{b} = \boldsymbol{c}^\top \boldsymbol{A}\boldsymbol{b} = 0$ and $\boldsymbol{c}^\top \boldsymbol{A}^2\boldsymbol{b} \neq 0$, but $\boldsymbol{c}^\top \frac{\partial \boldsymbol{f}(t,\boldsymbol{x})}{\partial \boldsymbol{x}}\big|_{(\boldsymbol{x}^\star,t^\star)} \boldsymbol{b} \neq 0$ is possible for some $\boldsymbol{x}^\star \in \mathbb{R}^n$ or some $t^\star \geq 0$. Hence at $(\boldsymbol{x}^\star, t^\star) \in \mathbb{R}^n \times \mathbb{R}_{\geq 0}$ the relative degree $r^\star = 2$ of the perturbed system is smaller than $r = 3$. Ye permits this case.*

Ye's controller consists of a stable $(r-1)$-th order compensator (in view of Bullinger [33] a reduced-state observer) and an adaptive λ-tracking controller with slightly modified gain adaption rule (both to be specified later). To achieve sign-correct control action he implements a Nussbaum function $f_{NB}\colon \mathbb{R} \to \mathbb{R}$ with properties as in (2.48). For $y_{\text{ref}}(\cdot) \in \mathcal{W}^{1,\infty}(\mathbb{R}_{\geq 0};\mathbb{R})$, his controller assures control objectives (co_1) and (co_2). For presentation measurement noise in the output is neglected, even though measurement noise $n_m(\cdot) \in \mathcal{W}^{1,\infty}(\mathbb{R}_{\geq 0};\mathbb{R})$ is tolerated but yields asymptotic tracking of the "deteriorated reference" $y_{\text{ref}}(\cdot) - n_m(\cdot)$ (see [190]).

In the following, to account for the exponent q in (3.32), choose

$$\bar{q} := \begin{cases} q & , q \quad \text{odd} \\ q+1 & , q \quad \text{even}, \end{cases} \tag{3.33}$$

and, conform to system class $\mathcal{S}_2$, only consider systems of form (3.31) with relative degree two, i.e. $r = 2$, and known sign of the high-frequency gain. Due to backstepping, Ye's controller is recursively defined and, already in the relative degree two case, becomes quite complex. For tracking error $e(t) = y_{\text{ref}}(t) - y(t)$, controller gain $k(t)$ and compensator state $\zeta_1(t)$ (both to be specified in (3.37)), introduce

$$\forall\, t \geq 0\colon \qquad \zeta_1^\star(t) := k(t)\big(e(t) + e(t)^{\bar{q}}\big) \qquad \text{and} \qquad \tilde{\zeta}_1(t) := \zeta_1^\star(t) - \zeta_1(t). \tag{3.34}$$

For compensator gain $k_F > 0$ and "design functions" $q_1(\cdot) \in \mathcal{C}^\infty(\mathbb{R};\mathbb{R}_{\geq 0})$ and $q_2(\cdot) \in \mathcal{C}^\infty(\mathbb{R};[1,\infty))$, satisfying

$$\forall\, e \in \mathbb{R}\colon \qquad q_1(e) \geq d_\lambda(|e|)^{\bar{q}}\big(|e| + |e|^{\bar{q}}\big) \qquad \text{and} \qquad q_2(e) \geq 1 + d_\lambda(|e|)^{\bar{q}}, \tag{3.35}$$

define (see [190])

$$\begin{aligned} \forall\, t \geq 0\colon \quad \zeta_2^\star(k(t), e(t), \zeta_1(t)) := k_F\, \zeta_1(t) + \Big[& q_1(e(t))^2 \big(e(t) + e(t)^{\bar{q}}\big)^2 \\ & + \big(1 + \bar{q} e(t)^{\bar{q}-1}\big)^2 \big(k(t)^2\, \zeta_1(t)^2 + q_2(e(t))^2\big) + 1 \Big]\, \tilde{\zeta}_1(t). \end{aligned} \tag{3.36}$$

Then Ye's adaptive λ-tracking controller with compensator is given as follows

$$\left.\begin{array}{rcll} \dot{\zeta}_1(t) & = & -k_F\,\zeta_1(t) + u(t), & \zeta_1(0) = \zeta_1^0 \in \mathbb{R},\ k_F > 0, \\ u(t) & = & \operatorname{sign}(\boldsymbol{c}^\top \boldsymbol{A}\boldsymbol{b})\,\zeta_2^\star\big(k(t), e(t), \zeta_1(t)\big), & \text{where} \quad e(t) = y_{\text{ref}}(t) - y(t) \quad \text{and} \\ & & & \zeta_2^\star\big(k(t), e(t), \zeta_1(t)\big) \text{ as in (3.36)}, \\ \dot{k}(t) & = & d_\lambda(|e(t)|)^{\bar{q}}\Big(|e(t)| + |e(t)|^{\bar{q}}\Big), & k(0) = k_0 \geq 0. \end{array}\right\} \tag{3.37}$$

Combining altogether, Ye's result can be formulated in the following theorem.

Theorem 3.7. *Consider a system of form (3.31) satisfying assumptions (A1)-(A3) with relative degree two and known sign of the high-frequency gain. Then, for arbitrary initial value* $(\boldsymbol{x}^0, \zeta_1^0) \in \mathbb{R}^{n+1}$ *and reference* $y_{\text{ref}}(\cdot) \in \mathcal{W}^{1,\infty}(\mathbb{R}_{\geq 0}, \mathbb{R})$*, the adaptive λ-tracking controller (3.37), with design parameters* $\bar{q} \geq 1$ *as in (3.33),* $k_0 \geq 0$*,* $k_F > 0$*,* $\lambda > 0$ *and* $q_1(\cdot) \in \mathcal{C}^\infty(\mathbb{R}; \mathbb{R}_{\geq 0})$ *and* $q_2(\cdot) \in \mathcal{C}^\infty(\mathbb{R}; [1, \infty))$ *with properties as in (3.35), applied to (3.31) yields a closed-loop initial-value problem with the properties:*

(i) there exists a solution $(\boldsymbol{x}, \zeta_1, k) : [-h, T) \to \mathbb{R}^n \times \mathbb{R} \times \mathbb{R}_{>0}$ *which can be maximally extended and* $T \in (0, \infty]$*;*

(ii) the solution is global, i.e. $T = \infty$*;*

(iii) all signals are bounded, i.e. $(\boldsymbol{x}(\cdot), \zeta_1(\cdot)) \in \mathcal{L}^\infty(\mathbb{R}_{\geq 0}; \mathbb{R}^{n+1})$ *and* $k(\cdot) \in \mathcal{L}^\infty(\mathbb{R}_{\geq 0}; \mathbb{R}_{>0})$*;*

(iv) the λ-strip is asymptotically reached, i.e. $\lim_{t\to\infty} \operatorname{dist}\Big(|e(t)|, [0, \lambda]\Big) = 0$.

Proof. see the proof of Theorem 1 in [190]. □

The choice of $\bar{q}$ as in (3.33) is essential for the Lyapunov-like analysis in the proof of Theorem 1 in [190]. It guarantees domination of the gain adaption over the nonlinear perturbation $\|\boldsymbol{f}(\cdot, \boldsymbol{x}(\cdot))\|$ (similar to (3.5) as introduced in [87]).

Remark 3.8 (Design parameters $\bar{q}$, k_0, λ, k_F, ζ_1^0, $q_1(\cdot)$ and $q_2(\cdot)$)**.**
Ye's adaptive λ-tracking controller (3.37) is set up by seven design parameters. In [190] Ye does not offer recommendations on parameter tuning. The parameter $\bar{q} \geq 1$ *(must be odd) will increase gain adaption speed and, clearly,* λ *and* k_0 *specify asymptotic accuracy and initial gain, respectively. Influence of* k_F*,* ζ_1^0*,* $q_1(\cdot)$ *and* $q_2(\cdot)$ *on the control performance is not easy to predict (see simulations in Section 3.5.4). The smooth functions* $q_1(\cdot)$ *and* $q_2(\cdot)$ *scale* $\tilde{\zeta}_1(\cdot)$ *in (3.36) and should be chosen "as small as" possible (but such that (3.35) holds) to avoid unnecessarily large control action. Large values in* k_F *yield a sensitive filter—in the sense that already "small" changes in* $u(\cdot)$ *will affect the filter state—and so the closed-loop system might exhibit oscillations with large amplitude and frequency. The initial value* ζ_1^0 *might be helpful to fix a non-zero control action at startup independently of the error. Simulations show that Ye's controller is sensitive to measurement noise and hence can hardly be implemented in "real world". Note that, in [190], Ye does not provide simulations results for* $u(\cdot)$ *(which should reveal high noise amplification).*

Remark 3.9. *The principle idea of Ye's approach becomes clearer by transforming system (3.31) into Byrnes-Isidori like form (similar to (3.7)). In [190, Lemma 1] it is shown that there exists an invertible, linear mapping* $\boldsymbol{T}\colon \mathbb{R}^{n+1} \to \mathbb{R}^{n+1}$ *which, if assumptions (A1)-(A3) hold, transforms the closed-loop system (3.31), (3.37) into the following equivalent form*

$$\begin{aligned} \dot{e}(t) &= f_1\, e(t) + \boldsymbol{f}_2^\top \boldsymbol{\eta}(t) + \beta\, \zeta_1(t) + d_1(t, e(t), \boldsymbol{\eta}(t), \zeta_1(t)) \\ \dot{\boldsymbol{\eta}}(t) &= \boldsymbol{f}_3\, e(t) + \boldsymbol{F}_4 \boldsymbol{\eta}(t) + \boldsymbol{d}_2(t, e(t), \boldsymbol{\eta}(t), \zeta_1(t)) \\ \dot{\zeta}_1(t) &= k_F\, \zeta_1(t) + u(t) \end{aligned} \quad , \quad \begin{pmatrix} e(0) \\ \boldsymbol{\eta}(0) \\ \zeta_1(0) \end{pmatrix} = \boldsymbol{T} \begin{pmatrix} \boldsymbol{x}^0 \\ \zeta_1^0 \end{pmatrix} \tag{3.38}$$

where $\beta > 0$, $f_1 \in \mathbb{R}$, $\boldsymbol{f}_2, \boldsymbol{f}_3 \in \mathbb{R}^{n-1}$, $\boldsymbol{F}_4 \in \mathbb{R}^{(n-1)\times(n-1)}$, $d_1\colon \mathbb{R}_{\geq 0} \times \mathbb{R} \times \mathbb{R}^{n-1} \times \mathbb{R} \to \mathbb{R}$ *and* $\boldsymbol{d}_2\colon \mathbb{R}_{\geq 0} \times \mathbb{R} \times \mathbb{R}^{n-1} \times \mathbb{R} \to \mathbb{R}^{n-1}$. *Moreover,* $\operatorname{spec}(\boldsymbol{F}_4) \subset \mathbb{C}_{<0}$ *and there exist* $\alpha_1, \alpha_2 > 0$ *such that* $|d_1(t, e, \boldsymbol{\eta}, \zeta_1)| \leq \alpha_1\big(1 + |e|^{\bar{q}}\big)$ *and* $\|\boldsymbol{d}_2(t, e, \boldsymbol{\eta}, \zeta_1)\| \leq \alpha_2\big(1 + |e|^{\bar{q}}\big)$ *for all* $(e, \boldsymbol{\eta}, \zeta_1) \in \mathbb{R} \times \mathbb{R}^{n-1} \times \mathbb{R}$ *and for almost all* $t \geq 0$.
Regarding ζ_1 *as (virtual) control input of system (3.38), it is easy to see that (3.38) can be interpreted as minimum-phase system with relative degree one and positive high-frequency gain* $\beta > 0$. *Thus adaptive* λ*-tracking control would be possible for*

$$\zeta_1(t) = \zeta_1^\star(k(t), e(t)) = k(t)\big(e(t) + e(t)^{\bar{q}}\big).$$

In general ζ_1 *will differ from the desired (virtual) control input* $\zeta_1^\star(k, e)$. *But if—loosely speaking—the "(virtual) control input error"* $\tilde{\zeta}_1(t)$ *as in (3.34) can be kept "small", then* λ*-tracking is still feasible. This intuition is exploited by Ye's approach.*

3.5.2 Adaptive λ-tracking controller with high-gain observer

Bullinger and Allgöwer present adaptive λ-tracking control for control-affine nonlinear SISO systems of the form

$$\begin{aligned} \dot{\boldsymbol{x}}(t) &= \boldsymbol{f}(\boldsymbol{x}(t)) + \boldsymbol{g}(\boldsymbol{x}(t))\, u(t), & \boldsymbol{x}(0) &= \boldsymbol{x}^0 \in \mathbb{R}^n, \\ y(t) &= h(\boldsymbol{x}(t)) & \boldsymbol{f}(\cdot),\, \boldsymbol{g}(\cdot) &\in \mathcal{C}^\infty(\mathbb{R}^n; \mathbb{R}^n),\ h(\cdot) \in \mathcal{C}^\infty(\mathbb{R}^n; \mathbb{R}) \end{aligned} \tag{3.39}$$

if, loosely speaking, the following assumptions hold (see [34]): (A1) the relative degree[1] $r \geq 1$ is arbitrary-but-known and globally defined, (A2) the high-frequency gain is positive, uniformly bounded away from zero and a lower bound $\underline{\gamma_0} > 0$ is known, i.e. $\gamma_0(\boldsymbol{x}) := L_{\boldsymbol{g}} L_{\boldsymbol{f}}^{r-1} h(\boldsymbol{x}) \geq \underline{\gamma_0}$ for all $\boldsymbol{x} \in \mathbb{R}^n$, (A3) the nonlinearities are "sector bounded" (see Definition 1 in [34]) and (A4) the zero-dynamics[2] of (3.39) can be decomposed into a "bounded and an exponentially stable part" (see Assumption 4 in [34]).

The controller proposed by Bullinger and Allgöwer consists of a r-th order high-gain adaptive observer and an adaptive λ-tracking controller with observer state feedback (instead of output feedback). For $y_{\text{ref}}(\cdot) \in \mathcal{W}^{1,\infty}(\mathbb{R}_{\geq 0}; \mathbb{R})$ their controller attains control objectives (co_1) and (co_2) (see Theorem 1 in [34]). Gain adaption affects observer and feedback gains. The observer states

[1] A system of form (3.39) is said to have relative degree r at a point $\boldsymbol{x}^\star \in \mathbb{R}^n$ if the following two conditions hold: (i) $L_{\boldsymbol{g}} L_{\boldsymbol{f}}^i h(\boldsymbol{x}) = 0$ for all $\boldsymbol{x}$ in a neighborhood of $\boldsymbol{x}^\star$ and all $i \in \{1, \dots r-1\}$ and (ii) $L_{\boldsymbol{g}} L_{\boldsymbol{f}}^{r-1} h(\boldsymbol{x}) \neq 0$ (see [107, p. 137]) where $L_{\boldsymbol{f}}^i h(\boldsymbol{x}) := (\partial L_{\boldsymbol{f}}^{i-1} h(\boldsymbol{x}) / \partial \boldsymbol{x}) \boldsymbol{f}(\boldsymbol{x})$ represents the i-th *Lie derivative* of $h(\cdot)$ along $\boldsymbol{f}(\boldsymbol{x})$ (see e.g. [115, p. 509,510]). If both conditions hold for any $\boldsymbol{x}^\star \in \mathbb{R}^n$, the relative degree r is globally defined.

[2] For a definition and a detailed discussion see [107, Section 4.3].

represent estimates of system output $y(\cdot)$ and its $r-1$ time derivatives. Note that neither measurement noise nor bounded (discontinuous) disturbances (in e.g. $\mathcal{L}^\infty(\mathbb{R}_{\geq 0};\mathbb{R})$) are explicitly permitted by Bullinger and Allgöwer (although those should be admissible).

Conform to system class $\mathcal{S}_2$, in the following assume that system (3.39) has global relative degree two (i.e. $r=2$). Then, under assumptions (A3) and (A4), system (3.39) can be transformed into (nonlinear) Bynres-Isidori form (see Remark 2 in [34]), i.e. there exists a global diffeomorphism[3] $\boldsymbol{\Phi}\colon\ \mathbb{R}^n \to \mathbb{R}^n,\ \boldsymbol{x} \mapsto ((y,\ \dot{y}),\ \boldsymbol{z}) := \boldsymbol{\Phi}(\boldsymbol{x})$ which yields

$$\left.\begin{aligned} \tfrac{\mathrm{d}}{\mathrm{d}t}\begin{pmatrix} y(t) \\ \dot{y}(t)\end{pmatrix} &= \begin{bmatrix} 0 & 1 \\ 0 & 0\end{bmatrix}\begin{pmatrix} y(t) \\ \dot{y}(t)\end{pmatrix} + \begin{pmatrix} 0 \\ 1\end{pmatrix}\Big(f_1\big((y(t),\,\dot{y}(t)),\boldsymbol{z}(t)\big) + \boldsymbol{f}_2\big((y(t),\,\dot{y}(t)),\boldsymbol{z}(t)\big)^\top \begin{pmatrix} y(t) \\ \dot{y}(t)\end{pmatrix} \\ &\qquad + \boldsymbol{f}_3\big((y(t),\,\dot{y}(t)),\boldsymbol{z}(t)\big)^\top \boldsymbol{z}(t) + \gamma_0\big((y(t),\,\dot{y}(t)),\boldsymbol{z}(t)\big)\,u(t)\Big), \\ \dot{\boldsymbol{z}}(t) &= \boldsymbol{f}_4\big((y(t),\,\dot{y}(t)),\boldsymbol{z}(t)\big)\,y(t) + \boldsymbol{f}_5\big(\boldsymbol{z}(t)\big) + \boldsymbol{f}_6\big((y(t),\,\dot{y}(t)),\boldsymbol{z}(t)\big), \\ (\boldsymbol{\xi}(0),\,\boldsymbol{z}(0)) &= \boldsymbol{\Phi}(\boldsymbol{x}^0) \end{aligned}\right\} \tag{3.40}$$

where

$$\left.\begin{aligned} &f_1(\cdot,\cdot) \in \mathcal{L}^\infty(\mathbb{R}^2\times\mathbb{R}^{n-2};\mathbb{R}),\ \boldsymbol{f}_2(\cdot,\cdot),\ \boldsymbol{f}_3(\cdot,\cdot) \in \mathcal{L}^\infty(\mathbb{R}^2\times\mathbb{R}^{n-2};\mathbb{R}^2), \\ &\boldsymbol{f}_4(\cdot,\cdot),\ \boldsymbol{f}_6(\cdot,\cdot) \in \mathcal{L}^\infty(\mathbb{R}^2\times\mathbb{R}^{n-2};\mathbb{R}^{n-2}),\ \forall\,(\boldsymbol{\xi},\boldsymbol{z}) \in \mathbb{R}^2\times\mathbb{R}^{n-2}\colon\ \gamma_0\big(\boldsymbol{\xi},\boldsymbol{z}\big) \geq \underline{\gamma_0} > 0 \\ &\text{and the dynamics } \dot{\boldsymbol{z}} = \boldsymbol{f}_5\big(\boldsymbol{z}\big) \text{ are globally exponentially stable.} \end{aligned}\right\} \tag{3.41}$$

Although system (3.40) is nonlinear, due to the restrictions in (3.41), it is structurally similar to the Byrnes-Isidori like form (3.8) of system class $\mathcal{S}_2$. Note that the admissible nonlinearities in $f_1(\cdot,\cdot)$ and $\boldsymbol{f}_6(\cdot,\cdot)$ are covered by the operator $\mathfrak{T}$.

To present Bullinger's and Allgöwer's adaptive λ-tracking controller with high-gain observer for systems of form (3.40) with (3.41) and relative degree two, introduce for $p_0, p_1 > 0$ and $g, q_0, q_1 > 0$ the polynomials

$$p(s) := s^2 + p_1 s + p_0 \qquad \text{and} \qquad q_g(s) := s^2 + g\,q_1\,s + g\,q_0 \tag{3.42}$$

and the following definition.

Definition 3.10. *Let $n \in \mathbb{N}$, $\epsilon > 0$ and $\mu > 0$. A polynomial $l(s) = s^n + \sum_{i=0}^{n-1} l_i s^i \in \mathbb{R}[s]$ is element of $H(\epsilon,\mu)$ if there exists a matrix $\boldsymbol{P} = \boldsymbol{P}^\top > 0$ which satisfies for*

$$\boldsymbol{A}_l := \begin{bmatrix} 0 & 1 & 0 & \dots & 0 \\ \vdots & \ddots & \ddots & \ddots & \vdots \\ \vdots & & \ddots & \ddots & 0 \\ 0 & \dots & \dots & 0 & 1 \\ -l_0 & -l_1 & \dots & -l_{n-2} & -l_{n-1} \end{bmatrix}$$

[3] Let $n \in \mathbb{N}$. A function $\boldsymbol{\Phi}\colon\ \mathbb{R}^n \to \mathbb{R}^n$ is called a global diffeomorphism if (i) $\boldsymbol{\Phi}$ is invertible, i.e. $\boldsymbol{\Phi}^{-1}(\boldsymbol{\Phi}(\boldsymbol{x})) = \boldsymbol{x}$ for all $\boldsymbol{x} \in \mathbb{R}^n$ and (ii) $\boldsymbol{\Phi}(\cdot),\ \boldsymbol{\Phi}(\cdot)^{-1} \in \mathcal{C}^\infty(\mathbb{R}^n;\mathbb{R}^n)$ (see e.g. [107, p. 11]).

and $\boldsymbol{\Psi}_n := \operatorname{diag}\{0, 1, \ldots, n-1\}$ *the two inequalities*

$$\left.\begin{aligned} \boldsymbol{A}_l^\top \boldsymbol{P} + \boldsymbol{P}\boldsymbol{A}_l &\leq -2\mu\boldsymbol{P}, \\ \boldsymbol{D} := \boldsymbol{\Psi}_n^\top \boldsymbol{P} + \boldsymbol{P}\boldsymbol{\Psi}_n &\geq -2\epsilon\boldsymbol{P}. \end{aligned}\right\} \tag{3.43}$$

Note that, in view of (3.43), $H(\epsilon, \mu)$ is a subset of the Hurwitz polynomials. In Appendix B.2 of [33] it is shown that for any Hurwitz polynomial $l(s)$ there exists a positive definite solution $\boldsymbol{P}$ which satisfies (3.43) and, moreover, there exist $\underline{\epsilon} > 0$ and $\overline{\mu} > 0$, such that $l(\cdot) \in H(\epsilon, \mu)$ for all $\epsilon \geq \underline{\epsilon}$ and $\mu \leq \overline{\mu}$, respectively.

Now Bullinger's and Allgöwer's main result can be formulated in the following theorem.

Theorem 3.11. *Consider a system of form (3.40) satisfying (3.41). Let $\alpha > \beta > 0$ and $p_0, p_1, q_0, q_1, \gamma > 0$, respectively. Choose $\epsilon > 0$ and $\mu > 0$ such that the polynomials $p(s)$ and $q_g(s)$ as in (3.42) are in $H(\epsilon, \mu)$ for all $g \geq \underline{\gamma_0}$ and*

$$\tilde{\gamma} > 2\alpha\epsilon + (\alpha - \beta) - \frac{1}{2}. \tag{3.44}$$

Then, for arbitrary initial value $(\boldsymbol{x}^0, \hat{\boldsymbol{x}}^0) \in \mathbb{R}^{n+2}$ and reference $y_{\mathrm{ref}}(\cdot) \in \mathcal{W}^{1,\infty}(\mathbb{R}_{\geq 0}, \mathbb{R})$, the adaptive λ-tracking controller with high-gain observer

$$\left.\begin{aligned} \dot{\hat{\boldsymbol{x}}}(t) &= \begin{bmatrix} -p_1\hat{\kappa}(t) & 1 \\ -p_0\hat{\kappa}^2(t) & 0 \end{bmatrix} \hat{\boldsymbol{x}}(t) - \begin{bmatrix} p_1\hat{\kappa}(t) \\ p_0\hat{\kappa}^2(t) \end{bmatrix} e(t), && \hat{\boldsymbol{x}}(0) = \hat{\boldsymbol{x}}^0 \in \mathbb{R}^2 \\ u(t) &= \begin{pmatrix} q_0\,\kappa(t)^2, & q_1\,\kappa(t) \end{pmatrix} \hat{\boldsymbol{x}}(t) && \text{where} \\ e(t) &= y_{\mathrm{ref}}(t) - y(t), \quad \hat{\kappa}(t) := k(t)^\alpha, \quad \kappa(t) := k(t)^\beta \\ \dot{k}(t) &= \gamma\, k(t)^{-2\tilde{\gamma}} d_\lambda(|e(t)|)^2, && k(0) = k_0 > 0 \end{aligned}\right\} \tag{3.45}$$

applied to (3.40) yields a closed-loop initial-value problem with the properties:

(i) there exists a solution $(\boldsymbol{x}, \hat{\boldsymbol{x}}, k) : [-h, T) \to \mathbb{R}^n \times \mathbb{R}^2 \times \mathbb{R}_{>0}$ which can be maximally extended and $T \in (0, \infty]$;

(ii) the solution is global, i.e. $T = \infty$;

(iii) all signals are bounded, i.e. $(\boldsymbol{x}(\cdot), \hat{\boldsymbol{x}}(\cdot)) \in \mathcal{L}^\infty(\mathbb{R}_{\geq 0}; \mathbb{R}^{n+1})$ and $k(\cdot) \in \mathcal{L}^\infty(\mathbb{R}_{\geq 0}; \mathbb{R}_{>0})$;

(iv) the λ-strip is asymptotically reached, i.e. $\lim_{t\to\infty} \operatorname{dist}\Big(|e(t)|, [0, \lambda]\Big) = 0$.

Proof. see proof of Theorem 1 in [34]. □

Remark 3.12 (Design parameters p_0, p_1, q_0, q_1, γ, $\tilde{\gamma}$, k_0, α and β)**.**
Controller (3.45) has nine design parameters which severely affect control performance. Bullinger and Allgöwer do not provide any rules of thumb for controller tuning. Clearly "fast observer dynamics" seem desirable, i.e. $p_0, p_1 \gg 1$ (see also simulations in Section 3.5.4). The influence of the feedback parameters q_0 and q_1 is not obvious and they must be chosen by trial and error (endangering application in real world, what if "bad" values are used?). The presuppositions in Theorem 3.11 make control design tedious. In particular the check for affiliation

of $p(s)$ and $q_g(s)$ as in (3.42) to the set $H(\epsilon, \mu)$ is unattractive. Any change in p_0, p_1 or q_0, q_1 may require revision of $\tilde{\gamma}$ as in (3.44) and so limit degrees of freedom in controller design (e.g. large values of $\tilde{\gamma}$ prevent rapid gain adaption). By γ and k_0 adaption speed and initial gain are varied. The exponents α and β allow tuning of observer and controller gains. Simulations show that a choice $\alpha > \beta \gg 1$ leads to "good" tracking performance and "fast" disturbance rejection but tremendous noise sensitivity and hence should be avoided.

3.5.3 Adaptive λ-tracking controller with derivative feedback

For relative degree $r \geq 2$, the proposed adaptive λ-tracking controllers with derivative feedback in [81, Section 2.3.3] require derivative feedback up to the r-th order. Systems of class $\mathcal{S}_2$ do not offer feedback of $\ddot{y}(\cdot)$. The following result is motivated by the high-gain adaptive controller proposed by Hoagg and Bernstein (see [80]), Theorem 2.36 (in Section 2.3.4.3) and the position control problem where $y(\cdot)$ and $\dot{y}(\cdot)$ are available for feedback.

Theorem 3.13 (Adaptive λ-tracking control with derivative feedback for systems of class $\mathcal{S}_2$)**.** *Consider a system of class $\mathcal{S}_2$ described by (1.36). Then, for arbitrary initial trajectories $\boldsymbol{x}^0(\cdot) \in \mathcal{C}^0([-h, 0]; \mathbb{R}^n)$ and $k^0(\cdot) \in \mathcal{C}^0([-h, 0]; \mathbb{R}_{>0})$ and reference $y_{\mathrm{ref}}(\cdot) \in \mathcal{W}^{2,\infty}(\mathbb{R}_{\geq 0}; \mathbb{R})$, the adaptive λ-tracking controller*

$$\left.\begin{aligned} u(t) &= \operatorname{sign}(\boldsymbol{c}^\top \boldsymbol{A}\boldsymbol{b})\Big(k(t)^2 e(t) + q_1\, k(t)\dot{e}(t)\Big) \quad \text{where} \quad e(t) = y_{\mathrm{ref}}(t) - y(t) \\ \dot{k}(t) &= q_2 \exp(-q_3\, q_4\, k(t))\, d_\lambda\Big(\left\|(e(t),\, \dot{e}(t)/k(t))^\top\right\|\Big)^{q_4}, \quad k(0) = k^0(0) \end{aligned}\right\} \tag{3.46}$$

with design parameters $q_1, q_2, q_3 > 0$, $q_4 \geq 2$, $k^0(0) > 0$ and $\lambda > 0$ applied to (1.36) yields a closed-loop initial-value problem with the properties:

(i) there exists a solution $(\boldsymbol{x}, k) : [-h, T) \to \mathbb{R}^n \times \mathbb{R}_{>0}$, $T \in (0, \infty]$ which can be maximally extended;

(ii) the solution is global, i.e. $T = \infty$;

(iii) all signals are bounded, i.e. $\boldsymbol{x}(\cdot) \in \mathcal{L}^\infty(\mathbb{R}_{\geq 0}; \mathbb{R}^n)$ and $k(\cdot) \in \mathcal{L}^\infty(\mathbb{R}_{\geq 0}; \mathbb{R}_{>0})$;

(iv) the λ-strip is asymptotically reached, i.e. $\lim_{t\to\infty} \operatorname{dist}\Big(\left\|(e(t),\, \dot{e}(t)/k(t))^\top\right\|, [0, \lambda]\Big) = 0$.

Remark 3.14 (Design parameters q_1, q_2, q_3, q_4, $k^0(0)$ and λ)**.**
The controller (3.46) is tuned by six parameters. Influence of the parameters q_1, q_2 and $k^0(0)$ on the closed-loop system response has already been discussed in Remark 2.37 (see also discussion in Section 2.3.4.4). The parameter $q_3 > 0$ scales the exponent in gain adaption (3.46) and should be chosen small, i.e. $q_3 \ll 1/(q_4 k^0(0))$. Practically, large initial exponents $q_3 q_4 k^0(0) \gg 1$ might stop gain adaption "too early" due to truncation of small numbers in binary format (in the real-time system). The exponent $q_4 \geq 2$ allows to accelerate gain adaption for large values of $\|(e(\cdot),\, \dot{e}(\cdot)/k(\cdot))\|$. The asymptotic accuracy is prescribed by $\lambda > 0$.

Proof of Theorem 3.13.

Step 1: It is shown that Assertion (i) holds true, i.e. existence of a maximally extended solution.

It suffices to consider system (1.36) in the form (3.9). Extend $y_{\mathrm{ref}}(\cdot)$ to $[-h,0)$ such that $y_{\mathrm{ref}}(\cdot) \in \mathcal{W}^{2,\infty}([-h,\infty);\mathbb{R})$ and define the open and non-empty set

$$\mathcal{D} := \mathbb{R}^2 \times \mathbb{R}^{n-2} \times \mathbb{R}_{>0},$$

the function

$$\begin{aligned}
\boldsymbol{f}\colon\ [-h,\infty) \times \mathcal{D} \times \mathbb{R}^m \ &\to\ \mathcal{D},\\
(t,(\boldsymbol{\mu},\boldsymbol{\xi},\kappa),\boldsymbol{\zeta}) \ &\mapsto\ \begin{pmatrix}
\begin{bmatrix} 0 & 1 \\ a_1 & a_2 \end{bmatrix} \left(\boldsymbol{\mu} - \begin{pmatrix} y_{\mathrm{ref}}(t) \\ \dot{y}_{\mathrm{ref}}(t) \end{pmatrix} \right) - |\gamma_0| \begin{pmatrix} 0 \\ \kappa^2\,\mu_1 + q_1\,\kappa\,\mu_2 \end{pmatrix} - \begin{pmatrix} 0 \\ \gamma_0 \end{pmatrix} u_d(t) \\
\qquad + \begin{pmatrix} \dot{y}_{\mathrm{ref}}(t) \\ \ddot{y}_{\mathrm{ref}}(t) \end{pmatrix} - \begin{bmatrix} \boldsymbol{0}^\top \\ \boldsymbol{a}_3^\top \end{bmatrix} \boldsymbol{\xi} - \begin{bmatrix} \boldsymbol{0}^\top \\ \boldsymbol{c}^\top \boldsymbol{A} \boldsymbol{B}_{\mathfrak{T}} \end{bmatrix} (\boldsymbol{\zeta} + \boldsymbol{d}(t)) \\
\begin{bmatrix} \boldsymbol{a}_4 & \boldsymbol{0} \end{bmatrix} \left(\begin{pmatrix} y_{\mathrm{ref}}(t) \\ \dot{y}_{\mathrm{ref}}(t) \end{pmatrix} - \boldsymbol{\mu} \right) + \boldsymbol{A}_5 \boldsymbol{\xi} + \boldsymbol{N} \boldsymbol{B}_{\mathfrak{T}} (\boldsymbol{\zeta} + \boldsymbol{d}(t)) \\
q_2\ \exp(-q_3\,q_4\,\kappa)\, d_\lambda(\|(\mu_1,\mu_2/\kappa)\|)^{q_4}
\end{pmatrix}
\end{aligned}$$

and the operator

$$\hat{\mathfrak{T}} : \mathcal{C}([-h,\infty);\mathbb{R}^{n+1}) \to \mathcal{L}^\infty_{\mathrm{loc}}(\mathbb{R}_{\geq 0};\mathbb{R}^m), \qquad (\hat{\mathfrak{T}}(\boldsymbol{\mu},\boldsymbol{\xi},\kappa))(t) := (\mathfrak{T}(\boldsymbol{S}^{-1} \begin{pmatrix} y_{\mathrm{ref}} - \mu_1 \\ \dot{y}_{\mathrm{ref}} - \mu_2 \\ \boldsymbol{\xi} \end{pmatrix}))(t).$$

Then, by introducing the expanded state variable $\hat{\boldsymbol{x}} := ((e,\dot{e}),\boldsymbol{z},k)$, the initial-value problem (3.9), (3.46) may be expressed in the form

$$\frac{\mathrm{d}}{\mathrm{d}t}\,\hat{\boldsymbol{x}}(t) = \boldsymbol{f}(t,\hat{\boldsymbol{x}}(t),(\hat{\mathfrak{T}}\hat{\boldsymbol{x}})(t)), \qquad \hat{\boldsymbol{x}}|_{[-h,0]} = \begin{pmatrix} y_{\mathrm{ref}}|_{[-h,0]} - \boldsymbol{c}^\top \boldsymbol{x}^0 \\ \dot{y}_{\mathrm{ref}}|_{[-h,0]} - \boldsymbol{c}^\top \boldsymbol{A} \boldsymbol{x}^0 \\ \boldsymbol{N}\boldsymbol{x}^0 \\ k^0 \end{pmatrix}. \tag{3.47}$$

Choose a non-empty compact set $\mathfrak{C} \subset \mathcal{D} \times \mathbb{R}^m$ and note that

$$\exists\, M_{\mathfrak{C}} > 0\ \forall\, ((\boldsymbol{\mu},\boldsymbol{\xi},\kappa),\boldsymbol{\zeta}) \in \mathfrak{C}: \quad \|((\boldsymbol{\mu},\boldsymbol{\xi},\kappa),\boldsymbol{\zeta})\| \leq M_{\mathfrak{C}}. \tag{3.48}$$

Then, for $u_d(\cdot) \in \mathcal{L}^\infty([-h,\infty);\,\mathbb{R})$, $\boldsymbol{d}(\cdot) \in \mathcal{L}^\infty([-h,\infty);\,\mathbb{R}^m)$, and $y_{\mathrm{ref}}(\cdot) \in \mathcal{W}^{2,\infty}([-h,\infty);\,\mathbb{R})$, the function $\boldsymbol{f}(\cdot,\cdot,\cdot)$ has the following properties: (i) $\boldsymbol{f}(t,\cdot,\cdot)$ is continuous for each fixed $t \in [-h,\infty)$; (ii) for each fixed $((\boldsymbol{\mu},\boldsymbol{\xi},\kappa),\boldsymbol{\zeta}) \in \mathcal{D}\times\mathbb{R}^n$ the function $\boldsymbol{f}(\cdot,(\boldsymbol{\mu},\boldsymbol{\xi},\kappa),\boldsymbol{\zeta})$ is measurable; (iii) for almost all $t \in [-h,\infty)$ and for all $((\boldsymbol{\mu},\boldsymbol{\xi},\kappa),\boldsymbol{\zeta}) \in \mathfrak{C}$ the following holds

$$\begin{aligned}
\|\boldsymbol{f}(t,(\boldsymbol{\mu},\boldsymbol{\xi},\kappa),\boldsymbol{\zeta})\| \overset{(3.48)}{\leq}\ & \left\| \begin{bmatrix} 0 & 1 \\ a_1 & a_2 \end{bmatrix} \right\| (M_{\mathfrak{C}} + 2\max\{\|y_{\mathrm{ref}}\|_\infty, \|\dot{y}_{\mathrm{ref}}\|_\infty\}) + |\gamma_0|\, M_{\mathfrak{C}}^2\, (M_{\mathfrak{C}} + q_1) \\
& + |\gamma_0|\, \|u_d\|_\infty + 2(\max\{\|\dot{y}_{\mathrm{ref}}\|_\infty,\, \|\ddot{y}_{\mathrm{ref}}\|_\infty\} + \|\boldsymbol{a}_4\| \max\{\|y_{\mathrm{ref}}\|_\infty, \|\dot{y}_{\mathrm{ref}}\|_\infty\}) \\
& + (\|\boldsymbol{a}_3\| + \|\boldsymbol{a}_4\| + \|\boldsymbol{A}_5\|) M_{\mathfrak{C}} + (\|\boldsymbol{c}\|\,\|\boldsymbol{A}\| + \|\boldsymbol{N}\|)\,\|\boldsymbol{B}_{\mathfrak{T}}\|\,(M_{\mathfrak{C}} + \|\boldsymbol{d}\|_\infty) \\
& + q_2\ \exp(-q_3\,q_4\,k^0(0))\, \left(M_{\mathfrak{C}} \sqrt{1 + 1/k^0(0)^2} + \lambda \right)^{q_4} =: l_{\mathfrak{C}}.
\end{aligned}$$

Hence, $\boldsymbol{f}(\cdot,\cdot,\cdot)$ is a Carathéodory function (see Definition 3.1) and existence of a solution

$\hat{\boldsymbol{x}} : [-h, T) \to \mathbb{R}^2 \times \mathbb{R}^{n-2} \times \mathbb{R}_{\geq 0}$ of the initial-value problem (3.47) with $\hat{\boldsymbol{x}}([0,T)) \in \mathcal{D}$, $T \in (0, \infty]$ follows from Theorem 3.2. Every solution can be extended to a maximal solution. For the following, let $\hat{\boldsymbol{x}} := ((e, \dot{e}), \boldsymbol{z}, k) \colon [-h, T) \to \mathbb{R}^2 \times \mathbb{R}^{n-2} \times \mathbb{R}_{>0}$ be a fixed and maximally extended solution of the initial-value problem (3.47). Note that this implies that $((e, \dot{e}), \boldsymbol{z}, k) : [-h, T) \to \mathbb{R}^2 \times \mathbb{R}^{n-2} \times \mathbb{R}_{>0}$ solves the closed-loop initial-value problem (3.9), (3.46) for almost all $t \in [0, T)$. Hence Assertion (i) is shown.

Step 2: Some technical preliminaries are introduced.

Step 2a: Lyapunov equations, an inequality and a coordinate transformation.
For $q_1 > 0$ and $\gamma_0 \neq 0$ (see system property ($\mathcal{S}_2$-sp$_1$)) the matrix

$$\boldsymbol{A}_1 := \begin{bmatrix} 0 & 1 \\ -|\gamma_0| & -|\gamma_0| q_1 \end{bmatrix} \tag{3.49}$$

and by system property ($\mathcal{S}_2$-sp$_2$) the matrix $\boldsymbol{A}_5$ as in (3.9) are Hurwitz, resp. Hence there exist

$$\begin{aligned} &0 < \boldsymbol{P}_1^\top = \boldsymbol{P}_1 = \tfrac{1}{2\,|\gamma_0|\,q_1} \begin{bmatrix} |\gamma_0|\,q_1^2 + |\gamma_0| + 1 & q_1 \\ q_1 & \frac{1}{|\gamma_0|} + 1 \end{bmatrix} \text{ and } \; 0 < \boldsymbol{P}_5^\top = \boldsymbol{P}_5 \in \mathbb{R}^{(n-2)\times(n-2)} \\ &\text{such that} \quad \boldsymbol{A}_1^\top \boldsymbol{P}_1 + \boldsymbol{P}_1 \boldsymbol{A}_1 = -\boldsymbol{I}_2 \quad \text{and} \quad \boldsymbol{A}_5^\top \boldsymbol{P}_5 + \boldsymbol{P}_5 \boldsymbol{A}_5 = -\boldsymbol{I}_{n-2}. \end{aligned} \tag{3.50}$$

Note that $k(t) \geq k^0(0) > 0$ for all $t \in [0, T)$. Define

$$\boldsymbol{K}(k(t)) := \begin{bmatrix} 1 & 0 \\ 0 & k(t) \end{bmatrix} \tag{3.51}$$

and the (sub-)coordinate change

$$\boldsymbol{w}(t) := \boldsymbol{K}(k(t))^{-1} \begin{pmatrix} e(t) \\ \dot{e}(t) \end{pmatrix} \qquad \text{and} \qquad \forall\, \nu \in [1/2,\, 1] : \qquad \boldsymbol{v}(t) := k(t)^{-\nu} \boldsymbol{z}(t). \tag{3.52}$$

Then, for $\boldsymbol{A}_1$ as in (3.49), the closed-loop system (3.9), (3.46) can be written as

$$\left.\begin{aligned} \dot{\boldsymbol{w}}(t) &= \left(-\tfrac{\dot{k}(t)}{k(t)} \begin{bmatrix} 0 & 0 \\ 0 & 1 \end{bmatrix} + \begin{bmatrix} 0 & 0 \\ \frac{a_1}{k(t)} & a_2 \end{bmatrix} + k(t)\, \boldsymbol{A}_1 \right) \boldsymbol{w}(t) \\ &\quad + k(t)^{-1} \left\{ \begin{bmatrix} 0 & 0 \\ a_1 & a_2 \end{bmatrix} \begin{pmatrix} y_{\mathrm{ref}}(t) \\ \dot{y}_{\mathrm{ref}}(t) \end{pmatrix} + \begin{pmatrix} 0 \\ \ddot{y}_{\mathrm{ref}}(t) \end{pmatrix} - \begin{bmatrix} \boldsymbol{0}^\top \\ \boldsymbol{a}_3^\top \end{bmatrix} k(t)^\nu \boldsymbol{v}(t) - \begin{pmatrix} 0 \\ \gamma_0 \end{pmatrix} u_d(t) \right. \\ &\quad \left. - \begin{bmatrix} \boldsymbol{0}^\top \\ \boldsymbol{c}^\top \boldsymbol{A} \boldsymbol{B}_{\mathfrak{T}} \end{bmatrix} \left((\mathfrak{T}(\boldsymbol{S}^{-1} \begin{pmatrix} y_{\mathrm{ref}} - w_1 \\ \dot{y}_{\mathrm{ref}} - k\, w_2 \\ k^\nu \boldsymbol{v} \end{pmatrix}))(t) + \boldsymbol{d}(t) \right) \right\}, \\ &\qquad\qquad \boldsymbol{w}|_{[-h,0]} = \boldsymbol{K}(k^0)^{-1} \left(\begin{pmatrix} y_{\mathrm{ref}}|_{[-h,0]} \\ \dot{y}_{\mathrm{ref}}|_{[-h,0]} \end{pmatrix} - \boldsymbol{C} \boldsymbol{x}^0 \right) \\ \dot{\boldsymbol{v}}(t) &= \left(-\nu \tfrac{\dot{k}(t)}{k(t)} \boldsymbol{I}_{n-2} + \boldsymbol{A}_5 \right) \boldsymbol{v}(t) + k(t)^{-\nu} \left\{ \begin{bmatrix} \boldsymbol{a}_4 & \boldsymbol{0} \end{bmatrix} \left(\begin{pmatrix} y_{\mathrm{ref}}(t) \\ \dot{y}_{\mathrm{ref}}(t) \end{pmatrix} - \boldsymbol{w}(t) \right) \right. \\ &\quad \left. + \boldsymbol{N} \boldsymbol{B}_{\mathfrak{T}} \left((\mathfrak{T}(\boldsymbol{S}^{-1} \begin{pmatrix} y_{\mathrm{ref}} - w_1 \\ \dot{y}_{\mathrm{ref}} - k\, w_2 \\ k^\nu \boldsymbol{v} \end{pmatrix}))(t) + \boldsymbol{d}(t) \right) \right\}, \qquad \boldsymbol{z}|_{[-h,0]} = (k^0)^{-\nu} \boldsymbol{N} \boldsymbol{x}^0 \\ \dot{k}(t) &= q_2 \exp(-q_3\, q_4\, k(t))\, d_\lambda(\|\boldsymbol{w}(t)\|)^{q_4}, \qquad k|_{[-h,0]} = k^0 \end{aligned} \right\} \tag{3.53}$$

Step 2b: Introduction of a Lyapunov-like function.
For $\boldsymbol{P}_1^\top = \boldsymbol{P}_1 > 0$ and $\boldsymbol{P}_5^\top = \boldsymbol{P}_5 > 0$ as in (3.50), introduce the Lyapunov-like function

$$\begin{aligned} V_1 \colon \mathbb{R}^2 \times \mathbb{R}^{n-2} \times [k^0(0), \infty) &\to \mathbb{R}_{\geq 0}, \\ (\boldsymbol{w}, \boldsymbol{v}, k) &\mapsto V_1(\boldsymbol{w}, \boldsymbol{v}, k) := \exp(-2q_3 k) \left(\boldsymbol{w}^\top \boldsymbol{P}_1 \boldsymbol{w} + \boldsymbol{v}^\top \boldsymbol{P}_5 \boldsymbol{v} \right). \end{aligned}$$

and define the constants

$$\begin{aligned} M_{\boldsymbol{w}} &:= \|\boldsymbol{P}_1\| \left(\sqrt{a_1^2 + a_2^2} (\|y_{\mathrm{ref}}\|_\infty + \|\dot{y}_{\mathrm{ref}}\|_\infty) + \|\ddot{y}_{\mathrm{ref}}\|_\infty + |\gamma_0| \|u_d\|_\infty + \|\boldsymbol{c}\| \, \|\boldsymbol{A}\| \, \|\boldsymbol{B}_{\mathfrak{T}}\| \, (M_{\mathfrak{T}} + \|\boldsymbol{d}\|_\infty) \right), \\ M_{\boldsymbol{v}} &:= \|\boldsymbol{P}_5\| \, (\|\boldsymbol{a}_4\| \, \|y_{\mathrm{ref}}\|_\infty + \|\boldsymbol{N}\| \, \|\boldsymbol{B}_{\mathfrak{T}}\| \, (M_{\mathfrak{T}} + \|\boldsymbol{d}\|_\infty)) \end{aligned} \tag{3.54}$$

and

$$\forall\, t \in [0, T) \colon \qquad M_1(t) := k(t)^{-2} M_{\boldsymbol{w}}^2 + 8 k(t)^{-2\nu} \, M_{\boldsymbol{v}}^2 \geq 0. \tag{3.55}$$

For notational brevity, write

$$\begin{aligned} &\forall\, t \in [0, T) \colon \qquad V_1(t) := V_1(\boldsymbol{w}(t), \boldsymbol{v}(t), k(t)) \qquad \text{with derivative along (3.53):} \\ &\forall\, t \in [0, T) \colon \; \frac{\mathrm{d}}{\mathrm{d}t} V_1(t) = 2 \exp(-2q_3 k(t)) \Big(\boldsymbol{w}(t)^\top \boldsymbol{P}_1 \dot{\boldsymbol{w}}(t) + \boldsymbol{v}(t)^\top \boldsymbol{P}_5 \dot{\boldsymbol{v}}(t) \Big) - 2q_3 \dot{k}(t) V_1(t). \end{aligned} \tag{3.56}$$

In view of (3.53), the following holds for almost all $t \in [0, T)$

$$\begin{aligned} 2\boldsymbol{w}(t)^\top \boldsymbol{P}_1 \dot{\boldsymbol{w}}(t) &\overset{(3.50),(3.54)}{\leq} -\left(k(t) - 2 \|\boldsymbol{P}_1\| \, \sqrt{\tfrac{a_1^2}{k^0(0)^2} + a_2^2} \right) \|\boldsymbol{w}(t)\|^2 + 2 \frac{\dot{k}(t)}{k(t)} \|\boldsymbol{P}_1\| \, \|\boldsymbol{w}(t)\|^2 \\ &\quad + 2 k(t)^{-1} M_{\boldsymbol{w}} \|\boldsymbol{w}(t)\| + 2 k(t)^{-1+\nu} \|\boldsymbol{P}_1\| \, \|\boldsymbol{a}_3\| \, \|\boldsymbol{v}(t)\| \, \|\boldsymbol{w}(t)\| \\ &\overset{(2.62)}{\leq} -\left(k(t) - 2 \|\boldsymbol{P}_1\| \, \sqrt{\tfrac{a_1^2}{k^0(0)^2} + a_2^2} - 1 - 8 \tfrac{\|\boldsymbol{P}_1\|^2 \|\boldsymbol{a}_3\|^2}{k(t)^{2(1-\nu)}} \right) \|\boldsymbol{w}(t)\|^2 \\ &\quad + 2 \frac{\dot{k}(t)}{k(t)} \|\boldsymbol{P}_1\| \, \|\boldsymbol{w}(t)\|^2 + \frac{1}{8} \|\boldsymbol{v}(t)\|^2 + k(t)^{-2} M_{\boldsymbol{w}}^2 \end{aligned} \tag{3.57}$$

and

$$\begin{aligned} 2\boldsymbol{v}(t)^\top \boldsymbol{P}_5 \dot{\boldsymbol{v}}(t) &\overset{(3.50),(3.54)}{\leq} -\|\boldsymbol{v}(t)\|^2 + 2 \, k(t)^{-\nu} \big(M_{\boldsymbol{v}} + \|\boldsymbol{P}_5\| \, \|\boldsymbol{a}_4\| \, \|\boldsymbol{w}(t)\| \big) \, \|\boldsymbol{v}(t)\| \\ &\overset{(2.62)}{\leq} -\frac{3}{4} \|\boldsymbol{v}(t)\|^2 + 8 k(t)^{-2\nu} \big(M_{\boldsymbol{v}}^2 + \|\boldsymbol{P}_5\|^2 \, \|\boldsymbol{a}_4\|^2 \, \|\boldsymbol{w}(t)\|^2 \big) \end{aligned} \tag{3.58}$$

where '$-\frac{\dot{k}(t)}{k(t)} \boldsymbol{v}(t)^\top \boldsymbol{P}_5 \boldsymbol{v}(t) \leq 0$ for all $t \in [0, T)$' was used ($\dot{k}(t) \geq 0$ for all $t \in [0, T)$ see (3.46)). Furthermore, using

$$\forall\, t \in [0, T) \colon \; V_1(t) \overset{(3.50)}{\geq} \exp(-2q_3 k(t)) \left(\frac{\|\boldsymbol{w}(t)\|^2}{\|\boldsymbol{P}_1^{-1}\|} + \frac{\|\boldsymbol{v}(t)\|^2}{\|\boldsymbol{P}_5^{-1}\|} \right) \geq \exp(-2q_3 k(t)) \frac{\|\boldsymbol{w}(t)\|^2}{\|\boldsymbol{P}_1^{-1}\|} \tag{3.59}$$

yields

$$\forall\, t \in [0,T)\colon \quad -2\exp(-2q_3k(t))\frac{\dot{k}(t)}{k(t)}\left\|\boldsymbol{P}_1\right\|\left\|\boldsymbol{w}(t)\right\|^2 - q_3\dot{k}(t)V_1(t)$$
$$\overset{(3.59)}{\leq} -\dot{k}(t)\exp(-2q_3k(t))\left(\frac{q_3}{\left\|\boldsymbol{P}_1^{-1}\right\|} - \frac{2\left\|\boldsymbol{P}_1\right\|}{k(t)}\right)\left\|\boldsymbol{w}(t)\right\|^2. \quad (3.60)$$

Then the time derivative $\frac{\mathrm{d}}{\mathrm{d}t}V_1(t)$ as in (3.61) along the solution of the closed-loop system (3.53) is, for almost all $t \in [0,T)$, bounded from above as follows

$$\begin{aligned}\frac{\mathrm{d}}{\mathrm{d}t}V_1(t) \overset{(3.57),(3.58),(3.60)}{\leq}\ & \exp(-2q_3k(t))\Bigg\{-\Bigg(k(t) - 2\left\|\boldsymbol{P}_1\right\|\sqrt{\tfrac{a_1^2}{k^0(0)^2}+a_2^2} - 1\\ & -8k(t)^{-2(1-\nu)}\left\|\boldsymbol{P}_1\right\|^2\left\|\boldsymbol{a}_3\right\|^2 - 8k(t)^{-2\nu}\left\|\boldsymbol{P}_5\right\|^2\left\|\boldsymbol{a}_4\right\|^2\Bigg)\left\|\boldsymbol{w}(t)\right\|^2\\ & -\frac{1}{2}\left\|\boldsymbol{v}(t)\right\|^2 + \underbrace{k(t)^{-2}M_{\boldsymbol{w}}^2 + 8k(t)^{-2\nu}M_{\boldsymbol{v}}^2}_{=M_1(t)}\Bigg\} - q_3\dot{k}(t)V_1(t)\\ & -\dot{k}(t)\exp(-2q_3k(t))\left(\frac{q_3}{\left\|\boldsymbol{P}_1^{-1}\right\|} - \frac{2\left\|\boldsymbol{P}_1\right\|}{k(t)}\right)\left\|\boldsymbol{w}(t)\right\|^2. \end{aligned} \quad (3.61)$$

Step 3: It is shown that $k(\cdot)$ is bounded on $[0,T)$.
Seeking a contradiction, assume that $k(\cdot)$ is unbounded on $[0,T)$. In view of (3.46), $\dot{k}(t) \geq 0$ for all $t \in [0,T)$, hence $k(\cdot)$ is non-decreasing on $[0,T)$ and

$$\begin{aligned}&\exists\, t^\star \geq 0\ \forall\, t \in [t^\star,T)\colon\ k(t) \geq \max\Bigg\{\frac{2}{q_3}\left\|\boldsymbol{P}_1\right\|\left\|\boldsymbol{P}_1^{-1}\right\|,\ 4\frac{\left\|\boldsymbol{P}_1^{-1}\right\|}{\mu_V\lambda^2}(M_{\boldsymbol{w}}^2 + 8M_{\boldsymbol{v}}^2),\\ &2\left\|\boldsymbol{P}_1\right\|\sqrt{\tfrac{a_1^2}{k^0(0)^2}+a_2^2} + 1 + 8k^0(0)^{-2(1-\nu)}\left\|\boldsymbol{P}_1\right\|^2\left\|\boldsymbol{a}_3\right\|^2 + 8k^0(0)^{-2\nu}\left\|\boldsymbol{P}_5\right\|^2\left\|\boldsymbol{a}_4\right\|^2 + \frac{1}{2}\Bigg\}. \end{aligned} \quad (3.62)$$

For $M_1(t)$ as in (3.55) and

$$\mu_V := \min\left\{\frac{1}{2\left\|\boldsymbol{P}_1\right\|},\ \frac{1}{2\left\|\boldsymbol{P}_5\right\|}\right\} > 0, \quad (3.63)$$

invoking (3.61) and the facts '$-\left\|\boldsymbol{w}\right\|^2 \leq -\frac{1}{\left\|\boldsymbol{P}_1\right\|}\boldsymbol{w}^\top\boldsymbol{P}_1\boldsymbol{w}$', '$-\left\|\boldsymbol{v}\right\|^2 \leq -\frac{1}{\left\|\boldsymbol{P}_5\right\|}\boldsymbol{v}^\top\boldsymbol{P}_5\boldsymbol{v}$' and '$q_3/\left\|\boldsymbol{P}_1^{-1}\right\| - 2\left\|\boldsymbol{P}_1\right\|/k(t) \overset{(3.62)}{\geq} 0$' yields

$$\begin{aligned}\text{for a.a. } t \in [t^\star,T)\colon\ \frac{\mathrm{d}}{\mathrm{d}t}V_1(t) &\overset{(3.62)}{\leq} \exp(-2q_3k(t))\Big\{-\tfrac{\left\|\boldsymbol{w}(t)\right\|^2+\left\|\boldsymbol{v}(t)\right\|^2}{2} + M_1(t)\Big\} - q_3\dot{k}(t)V_1(t)\\ &\leq -(\mu_V + q_3\dot{k}(t))\,V_1(t) + \exp(-2q_3k(t))M_1(t). \end{aligned} \quad (3.64)$$

Define

$$\forall\, t \in [0,T)\colon \quad \Lambda(t) := \frac{\lambda \exp(-q_3 k(t))}{2\sqrt{\left\|\boldsymbol{P}_1^{-1}\right\|}} > 0, \qquad \text{with derivative } \dot{\Lambda}(t) = -q_3 \dot{k}(t)\Lambda(t), \tag{3.65}$$

and, for $d_{\Lambda(t)}(\cdot)$ as in (N.5), note that the following holds

$$\begin{aligned}
\forall\, t \in [0,T)\colon \quad \|\boldsymbol{w}(t)\| &\overset{(3.59)}{\leq} \sqrt{\left\|\boldsymbol{P}_1^{-1}\right\|}\exp(q_3 k(t))\sqrt{V_1(t)} - \frac{\sqrt{\left\|\boldsymbol{P}_1^{-1}\right\|}\exp(q_3 k(t))}{\sqrt{\left\|\boldsymbol{P}_1^{-1}\right\|}\exp(q_3 k(t))}\frac{\lambda}{2} + \frac{\lambda}{2} \\
&\overset{(3.65)}{=} \sqrt{\left\|\boldsymbol{P}_1^{-1}\right\|}\exp(q_3 k(t))\left(\sqrt{V_1(t)} - \Lambda(t)\right) + \frac{\lambda}{2} \qquad (3.66) \\
&\leq \sqrt{\left\|\boldsymbol{P}_1^{-1}\right\|}\exp(q_3 k(t))\, d_{\Lambda(t)}\left(\sqrt{V_1(t)}\right) + \lambda. \qquad (3.67)
\end{aligned}$$

Since $d_\lambda(x) \leq d_\lambda(y)$ for all $0 \leq x \leq y$ it follows that

$$\forall\, t \in [0,T)\colon \ \dot{k}(t) \overset{(3.46)}{=} q_2 \exp(-q_3 q_4 k(t))\, d_\lambda(\|\boldsymbol{w}(t)\|)^{q_4} \overset{(3.67)}{\leq} q_2 \left\|\boldsymbol{P}_1^{-1}\right\|^{q_4/2} d_{\Lambda(t)}\left(\sqrt{V_1(t)}\right)^{q_4}. \tag{3.68}$$

Furthermore, observe that

$$\begin{aligned}
\text{for a.a. } t \in [t^\star, T)\colon \quad & \exp(-2q_3 k(t))M_1(t) - \mu_V \Lambda(t)^2 \\
&\overset{(3.55),(3.52),(3.65)}{\leq} \exp(-2q_3 k(t))\left(\frac{M_{\boldsymbol{w}}^2 + 4M_{\boldsymbol{v}}^2}{k(t)} - \frac{\mu_V}{4}\frac{\lambda^2}{\left\|\boldsymbol{P}_1^{-1}\right\|}\right) \overset{(3.62)}{\leq} 0
\end{aligned} \tag{3.69}$$

and, since for any $t \in [0,T)$, the following implications hold

$$\left[\!\left[\ \sqrt{V_1(t)} \leq 2\Lambda(t)\ \right]\!\right] \overset{(3.65),(3.66)}{\Longrightarrow} \left[\!\left[\ \|\boldsymbol{w}(t)\| \leq \lambda\ \right]\!\right] \overset{(3.46)}{\Longrightarrow} \left[\!\left[\ \dot{k}(t) = 0\ \right]\!\right]$$

and

$$\left[\!\left[\ \sqrt{V_1(t)} > 2\Lambda(t)\ \right]\!\right] \implies \left[\!\left[\ \left(V_1(t) - 2\Lambda(t)\sqrt{V_1(t)}\right) = \sqrt{V_1(t)}\left(\sqrt{V_1(t)} - 2\Lambda(t)\right) > 0\ \right]\!\right],$$

it follows that

$$\forall\, t \in [0,T)\colon \quad -\dot{k}(t)\left(V_1(t) - 2\Lambda(t)\sqrt{V_1(t)}\right) \leq 0. \tag{3.70}$$

Now it is easy to see that the time derivative $\frac{1}{2}\frac{\mathrm{d}}{\mathrm{d}t}\, d_{\Lambda(t)}\Big(\sqrt{V_1(t)}\Big)^2$ along the solution of the closed-loop initial-value problem (3.53) is, for almost all $t \in [t^\star, T)$, bounded from above as follows

$$\begin{aligned}
\frac{1}{2}\frac{\mathrm{d}}{\mathrm{d}t}\, d_{\Lambda(t)}\Big(\sqrt{V_1(t)}\Big)^2 &= d_{\Lambda(t)}\left(\sqrt{V_1(t)}\right)\frac{\mathrm{d}}{\mathrm{d}t}\left(\sqrt{V_1(t)} - \Lambda(t)\right) \\
&= \frac{d_{\Lambda(t)}\left(\sqrt{V_1(t)}\right)}{2\sqrt{V_1(t)}}\left(\frac{\mathrm{d}}{\mathrm{d}t}V_1(t) - 2\dot{\Lambda}(t)\sqrt{V_1(t)}\right) \\
&\overset{(3.64),(3.65)}{\leq} \frac{d_{\Lambda(t)}\left(\sqrt{V_1(t)}\right)}{2\sqrt{V_1(t)}}\Bigg(-\mu_V V_1(t) + \exp(-2q_3k(t))M_1(t) \\
&\qquad -q_3\dot{k}(t)\left(V_1(t) - 2\Lambda(t)\sqrt{V_1(t)}\right)\Bigg) \\
&\overset{(3.70)}{\leq} -\frac{d_{\Lambda(t)}\left(\sqrt{V_1(t)}\right)}{2\sqrt{V_1(t)}}\left(\mu_V V_1(t) - \exp(-2q_3k(t))M_1(t)\right) \\
&\overset{(3.69)}{\leq} -\frac{d_{\Lambda(t)}\left(\sqrt{V_1(t)}\right)}{2\sqrt{V_1(t)}}\left(\mu_V V_1(t) - \mu_V\Lambda(t)^2\right) \\
&= -\frac{\mu_V}{2}d_{\Lambda(t)}\left(\sqrt{V_1(t)}\right)\left(\sqrt{V_1(t)} - \Lambda(t)\right)\left(1 + \frac{\Lambda(t)}{\sqrt{V_1(t)}}\right) \\
&\leq -\frac{\mu_V}{2}d_{\Lambda(t)}\left(\sqrt{V_1(t)}\right)^2.
\end{aligned}$$

Integration yields

$$\forall\, t \in [t^\star, T)\colon \qquad d_{\Lambda(t)}\left(\sqrt{V_1(t)}\right)^2 \leq d_{\Lambda(t^\star)}\left(\sqrt{V_1(t^\star)}\right)^2 \exp\Big(-q_4\mu_V\,(\tau - t^\star)\Big) \tag{3.71}$$

and so the contradiction follows

$$\begin{aligned}
\forall\, t \in [t^\star, T)\colon \quad k(t) - k(t^\star) &= \int_{t^\star}^{t}\dot{k}(\tau)\,\mathrm{d}\tau \overset{(3.68)}{\leq} q_2\left\|\boldsymbol{P}_1^{-1}\right\|^{q_4/2}\int_{t^\star}^{t} d_{\Lambda(\tau)}\left(\sqrt{V_1(\tau)}\right)^{q_4}\mathrm{d}\tau \\
&\overset{(3.71)}{\leq} q_2\left\|\boldsymbol{P}_1^{-1}\right\|^{q_4/2} d_{\Lambda(t^\star)}\left(\sqrt{V_1(t^\star)}\right)^{q_4}\int_{t^\star}^{t}\exp\left(-\tfrac{q_4\mu_V}{2}\,(\tau - t^\star)\right)\mathrm{d}\tau \\
&\leq \frac{2q_2\left\|\boldsymbol{P}_1^{-1}\right\|^{q_4/2}}{q_4\mu_V} d_{\Lambda(t^\star)}\left(\sqrt{V_1(t^\star)}\right)^{q_4}\left(1 - \exp\left(-\tfrac{q_4\mu_V}{2}\,(t - t^\star)\right)\right) \\
&< \infty.
\end{aligned}$$

Step 4: It is shown that Assertions (ii) holds true, i.e. $T = \infty$.
From Step 3 and (3.46) it follows that $k(\cdot)$ is continuous, non-increasing and bounded on $[0, T)$. Therefore the limit

$$k_\infty := \lim_{t\to T} k(t) \geq k(0) > 0$$

exists and the following holds for almost all $t \in [0, T)$

$$\begin{aligned}\left\| \frac{\mathrm{d}}{\mathrm{d}t} \begin{pmatrix} \begin{pmatrix} e(t) \\ \dot{e}(t) \end{pmatrix} \\ \boldsymbol{z}(t) \end{pmatrix} \right\| \;\leq\; & \left(\left\| \begin{bmatrix} 0 & 1 \\ a_1 & a_2 \end{bmatrix} \right\| + |\gamma_0|\, k_\infty (k_\infty + q_1) + \|\boldsymbol{a}_3\| + \|\boldsymbol{a}_4\| + \|\boldsymbol{A}_5\| \right) \left\| \begin{pmatrix} \begin{pmatrix} e(t) \\ \dot{e}(t) \end{pmatrix} \\ \boldsymbol{z}(t) \end{pmatrix} \right\| \\ & + \left\| \begin{bmatrix} 0 & 1 \\ a_1 & a_2 \end{bmatrix} \right\| (\|y_{\mathrm{ref}}\|_\infty + \|\dot{y}_{\mathrm{ref}}\|_\infty) + |\gamma_0| \|u_d\|_\infty + \|\dot{y}_{\mathrm{ref}}\|_\infty + \|\ddot{y}_{\mathrm{ref}}\|_\infty \\ & + \|\boldsymbol{a}_4\|\, \|y_{\mathrm{ref}}\|_\infty + (\|\boldsymbol{c}\|\, \|\boldsymbol{A}_5\| + \|\boldsymbol{N}\|)\, \|\boldsymbol{B}_{\mathfrak{T}}\|\, (M_{\mathfrak{T}} + \|\boldsymbol{d}\|_\infty)\end{aligned}$$

which in combination with Proposition 2.1.19 in [77, p. 86] implies, by maximality of T, that $T = \infty$. This shows Assertion (ii) and completes Step 4.

Step 5: It is shown that Assertion (iii) holds true, i.e. $k(\cdot) \in \mathcal{L}^\infty(\mathbb{R}_{\geq 0}; \mathbb{R}_{>0})$ *and* $\boldsymbol{x}(\cdot) \in \mathcal{L}^\infty(\mathbb{R}_{\geq 0}; \mathbb{R}^n)$.
Note that $k(\cdot) \in \mathcal{L}^\infty(\mathbb{R}_{\geq 0}; \mathbb{R}_{>0})$ follows from Step 3 and 4.

Step 5a: It is shown that $\boldsymbol{z}(\cdot)$ *is bounded on* $\mathbb{R}_{\geq 0}$.
For k_∞ as in Step 4 observe that the following holds

$$\begin{aligned}\forall\, t \geq 0\colon \qquad \exp(-q_3 q_4 k_\infty) \int_0^t d_\lambda(\|\boldsymbol{w}(\tau)\|)^{q_4}\, \mathrm{d}\tau \;&\leq \int_0^t \exp(-q_3 q_4 k(\tau)) d_\lambda(\|\boldsymbol{w}(\tau)\|)^{q_4}\, \mathrm{d}\tau \\ &\overset{(3.46)}{=} \frac{1}{q_2} \int_0^t \dot{k}(\tau)\, \mathrm{d}\tau \;\leq \frac{1}{q_2}(k_\infty - k^0(0)) < \infty\end{aligned}$$

which implies

$$\dot{k}(\cdot) \in \mathcal{L}^1(\mathbb{R}_{\geq 0}; \mathbb{R}_{\geq 0}) \qquad \text{and} \qquad d_\lambda(\|\boldsymbol{w}(\cdot)\|) \in \mathcal{L}^{q_4}(\mathbb{R}_{\geq 0}; \mathbb{R}_{\geq 0}). \tag{3.72}$$

Define

$$\begin{aligned}\boldsymbol{\delta}_2\colon\; \mathbb{R}^2 \to \mathbb{R}^2, \quad \boldsymbol{w} \mapsto \boldsymbol{\delta}_2(\boldsymbol{w}) &:= \begin{cases} d_\lambda(\|\boldsymbol{w}\|) \frac{\boldsymbol{w}}{\|\boldsymbol{w}\|} & , \|\boldsymbol{w}\| > \lambda \\ \boldsymbol{0} & , \|\boldsymbol{w}\| \leq \lambda \end{cases} \qquad \text{and} \\ \boldsymbol{\delta}_\infty\colon\; \mathbb{R}^2 \to \mathbb{R}^2, \quad \boldsymbol{w} \mapsto \boldsymbol{\delta}_\infty(\boldsymbol{w}) &:= \begin{cases} \left(1 - \frac{d_\lambda(\|\boldsymbol{w}\|)}{\|\boldsymbol{w}\|}\right) \boldsymbol{w} & , \|\boldsymbol{w}\| > \lambda \\ \boldsymbol{w} & , \|\boldsymbol{w}\| \leq \lambda \end{cases}\end{aligned} \tag{3.73}$$

and note that, in view of (3.72) and (3.73), the following holds

$$\forall\, t \geq 0\colon\; \boldsymbol{w}(t) = \boldsymbol{\delta}_2(\boldsymbol{w}(t)) + \boldsymbol{\delta}_\infty(\boldsymbol{w}(t)) \;\wedge\; \|\boldsymbol{\delta}_\infty(\boldsymbol{w}(t))\| \leq \lambda \text{ and } \boldsymbol{\delta}_2(\boldsymbol{w}(\cdot)) \in \mathcal{L}^{q_4}(\mathbb{R}_{\geq 0}; \mathbb{R}^2). \tag{3.74}$$

Introduce the Lyapunov candidate

$$V_2\colon \mathbb{R}^{n-2} \to \mathbb{R}_{\geq 0}, \quad \boldsymbol{v} \mapsto V_2(\boldsymbol{v}) := \boldsymbol{v}^\top \boldsymbol{P}_5 \boldsymbol{v}.$$

For $M_{\boldsymbol{v}}$ as in (3.54),

$$M_2 := 8\,k^0(0)^{-2\nu}\Big(\|\boldsymbol{P}_5\|^2\,\|\boldsymbol{a}_4\|^2\,\lambda^2 + M_{\boldsymbol{v}}^2\Big) \quad \text{and} \quad M_3 := 8\,k^0(0)^{-2\nu}\,\|\boldsymbol{P}_5\|^2\,\|\boldsymbol{a}_4\|^2\,, \tag{3.75}$$

the time derivative $\frac{\mathrm{d}}{\mathrm{d}t}V_2(\boldsymbol{v}(t))$ along the solution of the (second equation of) closed-loop system (3.53) is, for almost all $t \geq 0$, bounded from above as follows

$$\begin{aligned}
\frac{\mathrm{d}}{\mathrm{d}t}V_2(\boldsymbol{v}(t)) &\leq -\|\boldsymbol{v}(t)\|^2 + 2\,k^0(0)^{-\nu}\,\|\boldsymbol{v}(t)\|\,(\|\boldsymbol{P}_5\|\,\|\boldsymbol{a}_4\|\,\|\boldsymbol{w}(t)\| + M_{\boldsymbol{v}}) \\
&\overset{(3.74)}{\leq} -\|\boldsymbol{v}(t)\|^2 + 2\,k^0(0)^{-\nu}\,\|\boldsymbol{v}(t)\|\,\Big(\|\boldsymbol{P}_5\|\,\|\boldsymbol{a}_4\|\,(\|\boldsymbol{\delta}_2(\boldsymbol{w}(t))\| + \lambda) + M_{\boldsymbol{v}}\Big) \\
&\overset{(2.62)}{\leq} -\frac{1}{2}\,\|\boldsymbol{v}(t)\|^2 + 8\,k^0(0)^{-2\nu}\Big(\|\boldsymbol{P}_5\|^2\,\|\boldsymbol{a}_4\|^2\,(\|\boldsymbol{\delta}_2(\boldsymbol{w}(t))\|^2 + \lambda^2) + M_{\boldsymbol{v}}^2\Big) \\
&\overset{(3.63),(3.75)}{\leq} -\mu_V V_2(\boldsymbol{v}(t)) + M_2 + M_3\,\|\boldsymbol{\delta}_2(\boldsymbol{w}(t))\|^2 \\
&\leq -\mu_V V_2(\boldsymbol{v}(t)) + M_2 + M_3(1 + \|\boldsymbol{\delta}_2(\boldsymbol{w}(t))\|^{q_4})
\end{aligned}$$

where in the last step Fact 1.12.31 in [24, p. 39] was used. Now application of the Bellman-Gronwall Lemma (in its differential form [18, Lemma 1.1, p. 2]) yields

$$\forall\, t \geq 0\colon \quad V_2(\boldsymbol{v}(t)) \overset{(3.74)}{\leq} V_2(\boldsymbol{v}(0)) + \frac{M_2 + M_3}{\mu_V} + M_3 \underbrace{\int_0^t \overbrace{\exp\left(-\frac{t-\tau}{2\,\|\boldsymbol{P}_5\|}\right)}^{\leq 1} \|\boldsymbol{\delta}_2(\boldsymbol{w}(\tau))\|^{q_4}\,\mathrm{d}\tau}_{\leq \|\boldsymbol{\delta}_2(\boldsymbol{w})\|_{\mathcal{L}^{q_4}}^{q_4} < \infty}.$$

Hence $V_2(\boldsymbol{v}(\cdot))$ is bounded on $\mathbb{R}_{\geq 0}$, which implies $\boldsymbol{v}(\cdot) \in \mathcal{L}^\infty(\mathbb{R}_{\geq 0}; \mathbb{R}^{n-2})$. From this, combined with $k(\cdot) \in \mathcal{L}^\infty(\mathbb{R}_{\geq 0}; \mathbb{R}_{>0})$ and (3.52), it follows that $\boldsymbol{z}(\cdot) = k(\cdot)^\nu \boldsymbol{v}(\cdot) \in \mathcal{L}^\infty(\mathbb{R}_{\geq 0}; \mathbb{R}^{n-2})$, which completes Step 5a.

Step 5b: It is shown that $(e(\cdot), \dot{e}(\cdot))^\top$ is bounded on $\mathbb{R}_{\geq 0}$.
For $k_\infty > 0$ as in Step 4, consider the first equation of the closed-loop system (3.9), (3.46) and note that

$$\forall\, a_1,\, a_2 \in \mathbb{R}\colon \quad \operatorname{rank}\left[\begin{pmatrix} 0 \\ \gamma_0 \end{pmatrix}, \begin{bmatrix} 0 & 1 \\ a_1 & a_2 \end{bmatrix}\begin{pmatrix} 0 \\ \gamma_0 \end{pmatrix}\right] = \operatorname{rank}\begin{bmatrix} 0 & \gamma_0 \\ \gamma_0 & a_2 \end{bmatrix} = 2,$$

where, by system property (sp_1), $\gamma_0 \neq 0$ is satisfied. Hence the "first sub-system" in (3.9), (3.46) is controllable and there exists $\boldsymbol{l} \in \mathbb{R}^2$ such that

$$\boldsymbol{A}_{\boldsymbol{l}} := \begin{bmatrix} 0 & 1 \\ a_1 - |\gamma_0| k_\infty^2 & a_2 - q_1 |\gamma_0| k_\infty \end{bmatrix} - \begin{pmatrix} 0 \\ \gamma_0 \end{pmatrix} \boldsymbol{l} \tag{3.76}$$

is a Hurwitz matrix and furthermore there exists a unique $\boldsymbol{P}_{\boldsymbol{l}} = \boldsymbol{P}_{\boldsymbol{l}}^\top > 0$ such that $\boldsymbol{A}_{\boldsymbol{l}}^\top \boldsymbol{P}_{\boldsymbol{l}} +$

$\boldsymbol{P_l A_l} = -\boldsymbol{I}_2$. Now, for $\boldsymbol{A_l}$ as in (3.76), $\boldsymbol{w}(t)$ as in (3.52) and by defining

$$\forall\, t \geq 0\colon\ \boldsymbol{e}(t) := \begin{pmatrix} e(t) \\ \dot{e}(t) \end{pmatrix} \quad \text{and} \quad \boldsymbol{g}(t) := \begin{bmatrix} 0 & 0 \\ a_1 & a_2 \end{bmatrix} \begin{pmatrix} y_{\mathrm{ref}}(t) \\ \dot{y}_{\mathrm{ref}}(t) \end{pmatrix} + \begin{pmatrix} 0 \\ \ddot{y}_{\mathrm{ref}}(t) \end{pmatrix} - \begin{bmatrix} \boldsymbol{0}^\top \\ \boldsymbol{a}_3^\top \end{bmatrix} \boldsymbol{z}(t) - \begin{pmatrix} 0 \\ \gamma_0 \end{pmatrix} u_d(t) - \begin{bmatrix} \boldsymbol{0}^\top \\ \boldsymbol{c}^\top \boldsymbol{A}\boldsymbol{B}_{\mathfrak{T}} \end{bmatrix} \left((\mathfrak{T}(\boldsymbol{S}^{-1} \begin{pmatrix} y_{\mathrm{ref}} - e \\ \dot{y}_{\mathrm{ref}} - \dot{e} \\ \boldsymbol{z} \end{pmatrix}))(t) + \boldsymbol{d}(t) \right),$$

rewrite the first equation of the closed-loop system (3.9), (3.46) as follows

$$\tfrac{\mathrm{d}}{\mathrm{d}t}\, \boldsymbol{e}(t) \;=\; \left(\boldsymbol{A_l} + |\gamma_0| \underbrace{\begin{bmatrix} 0 & 0 \\ k_\infty^2 - k(t)^2 & q_1(k_\infty - k(t)) \end{bmatrix}}_{=:\boldsymbol{F}(t)} \right) \boldsymbol{e}(t) + \begin{pmatrix} 0 \\ \gamma_0 \end{pmatrix} \boldsymbol{l}\, \boldsymbol{K}(k(t)) \boldsymbol{w}(t) + \boldsymbol{g}(t), \tag{3.77}$$

where $\boldsymbol{w}(\cdot) = \boldsymbol{\delta}_2(\boldsymbol{w}(\cdot)) + \boldsymbol{\delta}_\infty(\boldsymbol{w}(\cdot))$ and $\boldsymbol{z}(\cdot) \in \mathcal{L}^\infty(\mathbb{R}_{\geq 0}; \mathbb{R}^{n-2})$ are considered as continuous external signals, resp. For $M_{\boldsymbol{w}}$ as in (3.54), $\boldsymbol{K}(k(t))$ as in (3.51) and $\boldsymbol{P}_1$ as in (3.50), note that

$$\begin{aligned} &\forall\, t \geq 0\colon\ \ \|\boldsymbol{g}(t)\| \leq \tfrac{M_{\boldsymbol{w}}}{\|\boldsymbol{P}_1\|} + \|\boldsymbol{a}_3\|\, \|\boldsymbol{z}\|_\infty =: M_{\boldsymbol{g}}, \quad \|\boldsymbol{K}(k(t))\| \leq \max\{1, k_\infty\} =: K_\infty \\ &\text{and} \quad [\![\, \lim_{t\to\infty} \boldsymbol{F}(t) = 0 \,]\!] \quad \Longrightarrow \quad \Big[\!\!\Big[\, \exists\, \tilde{t}_1 \geq 0\, \forall t \geq \tilde{t}_1\colon \quad \|\boldsymbol{F}(t)\| \leq \tfrac{1}{16} \tfrac{1}{|\gamma_0| \|\boldsymbol{P_l}\|} \Big]\!\!\Big]. \end{aligned} \tag{3.78}$$

Now introduce the Lyapunov candidate

$$V_3\colon \mathbb{R}^2 \to \mathbb{R}_{\geq 0},\ \boldsymbol{e} \mapsto V_3(\boldsymbol{e}) := \boldsymbol{e}^\top \boldsymbol{P_l} \boldsymbol{e} \geq 0$$

and, for

$$M_4 := 8\, \|\boldsymbol{P_l}\|^2 \left(M_{\boldsymbol{g}}^2 + |\gamma_0|^2\, \|\boldsymbol{l}\|^2\, K_\infty^2 \lambda^2 \right) \quad \text{and} \quad M_5 := 8\, \|\boldsymbol{P_l}\|^2\, |\gamma_0|^2\, \|\boldsymbol{l}\|^2\, K_\infty^2 \tag{3.79}$$

observe that the time derivative $\frac{\mathrm{d}}{\mathrm{d}t}\, V_3(\boldsymbol{e}(t))$ along the solution of (3.77) is, for almost all $t \geq \tilde{t}_1$, bounded from above as follows

$$\begin{aligned} \tfrac{\mathrm{d}}{\mathrm{d}t}\, V_3(\boldsymbol{e}(t)) \overset{(3.77),(3.78)}{\leq}\ & -\big(1 - 2|\gamma_0|\, \|\boldsymbol{P_l}\|\, \|\boldsymbol{F}(t)\|\, \big)\, \|\boldsymbol{e}(t)\|^2 \\ & +2\, \|\boldsymbol{P_l}\|\, \|\boldsymbol{e}(t)\| \left(M_{\boldsymbol{g}} + |\gamma_0|\, \|\boldsymbol{l}\|\, K_\infty\, \|\boldsymbol{w}(t)\| \right) \\ \overset{(3.78),(3.74)}{\leq}\ & -\tfrac{7}{8}\, \|\boldsymbol{e}(t)\|^2 + 2\, \|\boldsymbol{P_l}\|\, \|\boldsymbol{e}(t)\| \left(M_{\boldsymbol{g}} + |\gamma_0|\, \|\boldsymbol{l}\|\, K_\infty (\|\boldsymbol{\delta}_2(\boldsymbol{w}(t))\| + \lambda) \right) \\ \overset{(2.62)}{\leq}\ & -\frac{1}{2\, \|\boldsymbol{P_l}\|} V_3(\boldsymbol{e}(t)) + 8\, \|\boldsymbol{P_l}\|^2 \left(M_{\boldsymbol{g}}^2 + |\gamma_0|^2\, \|\boldsymbol{l}\|^2\, K_\infty^2 \big(\|\boldsymbol{\delta}_2(\boldsymbol{w}(t))\|^2 + \lambda^2 \big) \right) \\ \overset{(3.79)}{\leq}\ & -\frac{1}{2\, \|\boldsymbol{P_l}\|} V_3(\boldsymbol{e}(t)) + M_4 + M_5 (1 + \|\boldsymbol{\delta}_2(\boldsymbol{w}(t))\|^{q_4}). \end{aligned}$$

Invoking the Bellman-Gronwall Lemma and Theorem C.2.14 in [46, p. 241] again yields

$$\forall\, t \;\geq\; \tilde{t}_1\colon \quad V_3(\boldsymbol{e}(t)) \;\overset{(3.74)}{\leq}\; V_3(\boldsymbol{e}(\tilde{t}_1)) \;+\; 2\, \|\boldsymbol{P_l}\|\, (M_4 \;+\; M_5) \;+\; M_5 \|\boldsymbol{\delta}_2(\boldsymbol{w})\|_{\mathcal{L}^{q_4}}^{q_4} \;<\; \infty,$$

which by continuity of $\boldsymbol{e}(\cdot) = (e(\cdot), \dot{e}(\cdot))^\top$ on $\mathbb{R}_{\geq 0}$ and by compactness of $[0, \tilde{t}_1]$ implies $(e(\cdot), \dot{e}(\cdot))^\top \in \mathcal{L}^\infty(\mathbb{R}_{\geq 0}; \mathbb{R}^2)$.

Step 5c: It is shown that $\boldsymbol{x}(\cdot) \in \mathcal{L}^\infty(\mathbb{R}_{\geq 0}; \mathbb{R}^n)$.
From Step 3 and 4 it follows that $k(\cdot) \in \mathcal{L}^\infty(\mathbb{R}_{\geq 0}; \mathbb{R}_{>0})$. From Step 5b & 5a it follows that $(e(\cdot), \dot{e}(\cdot))^\top \in \mathcal{L}^\infty(\mathbb{R}_{\geq 0}; \mathbb{R}^2)$ and $\boldsymbol{z}(\cdot) \in \mathcal{L}^\infty(\mathbb{R}_{\geq 0}; \mathbb{R}^{n-2})$, resp. This combined with $y_{\mathrm{ref}}(\cdot) \in \mathcal{W}^{2,\infty}(\mathbb{R}_{\geq 0}; \mathbb{R})$ and $\boldsymbol{S}^{-1}$ as in (2.24) yields

$$\boldsymbol{x}(\cdot) = \boldsymbol{S}^{-1}(e(\cdot) - y_{\mathrm{ref}}(\cdot), \dot{e}(\cdot) - \dot{y}_{\mathrm{ref}}(\cdot), \boldsymbol{z}(\cdot)^\top)^\top \in \mathcal{L}^\infty(\mathbb{R}_{\geq 0}; \mathbb{R}^n).$$

This shows Assertion (iii) and completes Step 5.

Step 6: It is shown that Assertion (iv) holds true, i.e. $\lim_{t\to\infty} \operatorname{dist}\Big(\Big\| \Big(e(t),\ \frac{\dot{e}(t)}{k(t)} \Big)^\top \Big\|, [0, \lambda] \Big) = 0$.

First note that $k(\cdot) \in \mathcal{L}^\infty(\mathbb{R}_{\geq 0}; \mathbb{R}_{>0})$ and $(e(\cdot), \dot{e}(\cdot))^\top \in \mathcal{L}^\infty(\mathbb{R}_{\geq 0}; \mathbb{R}^2)$ imply

$$\boldsymbol{w}(\cdot) = \boldsymbol{K}(k(\cdot))(e(\cdot), \dot{e}(\cdot))^\top \in \mathcal{L}^\infty(\mathbb{R}_{\geq 0}; \mathbb{R}^2)$$

and hence, by (3.46), $\dot{k}(\cdot) \in \mathcal{L}^\infty(\mathbb{R}_{\geq 0}; \mathbb{R}_{>0})$. From Step 5a recall that $\boldsymbol{v}(\cdot) \in \mathcal{L}^\infty(\mathbb{R}_{\geq 0}; \mathbb{R}^{n-2})$. Combining this with $\boldsymbol{d}(\cdot) \in \mathcal{L}^\infty(\mathbb{R}_{\geq 0}; \mathbb{R}^m)$, $y_{\mathrm{ref}}(\cdot) \in \mathcal{W}^{2,\infty}(\mathbb{R}_{\geq 0}; \mathbb{R})$, $u_d(\cdot) \in \mathcal{L}^\infty(\mathbb{R}_{\geq 0}; \mathbb{R})$ and global boundedness of the operator $\mathfrak{T}$ (see system property $(\mathcal{S}_2\text{-sp}_3)$) gives, in view of (3.53), $\dot{\boldsymbol{w}}(\cdot) \in \mathcal{L}^\infty(\mathbb{R}_{\geq 0}; \mathbb{R}^2)$ and $\dot{\boldsymbol{v}}(\cdot) \in \mathcal{L}^\infty(\mathbb{R}_{\geq 0}; \mathbb{R}^{n-2})$, resp. Furthermore it holds that

$$\begin{aligned}
\text{for a.a. } t \geq 0\colon \quad \ddot{k}(t) &= \frac{\mathrm{d}}{\mathrm{d}t}\dot{k}(t) = \frac{\mathrm{d}}{\mathrm{d}t}\left(q_2 \exp(-q_3 q_4 k(t)) d_\lambda\left(\|\boldsymbol{w}(t)\|\right)^{q_4}\right) \\
&= \begin{cases} 0 & , \|\boldsymbol{w}(t)\| = 0 \\ -q_3 q_4 \dot{k}(t)^2 + q_2 q_4 \exp(-q_3 q_4 k(t)) d_\lambda\left(\|\boldsymbol{w}(t)\|\right)^{q_4 - 1} \frac{\boldsymbol{w}(t)^\top \frac{\mathrm{d}}{\mathrm{d}t}\boldsymbol{w}(t)}{\|\boldsymbol{w}(t)\|} & , \|\boldsymbol{w}(t)\| > 0. \end{cases}
\end{aligned}$$

Hence, $\ddot{k}(\cdot) \in \mathcal{L}^\infty(\mathbb{R}_{\geq 0}; \mathbb{R})$ and moreover, in view of (3.72), Lemma 2.1.7 in [86, p. 17] gives $\lim_{t\to\infty} \dot{k}(t) = 0$. Therefore $\lim_{t\to\infty} d_\lambda(\|\boldsymbol{w}(t)\|) = \lim_{t\to\infty} d_\lambda(\|(e(t), \dot{e}(t)/k(t))^\top\|) = 0$, which shows Assertion (iv). This completes Step 6 and the proof of Theorem 3.13. □

3.5.4 Simulations

In this subsection, the controllers (3.37), (3.45) and (3.46) are applied to the following simple second order system, given by

$$\ddot{y}(t) \quad = \quad \gamma_0\big(u(t) + u_d(t)\big), \qquad \begin{array}{l} (y(0),\ \dot{y}(0)) = (y_0,\ y_1) \in \mathbb{R}^2, \\ \gamma_0 \neq 0,\ u_d(\cdot) \in \mathcal{L}^\infty(\mathbb{R}_{\geq 0}; \mathbb{R}), \end{array} \tag{3.80}$$

to try for a direct comparison of their control performance. System (3.80) is subject to input disturbance $u_d(\cdot)$. Output $y(\cdot)$ and output derivative $\dot{y}(\cdot)$ are assumed to be available for feedback and deteriorated by measurement noise $n_m(\cdot) \in \mathcal{W}^{2,\infty}(\mathbb{R}_{\geq 0}; \mathbb{R})$ and its derivative $\dot{n}_m(\cdot)$, respectively. Clearly, for known $\operatorname{sign}(\gamma_0)$, system (3.80) is element of class $\mathcal{S}_2$ and hence application of the controllers (3.37), (3.45) and (3.46) is admissible. System (3.80) represents the simplest model for any position control problem: a double integrator with inertia $1/\gamma_0$.

The closed-loop systems (3.80),(3.37), (3.80),(3.45) and (3.80),(3.46) are implemented in Matlab/Simulink. The comparative simulations are performed for 30 [s]. Control objective is set-point tracking of $y_{\text{ref}}(\cdot) = 1$ on [0, 5] [s], set-point tracking under constant load $u_d(\cdot) = -1$ on [5, 10] [s] (see Fig. 3.3) and reference tracking under changing load on [10, 30] [s] (see Fig. 3.4). The set-point tracking problem on [0, 5] [s] is formulated in terms of motion control objectives (mco_1)-(mco_3) (see Section 1.1) where maximum rise time, maximum settling time and maximum overshoot are (arbitrarily) specified as follow

$$t^r_{\text{ref},0.8} = 1.0 \text{ [s]}\,, \qquad t^s_{\text{ref},0.1} = 2.0 \text{ [s]} \qquad \text{and} \qquad \Delta^{os}_{\text{ref}} = 50 \text{ [\%]}\,. \tag{3.81}$$

The controllers (3.37), (3.45) and (3.46) are designed such that (3.81) (with overshoot as small as possible) and the presuppositions in Theorem 3.7, 3.11 and 3.13 hold, respectively. Tuning of (3.37) and (3.45) is performed by trial and error. Controller design of (3.46) is based on Remark 3.14 (and Remark 2.37). Clearly, a comparison always lakes of objectivity. But, to the best knowledge of the author, each controller is tuned such that "best performance" is achieved in a comparable setting (e.g. all controllers have an initial gain of 2).

System data and design parameters are collected in Tab. 3.1. The simulation results for the closed-loop systems ——(3.80), (3.37), ——(3.80), (3.45) and ——(3.80), (3.46) are depicted in Fig. 3.3 for set-point tracking and in Fig. 3.4 for (overall) reference tracking. Due to measurement noise $n_m(\cdot)$, the tracking error is given by $e(\cdot) = \big(y_{\text{ref}}(\cdot) - n_m(\cdot)\big) - y(\cdot)$ (similarly its derivative) and so, at most, "exact" tracking of the corrupted reference $y_{\text{ref}}(\cdot) - n_m(\cdot)$ is feasible.

Control performance of each controller is evaluated by means of rise time $t^r_{y(\cdot),0.8}$, overshoot $\Delta^{os}_{y(\cdot)}$, settling time $t^s_{y(\cdot),0.1}$, maximal required control action $\max_{t\geq 0} |u(t)|$ and integral time absolute error (ITAE[4]) criterion

$$ITAE := \int_0^{t_{end}} \tau \cdot |e(\tau)|\, \mathrm{d}\tau \qquad \text{for} \qquad t_{end} \geq 0. \tag{3.82}$$

where, for the simulations, $t_{end} = 30$ [s]. Evaluation results and maximal gains are summarized in Tab. 3.2 (values are rounded). All controllers accomplish specification (3.81).

Discussion for adaptive λ-tracking controller (3.37) *with backstepping:* Ye's controller yields the second best ITAE value. Especially rise and settling time beat the other two concepts. Overshoot is within the admissible range. Although the generated maximal gain is the lowest in the study, due to (3.36), the highest control action is generated at startup and noise sensitivity is unacceptable (see Fig. 3.4(c)). In conclusion, Ye's controller seems not applicable in real world.

Discussion for adaptive λ-tracking controller (3.45) *with high-gain observer:* The controller of Bullinger and Allgöwer is the second best of this study concerning rise and settling time. In contrast overshoot and ITAE value are the highest. Albeit generating the largest control gain,

[4]ITAE is used in favor of integral squared error (ISE) or integral absolute error (IAE) (see e.g. [120, p. 218]) due to time-weighting: non-zero errors at future times have greater influence on the performance measure than those at earlier times.

	data/parametrization
Matlab solver	`ode15s (stiff/NDF)` with variable step size (maximum 10^{-3} [s])
system (3.80)	$\gamma_0 = 3$, $(y_0,\, y_1) = (0,\, 0)$, $\|u_d\|_\infty \leq 2$ (see Fig. 3.4(c)), $\|n_m\|_\infty \leq 5 \cdot 10^{-3}$ and $\|\dot{n}_m\|_\infty \leq 5 \cdot 10^{-2}$ [1/s]
reference $y_{\mathrm{ref}}(\cdot)$	$\|y_{\mathrm{ref}}\|_\infty = 5$ (see Fig. 3.4(a)), $\|\dot{y}_{\mathrm{ref}}\|_\infty = 1$ and $\|\ddot{y}_{\mathrm{ref}}\|_\infty = 10$
controller (3.37)	$\bar{q} = 1$, $k_F = 1$, $k_0 = 2$, $\lambda = 0.1$, $\zeta_1^0 = 0$, $q_1(e) = 2\,e^2$, $q_2(e) = 2 + e^2$
controller (3.45)	$\underline{\gamma_0} = \gamma_0$, $q_0 = 1$, $q_1 = 2/\sqrt{\underline{\gamma_0}}$, $p_0 = 100$, $p_1 = 20$, $\epsilon = 1$, $\mu = 0.19$, $\alpha = 1$, $\beta = 0.5$, $\hat{\boldsymbol{x}}^0 = \mathbf{0}_2$, $\gamma = 10$, $\tilde{\gamma} = 2$, $k_0 = 2$
controller (3.46)	$\underline{\gamma_0} = \gamma_0/3$, $q_1 = 2/\sqrt{\gamma_0}$, $q_2 = 10$, $q_3 = 0.1$, $q_4 = 2$, $k^0(0) = 2$

Table 3.1: *System data and design parameters for comparative simulations.*

the controller reacts somehow "slowly" on varying references and disturbances. Its ITAE value could be reduced by choosing larger values for $\alpha > \beta \gg 1$ (e.g. $\alpha = 2$ and $\beta = 1$), however this would imply increased noise sensitivity. For the parametrization in Tab. 3.1 noise sensitivity is the lowest in the study. Due to tedious controller design (with too many tuning parameters) and bad control performance (ITAE and overshoot), the controller (3.45) seems not suitable for real application.

Discussion for adaptive λ-tracking controller (3.46) with derivative feedback: The proposed controller is the slowest concerning rise and settling time but yields a closed-loop system response with the smallest overshoot. This is due to the special choice of $q_1 \geq 2/\sqrt{\underline{\gamma_0}}$ (recall Remarks 3.14 and 2.37). Without noise, the response is "overdamped" (i.e. no overshoot). Maximal control gain is comparable to that of controller (3.45). Maximal control action is the smallest in the study. Good tracking performance and disturbance rejection give the smallest ITAE value. Noise sensitivity is acceptable and but slightly higher than that of (3.45). Since design parameters have a clear and easy to understand influence on the closed-loop system response, controller tuning of (3.46) is the most intuitive in this study (an attractive feature for implementation). Controller (3.46) will be implemented for position control of 1MS and 2MS (see Section 5.2.3).

Controller	$t^r_{y(\cdot),0.8}$ [s]	$t^s_{y(\cdot),0.1}$ [s]	$\Delta^{os}_{y(\cdot)}$ [%]	$\max_{t\in I} \|u(t)\|$ [1]	ITAE [s^2]	$\max_{t\in I} k(t)$
(3.37)	0.11	0.15	6.53	644.0	70.8	3.49
(3.45)	0.26	0.69	14.43	15.0	113.7	4.02
(3.46)	0.95	1.28	0.28	4.0	26.9	3.87

Table 3.2: *Performance evaluation of closed-loop systems* ——(3.80),(3.37), ——(3.80),(3.45) *and* ——(3.80),(3.46) *with parametrization as in Tab. 3.1 and* $I = [0,\, 30]$ [s].

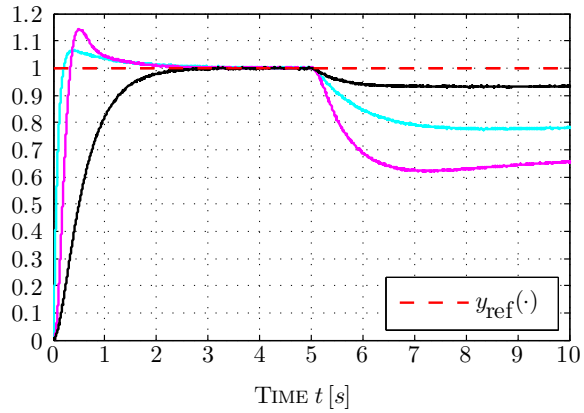

(a) *output* $y(\cdot) + n_m(\cdot)$ *and reference* $y_{\text{ref}}(\cdot)$

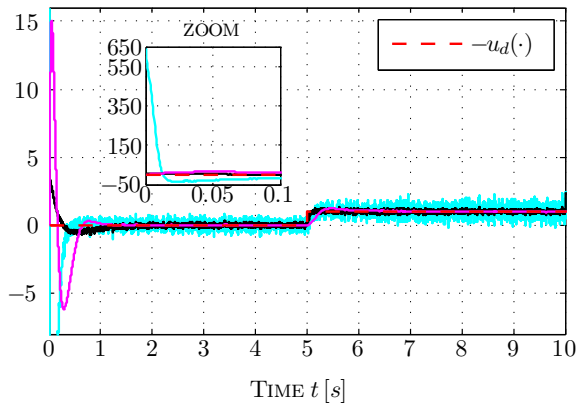

(b) *control action* $u(\cdot)$

Figure 3.3: *Simulation results for set-point tracking under load of closed-loop systems* —(3.80),(3.37), —(3.80),(3.45) *and* —(3.80),(3.46) *with parametrization as in Tab. 3.1.*

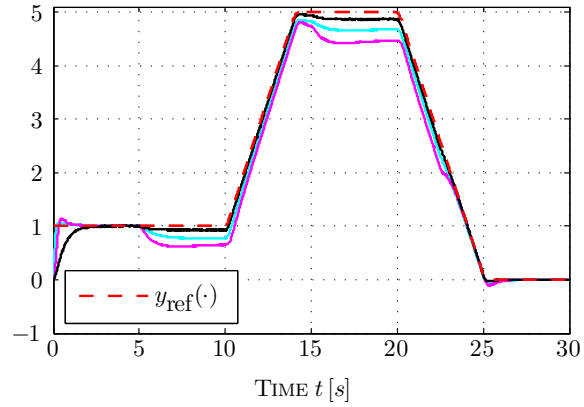

(a) *output* $y(\cdot) + n_m(\cdot)$ *and reference* $y_{\text{ref}}(\cdot)$

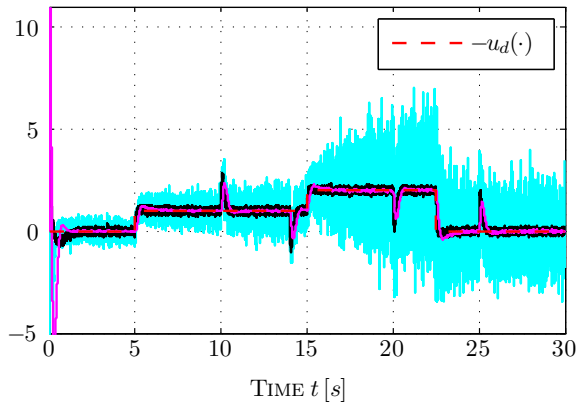

(b) *control action* $u(\cdot)$ *and disturbance* $-u_d(\cdot)$

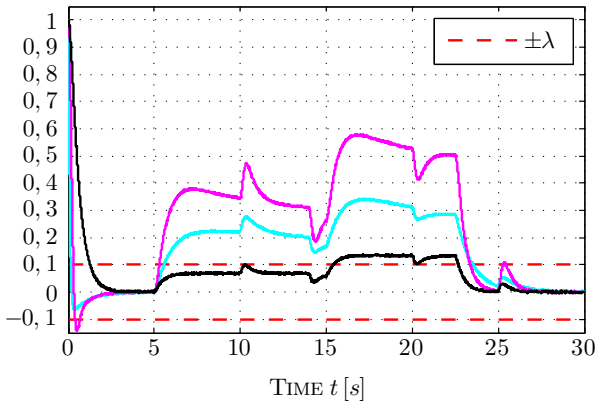

(c) *error* $e(\cdot)$ *and* λ*-strip*

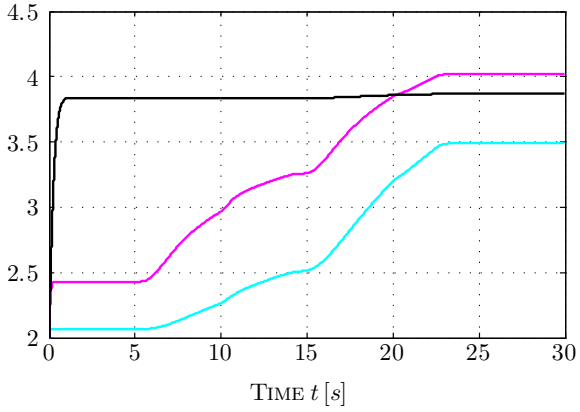

(d) *gain* $k(\cdot)$

Figure 3.4: *Simulation results for reference tracking under load of closed-loop systems* —(3.80),(3.37), —(3.80),(3.45) *and* —(3.80),(3.46) *with parametrization as in Tab. 3.1.*

Chapter 4

Funnel control

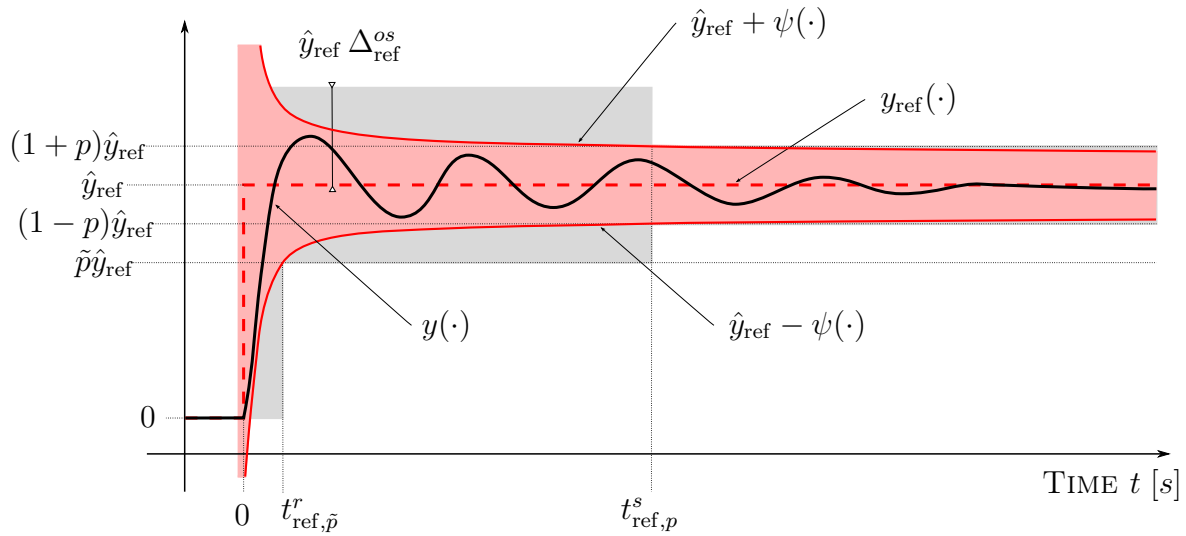

Figure 4.1: *Set-point tracking problem of reference step $y_{\text{ref}}(\cdot)$ with amplitude $\hat{y}_{\text{ref}} > 0$: exemplary evolution of system output $y(\cdot)$ constrained by prescribed limiting function $\psi(\cdot)$.*

In this chapter, funnel control is introduced for systems of class $\mathcal{S}_1$ and for systems of class $\mathcal{S}_2$. It will be shown that, for reference $y_{\text{ref}}(\cdot) \in \mathcal{W}^{1,\infty}(\mathbb{R}_{\geq 0};\mathbb{R})$ (or $\mathcal{W}^{2,\infty}(\mathbb{R}_{\geq 0};\mathbb{R})$), regulated output $y(\cdot)$, tracking error $e(\cdot) = y_{\text{ref}}(\cdot) - y(\cdot)$ and (prescribed) limiting function $\psi(\cdot)$, the presented funnel controllers achieve tracking with prescribed transient accuracy if the initial error is enclosed by the limiting function, i.e.

$$\forall\, \lambda > 0\ \forall\, \psi(\cdot) \in \mathcal{W}^{1,\infty}(\mathbb{R}_{\geq 0};[\lambda,\infty))\ \forall\, |e(0)| < \psi(0)\ \forall\, t \geq 0\colon \qquad |e(t)| < \psi(t). \tag{4.1}$$

According to this, the system output $y(\cdot)$ is constrained by the function $\psi(\cdot)$ (later on called funnel boundary) and the reference $y_{\text{ref}}(\cdot)$ (see Fig. 4.1), i.e.

$$\forall\, t \geq 0\colon \qquad y_{\text{ref}}(t) - \psi(t) < y(t) < y_{\text{ref}}(t) + \psi(t).$$

Clearly, (4.1) is stronger than control objective (co_2) (see Section 1.6.2.3). Moreover, it will be shown that funnel control assures boundedness of system state and control action, i.e.

$$\boldsymbol{x}(\cdot) \in \mathcal{L}^\infty(\mathbb{R}_{\geq 0};\mathbb{R}^n) \qquad \text{and} \qquad u(\cdot) \in \mathcal{L}^\infty(\mathbb{R}_{\geq 0};\mathbb{R}). \tag{4.2}$$

Hence, control objectives (co_1)-(co_3) are accomplished simultaneously by funnel control.

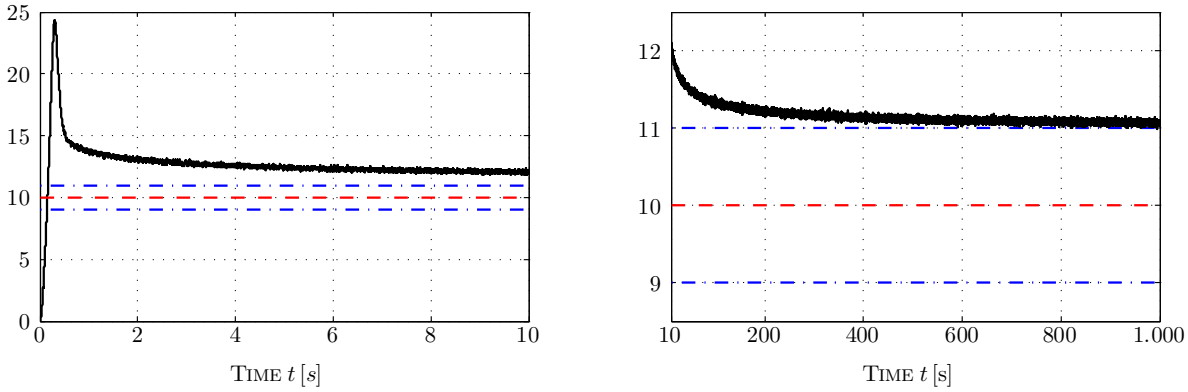

(a) *shortrun:* ——*noisy output* $y(\cdot) + n_m(\cdot)$, - - - *reference* $y_{\mathrm{ref}}(\cdot)$, ·-·-·$y_{\mathrm{ref}}(\cdot) \pm \lambda$. (b) *longrun:* ——*noisy output* $y(\cdot) + n_m(\cdot)$, - - - *reference* $y_{\mathrm{ref}}(\cdot)$, ·-·-·$y_{\mathrm{ref}}(\cdot) \pm \lambda$.

Figure 4.2: *Simulation results for closed-loop system* (3.2), (3.11) *with* $y_{\mathrm{ref}}(\cdot) = 10$, $\lambda = k(0) = q_1 = 1$, $q_2 = 2$, $y(0) = 0$, *noise* $n_m(\cdot) \in \mathcal{W}^{1,\infty}(\mathbb{R}_{\geq 0}; [-0.1, 0.1])$ *and disturbance* $u_d(\cdot) = 0$.

4.1 Motivation

The adaptive λ-tracking controllers in Chapter 3 achieve control objectives (co_1) and (co_2), tolerate disturbances and measurement noise and therefore are indeed applicable in real world. However, two major limitations remain which motivate for introduction of funnel control:

Motivation 1: Adaptive λ-tracking (and high-gain adaptive) control exhibit a non-decreasing gain and so, as time tends to infinity, it is likely that e.g. noise sensitivity permanently exceeds an acceptable level (if gain adaption is not stopped).

Motivation 2: Adaptive λ-tracking control assures tracking with prescribed asymptotic accuracy, however statements on the transient accuracy are not possible: e.g. albeit bounded large overshoots might occur[1] (see Fig. 4.2(a)) and, in general, the λ-strip is not reached in finite time (see Fig. 4.2(b)).

It will be shown that, for both system classes $\mathcal{S}_1$ and $\mathcal{S}_2$, funnel control achieves tracking with prescribed transient accuracy (4.1) and also permits gain decrease. For instance, for systems of class $\mathcal{S}_1$, a simple funnel controller is given by

$$u(t) = \operatorname{sign}(\boldsymbol{c}^\top \boldsymbol{b}) k(t) e(t) \quad \text{where} \quad e(t) = y_{\mathrm{ref}}(t) - y(t) \quad \text{and} \quad k(t) = \frac{1}{\psi(t) - |e(t)|}. \tag{4.3}$$

That is a proportional but time-varying controller. Note that gain $k(\cdot)$ in (4.3) is instantaneously adjusted and *not* dynamically tuned. Principle idea behind gain adaption is as follows: the gain $k(\cdot)$ becomes "time-varying" and is inversely proportional to the (actual) distance $\psi(t) - |e(t)|$ between limiting function $\psi(\cdot)$ and absolute value $|e(\cdot)|$ of the error. Hence, the gain $k(\cdot)$ increases only if absolute error $|e(\cdot)|$ advances on the boundary $\psi(\cdot)$ (critical situation) and may decrease again as soon as $|e(\cdot)|$ departs from $\psi(\cdot)$ (noncritical situation). Hence, funnel gain $k(\cdot)$ in (4.3) is *not* necessarily non-decreasing in contrast to the gain in adaptive λ-tracking

[1] Clearly, the overshoot might be decreased by accelerating gain adaption (i.e. $\dot{k}(t) = q_1 d_\lambda(|e(t)|)^{q_2}$ with $q_1 \gg 1$ and/or $q_2 \gg 2$). However, no bound on output (or states) can be specified a priori.

(or high-gain adaptive) control. Class $\mathcal{S}_2$ necessitates an augmented funnel controller, but the principle idea is similar (see Section 4.4).

Clearly, by adequate choice of the limiting function $\psi(\cdot)$, funnel control directly allows to account for motion control objectives (mco_1), (mco_3) and (mco_4) in controller design. Hence implementation effort is reduced. Iterations in controller tuning are not necessary. For illustration, let $\psi(\cdot) \in \mathcal{W}^{1,\infty}(\mathbb{R}_{\geq 0}; \mathbb{R}_{>0})$, consider the set-point tracking problem depicted in Fig. 4.1 and assume that $\hat{y}_{\text{ref}} > 0$, $\tilde{p} \in (0,1]$, $p \in (0,1)$, $0 \leq t^r_{\text{ref},\tilde{p}} \leq t^s_{\text{ref},p} = \tau_\lambda$ and $0 < \lambda = p\,\hat{y}_{\text{ref}}$ are specified. If $\psi(\cdot)$ is designed such that the following hold

$$\psi(0) > |\hat{y}_{\text{ref}} - y(0)|, \quad \forall\, t \geq t^r_{\text{ref},\tilde{p}}\colon\ \psi(t) \leq \tilde{p}\hat{y}_{\text{ref}} \quad \text{and} \quad \forall\, t \geq \tau_\lambda = t^s_{\text{ref},p}\colon\ \psi(t) \leq \lambda = p\,\hat{y}_{\text{ref}},$$

then the motion control objectives (mco_1), (mco_3) and (mco_4) are clearly met (see grey-shaded region in Fig. 4.1). Note that motion control objective (mco_2) cannot be addressed in general: suppose $\Delta^{os}_{\text{ref}} > 0$ and $\hat{y}_{\text{ref}} > 0$ such that $\Delta^{os}_{\text{ref}}\hat{y}_{\text{ref}} < \psi(0) + \hat{y}_{\text{ref}}$, then there might exist $t \geq 0$ such that $y(t) > \hat{y}_{\text{ref}}\Delta^{os}_{\text{ref}}$ (see Fig. 4.1).

4.2 Brief historical overview

In 1991 a contribution by Miller and Davison [134] addressed the problem of prescribed transient accuracy for disturbed minimum-phase LTI SISO systems with known high-frequency and arbitrary relative degree. Their proposed controller guarantees prescribed bounded overshoot and tracking with prescribed accuracy after some prescribed time. However, it has a non-increasing piecewise-constant gain adjusted by a switching strategy which yields a discontinuous control action. Moreover, the prescribed error bound is piecewise constant and hence limited in shaping the prescribed transient accuracy.

Funnel control is still a "young idea". It was introduced in 2002 by Ilchmann, Ryan and Sangwin for nonlinear functional differential equations with relative degree one and positive (generalized) high-frequency gain (see [99]). In [101] the concept was equipped with two extensions in gain adjustment: (i) gain scaling (introduced as distance scaling) and (ii) "future distance" evaluation taking into account that the future evolution of the prescribed funnel boundary is a priori known. The extensions may help to improve the transient behavior of the closed-loop system.

In [102] (2006) and in [103] (2007), funnel control was introduced for systems with known-but-arbitrary relative degree: in [102] for nonlinearly perturbed minimum-phase LTI MIMO systems and in [103] for nonlinear MIMO systems. However, the proposed controllers are complex due to the use of a dynamic compensator (input filter) and a back-stepping procedure. Moreover, already in the relative degree two case, the controller gain occurs with $k(t)^7$ and hence the controller is extremely sensitive to noise—an insuperable obstacle for real implementation (see Section 4.4.3). In 2010 funnel control with derivative feedback for nonlinear systems with relative degree two was developed. The results have been submitted for publication to "SIAM Journal of Control and Optimization" (see the joint work in [72]). In the same year bang-bang funnel control was introduced for nonlinear SISO system with relative degree one and two (see [121]). The bang-bang controller generates a discontinuous two-point like control action

(switching between two values) and is not appropriate for motion control (due to switching, it would entail an unnecessarily high power consumption and, in particular for systems with elasticity, it would excite oscillations). In [104] funnel control was successfully applied to nonlinear SISO systems with relative degree one and hysteresis in the control input.

Funnel control with input saturation was first addressed in 2004 for a class of exothermic reactor models (see [98]). More general results for LTI MIMO systems (see [82]) and for nonlinear SISO systems (see [83]) were published in 2010 for the relative degree one case. Results for the relative degree two case (if derivative feedback is admissible) have been submitted for publication to "SIAM Journal of Control and Optimization" (see the joint work in [72]).

Funnel control is robust in terms of the gap metric (see [90] for LTI MIMO systems with relative degree one and see [72] for LTI SISO systems with relative degree two). Loosely speaking (for the SISO case), by defining a measure for the "gap" between a nominal system $\mathfrak{S}_0$ element of class $\mathcal{S}_1^{\text{lin}}$ (or $\mathcal{S}_2^{\text{lin}}$) and a system $\mathfrak{S}$ not element of $\mathcal{S}_1^{\text{lin}}$ (or $\mathcal{S}_2^{\text{lin}}$), it can be shown that, if the initial value of $\mathfrak{S}$ and the gap are sufficiently small, then funnel control is still applicable for system $\mathfrak{S}$.

There exist some few applications. Funnel control works for set-point temperature control of chemical reactor models (see [98]) and it was successfully implemented for speed and position control of electrical drives (see [96] (2009) and [72] (2010) and [65] (2011)). First results for position control of 1MS and 2MS have been accepted for publication in "International Journal of Control" and will be discussed (with slight modifications and improvements) in Section 5.2.3.

4.3 Relative degree one systems

First funnel control for systems element of class $\mathcal{S}_1$ is introduced. The following results are well known (see e.g. [99, 101]), nevertheless they will be discussed in detail to achieve a self-contained presentation and a unified framework for systems of class $\mathcal{S}_1$. In literature the operator $\mathfrak{T}\colon \mathcal{C}([-h,\infty);\mathbb{R}) \to \mathcal{L}^\infty_{\text{loc}}(\mathbb{R}_{\geq 0};\mathbb{R}^m)$ is "solely" allowed to map output $y(\cdot)$ to $(\mathfrak{T}y)(\cdot)$. In the present work an operator mapping $\mathfrak{T}\colon \mathcal{C}([-h,\infty);\mathbb{R}^n) \to \mathcal{L}^\infty(\mathbb{R}_{\geq 0};\mathbb{R}^m)$ from state $\boldsymbol{x}(\cdot)$ to $(\mathfrak{T}\boldsymbol{x})(\cdot)$ is feasible, but it must be globally bounded.

4.3.1 Performance funnel

In this subsection, the admissible set of limiting functions $\psi(\cdot)$ is formalized and the notions of "performance funnel" and "funnel boundary" are introduced. Clearly, the limiting function $\psi(\cdot)$ should be continuous, class $\mathcal{S}_1$ precludes "jumps" in the output. Moreover, in view of application in "real world", the limiting function should have a bounded derivative. The output derivative is constrained e.g. due to actuator saturation. So, for $\psi(\cdot)$ belonging to the set

$$\mathcal{B}_1 := \left\{ \psi\colon \mathbb{R}_{\geq 0} \to \mathbb{R}_{>0} \quad \middle| \quad \exists\, c > 0 : \quad \psi(\cdot) \in \mathcal{W}^{1,\infty}(\mathbb{R}_{\geq 0}, [c,\infty)) \right\}, \tag{4.4}$$

introduce the performance funnel (see Fig. 4.3)

$$\mathcal{F}_\psi := \{ (t,e) \in \mathbb{R}_{\geq 0} \times \mathbb{R} \quad | \quad |e| < \psi(t) \} \tag{4.5}$$

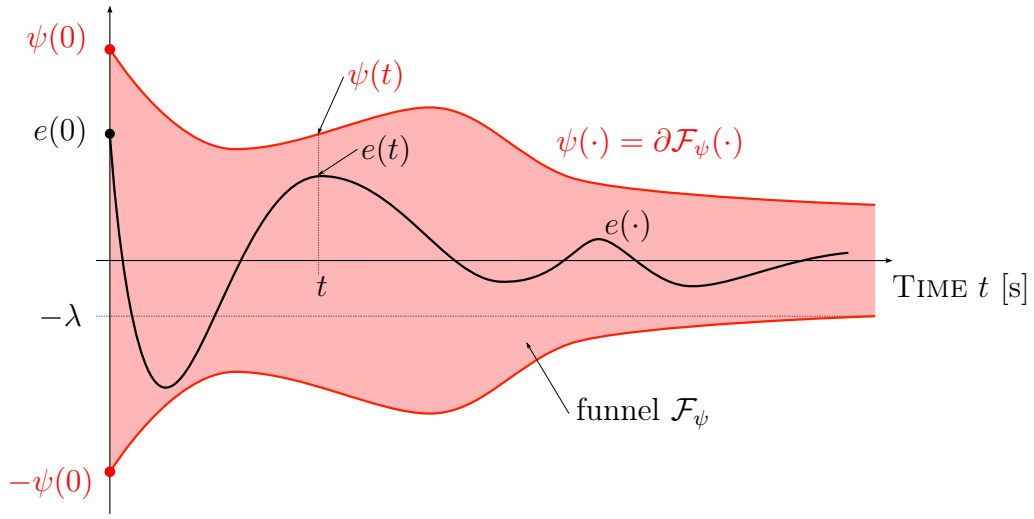

Figure 4.3: *Illustration of performance funnel $\mathcal{F}_\psi$ with boundary $\psi(\cdot)$, asymptotic accuracy λ and exemplary error evolution $e(\cdot)$.*

with funnel boundary

$$\forall\, t \geq 0\colon \qquad \partial\mathcal{F}_\psi(t) = \psi(t). \tag{4.6}$$

Any $\psi(\cdot) \in \mathcal{B}_1$ is bounded and has an (essentially) bounded derivative. Hence, any $\psi(\cdot) \in \mathcal{B}_1$ is (globally) Lipschitz continuous. Moreover, for any $\psi(\cdot) \in \mathcal{B}_1$, the (prescribed) asymptotic accuracy is given by

$$\lambda := \liminf_{t\to\infty} \psi(t) > 0.$$

Note that $\mathcal{B}_1$ as in (4.4) also allows for increasing funnel boundaries $\psi(\cdot)$ and so the width of the performance funnel $\mathcal{F}_\psi$ does not necessarily decrease. In most applications a non-increasing boundary $\psi(\cdot)$ and so a shrinking funnel $\mathcal{F}_\psi$ is desirable. Nevertheless, a temporarily increasing boundary might be reasonable, e.g. to avoid unacceptable large control actions due to (a priori known) rapid changes in reference (or disturbance) or events like sensor calibration/reset.

Examples 4.1. *Let T_L, $T_E > 0$ [s] and $\Lambda \geq \lambda > 0$. Then admissible funnel boundaries are given by*

$$\psi_L\colon \mathbb{R}_{\geq 0} \to [\lambda,\, \Lambda], \qquad t \mapsto \psi_L(t) := \max\left\{\Lambda - t/T_L,\ \lambda\right\} \tag{4.7}$$

and

$$\psi_E\colon \mathbb{R}_{\geq 0} \to (\lambda,\, \Lambda], \qquad t \mapsto \psi_E(t) := (\Lambda - \lambda)\exp\left(-t/T_E\right) + \lambda. \tag{4.8}$$

Both, $\psi_L(\cdot)$ and $\psi_E(\cdot)$, are non-increasing, have asymptotic accuracy $\lambda > 0$ and start at $\Lambda = \psi_L(0) = \|\psi_L\|_\infty = \psi_E(0) = \|\psi_E\|_\infty$. Their derivatives are bounded by $\|\dot\psi_L\|_\infty = 1/T_L$ and $\|\dot\psi_E\|_\infty = (\Lambda - \lambda)/T_E$, respectively.

Remark 4.2 (Infinite funnels)**.** *In [99] (or [72]) also performance funnels with "infinite initial width" (i.e. $\lim_{t\to 0+}\psi(t) = \infty$) are considered, which allows to show global results, in the sense that the assumption on the initial error can be dropped: any initial error $e(0) \in \mathbb{R}$ will "start" inside the "infinite performance funnel". Such a generalization is mainly of theoretical interest. In "real world" the initial error $e(0)$ is (at least) roughly known and hence there always exists an*

adequate choice $\psi(\cdot) \in \mathcal{B}_1$ such that $|e(0)| < \psi(0) \leq \|\psi\|_\infty < \infty$. Furthermore, even for non-zero initial errors (i.e. $e(0) \neq 0$), infinite boundaries yield zero initial control action (without gain scaling), i.e. $\lim_{t\to 0+} u(t) = 1/(\psi(t) - |e(0)|) = 0$ and so a "delayed" closed-loop system response.

4.3.2 Proportional controller with prescribed transient accuracy

Before presenting the main result for systems of class $\mathcal{S}_1$, an astonishing observation is discussed. Tracking with prescribed transient accuracy is already established by simple proportional output feedback of the following form

$$u(t) = \operatorname{sign}(\boldsymbol{c}^\top \boldsymbol{b})\, k\, e(t) \quad \text{where} \quad e(t) = y_{\mathrm{ref}}(t) - y(t) \quad \text{and} \quad k > 0, \tag{4.9}$$

if the constant controller gain k is fixed sufficiently large. Loosely speaking, the "output dynamics" of the closed-loop system (1.36), (4.9) become faster and faster for larger and larger values of k. Thus tracking of an arbitrary reference $y_{\mathrm{ref}}(\cdot) \in \mathcal{W}^{1,\infty}(\mathbb{R}_{\geq 0}; \mathbb{R})$ with prescribed transient accuracy is feasible. This formulated more precisely gives the following proposition (see [99]).

Proposition 4.3. *Consider a system of class $\mathcal{S}_1$ given by (1.36). Then, for non-increasing funnel boundary $\psi(\cdot) \in \mathcal{B}_1$, reference $y_{\mathrm{ref}}(\cdot) \in \mathcal{W}^{1,\infty}(\mathbb{R}_{\geq 0}; \mathbb{R})$ and initial trajectory $\boldsymbol{x}^0 \in \mathcal{C}([-h, 0]; \mathbb{R}^n)$ satisfying*

$$|y_{\mathrm{ref}}(0) - \boldsymbol{c}^\top \boldsymbol{x}^0(0)| < \psi(0), \tag{4.10}$$

there exists a threshold gain $k^\star > 0$ such that, for all $k \geq k^\star$, the proportional controller (4.9) applied to system (1.36) yields a closed-loop initial-value problem with the properties:

(i) there exists a solution $\boldsymbol{x} : [-h, T) \to \mathbb{R}^n$ which can be maximally extended and $T \in (0, \infty]$;

(ii) the solution is global, i.e. $T = \infty$;

(iii) the state variable is bounded, i.e. $\boldsymbol{x}(\cdot) \in \mathcal{L}^\infty(\mathbb{R}_{\geq 0}; \mathbb{R}^n)$;

(iv) and the tracking error evolves within the funnel, i.e. $|e(t)| < \psi(t)$ for all $t \geq 0$.

The proof is similar to that given in [99]. It is adjusted to fit for system class $\mathcal{S}_1$.

Proof of Proposition 4.3.

Step 1: It is shown that Assertion (i) holds true, i.e. existence of a maximally extended solution. It suffices to consider the system (1.36) of class $\mathcal{S}_1$ in the Byrnes-Isidori like form (3.7). Extend $y_{\mathrm{ref}}(\cdot)$ to $[-h, 0)$ such that $y_{\mathrm{ref}}(\cdot) \in \mathcal{W}^{1,\infty}([-h, \infty); \mathbb{R})$ and $|y_{\mathrm{ref}}(t) - \boldsymbol{c}^\top \boldsymbol{x}^0(t)| < \psi(|t|)$ for all $t \in [-h, 0]$. This is possible since $\boldsymbol{x}^0(\cdot)$ and $\psi(\cdot)$ are continuous. Define the open set

$$\mathcal{D} := \mathbb{R} \times \mathbb{R}^{n-1},$$

the function

$$\begin{aligned} \boldsymbol{f} \colon [-h, \infty) \times \mathcal{D} \times \mathbb{R}^m &\to \mathbb{R} \times \mathbb{R}^{n-1}, \\ (t, (\mu, \boldsymbol{\xi}), \boldsymbol{w}) &\mapsto \begin{pmatrix} a_1(\mu - y_{\mathrm{ref}}(t)) + \dot{y}_{\mathrm{ref}}(t) - \boldsymbol{a}_2^\top \boldsymbol{\xi} - |\gamma_0|\, k\, \mu \\ -\gamma_0\, u_d(t) - \boldsymbol{c}^\top \boldsymbol{B}_{\mathfrak{T}}(\boldsymbol{w} + \boldsymbol{d}(t)) \\ \boldsymbol{a}_3(y_{\mathrm{ref}}(t) - \mu) + \boldsymbol{A}_4 \boldsymbol{\xi} + \boldsymbol{N} \boldsymbol{B}_{\mathfrak{T}}(\boldsymbol{w} + \boldsymbol{d}(t)) \end{pmatrix} \end{aligned}$$

and the operator

$$\hat{\mathfrak{T}}\colon\ \mathcal{C}([-h,\infty);\mathbb{R}^n) \to \mathcal{L}^\infty_{\mathrm{loc}}(\mathbb{R}_{\geq 0};\mathbb{R}^m), \qquad (\hat{\mathfrak{T}}(\mu,\boldsymbol{\xi}))(t) := (\mathfrak{T}(\boldsymbol{S}^{-1}\left(\begin{smallmatrix} y_{\mathrm{ref}} - \mu \\ \boldsymbol{\xi} \end{smallmatrix}\right)))(t).$$

For $\hat{\boldsymbol{x}} := (\mu,\, \boldsymbol{\xi}^\top)^\top$ rewrite the closed-loop initial-value problem (3.7), (4.9) as follows

$$\frac{\mathrm{d}}{\mathrm{d}t}\,\hat{\boldsymbol{x}}(t) = \boldsymbol{f}(t, \hat{\boldsymbol{x}}(t), (\hat{\mathfrak{T}}\hat{\boldsymbol{x}})(t)), \qquad \hat{\boldsymbol{x}}|_{[-h,0]} = \begin{pmatrix} y_{\mathrm{ref}}|_{[-h,0]} - \boldsymbol{c}^\top \boldsymbol{x}^0 \\ \boldsymbol{N}\boldsymbol{x}^0 \end{pmatrix}. \tag{4.11}$$

For any non-empty compact set $\mathfrak{C} \subset \mathcal{D} \times \mathbb{R}^m$ note that

$$\exists\, M_{\mathfrak{C}} > 0\ \forall\, ((\mu,\boldsymbol{\xi}),\boldsymbol{w}) \in \mathfrak{C}: \quad \|((\mu,\boldsymbol{\xi}),\boldsymbol{w})\| \leq M_{\mathfrak{C}} \tag{4.12}$$

and thus it is easy to see that, for $u_d(\cdot) \in \mathcal{L}^\infty([-h,\infty);\mathbb{R})$, $\boldsymbol{d}(\cdot) \in \mathcal{L}^\infty([-h,\infty);\mathbb{R}^m)$ and $y_{\mathrm{ref}}(\cdot) \in \mathcal{W}^{1,\infty}([-h,\infty);\mathbb{R})$, the function $\boldsymbol{f}(\cdot,\cdot,\cdot)$ is a Carathéodory function (see Definition 3.1), since (i) $\boldsymbol{f}(t,\cdot,\cdot)$ is continuous for each fixed $t \in [-h,\infty)$, (ii) for each fixed $((\mu,\boldsymbol{\xi}),\boldsymbol{w}) \in \mathcal{D}\times\mathbb{R}^m$ the function $\boldsymbol{f}(\cdot,(\mu,\boldsymbol{\xi}),\boldsymbol{w})$ is measurable and (iii) for almost all $t \in [-h,\infty)$ and for all $((\mu,\boldsymbol{\xi}),\boldsymbol{w}) \in \mathfrak{C}$ the following holds

$$\begin{aligned}\|\boldsymbol{f}(t,(\mu,\boldsymbol{\xi}),\boldsymbol{w})\| \overset{(4.12)}{\leq}\ & M_{\mathfrak{C}}(|a_1| + \|\boldsymbol{a}_2\| + |\gamma_0|\, k + \|\boldsymbol{c}\|\, \|\boldsymbol{B}_{\mathfrak{T}}\| + \|\boldsymbol{a}_3\| + \|\boldsymbol{A}_4\| + \|\boldsymbol{N}\|\, \|\boldsymbol{B}_{\mathfrak{T}}\|) \\ & + (|a_1| + \|\boldsymbol{a}_3\|)\|y_{\mathrm{ref}}\|_\infty + \|\dot{y}_{\mathrm{ref}}\|_\infty + |\gamma_0|\, \|u_d\|_\infty \\ & + (\|\boldsymbol{c}\| + \|\boldsymbol{N}\|)\, \|\boldsymbol{B}_{\mathfrak{T}}\|\, \|\boldsymbol{d}\|_\infty =: l_{\mathfrak{C}}.\end{aligned}$$

Now Theorem 3.2 ensures existence of a solution $\hat{\boldsymbol{x}} : [-h,T) \to \mathbb{R}\times\mathbb{R}^{n-1}$ of the initial-value problem (4.11), with $\hat{\boldsymbol{x}}([0,T)) \in \mathcal{D}$, $T \in (0,\infty]$. Every solution can be extended to a maximal solution.

In the following, let $\hat{\boldsymbol{x}} := (e,\boldsymbol{z})\colon [-h,T) \to \mathbb{R}\times\mathbb{R}^{n-1}$ be a fixed and maximally extended solution of the initial-value problem (4.11), where $(e,\boldsymbol{z}) : [-h,T) \to \mathbb{R}\times\mathbb{R}^{n-1}$ solves the closed-loop initial-value problem (3.7), (4.9) for almost all $t \in [0,T)$. Hence Assertion (i) is shown.

Step 2: It is shown that $|e(t)| < \psi(0)$ for all $t \in [0,T)$.
Since $\psi(\cdot) \in \mathcal{B}_1$ and is non-increasing, it follows that

$$\forall\, t \geq 0\colon \qquad 0 < \lambda := \inf_{t\geq 0} \psi(t) \leq \psi(t) \leq \psi(0) = \|\psi\|_\infty.$$

Seeking a contradiction, assume there exists

$$t^\star := \min\{\, t \in [0,T) \quad | \quad |e(t)| = \|\psi\|_\infty \,\}. \tag{4.13}$$

Then, by continuity of $e(\cdot)$ on $[0,T)$, there exists

$$t_\star := \max\{\, t \in [0,t^\star) \quad | \quad |e(t)| = \lambda/2 \,\} \tag{4.14}$$

and the following holds

$$\forall\, t \in [t_\star,t^\star]\colon \qquad \lambda/2 \leq |e(t)| \leq \|\psi\|_\infty \qquad \text{and} \qquad \forall\, t \in [0,t^\star]\colon \qquad |e(t)| \leq \|\psi\|_\infty. \tag{4.15}$$

Due to system property ($\mathcal{S}_1$-sp$_2$) and Lemma 2.12, the matrix $\boldsymbol{A}_4$ is Hurwitz, hence there exists $\boldsymbol{P}_4 = \boldsymbol{P}_4^\top > 0$ such that $\boldsymbol{A}_4^\top \boldsymbol{P}_4 + \boldsymbol{P}_4 \boldsymbol{A}_4 = -\boldsymbol{I}_{n-1}$ is satisfied, i.e. (2.63). Now, for $\boldsymbol{P}_4 = \boldsymbol{P}_4^\top > 0$ as in (2.63), introduce the Lyapunov candidate

$$V : \mathbb{R}^{n-1} \to \mathbb{R}_{\geq 0}, \qquad \boldsymbol{z} \mapsto V(\boldsymbol{z}) := \boldsymbol{z}^\top \boldsymbol{P}_4 \boldsymbol{z} \geq 0 \tag{4.16}$$

and define

$$M_{\dot V} := \|\boldsymbol{P}_4\| \left(\|\boldsymbol{a}_3\| \left(\|\psi\|_\infty + \|y_{\mathrm{ref}}\|_\infty\right) + \|\boldsymbol{N}\| \, \|\boldsymbol{B}_{\mathfrak{T}}\| \left(M_{\mathfrak{T}} + \|\boldsymbol{d}\|_\infty\right)\right) \geq 0. \tag{4.17}$$

The time derivative $\frac{\mathrm{d}}{\mathrm{d}t} V(\boldsymbol{z}(t))$ along the solution of the closed-loop system (3.7), (4.9) is, for almost all $t \in [0, t^\star)$, given by

$$\begin{aligned} \frac{\mathrm{d}}{\mathrm{d}t} V(\boldsymbol{z}(t)) \quad &\leq \quad - \|\boldsymbol{z}(t)\|^2 + 2 \|\boldsymbol{z}(t)\| \, \|\boldsymbol{P}_4\| \Big(\|\boldsymbol{a}_4\| \left(\|y_{\mathrm{ref}}\|_\infty + \|\psi\|_\infty\right) \\ &\qquad + \|\boldsymbol{N}\| \, \|\boldsymbol{B}_{\mathfrak{T}}\| \left(M_{\mathfrak{T}} + \|\boldsymbol{d}\|_\infty\right)\Big) \\ &\overset{(4.17)}{\leq} \quad -\frac{1}{2} \|\boldsymbol{z}(t)\|^2 + 2M_{\dot V}^2 \leq -\frac{1}{2 \, \|\boldsymbol{P}_4\|} V(\boldsymbol{z}(t)) + 2M_{\dot V}^2 \end{aligned} \tag{4.18}$$

Hence, for $M_{\dot V}$ as in (4.17), the Belman-Gronwall Lemma (in its differential form (see e.g. [18, Lemma 1.1, p. 2])) gives

$$\begin{aligned} \forall t \in [0, t^\star): \qquad V(\boldsymbol{z}(t)) &\leq V(\boldsymbol{z}(0)) \exp\left(-\frac{t}{2 \, \|\boldsymbol{P}_4\|}\right) + \int_0^t 2M_{\dot V}^2 \exp\left(-\frac{t-s}{2 \, \|\boldsymbol{P}_4\|}\right) \mathrm{d}s \\ &\leq V(\boldsymbol{z}(0)) + 4 \, \|\boldsymbol{P}_4\| \, M_{\dot V}^2 \leq \|\boldsymbol{P}_4\| \left(\|\boldsymbol{z}(0)\|^2 + 4 \, M_{\dot V}^2\right), \end{aligned}$$

and, moreover, the following holds

$$\forall \, t \in [0, t^\star): \quad \|\boldsymbol{z}(t)\| \leq \sqrt{\|\boldsymbol{P}_4\| \left\|\boldsymbol{P}_4^{-1}\right\|} \sqrt{\|\boldsymbol{z}(0)\|^2 + 4 \, M_{\dot V}^2} =: M_{\boldsymbol{z}}. \tag{4.19}$$

For $\delta > 0$ and $M_{\boldsymbol{z}}$ as in (4.19) define

$$M := |a_1| (\|\psi\|_\infty + \|y_{\mathrm{ref}}\|_\infty) + \|\dot y_{\mathrm{ref}}\|_\infty + \|\boldsymbol{a}_2\| \, M_{\boldsymbol{z}} + |\gamma_0| \|u_d\|_\infty + \|\boldsymbol{c}\| \, \|\boldsymbol{B}_{\mathfrak{T}}\| \left(M_{\mathfrak{T}} + \|\boldsymbol{d}\|_\infty\right) \tag{4.20}$$

and

$$k^\star := 2(\delta + M + \|\dot\psi\|_\infty)/(\gamma_0 \, \lambda). \tag{4.21}$$

In view of the first equation in (3.7) note that

$$\begin{aligned} \text{for a.a. } t \in [0, T): \; \dot e(t) = a_1 (e(t) - y_{\mathrm{ref}}(t)) + \dot y_{\mathrm{ref}}(t) - \boldsymbol{a}_2^\top \boldsymbol{z}(t) - \gamma_0 (u(t) + u_d(t)) \\ - \boldsymbol{c}^\top \boldsymbol{B}_{\mathfrak{T}} \Big(\left(\mathfrak{T}\left(\boldsymbol{S}^{-1} \begin{pmatrix} y_{\mathrm{ref}} - e \\ \boldsymbol{z} \end{pmatrix}\right)\right)(t) + \boldsymbol{d}(t) \Big) \end{aligned}$$

which, with M as in (4.20), yields

$$\text{for a.a. } t \in [0, t^\star): \quad -M - \gamma_0\, u(t) \leq \dot{e}(t) \leq M - \gamma_0\, u(t). \tag{4.22}$$

Observe that (4.15) precludes a sign change on $[t_\star, t^\star]$. Consider only the case $e(\cdot) > 0$ on $[t_\star, t^\star]$, the other case follows analogously. Then inserting (4.9) into (4.22) gives

$$\text{for a.a. } t \in [t_\star, t^\star]: \quad \dot{e}(t) \leq M - |\gamma_0| k e(t) \overset{(4.15)}{\leq} M - |\gamma_0| k \frac{\lambda}{2} \overset{(4.21)}{\leq} -(\delta + \|\dot{\psi}\|_\infty). \tag{4.23}$$

Since $e(t_\star) \leq \lambda/2 < \psi(0)$, the contradiction follows by integration

$$\forall\, t \in (t_\star, t^\star]: \quad 0 \leq e(t) - e(t_\star) = \int_{t_\star}^{t} \dot{e}(\tau)\, \mathrm{d}\tau \overset{(4.14)}{=} e(t) - \lambda/2 \overset{(4.23)}{\leq} -\delta(t - t_\star) < 0.$$

Step 3: It is shown that Assertions (ii) and (iii) hold true, i.e. $T = \infty$ and $\boldsymbol{x}(\cdot) \in \mathcal{L}^\infty(\mathbb{R}_{\geq 0}; \mathbb{R})$.

From Step 2, it follows that $|e(t)| < \|\psi\|_\infty$ for all $t \in [0, T)$ and hence $\|\boldsymbol{z}(t)\| \leq M_{\boldsymbol{z}}$ for all $t \in [0, T)$ which, by maximality of $T \in (0, \infty]$, implies $T = \infty$. Hence Assertion (ii) is shown. From $y_{\mathrm{ref}}(\cdot) \in \mathcal{W}^{1,\infty}(\mathbb{R}_{\geq 0}; \mathbb{R})$ and $\|\psi\|_\infty > |e(t)| = |y_{\mathrm{ref}}(t) - y(t)|$ for all $t \geq 0$ it follows that $y(\cdot) \in \mathcal{L}^\infty(\mathbb{R}_{\geq 0}; \mathbb{R})$. Combining this with $\boldsymbol{z}(\cdot) \in \mathcal{L}^\infty(\mathbb{R}_{\geq 0}; \mathbb{R}^{n-1})$ yields $\boldsymbol{x}(\cdot) = \boldsymbol{S}^{-1}(y(\cdot), \boldsymbol{z}(\cdot))^\top \in \mathcal{L}^\infty(\mathbb{R}_{\geq 0}; \mathbb{R}^n)$, which shows Assertion (iii) and completes Step 3.

Step 4: It is shown that Assertion (iv) holds true, i.e. $|e(t)| < \psi(t)$ for all $t \geq 0$
Claim there exists $s \geq 0$ such that $|e(s)| < \lambda/2$. Seeking a contradiction, suppose otherwise. Then $\|\psi\|_\infty > |e(t)| \geq \lambda/2$ for all $t \geq 0$ and either $e(\cdot) > 0$ or $e(\cdot) < 0$ on $\mathbb{R}_{\geq 0}$. Consider only the case $\operatorname{sign} e(t) = 1$ for all $t \geq 0$, the other case follows analogously. Hence inequality (4.23) holds for almost all $t \geq 0$ and integration yields the contradiction

$$\forall\, t \geq 0: \qquad \int_0^t \dot{e}(\tau)\, \mathrm{d}\tau \overset{(4.23)}{\leq} -\delta\, t \qquad \Longrightarrow \qquad e(t) \leq e(0) - \delta\, t,$$

whence there exists $s \geq 0$ such that $|e(s)| < \lambda/2$. Now fix $\hat{t} := \min\{\, t \geq 0 \,|\, |e(t)| \leq \lambda/2 \,\}$ and claim that $|e(t)| < \lambda$ for all $t \geq \hat{t}$. Seeking a contradiction, assume there exist $s > \hat{t}$ such that $|e(s)| \geq \lambda$. Then, by continuity of $e(\cdot)$ on $\mathbb{R}_{\geq 0}$, there exists

$$s^\star := \min\{\, t \in [\hat{t}, s) \,|\, |e(t)| = \lambda \,\} \quad \text{and} \quad s_\star := \max\{\, t \in [\hat{t}, s^\star) \,|\, |e(t)| = \lambda/2 \,\}.$$

Clearly, $\lambda/2 \leq |e(t)| \leq \lambda$ for all $t \in [s_\star, s^\star]$, which precludes a sign change of $e(\cdot)$ on $[s_\star, s^\star]$. Again consider only the case $e(\cdot) > 0$ on $[s_\star, s^\star]$, the other case follows analogously. Hence (4.23) holds on $[s_\star, s^\star]$ and the contradiction follows

$$\lambda/2 < \lambda = e(s^\star) \overset{(4.23)}{<} e(s_\star) = \lambda/2.$$

Furthermore, since $\|\psi\|_\infty \geq \psi(t) \geq \lambda$ for all $t \geq \hat{t}$ it follows that $|e(t)| < \psi(t)$ for all $t \geq \hat{t}$. The remainder of Step 4 is to show that $|e(t)| < \psi(t)$ for all $t \in [0, \hat{t}]$. If $\hat{t} = 0$ then $|e(0)| < \psi(0)$ trivially holds. Suppose $\hat{t} > 0$, then $\|\psi\|_\infty > |e(t)| \geq \lambda/2$ for all $t \in [0, \hat{t}]$ precluding a sign change of $e(\cdot)$ on $[0, \hat{t}]$. Again only consider the case $\operatorname{sign} e(\cdot) = 1$, the other case follows

analogously. Note that (4.23) holds on $[0, \hat{t}]$ and, since $\psi(\cdot) \in \mathcal{W}^{1,\infty}(\mathbb{R}_{\geq 0}; [\lambda, \infty))$, it follows that $\psi(t) \geq \psi(0) - \|\dot{\psi}\|_\infty t$ for all $t \in [0, \hat{t}]$, whence

$$\forall\, t \in [0, \hat{t}]: \quad e(t) - e(0) = \int_0^t \dot{e}(\tau)\,\mathrm{d}\tau \overset{(4.23)}{<} -\|\dot{\psi}\|_\infty t \leq \psi(t) - \psi(0)$$
$$\implies 0 < \psi(0) - e(0) < \psi(t) - e(t).$$

This shows Assertion (iv) and completes the proof. □

4.3.3 Funnel controller

Proposition 4.3 shows that for all $k \geq k^\star$ with $k^\star$ as in (4.21) the state variable of the closed-loop system (1.36), (4.9) remains bounded and furthermore, if $|e(0)| < \psi(0)$, any admissible reference $y_{\mathrm{ref}}(\cdot) \in \mathcal{W}^{1,\infty}(\mathbb{R}_{\geq 0}; \mathbb{R})$ may be tracked with prescribed transient accuracy specified by the (non-increasing) funnel boundary $\psi(\cdot) \in \mathcal{B}_1$. The threshold $k^\star$ in (4.21) obviously depends on system data, disturbance, reference signal and funnel boundary and must be known a priori.

The following well known result (see e.g. [99, 101]) shows that for systems of class $\mathcal{S}_1$ tracking with prescribed transient accuracy is feasible without a priori knowledge of $k^\star$. Solely the gain must be adapted appropriately.

Theorem 4.4 (Funnel control for systems of class $\mathcal{S}_1$)**.**
Consider a system of class $\mathcal{S}_1$ described by (1.36). Then, for arbitrary funnel boundary $\psi(\cdot) \in \mathcal{B}_1$, gain scaling function $\varsigma(\cdot) \in \mathcal{B}_1$, reference $y_{\mathrm{ref}}(\cdot) \in \mathcal{W}^{1,\infty}(\mathbb{R}_{\geq 0}; \mathbb{R})$ and initial trajectory $\boldsymbol{x}^0(\cdot) \in \mathcal{C}([-h, 0]; \mathbb{R}^n)$ satisfying (4.10), the funnel controller

$$u(t) = \operatorname{sign}(\boldsymbol{c}^\top \boldsymbol{b}) k(t) e(t) \quad \text{where} \quad e(t) = y_{\mathrm{ref}}(t) - y(t) \quad \text{and} \quad k(t) = \frac{\varsigma(t)}{\psi(t) - |e(t)|} \tag{4.24}$$

applied to (1.36) yields a closed-loop initial-value problem with the properties

(i) there exists a solution $\boldsymbol{x} : [-h, T) \to \mathbb{R}^n$ which can be maximally extended and $T \in (0, \infty]$;

(ii) the solution $\boldsymbol{x}(\cdot)$ does not have finite escape time, i.e. $T = \infty$;

(iii) the tracking error is uniformly bounded away from the funnel boundary, i.e.

$$\exists\, \varepsilon > 0\ \forall\, t \geq 0: \qquad \psi(t) - |e(t)| \geq \varepsilon;$$

(iv) gain and control action are uniformly bounded, i.e. $k(\cdot), u(\cdot) \in \mathcal{L}^\infty(\mathbb{R}_{\geq 0}; \mathbb{R})$.

Remark 4.5. *The performance funnel must not shrink to zero. More precisely, for any $\psi(\cdot) \in \mathcal{B}_1$, there exists $\varepsilon > 0$ such that $\partial \mathcal{F}_\psi(t) = \psi(t) \geq \varepsilon$ for all $t \geq 0$. Hence, funnel control may not guarantee asymptotic stabilization (i.e. $\lim_{t\to\infty} y(t) = 0$ for $y_{\mathrm{ref}}(\cdot) = 0$) or asymptotic tracking (i.e. $\lim_{t\to\infty} e(t) = 0$). However, in [99, Proposition 9] and [94, Theorem 2.3] it is shown that asymptotic stabilization and asymptotic tracking is feasible for linear systems if the funnel boundary $\psi(\cdot)$ possesses certain properties (e.g. $\lim_{t\to\infty} \psi(t) = 0$) and an internal model is applied, respectively.*

Note the potential singularity in gain adaption (4.24): if there exists $t^\star < \infty$ such that $\lim_{t\to t^\star} \psi(t) - |e(t)| = 0$, then the closed-loop system (1.36), (4.24) will exhibit finite escape time. Fortunately, a precise analysis invoking Theorem 3.2 yields that the closed-loop initial-value problem (1.36), (4.24) is well-posed and the solution exists globally.

Proof of Theorem 4.4.

Step 1: It is shown that Assertion (i) holds true, i.e. existence of a maximally extended solution. It suffices to consider the system (1.36) in the form (3.7). Extend $\varsigma(\cdot)$ and $y_{\mathrm{ref}}(\cdot)$ to $[-h, 0)$ such that

$$\varsigma(\cdot) \in \mathcal{W}^{1,\infty}([-h,\infty);\mathbb{R}_{>0}) \quad \text{and} \quad y_{\mathrm{ref}}(\cdot) \in \mathcal{W}^{1,\infty}([-h,\infty);\mathbb{R}), \tag{4.25}$$

respectively, and furthermore, such that the following holds

$$\forall\, t \in [-h, 0]\colon \qquad |y_{\mathrm{ref}}(t) - \boldsymbol{c}^\top \boldsymbol{x}^0(t)| < \psi(|t|) \tag{4.26}$$

which is possible since $\psi(\cdot) \in \mathcal{B}_1$ and $y_{\mathrm{ref}}(\cdot)$ are both continuous. For $\mathcal{F}_\psi$ as in (4.5), define the non-empty and open set

$$\mathcal{D} := \left\{ (\tau, \mu, \boldsymbol{\xi}) \in \mathbb{R} \times \mathbb{R} \times \mathbb{R}^{n-1} \mid (|\tau|, \mu) \in \mathcal{F}_\psi \right\}, \tag{4.27}$$

the function

$$\begin{aligned} \boldsymbol{f}\colon\ [-h,\infty) \times \mathcal{D} \times \mathbb{R}^m \ &\to\ \mathbb{R} \times \mathbb{R} \times \mathbb{R}^{n-1}, \\ (t, (\tau, \mu, \boldsymbol{\xi}), \boldsymbol{w}) \ &\mapsto\ \begin{pmatrix} 1 \\ a_1\,(\mu - y_{\mathrm{ref}}(t)) + \dot{y}_{\mathrm{ref}}(t) - |\gamma_0| \frac{\varsigma(t)\,\mu}{\psi(|\tau|) - |\mu|} - \gamma_0 u_d(t) \\ -\boldsymbol{a}_2^\top \boldsymbol{\xi} - \boldsymbol{c}^\top \boldsymbol{B}_{\mathfrak{T}}\,(\boldsymbol{w} + \boldsymbol{d}(t)) \\ \boldsymbol{a}_3\,(y_{\mathrm{ref}}(t) - \mu) + \boldsymbol{A}_4 \boldsymbol{\xi} + \boldsymbol{N} \boldsymbol{B}_{\mathfrak{T}}\,(\boldsymbol{w} + \boldsymbol{d}(t)) \end{pmatrix} \end{aligned}$$

and the operator

$$\hat{\mathfrak{T}} : \mathcal{C}([-h,\infty);\mathbb{R}\times\mathbb{R}^n) \to \mathcal{L}^\infty_{\mathrm{loc}}(\mathbb{R}_{\geq 0};\mathbb{R}^m), \qquad (\hat{\mathfrak{T}}(\tau,\mu,\boldsymbol{\xi}))(t) := (\mathfrak{T}(\boldsymbol{S}^{-1}\left(\begin{smallmatrix} y_{\mathrm{ref}} - \mu \\ \boldsymbol{\xi} \end{smallmatrix}\right)))(t). \tag{4.28}$$

Then, introducing the artifact $\tau\colon [-h,\infty) \to \mathbb{R},\ t \mapsto t$ and the augmented state variable $\hat{\boldsymbol{x}} := (\tau, e, \boldsymbol{z})$ and writing $\tau^0 := \tau|_{[-h,0]}$, the initial-value problem (3.7), (4.24) may be expressed in the form

$$\frac{\mathrm{d}}{\mathrm{d}t}\,\hat{\boldsymbol{x}}(t) = \boldsymbol{f}(t, \hat{\boldsymbol{x}}(t), (\hat{\mathfrak{T}}\hat{\boldsymbol{x}})(t)), \qquad \hat{\boldsymbol{x}}|_{[-h,0]} = \begin{pmatrix} \tau^0 \\ y_{\mathrm{ref}}|_{[-h,0]} - \boldsymbol{c}^\top \boldsymbol{x}^0 \\ \boldsymbol{N}\boldsymbol{x}^0 \end{pmatrix}. \tag{4.29}$$

Choose a compact set $\mathfrak{C} \subset \mathcal{D} \times \mathbb{R}^m$ and note that

$$\begin{aligned} &\exists\, M_{\mathfrak{C}} > 0\ \forall\, ((\tau,\mu,\boldsymbol{\xi}),\boldsymbol{w}) \in \mathfrak{C}\colon \quad \|((\tau,\mu,\boldsymbol{\xi}),\boldsymbol{w})\| \leq M_{\mathfrak{C}} \\ &\exists\, m_{\mathfrak{C}} > 0\ \forall\, ((\tau,\mu,\boldsymbol{\xi}),\boldsymbol{w}) \in \mathfrak{C}\colon \quad \min\{\psi(|\tau|) - \mu\} \geq m_{\mathfrak{C}}. \end{aligned} \tag{4.30}$$

Then it is easy to see that, for $u_d(\cdot), y_{\mathrm{ref}}(\cdot) \in \mathcal{L}^\infty([-h,\infty);\,\mathbb{R})$, $\boldsymbol{d}(\cdot) \in \mathcal{L}^\infty([-h,\infty);\,\mathbb{R}^n)$ and $\varsigma(\cdot) \in \mathcal{W}^{1,\infty}([-h,\infty),\mathbb{R}_{>0})$, the function $\boldsymbol{f}(\cdot,\cdot,\cdot)$ has following properties (i) $\boldsymbol{f}(t,\cdot,\cdot)$ is con-

tinuous for each fixed $t \in [-h, \infty)$, (ii) for each fixed $((\tau, \mu, \boldsymbol{\xi}), \boldsymbol{w}) \in \mathcal{D} \times \mathbb{R}^m$ the function $\boldsymbol{f}(\cdot, (\tau, \mu, \boldsymbol{\xi}), \boldsymbol{w})$ is measurable and (iii) for almost all $t \in [-h, \infty)$ and for all $((\tau, \mu, \boldsymbol{\xi}), \boldsymbol{w}) \in \mathfrak{C}$:

$$\begin{aligned}\|\boldsymbol{f}(t, (\tau, \mu, \boldsymbol{\xi}), \boldsymbol{w})\| \overset{(4.30)}{\leq}\ & 1 + (|a_1| + \|\boldsymbol{a}_3\|)\, \|y_{\mathrm{ref}}\|_\infty + \|\dot{y}_{\mathrm{ref}}\|_\infty + |\gamma_0|\, \|u_d\|_\infty \\ & + M_{\mathfrak{C}}\, (|a_1| + \|\boldsymbol{a}_2\| + (\|\boldsymbol{c}\| + \|\boldsymbol{N}\|)\, \|\boldsymbol{B}_{\mathfrak{T}}\| + \|\boldsymbol{a}_3\| + \|\boldsymbol{A}_4\|) \\ & + (\|\boldsymbol{c}\| + \|\boldsymbol{N}\|)\, \|\boldsymbol{B}_{\mathfrak{T}}\|\, \|\boldsymbol{d}\|_\infty + |\gamma_0| m_{\mathfrak{C}} M_{\mathfrak{C}} \|\varsigma\|_\infty =: l_{\mathfrak{C}}. \end{aligned} \tag{4.31}$$

Hence, $\boldsymbol{f}(\cdot, \cdot, \cdot)$ is a Carathéodory function (see Definition 3.1) and Theorem 3.2 yields existence of a solution $\hat{\boldsymbol{x}} : [-h, T) \to \mathbb{R} \times \mathbb{R}^n$ of the initial-value problem (4.29) with $\hat{\boldsymbol{x}}([0, T)) \in \mathcal{D}$, $T \in (0, \infty]$. Every solution can be extended to a maximal solution. Moreover, since $\boldsymbol{f}(\cdot, \cdot, \cdot)$ is locally essentially bounded, it follows from Theorem 3.2 that if $T < \infty$ then for every compact set $\widetilde{\mathfrak{C}} \subset \mathcal{D}$, there exists $\tilde{t} \in [0, T)$ such that $\hat{\boldsymbol{x}}(\tilde{t}) \notin \widetilde{\mathfrak{C}}$.

In the following, let $\hat{\boldsymbol{x}} := (\tau, e, \boldsymbol{z}) \colon [-h, T) \to \mathbb{R} \times \mathbb{R} \times \mathbb{R}^{n-1}$ be a fixed and maximally extended solution of the initial-value problem (4.29), where $(e, \boldsymbol{z}) : [-h, T) \to \mathbb{R} \times \mathbb{R}^{n-1}$ solves the closed-loop initial-value problem (3.7), (4.24) for almost all $t \in [0, T)$.

Step 2: It is shown that $\boldsymbol{z}(\cdot)$ is bounded on $[0, T)$ and an essential inequality holds true.
In view of Step 1, $e(\cdot)$ is continuous on $[0, T)$ and evolves within the funnel $\mathcal{F}_\psi$, hence by properties of $\mathcal{B}_1$, it follows that

$$\forall\, t \in [0, T) : \qquad |e(t)| < \psi(t) \leq \|\psi\|_\infty. \tag{4.32}$$

Now similar arguments as in Step 2 of the proof of Proposition 4.3 with $[0, t^\star)$ replaced by $[0, T)$ yield, for $M_{\boldsymbol{z}}$ as in (4.19),

$$\forall\, t \in [0, T) \colon \qquad \|\boldsymbol{z}(t)\| \leq M_{\boldsymbol{z}}. \tag{4.33}$$

Moreover note that identical arguments as in Step 2 of the proof of Proposition 4.3 yield, for M as in (4.20),

$$\text{for a.a. } t \in [0, T) : \ -M - \gamma_0 u(t) \leq \dot{e}(t) \leq M - \gamma_0 u(t). \tag{4.34}$$

This completes Step 2. For the following define

$$\underline{\varsigma} := \inf_{t \geq 0} \varsigma(t) \qquad \text{and} \qquad \lambda := \inf_{t \geq 0} \psi(t). \tag{4.35}$$

Step 3: For M as in (4.20) and $\underline{\varsigma}, \lambda$ as in (4.35), it is shown that there exists a positive

$$\varepsilon \leq \min \left\{ \frac{\lambda}{2},\ \psi(0) - |e(0)|,\ \frac{|\gamma_0| \underline{\varsigma}\, \lambda}{2(M + \|\dot{\psi}\|_\infty)} \right\} \tag{4.36}$$

such that $\psi(t) - |e(t)| \geq \varepsilon$ for all $t \in [0, T)$.

Seeking a contradiction, assume there exists

$$t_1 := \min\{\, t \in [0, T) \quad | \quad \psi(t) - |e(t)| < \varepsilon \,\}. \tag{4.37}$$

Then, by continuity of $\psi(\cdot) - |e(\cdot)|$ on $[0, T)$, there exists

$$t_0 := \max\{\, t \in [0, t_1) \quad | \quad \psi(t) - |e(t)| = \varepsilon \,\}. \tag{4.38}$$

Furthermore, for $\varepsilon > 0$ as in (4.36) and λ as in (4.35), the following holds

$$\forall\, t \in [t_0,\, t_1]\colon \qquad |e(t)| \geq \psi(t) - \varepsilon \overset{(4.36)}{\geq} \lambda - \lambda/2 = \lambda/2 \tag{4.39}$$

and hence $\operatorname{sign} e(\cdot)$ is constant on $[t_0,\, t_1] \subset [0, T)$. Consider only the case $e(\cdot)$ on $[t_0,\, t_1]$, the other case follows analogously. Then inserting (4.24) into (4.34) yields

$$\text{for a.a. } t \in [t_0,\, t_1]\colon \quad \dot{e}(t) \leq M - |\gamma_0| \frac{\varsigma(t)}{\psi(t) - |e(t)|} e(t) \overset{(4.39)}{\leq} M - |\gamma_0| \frac{\varsigma}{\varepsilon} \frac{\lambda}{2} \overset{(4.36)}{\leq} -\|\dot{\psi}\|_\infty.$$

Integration and recalling '$\psi(t) \geq \psi(t_0) - \|\dot{\psi}\|_\infty (t - t_0)$ for all $t \in [t_0, t_1]$' (see properties of $\mathcal{B}_1$) gives

$$\forall\, t \in [t_0,\, t_1]\colon \qquad e(t) - e(t_0) = \int_{t_0}^{t} \dot{e}(\tau)\, \mathrm{d}\tau \;\leq -\|\dot{\psi}\|_\infty (t - t_0) \leq \psi(t) - \psi(t_0)$$

with which the contradiction follows

$$\varepsilon = \psi(t_0) - e(t_0) \leq \psi(t_1) - e(t_1) < \varepsilon.$$

This completes Step 3.

Step 4: It is shown that Assertions (ii), (iii) and (iv) hold true.
At first Assertion (ii) will be shown. For ε as in (4.36) and $M_{\boldsymbol{z}}$ as in (4.19) define the compact set

$$\widetilde{\mathfrak{C}} := \left\{\; (t, e, \boldsymbol{z}) \in [0, T] \times \mathbb{R} \times \mathbb{R}^{n-1} \;\middle|\; |e| \leq \psi(t) - \varepsilon \;\wedge\; \|\boldsymbol{z}\| \leq M_{\boldsymbol{z}} \;\right\} \tag{4.40}$$

and let $\mathcal{D}$ be as in Step 1. If $T < \infty$ then $\widetilde{\mathfrak{C}} \subset \mathcal{D}$ is a compact subset of $\mathcal{D}$ which contains the whole graph of the solution $t \mapsto (e(t), \boldsymbol{z}(t))$, which contradicts maximality of the solution. Hence $T = \infty$ and Assertion (ii) is shown. Now, Assertion (iii) follows from Step 3 with $\varepsilon > 0$ as in (4.36). Furthermore, Step 4 ensures that $k(\cdot)$ is uniformly bounded on $\mathbb{R}_{\geq 0}$ and from (4.32) it follows that $u(\cdot) = k(\cdot)e(\cdot)$ is uniformly bounded on $\mathbb{R}_{\geq 0}$. This shows Assertion (iv) and completes the proof. □

4.3.3.1 Minimal future distance

As already noted, gain adaption in (4.24) is inversely proportional to the actual or "vertical" distance $\psi(t) - |e(t)|$. Since $\psi(\cdot)$ is known a priori (it is chosen by the control designer), the (minimal) future distance

$$d_F\colon\; \mathbb{R}_{\geq 0} \times \mathbb{R} \to \mathbb{R}_{>0}, \qquad (t, e) \mapsto d_F(t, e) := \min_{t_F \geq 0} \sqrt{\big(\psi(t_F) - |e|\big)^2 + \big(t_F - t\big)^2} \tag{4.41}$$

may be evaluated. Note that $d_F(t, e(t)) \leq \psi(t) - |e(t)|$ and $t_F \in [t,\, t + \psi(t) - |e(t)|)$ for all $t \geq 0$. In [101] it is shown that

$$k(t) = \frac{\varsigma(t)}{d_F(t, e(t))} \qquad \text{where} \qquad e(t) = y_{\text{ref}}(t) - y(t) \tag{4.42}$$

is also feasible. The gain adaption in (4.42) might be advantageous, since the future prescribed transient accuracy $\psi(t_F)$ for $t_F \geq t$ is already considered at actual time $t \geq 0$. Concerning implementation, a computational effective numerical approximation of (4.41) must be found. This issue is out of the scope of this thesis. In [101] or [68, 69] several numerical algorithms to approximate the future distance (4.41) are proposed. A comparison can be found in [167, p. 731-741]. For the remainder of this thesis, minimal future distance evaluation is not considered.

4.3.3.2 Gain scaling

The gain adaption in (4.24) is similar to (4.3) but, in addition, allows for gain scaling. Gain scaling was introduced in [101] as distance scaling and is helpful for implementation: it increases the degrees of freedom for controller tuning. For example, adequate gain scaling permits (independently of boundary design):

(i) to specify a minimal gain permanently, i.e.

$$\forall\, (t,\, e) \in \mathcal{F}_\psi\colon \qquad k(t) = \frac{\varsigma(t)}{\psi(t) - |e|} \geq \frac{\inf_{t\geq 0} \varsigma(t)}{\|\psi\|_\infty} > 0; \tag{4.43}$$

(ii) to fix an (arbitrary) initial control action, i.e.

$$|u(0)| = \frac{\varsigma(0)}{\psi(0) - |e(0)|}|e(0)|,$$

e.g. to accelerate (or decelerate) the closed-loop system response at startup.

Simulation results are presented in Section 4.3.3.4. More illustrative examples are discussed in e.g. [68, 69, 99] or [167, Sections 17.2-17.4]. In Section 5.2.2 the funnel controller (4.24) will be applied for speed control of 1MS and 2MS.

4.3.3.3 Asymmetric funnel

For the set-point tracking problem (see Fig. 4.1) with step magnitude $\hat{y}_{\text{ref}} > 0$ and maximum overshoot $\Delta^{os}_{\text{ref}} \geq 0$, it was already noted that, in general, motion control objective (co_2) cannot be included in boundary design. In particular, since $\psi(0) > |e(0)|$ must hold, a too large initial error $|e(0)| > \hat{y}_{\text{ref}}\Delta^{os}_{\text{ref}}$ precludes appropriate boundary design assuring $y(\cdot) \leq \hat{y}_{\text{ref}}\Delta^{os}_{\text{ref}}$. There might exist $t \geq 0$ such that $y(t) > \hat{y}_{\text{ref}}\Delta^{os}_{\text{ref}}$. If an asymmetric funnel is admitted and $\Delta^{os}_{\text{ref}} > 0$, then funnel control can assure motion control objective (co_2) independently of the initial error. For the design of an asymmetric funnel, two (differing) limiting function must be introduced (see Fig. 4.4). Denote "upper" and "lower" limiting function by $\psi^+(\cdot)$ and $\psi^-(\cdot)$, respectively, and assume that $\psi^+(\cdot)$, $-\psi^-(\cdot) \in \mathcal{B}_1$, then the asymmetric performance funnel is defined by

$$\mathcal{F}_{(\psi^+,\psi^-)} := \left\{\, (t, e) \in \mathbb{R}_{\geq 0} \times \mathbb{R} \quad | \quad \psi^-(t) < e < \psi^+(t) \,\right\}. \tag{4.44}$$

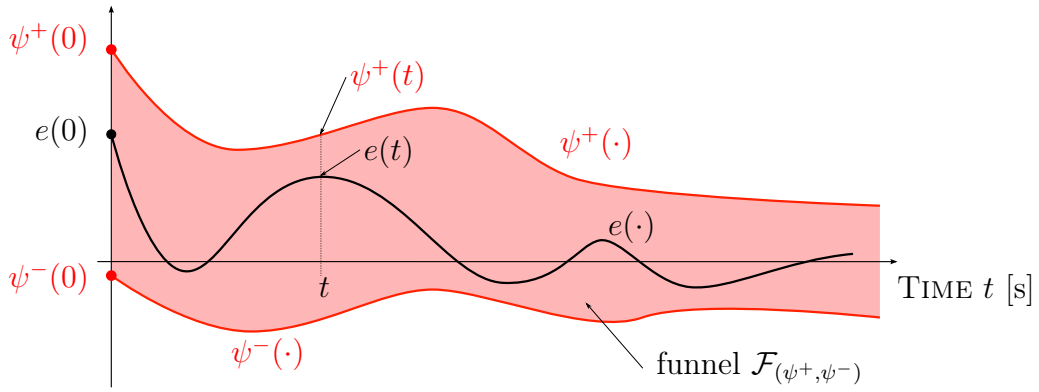

Figure 4.4: *Illustration of asymmetric performance funnel $\mathcal{F}_{(\psi^+,\psi^-)}$ with "upper" and "lower" limiting functions $\psi^+(\cdot)$ and $\psi^-(\cdot)$ and exemplary error evolution $e(\cdot)$.*

Moreover, by introducing the function

$$u_{AS}\colon \mathcal{F}_{(\psi^+,\psi^-)} \to \mathbb{R}, \qquad (t,e) \mapsto u_{AS}(t,e) := \begin{cases} \dfrac{e}{\psi^+(t)-e} & , e \geq 0 \\ \dfrac{e}{e-\psi^-(t)} & , e < 0 \end{cases} \tag{4.45}$$

an asymmetric funnel controller for system class $\mathcal{S}_1$ can be proposed.

Theorem 4.6. *Consider a system of class $\mathcal{S}_1$ described by (1.36). Then, for arbitrary limiting functions $\psi^+(\cdot)$, $-\psi^-(\cdot) \in \mathcal{B}_1$, gain scaling function $\varsigma(\cdot) \in \mathcal{B}_1$, reference $y_{\mathrm{ref}}(\cdot) \in \mathcal{W}^{1,\infty}(\mathbb{R}_{\geq 0};\mathbb{R})$ and initial trajectory $\boldsymbol{x}^0(\cdot) \in \mathcal{C}([-h,0];\mathbb{R}^n)$ satisfying*

$$\psi^-(0) < y_{\mathrm{ref}}(0) - \boldsymbol{c}^\top \boldsymbol{x}^0(0) < \psi^+(0), \tag{4.46}$$

the "asymmetric" funnel controller

$$u(t) = \operatorname{sign}(\boldsymbol{c}^\top \boldsymbol{b})\varsigma(t)\, u_{AS}\big(t, e(t)\big) \text{ with } e(t) = y_{\mathrm{ref}}(t) - y(t) \text{ and } u_{AS}(\cdot,\cdot) \text{ as in (4.45)}, \tag{4.47}$$

applied to (1.36) yields a closed-loop initial-value problem with the properties (i), (ii) and (iv) of Theorem 4.4 and (iii) the tracking error is uniformly bounded away from the limiting functions, i.e.

$$\exists\, \varepsilon > 0\ \forall\, t \geq 0: \qquad \psi^-(t) + \varepsilon < e(t) < \psi^+(t) - \varepsilon.$$

Clearly, for adequate funnel design, Theorem 4.6 assures control objectives (co_1)-(co_3) and hence motion control objectives (mco_1), (mco_3) and (mco_4) may be accomplished. Moreover, for given maximum overshoot $\Delta^{os}_{\mathrm{ref}} > 0$ and positive (or negative) reference step (1.2) with $\hat{y}_{\mathrm{ref}} > 0$ (or $\hat{y}_{\mathrm{ref}} < 0$), the choice $\psi^-(t) \geq -\hat{y}_{\mathrm{ref}}\Delta^{os}_{\mathrm{ref}}$ (or $\psi^+(t) \leq -\hat{y}_{\mathrm{ref}}\Delta^{os}_{\mathrm{ref}}$) guarantees that motion control objective (mco_2) is met, i.e. $\Delta^{os}_{y(\cdot)} \leq \Delta^{os}_{\mathrm{ref}}$. Simulations are performed in Section 4.3.3.4. In [70] an asymmetric funnel in combination with gain scaling is introduced for speed control of a flexible servos-system to avoid overshoots in the closed-loop system response.

Proof of Theorem 4.6.
The proof is similar to the proof of Theorem 4.4, only the essential changes are presented. It suffices to consider system (1.36) in the form (3.7).

Step 1: It is shown that Assertion (i) holds true, i.e. existence of a maximally extended solution. Extend $\varsigma(\cdot)$ and $y_{\mathrm{ref}}(\cdot)$ to $[-h,0)$ such that (4.25) and

$$\forall\, t \in [-h,0]\colon \qquad \psi^-(|t|) < y_{\mathrm{ref}}(t) - \boldsymbol{c}^\top \boldsymbol{x}^0(t) < \psi^+(|t|)$$

hold. This is feasible since $\psi^+(\cdot)$, $-\psi^-(\cdot) \in \mathcal{B}_1$ and $y_{\mathrm{ref}}(\cdot)$ are continuous, respectively. For $\mathcal{F}_{(\psi^+,\psi^-)}$ as in (4.44), define the non-empty and open set

$$\mathcal{D} := \left\{ (\tau, \mu, \boldsymbol{\xi}) \in \mathbb{R} \times \mathbb{R} \times \mathbb{R}^{n-1} \;\middle|\; (|\tau|, \mu) \in \mathcal{F}_{(\psi^+,\psi^-)} \right\}$$

and the function

$$\begin{aligned} \boldsymbol{f}\colon\ [-h,\infty) \times \mathcal{D} \times \mathbb{R}^m \ &\to\ \mathbb{R} \times \mathbb{R} \times \mathbb{R}^{n-1}, \\ (t, (\tau, \mu, \boldsymbol{\xi}), \boldsymbol{w}) \ &\mapsto\ \begin{pmatrix} 1 \\ a_1\left(\mu - y_{\mathrm{ref}}(t)\right) + \dot{y}_{\mathrm{ref}}(t) - |\gamma_0|\varsigma(t) u_{AS}(|\tau|,\mu) - \gamma_0 u_d(t) \\ -\boldsymbol{a}_2^\top \boldsymbol{\xi} - \boldsymbol{c}^\top \boldsymbol{B}_{\mathfrak{T}}\left(\boldsymbol{w} + \boldsymbol{d}(t)\right) \\ \boldsymbol{a}_3\left(y_{\mathrm{ref}}(t) - \mu\right) + \boldsymbol{A}_4 \boldsymbol{\xi} + \boldsymbol{N} \boldsymbol{B}_{\mathfrak{T}}\left(\boldsymbol{w} + \boldsymbol{d}(t)\right) \end{pmatrix}. \end{aligned}$$

Now, for $\hat{\mathfrak{T}}$ as in (4.28) and by introducing $\tau\colon [-h,\infty) \to \mathbb{R},\ t \mapsto t$, $\hat{\boldsymbol{x}} := (\tau, (e, \boldsymbol{z})$ and $\tau^0 := \tau|_{[-h,0]}$, the initial-value problem (3.7), (4.47) may be written in the form (4.29). Note that $u_{AS}(t,0) = 0$ for all $t \geq 0$ and so $u_{AS}(\cdot,\cdot)$ is locally Lipschitz continuous on $\mathcal{F}_{(\psi^+,\psi^-)}$. Moreover, since $-\psi^-(\cdot) \in \mathcal{B}_1$ it follows that $\psi^-(t) < 0$ for all $t \geq 0$ and so, for every compact $\mathfrak{C} \subset \mathcal{D} \times \mathbb{R}^m$, there exists $M_{\mathfrak{C}}, m_{\mathfrak{C}} > 0$ such that $\|((\tau,\mu,\boldsymbol{\xi}),\boldsymbol{w})\| \leq M_{\mathfrak{C}}$ and $\min\{\psi^+(|\tau|)-\mu,\ \mu-\psi^-(|\tau|)\} \geq m_{\mathfrak{C}}$ for all $((\tau,\mu,\boldsymbol{\xi}),\boldsymbol{w}) \in \mathfrak{C}$, respectively. Now identical arguments as in Step 1 of Theorem 4.4 show that (4.31) holds and that $\boldsymbol{f}(\cdot,\cdot,\cdot)$ is a Carathéodory function. Hence there exists a maximally extended solution $\hat{\boldsymbol{x}} : [-h,T) \to \mathbb{R} \times \mathbb{R}^n$ of the initial-value problem (4.29) with $\hat{\boldsymbol{x}}([0,T)) \in \mathcal{D}$, $T \in (0,\infty]$, where $(e,\boldsymbol{z}) : [-h,T) \to \mathbb{R} \times \mathbb{R}^{n-1}$ solves the closed-loop initial-value problem (3.7), (4.47) for almost all $t \in [0,T)$.

Step 2: It is shown that $\boldsymbol{z}(\cdot)$ is bounded on $[0,T)$ and an essential inequality holds true. Define

$$\varsigma := \inf_{t\geq 0} \varsigma(t) \qquad \text{and} \qquad \lambda := \min\left\{ \inf_{t\geq 0} \psi^+(t),\ \inf_{t\geq 0} -\psi^-(t) \right\} \tag{4.48}$$

and (by abuse of notation)

$$\|\psi\|_\infty := \max\{\|\psi^-\|_\infty,\ \|\psi^+\|_\infty\} \qquad \text{and} \qquad \|\dot{\psi}\|_\infty := \max\{\|\dot{\psi^-}\|_\infty,\ \|\dot{\psi^+}\|_\infty\}. \tag{4.49}$$

In view of Step 1, $e(\cdot)$ is continuous on $[0,T)$ and the following holds

$$\forall\, t \in [0,T)\colon \qquad \|\psi^-\|_\infty \leq \psi^-(t) < e(t) < \psi^+(t) \leq \|\psi^+\|_\infty, \tag{4.50}$$

hence, for $\|\psi\|_\infty$ as in (4.49), $M_{\boldsymbol{z}}$ as in (4.19) and M as in (4.20), the inequalities (4.33) and (4.34) hold true, respectively. This completes Step 2.

Step 3: For M as in (4.20), ς, λ as in (4.48) and $\|\dot{\psi}\|_\infty$ as in (4.49), it is shown that there exists a positive

$$\varepsilon \leq \min\left\{\frac{\lambda}{2},\ \psi^+(0) - e(0),\ e(0) - \psi^-(0),\ \frac{|\gamma_0|\varsigma\,\lambda}{2(M + \|\dot{\psi}\|_\infty)}\right\} \tag{4.51}$$

such that $\psi^-(t) + \varepsilon \leq e(t) \leq \psi^+(t) - \varepsilon$ for all $t \in [0, T)$.

Seeking a contradiction, assume there exists

$$t_1^+ := \min\{\, t \in [0,T) \mid \psi^+(t) - e(t) < \varepsilon \,\} \quad \text{or} \quad t_1^- := \min\{\, t \in [0,T) \mid e(t) - \psi^-(t) < \varepsilon \,\}.$$

Then a case-by-case analysis and invoking similar arguments as in Step 3 of the proof of Theorem 4.4 prove the claim of Step 3. The details are omitted.

Step 4: It is shown that Assertions (ii), (iii) and (iv) hold true.
For ε as in (4.51) and $M_{\boldsymbol{z}}$ as in (4.19), replace $\tilde{\mathfrak{C}}$ in (4.40) by

$$\tilde{\mathfrak{C}} := \left\{\ (t, e, \boldsymbol{z}) \in [0,T] \times \mathbb{R} \times \mathbb{R}^{n-1} \ \middle|\ \psi^-(t) + \varepsilon \leq e \leq \psi^+(t) - \varepsilon \ \wedge\ \|\boldsymbol{z}\| \leq M_{\boldsymbol{z}}\ \right\},$$

then identical arguments as in Step 4 of the proof of Theorem 4.4 show that the claim of Step 4 holds true. This completes the proof. □

4.3.3.4 Simulations

In this section, the funnel controller (4.24) with and without scaling (i.e. $\varsigma(\cdot) = 1$) and the asymmetric funnel controller (4.47) are applied to the following third order system

$$F(s) = \frac{(1 + 0.5\,s)\,(1 + 0.1\,s)}{s^3 + 1}. \tag{4.52}$$

The system has relative degree $r = 1$ and positive high-frequency gain $\gamma_0 = \lim_{s\to\infty} s\,F(s) = 0.05$. It is minimum-phase with transmission zeros $z_1 = -10$ [1/s] and $z_2 = -2$ [1/s]. Hence the system is element of class $\mathcal{S}_1^{\text{lin}} \subset \mathcal{S}_1$ and application of the funnel controllers is admissible.

Control task is the set-point tracking of $y_{\text{ref}}(\cdot) = \hat{y}_{\text{ref}} = 1$ on $[0, 5]$ [s]. The control objective is formulated in terms of maximum rise time $t^r_{\text{ref},0.8} = 1.0$ [s] and maximum settling time $t^s_{\text{ref},0.1} = 2.0$ [s]. In addition, the asymmetric funnel controller (4.47) must guarantee a maximum overshoot $\Delta^{os}_{\text{ref}} = 0.1$.

The "symmetric" funnel controllers (4.24) with and without scaling are equipped with boundary $\psi(\cdot) = \psi_E(\cdot)$ as in (4.8), respectively. For the asymmetric funnel controller (4.47), upper and lower limiting function are chosen as follows

$$\forall\, t \geq 0\colon \qquad \psi^+(t) = \psi_E(t) \qquad \text{and} \qquad \psi^-(t) = -\min\{\psi_E(t),\, \hat{y}_{\text{ref}}\Delta^{os}_{\text{ref}}\}.$$

Gain scaling is given by $\varsigma(\cdot) = 10\,\psi(\cdot) = 10\,\psi^+(\cdot)$. Exponential boundary $\psi_E(\cdot)$ as in (4.8) is parametrized by $\Lambda = 2$, $\lambda = 0.05$ and $T_E = 0.39$ [s].

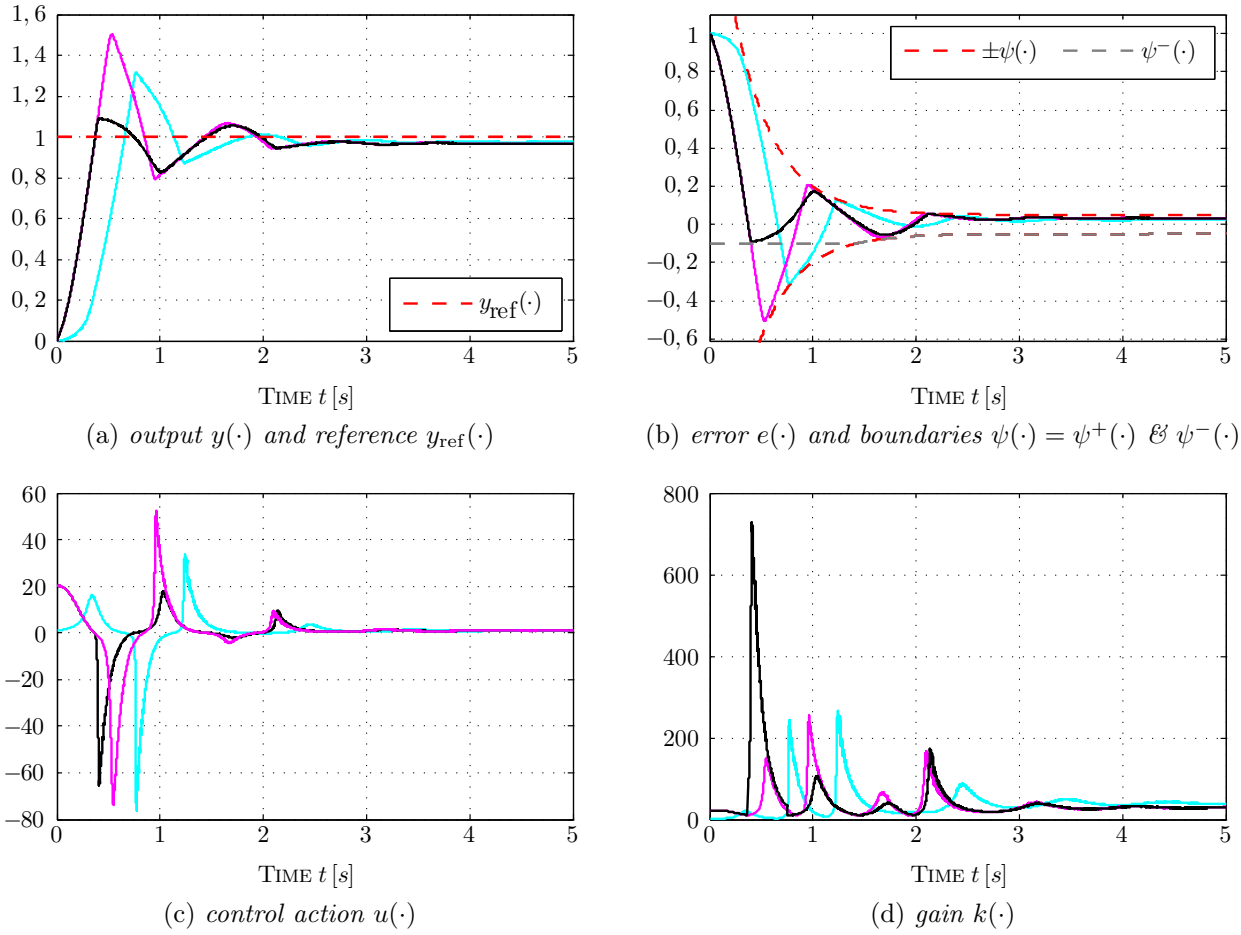

(a) *output* $y(\cdot)$ *and reference* $y_{\text{ref}}(\cdot)$

(b) *error* $e(\cdot)$ *and boundaries* $\psi(\cdot) = \psi^+(\cdot)$ *&* $\psi^-(\cdot)$

(c) *control action* $u(\cdot)$

(d) *gain* $k(\cdot)$

Figure 4.5: *Simulation results for closed-loop systems* ——(4.52), (4.24) *without scaling (i.e.* $\varsigma(\cdot) = 1$*),* ——(4.52), (4.24) *with scaling* $\varsigma(\cdot) = 10\,\psi(\cdot)$ *and* ——(4.52), (4.47) *with scaling* $\varsigma(\cdot) = 10\,\psi^+(\cdot)$.

The control-loops are implemented in Matlab/Simulink using solver `ode4 (Runge-Kutta)` with (fixed) step size 10^{-5} [s]. Simulation results for the closed-loop systems ——(4.52), (4.24) without scaling (i.e. $\varsigma(\cdot) = 1$), ——(4.52), (4.24) with scaling $\varsigma(\cdot) = 10\,\psi(\cdot)$ and ——(4.52), (4.47) with scaling $\varsigma(\cdot) = 10\,\psi^+(\cdot)$ are depicted in Fig. 4.5.

All closed-loop systems accomplish $t^r_{y(\cdot),0.8} \leq t^r_{\text{ref},0.8}$ and $t^s_{y(\cdot),0.1} \leq t^s_{\text{ref},0.1}$ (see Fig. 4.5(a)) and each control error $e(\cdot)$ evolves within its prescribed performance funnel (see Fig. 4.5(b)). Due to the asymmetric funnel design, controller (4.47) assures the specified maximum overshoot, whereas the other controllers with and without scaling, by far, exceed the limit (see Fig. 4.5(a), (b)). All three controllers generate a comparable magnitude in control action (see Fig. 4.5(c)), nevertheless, due to the choice of $\psi^-(\cdot)$, the asymmetric controller (4.47) exhibits a huge peak in the control gain (see Fig. 4.5(d)). Due to gain scaling, the controllers ——(4.24) and ——(4.47) generate a larger initial control action than the "unscaled" controller ——(4.24) (see Fig. 4.5(c)). Gain scaling accelerates their closed-loop system response and yields a smaller rise time.

4.3.4 Funnel controller with saturation

In "real world" the actuator limits the available control action. Although Theorem 4.4 ensures a bounded control action, the funnel controller (4.24) might generate control actions by far exceeding the available range. The following theorem gives a sufficient condition for funnel control to work even under actuator saturation. In addition, bounded control input disturbances $u_F\colon \mathbb{R}_{\geq 0} \to \mathbb{R}$ are considered to account e.g. for actuator deviations or feedforward control. The following theorem is similar to the results published in [82, 83]. It is tailored for system class $\mathcal{S}_1$.

Theorem 4.7 (Funnel control with saturation for systems of class $\mathcal{S}_1$)**.**
Consider a system of class $\mathcal{S}_1$ described by (1.36). Then, for arbitrary input disturbance $u_F(\cdot) \in \mathcal{L}^\infty(\mathbb{R}_{\geq 0};\mathbb{R})$, funnel boundary $\psi(\cdot) \in \mathcal{B}_1$, scaling function $\varsigma(\cdot) \in \mathcal{B}_1$, reference $y_{\mathrm{ref}}(\cdot) \in \mathcal{W}^{1,\infty}(\mathbb{R}_{\geq 0};\mathbb{R})$, initial trajectory $\boldsymbol{x}^0(\cdot) \in \mathcal{C}([-h,0];\mathbb{R}^n)$ satisfying (4.10) there exists a feasibility number $u_{\mathrm{feas}} > 0$ such that, for all $\hat{u} \geq u_{\mathrm{feas}}$, the saturated funnel controller

$$\left.\begin{aligned} u(t) &= \operatorname{sign}(\boldsymbol{c}^\top \boldsymbol{b})\, \operatorname{sat}_{\hat{u}}\Big(k(t)\, e(t) + u_F(t)\Big) \qquad \textit{where} \\ k(t) &= \frac{\varsigma(t)}{\psi(t) - |e(t)|} \qquad \textit{and} \qquad e(t) = y_{\mathrm{ref}}(t) - y(t) \end{aligned}\right\} \tag{4.53}$$

applied to (1.36) yields a closed-loop initial-value problem with the properties (i)-(iii) as in Theorem 4.4,

(iv) the gain is uniformly bounded, i.e. $k(\cdot) \in \mathcal{L}^\infty(\mathbb{R}_{\geq 0};\mathbb{R}_{>0})$;

(v) the control action $u(\cdot)$ is unsaturated at some time, i.e.

$$\exists\, t_{us} \geq 0\colon \qquad |u(t_{us})| < \hat{u}$$

(vi) and, if $\varsigma(\cdot)$ is non-increasing, then it remains unsaturated thereafter, i.e.

$$\exists\, t_{us} \geq 0\ \forall t \geq t_{us}\colon \qquad |u(t)| < \hat{u}.$$

A direct consequence of Assertion (vi) of Theorem 4.7 is that the following implication holds

$$\Big[\!\!\Big[\ \forall\, t \geq 0\colon\ |u(t)| < \hat{u}\ \Big]\!\!\Big] \qquad \Longleftrightarrow \qquad \Big[\!\!\Big[\ |e(0)| < \frac{\psi(0)}{\varsigma(0)}\,\frac{\hat{u}}{1+\hat{u}}\ \Big]\!\!\Big].$$

Hence, if the control action is initially not saturated, it will never become saturated. The feasibility number u_{feas} depends on system data, reference, disturbances, funnel design and scaling function; more precisely, for M as in (4.20) and some $\delta > 0$ (arbitrarily small), it is given by

$$u_{\mathrm{feas}} := \big(M + \delta + \|\dot{\psi}\|_\infty\big)/|\gamma_0| > 0. \tag{4.54}$$

Clearly, to verify $\hat{u} \geq u_{\mathrm{feas}}$, rough system knowledge is required which foils the striking advantage of high-gain adaptive control. Nevertheless, Theorem 4.7 underpins applicability of funnel control for plants with saturated actuators. Moreover, at least for low order systems, evaluation of (4.54) is feasible even though the computed value might be conservative (see Section 5.2.2).

Proof of Theorem 4.7.

Step 1: It is shown that Assertion (i) holds true, i.e. existence of a maximally extended solution. It suffices to consider the system (1.36) in the form (3.7). Extend $u_F(\cdot)$, $\varsigma(\cdot)$ and $y_{\mathrm{ref}}(\cdot)$ to $[-h,0)$ such that

$$u_F(\cdot) \in \mathcal{W}^{1,\infty}([-h,\infty);\mathbb{R}),\ \varsigma(\cdot) \in \mathcal{W}^{1,\infty}([-h,\infty);\mathbb{R}_{>0}) \ \text{ and } \ y_{\mathrm{ref}}(\cdot) \in \mathcal{W}^{1,\infty}([-h,\infty);\mathbb{R}),$$

respectively, and furthermore, such that (4.26) holds. Clearly, this is possible since $\psi(\cdot) \in \mathcal{B}_1$ and $y_{\mathrm{ref}}(\cdot)$ are continuous. Let $\mathcal{D}$ and $\hat{\mathfrak{T}}$ be defined as in (4.27) and (4.28), respectively. Introduce the function

$$\begin{aligned} \boldsymbol{f}\colon\ [-h,\infty)\times\mathcal{D}\times\mathbb{R}^m \ &\to\ \mathbb{R}\times\mathbb{R}\times\mathbb{R}^{n-1},\\ (t,(\tau,\mu,\boldsymbol{\xi}),\boldsymbol{w}) \ &\mapsto\ \begin{pmatrix} 1 \\ a_1\left(\mu - y_{\mathrm{ref}}(t)\right) + \dot{y}_{\mathrm{ref}}(t) - |\gamma_0|\operatorname{sat}_{\hat{u}}\left(\frac{\varsigma(t)\,\mu}{\psi(|\tau|)-|\mu|} + u_F(t)\right) - \gamma_0 u_d(t) \\ -\boldsymbol{a}_3^\top\boldsymbol{\xi} - \boldsymbol{c}^\top\boldsymbol{B}_{\mathfrak{T}}\left(\boldsymbol{w}+\boldsymbol{d}(t)\right) \\ \boldsymbol{a}_3\left(y_{\mathrm{ref}}(t)-\mu\right) + \boldsymbol{A}_4\boldsymbol{\xi} + \boldsymbol{N}\boldsymbol{B}_{\mathfrak{T}}\left(\boldsymbol{w}+\boldsymbol{d}(t)\right) \end{pmatrix}. \end{aligned}$$

Then, for $\tau\colon\ [-h,\infty)\to\mathbb{R},\ t\mapsto t$ and $\hat{\boldsymbol{x}} := (\tau,(e,\dot{e}),\boldsymbol{z})$ and writing $\tau^0 := \tau|_{[-h,0]}$, the initial-value problem (3.7), (4.53) may be expressed in the form (4.29). Note that, for $M_{\mathfrak{C}}$ as in (4.30), $u_d(\cdot), y_{\mathrm{ref}}(\cdot) \in \mathcal{L}^\infty([-h,\infty);\,\mathbb{R})$, $\boldsymbol{d}(\cdot) \in \mathcal{L}^\infty([-h,\infty);\,\mathbb{R}^n)$ and $\varsigma(\cdot) \in \mathcal{W}^{1,\infty}\left([-h,\infty),\mathbb{R}_{>0}\right)$, the function $\boldsymbol{f}(\cdot,\cdot,\cdot)$ is a Carathéodory function (see Definition 3.1), since (i) $\boldsymbol{f}(t,\cdot,\cdot)$ is continuous for each fixed $t\in[-h,\infty)$, (ii) for each fixed $((\tau,\mu,\boldsymbol{\xi}),\boldsymbol{w})\in\mathcal{D}\times\mathbb{R}^m$ the function $\boldsymbol{f}(\cdot,(\tau,\mu,\boldsymbol{\xi}),\boldsymbol{w})$ is measurable and (iii) for almost all $t\in[-h,\infty)$ and for all $((\tau,\mu,\boldsymbol{\xi}),\boldsymbol{w})\in\mathfrak{C}$:

$$\begin{aligned} \|\boldsymbol{f}(t,(\tau,\mu,\boldsymbol{\xi}),\boldsymbol{w})\| \overset{(4.30)}{\leq}\ & 1 + \left(|a_1| + \|\boldsymbol{a}_3\|\right)\|y_{\mathrm{ref}}\|_\infty + \|\dot{y}_{\mathrm{ref}}\|_\infty + |\gamma_0|\,\|u_d\|_\infty \\ & + M_{\mathfrak{C}}\left(|a_1| + \|\boldsymbol{a}_2\| + \left(\|\boldsymbol{c}\| + \|\boldsymbol{N}\|\right)\|\boldsymbol{B}_{\mathfrak{T}}\| + \|\boldsymbol{a}_3\| + \|\boldsymbol{A}_4\|\right) \\ & + \left(\|\boldsymbol{c}\| + \|\boldsymbol{N}\|\right)\|\boldsymbol{B}_{\mathfrak{T}}\|\,\|\boldsymbol{d}\|_\infty + |\gamma_0|\hat{u} =: l_{\mathfrak{C}}. \end{aligned}$$

Hence, in view of Theorem 3.2 there exists a solution $\hat{\boldsymbol{x}} : [-h,T)\to\mathbb{R}\times\mathbb{R}^n$ of the initial-value problem (4.29) with $\hat{\boldsymbol{x}}([0,T))\in\mathcal{D}$, $T\in(0,\infty]$. Every solution can be extended to a maximal solution. Moreover, since $\boldsymbol{f}(\cdot,\cdot,\cdot)$ is locally essentially bounded, it follows from Theorem 3.2 that if $T<\infty$ then for every compact set $\widetilde{\mathfrak{C}}\subset\mathcal{D}$, there exists $\tilde{t}\in[0,T)$ such that $\hat{\boldsymbol{x}}(\tilde{t})\notin\widetilde{\mathfrak{C}}$.

For the remainder of the proof, let $\hat{\boldsymbol{x}} := (\tau,e,\boldsymbol{z})\colon [-h,T)\to\mathbb{R}\times\mathbb{R}\times\mathbb{R}^{n-1}$ be a fixed and maximally extended solution of the initial-value problem (4.29) and observe that this implies that $(e,\boldsymbol{z}) : [-h,T)\to\mathbb{R}\times\mathbb{R}^{n-1}$ solves the closed-loop initial-value problem (3.7), (4.24) for almost all $t\in[0,T)$.

Step 2: Some technical preliminaries are introduced.
From Step 1 it follows that $e(\cdot)$ is continuous on $[0,T)$ and evolves within the funnel $\mathcal{F}_\psi$, hence $e(\cdot)$ is bounded on $[0,T)$, i.e. (4.32) holds. Similar arguments as in Step 2 of the proof of Theorem 4.4 yield boundedness of $\boldsymbol{z}(\cdot)$ on $[0,T)$, i.e. (4.33) holds, and, moreover, show that

inequality (4.34) also holds. Inserting (4.53) into (4.34) gives for M as in (4.20)

$$\text{for a.a. } t \in [0,T): \ -M - |\gamma_0| \operatorname{sat}_{\hat{u}}\Big(k(t)e(t)+u_F(t)\Big) \le \dot{e}(t) \le M - |\gamma_0| \operatorname{sat}_{\hat{u}}\Big(k(t)e(t)+u_F(t)\Big). \tag{4.55}$$

Since $\psi(\cdot), \varsigma(\cdot) \in \mathcal{B}_1$ the infima $\underline{\varsigma} > 0$ and $\lambda > 0$ as in (4.35) exist.

Step 3: It is shown that there exists a positive

$$\varepsilon \le \min\big\{\lambda/2,\ \psi(0) - |e(0)|,\ \underline{\varsigma}\,\lambda/\big(2(\hat{u} + \|u_F\|_\infty)\big)\big\} \tag{4.56}$$

where M as in (4.20) and $\underline{\varsigma}, \lambda$ as in (4.35) such that $\psi(t) - |e(t)| \ge \varepsilon$ for all $t \in [0,T)$.

Seeking a contradiction, assume there exists $t_1 \ge 0$ as in (4.37). Clearly, by continuity of $\psi(\cdot) - |e(\cdot)|$ on $[0,T)$ there exists $t_0 < t_1$ as in (4.38) and, in view of (4.39), $\operatorname{sign} e(\cdot)$ is constant on $[t_0,\, t_1] \subset [0,T)$. Consider only the case $e(\cdot) > 0$ on $[t_0,\, t_1]$, the other case follows analogously. Then in view of (4.55), (4.39) and since $\hat{u} \ge u_{\text{feas}}$ by assumption the following holds

$$\text{for a.a. } t \in [t_0,\, t_1]\colon \quad \dot{e}(t) \le M - |\gamma_0| \operatorname{sat}_{\hat{u}}\Big(\frac{\underline{\varsigma}\,\lambda}{2\,\varepsilon} - \|u_F\|_\infty\Big) \overset{(4.56)}{\le} M - |\gamma_0|\hat{u} \overset{(4.54)}{\le} -\|\dot{\psi}\|_\infty - \delta. \tag{4.57}$$

Now identical arguments as in Step 3 of the proof of Theorem 4.4 yield the contradiction which completes Step 3.

Step 4: It is shown that Assertions (ii), (iii) and (iv) hold true.
For ε as in (4.56), identical arguments as in Step 4 of the proof of Theorem 4.4 show Assertion (ii)-(iv), respectively.

Step 5: It is shown that Assertions (v) and (vi) hold true.
Seeking a contradiction, assume that $|u(t)| \ge \hat{u}$ for all $t \ge 0$. Note that this precludes a sign change of $e(\cdot)$ on $\mathbb{R}_{\ge 0}$. Consider only the case $e(t) > 0$ for all $t \ge 0$, the other case follows analogously. Then (4.57) clearly holds on $\mathbb{R}_{\ge 0}$. Since $\delta > 0$ in (4.54) integration yields the contradiction

$$\forall\, t \ge 0\colon \qquad 0 < e(t) = e(0) + \int_0^t \dot{e}(\tau) \overset{(4.57)}{\le} e(0) - \delta\, t,$$

hence there exists $t_{us} \ge 0$ such that $|u(t_{us})| < \hat{u}$ which shows Assertion (v). Now suppose there exists $\hat{t}_1 > t_{us}$ such that $|u(\hat{t}_1)| = \hat{u}$ and, for $\delta > 0$ as in (4.54), choose $\hat{\delta} \in (0, \delta/2]$. By continuity of $u(\cdot)$ on $\mathbb{R}_{\ge 0}$, there exists

$$\hat{t}_0 := \max\{\, t \in [t_{us}, \hat{t}_1) \quad | \quad |u(t)| = \hat{u} - \hat{\delta}/|\gamma_0| \,\}.$$

In view of $\hat{u} \ge u_{\text{feas}} > 0$ the choice of $\hat{\delta}$ precludes a sign change of $e(\cdot)$ on $[\hat{t}_0,\, \hat{t}_1]$. Again consider only the case $\operatorname{sign} e(t) = 1$ for all $t \in [\hat{t}_0,\, \hat{t}_1]$, the other case follows analogously. Then, (4.57) holds with δ replaced by $\delta/2$ which implies $|e(t)| < |e(\hat{t}_0)|$ for all $t \in [\hat{t}_0,\, \hat{t}_1]$. Moreover, since $\varsigma(\cdot)$ is non-increasing it follows that $\varsigma(t) \le \varsigma(\hat{t}_0)$ for all $t \in [\hat{t}_0,\, \hat{t}_1]$. Integration and recalling '$\psi(t) \ge \psi(t_0) - \|\dot{\psi}\|_\infty (t - \hat{t}_0)$ for all $t \in [\hat{t}_0,\, \hat{t}_1]$' (see properties of $\mathcal{B}_1$) yields

$$\forall\, t \in [\hat{t}_0,\, \hat{t}_1]\colon \qquad e(t) - e(\hat{t}_0) \le (-\|\dot{\psi}\|_\infty - \delta/2)(t - \hat{t}_0) < \psi(t) - \psi(\hat{t}_0)$$

whence the contradiction

$$\hat{u} = u(\hat{t}_1) = \frac{\varsigma(\hat{t}_1)|e(\hat{t}_1)|}{\psi(\hat{t}_1) - |e(\hat{t}_1)|} < \frac{\varsigma(\hat{t}_0)|e(\hat{t}_0)|}{\psi(\hat{t}_0) - |e(\hat{t}_0)|} = u(\hat{t}_0) = \hat{u} - \hat{\delta} < \hat{u}.$$

This completes the proof. □

Remark 4.8 (Relaxation of system property ($\mathcal{S}_1$-sp$_3$) of class $\mathcal{S}_1$).
Let $h \geq 0$, $\hat{\mathfrak{T}}\colon \mathcal{C}([-h,\infty);\mathbb{R}) \to \mathcal{L}^\infty_{\mathrm{loc}}([-h,\infty);\mathbb{R}^m)$, $\mathfrak{T}\colon \mathcal{C}([-h,\infty);\mathbb{R}^n) \to \mathcal{L}^\infty_{\mathrm{loc}}([-h,\infty);\mathbb{R}^m)$ and $\hat{\mathfrak{T}}, \mathfrak{T} \in \mathcal{T}$ (see Definition 1.5) and consider a system (1.36) of class $\mathcal{S}_1$. If the operator in (1.36) "only" maps the output, i.e. $\mathfrak{T}\boldsymbol{x} = \hat{\mathfrak{T}}y$ in (1.36), and funnel controller (4.24) (or (4.53)) is applied to the system, then system property ($\mathcal{S}_1$-sp$_3$) in Definition 1.6 may be relaxed as follows: in view of (4.32) in the proof of Theorem 4.4, it follows that

$$\forall\, t \in [0,T)\colon \qquad |y(t)| \leq \psi(t) + \|y_{\mathrm{ref}}\|_\infty,$$

which due to property (op$_2$) of operator class $\mathcal{T}$ implies that there exists $\Delta > 0$ such that $\|(\hat{\mathfrak{T}}y)(t)\| \leq \Delta$ for all $t \in [0,T)$. Replace $M_{\mathfrak{T}}$ by Δ in (4.20). Then it is easy to see that the proof of Theorem 4.4 (or Theorem 4.7) goes through without global boundedness of the operator. Hence presupposition $M_{\mathfrak{T}} < \infty$ in ($\mathcal{S}_1$-sp$_3$) of Definition 1.6 can be dropped: the nonlinear perturbation $\hat{\mathfrak{T}}y$ may grow without bound.

4.4 Relative degree two systems

In this section, funnel control with derivative feedback for systems of class $\mathcal{S}_2$ is developed. At first, a result without derivative feedback is revisited which was introduced in [103] and which achieves tracking with prescribed transient accuracy for systems with arbitrary-but-known relative degree. Due to its complexity and noise sensitivity, this approach seems not reasonable for implementation. In Section 4.4.2, funnel control with derivative feedback is discussed. On the basis of the "original" funnel controller with derivative feedback (introduced in the joint work [72]), a slightly extended and altered controller is proposed. The "modified" funnel controller is easy to tune and simple in structure and allows for a well-damped closed-loop system response. The proposed controller also works under constrained inputs if a feasibility condition is satisfied. In Section 4.4.3, comparative simulations are presented.

4.4.1 Funnel controller with backstepping

In [103] Ilchmann, Ryan and Townsend present funnel control for nonlinear MIMO systems modeled by a functional differential equation with arbitrary-but-known relative degree $r \geq 1$ and possibly unknown but sign definite high-frequency gain. The considered system class comprises finite and infinite dimensional linear systems, nonlinear delay systems and systems with hysteresis. The paper extends and generalizes the results in [102] (there for nonlinearly perturbed LTI MIMO systems).

The proposed controller incorporates a time-varying gain adaption (similar to (4.3)), a Nussbaum-like switching function (online detection of the correct sign of the control action) and a $(r-1)$-th order dynamic compensator (input filter). The system in conjunction with the

filter behaves like a system with (strict) relative degree one. Filter and controller construction emerge from a backstepping procedure, motivated by the intuition of reducing the relative degree to one and then exploiting the intrinsic high-gain property of minimum-phase systems with relative degree one (similar to Ye's approach, see Section 3.5.1). Due to backstepping the controller is recursively defined and yields a complex structure (already for the relative degree two case, see below). It will be illustrated in Section 4.4.3 that this controller is not reasonable for implementation and so the result is not transferred to system class $\mathcal{S}_2$. It is presented for the same system class as introduced in [103]. Ilchmann et al. consider systems of the form (only the SISO case is presented)

$$\left.\begin{aligned} \dot{\boldsymbol{x}}(t) &= \boldsymbol{A}\boldsymbol{x}(t) + \boldsymbol{f}\left(\boldsymbol{p}(t), (\mathfrak{T}y)(t), \boldsymbol{x}(t)\right) + \boldsymbol{b}\,u(t), \\ y(t) &= \boldsymbol{c}^\top \boldsymbol{x}(t), \qquad\qquad \boldsymbol{x}|_{[-h,0]} = \boldsymbol{x}^0(\cdot) \in \mathcal{C}([-h,0];\mathbb{R}^r) \end{aligned}\right\} \tag{4.58}$$

where $h \geq 0$, $l, m \in \mathbb{N}$, $\boldsymbol{p}\colon \mathbb{R}_{\geq 0} \to \mathbb{R}^l$, $\boldsymbol{f}\colon \mathbb{R}^l \times \mathbb{R}^m \times \mathbb{R}^r \to \mathbb{R}^r$, $\mathfrak{T}\colon \mathcal{C}([-h,\infty);\mathbb{R}^r) \to \mathcal{L}^\infty_{\mathrm{loc}}(\mathbb{R}_{\geq 0};\mathbb{R}^m)$ and

$$\boldsymbol{A} = \begin{bmatrix} 0 & 1 & 0 & \cdots & 0 \\ \vdots & \ddots & \ddots & \ddots & \vdots \\ \vdots & \ddots & \ddots & 1 & 0 \\ 0 & \cdots & \cdots & 0 & 1 \\ a_1 & \cdots & \cdots & a_{r-1} & a_r \end{bmatrix} \in \mathbb{R}^{r\times r}, \quad \boldsymbol{b} = \begin{pmatrix} 0 \\ \vdots \\ 0 \\ 0 \\ \gamma_0 \end{pmatrix} \in \mathbb{R}^r \quad \text{and} \quad \boldsymbol{c} = \begin{pmatrix} 1 \\ 0 \\ 0 \\ \vdots \\ 0 \end{pmatrix} \in \mathbb{R}^r \tag{4.59}$$

and impose the following assumptions on system (4.58): (A1) the unperturbed system (i.e. $\boldsymbol{f}(\cdot) = \boldsymbol{0}_r$) has a non-zero high-frequency gain, i.e. $\gamma_0 \neq 0$ and known relative degree $r \geq 1$, (A2) the exogenous disturbance is bounded, i.e. $\boldsymbol{p}(\cdot) \in \mathcal{L}^\infty(\mathbb{R}_{\geq 0};\mathbb{R}^l)$, (A3) the operator $\mathfrak{T}$ is element of class $\mathcal{T}$ and (A4) the function $\boldsymbol{f}\colon \mathbb{R}^l \times \mathbb{R}^m \times \mathbb{R}^r \to \mathbb{R}^r$ is continuous, and for all nonempty compact sets $P \subset \mathbb{R}^l$, $W \subset \mathbb{R}^m$ and $Y \subset \mathbb{R}$, there exists $c_0 = c_0(P, W, Y) > 0$ such that $\|\boldsymbol{f}(\boldsymbol{p}, \boldsymbol{w}, \boldsymbol{x})\| \leq c_0$ for all $(\boldsymbol{p}, \boldsymbol{w}, \boldsymbol{x}) \in P \times W \times \{\boldsymbol{x} \in \mathbb{R}^r \,|\, \boldsymbol{c}^\top \boldsymbol{x} \in Y\}$.

Note that the nonlinear perturbation $\boldsymbol{f}(\cdot,\cdot,\cdot)$ (and its dependence on $\boldsymbol{x}$ in particular) may entail that the relative degree of (4.58) is not defined at some point $\boldsymbol{x}^* \in \mathbb{R}^r$ (in terms of [107, p. 138]). However, in the unperturbed case, system (4.58) is a LTI SISO system and clearly has relative degree $r \geq 1$. Assumption (A4) is essential and constrains the influence of $\boldsymbol{f}(\cdot,\cdot,\cdot)$ on the state derivative in (4.58). In particular, if there exists a continuous function $c_{\boldsymbol{f}}\colon \mathbb{R}^l \times \mathbb{R}^m \times \mathbb{R} \to \mathbb{R}_{\geq 0}$ such that $\|\boldsymbol{f}(\boldsymbol{p}, \boldsymbol{w}, \boldsymbol{x})\| \leq c_{\boldsymbol{f}}(\boldsymbol{p}, \boldsymbol{w}, \boldsymbol{c}^\top \boldsymbol{x})$ for all $(\boldsymbol{p}, \boldsymbol{w}, \boldsymbol{x}) \in \mathbb{R}^l \times \mathbb{R}^m \times \mathbb{R}^r$ then (A4) holds. Loosely speaking, state dependence (third argument) of the function $\boldsymbol{f}(\boldsymbol{p}, \boldsymbol{w}, \cdot)$ is bounded in terms of the output $y(\cdot) = \boldsymbol{c}^\top \boldsymbol{x}(\cdot)$.

System description (4.58) is similar to the form (1.36). The nonlinear functional perturbation, in contrast to system class $\mathcal{S}_2$, is not required to be globally bounded but restricted to output mappings. Certain internal dynamics can be subsumed in the operator mapping $\mathfrak{T}y$ (see Example B.2).

In the following, conform to class $\mathcal{S}_2$, the presentation is restricted to systems of form (4.58) with relative degree two (i.e. $r = 2$) and known sign of the high-frequency gain. Then the Nussbaum-like sign switching in the controller is unnecessary, the filter simplifies to a first order system and the following simplified version of Theorem 5.5 in [103] can be stated.

Theorem 4.9. *Consider a system of form (4.58) with (4.59) satisfying assumptions (A1)-(A4) with relative degree two and known sign of the high-frequency gain $\gamma_0 = \boldsymbol{c}^\top \boldsymbol{A}\boldsymbol{b}$. Then, for arbitrary reference $y_{\mathrm{ref}}(\cdot) \in \mathcal{W}^{1,\infty}(\mathbb{R}_{\geq 0}, \mathbb{R})$, funnel boundary $\psi(\cdot) \in \mathcal{B}_1$, filter parameter $k_F > 0$ and initial trajectory $(\boldsymbol{x}^0, \zeta_1^0) \in \mathcal{C}([-h, 0]; \mathbb{R}^{n+1})$ satisfying $|y_{\mathrm{ref}}(0) - \boldsymbol{c}^\top \boldsymbol{x}^0(0)| < \psi(0)$, the funnel controller with filter*

$$\left.\begin{aligned} \dot{\zeta}_1(t) &= -k_F \zeta_1(t) + u(t), && \zeta_1(0) = \zeta_1^0(0) \\ u(t) &= \operatorname{sign}(\gamma_0)\, k_F\, k(t) e(t) \\ &\quad -k_F\, k(t)^4 \left(e(t)^2 + k(t)^2\right)\left(1 + \zeta_1(t)^2\right)\left(\zeta_1(t) - \operatorname{sign}(\gamma_0) k(t) e(t)\right) && \text{where} \\ k(t) &= \frac{\psi(t)^2}{\psi(t)^2 - e(t)^2} \qquad \text{and} \qquad e(t) = y_{\mathrm{ref}}(t) - y(t). \end{aligned}\right\} \tag{4.60}$$

applied to (4.58) yields a closed-loop initial-value problem with the properties:

(i) there exists a solution $(\boldsymbol{x}, \zeta_1) : [-h, T) \to \mathbb{R}^n \times \mathbb{R}$ which can be maximally extended and $T \in (0, \infty]$;

(ii) the solution is global, i.e. $T = \infty$;

(iii) the tracking error $e(\cdot)$ is uniformly bounded away from the funnel boundary $\psi(\cdot)$, i.e.

$$\exists\, \varepsilon > 0\ \forall\, t \geq 0 : \qquad \psi(t) - |e(t)| \geq \varepsilon;$$

(iv) all signals are bounded, i.e. $(\boldsymbol{x}(\cdot), \zeta_1(\cdot)) \in \mathcal{L}^\infty(\mathbb{R}_{\geq 0}; \mathbb{R}^{n+1})$, $k(\cdot) \in \mathcal{L}^\infty(\mathbb{R}_{\geq 0}; \mathbb{R}_{>0})$ and $u(\cdot) \in \mathcal{L}^\infty(\mathbb{R}_{\geq 0}; \mathbb{R})$.

Proof. see the proof of Theorem 5.5 in [103]. □

Note that the compensator in (4.60) is identical to the filter in (3.37) of Ye's approach (see Section 3.5.1). Moreover, the motivation for funnel controller (4.60) is based on the fact that there exists a similarity transformation (see Lemma 5.1 in [103]) which converts system (4.58) into a form similar to (3.38) which, regarding ζ_1 as (virtual) control input, has relative degree one and is minimum-phase. Thus control action $u(\cdot)$ in (4.60) can be interpreted as follows: the first term represents the "classical" funnel controller for relative degree one systems (scaled by k_F) whereas the second term compensates for the fact of higher relative degree (here two). Unfortunately, the controller gain occurs with $k(t)^7$ in (4.60) which will result in tremendous noise sensitivity (already for small gains larger than one) and so controller (4.60) is unattractive for application in real world (see also simulations in Section 4.4.3).

Remark 4.10 (Design parameters $\psi(\cdot)$, k_F and $\zeta_1^0(0)$)**.**
The funnel controller (4.60) with input filter and output feedback is set up by 3 "design parameters". Funnel boundary $\psi(\cdot) \in \mathcal{B}_1$ allows to account for costumer specifications (e.g. motion control objectives (mco_1), (mco_3) and (mco_4)). The value of $k_F > 0$ [1/s] specifies the cut-off frequency of the filter in (4.60). In [103] no recommendations are provided for filter design. Simulation studies show that the choice of k_F drastically influences the control performance, e.g. the closed-loop system response might exhibit high-frequent oscillations with large overshoot for very large or very small values of k_F. So an intuitive effect could not be deduced. The initial value $\zeta_1^0(0)$ of the filter might be useful to specify an initial control action independently of the initial error, however the choice $\zeta_1^0(0) = 0$ seems most adequate and simple.

4.4.2 Funnel controller with derivative feedback

In the previous section, a funnel controller was presented which works for systems with relative degree two, however due to backstepping and the use of a filter its structure is complex. So the striking simplicity of funnel controller (4.24) (for relative degree one systems) is lost. Moreover, the gain occurs with $k(t)^7$ in the control law which indicates high noise sensitivity.

In [72] funnel control with derivative feedback is introduced which retains a simple controller structure and works for nonlinear systems with relative degree two (and one). Moreover, error *and* error derivative are forced to evolve within a prescribed performance funnel. Based on this original idea, a slightly modified controller will be proposed for systems of class $\mathcal{S}_2$ which allows for easy tuning and overdamped transient behavior (at least for systems similar to the mechatronic systems introduced in Section 1.4). First the extended performance funnel for error and error derivative is presented.

4.4.2.1 Performance funnel

In contrast to the relative degree one case, *two* limiting functions $\psi_0(\cdot)$ and $\psi_1(\cdot)$ are introduced to limit the absolute value $|e(\cdot)|$ of the error and the absolute value $|\dot{e}(\cdot)|$ of the error derivative, respectively (see Fig. 4.6). Goal is to achieve tracking with prescribed transient accuracy for output *and* output derivative. Clearly, both limiting functions should be continuous and have a bounded derivative. System class $\mathcal{S}_2$ precludes "jumps" in error and error derivative. Moreover, in view of implementation, the second time derivative of the error is constrained (e.g. due to actuator saturation). More formerly, the limiting functions $\psi_0(\cdot)$ and $\psi_1(\cdot)$ are chosen from the set

$$\mathcal{B}_2 := \left\{ (\psi_0, \psi_1)\colon \mathbb{R}_{\geq 0} \to \mathbb{R}^2 \;\middle|\; \begin{array}{l} \text{(i) } \forall\, i \in \{0,1\}\ \exists\, c_i > 0\colon\ \psi_i(\cdot) \in \mathcal{W}^{1,\infty}(\mathbb{R}_{\geq 0}, [c_i, \infty)), \\ \text{(ii) } \exists\, \delta > 0 \text{ for a.a. } t \geq 0\colon\ \psi_1(t) \geq -\frac{\mathrm{d}}{\mathrm{d}t}\psi_0(t) + \delta \end{array} \right\} \tag{4.61}$$

and allow to introduce the performance funnel (see Fig. 4.6)

$$\mathcal{F}_{(\psi_0,\psi_1)} := \left\{ (t, e_0, e_1) \in \mathbb{R}_{\geq 0} \times \mathbb{R} \times \mathbb{R} \;\middle|\; |e_0| < \psi_0(t) \quad \text{and} \quad |e_1| < \psi_1(t) \right\} \tag{4.62}$$

with funnel boundary

$$\forall\, t \geq 0\colon \qquad \partial\mathcal{F}_{(\psi_0,\psi_1)}(t) = (\psi_0(t), \psi_1(t)).$$

Condition (i) in (4.61) implies that both limiting functions—i.e. the "subboundary" $\psi_0(\cdot)$ for $e(\cdot)$ and $\psi_1(\cdot)$ for $\dot{e}(\cdot)$—are (absolutely) continuous and differentiable almost everywhere (with essentially bounded derivative). The asymptotic accuracies of the subboundaries (see Fig. 4.6) are given by

$$\lambda_0 := \liminf_{t\to\infty} \psi_0(t) \qquad \text{and} \qquad \lambda_1 := \liminf_{t\to\infty} \psi_1(t),$$

respectively. In most applications non-increasing performance funnels are desirable, however the subboundaries may increase as well. This might be reasonable if, due to large reference changes or sensor calibration/reset, error or error derivative will increase drastically leading to unacceptably large control actions. Condition (ii) in (4.61) is essential: only if an error derivative with $\operatorname{sign}(e(t))\dot{e}(t) < \frac{\mathrm{d}}{\mathrm{d}t}\psi_0(t)$ is admissible, then the error $e(\cdot)$ "can depart" from the boundary $\psi_0(\cdot)$ (see Fig. 4.6).

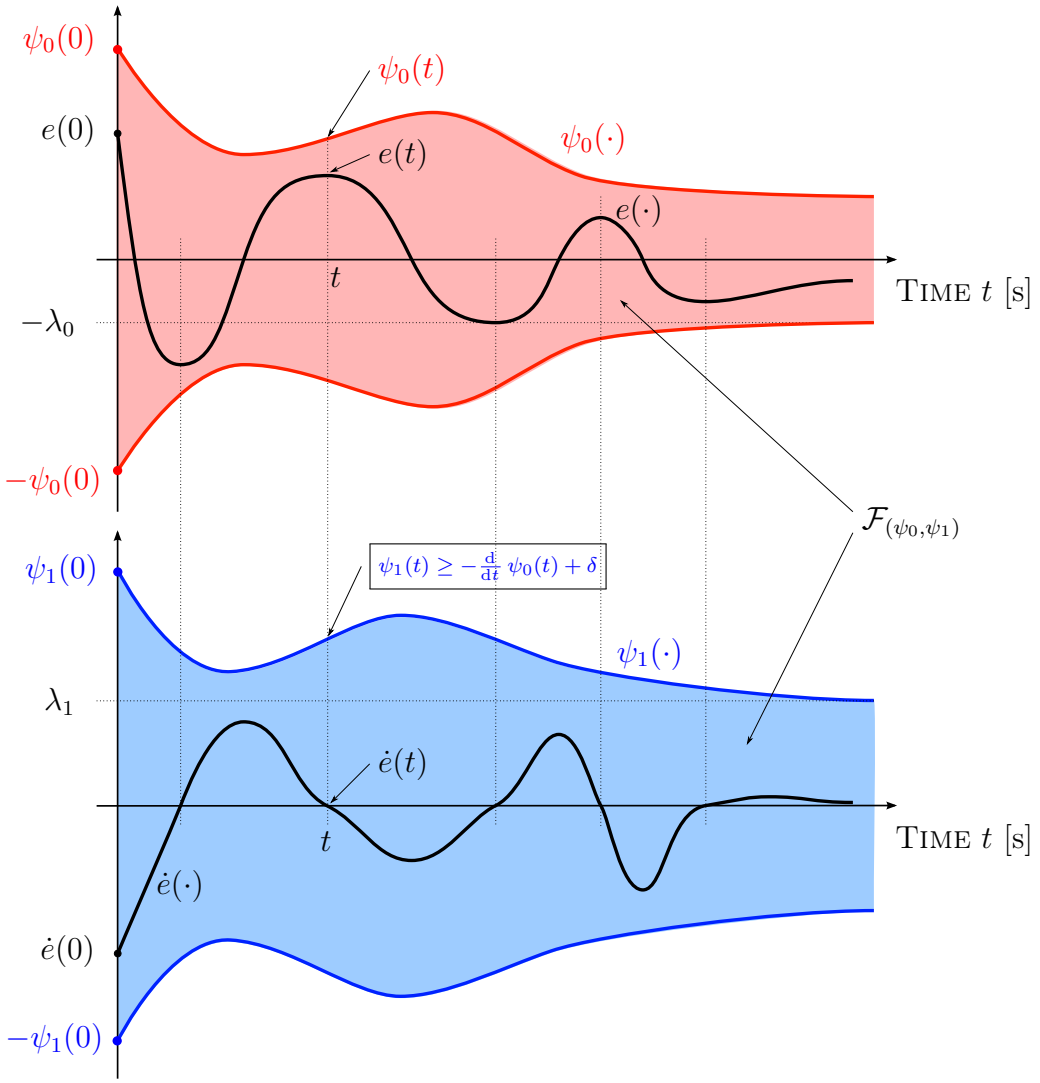

Figure 4.6: *Performance funnel for relative degree two systems: limiting function $\psi_0(\cdot)$ for error $e(\cdot)$ (top) and limiting function $\psi_1(\cdot)$ for error derivative $\dot{e}(\cdot)$ (bottom).*

Similar to the relative degree one case, motion control objectives (mco_1), (mco_3) and (mco_4) can easily be met by adequate boundary design, whereas (mco_2) cannot be accounted for in general (see Section 4.1). Nevertheless, it will be shown (by simulations and measurements) that the proposed funnel controller with derivative feedback allows for a closed-loop system response with (almost) no overshoot, i.e. $\Delta^{os}_{y(\cdot)} \ll 1\%$. Infinite performance funnels (i.e. $\psi_i(t) \to \infty$, $i = 0, 1$ as $t \to 0$) or asymmetric funnels (i.e. $\psi_i^+(t) > 0 > \psi_i^-(t)$, $i = 0, 1$ for all $t \geq 0$) are admissible (see [72] or [121], respectively) but not considered in the remainder of this thesis.

Examples 4.11. *According to the Examples 4.1, two simple funnel boundaries are presented. Let $\Lambda_0 \geq \lambda_0 > 0$, T_L, $T_E > 0$ [s] and $\lambda_1 > 0$ [s], then admissible boundaries are given by*

$$\begin{aligned}(\psi_0,\, \psi_1)\colon \mathbb{R}_{\geq 0} &\to [\lambda_0, \Lambda_0] \times \{1/T_L + \lambda_1\} \\ t &\mapsto (\psi_0(t),\, \psi_1(t)) := (\max\left\{\Lambda_0 - t/T_L,\ \lambda_0\right\},\, 1/T_L + \lambda_1)\end{aligned} \tag{4.63}$$

and

$$(\psi_0,\,\psi_1)\colon \mathbb{R}_{\geq 0} \to (\lambda_0, \Lambda_0] \times (\lambda_1,\, (\Lambda_0-\lambda_0)/T_E]$$
$$t \mapsto (\psi_0(t), \psi_1(t)) := \left((\Lambda_0-\lambda_0)\exp\left(-\frac{t}{T_E}\right)+\lambda_0,\; \frac{\Lambda_0-\lambda_0}{T_E}\exp\left(-\frac{t}{T_E}\right)+\lambda_1 \right). \tag{4.64}$$

Both boundaries are positive, non-increasing and bounded. $(\psi_0,\,\psi_1)$ *in* (4.64) *is actually smooth. The asymptotic accuracies of* (4.63) *and* (4.64) *are given by* $(\lambda_0,\, 1/T_L+\lambda_1)$ *and* $(\lambda_0,\, \lambda_1)$*, respectively. They start at* $(\Lambda_0, 1/T_L+\lambda_1)$ *and* $(\Lambda_0,\, \frac{\Lambda_0-\lambda_0}{T_E}+\lambda_1)$ *and their derivatives are (essentially) bounded by* $(1/T_L,\, 0)$ *and* $\big((\Lambda_0-\lambda_0)/T_E,\, (\Lambda_0-\lambda_0)/T_E^2\big)$*, respectively. By setting* $\delta := \lambda_1$ *and noting that* $\psi_1(t) \geq -\dot{\psi}_0(t)+\delta$ *for (almost) all* $t \geq 0$ *in* (4.63) *and* (4.64)*, respectively, it is easy to see that both boundaries are element of* $\mathcal{B}_2$*.*

4.4.2.2 Funnel controller

For $(\psi_0(\cdot),\, \psi_1(\cdot)) \in \mathcal{B}_2$ and $y_{\mathrm{ref}}(\cdot) \in \mathcal{W}^{2,\infty}(\mathbb{R}_{\geq 0}; \mathbb{R})$, the "original" funnel controller with derivative feedback proposed in [72] has the following form

$$\left.\begin{aligned} u(t) &= \operatorname{sign}(\boldsymbol{c}^\top \boldsymbol{A}\boldsymbol{b})\Big(k_0(t)^2 e(t) + k_1(t)\dot{e}(t)\Big) && \text{where} \\ k_i(t) &= \frac{1}{\psi_i(t) - |e^{(i)}(t)|},\; i \in \{0,1\} \quad \text{and} \quad e(t) &= y_{\mathrm{ref}}(t) - y(t) \end{aligned}\right\} \tag{4.65}$$

and may be applied to systems of form (1.36) being element of class $\mathcal{S}_2$. It guarantees that error $e(\cdot)$ and error derivative $\dot{e}(\cdot)$ are uniformly bounded away from the boundary $(\psi_0(\cdot),\, \psi_1(\cdot))$. Hence both controller gains $k_0(\cdot)$ and $k_1(\cdot)$ and control action $u(\cdot)$ are uniformly bounded (see [72]).

Remark 4.12. *In [72] it has been also shown that the funnel controller* (4.65) *can be applied to minimum-phase LTI SISO systems with relative degree one (i.e. systems of form* (2.45) *element of class* $\mathcal{S}_1^{\mathrm{lin}}$*). However, due to derivative feedback in* (4.65)*, application of* (4.65) *yields an implicit differential equation which necessitates to allow for arbitrary initial values for* $\dot{e}(0)$*, and hence infinite funnel boundaries are required. Moreover, in order to be able to utilize the Implicit Function Theorem the functions* $\psi_0(\cdot)$*,* $\psi_1(\cdot)$ *and* $\dot{y}_{\mathrm{ref}}(\cdot)$ *must be continuously differentiable (see Appendix A.3 in [72]).*

Clearly, control objectives (co_1)-(co_3) are accomplished. Moreover, the funnel controller (4.65) was successfully implemented for position control of a stiff one-mass system. However the control performance is rather disappointing. The closed-loop system response exhibits turbulent oscillations in error, error derivate, gains and control action. In particular, due to measurement noise, the asymptotic accuracy λ_1 of $\psi_1(\cdot)$ must be chosen "large" and so active damping is not feasible by the controller (4.65) (see Fig. 4.3(c)-(f) in [72] or the simulations presented in Section 4.4.3). Since oscillations lead to system wear, ineffective power consumption and possibly to deficient work pieces in machine tools, they are undesirable and should be avoided or damped.

With the goal to achieve a better damped closed-loop system response but retain the nice features and simplicity of the original funnel controller (4.65), the following "modified" funnel

controller is proposed. In addition, conform to the relative degree one case, gain scaling is considered.

Theorem 4.13 (Funnel control with derivative feedback for systems of class $\mathcal{S}_2$)**.**
Consider a system of class $\mathcal{S}_2$ described by (1.36). Then, for arbitrary funnel boundary $(\psi_0(\cdot), \psi_1(\cdot)) \in \mathcal{B}_2$, gain scaling functions $\varsigma_0(\cdot), \varsigma_1(\cdot) \in \mathcal{B}_1$, reference $y_{\mathrm{ref}}(\cdot) \in \mathcal{W}^{2,\infty}(\mathbb{R}_{\geq 0}; \mathbb{R})$ and initial trajectory $\boldsymbol{x}^0(\cdot) \in \mathcal{C}([-h, 0]; \mathbb{R}^n)$ satisfying

$$|y_{\mathrm{ref}}(0) - \boldsymbol{c}^\top \boldsymbol{x}^0(0)| < \psi_0(0) \qquad \text{and} \qquad |\dot{y}_{\mathrm{ref}}(0) - \boldsymbol{c}^\top \boldsymbol{A}\boldsymbol{x}^0(0)| < \psi_1(0), \tag{4.66}$$

the (modified) funnel controller

$$\left.\begin{aligned} u(t) &= \operatorname{sign}(\boldsymbol{c}^\top \boldsymbol{A}\boldsymbol{b})\Big(k_0(t)^2 e(t) + k_0(t) k_1(t) \dot{e}(t)\Big) && \text{where} \\ k_i(t) &= \frac{\varsigma_i(t)}{\psi_i(t) - |e^{(i)}(t)|},\ i \in \{0, 1\} \quad \text{and} \quad e(t) = y_{\mathrm{ref}}(t) - y(t) \end{aligned}\right\} \tag{4.67}$$

applied to (1.36) yields a closed-loop initial-value problem with the properties

(i) there exists a solution $\boldsymbol{x} : [-h, T) \to \mathbb{R}^n$ which can be maximally extended and $T \in (0, \infty]$;

(ii) the solution $\boldsymbol{x}(\cdot)$ does not have finite escape time, i.e. $T = \infty$;

(iii) the signals $e(\cdot)$, $\dot{e}(\cdot)$ are uniformly bounded away from the funnel boundary, i.e.

$$\forall\, i \in \{0, 1\}\ \exists\, \varepsilon_i > 0\ \forall\, t \geq 0 : \qquad \psi_i(t) - |e^{(i)}(t)| \geq \varepsilon_i$$

(iv) control action and control gains are uniformly bounded, i.e. $u(\cdot)$, $k_0(\cdot)$, $k_1(\cdot) \in \mathcal{L}^\infty(\mathbb{R}_{\geq 0}; \mathbb{R})$.

In Section 4.4.3 it will be shown (by comparative simulations) that the modified funnel controller (4.67) allows for active damping and, moreover, if an lower bound on the magnitude of the high-frequency gain is known a priori, overdamped transient behavior may be achieved (at least for a second order system).

Proof of Theorem 4.13.

Step 1: It is shown that Assertion (i) holds true, i.e. existence of a maximally extended solution.
It suffices to consider system (1.36) in the Byrnes-Isidori like form (3.9). Define

$$\forall\, i \in \{0, 1\}: \qquad \varsigma_i := \inf_{t \geq 0} \varsigma_i(t) \quad \text{and} \quad \lambda_i := \inf_{t \geq 0} \psi_i(t) \tag{4.68}$$

and extend $\varsigma_1(\cdot)$, $\varsigma_2(\cdot)$ and $y_{\mathrm{ref}}(\cdot)$ to $[-h, 0)$ such that

$$\varsigma_1(\cdot),\ \varsigma_2(\cdot) \in \mathcal{W}^{1,\infty}([-h, \infty); \mathbb{R}_{>0}) \quad \text{and} \quad y_{\mathrm{ref}}(\cdot) \in \mathcal{W}^{2,\infty}([-h, \infty); \mathbb{R}) \tag{4.69}$$

and furthermore such that

$$\forall\, t \in [-h, 0]: \quad |y_{\mathrm{ref}}(t) - \boldsymbol{c}^\top \boldsymbol{x}^0(t)| < \psi_0(|t|) \quad \text{and} \quad |\dot{y}_{\mathrm{ref}}(t) - \boldsymbol{c}^\top \boldsymbol{A}\boldsymbol{x}^0(t)| < \psi_1(|t|), \tag{4.70}$$

which is possible since (4.66) holds and $y_{\mathrm{ref}}(\cdot)$ is continuous and $(\psi_0(\cdot), \psi_1(\cdot)) \in \mathcal{B}_2$. For $\mathcal{F}_{(\psi_0,\psi_1)}$ as in (4.62), define the non-empty and open set

$$\mathcal{D} := \left\{ (\tau, \boldsymbol{\mu}, \boldsymbol{\xi}) \in \mathbb{R} \times \mathbb{R}^2 \times \mathbb{R}^{n-2} \;\middle|\; (|\tau|, \mu_1, \mu_2) \in \mathcal{F}_{(\psi_0,\psi_1)} \right\}, \tag{4.71}$$

the function

$$\boldsymbol{f} : [-h, \infty) \times \mathcal{D} \times \mathbb{R}^m \to \mathbb{R} \times \mathbb{R}^2 \times \mathbb{R}^{n-2},$$

$$(t, (\tau, \boldsymbol{\mu}, \boldsymbol{\xi}), \boldsymbol{w}) \mapsto \begin{pmatrix} 1 \\ \begin{bmatrix} 0 & 1 \\ a_1 & a_2 \end{bmatrix} \left(\boldsymbol{\mu} - \begin{pmatrix} y_{\mathrm{ref}}(t) \\ \dot{y}_{\mathrm{ref}}(t) \end{pmatrix} \right) - |\gamma_0| \begin{pmatrix} 0 \\ \frac{\varsigma_0(t)^2 \, \mu_1}{(\psi_0(|\tau|) - |\mu_1|)^2} + \frac{\varsigma_0(t)}{\psi_0(|\tau|) - |\mu_1|} \frac{\varsigma_1(t) \, \mu_2}{\psi_1(|\tau|) - |\mu_2|} \end{pmatrix} \\ - \begin{pmatrix} 0 \\ \gamma_0 \end{pmatrix} u_d(t) + \begin{pmatrix} \dot{y}_{\mathrm{ref}}(t) \\ \ddot{y}_{\mathrm{ref}}(t) \end{pmatrix} - \begin{bmatrix} \boldsymbol{0}^\top \\ \boldsymbol{a}_3^\top \end{bmatrix} \boldsymbol{\xi} - \begin{bmatrix} \boldsymbol{0}^\top \\ \boldsymbol{c}^\top \boldsymbol{A} \boldsymbol{B}_{\mathfrak{T}} \end{bmatrix} (\boldsymbol{w} + \boldsymbol{d}(t)) \\ \begin{bmatrix} \boldsymbol{a}_4 & \boldsymbol{0} \end{bmatrix} \left(\begin{pmatrix} y_{\mathrm{ref}}(t) \\ \dot{y}_{\mathrm{ref}}(t) \end{pmatrix} - \boldsymbol{\mu} \right) + \boldsymbol{A}_5 \boldsymbol{\xi} + \boldsymbol{N} \boldsymbol{B}_{\mathfrak{T}} (\boldsymbol{w} + \boldsymbol{d}(t)) \end{pmatrix}$$

and the operator

$$\hat{\mathfrak{T}} : \mathcal{C}([-h, \infty); \mathbb{R} \times \mathbb{R}^n) \to \mathcal{L}^\infty_{\mathrm{loc}}(\mathbb{R}_{\geq 0}; \mathbb{R}^m), \qquad (\hat{\mathfrak{T}}(\tau, \boldsymbol{\mu}, \boldsymbol{\xi}))(t) := (\mathfrak{T}(\boldsymbol{S}^{-1} \begin{pmatrix} y_{\mathrm{ref}} - \mu_1 \\ \dot{y}_{\mathrm{ref}} - \mu_2 \\ \boldsymbol{\xi} \end{pmatrix}))(t). \tag{4.72}$$

Then, for the artifact $\tau \colon [-h, \infty) \to \mathbb{R}$, $t \mapsto t$, $\hat{\boldsymbol{x}} := (\tau, (e, \dot{e}), \boldsymbol{z})$ and by writing $\tau^0 := \tau|_{[-h,0]}$ the initial-value problem (3.9), (4.67) can be written in the form

$$\frac{\mathrm{d}}{\mathrm{d}t} \hat{\boldsymbol{x}}(t) = \boldsymbol{f}(t, \hat{\boldsymbol{x}}(t), (\hat{\mathfrak{T}} \hat{\boldsymbol{x}})(t)), \qquad \hat{\boldsymbol{x}}|_{[-h,0]} = \begin{pmatrix} \tau^0 \\ y_{\mathrm{ref}}|_{[-h,0]} - \boldsymbol{c}^\top \boldsymbol{x}^0 \\ \dot{y}_{\mathrm{ref}}|_{[-h,0]} - \boldsymbol{c}^\top \boldsymbol{A} \boldsymbol{x}^0 \\ \boldsymbol{N} \boldsymbol{x}^0 \end{pmatrix}. \tag{4.73}$$

Choose a compact set $\mathfrak{C} \subset \mathcal{D} \times \mathbb{R}^m$ and note that

$$\begin{aligned} &\exists\, M_{\mathfrak{C}} > 0 \;\forall\, ((\tau, \boldsymbol{\mu}, \boldsymbol{\xi}), \boldsymbol{w}) \in \mathfrak{C} : \quad \|((\tau, \boldsymbol{\mu}, \boldsymbol{\xi}), \boldsymbol{w})\| \leq M_{\mathfrak{C}} \\ &\exists\, m_{\mathfrak{C}} > 0 \;\forall\, ((\tau, \boldsymbol{\mu}, \boldsymbol{\xi}), \boldsymbol{w}) \in \mathfrak{C} : \quad \min\{\psi_0(|\tau|) - |\mu_1|,\ \psi_1(|\tau|) - |\mu_2|\} \geq m_{\mathfrak{C}}. \end{aligned} \tag{4.74}$$

Then, for $u_d(\cdot) \in \mathcal{L}^\infty([-h, \infty); \mathbb{R})$, $\boldsymbol{d}(\cdot) \in \mathcal{L}^\infty([-h, \infty); \mathbb{R}^m)$, $y_{\mathrm{ref}}(\cdot) \in \mathcal{W}^{2,\infty}([-h, \infty); \mathbb{R})$ and $\varsigma_0(\cdot), \varsigma_1(\cdot) \in \mathcal{W}^{1,\infty}([-h, \infty), \mathbb{R}_{>0})$, observe that the function $\boldsymbol{f}(\cdot, \cdot, \cdot)$ has the following properties: (i) $\boldsymbol{f}(t, \cdot, \cdot)$ is continuous for each fixed $t \in [-h, \infty)$, (ii) for each fixed $((\tau, \boldsymbol{\mu}, \boldsymbol{\xi}), \boldsymbol{w}) \in \mathcal{D} \times \mathbb{R}^m$ the function $\boldsymbol{f}(\cdot, (\tau, \boldsymbol{\mu}, \boldsymbol{\xi}), \boldsymbol{w})$ is measurable and (iii) for almost all $t \in [-h, \infty)$ and for

all $((\tau, \boldsymbol{\mu}, \boldsymbol{\xi}), \boldsymbol{w}) \in \mathfrak{C}$ the following holds

$$\begin{aligned}\|\boldsymbol{f}(t,(\tau,\boldsymbol{\mu},\boldsymbol{\xi}),\boldsymbol{w})\| &\overset{(4.74)}{\leq} 1 + \left\|\begin{bmatrix}0 & 1\\ a_1 & a_2\end{bmatrix}\right\| (M_{\mathfrak{C}} + 2\max\{\|y_{\mathrm{ref}}\|_\infty, \|\dot{y}_{\mathrm{ref}}\|_\infty\}) + |\gamma_0|\,\|u_d\|_\infty \\ &\quad + \frac{2|\gamma_0|\,M_{\mathfrak{C}}\,\|\varsigma_0\|_\infty}{m_{\mathfrak{C}}^2}\max\{\|\varsigma_0\|_\infty, \|\varsigma_1\|_\infty\} + \big(\|\boldsymbol{a}_3\| + \|\boldsymbol{a}_4\| + \|\boldsymbol{A}_5\|\big) M_{\mathfrak{C}} \\ &\quad + 2(\max\{\|\dot{y}_{\mathrm{ref}}\|_\infty, \|\ddot{y}_{\mathrm{ref}}\|_\infty\} + \|\boldsymbol{a}_4\|\max\{\|y_{\mathrm{ref}}\|_\infty, \|\dot{y}_{\mathrm{ref}}\|_\infty\}) \\ &\quad + (\|\boldsymbol{c}\|\,\|\boldsymbol{A}\| + \|\boldsymbol{N}\|)\,\|\boldsymbol{B}_{\mathfrak{T}}\|\,(M_{\mathfrak{C}} + \|\boldsymbol{d}\|_\infty) =: l_{\mathfrak{C}}.\end{aligned}$$

Clearly $\boldsymbol{f}(\cdot,\cdot,\cdot)$ is a Carathéodory function (see Definition 3.1) and invoking Theorem 3.2 yields existence of a solution $\hat{\boldsymbol{x}} : [-h, T) \to \mathcal{D}$ of the initial-value problem (4.73) with $\hat{\boldsymbol{x}}([0,T)) \in \mathcal{D}$, $T \in (0, \infty]$. Each solution can be extended to a maximal solution. Moreover $\boldsymbol{f}(\cdot,\cdot,\cdot)$ is essentially bounded, hence if $T < \infty$ then for every compact $\tilde{\mathfrak{C}} \subset \mathcal{D}$, there exists $\tilde{t} \in [0,T)$ such that $\hat{\boldsymbol{x}}(\tilde{t}) \notin \tilde{\mathfrak{C}}$. In the following, let $\hat{\boldsymbol{x}} := (\tau, (e, \dot{e}), \boldsymbol{z}) \colon [-h, T) \to \mathbb{R} \times \mathbb{R}^2 \times \mathbb{R}^{n-2}$ be a fixed and maximally extended solution of the initial-value problem (4.73), where $((e, \dot{e}), \boldsymbol{z}) : [-h, T) \to \mathbb{R}^2 \times \mathbb{R}^{n-2}$ solves the closed-loop initial-value problem (3.9), (4.67) for almost all $t \in [0, T)$.

Step 2: Some technical inequalities are introduced.
In view of Step 1, $e(\cdot)$ and $\dot{e}(\cdot)$ are continuous on $[0,T)$ and evolve within the funnel $\mathcal{F}_{(\psi_0,\psi_1)}$, hence by the properties of $\mathcal{B}_2$, it follows that

$$\forall\, t \in [0,T): \quad |e(t)| < \psi_0(t) \leq \|\psi_0\|_\infty \qquad \wedge \qquad |\dot{e}(t)| < \psi_1(t) \leq \|\psi_1\|_\infty. \tag{4.75}$$

Due to ($\mathcal{S}_2$-sp$_2$) and Lemma 2.12, the matrix $\boldsymbol{A}_5$ is Hurwitz, hence there exists $\boldsymbol{P}_5 = \boldsymbol{P}_5^\top > 0$ such that $\boldsymbol{A}_5^\top \boldsymbol{P}_5 + \boldsymbol{P}_5 \boldsymbol{A}_5 = -\boldsymbol{I}_{n-2}$ is satisfied, i.e. (2.87). Now, define

$$M_{\dot{V}} := \|\boldsymbol{P}_5\| \Big(\|\boldsymbol{a}_4\|\,(\|\psi_0\|_\infty + \|y_{\mathrm{ref}}\|_\infty) + \|\boldsymbol{N}\|\,\|\boldsymbol{B}_{\mathfrak{T}}\|\,(M_{\mathfrak{T}} + \|\boldsymbol{d}\|_\infty)\Big). \tag{4.76}$$

and consider the Lyapunov candidate

$$V : \mathbb{R}^{n-2} \to \mathbb{R}_{\geq 0}, \qquad \boldsymbol{z} \mapsto V(\boldsymbol{z}) := \boldsymbol{z}^\top \boldsymbol{P}_5 \boldsymbol{z} \geq 0.$$

Taking the time derivative of $V(\cdot)$ along the solution of the closed-loop system (3.9), (4.67) gives

$$\begin{aligned}\text{for a.a. } t \in [0,T): \ \frac{\mathrm{d}}{\mathrm{d}t} V(\boldsymbol{z}(t)) &\overset{(2.87),(4.75)}{\leq} -\|\boldsymbol{z}(t)\|^2 + 2\,\|\boldsymbol{z}(t)\|\,\|\boldsymbol{P}_5\| \Big(\|\boldsymbol{a}_4\|\,(\|y_{\mathrm{ref}}\|_\infty + \|\psi_0\|_\infty) \\ &\qquad + \|\boldsymbol{N}\|\,\|\boldsymbol{B}_{\mathfrak{T}}\|\,(M_{\mathfrak{T}} + \|\boldsymbol{d}\|_\infty)\Big) \\ &\overset{(4.76)}{\leq} -\frac{1}{2}\|\boldsymbol{z}(t)\|^2 + 2M_{\dot{V}}^2 \leq -\frac{V(\boldsymbol{z}(t))}{2\,\|\boldsymbol{P}_5\|} + 2M_{\dot{V}}^2\end{aligned}$$

Applying the Bellman-Gronwall Lemma yields

$$\forall\, t \in [0,T): \quad V(\boldsymbol{z}(t)) \leq V(\boldsymbol{z}(0)) + 4\,\|\boldsymbol{P}_5\|\,M_{\dot{V}}^2 \leq \|\boldsymbol{P}_5\|\left(\|\boldsymbol{z}(0)\|^2 + 4\,M_{\dot{V}}^2\right),$$

and hence

$$\forall\, t \in [0,T): \quad \|\boldsymbol{z}(t)\| \le \sqrt{\|\boldsymbol{P}_5\|\,\|\boldsymbol{P}_5^{-1}\|}\sqrt{\|\boldsymbol{z}(0)\|^2 + 4\,M_{\dot V}^2} =: M_{\boldsymbol{z}} \tag{4.77}$$

where $M_{\boldsymbol{z}} \ge 0$. Moreover, invoking the first equation in (3.9) yields

$$\begin{aligned}\text{for a.a. } t \in [0,T): \ \ddot e(t) = a_1\,[e(t) - y_{\mathrm{ref}}(t)] + a_2\,[\dot e(t) - \dot y_{\mathrm{ref}}(t)] + \ddot y_{\mathrm{ref}}(t) - \boldsymbol{a}_3^\top \boldsymbol{z}(t)\\ - \gamma_0(u(t)+u_d(t)) - \boldsymbol{c}^\top \boldsymbol{A}\boldsymbol{B}_{\mathfrak{T}}\left((\mathfrak{T}(\boldsymbol{S}^{-1}\begin{pmatrix} y_{\mathrm{ref}} - e \\ \dot y_{\mathrm{ref}} - \dot e \\ \boldsymbol{z}\end{pmatrix}))(t) + \boldsymbol{d}(t)\right)\end{aligned}$$

and hence, for

$$\begin{aligned}M := |a_1|\big(\|\psi_0\|_\infty + \|y_{\mathrm{ref}}\|_\infty\big) + |a_2|\big(\|\psi_1\|_\infty + \|\dot y_{\mathrm{ref}}\|_\infty\big) + \|\boldsymbol{a}_3\| M_{\boldsymbol{z}}\\ + \|\ddot y_{\mathrm{ref}}\|_\infty + |\gamma_0|\|u_d\|_\infty + \|\boldsymbol{c}\|\ \|\boldsymbol{A}\|\ \|\boldsymbol{B}_{\mathfrak{T}}\|\,(M_{\mathfrak{T}} + \|\boldsymbol{d}\|_\infty) \ge 0\end{aligned} \tag{4.78}$$

with $M_{\boldsymbol{z}}$ as in (4.77), it follows that

$$\text{for a.a. } t \in [0,T): \ -M - \gamma_0 u(t) \le \ddot e(t) \le M - \gamma_0 u(t). \tag{4.79}$$

Step 3: It is shown that $|e(\cdot)|$ is uniformly bounded away from the boundary $\psi_0(\cdot)$; more precisely for positive

$$\begin{aligned}\varepsilon_0 \le \min\Bigg\{ &\tfrac{\lambda_0}{4}, \tfrac{\psi_0(0)-|e(0)|}{2}, \frac{\frac{1}{2}|\gamma_0|\delta_{\varsigma_0}\lambda_0}{2|\gamma_0|\|\varsigma_1\|_\infty\|\psi_1\|_\infty + \sqrt{4|\gamma_0|^2\|\varsigma_1\|_\infty^2\|\psi_1\|_\infty^2 + 2\delta^2\lambda_0|\gamma_0|(M+\|\dot\psi_1\|_\infty)}},\\ &\frac{\frac{1}{2}|\gamma_0|\delta_{\varsigma_0}^2\lambda_0}{2|\gamma_0|\varsigma_0\|\varsigma_1\|_\infty\|\psi_1\|_\infty + \delta\big(\|\psi_1\|_\infty + \|\dot\psi_0\|_\infty\big)^2 + \sqrt{\big(2|\gamma_0|\varsigma_0\|\varsigma_1\|_\infty\|\psi_1\|_\infty + \delta(\|\psi_1\|_\infty + \|\dot\psi_0\|_\infty)^2\big)^2 + 2|\gamma_0|\delta^2\varsigma_0^2\lambda_0 M}}\Bigg\}\end{aligned} \tag{4.80}$$

it holds that $\psi_0(t) - |e(t)| \ge \varepsilon_0$ for all $t \in [0,T)$.

Step 3a: It is shown that for $\varepsilon_0 \in (0, \lambda_0/2)$ the following implication holds on any interval $[t_0,t_1] \subseteq [0,T)$:

$$\begin{aligned}\Big[\!\Big[\ \psi_0(t_0) - |e(t_0)| = 2\varepsilon_0 \ \wedge\ \text{for a.a. } t \in [t_0,t_1]: \ \ddot e(t)\,\operatorname{sign} e(t) \le -(\|\psi_1\|_\infty + \|\dot\psi_0\|_\infty)^2/(2\varepsilon_0)\ \Big]\!\Big]\\ \Longrightarrow \quad \Big[\!\Big[\ \forall\, t \in [t_0,t_1]: \ \psi_0(t) - |e(t)| \ge \varepsilon_0\ \Big]\!\Big].\end{aligned} \tag{4.81}$$

First consider the case

$$\forall\, t \in [t_0,t_1]: \ \psi_0(t) - |e(t)| \le 2\varepsilon_0 \tag{4.82}$$

Then $\lambda_0 > 2\varepsilon_0$ implies that $\operatorname{sign} e(\cdot)$ is constant on $[t_0,t_1]$. Consider only the case $\operatorname{sign} e(\cdot) = 1$, the case $\operatorname{sign} e(\cdot) = -1$ follows analogously. Integrating the inequality $\ddot e(\cdot) \le -\frac{(\|\psi_1\|_\infty + \|\dot\psi_0\|_\infty)^2}{2\varepsilon_0}$ twice yields

$$\forall\, t \in [t_0,t_1]: \quad e(t) \le e(t_0) - \tfrac{(\|\psi_1\|_\infty + \|\dot\psi_0\|_\infty)^2}{4\varepsilon_0}(t-t_0)^2 + \underbrace{\dot e(t_0)}_{\le \|\psi_1\|_\infty}(t-t_0).$$

This combined with '$\psi_0(t) \geq \psi_0(t_0) - \|\dot{\psi}_0\|_\infty (t - t_0)$ for all $t \in [t_0, t_1]$' (see property i) in (4.61)) implies

$$\psi_0(t) - e(t) \geq \underbrace{\psi_0(t_0) - e(t_0)}_{=2\varepsilon_0} - \left((\|\psi_1\|_\infty + \|\dot{\psi}_0\|_\infty)(t - t_0) - \tfrac{(\|\psi_1\|_\infty + \|\dot{\psi}_0\|_\infty)^2}{4\varepsilon_0} (t - t_0)^2 \right).$$

for all $t \in [t_0, t_1]$. The parabola $t \mapsto (\|\psi_1\|_\infty + \|\dot{\psi}_0\|_\infty)(t - t_0) - \frac{(\|\psi_1\|_\infty + \|\dot{\psi}_0\|_\infty)^2}{4\varepsilon_0}(t - t_0)^2$ attains its maximum at $t - t_0 = \frac{2\varepsilon_0}{\|\psi_1\|_\infty + \|\dot{\psi}_0\|_\infty}$ with the maximum value ε_0, hence $\psi_0(t) - e(t) \geq \varepsilon_0$ for all $t \in [t_0, t_1]$. This proves Step 3a in case of (4.82). It remains to consider the case that there exists $t \in [t_0, t_1]$ such that $\psi_0(t) - |e(t)| > 2\varepsilon_0$. Now either $\psi_0(t) - |e(t)| \geq 2\varepsilon_0$ for all $t \in [t_0, t_1]$ in which case the claim of Step 3a holds anyway, or there exists $\hat{t} \in [t_0, t_1]$ such that $\psi_0(\hat{t}) - |e(\hat{t})| < 2\varepsilon_0$. Then, by continuity of $t \mapsto \psi_0(t) - |e(t)|$, one may choose $[\hat{t}_0, \hat{t}_1] \subset [t_0, t_1]$ such that $\hat{t} \in [\hat{t}_0, \hat{t}_1]$ and (4.82) holds for $[t_0, t_1]$ replaced by $[\hat{t}_0, \hat{t}_1]$. Now a contradiction follows as in the first case and the proof of Step 3a is complete.

Step 3b: It is shown that for positive ε_0 as in (4.80) the following implication holds on any interval $[t_0, t_1] \subset [0, T)$:

$$\begin{aligned} &[\![\, \forall\, t \in [t_0, t_1] :\ \text{i)}\ \psi_0(t) - \big|e(t)\big| \leq 2\varepsilon_0\ \wedge\ \text{ii)}\ \dot{e}(t) \operatorname{sign} e(t) \geq -\psi_1(t) + \delta/2 \,]\!] \\ &\qquad \Longrightarrow \quad [\![\, \text{for a.a. } t \in [t_0, t_1] :\ \ddot{e}(t) \operatorname{sign} e(t) \leq -(\|\psi_1\|_\infty + \|\dot{\psi}_0\|_\infty)^2/(2\varepsilon_0) \,]\!]. \end{aligned} \tag{4.83}$$

Due to presupposition i) in (4.83) and $0 < \varepsilon_0 \leq \lambda_0/4$, see (4.80), it follows that

$$\forall\, t \in [t_0, t_1] : \qquad |e\,(t)| \geq \psi_0\,(t) - 2\varepsilon_0 \geq \lambda_0 - \lambda_0/2 = \lambda_0/2 > 0, \tag{4.84}$$

which precludes a sign change of $e(\cdot)$ on $[t_0, t_1]$. Consider only the case $\operatorname{sign} e(\cdot) = 1$, $\operatorname{sign} e(\cdot) = -1$ follows analogously. Inserting (4.67) into (3.9) and invoking inequality (4.79) yields

$$\text{for a.a. } t \in [t_0, t_1] : \quad \ddot{e}(t) \leq M - |\gamma_0| k_0(t)^2 e(t) - |\gamma_0| k_0(t) k_1\,(t)\, \dot{e}(t). \tag{4.85}$$

Furthermore, presupposition i) in (4.83) implies

$$\forall\, t \in [t_0, t_1] : \qquad -k_0\,(t)\,/\varsigma_0 = -\varsigma_0(t)/(\varsigma_0(\psi_0(t) - |e(t)|)) \leq -1/(2\varepsilon_0) \tag{4.86}$$

and presupposition ii) in (4.83) implies, either $\dot{e}(t) \geq -\psi_1(t) + \delta/2 \geq 0$[2] for all $t \in [t_0,\, t_1]$, or $\dot{e}(t) \geq 0\ \vee\ 0 > \dot{e}(t) \geq -\psi_1(t) + \delta/2$ for all $t \in [t_0, t_1]$. Then, in view of (4.75), one obtains

$$\forall\, t \in [t_0, t_1] : \quad -k_0(t) k_1(t) \dot{e}(t) = -k_0(t) \frac{\varsigma_1(t)}{\psi_1(t) - |\dot{e}(t)|} \dot{e}(t) \leq k_0(t) \frac{2}{\delta} \|\varsigma_1\|_\infty \|\psi_1\|_\infty. \tag{4.87}$$

Inserting (4.87) into (4.85) and invoking (4.84) yields

$$\text{for a.a. } t \in [t_0, t_1] : \qquad \ddot{e}(t) \leq M + |\gamma_0| \frac{2}{\delta} \|\varsigma_1\|_\infty \|\psi_1\|_\infty\, k_0\,(t) - |\gamma_0| \frac{\lambda_0}{2}\, k_0\,(t)^2$$

[2] For e.g. $\dot{\psi}_0(t) = \delta$ and $\lambda_1 < \delta/2$, the case $-\psi_1(t) + \delta/2 \geq 0$ for all $t \in [t_0,\, t_1]$ is possible.

To show implication (4.83), due to (4.86), it is sufficient to show that

$$\forall\, t \in [t_0, t_1]: \; M + |\gamma_0|\frac{2}{\delta}\|\varsigma_1\|_\infty\|\psi_1\|_\infty\, k_0\,(t) - |\gamma_0|\frac{\lambda_0}{2}\, k_0\,(t)^2 \leq -\left(\|\psi_1\|_\infty + \|\dot\psi_0\|_\infty\right)^2 k_0(t)/\underline{\varsigma}_0,$$

rewriting gives

$$\underbrace{2\delta M\underline{\varsigma}_0}_{=:c>0} + \underbrace{2\left(2|\gamma_0|\underline{\varsigma}_0\|\varsigma_1\|_\infty\|\psi_1\|_\infty + \delta\left(\|\psi_1\|_\infty + \|\dot\psi_0\|_\infty\right)^2\right)}_{=:b>0} k_0\,(t) - \underbrace{|\gamma_0|\delta\underline{\varsigma}_0\lambda_0}_{=:a>0} k_0\,(t)^2 \leq 0. \quad (4.88)$$

Regard $k_0\,(t)$ as argument of the parabola $p \mapsto -ap^2+bp+c$ with $\frac{\mathrm{d}^2}{\mathrm{d}p^2}\,(-ap^2+bp+c) = -2a < 0$ having maximum $(2|\gamma_0|\underline{\varsigma}_0\|\varsigma_1\|_\infty\|\psi_1\|_\infty + \delta(\|\psi_1\|_\infty + \|\dot\psi_0\|_\infty)^2)^2/\left(|\gamma_0|\delta\underline{\varsigma}_0\lambda_0\right) + 2\delta M\underline{\varsigma}_0 > 0$. Hence for all

$$p \geq \frac{2|\gamma_0|\underline{\varsigma}_0\|\varsigma_1\|_\infty\|\psi_1\|_\infty + \delta\left(\|\psi_1\|_\infty + \|\dot\psi_0\|_\infty\right)^2 + \sqrt{\left(2|\gamma_0|\underline{\varsigma}_0\|\varsigma_1\|_\infty\|\psi_1\|_\infty + \delta(\|\psi_1\|_\infty + \|\dot\psi_0\|_\infty)^2\right)^2 + 2|\gamma_0|\delta^2\underline{\varsigma}_0^2\lambda_0 M}}{|\gamma_0|\delta\underline{\varsigma}_0\lambda_0} > 0$$

inequality (4.88) is fulfilled. This, with the choice of ε_0 as in (4.80), (4.86) and $1/(2\varepsilon_0) \geq p/\underline{\varsigma}_0$, implies (4.83).

Step 3c: It is shown that for $\varepsilon_0 \in (0,\, \lambda_0/2)$ the following implication holds for any $[t_0, t_1] \subset [0, T)$:

$$\begin{aligned}[\![\, \forall\, t \in [t_0, t_1]: \qquad & \dot e(t)\,\operatorname{sign} e(t) \leq -\psi_1(t) + \delta/2 \quad \wedge \quad \psi_0(t) - |e(t)| \leq 2\varepsilon_0 \,]\!] \\ \Longrightarrow \qquad & \left[\!\!\left[\, t \mapsto \psi_0(t) - |e(t)| \text{ is monotonically increasing on } [t_0, t_1] \,\right]\!\!\right] \end{aligned} \quad (4.89)$$

Again, only consider the case $\operatorname{sign} e(\cdot) = 1$, the other case follows analogously. Now, invoking '$\psi_1(t) \geq -\frac{\mathrm{d}}{\mathrm{d}t}\,\psi_0(t) + \delta$ for all $t \geq 0$' (see property (ii) in (4.61)) gives

$$\forall\, t \in (t_0, t_1]: \quad \frac{\mathrm{d}}{\mathrm{d}t}\,\psi_0(t) - \dot e(t) \geq \frac{\mathrm{d}}{\mathrm{d}t}\,\psi_0(t) + \psi_1(t) - \frac{\delta}{2} \geq \delta - \frac{\delta}{2} = \frac{\delta}{2} > 0$$

whence (4.89).

Step 3d: It is shown that for positive ε_0 as in (4.80) the following implication holds for any $t \in [t_0, t_1] \subset [0, T)$:

$$\begin{aligned}[\![\, \forall\, t \in [t_0,\, t_1]: \qquad & \psi_0(t) - |e(t)| \leq 2\,\varepsilon_0 \qquad \wedge \qquad \dot e(t_0)\,\operatorname{sign} e(t_0) = -\psi_1(t_0) + \delta/2 \,]\!] \\ \Longrightarrow \quad & [\![\, \forall\, t \in [t_0,\, t_1]: \qquad \dot e(t)\,\operatorname{sign} e(t) \leq -\psi_1(t) + \delta/2 \,]\!] \end{aligned} \quad (4.90)$$

Again, $\operatorname{sign} e(\cdot)$ is constant on $[t_0, t_1]$ and consider only the case $\operatorname{sign} e(\cdot) = 1$, the other case follows analogously. Seeking a contradiction, assume

$$\exists\, \hat t \in (t_0,\, t_1]: \qquad \dot e(\hat t) > -\psi_1(\hat t) + \delta/2. \quad (4.91)$$

Then, by continuity of $\dot{e}(\cdot)$ and $\psi_1(\cdot)$,

$$\exists\, \hat{t}_0 \in [t_0,\, \hat{t}) \colon\ \dot{e}(\hat{t}_0) = -\psi_1(\hat{t}_0) + \delta/2 \ \text{ and } \ \forall\, t \in [\hat{t}_0, \hat{t}] \colon\ \dot{e}(t) \geq -\psi_1(t) + \delta/2. \tag{4.92}$$

Furthermore, invoking (4.85) with (4.84) and (4.87) and recalling (4.86), i.e. $k_0(t) \geq \varsigma_0/(2\varepsilon_0)$ for all $t \in [\hat{t}_0, \hat{t}] \subseteq [t_0,\, t_1]$ gives

$$\text{for a.a. } t \in [\hat{t}_0, \hat{t}] : \ \ddot{e}(t) \leq M + |\gamma_0| \frac{2}{\delta} \|\varsigma_1\|_\infty \|\psi_1\|_\infty\, k_0\,(t) - |\gamma_0| \frac{\lambda_0}{2}\, k_0\,(t)^2 \overset{(4.80)}{\leq} -\|\dot{\psi}_1\|_\infty \tag{4.93}$$

with which and '$\psi_1(t) \leq \psi_1(\hat{t}_0) + \|\dot{\psi}_1\|_\infty (t - \hat{t}_0)$ for all $t \in [\hat{t}_0, \hat{t}]$' one arrives at the contradiction

$$\delta/2 \overset{(4.91)}{<} \dot{e}(\hat{t}) + \psi_1(\hat{t}) = \dot{e}(\hat{t}_0) + \psi_1(\hat{t}_0) + \int_{\hat{t}_0}^{\hat{t}} (\ddot{e}(s) + \dot{\psi}_1(s))\, \mathrm{d}s \overset{(4.93)}{\leq} \dot{e}(\hat{t}_0) + \psi_1(\hat{t}_0) \overset{(4.92)}{=} \delta/2. \tag{4.94}$$

Step 3e: Finally it is shown show that the claim of Step 3 holds true for positive ε_0 as in (4.80). Seeking a contradiction, assume

$$\exists\, \hat{t} \in [0, T) : \qquad \psi_0(\hat{t}) - |e(\hat{t})| < \varepsilon_0. \tag{4.95}$$

By continuity of $t \mapsto \psi_0(t) - |e(t)|$, the point in time

$$t_0 := \max\{t \in [0, \hat{t}) \,|\, \psi_0(t) - |e(t)| = 2\varepsilon_0\},$$

is well defined. It then follows that $\psi_0(t) - |e(t)| \leq 2\varepsilon_0$ for all $t \in [t_0, \hat{t}]$, hence, by $\varepsilon_0 \leq \lambda_0/4$, it holds that $\operatorname{sign} e(\cdot)$ is constant on $[t_0, \hat{t}]$. Only consider the case $\operatorname{sign} e(\cdot) = 1$, the other case follows analogously. Now for ε_0 as in (4.80), the following three cases yield a contradiction to assumption (4.95):

(i) $\dot{e}(t) > -\psi_1(t) + \delta/2$ for all $t \in [t_0, \hat{t}]$, then implication (4.83) together with (4.81) yields $\psi_0(t) - |e(t)| \geq \varepsilon_0$ for all $t \in [t_0, \hat{t}]$,

(ii) $\dot{e}(t) < -\psi_1(t) + \delta/2$ for all $t \in [t_0, \hat{t}]$, then implication (4.89) yields $\psi_0(t) - |e(t)| \geq \varepsilon_0$ for all $t \in [t_0, \hat{t}]$ and

(iii) $\dot{e}(t_0) = -\psi_1(t_0) + \delta/2$, then implication (4.90) together with (4.89) yields $\psi_0(t) - |e(t)| \geq \varepsilon_0$ for all $t \in [t_0, \hat{t}]$.

Therefore, assume that

$$\exists\, t^\star := \min\{\, t \in (t_0, \hat{t}] \mid \dot{e}(t) = -\psi_1(t) + \delta/2\} \ \text{ and } \ \forall\, t \in [t_0,\, t^\star) \colon\ \dot{e}(t) > -\psi_1(t) + \delta/2. \tag{4.96}$$

Then, by continuity of $\dot{e}(\cdot)$ and $\psi_1(\cdot)$, it follows that $\dot{e}(t) \geq -\psi_1(t) + \delta/2$ for all $t \in [t_0,\, t^\star]$. This, for ε_0 as in (4.80), combined with implication (4.83) and (4.81) yields $\psi_0(t^\star) - e(t^\star) \geq \varepsilon_0$. Furthermore, for ε_0 as in (4.80), the choice of $t^\star$ in (4.96) and implication (4.90) give $\dot{e}(t) \leq -\psi_1(t) + \delta/2$ for all $t \in [t^\star, \hat{t}]$, which together with implication (4.89) yields $\varepsilon_0 \leq \psi_0(t^\star) - |e(t^\star)| \leq \psi_0(t) - |e(t)|$ for all $t \in [t^\star, \hat{t}]$, contradicting the assumption (4.95). This completes the proof of Step 3.

Step 4: For positive

$$\varepsilon_1 \leq \min\left\{\frac{\lambda_1}{2},\, \psi_1(0) - |\dot{e}(0)|,\, \frac{\frac{1}{2}|\gamma_0|\underline{\varsigma}_0\underline{\varsigma}_1\lambda_1\varepsilon_0^2}{\|\psi_0\|_\infty(M + \|\dot{\psi}_1\|_\infty)\varepsilon_0^2 + |\gamma_0|\|\varsigma_0\|_\infty^2\|\psi_0\|_\infty^2}\right\}, \tag{4.97}$$

where M as in (4.79) and ε_0 as in (4.80), it is shown that $\psi_1(t) - |\dot{e}(t)| \geq \varepsilon_1$ for all $t \in [0,T)$. From Step 3, for $\varepsilon_0 > 0$ as in (4.80), it follows that $\psi_0(t) - |e(t)| \geq \varepsilon_0$ for all $t \in [0,T)$ and for $\varsigma_0(\cdot) \in \mathcal{W}^{1,\infty}(\mathbb{R}_{\geq 0}; [\underline{\varsigma}_0, \infty))$, one obtains

$$\forall\, t \in [0,T): \qquad \underline{\varsigma}_0/\|\psi_0\|_\infty \leq k_0(t) = \varsigma_0(t)/(\psi_0(t) - |e(t)|) \leq \|\varsigma_0\|_\infty/\varepsilon_0 \tag{4.98}$$

which together with (4.75) yields $-k_0(t)^2 e(t) \leq \|\varsigma_0\|_\infty^2\, \|\psi_0\|_\infty/\varepsilon_0^2$ for all $t \in [0,T)$. Now assume that there exists $\hat{t} \in [0,T)$ such that $\psi_1(\hat{t}) - |\dot{e}(\hat{t})| = \varepsilon_1$, then

$$|\dot{e}(\hat{t})| = \psi_1(\hat{t}) - \varepsilon_1 \geq \lambda_1/2 \qquad \wedge \qquad k_1(\hat{t}) = \varsigma_1(\hat{t})/\varepsilon_1 \geq \underline{\varsigma}_1/\varepsilon_1. \tag{4.99}$$

Again consider only the case $\operatorname{sign}\dot{e}(\hat{t}) = 1$, the case $\operatorname{sign}\dot{e}(\hat{t}) = -1$ follows analogously. Then in view of (4.79) and (4.67), simple calculations show that the choice of ε_1 in (4.97) implies

$$\begin{aligned} \text{for a.a. } \hat{t} \in [0,T): \qquad \ddot{e}(\hat{t}) &\leq M - |\gamma_0| k_0(\hat{t})^2 e(\hat{t}) - |\gamma_0| k_0(\hat{t}) k_1(\hat{t}) \dot{e}(\hat{t}) \\ &\overset{(4.98),(4.99)}{\leq} M + \frac{|\gamma_0|\|\varsigma_0\|_\infty^2\|\psi_0\|_\infty}{\varepsilon_0^2} - \frac{|\gamma_0|\underline{\varsigma}_0\underline{\varsigma}_1}{\|\psi_0\|_\infty \varepsilon_1}\frac{\lambda_1}{2} \overset{(4.97)}{\leq} -\|\dot{\psi}_1\|_\infty. \end{aligned}$$

Hence '$\psi_1(t) - |\dot{e}(t)| = \varepsilon_1$ for all $t \in [0,T)$' implies '$\ddot{e}(t)\operatorname{sign}\dot{e}(t) \leq -\|\dot{\psi}_1\|_\infty$ for almost all $t \in [0,T)$' and since $|\frac{\mathrm{d}}{\mathrm{d}t}\psi_1(t)| \leq \|\dot{\psi}_1\|_\infty$ for almost all $t \in [0,T)$ and $\psi_1(0) > |\dot{e}(0)|$, the set $\{(t,\xi) \in \mathbb{R}_{\geq 0} \times \mathbb{R} \mid \psi_1(t) - |\xi| \geq \varepsilon_1\}$ cannot be left by $\dot{e}(\cdot)$ which completes Step 4.

Step 5: It is shown that Assertions (ii)-(iv) hold true.
At first it is shown that Assertion (ii) holds, i.e. $T = \infty$. For ε_0 as in (4.80), ε_1 as in (4.97) and $M_{\boldsymbol{z}}$ as in (4.77) define the compact set

$$\tilde{\mathfrak{C}} := \left\{\, (t, e_0, e_1, \boldsymbol{z}) \in [0,T] \times \mathbb{R} \times \mathbb{R} \times \mathbb{R}^{n-2} \;\middle|\; \forall\, i \in \{0,1\}:\ |e_i| \leq \psi_i(t) - \varepsilon_i \ \wedge\ \|\boldsymbol{z}\| \leq M_{\boldsymbol{z}} \,\right\}.$$

Let $\mathcal{D}$ be as in Step 1. If $T < \infty$ then $\tilde{\mathfrak{C}}$ is a compact subset of $\mathcal{D}$ which contains the whole graph of the solution $t \mapsto (e(t), \dot{e}(t), \boldsymbol{z}(t))$, which contradicts the maximality of the solution. Hence $T = \infty$. Now, Assertion (iii) follows from Step 3 and Step 4, where ε_0 as in (4.80) and ε_1 as in (4.97). Step 3 and Step 4, respectively, ensure that $k_0(\cdot)$ and $k_1(\cdot)$ are uniformly bounded on $\mathbb{R}_{\geq 0}$. From (4.75) it also follows that $u(\cdot)$ is uniformly bounded on $\mathbb{R}_{\geq 0}$, hence Assertion (iv) is shown. This completes the proof. □

4.4.2.3 Motivation for the modified funnel controller

The original funnel controller (4.65)—introduced in [72]—applied for position control of a stiff servo-system yields a badly damped closed-loop system response (see Fig. 4.3(c)-(f) in [72]). Only for given non-increasing subboundary $\psi_0(\cdot)$ and small $\delta \ll 1$ in (4.61), e.g. the choice $\psi_1(\cdot) = -\dot{\psi}_0(\cdot) + \delta$ yields a well damped system response. Since speed measurement is (very) noisy, such a choice is not admissible for implementation. In contrast, for arbitrary $\delta > 1$, the

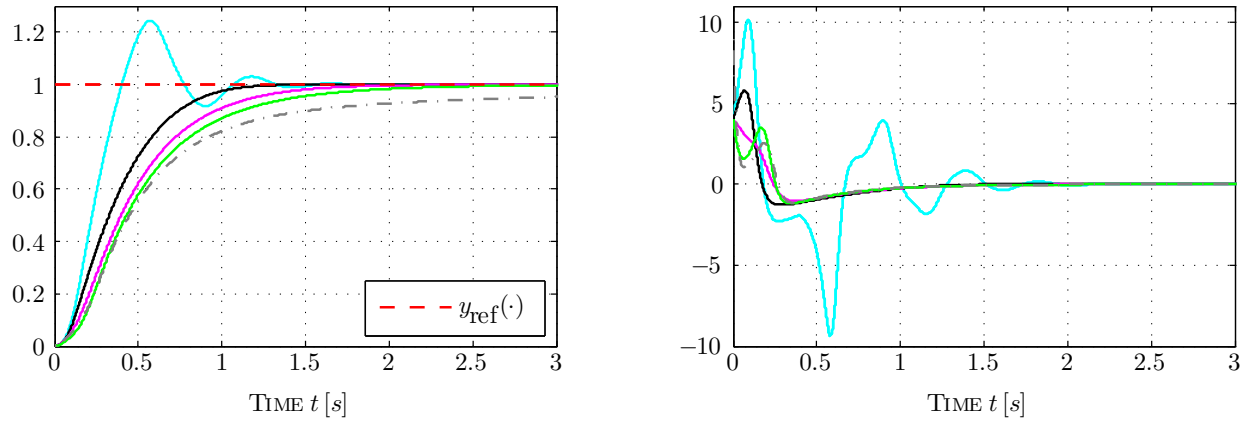

(a) *output* $y(\cdot)$ *and reference* $y_{\mathrm{ref}}(\cdot)$ (b) *control action* $u(\cdot)$

Figure 4.7: *Simulation results for closed-loop system* (3.80), (4.67) *with parametrization* $\gamma_0 = 3$, $(y_0, y_1) = (0, 0)$, $u_d(\cdot) = 0$, *funnel boundary* $(\psi_0(\cdot), \psi_1(\cdot))$ *as in* (4.64) *where* $\Lambda_0 = 1.5$, $\lambda_0 = 0.1$, $T_E = 0.379$ [s] *and* $\lambda_1 = 3$ [1/s] *and* different *gain scalings* $(\varsigma_0(\cdot), \varsigma_1(\cdot)) \in \{$——$(1,\, 1)$, ——$(1,\, 2/\sqrt{\gamma_0}\,\psi_1(\cdot))$, ——$(1,\, 5/\sqrt{\gamma_0}\,\psi_1(\cdot))$, ——$(1,\, 10/\sqrt{\gamma_0}\,\psi_1(\cdot))$, ·····$(\psi_0(\cdot),\, 10/\sqrt{\gamma_0}\,\psi_1(\cdot))\}$.

modified funnel controller (4.67) may achieve a better damped closed-loop system response (see Fig. 6(a)-(e) in [65] or the simulations presented in Section 4.4.3). Here the product $k_0(\cdot)k_1(\cdot)$ in (4.67) in combination with a special choice of $\varsigma_1(\cdot)$ seems to be essential. In simple simulation studies for the closed-loop system (3.80), (4.67) it was observed that, for (known) $\underline{\gamma_0} \leq \gamma_0$ and given subboundary $\psi_1(\cdot)$, the following gain scaling

$$[\![\, \forall\, t \geq 0\colon\ \varsigma_1(t) = 2\psi_1(t)/\sqrt{\underline{\gamma_0}}\,]\!] \implies [\![\, \forall\, (t, e(t), \dot{e}(t)) \in \mathcal{F}_{(\psi_0,\psi_1)}\colon\ k_1(t) \geq 2/\sqrt{\underline{\gamma_0}}\,]\!] \tag{4.100}$$

results in an "overdamped" system response (i.e. no overshoot). One exemplary simulation study is depicted in Fig. 4.7. Different gain scalings are implemented (for parametrization see figure caption). Qualitatively identical results as in Fig. 4.7 are also obtained for $(\psi_0(\cdot),\, \psi_1(\cdot))$ as in (4.63) (see Fig. 4.8) or for different values of high-frequency gain and/or reference magnitude (not shown). It was not possible to prove this "overdamped" behavior in general. Nevertheless, the observations above are noteworthy concerning application of the funnel controller (4.67) for position control of 1MS and 2MS (see Section 5.2.2 and 5.2.3, respectively). Oscillations and large overshoots should be avoided in "real world".

An intuitive explanation (stemming from linear analysis) for the advantageous effect of the product $k_0(\cdot)k_1(\cdot)$ in (4.67) on the closed-loop system response might be as follows: Application of the PD controller $u(t) = k_0^2 y(t) + k_0\, k_1\, \dot{y}(t)$ with *constant* $k_0,\, k_1 > 0$ to the double integrator (3.80), with $\gamma_0 > 0$, $(y_0,\, y_1) = (0, 0)$ and $u_d(\cdot)$, yields the harmonic oscillator

$$\ddot{y}(t) + \gamma_0 k_0 k_1 \dot{y}(t) + \gamma_0 k_0^2 y(t) = 0, \qquad (y(0),\, \dot{y}(0)) = (0,\, 0). \tag{4.101}$$

It is "overdamped" (or "critically damped", in the sense of Example 11.3.7 in [24, p. 717-718])

if its poles $p_{1,2}$ are *real* and negative, i.e.

$$p_{1,2} = -\gamma_0 k_0 k_1/2 \left(1 \pm \sqrt{1 - 4/(\gamma_0 k_1^2)}\right) < 0. \tag{4.102}$$

If $k_0 > 0$, $\gamma_0 \geq \underline{\gamma_0} > 0$ and $\underline{\gamma_0}$ is known, then

$$[\![\, k_1 \geq 2/\sqrt{\underline{\gamma_0}} \,]\!] \quad \Longrightarrow \quad [\![\, 0 \leq 1 - 4/(\gamma_0 k_1^2) < 1 \,]\!] \quad \Longrightarrow \quad (4.102). \tag{4.103}$$

The implication above motivated for the proposed gain scaling in (4.100), which can be regarded as "recommendation" or "rule of thumb" for controller design of (4.67). The fastest *but* "overdamped" closed-loop system response is obtained for $\underline{\gamma_0} = \gamma_0$ (see —— in Fig. 4.7). Hence "good" system knowledge is beneficial and may be incorporated in controller design directly.

Remark 4.14. *It can be shown that gain scaling is also admissible for the original funnel controller (4.65), i.e. replace gain adaption in (4.65) by gain adaption in (4.67). The proof is omitted, it is implicitly given in the proof of Theorem 4.4. Moreover, as simulations show, there also exist adequate choices for gain scaling to achieve an overdamped system response by the "scaled" original funnel controller (e.g. $\varsigma_1(\cdot) = c\,\psi_1(\cdot)$ with $c > 0$ sufficiently large). However, it was not possible to deduce a "rule of thumb" as in (4.100).*

4.4.2.4 Funnel controller with saturation

In [72] it is shown that the funnel controller (4.65) also works for constrained control inputs (e.g. due to actuator saturation) if the available control action matches a feasibility condition. In the following, based on the idea in [72], it will be shown that also the modified funnel controller (4.67) is feasible under input constraints which underpins its applicability in "real world". To account e.g. for actuator deviations or feedforward control in the saturated controller, the following theorem also considers arbitrary but bounded input disturbances.

Theorem 4.15 (Funnel control with derivative feedback & saturation for systems of class $\mathcal{S}_2$)**.** *Consider a system of class $\mathcal{S}_2$ described by (1.36). Then, for arbitrary funnel boundary $(\psi_0(\cdot), \psi_1(\cdot)) \in \mathcal{B}_2$, gain scaling functions $\varsigma_0(\cdot)$, $\varsigma_1(\cdot) \in \mathcal{B}_1$, input disturbance $u_F(\cdot) \in \mathcal{L}^\infty(\mathbb{R}_{\geq 0}; \mathbb{R})$, reference $y_{\mathrm{ref}}(\cdot) \in \mathcal{W}^{2,\infty}(\mathbb{R}_{\geq 0}; \mathbb{R})$ and initial trajectory $\boldsymbol{x}^0(\cdot) \in \mathcal{C}([-h, 0]; \mathbb{R}^n)$ satisfying (4.66), there exists a feasibility number u_{feas} such that, for all $\hat{u} \geq u_{\mathrm{feas}}$, the saturated funnel controller*

$$\left.\begin{aligned} u(t) &= \operatorname{sign}(\boldsymbol{c}^\top \boldsymbol{A}\boldsymbol{b})\, \operatorname{sat}_{\hat{u}}\Big(k_0(t)^2 e(t) + k_0(t) k_1(t) \dot{e}(t) + u_F(t)\Big) \qquad \text{where} \\ k_i(t) &= \frac{\varsigma_i(t)}{\psi_i(t) - |e^{(i)}(t)|},\ i = \{0, 1\} \quad \text{and} \quad e(t) = y_{\mathrm{ref}}(t) - y(t) \end{aligned}\right\} \tag{4.104}$$

applied to (1.36) yields a closed-loop initial-value problem with the properties

(i) there exists solution $\boldsymbol{x} : [-h, T) \to \mathbb{R}^n$ which can be maximally extended and $T \in (0, \infty]$;

(ii) the solution $\boldsymbol{x}(\cdot)$ does not have finite escape time, i.e. $T = \infty$;

(iii) the signals $e(\cdot)$, $\dot{e}(\cdot)$ are uniformly bounded away from the funnel boundary, i.e.

$$\forall\, i \in \{0, 1\}\ \exists\, \varepsilon_i > 0\ \forall\, t \geq 0 : \qquad \psi_i(t) - |e^{(i)}(t)| \geq \varepsilon_i$$

(iv) the gains are uniformly bounded, i.e. $k_0(\cdot),\, k_1(\cdot) \in \mathcal{L}^\infty(\mathbb{R}_{\geq 0}; \mathbb{R}_{>0})$ *and*

(v) the control input is unsaturated at some time, i.e. there exists $t \geq 0$ *such that* $|u(t)| < \hat{u}$.

The feasibility number u_{feas} can be quoted explicitly. In Section 5.2.3, it will be required for a feasibility check in application (position control of industrial servo-systems). For ς_0, ς_1, λ_0 and λ_1 as in (4.68), M as in (4.78) and $\gamma_0 = \boldsymbol{c}^\top \boldsymbol{A}\boldsymbol{b}$ define

$$\hat{u}_S := \frac{\delta^2 \lambda_0}{|\gamma_0|}\left\{\frac{(\|\psi_1\|_\infty + \|\dot{\psi}_0\|_\infty)^2}{\delta\, \varsigma_0\, \lambda_0} + \left(\frac{(\|\psi_1\|_\infty + \|\dot{\psi}_0\|_\infty)^4}{\delta^2\, \varsigma_0^2\, \lambda_0^2} + \frac{2|\gamma_0|}{\delta^2\, \lambda_0}\left[\frac{2|\gamma_0|\|\varsigma_1\|_\infty^2 \|\psi_1\|_\infty^2}{\delta^2\, \lambda_0} + |\gamma_0|\|u_F\|_\infty + M + 2\|\varsigma_1\|_\infty \|\psi_1\|_\infty \frac{(\|\psi_1\|_\infty + \|\dot{\psi}_0\|_\infty)^2}{\delta\, \varsigma_0\, \lambda_0}\right]\right)^{1/2}\right\} \tag{4.105}$$

and

$$L := \max\left\{\frac{2\,(\|\psi_1\|_\infty + \|\dot{\psi}_0\|_\infty)^2}{\lambda_0},\, \frac{(\|\psi_1\|_\infty + \|\dot{\psi}_0\|_\infty)^2}{\psi_0(0) - |e(0)|},\, \|\dot{\psi}_1\|_\infty,\, \frac{\hat{u}_S^2 - 4\|\varsigma_1\|_\infty^2\, \|\psi_1\|_\infty^2}{2\delta^2 \lambda_0} - \|u_F\|_\infty\right\}, \tag{4.106}$$

then the feasibility condition is given by

$$\hat{u} \geq u_{\text{feas}} := (M + L)\,/|\gamma_0| > 0. \tag{4.107}$$

Clearly, to validate (4.107), rough knowledge of the system parameters is necessary. In particular, rough bounds on M as in (4.78), the high-frequency gain γ_0 and the control input disturbance $u_F(\cdot)$ are needed. The other values in (4.105) and (4.106) are known to the control designer. The dependence on M in (4.107) is the most severe: the constant M subsumes "all" system data (e.g. $\boldsymbol{A}$ or $\boldsymbol{B}_{\mathfrak{T}}$), exogenous disturbances (e.g. $u_d(\cdot)$ or $\boldsymbol{d}(\cdot)$) and the bound $M_{\boldsymbol{z}}$ on the internal dynamics. At least, for systems with low order, evaluation of (4.107) is feasible and helpful in verifying that funnel control for systems with constrained inputs is admissible. In Section 5.2.3, it will be verified by experiments that the feasibility condition (4.107) is sufficient but not necessary and that the feasibility number $u_{\text{feas}} > 0$ is (often) a very conservative bound (see also [72]).

Proof of Theorem 4.15.

The outline of the proof of Theorem 4.15 is analogously to the proof of Theorem 4.13. Only the essential changes are presented. Again it suffices to consider system (1.36) in Byrnes-Isidori like form (3.9).

Step 1: It is shown that Assertion (i) holds true, i.e. existence of a maximally extended solution. For the open and non-empty set $\mathcal{D}$ as in (4.71) and the extended signals $\varsigma_0(\cdot)$, $\varsigma_1(\cdot)$ and $y_{\text{ref}}(\cdot)$

as in (4.69) and (4.70), introduce

$$\begin{aligned}\boldsymbol{f}\colon [-h,\infty)\times\mathcal{D}\times\mathbb{R}^n &\to \mathbb{R}_{\geq 0}\times\mathbb{R}^2\times\mathbb{R}^{n-2},\\ (t,(\tau,\boldsymbol{\mu},\boldsymbol{\xi}),\boldsymbol{w}) &\mapsto \begin{pmatrix} \begin{bmatrix} 0 & 1\\ a_1 & a_2\end{bmatrix}\left(\boldsymbol{\mu}-\begin{pmatrix} y_{\mathrm{ref}}(t)\\ \dot{y}_{\mathrm{ref}}(t)\end{pmatrix}\right)+\begin{pmatrix} \dot{y}_{\mathrm{ref}}(t)\\ \ddot{y}_{\mathrm{ref}}(t)\end{pmatrix}-\begin{bmatrix}\mathbf{0}^\top\\ \boldsymbol{a}_3^\top\end{bmatrix}\boldsymbol{\xi}-\begin{bmatrix}\mathbf{0}^\top\\ \boldsymbol{c}^\top\boldsymbol{A}\boldsymbol{B}_{\mathfrak{T}}\end{bmatrix}(\boldsymbol{w}+\boldsymbol{d}(t))\\ -|\gamma_0|\left(\mathrm{sat}_{\hat{u}}\left(\frac{\varsigma_0(t)^2\,\mu_1}{(\psi_0(|\tau|)-|\mu_1|)^2}+\frac{\varsigma_0(t)}{\psi_0(|\tau|)-|\mu_1|}\frac{\varsigma_1(t)\,\mu_2}{\psi_1(|\tau|)-|\mu_2|}+u_F(t)\right)+u_d(t)\right)\\ \begin{bmatrix}\boldsymbol{a}_4 & \mathbf{0}\end{bmatrix}\left(\begin{pmatrix} y_{\mathrm{ref}}(t)\\ \dot{y}_{\mathrm{ref}}(t)\end{pmatrix}-\boldsymbol{\mu}\right)+\boldsymbol{A}_5\boldsymbol{\xi}+\boldsymbol{N}\boldsymbol{B}_{\mathfrak{T}}(\boldsymbol{w}+\boldsymbol{d}(t))\end{pmatrix}\end{aligned}$$

and the operator $\hat{\mathfrak{T}}:\mathcal{C}([-h,\infty);\mathbb{R}\times\mathbb{R}^n)\to\mathcal{L}^\infty_{\mathrm{loc}}(\mathbb{R}_{\geq 0};\mathbb{R}^n)$ as in (4.72). Then, for $\tau\colon [-h,\infty)\to\mathbb{R}_{\geq 0}$, $t\mapsto t$ and $\hat{\boldsymbol{x}}:=(\tau,(e,\dot{e}),\boldsymbol{z})$ and $\tau^0:=\tau|_{[-h,0]}$, the initial-value problem (3.9), (4.104) can be written in the form (4.73).
Now a similar argumentation as in Step 1 of the Proof of Theorem 4.13 yields existence of a solution $(\tau,(e,\dot{e}),\boldsymbol{z})\colon[-h,T)\to\mathbb{R}_{\geq 0}\times\mathbb{R}^2\times\mathbb{R}^{n-2}$ of the initial-value problem(4.73), where $((e,\dot{e}),\boldsymbol{z})\colon[-h,T)\to\mathbb{R}^2\times\mathbb{R}^{n-2}$ solves the closed-loop initial-value problem (3.9), (4.104) for almost all $t\in[0,T)$. The solution can be maximally extended and, moreover, if $T<\infty$ then for every compact $\tilde{\mathfrak{C}}\subset\mathcal{D}$, there exists $\tilde{t}\in[0,T)$ such that $\hat{\boldsymbol{x}}(\tilde{t})\notin\tilde{\mathfrak{C}}$. For the remainder of the proof, let $((e,\dot{e}),\boldsymbol{z}):[-h,T)\to\mathbb{R}^2\times\mathbb{R}^{n-2}$ be a fixed and maximally extended solution of the closed-loop initial-value problem (3.9), (4.104).

Step 2: Some technical preliminaries are introduced.
Similar arguments as in Step 2 of the proof of Theorem 4.13 show that the inequalities (4.75), (4.77) and, for M as in (4.78), (4.79) hold, respectively.
Moreover, inserting (4.104) into (4.79) yields

$$\begin{aligned}\text{for a.a. } t\in[0,T):\ -M-|\gamma_0|\,\mathrm{sat}_{\hat{u}}\left(k_0(t)^2\,e(t)+k_0(t)k_1(t)\,\dot{e}(t)+u_F(t)\right)&\leq\ddot{e}(t)\\ &\leq M-|\gamma_0|\,\mathrm{sat}_{\hat{u}}\left(k_0(t)^2\,e(t)+k_0(t)k_1(t)\,\dot{e}(t)+u_F(t)\right)\end{aligned}\tag{4.108}$$

where M as in (4.78).

Step 3: It is shown that $|e(\cdot)|$ is uniformly bounded away from the boundary $\psi_0(\cdot)$, i.e.

$$\exists\,\varepsilon_0>0\ \forall\,t\in[0,T):\qquad \psi_0(t)-|e(t)|\geq\varepsilon_0$$

Step 3a: Note that identical argumentation as in Step 3a of the Proof of Theorem 4.13 show that, for $\varepsilon_0\in(0,\lambda_0/2)$, implication (4.81) holds on any interval $[t_0,t_1]\subseteq[0,T)$.

Step 3b: It is shown that for positive

$$\varepsilon_0:=\min\left\{\frac{\lambda_0}{4},\frac{\psi_0(0)-|e(0)|}{2},\frac{\frac{1}{2}\delta_{\varsigma_0}\lambda_0}{2\|\varsigma_1\|_\infty\|\psi_1\|_\infty+\sqrt{4\|\varsigma_1\|_\infty^2\|\psi_1\|_\infty^2+2\delta^2\lambda_0(\|u_F\|_\infty+\hat{u})}}\right\}\tag{4.109}$$

implication (4.83) holds on any interval $[t_0,t_1]\subseteq[0,T)$.
Due to presupposition i) in (4.83) and $0<\varepsilon_0\leq\lambda_0/4$, see (4.109), it is easy to see that (4.84) holds. Hence $\operatorname{sign}e(\cdot)$ is constant on $[t_0,t_1]$. Consider only the case $e(\cdot)>0$ on $[t_0,t_1]$, the other

case follows analogously. In view of (4.75), presupposition ii) in (4.83) implies (4.87).

Note that $k_0(t) \geq \varsigma_0/(2\varepsilon_0)$ for all $t \in [t_0, t_1]$, hence the following holds

$$\text{for a.a. } t \in [t_0,\, t_1]: \qquad k_0(t)^2\, e(t) + k_0(t)k_1(t)\, \dot{e}(t) + u_F(t) \overset{(4.84),(4.87)}{\geq} k_0(t)^2\, \frac{\lambda_0}{2} - k_0(t)\frac{2}{\delta}\, \|\varsigma_1\|_\infty \|\psi_1\|_\infty - \|u_F\|_\infty \overset{(4.109)}{\geq} \hat{u}. \quad (4.110)$$

To complete Step 3b, for ε_0 as in (4.109), u_{feas} as in (4.107) and $\hat{u} \geq u_{\text{feas}}$, one needs to verify that the following holds

$$\text{for a.a. } t \in [t_0, t_1]: \qquad \ddot{e}(t) \leq M - |\gamma_0|\, \hat{u} \leq -\frac{(\|\psi_1\|_\infty + \|\dot{\psi}_0\|_\infty)^2}{2\varepsilon_0}. \quad (4.111)$$

Simple calculations show that, for $\varepsilon_0 = \lambda_0/4$ or $\varepsilon_0 = (\psi_0(0) - |e(0)|)/2$, (4.111) holds. It remains to consider $\varepsilon_0 = (\frac{1}{2}\delta\varsigma_0\lambda_0)/(2\|\varsigma_1\|_\infty\|\psi_1\|_\infty + \sqrt{4\|\varsigma_1\|_\infty^2\|\psi_1\|_\infty^2 + 2\delta^2\lambda_0(\|u_F\|_\infty + \hat{u})})$. Substituting $(u_S^2 - 4\|\varsigma_1\|_\infty^2\|\psi_1\|_\infty^2)/(2\delta^2\lambda_0) - \|u_F\|_\infty$ for $\hat{u}$ in (4.111) yields

$$-\frac{|\gamma_0|}{2\delta^2\lambda_0}u_S^2 + \frac{(\|\psi_1\|_\infty + \|\dot{\psi}_0\|_\infty)^2}{\delta\varsigma_0\lambda_0}u_S + |\gamma_0|\left(\frac{2\|\varsigma_1\|_\infty^2\|\psi_1\|_\infty^2}{\delta^2\lambda_0} + \|u_F\|_\infty\right) + M + 2\|\varsigma_1\|_\infty\|\psi_1\|_\infty\frac{(\|\psi_1\|_\infty + \|\dot{\psi}_0\|_\infty)^2}{\delta\varsigma_0\lambda_0} \leq 0$$

which clearly holds for all $u_S \geq \hat{u}_S$ with $\hat{u}_S$ as in (4.105). This completes Step 3b.

Step 3c: The identical argumentation as in Step 3c of the Proof of Theorem 4.13 shows that implication (4.89) holds for any $[t_0, t_1] \subset [0, T)$.

Step 3d: It is shown that for positive ε_0 as in (4.109) implication (4.90) holds for any $t \in [t_0, t_1] \subset [0, T)$.
Presuppositions in (4.90) imply that $\operatorname{sign} e(\cdot)$ is constant on $[t_0, t_1]$. Consider only the case $\operatorname{sign} e(\cdot) = 1$, the other case follows analogously. Observe that, for ε_0 as in (4.109), inequality (4.110) holds on the whole interval $[t_0, t_1]$. Seeking a contradiction assume that (4.91) holds. Now identical arguments as in Step 3d of the proof of Theorem 4.13 lead to

$$\text{for a.a. } t \in [\tilde{t}_0, \tilde{t}]: \qquad \ddot{e}(t) \leq M - |\gamma_0|\hat{u} \overset{(4.107)}{\leq} -\|\dot{\psi}_1\|_\infty$$

and, by integration as in (4.94), the contradiction follows. This completes Step 3d.

Step 3e: Finally it is shown that the claim of Step 3 holds true for positive ε_0 as in (4.109). Replacing ε_0 in (4.80) by (4.109) and invoking implications (4.81), (4.83), (4.89) and (4.90) allow for the identical argumentation as in Step 3e of the proof of Theorem 4.13. Hence the claim of Step 3 holds true. This completes Step 3.

Step 4: For positive

$$\varepsilon_1 \leq \min\left\{\frac{\lambda_1}{2}, \psi_1(0) - |\dot{e}(0)|, \frac{\frac{1}{2}\varsigma_0\varsigma_1\lambda_1\varepsilon_0^2}{\varepsilon_0^2\|\psi_0\|_\infty(\|u_F\|_\infty + \hat{u}) + \|\varsigma_0\|_\infty^2\|\psi_0\|_\infty^2}\right\}, \tag{4.112}$$

where M as in (4.78) and ε_0 as in (4.109), it is shown that $\psi_1(t) - |\dot{e}(t)| \geq \varepsilon_1$ for all $t \in [0,T)$. Assume there exists $\hat{t} \in [0,T)$ such that $\psi_1(\hat{t}) - |\dot{e}(\hat{t})| = \varepsilon_1$, then clearly (4.99) holds and it follows that

$$\left|k_0(\hat{t})^2\, e(\hat{t}) + k_0(\hat{t})k_1(\hat{t})\, \dot{e}(\hat{t}) + u_F(\hat{t})\right| \overset{(4.98),(4.99)}{\geq} \left|\mp\frac{\|\varsigma_0\|_\infty^2}{\varepsilon_0^2}\|\psi_0\|_\infty \pm \frac{\varsigma_0\varsigma_1\lambda_1}{2\|\psi_0\|_\infty\varepsilon_1} \mp \|u_F\|_\infty\right| \overset{(4.112)}{\geq} \hat{u} \tag{4.113}$$

for almost all $\hat{t} \in [0,T)$. Consider only the case $\operatorname{sign}\dot{e}(\hat{t}) = 1$, the other case follows analogously. Then in view of (4.108), simple calculations show that for almost all $\hat{t} \in [0,T)$

$$\ddot{e}(\hat{t}) \leq M - |\gamma_0|\operatorname{sat}_{\hat{u}}\left(k_0(\hat{t})^2\, e(\hat{t}) + k_0(\hat{t})k_1(\hat{t})\, \dot{e}(\hat{t}) + u_F(\hat{t})\right) \overset{(4.113)}{=} M - |\gamma_0|\hat{u} \overset{(4.107)}{\leq} -\|\dot{\psi}_1\|_\infty.$$

Now identical arguments as in Step 4 of the proof of Theorem 4.13 show the claim which completes Step 4.

Step 5: It is shown that Assertions (ii)-(iv) hold true.
In Step 5 of the proof of Theorem 4.13 substitute (4.109) and (4.112) for (4.80) and (4.97), respectively. Then identical arguments show Assertions (ii)-(iv).

Step 6: It is shown that Assertion (v) holds true.
Seeking a contradiction, suppose that

$$\forall\, t \geq 0: \qquad |\operatorname{sat}_{\hat{u}}\left(k_0(t)^2 e(t) + k_0(t)k_1(t)\dot{e}(t) + u_F(t)\right)| = \hat{u} > 0,$$

which implies that $\operatorname{sign}(k_0(t)^2 e(t) + k_0(t)k_1(t)\dot{e}(t) + u_F(t))$ is constant for all $t \geq 0$. Consider only the case $\operatorname{sign}(k_0(\cdot)^2 e(\cdot) + k_0(\cdot)k_1(\cdot)\dot{e}(\cdot) + u_F(\cdot)) = 1$, the other case follows analogously. Since $\hat{u} \geq u_{\text{feas}}$ in (4.107) it follows that $\hat{u} \geq (M + 2(\|\psi_1\|_\infty + \|\dot{\psi}_0\|_\infty)^2/\lambda_0)/|\gamma_0| > 0$, which implies

$$\text{for a.a. } t \geq 0: \qquad \ddot{e}(t) \leq M - |\gamma_0|\,\hat{u} \leq -\frac{2(\|\psi_1\|_\infty + \|\dot{\psi}_0\|_\infty)^2}{\lambda_0} < 0$$

whence the contradiction follows

$$\forall\, t \geq 0: \qquad -\|\psi_1\|_\infty \leq -\psi_1(t) < \dot{e}(t) \leq \dot{e}(0) - \frac{2(\|\psi_1\|_\infty + \|\dot{\psi}_0\|_\infty)^2}{\lambda_0}\, t.$$

This completes the proof. □

Remark 4.16 (Relaxation of system property ($\mathcal{S}_2$-sp$_3$) of class $\mathcal{S}_2$)**.**
Let $h \geq 0$, $\hat{\mathfrak{T}}\colon \mathcal{C}([-h,\infty);\mathbb{R}^2) \to \mathcal{L}^\infty_{\text{loc}}([-h,\infty);\mathbb{R}^m)$, $\mathfrak{T}\colon \mathcal{C}([-h,\infty);\mathbb{R}^n) \to \mathcal{L}^\infty_{\text{loc}}([-h,\infty);\mathbb{R}^m)$ and $\hat{\mathfrak{T}}, \mathfrak{T} \in \mathcal{T}$ (see Definition 1.5). If funnel controller (4.67) (or (4.104)) is applied to system (1.36) of class $\mathcal{S}_2$ with $\mathfrak{T}\boldsymbol{x} = \hat{\mathfrak{T}}(y,\dot{y})$, then system property ($\mathcal{S}_2$-sp$_3$) in Definition 1.7 can

controller/funnel	parametrization
(4.60)	$\psi(\cdot) = \psi_0(\cdot)$ as in (4.63), $k_F = 1.5$ and $\zeta_{1,0} = 0$,
(4.65)	$\psi_0(\cdot)$ and $\psi_1(\cdot)$ as in (4.63)
(4.67)	$\psi_0(\cdot)$ and $\psi_1(\cdot)$ as in (4.63), $\underline{\gamma_0} = \gamma_0/3$, $\varsigma_0(\cdot) = 1$ and $\varsigma_1(\cdot) = 2\psi_1(\cdot)/\sqrt{\underline{\gamma_0}}$
boundary design	$\Lambda_0 = 1.5$, $\lambda_0 = 0.1$, $\lambda_1 = 1.7$ and $T_L = 0.77$ [s]

Table 4.1: *Controller and funnel design for comparative simulations.*

be relaxed: the global boundedness of operator $\mathfrak{T}$ can be dropped, i.e. $M_{\mathfrak{T}} < \infty$ in ($\mathcal{S}_2$-sp$_3$) is not necessary. This can be shown as follows (similar to Remark 4.8). It is easy to see that (4.75) holds independently of ($\mathcal{S}_2$-sp$_3$) and this implies that

$$\forall\, t \in [0,T)\colon \qquad |y(t)| \leq \|\psi_0\|_\infty + \|y_{\mathrm{ref}}\|_\infty \qquad \textit{and} \qquad |\dot{y}(t)| \leq \|\psi_1\|_\infty + \|\dot{y}_{\mathrm{ref}}\|_\infty.$$

Hence by property (op$_2$) of operator class $\mathcal{T}$, there exists $\Delta > 0$ such that $\|(\hat{\mathfrak{T}}\left(\begin{smallmatrix} y \\ \dot{y} \end{smallmatrix}\right))(t)\| \leq \Delta$ for all $t \in [0,T)$. Clearly, utilizing Δ instead of $M_{\mathfrak{T}}$ in (4.77) and (4.78), respectively, does not alter the argumentation in the proof and so the proof of Theorem 4.13 (or Theorem 4.15) goes through without any further changes.

4.4.3 Simulations

Control performance of the controllers (4.60), (4.65) and (4.67) will be investigated. For this the three controllers are applied to the double integrator (3.80). The closed-loop systems (3.80),(4.60), (3.80),(4.65) and (3.80),(4.67) are implemented in Matlab/Simulink with identical setup as in Section 3.5.4, e.g. system (3.80) is parametrized as in Tab. 3.1, reference $y_{\mathrm{ref}}(\cdot)$ and disturbance $u_d(\cdot)$ are as in Fig. 3.4(a) and Fig. 3.4(b), etc. Each closed-loop system must accomplish the set-point control objectives specified in (3.81). Control performance of each controller is evaluated by means of rise and settling time, maximal overshoot, maximal control action and ITAE as in (3.82). To obtain a comparable setting, the performance funnels of (4.60), (4.65) and (4.67) are designed with identical limiting functions. Implementation data of controllers and funnel design is collected in Tab. 4.1. Simulation results[3] for the closed-loop systems ——(3.80), (4.60), ——(3.80), (4.65) and ——(3.80), (4.67) are depicted in Fig. 4.8 for set-point tracking and in Fig. 4.9 for (overall) reference tracking. All three controllers achieve the specifications in (3.81). Performance evaluation is summarized in Tab. 4.2.

Discussion for funnel controller (4.60) with backstepping: Filter gain $k_F > 0$ in (4.60) is tuned by trial and error to meet the maximum overshoot $\Delta^{os}_{\mathrm{ref}} = 50\,\%$ (scarcely accomplished). With the largest initial control action $u(0) \approx 123$, the controller achieves the smallest rise time, however settling time and overshoot are the worst in this study. Moreover, controller (4.60) is outperformed by both other concepts concerning the ITAE criterion. This is due to "gain scaling" in (4.60) with $\psi(\cdot)^2$ which yields a "decreased" minimal gain of 1 compared to (4.65)

[3] Albeit not shown qualitatively similar results are obtained for the exponential boundary (4.64) with $\Lambda_0 = 1.5$, $\lambda_0 = 0.1$, $T_E = 0.379$ [s] and $\lambda_1 = 3$ [1/s].

Controller	$t^r_{y(\cdot),0.8}$ [s]	$t^s_{y(\cdot),0.1}$ [s]	$\Delta^{os}_{y(\cdot)}$ [%]	$\max_{t\in I}\lvert u(t)\rvert$ [1]	ITAE [s^2]	$\max_{t\in I}(k_0(t),\, k_1(t))$
(4.60)	0.22	1.06	48.40	1050.9	30.2	$(19.8, -)$
(4.65)	0.48	0.95	21.15	65.0	4.1	$(29.3, 4.9)$
(4.67)	0.94	1.05	0.37	8.3	3.3	$(38.2, 3.0)$

Table 4.2: *Performance evaluation of closed-loop systems* ——(3.80),(4.60), ——(3.80),(4.65) *and* ——(3.80),(4.67) *with parametrization as in Tab. 3.1 & 4.1 and* $I = [0, 30]$ [s].

and (4.67) (see e.g. Fig. 4.8(e)). The maximal control gain is the smallest in this study. Nevertheless, since control action in (4.60) is proportional to $k(t)^7$, this controller is extremely noise sensitive for gains greater than one (see interval (5, 23) [s] in Fig. 4.9(b) and (e)), which results in huge control actions alternating between $\approx \pm 1050$ (not shown). In Fig. 4.9(b) the ordinate is limited to $[-10, 10]$ to ensure visibility for the other controllers. Application of funnel controller (4.60) with backstepping seems not advisable in real world.

Discussion for (original) funnel controller (4.65) *with derivative feedback:* Controller (4.65) is designed by $\psi_0(\cdot)$ and $\psi_1(\cdot)$ as in Tab. 4.1, other options for controller tuning are not available. The boundary design yields the closed-loop system response as in Fig. 4.8 and 4.9. The controller performs acceptably well: rise time and ITAE value are the second best, settling time is the best and overshoot is within the admissible range. Noise sensitivity is slightly better than that of (4.67). However, due to turbulent oscillations, the controller requires the second largest control action. Moreover, without gain scaling the oscillations cannot be damped. Hence, in its simple form (4.65), the original funnel controller seems not suitable for industrial application.

Discussion for (modified) funnel controller (4.67) *with derivative feedback:* Based on the observations discussed in Section 4.4.2.3, gain scaling $\varsigma_1(\cdot)$ of (4.67) is fixed according to the recommendation in (4.100). So the closed-loop system ——(3.80),(4.67) exhibits a well-damped response with almost no overshoot. Although rise and settling time are the worst in this study and noise sensitivity is significant, the modified controller (4.67) achieves the best ITAE value and generates the smallest control action. By gain scaling the degrees of freedom for controller tuning are increased, which is effectively exploited to guarantee (almost) overdamped transient behavior (see also discussion in Section 4.4.2.3). Concluding, obeying the recommendation in (4.100), the modified controller (4.67) is easy to tune and performs reasonably well. It will be applied for position control of 1MS and 2MS (see Section 5.2.3).

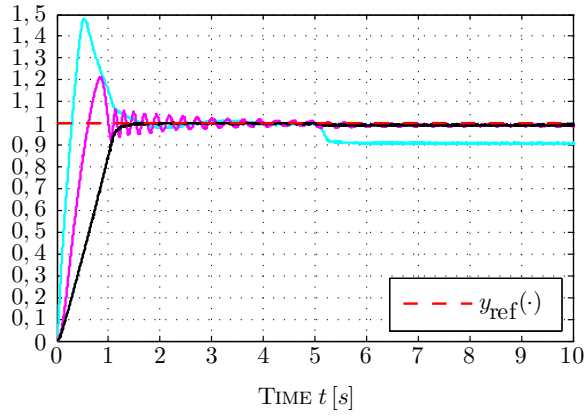

(a) *output* $y(\cdot)$ *and reference* $y_{\mathrm{ref}}(\cdot)$

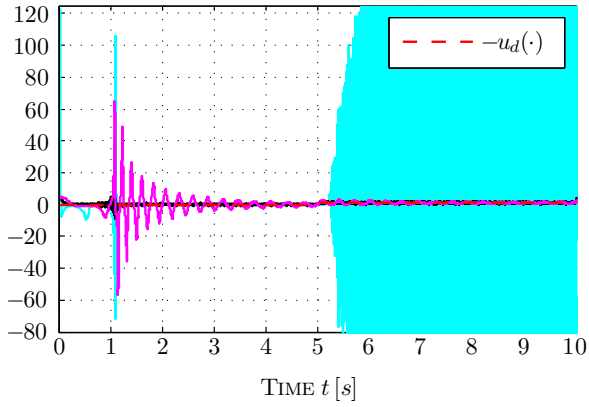

(b) *control action* $u(\cdot)$ *and disturbance* $-u_d(\cdot)$

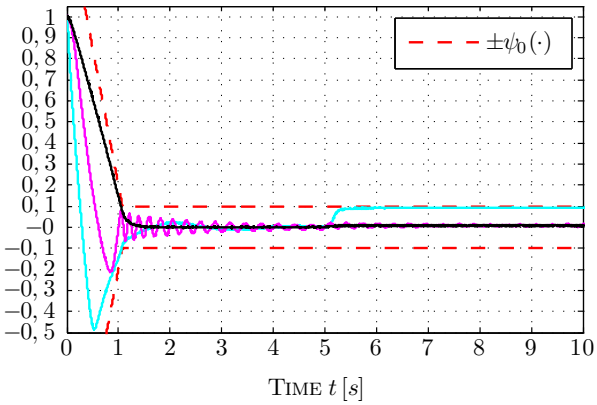

(c) *error* $e(\cdot)$ *and (sub)boundary* $\psi_0(\cdot) = \psi(\cdot)$

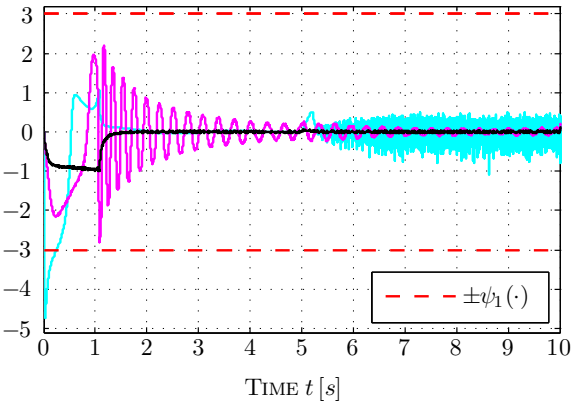

(d) *error derivative* $\dot{e}(\cdot)$ *and subboundary* $\psi_1(\cdot)$

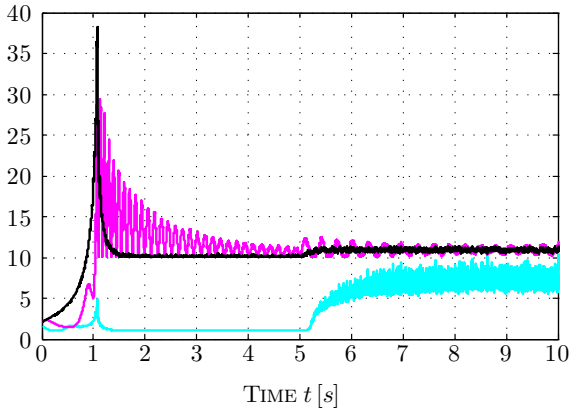

(e) *gain* $k_0(\cdot)$ *and* $k(\cdot)$

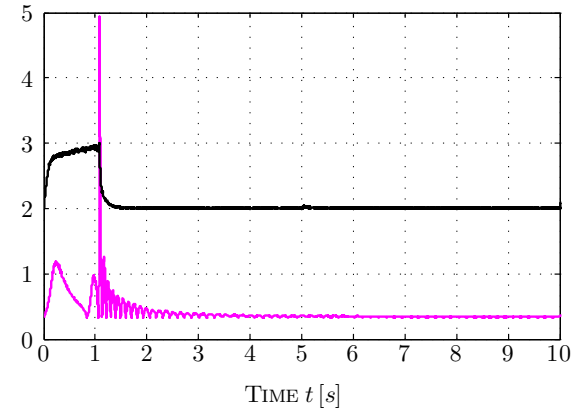

(f) *gain* $k_1(\cdot)$

Figure 4.8: *Simulation results for set-point tracking under load of closed-loop systems* ——(3.80),(4.60), ——(3.80),(4.65) *and* ——(3.80),(4.67) *with parametrization as in Tab. 3.1 & 4.1.*

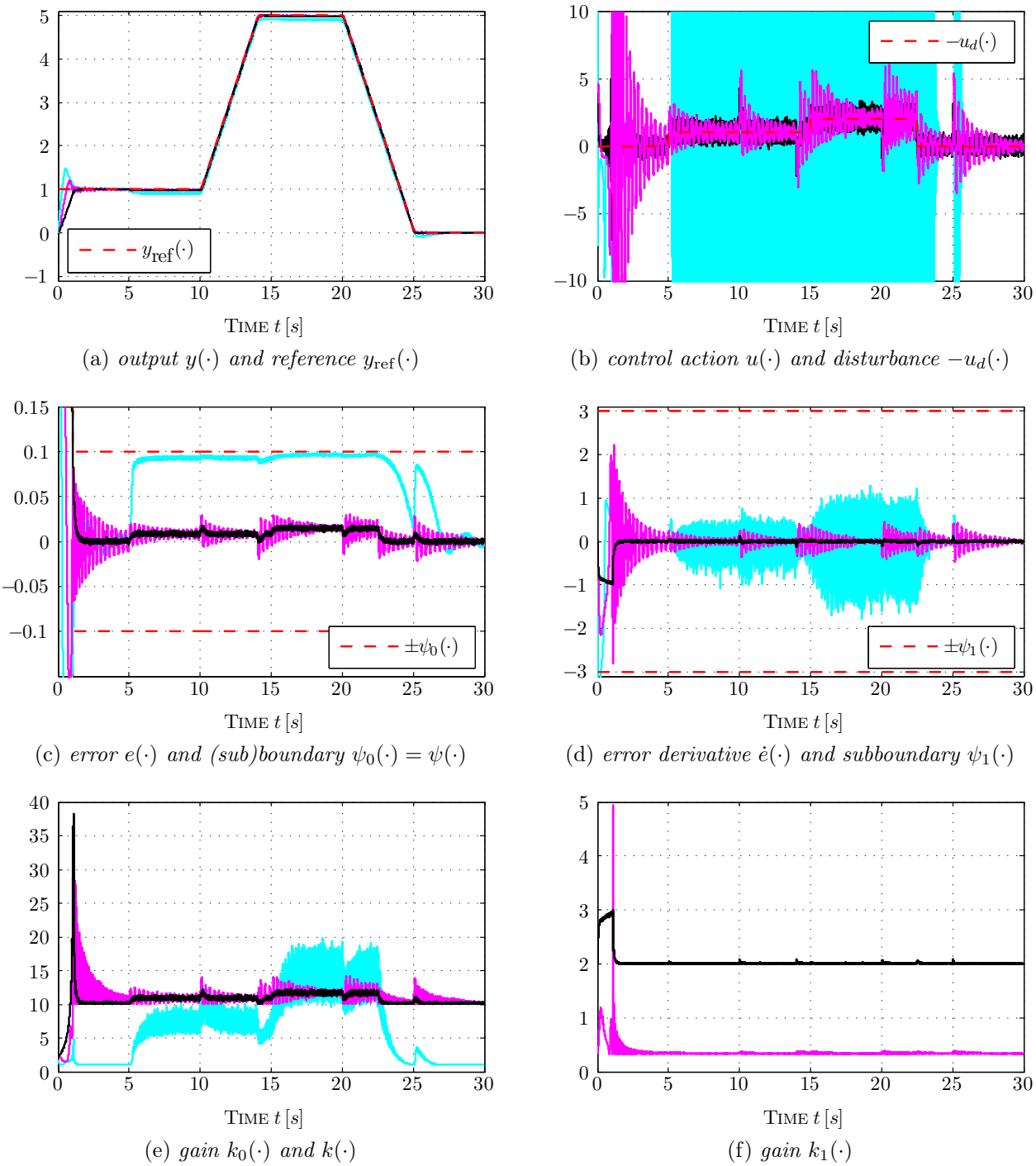

(a) *output* $y(\cdot)$ *and reference* $y_{\text{ref}}(\cdot)$

(b) *control action* $u(\cdot)$ *and disturbance* $-u_d(\cdot)$

(c) *error* $e(\cdot)$ *and (sub)boundary* $\psi_0(\cdot) = \psi(\cdot)$

(d) *error derivative* $\dot{e}(\cdot)$ *and subboundary* $\psi_1(\cdot)$

(e) *gain* $k_0(\cdot)$ *and* $k(\cdot)$

(f) *gain* $k_1(\cdot)$

Figure 4.9: *Simulation results for reference tracking under load of closed-loop systems* ——(3.80),(4.60), ——(3.80),(4.65) *and* ——(3.80),(4.67) *with parametrization as in Tab. 3.1 & 4.1.*

Chapter 5

Applications

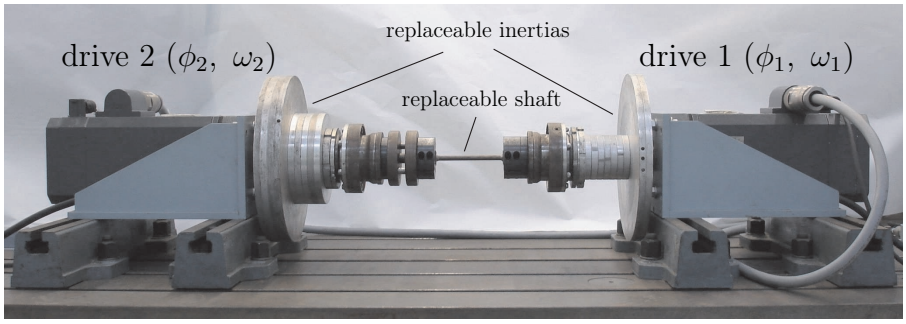

Figure 5.1: *Laboratory setup: coupled electrical drives.*

In the previous chapters, the *generalized high-gain adaptive control problem* has been solved for systems of class $\mathcal{S}_1$ and for systems of class $\mathcal{S}_2$. The presented adaptive λ-tracking controllers and funnel controllers guarantee that control objectives (co_1) & (co_2) and (co_1), (co_2) & (co_3) are accomplished, respectively, for any system of class $\mathcal{S}_1$ and class $\mathcal{S}_2$.

It remains to prove that these high-gain adaptive controllers are applicable in "real world"—e.g. at the laboratory setup depicted in Fig. 5.1—and so the *high-gain adaptive motion control problem* is solvable. In this chapter, it will be shown that the following applications are feasible:

- high-gain adaptive speed control of industrial servo-systems (see Section 5.2.2),
- high-gain adaptive position control of industrial servo-systems (see Section 5.2.3) and
- position funnel control of rigid revolute joint robotic manipulators (see Section 5.3).

5.1 Mathematical preliminaries

For the following argumentation and implementation, two more mathematical preliminaries are needed. It will be shown that (i) the use of internal models is also admissible for system classes $\mathcal{S}_1$ and $\mathcal{S}_2$ and (ii) the LuGre friction operators, introduced in Section 1.4.5, are element of operator class $\mathcal{T}$.

5.1.1 Internal model for system classes $\mathcal{S}_1$ and $\mathcal{S}_2$

The presented high-gain adaptive controllers in Chapters 3 & 4 are "memoryless" or "proportional" controllers (i.e. no dynamic control action is incorporated). As is well known (see e.g. [113]): for constant references and/or disturbances (or such exogenous signals approaching constant limits asymptotically) proportional controllers, in general, do not achieve steady state accuracy (i.e. $\lim_{t\to\infty} e(t) = 0$). Often integral control action is required. Therefore, following the internal model principle (see Section 2.4) a proportional-integral internal model is presented. It is similar to a PI controller and assures zero tracking errors for constant references and/or disturbances if steady state is reached.

First a general technicality is shown. In Section 2.4 it has been established that any minimum-phase LTI SISO system with relative degree zero and positive high-frequency gain connected in series to a system of class $\mathcal{S}_1^{\text{lin}}$ or class $\mathcal{S}_2^{\text{lin}}$ yields an inter-connected system of class $\mathcal{S}_1^{\text{lin}}$ or class $\mathcal{S}_2^{\text{lin}}$ (see Lemma 2.39). A similar result holds true for system classes $\mathcal{S}_1$ and $\mathcal{S}_2$.

Lemma 5.1 (Serial interconnection of internal model and system of class $\mathcal{S}_1$ (or $\mathcal{S}_2$))**.**
Consider a system of form (1.36) element of class $\mathcal{S}_1$ (or $\mathcal{S}_2$). If internal model (2.103) is a minimal realization of (2.101) and $\widehat{\boldsymbol{x}}^0(\cdot) \in \mathcal{C}([-h,0];\mathbb{R}^p)$ such that $\widehat{\boldsymbol{x}}^0(0) = \widehat{\boldsymbol{x}}_0$, then the serial interconnection of system (1.36) and internal model (2.103), given by

$$\left.\begin{aligned} \tfrac{d}{dt}\begin{pmatrix}\boldsymbol{x}(t)\\ \widehat{\boldsymbol{x}}(t)\end{pmatrix} &= \begin{bmatrix}\boldsymbol{A} & \boldsymbol{b}\widehat{\boldsymbol{c}}^\top\\ \boldsymbol{O}_{p\times n} & \widehat{\boldsymbol{A}}\end{bmatrix}\begin{pmatrix}\boldsymbol{x}(t)\\ \widehat{\boldsymbol{x}}(t)\end{pmatrix} + \begin{pmatrix}\widehat{\gamma}_0\boldsymbol{b}\\ \widehat{\boldsymbol{b}}\end{pmatrix} v(t) + \begin{pmatrix}\boldsymbol{b}\\ \boldsymbol{0}_p\end{pmatrix} u_d(t) + \begin{bmatrix}\boldsymbol{B}_{\mathfrak{T}}\\ \boldsymbol{O}_{p\times m}\end{bmatrix}\big((\mathfrak{T}\boldsymbol{x})(t) + \boldsymbol{d}(t)\big)\\ y(t) &= \big(\boldsymbol{c}^\top,\ \boldsymbol{0}_p^\top\big)\begin{pmatrix}\boldsymbol{x}(t)\\ \widehat{\boldsymbol{x}}(t)\end{pmatrix}, \qquad \begin{pmatrix}\boldsymbol{x}\\ \widehat{\boldsymbol{x}}\end{pmatrix}\Big|_{[-h,0]} = \begin{pmatrix}\boldsymbol{x}^0(\cdot)\\ \widehat{\boldsymbol{x}}^0(\cdot)\end{pmatrix} \in \mathcal{C}\big([-h,0];\,\mathbb{R}^{n+p}\big), \end{aligned}\right\} \tag{5.1}$$

is again element of system class $\mathcal{S}_1$ (or $\mathcal{S}_2$).

Proof of Lemma 5.1.
Define

$$\widetilde{\boldsymbol{x}} := \begin{pmatrix}\boldsymbol{x}\\ \widehat{\boldsymbol{x}}\end{pmatrix} \in \mathbb{R}^{n+p}, \quad \widetilde{\boldsymbol{A}} := \begin{bmatrix}\boldsymbol{A} & \boldsymbol{b}\widehat{\boldsymbol{c}}^\top\\ \boldsymbol{O}_{p\times n} & \widehat{\boldsymbol{A}}\end{bmatrix} \in \mathbb{R}^{(n+p)\times(n+p)}, \quad \widetilde{\boldsymbol{b}} := \begin{pmatrix}\widehat{\gamma}_0\boldsymbol{b}\\ \widehat{\boldsymbol{b}}\end{pmatrix} \in \mathbb{R}^{n+p},$$
$$\widetilde{\boldsymbol{B}}_{\mathfrak{T}} := \begin{bmatrix}\boldsymbol{b} & \boldsymbol{B}_{\mathfrak{T}}\\ \boldsymbol{0}_p & \boldsymbol{O}_{p\times m}\end{bmatrix} \in \mathbb{R}^{(n+p)\times(m+1)}, \quad \widetilde{\boldsymbol{c}} := \begin{pmatrix}\boldsymbol{c}\\ \boldsymbol{0}_p\end{pmatrix} \in \mathbb{R}^{n+p}, \quad \widetilde{u}_d(\cdot) = 0, \quad \widetilde{\boldsymbol{d}}(\cdot) := \begin{pmatrix}u_d(\cdot)\\ \boldsymbol{d}(\cdot)\end{pmatrix}$$

and

$$\widetilde{\mathfrak{T}}\colon \mathcal{C}([-h,\infty);\mathbb{R}^{n+p}) \to \mathcal{L}^\infty_{\text{loc}}(\mathbb{R}_{\geq 0};\mathbb{R}^{m+1}), \qquad (\widetilde{\mathfrak{T}}\widetilde{\boldsymbol{x}})(t) := \begin{pmatrix}0\\ (\mathfrak{T}\boldsymbol{x})(t)\end{pmatrix}.$$

Then it is easy to see that (5.1) may be expressed in the form (1.36). Moreover, system properties ($\mathcal{S}_1$-sp$_1$) and ($\mathcal{S}_1$-sp$_2$) (or ($\mathcal{S}_2$-sp$_1$) and ($\mathcal{S}_2$-sp$_2$)) follow from Lemma 2.39 (see Assertions (i)-(iii)). Since $\widetilde{\mathfrak{T}} \in \mathcal{T}$ with $M_{\widetilde{\mathfrak{T}}} := M_{\mathfrak{T}} < \infty$, $\widetilde{u}_d(\cdot) \in \mathcal{L}^\infty([-h,\infty);\mathbb{R})$ and $\widetilde{\boldsymbol{d}}(\cdot) \in \mathcal{L}^\infty([-h,\infty);\mathbb{R}^{m+1})$, system properties ($\mathcal{S}_1$-sp$_3$) and ($\mathcal{S}_1$-sp$_4$) (or ($\mathcal{S}_2$-sp$_3$) and ($\mathcal{S}_2$-sp$_4$)) are satisfied. Furthermore, ($\mathcal{S}_1$-sp$_5$) (or ($\mathcal{S}_2$-sp$_5$)) trivially holds. This completes the proof. □

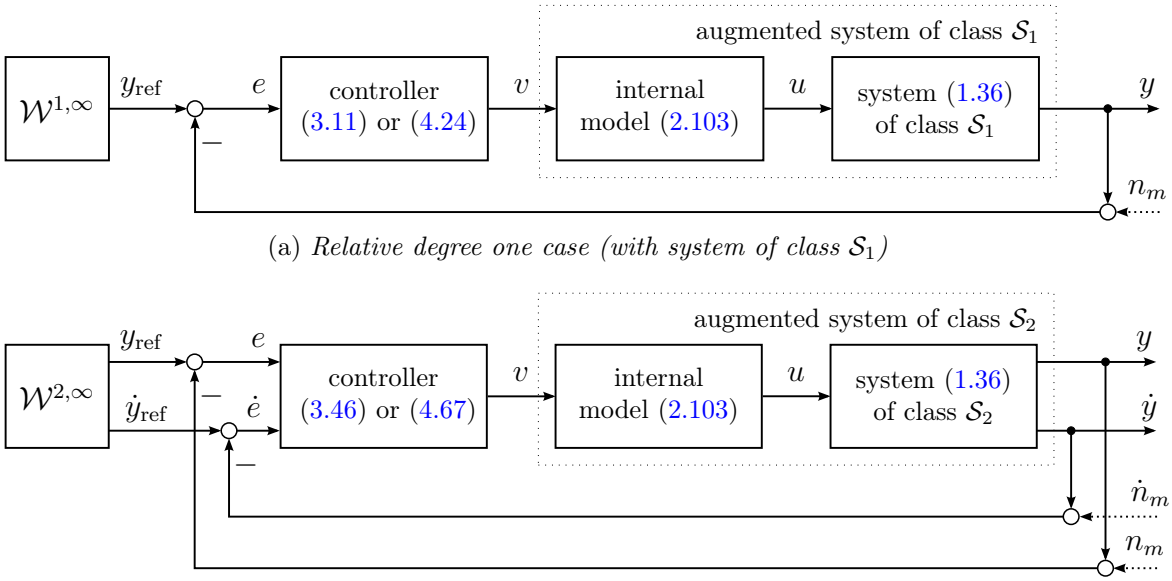

(a) *Relative degree one case (with system of class $\mathcal{S}_1$)*

(b) *Relative degree two case (with system of class $\mathcal{S}_2$)*

Figure 5.2: *High-gain adaptive closed-loop systems with internal model.*

For the following denote the "controller combination" (serial interconnection) of some controller (C) and some internal model (IM) by (C)+(IM), then

- Lemma 5.1 combined with Theorem 3.3 or Theorem 4.4 allows for application of controller combination (3.11)+(2.103) or (4.24)+(2.103) to system (1.36) of class $\mathcal{S}_1$;
- Lemma 5.1 combined with Theorem 3.13 or Theorem 4.13 allows for application of controller combination (3.46)+(2.103) or (4.67)+(2.103) to system (1.36) of class $\mathcal{S}_2$.

The resulting closed-loop systems are depicted in Fig. 5.2(a) and (b). Note that, for reference classes $\mathcal{W}^{1,\infty}(\mathbb{R}_{\geq 0};\mathbb{R})$ and $\mathcal{W}^{2,\infty}(\mathbb{R}_{\geq 0};\mathbb{R})$, an internal model of form (2.103) not necessarily guarantees asymptotic tracking.

However, if reference and/or disturbance are restricted to constant signals and the closed-loop system attains steady state, then a PI controller (as internal model) assures zero tracking errors. A PI controller has the following transfer function

$$F_{PI}(s) = \frac{u(s)}{v(s)} = k_P + \frac{k_I}{s} = \frac{k_I + k_P\, s}{s}, \qquad k_I, k_P > 0, \tag{5.2}$$

from input $v(s)$ to output $u(s)$. For $k_P > 0$, it is easy to see that $\deg(s) - \deg(k_I + k_P\, s) = 0$ and $\lim_{s\to\infty} k_P + k_I/s = k_P > 0$. Hence PI controller (5.2) has relative degree zero and positive high-frequency gain. Moreover, since $k_I + k_P\, s$ is Hurwitz for $k_I/k_P > 0$, the controller is minimum-phase. A minimal realization of (5.2) is given by

$$\left.\begin{aligned} \dot{x}_I(t) &= v(t), & x_I(0) &= 0, \\ u(t) &= k_P\, v(t) + k_I\, x_I(t), & k_I, k_P &> 0. \end{aligned}\right\} \tag{5.3}$$

The observations above are recorded in the following corollary.

Corollary 5.2. *Consider a serial interconnection of system (1.36) and proportional-integral internal model (5.3) with "new" control input $v(t)$.*

(i) If system (1.36) is element of class $\mathcal{S}_1$, $y_{\text{ref}}(\cdot) \in \mathcal{W}^{1,\infty}(\mathbb{R}_{\geq 0};\mathbb{R})$, $\varsigma(\cdot) \in \mathcal{B}_1$ and $\psi(\cdot) \in \mathcal{B}_1$ such that $\psi(0) > |y_{\text{ref}}(0) - \boldsymbol{c}^\top \boldsymbol{x}^0(0)|$, then

(a) application of adaptive λ-tracking controller (3.11) and funnel controller (4.24) is admissible, respectively, and

(b) for the closed-loop systems (1.36), (3.11)+(5.3) and (1.36), (4.24)+(5.3) with tracking error $e(t) = y_{\text{ref}}(t) - y(t)$ the following holds:

$$\forall\, t \geq 0\colon \qquad |e(t)| = \frac{|\dot{x}_I(t)|}{k(t)};$$

(ii) If system (1.36) is element of class $\mathcal{S}_2$, $y_{\text{ref}}(\cdot) \in \mathcal{W}^{2,\infty}(\mathbb{R}_{\geq 0};\mathbb{R})$, $\varsigma_0(\cdot), \varsigma_1(\cdot) \in \mathcal{B}_1$ and $(\psi_0(\cdot),\, \psi_1(\cdot)) \in \mathcal{B}_2$ such that $\psi_0(0) > |y_{\text{ref}}(0) - \boldsymbol{c}^\top \boldsymbol{x}^0(0)|$ and $\psi_1(0) > |\dot{y}_{\text{ref}}(0) - \boldsymbol{c}^\top \boldsymbol{A}\boldsymbol{x}^0(0)|$, then

(a) application of adaptive λ-tracking controller (3.46) and funnel controller (4.67) with derivative feedback is admissible, respectively, and

(b) for closed-loop system (1.36), (3.46)+(5.3) and (1.36), (4.67)+(5.3) with tracking error $e(t) = y_{\text{ref}}(t) - y(t)$ the following holds respectively:

$$\forall\, t \geq 0\colon \qquad |e(t)| \leq \frac{|\dot{x}_I(t)|}{k(t)^2} + q_1 \frac{|\dot{e}(t)|}{k(t)} \qquad \text{and} \qquad |e(t)| \leq \frac{|\dot{x}_I(t)|}{k_0(t)^2} + k_1(t) \frac{|\dot{e}(t)|}{k_0(t)};$$

(iii) if steady state is reached, i.e. $\lim_{t\to\infty} \frac{d}{dt}\left(\boldsymbol{x}(t), x_I(t)\right) = \boldsymbol{0}_{n+1}$, and $\lim_{t\to\infty} \dot{y}_{\text{ref}}(t) = 0$, then $\lim_{t\to\infty} e(t) = 0$ for each closed-loop system.

Proof of Corollary 5.2.

Substitute $v(t)$ for $u(t)$ in (3.11), (4.24), (3.46) and (4.67), then Assertions (i)(a) and (ii)(a) follow from Lemma 5.1 and Theorems 3.3, 4.4, 3.13 and 4.13, respectively. Inserting (3.11), (4.24), (3.46) and (4.67) (with $u(t)$ replaced by $v(t)$) into (5.3) and solving for $|e(t)|$ yields Assertions (i)(b) and (ii)(b), respectively. Note that, for $\lim_{t\to\infty} \dot{\boldsymbol{x}}(t) = \boldsymbol{0}_n$ and $\lim_{t\to\infty} \dot{y}_{\text{ref}}(t) = 0$, the following holds $\lim_{t\to\infty} \dot{e}(t) = \lim_{t\to\infty} \left(\dot{y}_{\text{ref}}(t) - \boldsymbol{c}^\top \dot{\boldsymbol{x}}(t)\right) = 0$. Then Assertion (iii) follows from $\lim_{t\to\infty} \dot{x}_I(t) = 0$ and Assertions (i)(b) and (ii)(b). □

The advantageous effect of a PI controller (or internal model (5.3)) on the control performance is well known in industry (see [166, p. 81-82]). Concerning high-gain adaptive speed control of electrical drives, the idea of connecting a PI controller in series to a high-gain adaptive controller was first noted in [64, Section 4.1.3] and then published in [170]. For position control a similar result has been accepted for publication in "International Journal of Control" (see [65]).

5.1.2 Friction operators element of operator class

In Section 1.4.5, based on the LuGre friction model introduced in [39], friction has been modeled as (dynamic) operator. It will be shown that operator class $\mathcal{T}$ (see Definition 1.5) subsumes both

friction operators: the (general) "LuGre friction operator" $\mathfrak{L}_{\vartheta^0}$ as in (1.21) and the "simplified LuGre friction operator" $\mathfrak{F}$ as in (1.22) (where viscous friction is excluded).

Lemma 5.3. *The "LuGre friction operator" $\mathfrak{L}_{\vartheta^0}$ as in (1.21), parametrized by $\vartheta^0 \in \mathbb{R}$, is element of operator class $\mathcal{T}$.*

Proof of Lemma 5.3.

It suffices to check operator properties (op_1), (op_2) and (op_3) of Definition 1.5.

Step 1: It is shown that (op_1), (op_2) and $(op_3)(a)$ hold true.
In view of (1.21) and Definition 1.5, Property (op_1) is readily verified and it follows that $h = 0$. To show Property (op_2), choose $\delta > 0$ arbitrarily and let $\omega(\cdot) \in \mathcal{C}(\mathbb{R}_{\geq 0}; \mathbb{R})$ such that $\sup_{t\geq 0} |\omega(t)| < \delta$, which with (1.16), (1.20), (1.14) and boundedness of the solution $\vartheta_{\omega(\cdot)}$ as in (1.19) implies

$$\forall\, t \geq 0\colon\ |(\mathfrak{L}_{\vartheta^0}\omega)(t)| \leq \sigma\, \max\{u_S/\sigma,\, |\vartheta^0|\} + \nu_D\, \delta \left(1 + \frac{\sigma}{u_C} \max\{u_S/\sigma,\, |\vartheta^0|\}\right) + \nu\delta^{\delta_V} =: \Delta.$$

Hence, Property (op_2) is satisfied. To show Property (op_3)(a), choose $\omega_1(\cdot), \omega_2(\cdot) \in \mathcal{C}(\mathbb{R}_{\geq 0}; \mathbb{R})$ such that the following holds

$$\forall t \geq 0\, \forall\, \tau \in [0, t]\colon \qquad \omega_1(\tau) = \omega_2(\tau). \tag{5.4}$$

Then, for any $\vartheta^0 \in \mathbb{R}$, uniqueness of the solution of the initial-value problem (1.18) and (5.4) imply

$$\forall \tau \in [0, t]\colon \qquad \vartheta_{\omega_1(\cdot)}(\tau) = \vartheta_{\omega_2(\cdot)}(\tau),$$

whence $(\mathfrak{L}_{\vartheta^0}\omega_1)(\tau) = (\mathfrak{L}_{\vartheta^0}\omega_2)(\tau)$ for all $\tau \in [0, t]$, i.e. Property (op_3)(a) and completes Step 1.

Step 2: It is shown that Property $(op_3)(b)$ holds true.
For $\sigma > 0$, $f_D(\cdot)$ as in (1.20), $\beta(\cdot)$ as in (1.16) and $f_V(\cdot)$ as in (1.14), define the functions

$$g_1\colon\ \mathbb{R} \times \mathbb{R} \to \mathbb{R}, \qquad (\omega,\, \vartheta) \mapsto g_1(\omega,\, \vartheta) := \omega - \sigma \frac{|\omega|}{\beta(\omega)} \vartheta$$

and

$$g_2\colon\ \mathbb{R} \times \mathbb{R} \to \mathbb{R}, \qquad (\omega, \vartheta) \mapsto g_2(\omega, \vartheta) := f_D(\omega) g_1(\omega,\, \vartheta) + f_V(\omega). \tag{5.5}$$

Observe that, $g_1(\cdot, \cdot)$ and $g_2(\cdot, \cdot)$ are locally Lipschitz in ω and ϑ, respectively. More precisely, for any compact $\mathfrak{C} \subset \mathbb{R} \times \mathbb{R}$, the following hold

$$\exists\, L_1 > 0\ \forall\, (\omega_1, \vartheta_1),\, (\omega_2, \vartheta_2) \in \mathfrak{C}\colon\ |g_1(\omega_1, \vartheta_1) - g_1(\omega_2, \vartheta_2)| \leq L_1 \left(|\omega_1 - \omega_2| + |\vartheta_1 - \vartheta_2|\right) \tag{5.6}$$

and

$$\exists\, L_2 > 0\ \forall\, (\omega_1, \vartheta_1),\, (\omega_2, \vartheta_2) \in \mathfrak{C}\colon\ |g_2(\omega_1, \vartheta_1) - g_2(\omega_2, \vartheta_2)| \leq L_2 \left(|\omega_1 - \omega_2| + |\vartheta_1 - \vartheta_2|\right). \tag{5.7}$$

Choose $\omega_1(\cdot), \omega_2(\cdot) \in \mathcal{C}(\mathbb{R}_{\geq 0}; \mathbb{R})$ such that, for arbitrary $t \geq 0$, the following is satisfied

$$\begin{array}{rll} \forall\, \tilde{\omega}(\cdot) \in \mathcal{C}([0,t];\mathbb{R}): & \omega_1|_{[0,t]} = \tilde{\omega} = \omega_2|_{[0,t]} & \text{and} \\ \exists \delta, \tau > 0\ \forall\, s \in [t, t+\tau]: & \omega_1(s), \omega_2(s) \in [\tilde{\omega}(t) - \delta,\, \tilde{\omega}(t) + \delta] \end{array} \tag{5.8}$$

and define

$$M := \max_{s \in [0,t]} |\tilde{\omega}(s)| + \delta.$$

For $\vartheta^0 \in \mathbb{R}$, denote the corresponding solution of the initial-value problem (1.18) by

$$\vartheta_1(\cdot) := \vartheta(\cdot, \vartheta^0, \omega_1(\cdot)) \quad \text{and} \quad \vartheta_2(\cdot) := \vartheta(\cdot, \vartheta^0, \omega_1(\cdot)),$$

respectively. Note that, due to (1.19), $\vartheta_1(\cdot)$ and $\vartheta_2(\cdot)$ are globally defined and uniformly bounded on $\mathbb{R}_{\geq 0}$. In view of (5.8), same argumentation as in Step 1 yields $\vartheta_1(\alpha) = \vartheta_2(\alpha)$ for all $\alpha \in [0, t]$. Hence, for

$$\mathfrak{C} := [-M,\, M] \times \Big[-\max\{u_S/\sigma,\, |\vartheta^0|\},\, \max\{u_S/\sigma,\, |\vartheta^0|\} \Big], \tag{5.9}$$

the following holds for all $s \in [t,\, t+\tau]$

$$\begin{aligned} |\vartheta_1(s) - \vartheta_2(s)| &\overset{(1.18)}{\leq} |\underbrace{\vartheta_1(t) - \vartheta_2(t)}_{=0}| + \int_t^s \big| g_1(\omega_1(\alpha), \vartheta_1(\alpha)) - g_1(\omega_2(\alpha), \vartheta_2(\alpha)) \big| \,\mathrm{d}\alpha \\ &\overset{(5.7)}{\leq} L_1 \int_t^s \big(|\omega_1(\alpha) - \omega_2(\alpha)| + |\vartheta_1(\alpha) - \vartheta_2(\alpha)| \big) \,\mathrm{d}\alpha\,. \end{aligned} \tag{5.10}$$

Applying Theorem 1.4 in [18, p. 5] (a special version of the Bellman-Gronwall Lemma) yields

$$\begin{aligned} \forall\, s \in [t,\, t+\tau]: \quad |\vartheta_1(s) - \vartheta_2(s)| &\leq L_1 \int_t^s \exp(L_1(s-\alpha))\, |\omega_1(\alpha) - \omega_2(\alpha)| \,\mathrm{d}\alpha \\ &\leq L_1 \max_{s \in [t,t+\tau]} |\omega_1(s) - \omega_2(s)| \int_t^s \exp(L_1(s-\alpha)) \,\mathrm{d}\alpha \\ &\leq \max_{s \in [t,t+\tau]} |\omega_1(s) - \omega_2(s)| \Big(\exp\left(L_1(s-t)\right) - 1 \Big) \\ &\leq \Big(\exp\left(L_1 \tau\right) - 1 \Big) \max_{s \in [t,t+\tau]} |\omega_1(s) - \omega_2(s)|. \end{aligned} \tag{5.11}$$

Now, for $\mathfrak{C}$ as in (5.9), it follows that for all $s \in [t,\, t+\tau]$

$$\begin{aligned}
|(\mathfrak{L}_{\vartheta^0}\omega_1)(s) - (\mathfrak{L}_{\vartheta^0}\omega_2)(s)| &\overset{(1.21)}{\leq} \sigma|\vartheta_1(s) - \vartheta_2(s)| + \big|g_2(\omega_1(s),\vartheta_1(s)) - g_2(\omega_2(s),\vartheta_2(s))\big| \\
&\overset{(5.6),(5.11)}{\leq} \sigma\left(\exp(L_1\tau) - 1\right) \max_{s\in[t,t+\tau]} |\omega_1(s) - \omega_2(s)| \\
&\quad + L_2\left(|\omega_1(s) - \omega_2(s)| + |\vartheta_1(s) - \vartheta_2(s)|\right) \\
&\overset{(5.11)}{\leq} \underbrace{\Big[(\sigma + L_2)\big(\exp(L_2\tau) - 1\big) + L_2\Big]}_{=:c_0} \max_{s\in[t,t+\tau]} |\omega_1(s) - \omega_2(s)|
\end{aligned}$$

which shows Property (op_3)(b) and completes the proof. □

For modeling of 1MS and 2MS as in (1.24) and (1.26), it is assumed that viscous friction is linear (i.e. $\delta_V = 1$ in (1.14)) on motor and load side. So the (general) "LuGre friction operator" $\mathfrak{L}_{\vartheta^0}$ as in (1.21) reduces to the "simplified LuGre friction operator" $\mathfrak{F}$ as in (1.22).

Corollary 5.4. *The "simplified LuGre friction operator" $\mathfrak{F}$ as in (1.22) is element of operator class $\mathcal{T}$.*

Proof of Corollary 5.4. Set $f_V(\cdot) = 0$ in (5.5), then it is easy to see that Corollary 5.4 directly follows from Lemma 5.3. □

5.2 Speed and position control of industrial servo-systems

In this section the *high-gain adaptive motion control problem* (see Section 1.6.1) will be solved for stiff and elastic industrial servo-systems.

From a theoretical point of view, to prove applicability of the high-gain adaptive controllers presented in Chapters 3 & 4 for speed and position control, it suffices to show that 1MS (1.24), (1.25) and 2MS (1.26), (1.27) (without saturation) are or "can be made" element of system classes $\mathcal{S}_1$ and $\mathcal{S}_2$. Corresponding proofs are presented in Section 5.2.2 for speed control and in Section 5.2.3 for position control. If affiliation is assured, then the results presented in Chapters 3 & 4 can directly be transferred to the high-gain adaptive motion control problem. Affiliation depends on application and instrumentation configuration. It will be shown that:

- the *high-gain adaptive speed control problem* of 1MS and 2MS is a subproblem of finding high-gain adaptive controllers for system class $\mathcal{S}_1$;
- the *high-gain adaptive position control problem* of 1MS and 2MS is a subproblem of finding high-gain adaptive controllers for system class $\mathcal{S}_2$;
- in the presence of actuator saturation, application of funnel controller (4.24) for speed control and application of funnel controller (4.67) with derivative feedback for position control is admissible. Theorem 4.7 and Theorem 4.15 cover input saturation: for $\hat{u} = \hat{u}_A$ and $u_A = u_F$, saturated funnel controller (4.53) or (4.104) incorporates the serial interconnection of funnel controller (4.24) or (4.67) and saturated actuator (1.9), respectively (see illustrations in Fig. 5.3).

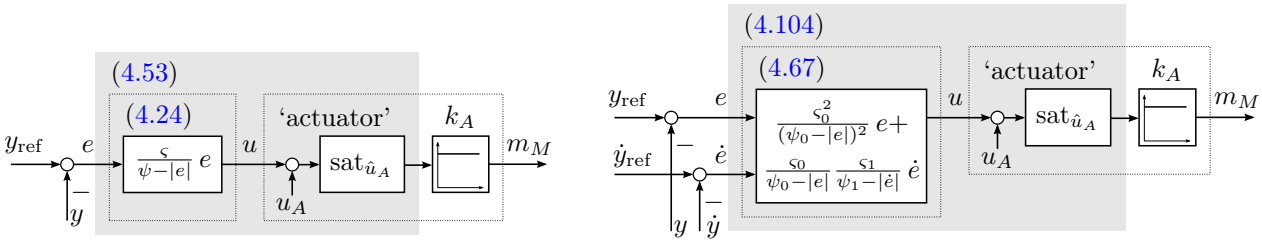

(a) *relative degree one case (speed control)* (b) *relative degree two case (position control)*

Figure 5.3: *Serial interconnection of funnel controller and 'actuator' with saturation.*

From a practical point of view, to prove applicability of the high-gain adaptive controllers for speed and position control of industrial servo-systems, implementation in "real world" is necessary. Comparative measurement results are presented in Section 5.2.2.3 for speed control and in Section 5.2.3.3 for position control of 1MS and 2MS, respectively. However, not all high-gain adaptive controllers, introduced in the previous chapters, are reasonable for application (recall e.g. simulation studies in Sections 3.5.4 and 4.4.3), only the most promising are selected for implementation:

- the *high-gain adaptive controllers with output feedback for systems of class* $\mathcal{S}_1$—i.e. the adaptive λ-tracking controller (3.11), the funnel controller (4.24) and the funnel controller with saturation (4.53)—are applied for *speed control of 1MS and 2MS*;
- the *high-gain adaptive controllers with derivative feedback for systems of class* $\mathcal{S}_2$—i.e. the adaptive λ-tracking controller (3.46), the funnel controller (4.67) and the funnel controller with saturation (4.104)—are applied for *position control of 1MS and 2MS*.

These controllers are implemented at the laboratory setup (see Fig. 5.1) of the Institute of Electrical Drive Systems and Power Electronics. To allow for a "fair" comparison with standard PI/PID control and to achieve steady state accuracy, also the controller combinations (3.11)+(5.3), (4.24)+(5.3), (3.46)+(5.3) and (4.67)+(5.3) with proportional-integral internal model (5.3) are implemented. First a brief description of the laboratory setup is given, then speed control and position control are discussed.

5.2.1 Laboratory setup: coupled electrical drives

The laboratory setup is depicted in Fig. 5.1. It consists of two permanent magnetic synchronous machines and power inverters coupled by a (flexible) shaft. The coupling is gear-less (i.e. $g_r = 1$). Both drives—machines and inverters—are identical in construction. Each machine is driven independently by its own power inverter. So drive 1 (with position ϕ_1 and speed ω_1) or drive 2 (with position ϕ_2 and speed ω_2) allows to emulate a motor drive or a load drive.

The motor drive generates the motor torque $m_M(\cdot)$ [Nm] and accelerates or decelerates the coupled load under speed or position control, whereas the load drive induces the load torque $m_L(\cdot)$ [Nm]. Both drives are subject to bounded actuator deviation $u_A(\cdot)$ [Nm] where $\|u_A\|_\infty < 0.6$ [Nm] (measured), have actuator gain $k_A \approx 1$ [1] (measured) and are constrained by saturation level $\hat{u}_A = 22$ [Nm] (specified for protection of the machines). Torque generation is (acceptably) fast: torque reference steps are tracked with delay times of $T_\sigma \approx 2 \cdot 10^{-3}$ [s] (see

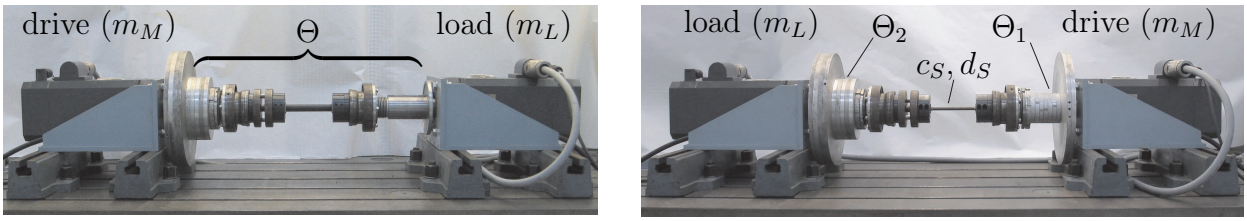

(a) *"stiff" one-mass system ('1MS')* (b) *elastic two-mass system (2MS)*

Figure 5.4: *Emulated industrial servo-systems at the laboratory setup.*

Fig. 5.5). Both drives are operated via a standard PC (*Intel Pentium 4, 3Ghz, 2GB Ram*) running the real-time operating system *xPC-Target v1.6* by *Mathworks* with fixed sampling time $T_S = 1{\cdot}10^{-3}$ [s]. Depending on the selection of the motor drive, reference torque $u(\cdot) = m_{M,\mathrm{ref}}(\cdot)$ (control input) is send to either inverter 1 or to inverter 2 via CAN-Bus (baud rate 1Mbps, *SOFTING CAN-AC2 PCI* board). An additional host computer (*Intel Pentium 4, 3Ghz, 2GB Ram, 80GB HD*), running *Windows XP SP1*, is used for monitoring, rapid-prototyping and data streaming. Rapid-prototyping is done in *MATLAB/SIMULINK (Version 7.0.1)*. The implemented controllers are compiled and then downloaded as executable program to the real-time xPC target system via *Ethernet (100Mbit LAN)*.

The build-in *HEIDENHAIN RON 3350 encoders*—with 2048 lines per revolution and 12-bit interpolation ($2^{12} = 4096$)—provide position information $\phi_1(\cdot)$ [rad] for drive 1 and $\phi_2(\cdot)$ [rad] for drive 2 which allows for field-oriented (torque) control of each drive. The installed PCI board *HEIDENHAIN IK220* (capturing interface) evaluates the encoder signals simultaneously and synchronously. By numeric differentiation, it computes the speed signals $\omega_1(\cdot)$ [rad/s] for drive 1 and $\omega_2(\cdot)$ [rad/s] for drive 2 with time delays smaller than $50 \cdot 10^{-6}$ [s] (see User's manual). Position measurement and speed measurement are deteriorated by bounded measurement errors (see Section 1.4.4) subsumed in $n_{m1}(\cdot)$ [rad] and $\dot{n}_{m1}(\cdot)$ [rad/s] for drive 1 and $n_{m2}(\cdot)$ [rad] and $\dot{n}_{m2}(\cdot)$ [rad/s] for drive 2, respectively, where $\|n_{m1}\|_\infty$, $\|n_{m2}\|_\infty < 6 \cdot 10^{-5}$ [rad] and $\|\dot{n}_{m1}\|_\infty$, $\|\dot{n}_{m2}\|_\infty < 4 \cdot 10^{-2}$ [rad/s] (measured).

The stiff 1MS (1.24), (1.25) and the elastic 2MS (1.26), (1.27) are emulated at the laboratory setup by using different shafts and different inertia ratios. Shaft and inertias are replaceable. Inertia Θ_1 and Θ_2 [kg m^2] can be modified via diverse mountable inertia wheels (e.g. differing in mass and radius, see Fig. 5.1 and Tab. D.2). The replaceable shafts differ in stiffness c_S [Nm/rad] and damping d_S [Nms/rad]. Two typical configurations are depicted in Fig. 5.4. The linearized models in the frequency domain (transfer functions) of these configurations are given by (see e.g. [166, p. 948 ff.])

$$F_{\text{'1MS'}}(s) = \frac{\omega_2(s)}{m_M(s)} = \frac{k_A}{s\,(\Theta_1+\Theta_2)} \cdot \frac{s^2 \frac{\Theta_2}{c_S} + s\,\frac{d_S}{c_S} + 1}{s^2 \frac{\Theta_1\Theta_2}{c_S(\Theta_1+\Theta_2)} + s\,\frac{d_S}{c_S} + 1} \quad \text{(for conf. in Fig. 5.4(a))}$$

and

$$F_{\text{2MS}}(s) = \frac{\omega_2(s)}{m_M(s)} = \frac{k_A}{s\,(\Theta_1+\Theta_2)} \cdot \frac{s\,\frac{d_S}{c_S} + 1}{s^2 \frac{\Theta_1\Theta_2}{c_S(\Theta_1+\Theta_2)} + s\,\frac{d_S}{c_S} + 1} \quad \text{(for conf. in Fig. 5.4(b))}$$

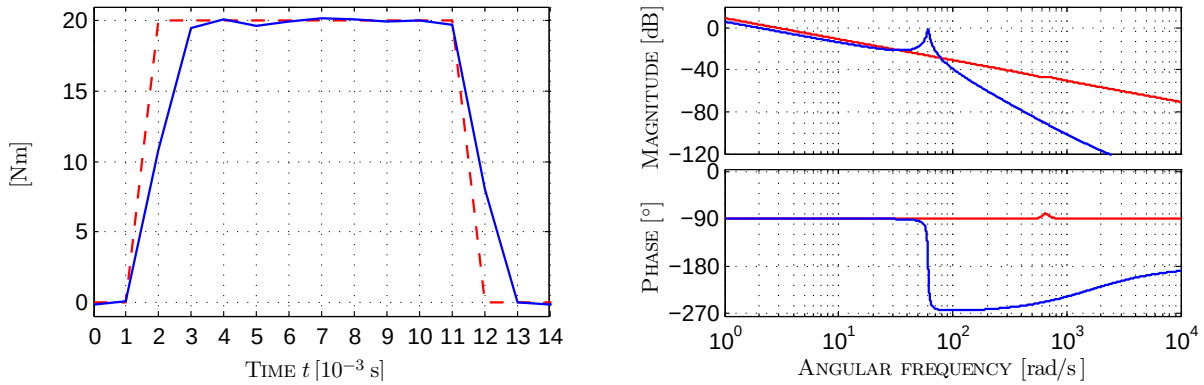

(a) *torque generation with delay of* $\approx 2 \cdot 10^{-3}$ [s]: - - - $u(\cdot) = m_{M,\mathrm{ref}}(\cdot)$ *and* — $m_M(\cdot) = \mathrm{sat}_{\hat{u}_A}\left(u(\cdot) + u_A(\cdot)\right)$

(b) *bode diagrams of* — $F_{\text{'1MS'}}(s)$ *and* — $F_{2MS}(s)$ *(with data in Tab. 5.1)*

Figure 5.5: *Torque generation at laboratory setup (left) and bode diagrams of the linearized models of the configurations depicted in Fig. 5.4 (right).*

with natural frequencies (see bode diagrams in Fig. 5.5(b) or use data in Tab. 5.1)

$$\omega_0^{\text{'1MS'}} = \sqrt{\frac{c_s(\Theta_1+\Theta_2)}{\Theta_1\Theta_2}} \approx 661 \text{ [rad/s]} \qquad \text{and} \qquad \omega_0^{2\text{MS}} \approx 61 \text{ [rad/s]}\,.$$

Natural frequency $\omega_0^{\text{'1MS'}}$ is high compared to the typical operation bandwidth (ranging from 0 to 200 [rad/s]) and yields a damped magnitude of ≈ -45 [dB] (see Fig. 5.5(b)), hence the configuration in Fig. 5.4(a) can be considered as "stiff" one-mass system with overall inertia $\Theta = \Theta_1 + \Theta_2$. The configuration in Fig. 5.4(b) represents an elastic two-mass system.

Several sets of the mechanical parameters c_S, d_S, Θ_1 and Θ_2 of the laboratory setup are estimated in [7], [151, Appendix A] and [78, Appendix C]. Moreover, in [151, p. 195] friction is identified using a *static* friction model (not covering e.g. presliding displacement). The available sensors do not provide the required resolution (see Section 1.5.3) to identify dynamic friction as in the LuGre friction model (1.22). For implementation friction will neither be compensated for nor identified or estimated. Conform to the models of stiff 1MS (1.24), (1.25) and elastic 2MS (1.26), (1.27), the key data of the two configurations of the laboratory setup is collected in Tab. 5.1, respectively. A complete list of technical data and a description of the electrical setup can be found in Appendix D.

5.2.2 Speed control

The *high-gain adaptive speed control problem* is solved in [169]. However, 1MS and 2MS are not modeled with gear, actuator saturation and motor side friction. Moreover, the presented measurement results for funnel control are tentative: the chosen asymptotic accuracy is almost three times larger than the chosen reference magnitude (see Section 6.4 in [169]).

In Sections 5.2.2.1 and 5.2.2.2, the available theoretical results are revisited and supplemented: it

	1MS (as in Fig. 5.4(a))	**2MS** (as in Fig. 5.4(b))
actuator	$\|u_A\|_\infty < 0.6$ [Nm], $k_A \approx 1$ [1] (measured), $\hat{u}_A = 22$ [Nm] (specified)	
real-time system	$T_S = 1 \cdot 10^{-3}$ [s] (sampling time specified in xPC target)	
mechanics	$\big(\Theta_1 = 0.0092$ [kg m^2], $\Theta_2 = 0.333$ [kg m^2], $c_S = 3870$ [Nm/rad], $d_S = 0.89$ [Nms/rad]$\big)$ $g_r = 1$ [1], $\Theta = \Theta_1 + \Theta_2 = 0.3422$ [kg m^2]	$\Theta_1 = 0.166$ [kg m^2], $\Theta_2 = 0.333$ [kg m^2], $c_S = 410$ [Nm/rad], $d_S = 0.25$ [Nms/rad], $g_r = 1$ [1]
instrumentation	$\|n_{m1}\|_\infty, \|n_m\|_\infty = \|n_{m2}\|_\infty < 6 \cdot 10^{-5}$ [rad] (position meas. error), $\|\dot{n}_{m1}\|_\infty, \|\dot{n}_m\|_\infty = \|\dot{n}_{m2}\|_\infty < 4 \cdot 10^{-2}$ [rad/s] (speed meas. error)	
friction	$\nu_1, \nu_2 < 0.005$ [Nms/rad] and $\mathfrak{F}_1$, $\mathfrak{F}_2$ as in (1.22) with $M_{\mathfrak{F}_1}, M_{\mathfrak{F}_2} < 1$ [Nm] (see [151, p. 195]), otherwise unknown	
initial values	$\boldsymbol{x}^0 = \mathbf{0}_2$ $\left[\frac{\text{rad}}{\text{s}}, \text{rad}\right]$	$\boldsymbol{x}^0 = \mathbf{0}_4$ $\left[\frac{\text{rad}}{\text{s}}, \text{rad}, \frac{\text{rad}}{\text{s}}, \text{rad}\right]$

Table 5.1: *Key data of laboratory setup (centered values hold for 1MS and 2MS, resp.)*

will be shown that 1MS and 2MS with gear and motor and load side friction are or can be rendered element of system class $\mathcal{S}_1$. In Section 5.2.2.3 comparative measurement results will be presented which underpin industrial applicability.

5.2.2.1 One-mass system of class $\mathcal{S}_1$

For speed control, model (1.24) of the rotatory 1MS may be simplified: the state variable of position $\phi(\cdot)$ is irrelevant and so negligible. The simplification yields a reduction of the system's order and is motivated by the observation illustrated in Example 2.23. Model (1.24), (1.25) is actually *not* element of system class $\mathcal{S}_1$. The reduced-order mathematical model for speed control is given by

$$\left.\begin{aligned} \dot{\omega}(t) &= -\tfrac{\nu_1+\nu_2/g_r^2}{\Theta}\omega(t) + \tfrac{k_A}{\Theta}\,\mathrm{sat}_{\hat{u}_A}\big(u(t)+u_A(t)\big) - \tfrac{(\mathfrak{F}_1\omega)(t)}{\Theta} - \tfrac{m_L(t)+(\mathfrak{F}_2\frac{\omega}{g_r})(t)}{g_r\Theta}, \\ y(t) &= c_1\,\omega(t), \qquad\qquad \omega(0) = \omega^0 \in \mathbb{R} \end{aligned}\right\} \tag{5.12}$$

where

$$\left.\begin{aligned} &\Theta > 0,\ g_r \in \mathbb{R}\setminus\{0\},\ \nu_1,\nu_2 > 0,\ \hat{u}_A, k_A > 0,\ u_A(\cdot), m_L(\cdot) \in \mathcal{L}^\infty(\mathbb{R}_{\geq 0};\mathbb{R}),\ c_1 \in \{1, 1/g_r\} \text{ and} \\ &\forall\, i \in \{1,2\}\colon\ \mathfrak{F}_i \text{ as in (1.22) with } M_{\mathfrak{F}_i} := \sup\{\,|(\mathfrak{F}_i\zeta)(t)| \mid t \geq 0,\ \zeta(\cdot) \in \mathcal{C}(\mathbb{R}_{\geq 0},\mathbb{R})\,\} < \infty. \end{aligned}\right\} \tag{5.13}$$

Conform to instrumentation configuration (1MS-ic$_1$) (see Section 1.4.6.1) either motor speed $\omega(\cdot)$ or load speed $\omega(\cdot)/g_r$ is available for feedback, i.e. $c_1 = 1$ or $c_1 = 1/g_r$ in (5.12).

Proposition 5.5. *Consider the 1MS given by (5.12), (5.13) with instrumentation configuration (1MS-ic$_1$). If actuator saturation is negligible, i.e. $\hat{u}_A \to \infty$ in (5.12), and if* sign(g_r) *is known, then it is element of system class $\mathcal{S}_1$.*

Proof of Proposition 5.5.

Consider only the case $c_1 = 1/g_r$, the other case follows analogously. For $u_A(\cdot)$, $m_L(\cdot)$, $\mathfrak{F}_1$ and $\mathfrak{F}_2$ as in (5.13), define $h := 0$, $x := \omega$, $A := -\frac{\nu_1+\nu_2/g_r^2}{\Theta}$, $b := \frac{k_A}{\Theta}$, $c := c_1 = 1/g_r$, $\boldsymbol{B}_{\mathfrak{T}} := \left[-\frac{1}{\Theta}, \ -\frac{1}{g_r\Theta}\right]$, $\mathfrak{T}\colon \mathcal{C}([-h,\infty),\mathbb{R}) \to \mathcal{L}^\infty_{\mathrm{loc}}(\mathbb{R}_{\geq 0};\mathbb{R}^2)$, $(\mathfrak{T}x)(t) := \big((\mathfrak{F}_1\, x)(t),\, (\mathfrak{F}_1\, x/g_r)(t)\big)^\top$, $u_d(\cdot) := u_A(\cdot)$ and $\boldsymbol{d}(\cdot) = (0,\, m_L(\cdot))^\top$. Then, for $\hat{u}_A \to \infty$, system (5.12) can be expressed in the form (1.36). Moreover, $\gamma_0 := c\,b = \frac{k_A}{g_r\Theta} \overset{(5.13)}{\neq} 0$, $\operatorname{sign}(\gamma_0) \overset{(5.13)}{=} \operatorname{sign}(g_r)$ and

$$\forall\, s \in \mathbb{C}_{\geq 0}\colon \quad \det \begin{bmatrix} s - A & b \\ c & 0 \end{bmatrix} = s + \frac{\nu_1 + \nu_2/g_r^2 + k_A}{\Theta} \overset{(5.13)}{\neq} 0,$$

which shows system properties ($\mathcal{S}_1$-sp$_1$) and ($\mathcal{S}_1$-sp$_2$), respectively. From Corollary 5.4 it follows that $\mathfrak{T} \in \mathcal{T}$. In view of (5.13), there exists $M_{\mathfrak{T}} := \sqrt{2}\max\{M_{\mathfrak{F}_1},\, M_{\mathfrak{F}_2}\} < \infty$, $u_d(\cdot) \in \mathcal{L}^\infty(\mathbb{R}_{\geq 0};\mathbb{R})$ and $\boldsymbol{d}(\cdot) \in \mathcal{L}^\infty(\mathbb{R}_{\geq 0};\mathbb{R}^2)$. Hence ($\mathcal{S}_1$-sp$_3$) and ($\mathcal{S}_1$-sp$_4$) are satisfied, respectively. Due to (1MS-ic$_1$), $y(\cdot) = \omega(\cdot)/g_r$ is available for feedback which shows ($\mathcal{S}_1$-sp$_5$). This completes the proof. □

Clearly, Proposition 5.5 with Theorem 3.3 or Theorem 4.4 assures that adaptive λ-tracking controller (3.11) or funnel controller (4.24) are applicable for speed control of the unconstrained 1MS (5.12), (5.13). For funnel control, Theorem 4.7 allows to account for the actuator saturation in (5.12). From Corollary 5.2 it follows that application of controller (3.11) and (4.24) in combination with internal model (5.3) is admissible and, moreover, if steady state is reached then both controller combinations guarantee asymptotic speed tracking.

5.2.2.2 Two-mass system of class $\mathcal{S}_1$

For speed control, the system order of 2MS (1.26), (1.27) may also be reduced. By introducing angle of twist ϕ_S in [rad], defined by

$$\forall\, t \geq 0\colon \qquad \phi_S(t) := \frac{\phi_1(t)}{g_r} - \phi_2(t) = \int_0^t \left(\frac{\omega_1(\tau)}{g_r} - \omega_2(\tau)\right) \mathrm{d}\tau \ \underbrace{-\frac{\phi_1(0)}{g_r} + \phi_2(0)}_{=-\phi_S(0)}, \tag{5.14}$$

and the reduced state variable

$$\boldsymbol{x}(t) = (\omega_1(t),\, \phi_S(t),\, \omega_2(t))^\top \in \mathbb{R}^3,$$

the mathematical model (1.26), (1.27) of the 2MS simplifies to

$$\left.\begin{aligned} \tfrac{\mathrm{d}}{\mathrm{d}t}\,\boldsymbol{x}(t) &= \boldsymbol{A}\boldsymbol{x}(t) + \boldsymbol{b}\,\mathrm{sat}_{\hat{u}_A}\big(u(t) + u_A(t)\big) + \boldsymbol{B}_L \begin{pmatrix} (\mathfrak{F}_1\omega_1)(t) \\ m_L(t) + (\mathfrak{F}_2\omega_2)(t) \end{pmatrix}, \\ y(t) &= \boldsymbol{c}^\top\boldsymbol{x}(t), \qquad\qquad \boldsymbol{x}(0) = \boldsymbol{x}^0 \in \mathbb{R}^3 \end{aligned}\right\} \tag{5.15}$$

where

$$\left.\begin{aligned} &\boldsymbol{A}=\begin{bmatrix} -\frac{d_S+g_r^2\nu_1}{g_r^2\Theta_1} & -\frac{c_S}{g_r\Theta_1} & \frac{d_S}{g_r\Theta_1} \\ \frac{1}{g_r} & 0 & -1 \\ \frac{d_S}{g_r\Theta_2} & \frac{c_S}{\Theta_2} & -\frac{d_S+\nu_2}{\Theta_2} \end{bmatrix},\ \boldsymbol{b}=\begin{pmatrix} \frac{k_A}{\Theta_1} \\ 0 \\ 0 \end{pmatrix},\ \boldsymbol{B}_L=\begin{bmatrix} -\frac{1}{\Theta_1} & 0 \\ 0 & 0 \\ 0 & -\frac{1}{\Theta_2} \end{bmatrix},\ \boldsymbol{c}=\begin{pmatrix} c_1 \\ c_2 \\ c_3 \end{pmatrix}, \\ &\Theta_1,\Theta_2>0,\quad c_S,d_S>0,\quad g_r\in\mathbb{R}\backslash\{0\},\quad \nu_1,\nu_2>0,\quad c_1,c_2,c_3\in\mathbb{R},\quad \hat{u}_A,k_A>0, \\ &u_A(\cdot),\,m_L(\cdot)\in\mathcal{L}^\infty(\mathbb{R}_{\geq 0};\mathbb{R})\ \text{ and }\ \forall\, i\in\{1,2\}:\ \mathfrak{F}_i \text{ as in (1.22) with } M_{\mathfrak{F}_i} \text{ as in (5.13).} \end{aligned}\right\} \tag{5.16}$$

Instrumentation configuration (2MS-ic$_1$)(c) (see Section 1.4.6.2) allows for feedback of all three states which is indicated by the "general" output coupling vector $\boldsymbol{c}$ in (5.16). In [169, Section 6.1.3]) it is shown that shaft oscillations can be actively damped if $c_2\neq 0$ in (5.16) (only then observability is retained). The following result was introduced in [96]. In contrast to the model in [96] the 2MS (5.15), (5.16) includes (dynamic) friction on motor and load side and a gear with ratio $g_r\neq 0$.

Proposition 5.6. *Consider the 2MS given by (5.15), (5.16) with instrumentation configuration (2MS-ic$_1$)(c) and assume that actuator saturation is negligible, i.e. $\hat{u}_A\to\infty$ in (5.15). If gear ratio g_r and initial value $\phi_S(0)$ of angle of twist are known then, for*

$$c_1>0,\qquad \frac{c_2}{g_r}\geq 0\qquad \textit{and}\qquad \frac{c_3}{g_r}>-c_1, \tag{5.17}$$

the 2MS (5.15), (5.16) is element of system class $\mathcal{S}_1$.

Note that knowledge of gear ratio g_r is actually a mild presupposition. Typically, the value of g_r can be read off on the gear box and so, without loss of generality, may be assumed to be known to the control designer.

Proof of Proposition 5.6.

Step 1: It is shown that properties ($\mathcal{S}_1$-sp$_1$), ($\mathcal{S}_1$-sp$_3$), ($\mathcal{S}_1$-sp$_4$) and ($\mathcal{S}_1$-sp$_5$) of system class $\mathcal{S}_1$ are satisfied.

For $\boldsymbol{B}_L$, $u_A(\cdot)$, $m_L(\cdot)$, $\mathfrak{F}_1$ and $\mathfrak{F}_2$ as in (5.16), define $h:=0$, $u_d(\cdot):=u_A(\cdot)$, $\boldsymbol{B}_{\mathfrak{T}}:=\boldsymbol{B}_L$, $\boldsymbol{d}(\cdot):=(0,\,m_L(\cdot))^\top$ and

$$\mathfrak{T}\colon \mathcal{C}([-h,\infty);\mathbb{R}^3)\to\mathcal{L}^\infty_{\mathrm{loc}}(\mathbb{R}_{\geq 0};\mathbb{R}^2),\qquad (\mathfrak{T}\boldsymbol{x})(t):=\big((\mathfrak{F}_1\omega_1)(t),\quad (\mathfrak{F}_2\omega_2)(t)\big)^\top.$$

Then, for $\hat{u}_A\to\infty$, system (5.15), (5.16) may be written in the form (1.36). Moreover, the following hold

(i) $\gamma_0:=\boldsymbol{c}^\top\boldsymbol{b}=c_1\,k_A/\Theta_1\overset{(5.17),(5.16)}{>}0$ and $\operatorname{sign}(\gamma_0)=\operatorname{sign}(c_1)$,

(ii) from Corollary 5.4 it follows that $\mathfrak{T}\in\mathcal{T}$,

(iii) in view of (5.16), $M_{\mathfrak{T}}\leq\sqrt{2}\max\{M_{\mathfrak{F}_1},\,M_{\mathfrak{F}_2}\}<\infty$ and $u_d(\cdot)\in\mathcal{L}^\infty(\mathbb{R}_{\geq 0};\mathbb{R})$ and $\boldsymbol{d}(\cdot)\in\mathcal{L}^\infty(\mathbb{R}_{\geq 0};\mathbb{R}^2)$, respectively and

(iv) instrumentation configuration (2MS-ic$_1$)(c) allows for feedback of $\omega_1(t)$, $\omega_2(t)$ and, since g_r and $\phi_S(0)$ are known, of $\phi_S(t) = \int_0^t (\omega_1(\tau)/g_r - \omega_2(\tau))\,\mathrm{d}\tau - \phi_S(0)$, respectively.

Hence, system properties ($\mathcal{S}_1$-sp$_1$), ($\mathcal{S}_1$-sp$_3$), ($\mathcal{S}_1$-sp$_4$) and ($\mathcal{S}_1$-sp$_5$) are satisfied. This completes Step 1.

Step 2: It is shown that property ($\mathcal{S}_1$-sp$_2$) of system class $\mathcal{S}_1$ is satisfied.
Since $\gamma_0 \neq 0$ there exists a similarity transformation (see Section 3.3.1)

$$\boldsymbol{S}\colon \mathbb{R}^3 \to \mathbb{R}^3, \qquad \boldsymbol{x} \mapsto \big(y, \quad z_1, \quad z_2\big)^\top := \boldsymbol{S}\boldsymbol{x}$$

which converts (5.15), (5.16) into Byrnes-Isidori like form (3.6). Invoking (2.49) with

$$\boldsymbol{V} = \ker \boldsymbol{c}^\top = \begin{bmatrix} -\frac{c_2}{c_1} & -\frac{c_3}{c_1} \\ 1 & 0 \\ 0 & 1 \end{bmatrix} \qquad \text{and} \qquad \boldsymbol{N} = (\boldsymbol{V}^\top\boldsymbol{V})^{-1}\boldsymbol{V}^\top[\boldsymbol{I}_4 - \boldsymbol{b}(\boldsymbol{c}^\top\boldsymbol{b})^{-1}\boldsymbol{c}] = \begin{bmatrix} 0 & 1 & 0 \\ 0 & 0 & 1 \end{bmatrix},$$

yields the transformation matrix

$$\boldsymbol{S} = \begin{bmatrix} c_1 & c_2 & c_3 \\ 0 & 1 & 0 \\ 0 & 0 & 1 \end{bmatrix} \qquad \text{and} \qquad \boldsymbol{S}^{-1} = \begin{bmatrix} -\frac{1}{c_1} & -\frac{c_2}{c_1} & -\frac{c_3}{c_1} \\ 0 & 1 & 0 \\ 0 & 0 & 1 \end{bmatrix}.$$

Hence, conform to (3.6), one arrives at

$$\begin{aligned} \frac{\mathrm{d}}{\mathrm{d}t}\begin{pmatrix} y(t) \\ z_1(t) \\ z_2(t) \end{pmatrix} &= \boldsymbol{S}\boldsymbol{A}\boldsymbol{S}^{-1}\begin{pmatrix} y(t) \\ z_1(t) \\ z_2(t) \end{pmatrix} + \boldsymbol{S}\boldsymbol{b}\big(u(t) + u_A(t)\big) + \boldsymbol{S}\boldsymbol{B}_L \begin{pmatrix} (\mathfrak{F}_1\,\mathrm{row}_1(\boldsymbol{S}^{-1})\begin{pmatrix} y \\ z_1 \\ z_2 \end{pmatrix})(t) \\ m_L(t) + (\mathfrak{F}_2\,\mathrm{row}_3(\boldsymbol{S}^{-1})\begin{pmatrix} y \\ z_1 \\ z_2 \end{pmatrix})(t) \end{pmatrix}, \\ \big(y(0), \quad z_1(0), \quad z_2(0)\big)^\top &= \boldsymbol{S}\boldsymbol{x}^0 \end{aligned}$$

where

$$\boldsymbol{S}\boldsymbol{A}\boldsymbol{S}^{-1} =: \begin{bmatrix} a_1 & \boldsymbol{a}_2^\top \\ \boldsymbol{a}_3 & \boldsymbol{A}_4 \end{bmatrix} \in \mathbb{R}^{3\times 3}, \quad \boldsymbol{S}\boldsymbol{b} = \begin{pmatrix} \gamma_0 \\ 0 \\ 0 \end{pmatrix} \in \mathbb{R}^3 \quad \text{and} \quad \boldsymbol{S}\boldsymbol{B}_L = \begin{bmatrix} -\frac{c_1}{\Theta_1} & -\frac{c_3}{\Theta_2} \\ 0 & 0 \\ 0 & -\frac{1}{\Theta_2} \end{bmatrix} \in \mathbb{R}^{3\times 2}.$$

More precisely, in view of (2.51), one obtains

$$\left.\begin{aligned} a_1 &= -\tfrac{d_S+g_r^2\nu_1}{g_r^2\Theta_1} + \tfrac{1}{g_r}\tfrac{c_2}{c_1} + \tfrac{d_S}{g_r\Theta_2}\tfrac{c_3}{c_1} \in \mathbb{R}, \\ \boldsymbol{a}_2 &= \begin{pmatrix} c_2\left(\tfrac{d_S+\nu_1 g_r^2}{g_r^2\Theta_1} - \tfrac{d_S}{g_r\Theta_2}\tfrac{c_3}{c_1} - \tfrac{1}{c_1}\tfrac{c_2}{g_r}\right) + c_S\left(\tfrac{c_3}{\Theta_2} - \tfrac{c_2}{g_r\Theta_1}\right) \\ c_3\left(\tfrac{d_S+\nu_1 g_r^2}{g_r^2\Theta_1} - \tfrac{d_S+\nu_2}{\Theta_2} - \tfrac{1}{g_r c_1}\left(c_2 + c_3\tfrac{d_S}{\Theta_2}\right)\right) - c_2 + c_1\tfrac{d_S}{g_r\Theta_1} \end{pmatrix} \in \mathbb{R}^2, \\ \boldsymbol{a}_3 &= \left(\tfrac{1}{g_r c_1}, \quad \tfrac{d_S}{g_r c_1\Theta_2}\right)^\top \in \mathbb{R}^2 \end{aligned}\right\} \qquad (5.18)$$

and

$$\boldsymbol{A}_4 = \boldsymbol{N}\boldsymbol{A}\boldsymbol{V} = \begin{bmatrix} -\frac{1}{g_r}\frac{c_2}{c_1} & -\frac{1}{g_r}\frac{c_3}{c_1} - 1 \\ -\frac{d_S}{g_r\Theta_2}\frac{c_2}{c_1} + \frac{c_S}{\Theta_2} & -\frac{d_S}{g_r\Theta_2}\frac{c_3}{c_1} - \frac{d_S+\nu_2}{\Theta_2} \end{bmatrix} \in \mathbb{R}^{2\times 2}. \tag{5.19}$$

It is easy to see that the characteristic polynomial of $\boldsymbol{A}_4$, given by

$$\chi_{\boldsymbol{A}_4}(s) = s^2 + \left(\frac{d_S}{c_1\Theta_2}\left(c_1 + \frac{c_3}{g_r}\right) + \frac{1}{c_1}\frac{c_2}{g_r} + \frac{\nu_2}{\Theta_2}\right)s + \left(\frac{c_S}{c_1\Theta_2}\left(c_1 + \frac{c_3}{g_r}\right) + \frac{\nu_2}{c_1\Theta_2}\frac{c_2}{g_r}\right),$$

is Hurwitz for c_1, c_2 and c_3 as in (5.17), hence

$$(5.17) \qquad \Longrightarrow \qquad \operatorname{spec}(\boldsymbol{A}_4) \subset \mathbb{C}_{<0}. \tag{5.20}$$

Since

$$\begin{aligned} \det \begin{bmatrix} \boldsymbol{S}(s\boldsymbol{I}_3 - \boldsymbol{A})\boldsymbol{S}^{-1} & \boldsymbol{S}\boldsymbol{b} \\ \boldsymbol{c}^\top\boldsymbol{S}^{-1} & 0 \end{bmatrix} &= \det\left(\begin{bmatrix} \boldsymbol{S} & \boldsymbol{0}_3 \\ \boldsymbol{0}_3^\top & 1 \end{bmatrix}\begin{bmatrix} s\boldsymbol{I}_3 - \boldsymbol{A} & \boldsymbol{b} \\ \boldsymbol{c}^\top & 0 \end{bmatrix}\begin{bmatrix} \boldsymbol{S}^{-1} & \boldsymbol{0}_3 \\ \boldsymbol{0}_3^\top & 1 \end{bmatrix}\right) \\ &= \underbrace{\det(\boldsymbol{S})\det(\boldsymbol{S}^{-1})}_{=1}\det\begin{bmatrix} s\boldsymbol{I}_3 - \boldsymbol{A} & \boldsymbol{b} \\ \boldsymbol{c}^\top & 0 \end{bmatrix}, \end{aligned}$$

note that, for $\gamma_0 = c_1 k_A/\Theta_1 > 0$, a_1, $\boldsymbol{a}_2$ and $\boldsymbol{a}_3$ as in (5.18) and $\boldsymbol{A}_4$ as in (5.19), the following holds

$$\det\begin{bmatrix} s\boldsymbol{I}_3 - \boldsymbol{A} & \boldsymbol{b} \\ \boldsymbol{c}^\top & 0 \end{bmatrix} = \det\begin{bmatrix} s - a_1 & -\boldsymbol{a}_2^\top & \gamma_0 \\ -\boldsymbol{a}_3 & s\boldsymbol{I}_2 - \boldsymbol{A}_4 & \boldsymbol{0}_2 \\ 1 & \boldsymbol{0}_2^\top & 0 \end{bmatrix} = -\gamma_0 \det\left[s\boldsymbol{I}_2 - \boldsymbol{A}_4\right] \overset{(5.20)}{\neq} 0 \quad \forall\, s \in \mathbb{C}_{\geq 0},$$

which shows property ($\mathcal{S}_1$-sp$_2$) of system class $\mathcal{S}_1$. Combining Step 1 and Step 2 completes the proof of Proposition 5.5. □

Clearly, Proposition 5.6 with e.g. Theorem 4.4 allows for application of funnel controller (4.24) for speed control of 2MS (5.15), (5.16) and, from Corollary 5.2, it follows that e.g. controller combination (4.24)+(5.3) is admissible. Note that only if angle of twist $\phi_S(\cdot)$ is used for feedback (i.e. $c_2 \neq 0$ in (5.17)), then its initial value $\phi_S(0)$ and g_r must be known a priori. For the case $c_2 = 0$ in (5.17), knowledge of the sign of gear ratio g_r is sufficient to satisfy the presuppositions in (5.17).

To achieve a well damped system response, (positive) feedback of angle of twist $\phi_S(\cdot)$ is necessary (see [169, Section 6.1.3]). Any choice $c_2/g_r > 0$ increases damping of e.g. the closed-loop system (5.15), (5.16), (4.24)+(5.3) *but* precludes asymptotic disturbance rejection of constant loads (see Section 6.1.3 in [169]). To circumvent this conflict of objectives, Ilchmann and Schuster propose the use of dynamic state feedback incorporating a high-pass filter for the angle of twist (see [96] or in great detail [169, Section 6.2]). Their result is recapitulated in the following proposition (again gear and motor side friction are supplemented).

Proposition 5.7. *Consider the 2MS given by (5.15), (5.16) with instrumentation configuration (2MS-ic$_1$)(c) and assume that actuator saturation is negligible, i.e. $\hat{u}_A \to \infty$ in (5.15), and let gear ratio g_r and initial value $\phi_S(0)$ of angle of twist be known. Then, for*

$$c_1 > 0, \qquad \frac{c_2}{g_r} \geq 0, \qquad \frac{c_3}{g_r} > -c_1 \qquad \text{and} \qquad k_F > 0, \tag{5.21}$$

and with filter and augmented output, given by

$$\left.\begin{aligned} \dot{x}_F(t) &= -k_F\big(x_F(t) + \phi_S(t)\big), & x_F(0) = 0, \\ y(t) &:= \begin{pmatrix} c_1, & c_2, & c_3, & c_2 \end{pmatrix} \begin{pmatrix} \boldsymbol{x}(t) \\ x_F(t) \end{pmatrix}, \end{aligned}\right\} \tag{5.22}$$

the augmented 2MS (5.15), (5.16), (5.22) is element of system class $\mathcal{S}_1$.

Proof of Proposition 5.7.

The proof is similar to the proof of Proposition 5.6. Only the essential changes are presented.
Step 1: It is shown that properties ($\mathcal{S}_1$-sp$_1$), ($\mathcal{S}_1$-sp$_3$), ($\mathcal{S}_1$-sp$_4$) and ($\mathcal{S}_1$-sp$_5$) of system class $\mathcal{S}_1$ are satisfied.
For $\boldsymbol{A}, \boldsymbol{b}$, $\boldsymbol{B}_L$ and $\boldsymbol{c}$ as in (5.15), define

$$\widehat{\boldsymbol{A}} := \begin{bmatrix} \boldsymbol{A} & \boldsymbol{0}_3 \\ (\ 0, & -k_F, \quad 0\ ) \quad -k_F \end{bmatrix}, \quad \widehat{\boldsymbol{b}} := \begin{pmatrix} \boldsymbol{b} \\ 0 \end{pmatrix}, \quad \widehat{\boldsymbol{B}}_L := \begin{bmatrix} \boldsymbol{B}_L \\ \boldsymbol{0}_2^\top \end{bmatrix} \quad \text{and} \quad \widehat{\boldsymbol{c}} := \begin{pmatrix} \boldsymbol{c} \\ c_2 \end{pmatrix}$$

and express system (5.15), (5.16) with (5.22) as follows

$$\left.\begin{aligned} \tfrac{\mathrm{d}}{\mathrm{d}t} \begin{pmatrix} \boldsymbol{x}(t) \\ x_F(t) \end{pmatrix} &= \widehat{\boldsymbol{A}} \begin{pmatrix} \boldsymbol{x}(t) \\ x_F(t) \end{pmatrix} + \widehat{\boldsymbol{b}}\, \mathrm{sat}_{\hat{u}_A}\big(u(t) + u_A(t)\big) + \widehat{\boldsymbol{B}}_L \begin{pmatrix} (\mathfrak{F}_1\omega_1)(t) \\ m_L(t) + (\mathfrak{F}_2\omega_2)(t) \end{pmatrix} \\ y(t) &= \widehat{\boldsymbol{c}}^\top \begin{pmatrix} \boldsymbol{x}(t) \\ x_F(t) \end{pmatrix}, \qquad \begin{pmatrix} \boldsymbol{x}(0) \\ x_F(0) \end{pmatrix} = \begin{pmatrix} \boldsymbol{x}^0 \\ x_F^0 \end{pmatrix} \in \mathbb{R}^4. \end{aligned}\right\} \tag{5.23}$$

For $u_A(\cdot)$, $m_L(\cdot)$, $\mathfrak{F}_1$ and $\mathfrak{F}_2$ as in (5.16), define $h := 0$, $u_d(\cdot) := u_A(\cdot)$, $\boldsymbol{B}_{\mathfrak{T}} := \widehat{\boldsymbol{B}}_L$, $\boldsymbol{d}(\cdot) := (0,\, m_L(\cdot))^\top$ and

$$\mathfrak{T}\colon\ \mathcal{C}([-h,\infty);\mathbb{R}^4) \to \mathcal{L}^\infty_{\mathrm{loc}}(\mathbb{R}_{\geq 0};\mathbb{R}^2), \qquad (\mathfrak{T}\begin{pmatrix} \boldsymbol{x} \\ x_F \end{pmatrix})(t) := \big((\mathfrak{F}_1\omega_1)(t),\ \ (\mathfrak{F}_2\omega_2)(t)\big)^\top.$$

Then, for $\hat{u}_A \to \infty$, system (5.23) may be written in the form (1.36). Moreover, invoking similar arguments as in Step 1 of the proof of Proposition 5.6 yields that properties ($\mathcal{S}_1$-sp$_1$), ($\mathcal{S}_1$-sp$_3$), ($\mathcal{S}_1$-sp$_4$) and ($\mathcal{S}_1$-sp$_5$) are satisfied, which completes Step 1.

Step 2: It is shown that property ($\mathcal{S}_1$-sp$_2$) of system class $\mathcal{S}_1$ is satisfied.
Note that $\gamma_0 := \widehat{\boldsymbol{c}}^\top \widehat{\boldsymbol{A}}\widehat{\boldsymbol{b}} = c_1 k_A/\Theta_1 > 0$. Hence there exists a similarity transformation

$$\widehat{\boldsymbol{S}}\colon \mathbb{R}^5 \to \mathbb{R}^5, \qquad \begin{pmatrix} \boldsymbol{x} \\ x_F \end{pmatrix} \mapsto \boldsymbol{w} := \begin{pmatrix} y, & z_1, & z_2, & z_3 \end{pmatrix}^\top := \widehat{\boldsymbol{S}} \begin{pmatrix} \boldsymbol{x} \\ x_F \end{pmatrix}$$

which takes (5.23) into Byrnes-Isidori like form (3.6). More precisely, for

$$\widehat{\boldsymbol{V}} = \ker \widehat{\boldsymbol{c}} = \begin{bmatrix} -\frac{c_2}{c_1} & -\frac{c_3}{c_1} & -\frac{c_2}{c_1} \\ 1 & 0 & 0 \\ 0 & 1 & 0 \\ 0 & 0 & 1 \end{bmatrix} \quad \text{and} \quad \widehat{\boldsymbol{N}} = (\widehat{\boldsymbol{V}}^\top \widehat{\boldsymbol{V}})^{-1} \widehat{\boldsymbol{V}}^\top [\boldsymbol{I}_4 - \frac{\widehat{\boldsymbol{b}}\widehat{\boldsymbol{c}}^\top}{\gamma_0}] = \begin{bmatrix} 0 & 1 & 0 & 0 \\ 0 & 0 & 1 & 0 \\ 0 & 0 & 0 & 1 \end{bmatrix}$$

the transformation matrix is given by

$$\widehat{\boldsymbol{S}} = \begin{bmatrix} \widehat{\boldsymbol{c}}^\top \\ \widehat{\boldsymbol{N}} \end{bmatrix} = \begin{bmatrix} c_1 & c_2 & c_3 & c_2 \\ 0 & 1 & 0 & 0 \\ 0 & 0 & 1 & 0 \\ 0 & 0 & 0 & 1 \end{bmatrix} \quad \text{with inverse} \quad \widehat{\boldsymbol{S}}^{-1} = \begin{bmatrix} \frac{1}{c_1} & -\frac{c_2}{c_1} & -\frac{c_3}{c_1} & -\frac{c_2}{c_1} \\ 0 & 1 & 0 & 0 \\ 0 & 0 & 1 & 0 \\ 0 & 0 & 0 & 1 \end{bmatrix}.$$

Conform to (3.8), one obtains

$$\dot{\boldsymbol{w}}(t) = \widehat{\boldsymbol{S}}\widehat{\boldsymbol{A}}\widehat{\boldsymbol{S}}^{-1}\boldsymbol{w}(t) + \widehat{\boldsymbol{S}}\widehat{\boldsymbol{b}}\big(u(t) + u_A(t)\big) + \widehat{\boldsymbol{S}}\widehat{\boldsymbol{B}}_L \begin{pmatrix} (\mathfrak{F}_1 \operatorname{row}_1(\widehat{\boldsymbol{S}}^{-1})\boldsymbol{w})(t) \\ m_L(t) + (\mathfrak{F}_2 \operatorname{row}_3(\widehat{\boldsymbol{S}}^{-1})\boldsymbol{w})(t) \end{pmatrix},$$
$$\boldsymbol{w}(0) = \widehat{\boldsymbol{S}} \begin{pmatrix} \boldsymbol{x}^0 \\ x_F^0 \end{pmatrix},$$

where

$$\widehat{\boldsymbol{S}}\widehat{\boldsymbol{A}}\widehat{\boldsymbol{S}}^{-1} =: \begin{bmatrix} \widehat{a}_1 & \widehat{\boldsymbol{a}}_2^\top \\ \widehat{\boldsymbol{a}}_3 & \widehat{\boldsymbol{A}}_4 \end{bmatrix} \in \mathbb{R}^{4\times 4}, \quad \widehat{\boldsymbol{S}}\widehat{\boldsymbol{b}} = \begin{pmatrix} \gamma_0 \\ 0 \\ 0 \\ 0 \end{pmatrix} \in \mathbb{R}^4 \quad \text{and} \quad \widehat{\boldsymbol{S}}\widehat{\boldsymbol{B}}_L = \begin{bmatrix} -\frac{c_1}{\Theta_1} & -\frac{c_3}{\Theta_2} \\ 0 & 0 \\ 0 & -\frac{1}{\Theta_2} \\ 0 & 0 \end{bmatrix} \in \mathbb{R}^{4\times 2}.$$

For a_1, $\boldsymbol{a}_2$ and $\boldsymbol{a}_3$ as in (5.18), invoking (2.51) yields $\widehat{a}_1 = a_1 \in \mathbb{R}$,

$$\widehat{\boldsymbol{a}}_2 = \left(\begin{pmatrix} \boldsymbol{a}_2 \\ 0 \end{pmatrix} + \begin{pmatrix} -c_2 k_F \\ 0 \\ -c_2 \left(\frac{d_S + g_r^2 \nu_1}{g_r^2 \Theta_1} - k_F - \frac{d_S}{g_r \Theta_2} \frac{c_3}{c_1} - \frac{1}{c_1} \frac{c_2}{g_r} \right) \end{pmatrix} \right) \in \mathbb{R}^3,$$

$\widehat{\boldsymbol{a}}_3 = \big(\boldsymbol{a}_3^\top, \ \ 0\big)^\top \in \mathbb{R}^3$ and

$$\widehat{\boldsymbol{A}}_4 = \widehat{\boldsymbol{N}}\widehat{\boldsymbol{A}}\widehat{\boldsymbol{V}} = \begin{bmatrix} -\frac{1}{g_r}\frac{c_2}{c_1} & -\frac{1}{g_r}\frac{c_3}{c_1} - 1 & -\frac{1}{c_1}\frac{c_2}{g_r} \\ -\frac{d_S}{g_r \Theta_2}\frac{c_2}{c_1} + \frac{c_S}{\Theta_2} & -\frac{d_S}{g_r \Theta_2}\frac{c_3}{c_1} - \frac{d_S + \nu_2}{\Theta_2} & -\frac{d_S}{g_r \Theta_2}\frac{c_2}{c_1} \\ -k_F & 0 & -k_F \end{bmatrix} \in \mathbb{R}^{3\times 3}.$$

Note that the following hold

$$\begin{aligned} m_0 &:= k_F \tfrac{c_S}{c_1\Theta_2}\left(c_1+\tfrac{c_3}{g_r}\right) \overset{(5.21)}{>} 0, \\ m_1 &:= k_F \tfrac{d_S}{c_1\Theta_2}\left(c_1+\tfrac{c_3}{g_r}\right) + \overbrace{\tfrac{c_S}{c_1\Theta_2}\left(c_1+\tfrac{c_3}{g_r}\right)}^{m_0/k_F} + \tfrac{\nu_2}{\Theta_2}\left(k_F+\tfrac{1}{c_1}\tfrac{c_2}{g_r}\right) \overset{(5.21)}{>} 0, \\ m_2 &:= \tfrac{d_S}{c_1\Theta_2}\left(c_1+\tfrac{c_3}{g_r}\right) + k_F + \tfrac{\nu_2}{\Theta_2} + \tfrac{1}{c_1}\tfrac{c_2}{g_r} \overset{(5.21)}{>} 0 \qquad \text{and} \qquad m_2\, m_1 - m_0 > 0. \end{aligned}$$

Hence the characteristic polynomial of $\widehat{\boldsymbol{A}}_4$, i.e. $\chi_{\widehat{\boldsymbol{A}}_5}(s) = s^3 + m_2 s^2 + m_1 s + m_0$, is Hurwitz [77, Theorem 3.4.71, p. 339] and $\operatorname{spec}(\widehat{\boldsymbol{A}}_4) \subset \mathbb{C}_{<0}$. Now a similar argumentation as in Step 2 of the proof of Proposition 5.6 shows that property ($\mathcal{S}_1$-sp$_2$) is satisfied, which completes Step 2. Combining Step 1 and Step 2 completes the proof of Proposition 5.7. □

Clearly, Proposition 5.7 in conjunction with Theorem 3.3, Theorem 4.4 or Theorem 4.7 assures that the high-gain adaptive controllers (3.11), (4.24) or (4.53) are applicable for speed control of augmented 2MS (5.12), (5.13), (5.22), respectively. Furthermore, in view of Corollary 5.2, the controller combinations (3.11)+(5.3) and (4.24)+(5.3) are also admissible. Due to the augmented output

$$\forall\, t \geq 0\colon \qquad y(t) = c_1\omega_1(t) + c_2\phi_S(t) + c_3\omega_2(t) + c_2 x_F(t)$$

and since load speed tracking is the control task, it is necessary to scale load speed reference $\omega_{2,\mathrm{ref}}(\cdot)$ and introduce the augmented reference given by (see [169, p. 176])

$$\forall\, t \geq 0\colon \qquad y_{\mathrm{ref}}(t) := (c_1/g_r + c_3)\,\omega_{2,\mathrm{ref}}(t).$$

It is easy to see that e.g. funnel controller (4.24) with boundary $\psi(\cdot) \in \mathcal{B}_1$ assures that the augmented error $e(\cdot) = y_{\mathrm{ref}}(\cdot) - y(\cdot)$ evolves within the performance funnel (i.e. $|e(t)| < \psi(t)$ for all $t \geq 0$) however this does *not* imply that load speed error $\omega_{2,\mathrm{ref}}(\cdot) - \omega_2(\cdot)$ remains within the prescribed region. Only if steady state is reached and controller combination (4.24)+(5.3) (or (3.11)+(5.3)) is applied to the augmented 2MS (5.15), (5.16), (5.22), then $\lim_{t\to\infty} e(t) = 0$ implies also $\lim_{t\to\infty} \omega_{2,\mathrm{ref}}(t) - \omega_2(t) = 0$ (see Theorem 6.11 in [169]).

Remark 5.8 (Design parameters c_1, c_2, c_3 and k_F)**.**
Besides the presuppositions in (5.21), the constants c_1, c_2, c_3 and k_F are free design parameters. Some recommendations are given for controller implementation: The augmented output in (5.22) incorporates filter state $x_F(\cdot)$. An analysis in the frequency domain reveals the idea behind the filter: denote the Laplace transforms of angle of twist and of filter state by $\phi_S(s)$ and $x_F(s)$, respectively. Then, from (5.22), it follows that

$$x_F(s) = \frac{-k_F}{s + k_F}\phi_S(s), \tag{5.24}$$

which is a first-order low-pass filter of negative angle of twist $\phi_S(\cdot)$ with cut-off frequency

k_F [rad/s]. *Moreover, it is easy to see that the following holds*

$$\phi_S(s) + x_F(s) = \left(1 + \frac{-k_F}{s + k_F}\right) \phi_S(s) = \frac{1}{k_F} \underbrace{\frac{s}{1 + s/k_F} \phi_S(s)}_{\approx \dot{\phi}_S(\cdot) \text{ for } k_F \gg 1} . \tag{5.25}$$

The transfer function in (5.25) *can be regarded as high-pass filter of angle of twist* $\phi_S(\cdot)$*. Clearly, feedback of* $\dot{\phi}_S(\cdot)$ *increases damping of the closed-loop system (see e.g. [166, p. 962]). The observation in* (5.25) *(or see a detailed discussion in Section 6.1.3 in [169]) indicates that large values for* c_2 *and* k_F *support system damping. Simulation and measurement results reveal that a choice* $0 > c_3/g_r > -c_1$ *increases damping additionally.*

5.2.2.3 Measurements

In the previous sections, it has been shown that high-gain adaptive speed control of (the models of) 1MS (5.12), (5.13) and 2MS (5.15), (5.16) is admissible, respectively. Now it will be shown that high-gain adaptive speed control of stiff and flexible industrial servo-systems in "real world" is indeed feasible. Therefore, three speed control (SC) experiments are carried out at the laboratory setup (see Section 5.2.1). The measurement results will show that

- adaptive λ-tracking controller (3.11) and funnel controller (4.24) in combination with proportional-integral internal model (5.3) can keep up with standard PI speed control of stiff servo-systems (1MS),
- high-gain adaptive speed control and, in addition, active damping of shaft oscillations of flexible servo-systems (2MS) is practicable and
- speed funnel control of 1MS and 2MS in the presence of actuator saturation may work even if feasibility condition (4.54) is violated.

Experiment SC1 — speed control of 1MS:
Five controllers are implemented at the laboratory setup for speed control of the emulated 1MS (see Fig. 5.4(a)). Benchmark controller is a standard PI controller as in (1.28) (with $k_D = 0$ and $u_F(\cdot) = 0$), whereas the other four controllers are the adaptive λ-tracking controller (3.11), the funnel controller (4.24) and the serial interconnections (3.11)+(5.3) and (4.24)+(5.3) with proportional-integral internal model (5.3).

Control task is set-point and reference tracking under changing disturbances (load torques). Reference $y_{\text{ref}}(\cdot) = \omega_{\text{ref}}(\cdot) \in \mathcal{W}^{1,\infty}(\mathbb{R}_{\geq 0}; \mathbb{R})$ and load torque $m_L(\cdot) \in \mathcal{L}^{\infty}(\mathbb{R}_{\geq 0}; \mathbb{R})$ are depicted in Fig. 5.8 (see top and bottom, respectively). Controller implementation in the xPC target real-time system is illustrated in Fig. 5.6. For each run the 'speed controller' in Fig. 5.6 corresponds to one of the five controllers above. So Experiment SC1 consists of five runs in total. A single run takes 50 [s].

To achieve comparable runs, all controllers are designed under the same circumstances:

(i) the available drive torque of the laboratory setup is *not* to be exceeded, i.e. $u(t) \leq \hat{u}_A = 22$ [Nm] for all $t \geq 0$,

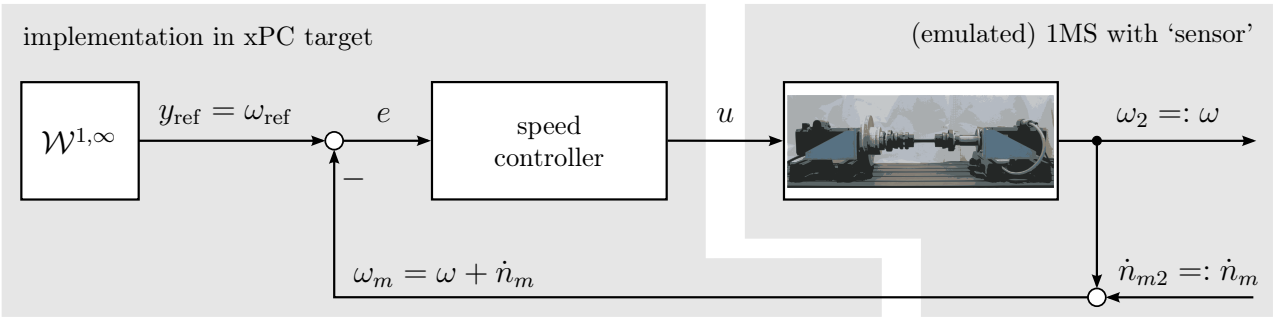

Figure 5.6: *Block diagram of implementation at laboratory setup for speed control of (emulated) 1MS.*

(ii) the generated reference torque at startup equals the maximal admissible torque, i.e. $u(0) = m_{M,\text{ref}}(0) = 22\,[\text{Nm}]$ (to achieve the fastest possible initial acceleration). Note that actuator deviations deteriorate the initial drive torque, hence solely $m_M(0) \approx 22\,[\text{Nm}]$ is to be expected and

(iii) the following motion control objectives—formulated in terms of maximum rise and settling time and maximum overshoot (similar to (mco_1), (mco_2) and (mco_3) in Section 1.1)—must be accomplished for set-point tracking without load (i.e. the interval $[0,\,5]\,[\text{s}]$):

$$t^r_{\text{ref},0.8} = 0.5\,[\text{s}]\,, \quad t^s_{\text{ref},0.1} = 1.0\,[\text{s}] \quad \text{and} \quad \Delta^{os}_{\text{ref}} = 25\,[\%] \quad \text{for} \quad \hat{y}_{\text{ref}} = 10\,[\text{rad/s}]\,. \tag{5.26}$$

To accomplish the motion control objectives in (5.26), the PI controller (1.28) and the adaptive λ-tracking controller (3.11) with and without internal model (5.3) are tuned by trial and error and so several implementation attempts are required to meet the specifications. In contrast, funnel controller (4.24) with and without internal model (5.3) directly allows to include control objectives (5.26) in boundary design and, consequently, the first implementation yields a successful run (fulfilling the control objectives), respectively. Data of reference, disturbance and controller design is collected in Tab. 5.4.

Control performance of each controller is evaluated by means of rise time $t^r_{y(\cdot),0.8}$, settling time $t^s_{y(\cdot),0.1}$ and overshoot $\Delta^{os}_{y(\cdot)}$ for set-point tracking (i.e. the interval $[0,\,5]\,[\text{s}]$) and by the ITAE criterion as in (3.82) for reference tracking under (varying) load (i.e. the overall interval $[0,\,50]\,[\text{s}]$). Performance evaluation is summarized in Tab. 5.3. Measurement results are depicted in Fig. 5.7(a) for set-point tracking and in Fig. 5.8 for reference tracking under varying load. The results are distinguishable from one another by the following color and line style assignment (to improve readability the controllers are restated):

——— (1.28) with $k_D = 0$ and $u_F(\cdot) = 0$, i.e. PI controller:

$$u(t) = k_P\, e(t) + k_I \int_0^t e(\tau)\,\mathrm{d}\tau\,;$$

-·-·-·-· (3.11), i.e. adaptive λ-tracking controller:

$$u(t) = k(t)\, e(t) \qquad \text{where} \qquad \dot{k}(t) = q_1\, d_\lambda\big(|e(t)|\big)^{q_2}, \quad k(0) = k_0;$$

controller/system	Experiment SC1 (1MS)	Experiment SC2 (2MS)
reference	$\hat{y}_{\text{ref}} = 10$ [rad/s], for $y_{\text{ref}}(\cdot)$ see top of Fig. 5.8 & 5.10, resp.	
	$\|y_{\text{ref}}\|_\infty = 50$ [rad/s],	$\|y_{\text{ref}}\|_\infty = 30$ [rad/s],
	$\|\dot{y}_{\text{ref}}\|_\infty = 4$ [rad/s^2]	$\|\dot{y}_{\text{ref}}\|_\infty = 2$ [rad/s^2]
load torque	for $m_L(\cdot)$ see bottom of Fig. 5.8, $\|m_L\|_\infty = 10$ [Nm]	
augmented output & filter as in (5.22)	—	$c_1 = 1$ [1], $c_2 = 100$ $\left[\frac{1}{\text{s}}\right]$, $c_3 = -0.1$ [s], $k_F = 5$ $\left[\frac{\text{rad}}{\text{s}}\right]$
initial error	$e(0) = 10$ $\left[\frac{\text{rad}}{\text{s}}\right]$	$e(0) = (c_1 + c_3)\hat{y}_{\text{ref}} = 9$ $\left[\frac{\text{rad}}{\text{s}}\right]$
PI controller as in (1.28)	$k_P = 2.2$ $\left[\frac{\text{Nms}}{\text{rad}}\right]$, $k_I = 6.0$ $\left[\frac{\text{Nm}}{\text{rad}}\right]$	—
	$k_D = 0$ $\left[\frac{\text{Nms}^2}{\text{rad}}\right]$, $u_F(\cdot) = 0$ [Nm]	
λ-tracking controller as in (3.11)	$q_1 = 0.1$ [1], $q_2 = 2$ [1], $\lambda = 0.99$ $\left[\frac{\text{rad}}{\text{s}}\right]$	
	$k_0 = \frac{\hat{u}_A}{e(0)} = 2.2$ $\left[\frac{\text{Nms}}{\text{rad}}\right]$	$k_0 = \frac{\hat{u}_A}{e(0)} = 2.44$ $\left[\frac{\text{Nms}}{\text{rad}}\right]$
funnel controller as in (4.24)	$\psi(\cdot)$ as in (4.8) and $\varsigma(\cdot) = \frac{\hat{u}_A(\Lambda - e(0))}{\Lambda e(0)}\,\psi(\cdot)$ where	
	$\Lambda = 2e(0) = 20$ $\left[\frac{\text{rad}}{\text{s}}\right]$	$\Lambda = 2e(0) = 18$ $\left[\frac{\text{rad}}{\text{s}}\right]$
	$\lambda = 0.99$ $\left[\frac{\text{rad}}{\text{s}}\right]$	$\lambda = 0.99$ $\left[\frac{\text{rad}}{\text{s}}\right]$
	$T_E = 0.134$ [s]	$T_E = 0.154$ [s]
internal model as in (5.3)	$k_P = 1$ [1], $k_I = 3$ $\left[\frac{1}{\text{s}}\right]$	$k_P = 1$ [1], $k_I = 2$ $\left[\frac{1}{\text{s}}\right]$

Table 5.2: *Implementation data of Experiment SC1 (speed control of 1MS) and Experiment SC2 (speed control of 2MS). Centered values hold for both experiments.*

(4.24), i.e. funnel controller:

$$u(t) = k(t)\,e(t) \qquad \text{where} \qquad k(t) = \frac{\varsigma(t)}{\psi(t) - |e(t)|};$$

(3.11)+(5.3), i.e. adaptive λ-tracking controller with internal model ($k_P = 1$):

$$u(t) = k(t)\,e(t) + k_I \int_0^t k(\tau)e(\tau)\,\mathrm{d}\tau \qquad \text{where} \qquad \dot{k}(t) = q_1\, d_\lambda\big(|e(t)|\big)^{q_2}, \quad k(0) = k_0;$$

(4.24)+(5.3), i.e. funnel controller with internal model ($k_P = 1$):

$$u(t) = k(t)\,e(t) + k_I \int_0^t k(\tau)e(\tau)\,\mathrm{d}\tau \qquad \text{where} \qquad k(t) = \frac{\varsigma(t)}{\psi(t) - |e(t)|}.$$

Discussion of the measurement results for set-point tracking (see Fig. 5.7(a)):
Clearly, all five controllers accomplish the motion control objectives specified in (5.26) (see Tab. 5.3). The high-gain adaptive controllers (3.11) and (4.24) without internal model yield no overshoots and the fastest settling times, but do not achieve steady state accu-

experiment	controller	$t^r_{y(\cdot),0.8}$ [s]	$t^s_{y(\cdot),0.1}$ [s]	$\Delta^{os}_{y(\cdot)}$ [%]	ITAE [rad s]
SC1 (1MS)	(1.28)	0.22	0.98	18.2	96.5
	(3.11)	0.30	0.48	0.0	1539.0
	(4.24)	0.29	0.46	0.0	(aborted run)
	(3.11)+(5.3)	0.19	0.82	17.7	70.3
	(4.24)+(5.3)	0.21	0.55	13.3	80.9
SC2 (2MS)	(3.11)	0.46	0.63	0.0	1709.2
	(4.24)	0.36	0.45	0.0	(aborted run)
	(3.11)+(5.3)	0.33	1.37	22.3	121.3
	(4.24)+(5.3)	0.33	1.05	18.9	120.6

Table 5.3: *Controller performance for Experiment SC1 (speed control of 1MS) and Experiment SC2 (speed control of 2MS).*

racy. PI controller ——(1.28) and the high-gain adaptive controllers ——(3.11)+(5.3) and ——(4.24)+(5.3) with internal model have comparable control performance and assure that the control error asymptotically vanishes, respectively. The funnel controller ——(4.24)+(5.3) with internal model shows the smallest settling time and the lowest overshoot but, to reach steady state, this controller combination takes the longest time.

Discussion of the measurement results for reference tracking under varying load (see Fig. 5.8): Adaptive λ-tracking controller ·····(3.11) without internal model produces large contouring errors and so has the worst ITAE value (see Tab. 5.3). Moreover, this controller does not attain standstill at 50 [s]. Funnel controller ·····(4.24) *without* internal model *cannot assure* error evolution within the performance funnel. Due to the step-like load torque $m_L(\cdot)$ at 5 [s] the tracking error approaches the boundary very closely and modeling assumptions (ma_1) and (ma_4) are violated (see Section 1.6.1): near the boundary, due to large gains (> 20, not shown), noise amplification is drastically increased, real-time execution in "quasi-continuous time" does not hold anymore and the actuator cannot provide the required drive torque sufficiently fast. As a consequence the error suddenly "jumps" out of the prescribed region which results in reversed control action (sign change in the gain). Hence this run is aborted after ≈ 12 [s]. The chosen asymptotic accuracy $\lambda = 0.99$ [rad/s] is too demanding for funnel control under load: at the laboratory setup, speed measurement is too noisy and torque generation is too slow. In Experiment SC3 it will be shown that funnel control without internal model works for speed control of the 1MS if funnel design is more relaxed.

Control performance of the controllers ——(1.28), ——(3.11)+(5.3) and ——(4.24)+(5.3) with integral control action is similar (see evaluation of ITAE criterion in Tab. 5.3). The funnel controller ——(4.24)+(5.3) with internal model assures error evolution within the performance funnel (by adequate gain adaption) whereas, for PI controller ——(1.28) and adaptive λ-tracking controller ——(3.11)+(5.3) with internal model, the tracking error leaves the prescribed region when step-like load torques are induced at 5, 15 and 35 [s], respectively. Nevertheless (and interesting to note that), the adaptive λ-tracking controller ——(3.11)+(5.3) with internal model gives the best ITAE value. Noise amplification of the high-gain adaptive controllers ·····(3.11), ——(3.11)+(5.3) and ——(4.24)+(5.3) is slightly higher than that of

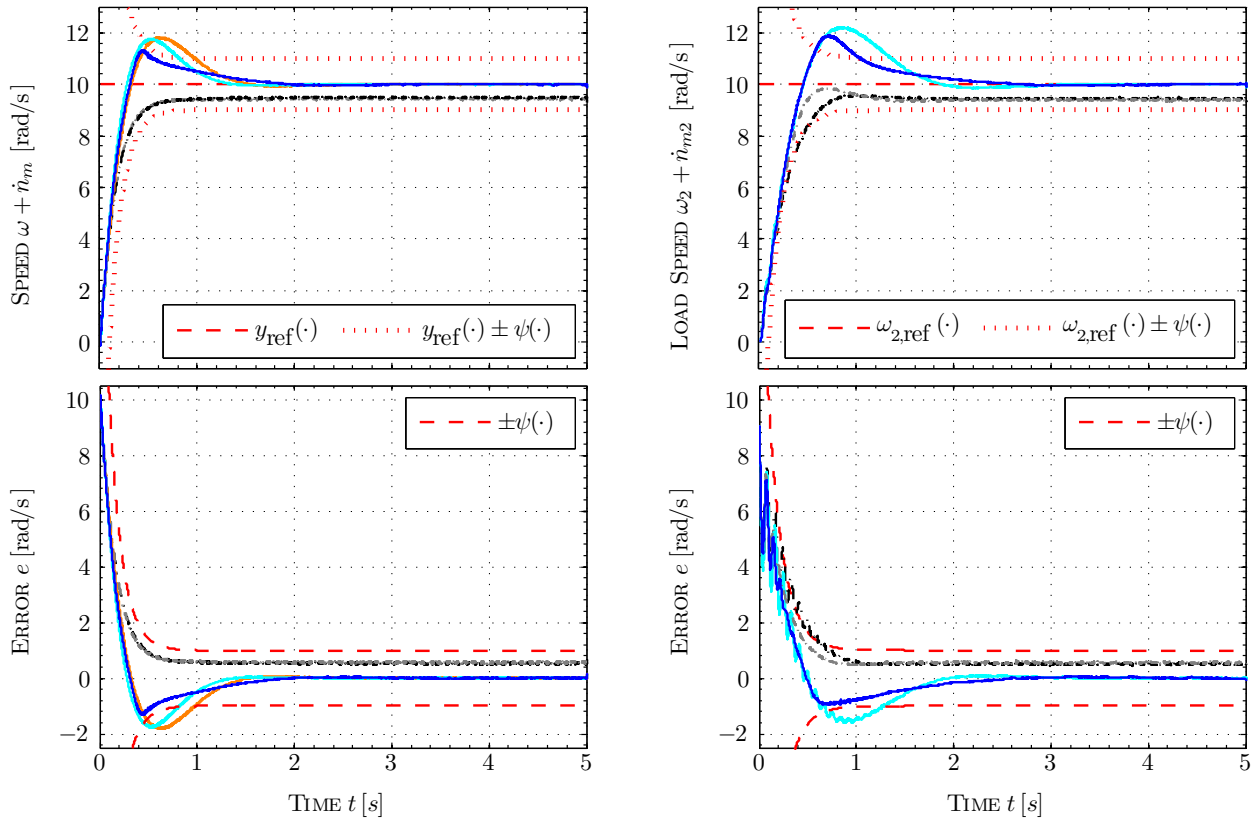

(a) *Experiment SC1 (1MS) — top: measured speed* $\omega(\cdot) + \dot{n}_m(\cdot)$*; bottom: speed error* $e(\cdot)$

(b) *Experiment SC2 (2MS) — top: measured load speed* $\omega_2(\cdot) + \dot{n}_{m2}(\cdot)$*; bottom: (augmented) error* $e(\cdot)$

Figure 5.7: *Measurement results of Experiment SC1 & SC2: set-point tracking speed control of emulated 1MS (left) and 2MS (right) for different controllers (see p. 194):* ——(1.28) *(only for 1MS),* ·····(3.11), ·····(4.24), ——(3.11)+(5.3), ——(4.24)+(5.3) *with parametrization as in Tab. 5.2.*

PI controller ——(1.28). Note that, only the gain of λ-tracking controller ·····(3.11) drastically and permanently exceeds gain $k_P = 2.2\,[\text{Nms/rad}]$ of PI controller ——(1.28) with $\lim_{t\to 50} k(t) \approx 7\,[\text{Nms/rad}]$. For the interval $[5-35]$ [s] the tracking error cannot be kept within the λ-strip. In contrast, for adaptive λ-tracking controller combination ——(3.11)+(5.3), the error remains within the λ-strip for almost all time. After a fast adaption phase within the interval $[0,\ 1]$ [s], the controller gain of ——(3.11)+(5.3) stays almost constant ($\approx 2.9\,[\text{Nms/rad}]$) and is slightly larger than $k_P = 2.2$ of PI controller ——(1.28). The time-varying gain of funnel controller combination ——(4.24)+(5.3) only increases if necessary, e.g. see the peak at 35 [s] with $k(35) = \max_{t\in[0,\,50]} k(t) \approx 7.9\,[\text{Nms/rad}]$ when the load torque is reduced step-like. Most of the time, its gain is even smaller than gain k_P of PI controller ——(1.28).

Remark 5.9. *Obviously, the PI controller* (1.28) *could be designed more properly, using e.g. anti-wind up strategies (see [166, Section 5.6]), such that better tracking performance and disturbance rejection is to be expected. But for the comparison here, the intention is to show the limits of classical PI speed control with constant gains: adaption to changing disturbances is not possible.*

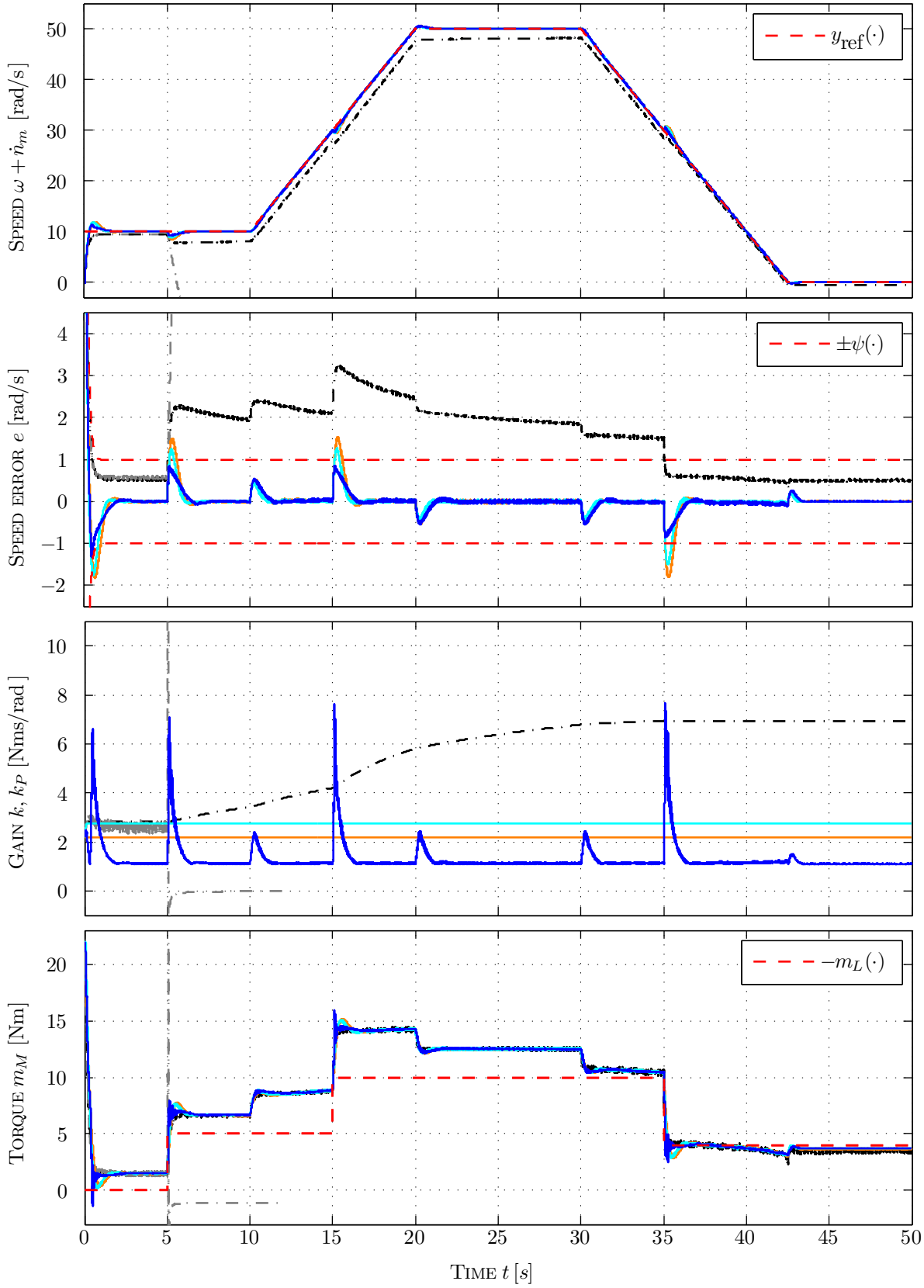

Figure 5.8: *Measurement results of Experiment SC1 (speed control of 1MS) for different controllers (see p. 194):* —(1.28), -·-·-(3.11), -·-·-(4.24), —(3.11)+(5.3), —(4.24)+(5.3) *with parametrization as in Tab. 5.2 (from top to bottom: measured speed* $\omega(\cdot) + \dot{n}_m(\cdot)$*, speed error* $e(\cdot)$*, gain* k_P *&* $k(\cdot)$ *and drive torque* $m_M(\cdot) = \text{sat}_{\hat{u}_A}\big(u(\cdot) + u_A(\cdot)\big)$*).*

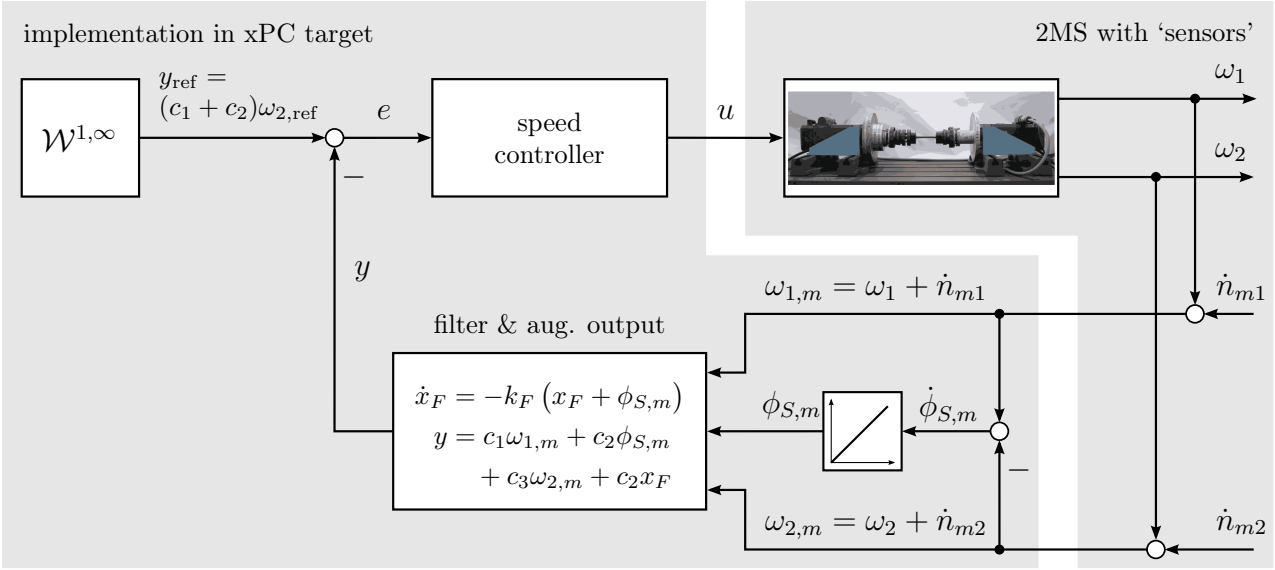

Figure 5.9: *Block diagram of implementation at laboratory setup for speed control of 2MS.*

Experiment SC2 — speed control of 2MS:
Experiment SC2 is similar to Experiment SC1. Control task is load speed set-point tracking without load and reference tracking under varying loads. Load speed reference $\omega_{2,\text{ref}}(\cdot) \in \mathcal{W}^{1,\infty}(\mathbb{R}_{\geq 0};\mathbb{R})$ and disturbance torque $m_L(\cdot) \in \mathcal{L}^{\infty}(\mathbb{R}_{\geq 0};\mathbb{R})$ are depicted in Fig. 5.10 (see top and bottom, respectively). Since

$$\omega_0^{\text{2MS}} = 61\,[\text{rad/s}] \ll 1/(2T_\sigma) = 1/(4\cdot 10^{-3})\,[\text{rad/s}] = 250\,[\text{rad/s}]$$

(see Section 5.2.1), the implementation of PI controller (1.28) (with $k_D = 0$ and $u_F(\cdot) = 0$) requires re-design (deceleration) of torque controller in the inverter to assure stability of the overall closed-loop system (see [166, Section 19.1]). Hence a comparison with standard PI control is omitted and only the four high-gain adaptive controllers ·····(3.11), ·····(4.24), ——(3.11)+(5.3) and ——(4.24)+(5.3) in conjunction with augmented output and high-pass filter as in (5.22) are applied for speed control of the 2MS. Color assignment is identical to Experiment SC1 (see p. 194). Again a single run takes 50 [s].

The implementation of the high-gain adaptive speed controllers is illustrated in Fig. 5.9. Filter and augmented output are shown for measured signals (with index $_m$) deteriorated by measurement errors. In comparison to Experiment SC1, due to the increased overall inertia $\Theta_1 + \Theta_2 = 0.499$ [kg m^2], the reference $\omega_{2,\text{ref}}(\cdot)$ is slightly adjusted: its slope and so its maximal magnitude $\|\omega_{2,\text{ref}}\|_\infty = 30$ [rad/s] are reduced (see top of Fig. 5.10). Also the motion control objectives are relaxed as follows:

$$t^r_{\text{ref},0.8} = 1.0\,[\text{s}]\,, \quad t^s_{\text{ref},0.1} = 1.5\,[\text{s}] \quad \text{and} \quad \Delta^{os}_{\text{ref}} = 25\,[\%] \quad \text{for} \quad \hat{y}_{\text{ref}} = 10\,[\text{rad/s}]\,. \tag{5.27}$$

All controllers are designed such that $u(0) = m_{M,\text{ref}}(0) = 22\,[\text{Nm}]$ and $|u(t)| \leq 22\,[\text{Nm}]$ for all $t \geq 0$. Design parameters of each implementation are listed in Tab. 5.2. Measurement results are shown in Fig. 5.7(b) for set-point tracking without load (i.e. the interval [0, 5] [s]) and in Fig. 5.10 for reference tracking under changing load (i.e. the interval [0, 50] [s]). Eval-

uation of control performance is done by means of rise time $t^r_{y(\cdot),0.8}$, settling time $t^s_{y(\cdot),0.1}$ and overshoot $\Delta^{os}_{y(\cdot)}$ for load speed set-point tracking and by the ITAE criterion for load speed reference tracking. To compute the ITAE criterion, $e(\tau)$ in (3.82) is replaced by load speed error $\omega_{2,\mathrm{ref}}(\tau) - \omega_2(\tau)$. Evaluation results are summarized in Tab. 5.3.

Discussion of the measurement results for load speed set-point tracking (see Fig. 5.7(b)):
First observe that all closed-loop systems exhibit noticeable oscillations in augmented error $e(\cdot)$ whereas load speed $\omega_2(\cdot)$ is well damped (see bottom and top of Fig. 5.7(b), respectively). Clearly, all four controllers accomplish the motion control objectives specified in (5.27) (see Tab. 5.8). But for the 2MS, due to the augmented output, even funnel controller design requires several tuning iterations: error evolution within the performance funnel does not imply that load speed error $\omega_{2,\mathrm{ref}}(\cdot) - \omega_2(\cdot)$ evolves within the prescribed region (see top of Fig. 5.7(b)!).

Discussion of the measurement results for load speed reference tracking (see Fig. 5.10):
The measurement results are similar to Experiment SC1. The adaptive λ-tracking controller ·····(3.11) without internal model yields bad transient tracking accuracy (large contouring errors) and so the largest ITAE value (see Tab. 5.3). After the load step at 5 [s], funnel controller ·····(4.24) *without* internal model is *not* capable to keep the augmented error within the performance funnel. The run is aborted after $\approx$ 11 [s]. Again, boundary design (asymptotic accuracy) is too demanding for the noisy speed sensor signal at the laboratory setup. The controller combinations with internal model, i.e. ——(3.11)+(5.3) and ——(4.24)+(5.3), have comparable control performance and achieve steady state accuracy (in augmented error *and* load speed error!). Evaluation of the ITAE criterion yields similar values for both high-gain adaptive controller combinations (see Tab. 5.3). Noise amplification of the high-gain adaptive controllers ·····(3.11) , ——(3.11)+(5.3) and ——(4.24)+(5.3) is acceptable.

Experiment SC3 — saturated funnel controller for speed control of 1MS and 2MS:
Experiment SC3 is similar to the runs of Experiment SC1 & SC2 with funnel controller (4.24). Now, instead of (4.24), the saturated funnel controller (4.53) (with $u_F(\cdot) = 0$), i.e.

$$u(t) = \mathrm{sat}_{\hat{u}}\Big(k(t)\,e(t)\Big) \quad \text{where} \quad k(t) = \frac{\varsigma(t)}{\psi(t) - |e(t)|} \quad \text{and} \quad \begin{array}{l}\varsigma(\cdot) \text{ as in Tab. 5.2,}\\ \psi(\cdot) \text{ as in (4.8),}\end{array}$$

is implemented for speed control of 1MS and 2MS (see implementation in Fig. 5.6 and Fig. 5.9, respectively). Reference and disturbance are as in Experiments SC1 & SC2 (see top and bottom of Fig. 5.11(a) and (b), respectively). The purpose of this experiment is to illustrate that

(a) funnel control *without* proportional-integral internal model is feasible for speed control of 1MS and 2MS, if boundary design is not too demanding and

(b) funnel control with saturation is feasible for speed control of 1MS and 2MS, even if feasibility condition (4.54) is violated.

To show (a), in contrast to Experiment SC1 & SC2, the funnel boundary of saturated funnel controller (4.53) is designed with larger asymptotic accuracy (otherwise similar to the design in Tab. 5.2). More precisely, for exponential boundary $\psi(\cdot)$ as in (4.8), the following parameters

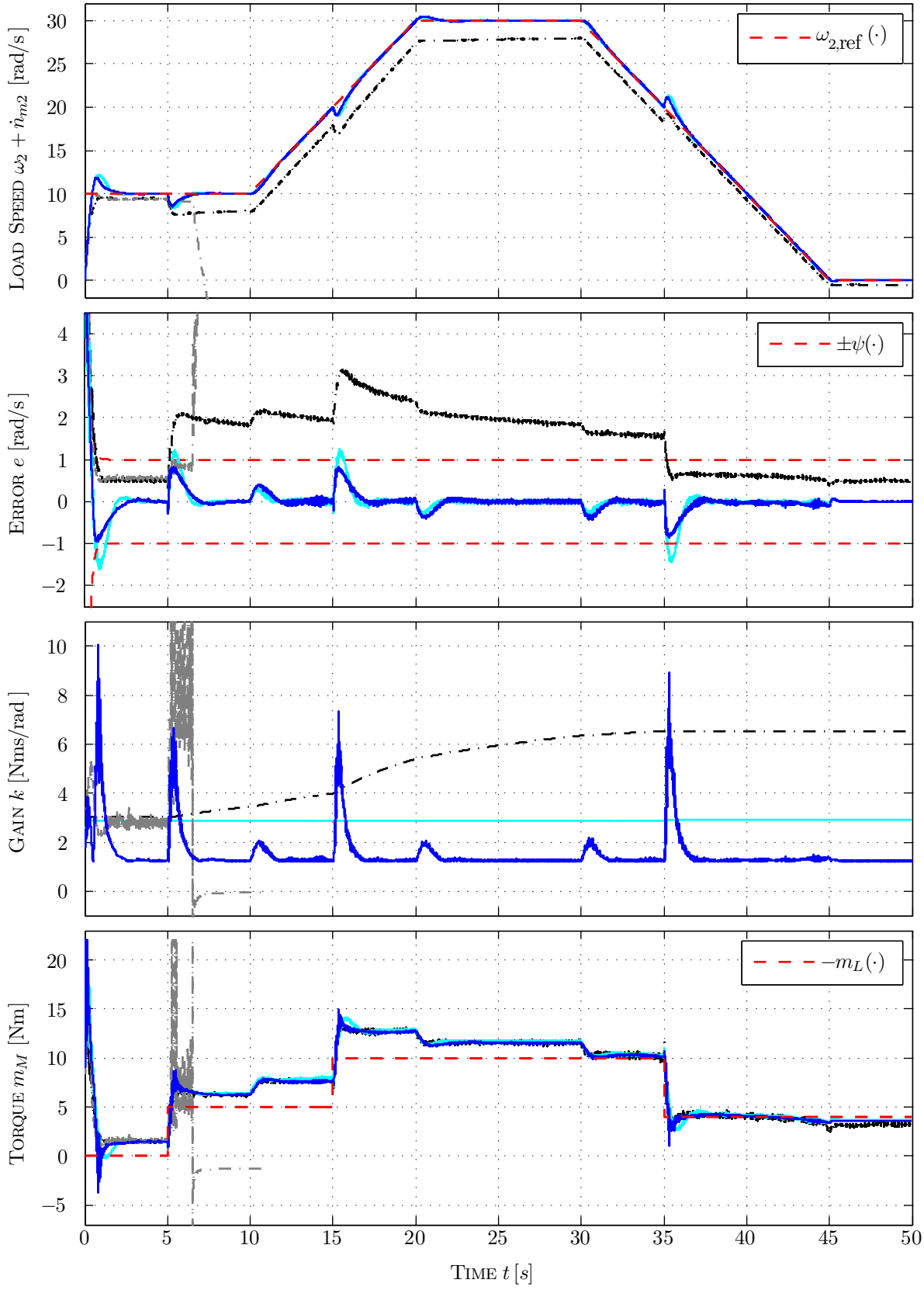

Figure 5.10: *Measurement results of Experiment SC2 (speed control of 2MS) for different controllers (see p. 194):* ·-·-(3.11), ·····(4.24), ——(3.11)+(5.3), ——(4.24)+(5.3) *with parametrization as in Tab. 5.2 (from top to bottom: measured load speed* $\omega_2(\cdot) + \dot{n}_{m2}(\cdot)$*, (augmented) error* $e(\cdot)$*, gain* $k(\cdot)$ *and drive torque* $m_M(\cdot) = \mathrm{sat}_{\hat{u}_A}\left(u(\cdot) + u_A(\cdot)\right)$*).*

are chosen:

$$\left.\begin{array}{lllll} \text{for 1MS:} & \Lambda = 20\,[\text{rad/s}]\,, & \lambda = 2.99\,[\text{rad/s}] & \text{and} & T_E = 0.134\,[\text{s}] \quad \text{and} \\ \text{for 2MS:} & \Lambda = 18\,[\text{rad/s}]\,, & \lambda = 2.99\,[\text{rad/s}] & \text{and} & T_E = 0.137\,[\text{s}]\,. \end{array}\right\} \tag{5.28}$$

The choice $\lambda = 2.99\,[\text{rad/s}]$ is the smallest possible to make funnel control *without* internal model work at the laboratory setup.
To show (b), feasibility condition (4.54) is evaluated and saturation level $\hat{u}$ of saturated funnel controller (4.53) is successively reduced until speed funnel control fails for 1MS and 2MS. So a sufficient and a necessary condition for saturation level $\hat{u}$ is obtained, respectively.

The measurement results are depicted in Fig. 5.11 for 1MS and 2MS. The results underpin that (load) speed tracking with prescribed transient accuracy for industrial servo-systems with constrained control action is feasible. For the settings of Experiment SC3, the measurements indicate that the following saturation levels are necessary: $\hat{u} = 15\,[\text{Nm}]$ for 1MS and $\hat{u} = 13.5\,[\text{Nm}]$ for 2MS. To check sufficiency the feasibility condition (4.54) is evaluated for 1MS (5.12), (5.13) and for augmented 2MS (5.15), (5.16), (5.22) (with filter). To ease computation, assume that both systems are exactly known. Then collecting the system data in Tab. 5.1, the implementation data in Tab. 5.2 (reference, disturbance, etc.) and the data of boundary design as in (5.28), invoking M as in (4.20) and choosing $\delta = 0.01\ [1/\text{s}^2]$ in (4.54) (arbitrarily) yields:

$$\begin{array}{lll} \text{for 1MS:} & \|\dot{\psi}\|_\infty = 126.95\ \left[\text{rad/s}^2\right]\,,\ \gamma_0 = 2.92\ \left[1/\text{kg}\,\text{m}^2\right] \ \text{ and } \ M = 53.99\ \left[1/\text{s}^2\right] \\ & \Longrightarrow \quad \boxed{u_{\text{feas}} = 61.97\ [\text{Nm}] \quad \text{whereas} \quad \hat{u} = 15\ [\text{Nm}]\,!} \\ \text{for 2MS:} & \|\dot{\psi}\|_\infty = 109.57\ \left[\text{rad/s}^2\right]\,,\ \gamma_0 = 6.02\ \left[1/\text{kg}\,\text{m}^2\right] \ \text{ and } \ M = 3.97 \cdot 10^{13}\ \left[1/\text{s}^2\right] \\ & \Longrightarrow \quad \boxed{u_{\text{feas}} = 6.60 \cdot 10^{12}\ [\text{Nm}] \quad \text{whereas} \quad \hat{u} = 13.5\ [\text{Nm}]\,!} \end{array}$$

All values are rounded. Both feasibility numbers are much larger than the actually required maximal torque. For the 1MS, the computed value of u_{feas} is still reasonable and realistic. In contrast, for the 2MS, u_{feas} is extremely huge. This is due to the very rough bound $M_{\boldsymbol{z}} = 2.16 \cdot 10^{10}$ as in (4.19) (with $M_{\dot{V}} = 2.02 \cdot 10^7$ as in (4.17)) on the internal dynamics[1]. Concluding, evaluation of feasibility condition (4.54) gives very conservative bounds and might not be useful (or helpful) for application. Nevertheless, the measurement results indicate that funnel control works even in the presence of actuator saturation if the motion control objectives are reasonable.

5.2.3 Position control

In this section, a solution to the *high-gain adaptive position control problem* will be presented. It will be shown that the high-gain adaptive controllers with derivative feedback for system class $\mathcal{S}_2$ (presented in Chapters 3 & 4) are applicable for position control of stiff and flexible industrial servo-systems. By adequate tuning the controllers assure fulfillment of e.g. motion control objectives (mco_1)-(mco_3).

First, in Sections 5.2.3.1 and 5.2.3.2, affiliation of 1MS (1.24), (1.25) and 2MS (1.26), (1.27) to

[1] To obtain $M_{\boldsymbol{z}}$ and $M_{\dot{V}}$, the augmented 2MS (5.15), (5.16), (5.22) must be transformed into BIF to allow for computation of $|\hat{a}_1|$, $\|\hat{\boldsymbol{a}}_2\|$, $\|\hat{\boldsymbol{a}}_3\|$, etc. (see proof of Proposition 5.7). The details are omitted.

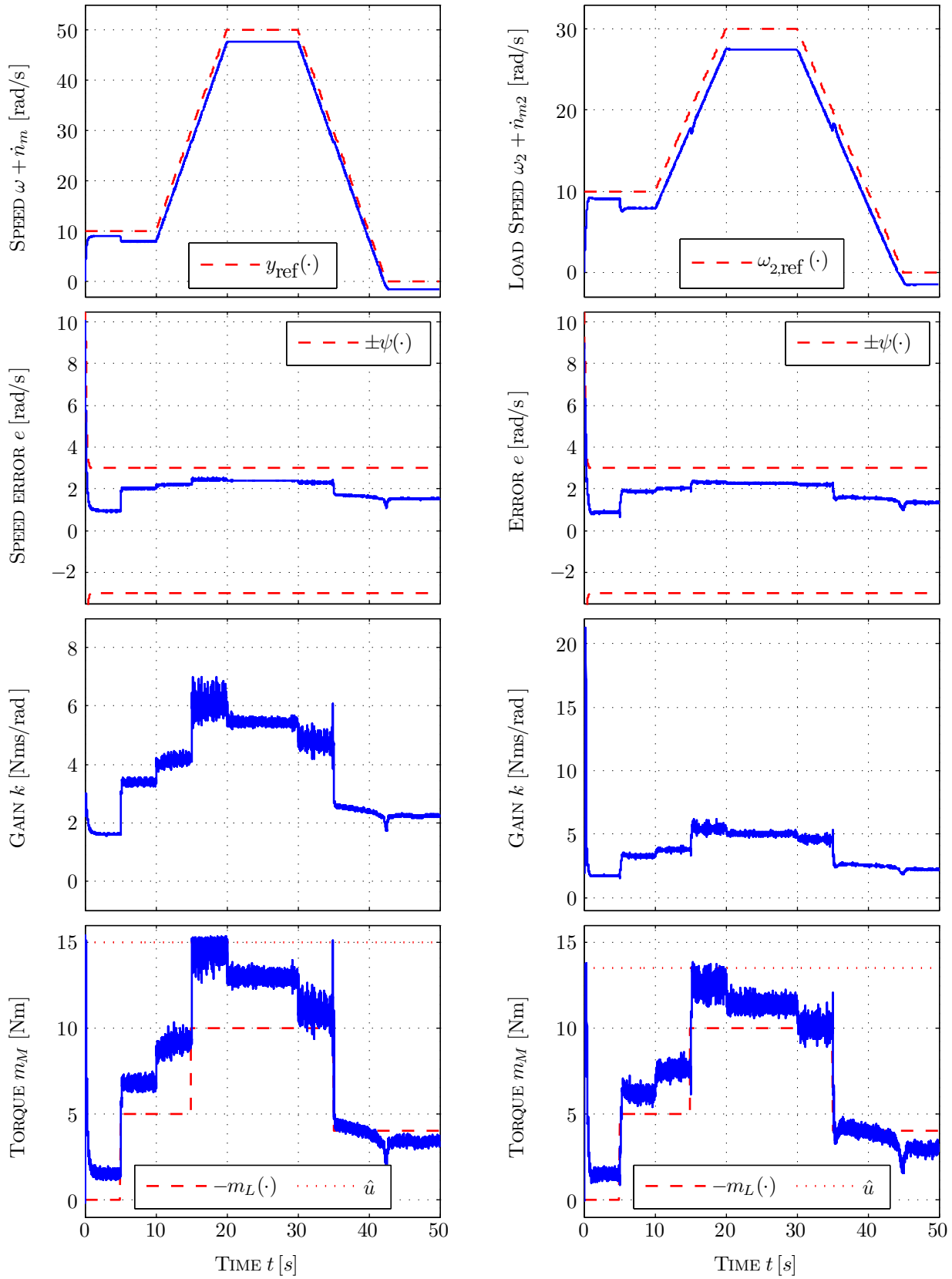

(a) *one-mass system (1MS):* $\hat{u} = 15$ [Nm]

(b) *two-mass system (2MS):* $\hat{u} = 13.5$ [Nm]

Figure 5.11: *Measurement results of Experiment SC3: saturated funnel controller* (4.53) *for speed control of 1MS (——left) and 2MS (——right).*

system class $\mathcal{S}_2$ is established, respectively. Hence, from a theoretical point of view, high-gain adaptive position control is admissible. To underpin industrial applicability, in Section 5.2.3.3, the high-gain adaptive (position) controllers are implemented at the laboratory setup and comparative measurement results are presented for a stiff and a flexible servo-system.

5.2.3.1 One-mass system of class $\mathcal{S}_2$

The 1MS (1.24), (1.25) represents the fundamental plant model for position control problems in mechatronics. Neglecting actuator saturation, affiliation to system class $\mathcal{S}_2$ can be established easily.

Proposition 5.10. *Consider the 1MS given by (1.24), (1.25) with instrumentation configuration (1MS-ic$_2$) and output coupling $\boldsymbol{c}^\top = (0,\, c_2)$, $c_2 \in \{1,\, 1/g_r\}$. If actuator saturation is negligible, i.e. $\hat{u}_A \to \infty$ in (1.24), and $\operatorname{sign}(g_r)$ is known, then 1MS (1.24), (1.25) is element of system class $\mathcal{S}_2$.*

Note that gear ratio g_r is written on the gear box. Hence its value and, clearly, its sign are available to the control designer.

Proof of Proposition 5.10.

Only the case $c_2 = 1/g_r$ is considered, the case $c_2 = 1$ follows analogously. For $\boldsymbol{B}_L$, $u_A(\cdot)$, $m_L(\cdot)$, $\mathfrak{F}_1$ and $\mathfrak{F}_2$ as in (1.25), define $h := 0$, $u_d(\cdot) := u_A(\cdot)$, $\boldsymbol{B}_{\mathfrak{T}} := \boldsymbol{B}_L$, $\boldsymbol{d}(\cdot) := (0,\, m_L(\cdot))^\top$ and $\mathfrak{T}\colon \mathcal{C}([-h,\infty);\mathbb{R}^2) \to \mathcal{L}^\infty_{\mathrm{loc}}(\mathbb{R}_{\geq 0};\mathbb{R}^2)$, $(\mathfrak{T}\boldsymbol{x})(t) := \big((\mathfrak{F}_1\omega)(t),\ (\mathfrak{F}_2\omega/g_r)(t)\big)^\top$. Then, for $\hat{u}_A \to \infty$, system (1.24) with (1.25) can be written in the form (1.36) and the following hold:

(i) $\boldsymbol{c}^\top\boldsymbol{b} = 0$, $\boldsymbol{c}^\top\boldsymbol{B}_{\mathfrak{T}} = \boldsymbol{0}_2^\top$, $\gamma_0 := \boldsymbol{c}^\top\boldsymbol{A}\boldsymbol{b} \overset{(1.24)}{=} \frac{k_A}{g_r\Theta} \overset{(1.25)}{\neq} 0$ and $\operatorname{sign}(\gamma_0) \overset{(1.25)}{=} \operatorname{sign}(g_r)$,

(ii)
$$\det\begin{bmatrix} s + \frac{\nu_1+\nu_2/g_r^2}{\Theta} & 0 & \frac{k_A}{\Theta} \\ -1 & s & 0 \\ 0 & \frac{1}{g_r} & 0 \end{bmatrix} = (-1)^{(1+3)}\frac{k_A}{\Theta}\det\begin{bmatrix} -1 & s \\ 0 & \frac{1}{g_r} \end{bmatrix} = -\frac{k_A}{g_r\Theta} \overset{(1.25)}{\neq} 0,$$

(iii) Corollary 5.4 gives $\mathfrak{F}_1, \mathfrak{F}_2 \in \mathcal{T}$, hence $\mathfrak{T} \in \mathcal{T}$ and, in view of (1.25), there exists $M_{\mathfrak{T}} := \sqrt{2}\max\{M_{\mathfrak{F}_1},\, M_{\mathfrak{F}_2}\} < \infty$ and $u_d(\cdot) \in \mathcal{L}^\infty(\mathbb{R}_{\geq 0};\mathbb{R})$ and $\boldsymbol{d}(\cdot) \in \mathcal{L}^\infty(\mathbb{R}_{\geq 0};\mathbb{R}^2)$ and

(iv) in view of instrumentation configuration (1MS-ic$_2$), output $y(\cdot) = \phi(\cdot)/g_r$ and derivative $\dot{y}(\cdot) = \omega(\cdot)/g_r$ are available for feedback.

Hence, all properties ($\mathcal{S}_2$-sp$_1$)–($\mathcal{S}_2$-sp$_5$) of system class $\mathcal{S}_2$ are satisfied. This completes the proof. □

Clearly, Proposition 5.10 with Theorem 3.13 and Theorem 4.13 allows for application of adaptive λ-tracking controller (3.46) and funnel controller (4.67) with derivative feedback for position control of 1MS (1.24), (1.25). In view of Corollary 5.2, the controller combinations (3.46)+(5.3) and (4.67)+(5.3) with proportional-integral internal model (5.3) are admissible and moreover, if steady state is reached, guarantee steady state accuracy. Theorem 4.7 allows to account for actuator saturation and assures tracking with prescribed transient accuracy if feasibility condition (4.107) is satisfied.

5.2.3.2 Two-mass system of class $\mathcal{S}_2$

Model (1.26), (1.27) of the 2MS is not in general element of system class $\mathcal{S}_2$, even if actuator saturation is negligible. Affiliation depends on the chosen output $y(\cdot)$. More precisely, output coupling vector $\boldsymbol{c}$ in (1.26) determines the relative degree and affects the minimum-phase condition. Under mild assumptions the 2MS (1.26), (1.27) without constrained actuator "can be made" element of system class $\mathcal{S}_2$.

Proposition 5.11. *Consider the 2MS given by (1.26), (1.27) with instrumentation configuration (2MS-ic$_2$)(c) and assume that actuator saturation is negligible, i.e. $\hat{u}_A \to \infty$ in (1.26). Then, for*

$$\boldsymbol{c}^\top = \begin{pmatrix} 0, & c_1, & 0, & c_2 \end{pmatrix}, \qquad c_1 > 0 \qquad \text{and} \qquad \frac{c_2}{g_r} > -c_1, \tag{5.29}$$

the 2MS (1.26), (1.27) is element of system class $\mathcal{S}_2$.

The output coupling vector $\boldsymbol{c}$ in (5.29) yields the "auxiliary" output

$$\forall t \geq 0\colon \qquad y(t) = c_1\phi_1(t) + c_2\phi_2(t) \tag{5.30}$$

(i.e. a linear combination of motor and load position) and assures, with the presuppositions in (5.29), that 2MS (1.26), (1.27) is minimum-phase and has relative degree two and positive high-frequency gain. Note that only the sign of gear ratio g_r is required to satisfy the presuppositions in (5.29).

Proof of Proposition 5.11.

Step 1: It is shown that properties ($\mathcal{S}_2$-sp$_1$), ($\mathcal{S}_2$-sp$_3$), ($\mathcal{S}_2$-sp$_4$) and ($\mathcal{S}_2$-sp$_5$) of system class $\mathcal{S}_2$ are satisfied.
For $\boldsymbol{B}_L$, $u_A(\cdot)$, $m_L(\cdot)$, $\mathfrak{F}_1$ and $\mathfrak{F}_2$ as in (1.27), define $h := 0$, $u_d(\cdot) := u_A(\cdot)$, $\boldsymbol{B}_{\mathfrak{T}} := \boldsymbol{B}_L$, $\boldsymbol{d}(\cdot) := (0,\, m_L(\cdot))^\top$ and

$$\mathfrak{T}\colon \mathcal{C}([-h,\infty);\mathbb{R}^4) \to \mathcal{L}^\infty_{\mathrm{loc}}(\mathbb{R}_{\geq 0};\mathbb{R}^2), \qquad (\mathfrak{T}\boldsymbol{x})(t) := \begin{pmatrix} (\mathfrak{F}_1\omega_1)(t), & (\mathfrak{F}_2\omega_2)(t) \end{pmatrix}^\top.$$

Then, for $\hat{u}_A \to \infty$, system (1.26) with (1.27) may be expressed in the form (1.36). Simple calculations give

$$\boldsymbol{c}^\top\boldsymbol{b} = 0,\ \boldsymbol{c}^\top\boldsymbol{B}_{\mathfrak{T}} = \boldsymbol{0}_2^\top,\ \gamma_0 := \boldsymbol{c}^\top\boldsymbol{A}\boldsymbol{b} = c_1\, k_A/\Theta_1 \overset{(5.29),(1.27)}{>} 0 \ \text{ and } \ \operatorname{sign}(\gamma_0) = \operatorname{sign}(c_1), \tag{5.31}$$

which shows system property ($\mathcal{S}_2$-sp$_1$). Furthermore, in view of Corollary 5.4 and (1.27), $\mathfrak{T} \in \mathcal{T}$, $M_{\mathfrak{T}} \leq \sqrt{2}\max\{M_{\mathfrak{F}_1},\, M_{\mathfrak{F}_2}\} < \infty$ and $u_d(\cdot) \in \mathcal{L}^\infty(\mathbb{R}_{\geq 0};\mathbb{R})$ and $\boldsymbol{d}(\cdot) \in \mathcal{L}^\infty(\mathbb{R}_{\geq 0};\mathbb{R}^2)$, respectively. Hence system properties ($\mathcal{S}_2$-sp$_3$) and ($\mathcal{S}_2$-sp$_4$) are fulfilled. Due to instrumentation configuration (2MS-ic$_2$)(c), output $y(\cdot) = c_1\,\phi_1(\cdot) + c_2\,\phi_2(\cdot)$ and derivative $\dot{y}(\cdot) = c_1\,\omega_1(\cdot) + c_2\,\omega_2(\cdot)$ are available for feedback which gives property ($\mathcal{S}_2$-sp$_5$). This completes Step 1.

Step 2: It is shown that property ($\mathcal{S}_2$-sp$_2$) of system class $\mathcal{S}_2$ is satisfied.
Since (5.31) holds, there exists a similarity transformation (see Section 3.3.2)

$$\boldsymbol{S}\colon \mathbb{R}^4 \to \mathbb{R}^4, \qquad \boldsymbol{x} \mapsto \begin{pmatrix} y, & \dot{y}, & z_1, & z_2 \end{pmatrix}^\top := \boldsymbol{S}\boldsymbol{x}$$

which takes (1.26), (1.27) with (5.29) into Byrnes-Isidori like form (3.8). For

$$\boldsymbol{C} = \begin{bmatrix} 0 & c_1 & 0 & c_2 \\ c_1 & 0 & c_2 & 0 \end{bmatrix} \qquad \text{and} \qquad \boldsymbol{B} = \begin{bmatrix} \frac{k_A}{\Theta_1} & 0 & 0 & 0 \\ -k_A \frac{d_S + g_r^2 \nu_1}{g_r^2 \Theta_1^2} & \frac{k_A}{\Theta_1} & \frac{k_A d_S}{g_r \Theta_1 \Theta_2} & 0 \end{bmatrix}^\top,$$

the "subtransformation" matrices are given by

$$\boldsymbol{V} = \ker \boldsymbol{C} = \begin{bmatrix} -\frac{c_2}{c_1} & 0 \\ 0 & -\frac{c_2}{c_1} \\ 1 & 0 \\ 0 & 1 \end{bmatrix} \qquad \text{and}$$

$$\boldsymbol{N} = (\boldsymbol{V}^\top \boldsymbol{V})^{-1} \boldsymbol{V}^\top [\boldsymbol{I}_4 - \boldsymbol{B}(\boldsymbol{C}\boldsymbol{B})^{-1}\boldsymbol{C}] = \begin{bmatrix} 0 & -\frac{d_S}{g_r \Theta_2} & 1 & -\frac{d_S c_2}{g_r \Theta_2 c_1} \\ 0 & 0 & 0 & 1 \end{bmatrix},$$

which, in view of (2.24), yields

$$\boldsymbol{S} = \begin{bmatrix} 0 & c_1 & 0 & c_2 \\ c_1 & 0 & c_2 & 0 \\ 0 & -\frac{d_S}{g_r \Theta_2} & 1 & -\frac{d_S c_2}{g_r \Theta_2 c_1} \\ 0 & 0 & 0 & 1 \end{bmatrix} \qquad \text{and} \qquad \boldsymbol{S}^{-1} = \begin{bmatrix} -\frac{d_S c_2}{g_r \Theta_2 c_1^2} & \frac{1}{c_1} & -\frac{c_2}{c_1} & 0 \\ \frac{1}{c_1} & 0 & 0 & -\frac{c_2}{c_1} \\ \frac{d_S}{g_r \Theta_2 c_1} & 0 & 1 & 0 \\ 0 & 0 & 0 & 1 \end{bmatrix}.$$

Hence, conform to (3.8), the system in new coordinates has the following form

$$\frac{\mathrm{d}}{\mathrm{d}t} \begin{pmatrix} y(t) \\ \dot{y}(t) \\ z_1(t) \\ z_2(t) \end{pmatrix} = \boldsymbol{S}\boldsymbol{A}\boldsymbol{S}^{-1} \begin{pmatrix} y(t) \\ \dot{y}(t) \\ z_1(t) \\ z_2(t) \end{pmatrix} + \boldsymbol{S}\boldsymbol{b}\big(u(t) + u_A(t)\big) + \boldsymbol{S}\boldsymbol{B}_L \begin{pmatrix} (\mathfrak{F}_1 \operatorname{row}_1(\boldsymbol{S}^{-1}) \begin{pmatrix} y \\ \dot{y} \\ z_1 \\ z_2 \end{pmatrix})(t) \\ m_L(t) + (\mathfrak{F}_2 \operatorname{row}_3(\boldsymbol{S}^{-1}) \begin{pmatrix} y \\ \dot{y} \\ z_1 \\ z_2 \end{pmatrix})(t) \end{pmatrix},$$

$$\big(y(0), \quad \dot{y}(0), \quad z_1(0), \quad z_2(0)\big)^\top = \boldsymbol{S}\boldsymbol{x}^0,$$

where

$$\boldsymbol{S}\boldsymbol{A}\boldsymbol{S}^{-1} =: \begin{bmatrix} 0 & 1 & \boldsymbol{0}_2^\top \\ a_1 & a_2 & \boldsymbol{a}_3^\top \\ \boldsymbol{a}_4 & \boldsymbol{0}_2 & \boldsymbol{A}_5 \end{bmatrix} \in \mathbb{R}^{4\times 4}, \ \boldsymbol{S}\boldsymbol{b} = \begin{pmatrix} 0 \\ \gamma_0 \\ 0 \\ 0 \end{pmatrix} \in \mathbb{R}^4 \ \text{ and } \ \boldsymbol{S}\boldsymbol{B}_L = \begin{bmatrix} 0 & 0 \\ -\frac{c_1}{\Theta_1} & -\frac{c_2}{\Theta_2} \\ 0 & -\frac{1}{\Theta_2} \\ 0 & 0 \end{bmatrix} \in \mathbb{R}^{4\times 2}.$$

Moreover, in view of (2.55), the entries of $\boldsymbol{S}\boldsymbol{A}\boldsymbol{S}^{-1}$ are given by

$$\begin{aligned}
a_1 &= \tfrac{c_S}{g_r}\left(\tfrac{1}{\Theta_2}\tfrac{c_2}{c_1} - \tfrac{1}{g_r\Theta_1}\right) + \tfrac{d_S}{g_r\Theta_1\Theta_2}\left(\tfrac{d_S}{g_r}\left(1+\tfrac{1}{g_r}\tfrac{c_2}{c_1}\right)+\nu_1\tfrac{c_2}{c_1}\right) \\
&\quad -\tfrac{d_S}{g_r\Theta_2^2}\tfrac{c_2}{c_1}\left(d_S\left(1+\tfrac{1}{g_r}\tfrac{c_2}{c_1}\right)+\nu_2\right) \in \mathbb{R}, \\
a_2 &= \tfrac{d_S}{g_r}\left(\tfrac{1}{\Theta_2}\tfrac{c_2}{c_1} - \tfrac{1}{g_r\Theta_1}\right) - \tfrac{\nu_1}{\Theta_1} \in \mathbb{R}, \\
\boldsymbol{a}_3 &= \begin{pmatrix} -d_S c_1\left(1+\tfrac{1}{g_r}\tfrac{c_2}{c_1}\right)\left(\tfrac{1}{\Theta_2}\tfrac{c_2}{c_1} - \tfrac{1}{g_r\Theta_1}\right) + c_2\left(\tfrac{\nu_1}{\Theta_1} - \tfrac{\nu_2}{\Theta_2}\right) \\ -c_S c_1\left(1+\tfrac{1}{g_r}\tfrac{c_2}{c_1}\right)\left(\tfrac{1}{\Theta_2}\tfrac{c_2}{c_1} - \tfrac{1}{g_r\Theta_1}\right) \end{pmatrix} \in \mathbb{R}^2, \\
\boldsymbol{a}_4 &= \tfrac{1}{g_r\Theta_2 c_1}\begin{pmatrix} c_S - \tfrac{d_S}{\Theta_2}\left(d_S\left(1+\tfrac{1}{g_r}\tfrac{c_2}{c_1}\right)+\nu_2\right) \\ d_S \end{pmatrix} \in \mathbb{R}^2
\end{aligned}$$

and

$$\boldsymbol{A}_5 = \boldsymbol{N}\boldsymbol{A}\boldsymbol{V} = \begin{bmatrix} -\tfrac{d_S}{\Theta_2}\left(1+\tfrac{1}{g_r}\tfrac{c_2}{c_1}\right) - \tfrac{\nu_2}{\Theta_2} & -\tfrac{c_S}{\Theta_2}\left(1+\tfrac{1}{g_r}\tfrac{c_2}{c_1}\right) \\ 1 & 0 \end{bmatrix} \in \mathbb{R}^{2\times 2}. \tag{5.32}$$

The characteristic polynomial of $\boldsymbol{A}_5$ is computed to

$$\chi_{\boldsymbol{A}_5}(s) = s^2 + \left(\frac{d_S}{\Theta_2}\left(1+\frac{1}{g_r}\frac{c_2}{c_1}\right) + \frac{\nu_2}{\Theta_2}\right)s + \frac{c_S}{\Theta_2}\left(1+\frac{1}{g_r}\frac{c_2}{c_1}\right)$$

and therefore

$$(5.29) \quad \Longrightarrow \quad \operatorname{spec}(\boldsymbol{A}_5) \subset \mathbb{C}_{<0}. \tag{5.33}$$

Invoking

$$\begin{aligned}
\det\begin{bmatrix} \boldsymbol{S}(s\boldsymbol{I}_4 - \boldsymbol{A})\boldsymbol{S}^{-1} & \boldsymbol{S}\boldsymbol{b} \\ \boldsymbol{c}^\top\boldsymbol{S}^{-1} & 0 \end{bmatrix} &= \det\left(\begin{bmatrix} \boldsymbol{S} & \boldsymbol{0}_4 \\ \boldsymbol{0}_4^\top & 1 \end{bmatrix}\begin{bmatrix} s\boldsymbol{I}_4 - \boldsymbol{A} & \boldsymbol{b} \\ \boldsymbol{c}^\top & 0 \end{bmatrix}\begin{bmatrix} \boldsymbol{S}^{-1} & \boldsymbol{0}_4 \\ \boldsymbol{0}_4^\top & 1 \end{bmatrix}\right) \\
&= \underbrace{\det(\boldsymbol{S})\det(\boldsymbol{S}^{-1})}_{=1}\det\begin{bmatrix} s\boldsymbol{I}_4 - \boldsymbol{A} & \boldsymbol{b} \\ \boldsymbol{c}^\top & 0 \end{bmatrix}
\end{aligned}$$

yields

$$\begin{aligned}
\det\begin{bmatrix} s\boldsymbol{I}_4 - \boldsymbol{A} & \boldsymbol{b} \\ \boldsymbol{c}^\top & 0 \end{bmatrix} &= \det\begin{bmatrix} s & -1 & \boldsymbol{0}_2^\top & 0 \\ -a_1 & s-a_2 & -\boldsymbol{a}_3^\top & \gamma_0 \\ -\boldsymbol{a}_4 & \boldsymbol{0}_2 & s\boldsymbol{I}_2 - \boldsymbol{A}_5 & 0 \\ 1 & 0 & \boldsymbol{0}_2^\top & 0 \end{bmatrix} = -\det\begin{bmatrix} -1 & \boldsymbol{0}_2^\top & 0 \\ s-a_2 & -\boldsymbol{a}_3^\top & \gamma_0 \\ \boldsymbol{0}_2 & s\boldsymbol{I}_2 - \boldsymbol{A}_5 & 0 \end{bmatrix} \\
&= \det\begin{bmatrix} -\boldsymbol{a}_3^\top & \gamma_0 \\ s\boldsymbol{I}_2 - \boldsymbol{A}_5 & 0 \end{bmatrix} = -\gamma_0\det\left[s\boldsymbol{I}_2 - \boldsymbol{A}_5\right] \overset{(5.33)}{\neq} 0 \quad \forall\, s \in \mathbb{C}_{\geq 0},
\end{aligned}$$

which shows property ($\mathcal{S}_2$-sp$_2$) of system class $\mathcal{S}_2$. Combining Step 1 and Step 2 completes the proof of Proposition 5.11. □

Clearly, Proposition 5.11 with Theorem 3.13, Theorem 4.13 or Corollary 5.2 ensures applicability of adaptive λ-tracking controller (3.46), funnel controller (4.67) or controller combinations (3.46)+(5.3) and (4.67)+(5.3) for position control of 2MS (1.26), (1.27) with auxiliary output (5.30). Position funnel control in the presence of actuator saturation is covered by Theorem 4.15.

Remark 5.12 (Controllability and observability of linear 2MS without friction)**.**
Neglecting friction (viscous and nonlinear, dynamic terms), actuator saturation and disturbances in (1.26), (1.27) *with* (5.29)*, i.e.* $u_A \to \infty$, $m_L(\cdot) = u_A(\cdot) = 0$, $(\mathfrak{F}_1\omega_1)(\cdot) = (\mathfrak{F}_2\omega_2)(\cdot) = 0$ *and* $\nu_1 = \nu_2 = 0$*, yields the linear model of a flexible 2MS. For the linear model, controllability and observability matrix are given by*

$$\boldsymbol{Q}_c = \begin{bmatrix} \boldsymbol{b} & \boldsymbol{A}\boldsymbol{b} & \boldsymbol{A}^2\boldsymbol{b} & \boldsymbol{A}^3\boldsymbol{b} \end{bmatrix} = k_A \begin{bmatrix} \frac{1}{\Theta_1} & -\frac{d_S}{g_r^2\Theta_1^2} & \frac{d_S^2\left(\Theta_1+\frac{\Theta_2}{g_r^2}\right)-c_S\Theta_1\Theta_2}{g_r^2\Theta_1^3\Theta_2} & \frac{d_S\left(\Theta_1+\frac{\Theta_2}{g_r^2}\right)\left(2c_S\Theta_1\Theta_2-d_S^2\left(\Theta_1+\frac{\Theta_2}{g_r^2}\right)\right)}{g_r^2\Theta_1^4\Theta_2^2} \\ 0 & \frac{1}{\Theta_1} & -\frac{d_S}{g_r^2\Theta_1^2} & \frac{d_S^2\left(\Theta_1+\frac{\Theta_2}{g_r^2}\right)-c_S\Theta_1\Theta_2}{g_r^2\Theta_1^3\Theta_2} \\ 0 & \frac{d_S}{g_r\Theta_1\Theta_2} & -\frac{d_S^2\left(\Theta_1+\frac{\Theta_2}{g_r^2}\right)-c_S\Theta_1\Theta_2}{g_r\Theta_1^2\Theta_2^2} & -\frac{d_S\left(\Theta_1+\frac{\Theta_2}{g_r^2}\right)\left(2c_S\Theta_1\Theta_2-d_S^2\left(\Theta_1+\frac{\Theta_2}{g_r^2}\right)\right)}{g_r\Theta_1^3\Theta_2^3} \\ 0 & 0 & \frac{d_S}{g_r\Theta_1\Theta_2} & -\frac{d_S^2\left(\Theta_1+\frac{\Theta_2}{g_r^2}\right)-c_S\Theta_1\Theta_2}{g_r\Theta_1^2\Theta_2^2} \end{bmatrix}$$

and

$$\boldsymbol{Q}_o := \begin{bmatrix} \boldsymbol{c}^\top \\ \boldsymbol{c}^\top\boldsymbol{A} \\ \boldsymbol{c}^\top\boldsymbol{A}^2 \\ \boldsymbol{c}^\top\boldsymbol{A}^3 \end{bmatrix} =$$

$$\begin{bmatrix} 0 & c_1 & 0 & c_2 \\ c_1 & 0 & c_2 & 0 \\ \frac{d_S\left(c_2-\frac{c_1\Theta_2}{g_r\Theta_1}\right)}{g_r\Theta_2} & \frac{c_S\left(c_2-\frac{c_1\Theta_2}{g_r\Theta_1}\right)}{g_r\Theta_2} & \frac{-d_S\left(c_2-\frac{c_1\Theta_2}{g_r\Theta_1}\right)}{\Theta_2} & \frac{-c_S\left(c_2-\frac{c_1\Theta_2}{g_r\Theta_1}\right)}{\Theta_2} \\ \frac{\left(c_2-\frac{c_1\Theta_2}{g_r\Theta_1}\right)(c_S\Theta_1-d_S^2\left(\frac{1}{g_r^2}+\frac{\Theta_1}{\Theta_2}\right))}{g_r\Theta_1\Theta_2} & \frac{-c_Sd_S\left(c_2-\frac{c_1\Theta_2}{g_r\Theta_1}\right)\left(\frac{1}{g_r^2}+\frac{\Theta_1}{\Theta_2}\right)}{g_r\Theta_1\Theta_2} & \frac{-\left(c_2-\frac{c_1\Theta_2}{g_r\Theta_1}\right)(c_S\Theta_1-d_S^2\left(\frac{1}{g_r^2}+\frac{\Theta_1}{\Theta_2}\right))}{\Theta_1\Theta_2} & \frac{c_Sd_S\left(c_2-\frac{c_1\Theta_2}{g_r\Theta_1}\right)\left(\frac{1}{g_r^2}+\frac{\Theta_1}{\Theta_2}\right)}{\Theta_1\Theta_2} \end{bmatrix},$$

respectively. Elementary row and column operations yield

$$\det(\boldsymbol{Q}_c) = \frac{k_A^4 c_S^2}{g_r^2\Theta_1^4\Theta_2^2} \overset{(1.27)}{\neq} 0 \qquad \textit{and} \qquad |\det(\boldsymbol{Q}_o)| = \left|\frac{c_S^2}{\Theta_2^2}\left(c_2 - c_1\frac{\Theta_2}{g_r\Theta_1}\right)^2\left(c_1+\frac{c_2}{g_r}\right)^2\right|.$$

Hence, the following implication holds

$$\left[\!\!\left[(1.27) \ \wedge \ \frac{c_2}{g_r} \neq -c_1 \ \wedge \ c_2 \neq c_1\frac{\Theta_2}{g_r\,\Theta_1} \right]\!\!\right] \qquad \Longrightarrow \qquad \left[\!\!\left[\det(\boldsymbol{Q}_o) \neq 0 \right]\!\!\right].$$

Controllability and observability are necessary for active damping of shaft oscillations. Loosely speaking, it has to be assured that the drive torque (control input) may affect angle of twist and that shaft oscillations are "visible" in the auxiliary output (5.30)*.*

Due to auxiliary output (5.30) and to allow for load position tracking of reference $\phi_{2,\mathrm{ref}}(\cdot) \in \mathcal{W}^{2,\infty}(\mathbb{R}_{\geq 0};\mathbb{R})$, the "auxiliary" reference

$$\forall t \geq 0\colon \qquad y_{\mathrm{ref}}(t) := (c_1/g_r + c_2)\phi_{2,\mathrm{ref}}(t) \tag{5.34}$$

should be implemented accordingly. Note that in many industrial applications solely motor position $\phi_1(\cdot)$ and motor speed $\omega_1(\cdot)$ are available for feedback. Setting $c_1 = 1$ and $c_2 = 0$ in (5.29), this case is covered by Proposition 5.11. However then, active damping of shaft oscillations is not possible (see e.g. [140]). Moreover, asymptotic load position tracking (i.e. $\lim_{t\to\infty} \phi_{2,\mathrm{ref}}(t) - \phi_2(t) = 0$) cannot be assured in general (see [65]). This also holds if load position $\phi_2(\cdot)$ is available for feedback, i.e. $c_1 > 0$ and $0 \neq c_2/g_r > -c_1$ in (5.29). To show this, suppose that the following assumptions are satisfied

(i) controller combination (3.46)+(5.3) or (4.67)+(5.3) is applied for position control of 2MS (1.26), (1.27) with auxiliary output (5.30) and

(ii) steady state is reached and, for $y_{\mathrm{ref}}(t)$ as in (5.34), the "auxiliary error" tends to zero, i.e.

$$\lim_{t\to\infty} e(t) = \lim_{t\to\infty} \left(y_{\mathrm{ref}}(t) - c_1\phi_1(t) - c_2\phi_2(t)\right) = 0.$$

Then it is easy to see that these assumptions do *not* imply $\lim_{t\to\infty} \phi_{2,\mathrm{ref}}(t) - \phi_2(t) = 0$. The load position error does not necessarily tend to zero asymptotically. To overcome this drawback and to achieve steady state accuracy *and* active damping of shaft oscillations, the restriction to the qualitative system knowledge as in (1.27) must be weakened.

If the system parameters d_S and Θ_2 in (1.27) are roughly and gear ratio g_r is exactly known (recall it can be read off on the gear box), then simulations and measurements show that active damping and, simultaneously, asymptotic load position tracking of constant reference signals can be achieved. Therefore dynamic feedback of angle of twist $\phi_S(\cdot) = \phi_1(\cdot)/g_r - \phi_2(\cdot)$ is necessary (similar to high-gain adaptive speed control of the 2MS). The following result may be formulated.

Proposition 5.13. *Consider the 2MS given by (1.26), (1.27) with instrumentation configuration (2MS-ic$_2$)(c). Suppose that actuator saturation is negligible, i.e. $\hat{u}_A \to \infty$ in (1.26), and introduce, for*

$$\frac{c_1}{g_r} > 0, \qquad 1 + \frac{c_2}{c_1} > 0 \qquad \textit{and} \qquad 0 < k_F < \frac{d_S}{\Theta_2}\left(1 + \frac{c_2}{c_1}\right), \tag{5.35}$$

the filter and the augmented output as follows

$$\left.\begin{aligned} \dot{x}_F(t) &= -k_F\left(x_F(t) + \tfrac{\phi_1(t)}{g_r} - \phi_2(t)\right), \qquad x_F(0) = 0, \\ y(t) &:= \underbrace{\left(0, \ \tfrac{c_1}{g_r}, \ 0, \ c_2, \ c_1\right)}_{=:\widehat{\boldsymbol{c}}^\top} \begin{pmatrix} \boldsymbol{x}(t) \\ x_F(t) \end{pmatrix}. \end{aligned}\right\} \tag{5.36}$$

Then the augmented 2MS (1.26), (1.27), (5.36) is element of system class $\mathcal{S}_2$.

The filter in (5.36) with state variable x_F [rad] represents a low-pass filter as in (5.24) of (negative) angle of twist $\phi_S(\cdot) = \phi_1(\cdot)/g_r - \phi_2(\cdot)$, whereas the sum $\phi_1(\cdot)/g_r - \phi_2(\cdot) + x_F(\cdot)$ in the augmented output (5.36) can be considered as high-pass filter (5.25) of $\phi_S(\cdot)$ with cutoff frequency k_F [rad/s]. The augmented output in (5.36) and the presuppositions in (5.35) yield a minimum-phase 2MS (1.26), (1.27), (5.36) with relative degree two and positive high-frequency gain.

Proof of Proposition 5.13.
The proof is similar to the proof of Proposition 5.11. Only the essential changes are highlighted.

Step 1: It is shown that properties ($\mathcal{S}_2$-sp$_1$), ($\mathcal{S}_2$-sp$_3$), ($\mathcal{S}_2$-sp$_4$) and ($\mathcal{S}_2$-sp$_5$) of system class $\mathcal{S}_2$ are satisfied.
For $\boldsymbol{A}, \boldsymbol{b}$ and $\boldsymbol{B}_L$ as in (1.26), introduce

$$\widehat{\boldsymbol{A}} := \begin{bmatrix} & \boldsymbol{A} & & \boldsymbol{0}_4 \\ (\ 0, & -\frac{k_F}{g_r}, \ 0, & k_F\ ) & -k_F \end{bmatrix} \in \mathbb{R}^{5\times 5}, \quad \widehat{\boldsymbol{b}} := \begin{pmatrix} \boldsymbol{b} \\ 0 \end{pmatrix} \in \mathbb{R}^5 \quad \text{and} \quad \widehat{\boldsymbol{B}}_L := \begin{bmatrix} \boldsymbol{B}_L \\ \boldsymbol{0}_2^\top \end{bmatrix} \in \mathbb{R}^{5\times 2}, \tag{5.37}$$

and with $\widehat{\boldsymbol{c}}$ as in (5.36) rewrite system (1.26), (1.27) with (5.36) as follows

$$\left.\begin{aligned} \tfrac{\mathrm{d}}{\mathrm{d}t}\begin{pmatrix} \boldsymbol{x}(t) \\ x_F(t) \end{pmatrix} &= \widehat{\boldsymbol{A}}\begin{pmatrix} \boldsymbol{x}(t) \\ x_F(t) \end{pmatrix} + \widehat{\boldsymbol{b}}\,\mathrm{sat}_{\hat{u}_A}\big(u(t)+u_A(t)\big) + \widehat{\boldsymbol{B}}_L\begin{pmatrix} (\mathfrak{F}_1\omega_1)(t) \\ m_L(t)+(\mathfrak{F}_2\omega_2)(t) \end{pmatrix}, \\ y(t) &= \widehat{\boldsymbol{c}}^\top\begin{pmatrix} \boldsymbol{x}(t) \\ x_F(t) \end{pmatrix}, \qquad \begin{pmatrix} \boldsymbol{x}(0) \\ x_F(0) \end{pmatrix} = \begin{pmatrix} \boldsymbol{x}^0 \\ x_F^0 \end{pmatrix} \in \mathbb{R}^5. \end{aligned}\right\} \tag{5.38}$$

Define $h := 0$, $u_d(\cdot) := u_A(\cdot)$, $\boldsymbol{B}_{\mathfrak{T}} := \widehat{\boldsymbol{B}}_L$, $\boldsymbol{d}(\cdot) := (0,\, m_L(\cdot))^\top$ and

$$\mathfrak{T}\colon\ \mathcal{C}([-h,\infty);\mathbb{R}^5) \to \mathcal{L}^\infty_{\mathrm{loc}}(\mathbb{R}_{\geq 0};\mathbb{R}^2), \qquad (\mathfrak{T}\begin{pmatrix} \boldsymbol{x} \\ x_F \end{pmatrix})(t) := \big((\mathfrak{F}_1\omega_1)(t),\ \ (\mathfrak{F}_2\omega_2)(t)\big)^\top.$$

Then, for $\hat{u}_A \to \infty$, system (5.38) can be expressed in the form (1.36). Moreover, similar arguments as in Step 1 of the proof of Proposition 5.11 show that properties ($\mathcal{S}_2$-sp$_1$), ($\mathcal{S}_2$-sp$_3$), ($\mathcal{S}_2$-sp$_4$) and ($\mathcal{S}_2$-sp$_5$) are satisfied. This completes Step 1.

Step 2: It is shown that property ($\mathcal{S}_2$-sp$_2$) of system class $\mathcal{S}_2$ is satisfied.
Since

$$\gamma_0 := \widehat{\boldsymbol{c}}^\top\widehat{\boldsymbol{A}}\widehat{\boldsymbol{b}} = \frac{c_1\,k_A}{g_r\,\Theta_1} \overset{(5.35)}{>} 0, \tag{5.39}$$

there exists a similarity transformation

$$\widehat{\boldsymbol{S}}\colon \mathbb{R}^5 \to \mathbb{R}^5, \qquad \begin{pmatrix} \boldsymbol{x} \\ x_F \end{pmatrix} \mapsto \boldsymbol{w} := \big(y,\ \ \dot{y},\ \ z_1,\ \ z_2,\ \ z_3\big)^\top := \widehat{\boldsymbol{S}}\begin{pmatrix} \boldsymbol{x} \\ x_F \end{pmatrix}$$

which transform (5.38) into Byrnes-Isidori like form (3.8). For

$$\widehat{\boldsymbol{C}} = \begin{bmatrix} 0 & \frac{c_1}{g_r} & 0 & c_2 & c_1 \\ \frac{c_1}{g_r} & -\frac{c_1}{g_r}k_F & c_2 & c_1k_F & -c_1k_F \end{bmatrix} \quad \text{and} \quad \widehat{\boldsymbol{B}} = \begin{bmatrix} \frac{k_A}{\Theta_1} & 0 & 0 & 0 & 0 \\ -k_A\frac{d_S+g_r^2\nu_1}{g_r^2\Theta_1^2} & \frac{k_A}{\Theta_1} & \frac{k_Ad_S}{g_r\Theta_1\Theta_2} & 0 & 0 \end{bmatrix}^\top,$$

one obtains

$$\widehat{\boldsymbol{V}} = \ker \widehat{\boldsymbol{C}} = \begin{bmatrix} -\frac{g_r c_2}{c_1} & -g_r k_F \left(1 + \frac{c_2}{c_1}\right) & 0 \\ 0 & -\frac{g_r c_2}{c_1} & -g_r \\ 1 & 0 & 0 \\ 0 & 1 & 0 \\ 0 & 0 & 1 \end{bmatrix}$$

and

$$\widehat{\boldsymbol{N}} = (\widehat{\boldsymbol{V}}^\top \widehat{\boldsymbol{V}})^{-1} \widehat{\boldsymbol{V}}^\top [\boldsymbol{I}_5 - \widehat{\boldsymbol{B}}(\widehat{\boldsymbol{C}}\widehat{\boldsymbol{B}})^{-1}\widehat{\boldsymbol{C}}] = \begin{bmatrix} 0 & -\frac{d_S}{g_r \Theta_2} & 1 & -\frac{c_2 d_S}{c_1 \Theta_2} & -\frac{d_S}{\Theta_2} \\ 0 & 0 & 0 & 1 & 0 \\ 0 & 0 & 0 & 0 & 1 \end{bmatrix}.$$

Then, invoking (2.24), gives

$$\widehat{\boldsymbol{S}} = \begin{bmatrix} \widehat{\boldsymbol{C}} \\ \widehat{\boldsymbol{N}} \end{bmatrix} = \begin{bmatrix} 0 & \frac{c_1}{g_r} & 0 & c_2 & c_1 \\ \frac{c_1}{g_r} & -\frac{c_1}{g_r} k_F & c_2 & c_1 k_F & -c_1 k_F \\ 0 & -\frac{d_S}{g_r \Theta_2} & 1 & -\frac{c_2 d_S}{c_1 \Theta_2} & -\frac{d_S}{\Theta_2} \\ 0 & 0 & 0 & 1 & 0 \\ 0 & 0 & 0 & 0 & 1 \end{bmatrix} \quad \text{and}$$

$$\widehat{\boldsymbol{S}}^{-1} = [\widehat{\boldsymbol{B}}(\widehat{\boldsymbol{C}}\widehat{\boldsymbol{B}})^{-1}, \widehat{\boldsymbol{V}}] = \begin{bmatrix} -g_r \frac{d_S c_2 - c_1 k_F \Theta_2}{c_1^2 \Theta_2} & \frac{g_r}{c_1} & -\frac{g_r c_2}{c_1} & -g_r k_F \left(1 + \frac{c_2}{c_1}\right) & 0 \\ \frac{g_r}{c_1} & 0 & 0 & -\frac{g_r c_2}{c_1} & -g_r \\ \frac{d_S}{c_1 \Theta_2} & 0 & 1 & 0 & 0 \\ 0 & 0 & 0 & 1 & 0 \\ 0 & 0 & 0 & 0 & 1 \end{bmatrix}$$

which allows for the coordinate change to the following form

$$\dot{\boldsymbol{w}}(t) = \widehat{\boldsymbol{S}}\widehat{\boldsymbol{A}}\widehat{\boldsymbol{S}}^{-1}\boldsymbol{w}(t) + \widehat{\boldsymbol{S}}\widehat{\boldsymbol{b}}\big(u(t) + u_A(t)\big) + \widehat{\boldsymbol{S}}\widehat{\boldsymbol{B}}_L \begin{pmatrix} (\mathfrak{F}_1 \operatorname{row}_1(\widehat{\boldsymbol{S}}^{-1})\boldsymbol{w})(t) \\ m_L(t) + (\mathfrak{F}_2 \operatorname{row}_3(\widehat{\boldsymbol{S}}^{-1})\boldsymbol{w})(t) \end{pmatrix},$$

$$\boldsymbol{w}(0) = \widehat{\boldsymbol{S}}\left(\boldsymbol{x}^0, x_F^0\right),$$

conform to (3.8), where

$$\widehat{\boldsymbol{S}}\widehat{\boldsymbol{A}}\widehat{\boldsymbol{S}}^{-1} =: \begin{bmatrix} 0 & 1 & \boldsymbol{0}_3^\top \\ \widehat{a}_1 & \widehat{a}_2 & \widehat{\boldsymbol{a}}_3^\top \\ \widehat{\boldsymbol{a}}_4 & \boldsymbol{0}_3 & \widehat{\boldsymbol{A}}_5 \end{bmatrix} \in \mathbb{R}^{5\times 5}, \ \widehat{\boldsymbol{S}}\widehat{\boldsymbol{b}} = \begin{pmatrix} 0 \\ \gamma_0 \\ 0 \\ 0 \\ 0 \end{pmatrix} \in \mathbb{R}^5 \ \text{ and } \ \widehat{\boldsymbol{S}}\widehat{\boldsymbol{B}}_L = \begin{bmatrix} 0 & 0 \\ -\frac{c_1}{g_r \Theta_1} & -\frac{c_2}{\Theta_2} \\ 0 & -\frac{1}{\Theta_2} \\ 0 & 0 \\ 0 & 0 \end{bmatrix} \in \mathbb{R}^{5\times 2}.$$

Invoking (2.55) yields

$$\begin{aligned}
\widehat{a}_1 &= c_S\left(\tfrac{1}{\Theta_2}\tfrac{c_2}{c_1}-\tfrac{1}{g_r^2\Theta_1}\right)+\tfrac{d_S^2}{g_r^2\Theta_1\Theta_2}\left(1+\tfrac{c_2}{c_1}\left(1+g_r^2\tfrac{\nu_1}{d_S}\right)\right)-\tfrac{d_S^2}{\Theta_2^2}\tfrac{c_2}{c_1}\left(1+\tfrac{c_2}{c_1}+\tfrac{\nu_2}{d_S}\right)\\
&\quad -\tfrac{k_F}{\Theta_1}\left(\tfrac{d_S}{g_r^2}+\nu_1\right)+k_F\tfrac{d_S}{\Theta_2}\left(1+2\tfrac{c_2}{c_1}\right)\in\mathbb{R},\\
\widehat{a}_2 &= d_S\left(\tfrac{1}{\Theta_2}\tfrac{c_2}{c_1}-\tfrac{1}{g_r^2\Theta_1}\right)-\tfrac{\nu_1}{\Theta_1}-k_F\in\mathbb{R},\\
\widehat{\boldsymbol{a}}_3 &= \begin{pmatrix} -c_2\left(\tfrac{d_S}{\Theta_2}\left(1+\tfrac{c_2}{c_1}\right)+\tfrac{\nu_2}{\Theta_2}-\tfrac{\nu_1}{\Theta_1}\right)+(c_1+c_2)\left(k_F+\tfrac{d_S}{g_r^2\Theta_1}\right)\\ -c_2\left(1+\tfrac{c_2}{c_1}\right)\tfrac{c_S+k_Fd_S}{\Theta_2}+(c_1+c_2)\left(k_F\tfrac{\nu_1}{\Theta_1}+\tfrac{c_S+k_Fd_S}{g_r^2\Theta_1}\right)\\ c_S\left(\tfrac{c_1}{g_r^2\Theta_1}-\tfrac{c_2}{\Theta_2}\right)\end{pmatrix}\in\mathbb{R}^3,\\
\widehat{\boldsymbol{a}}_4 &= \begin{pmatrix}\tfrac{1}{c_1\Theta_2}\left(c_S+k_Fd_S-\tfrac{d_S}{\Theta_2}\left(d_S\left(1+\tfrac{c_2}{c_1}\right)+\nu_2\right)\right)\\ \tfrac{d_S}{c_1\Theta_2}\\ -\tfrac{k_F}{c_1}\end{pmatrix}\in\mathbb{R}^3
\end{aligned}$$

and

$$\widehat{\boldsymbol{A}}_5=\widehat{\boldsymbol{N}}\widehat{\boldsymbol{A}}\widehat{\boldsymbol{V}}=\begin{bmatrix}-\tfrac{d_S}{\Theta_2}\left(1+\tfrac{c_2}{c_1}\right)-\tfrac{\nu_2}{\Theta_2} & -\left(1+\tfrac{c_2}{c_1}\right)\tfrac{c_S+k_Fd_S}{\Theta_2} & -\tfrac{c_S}{\Theta_2}\\ 1 & 0 & 0\\ 0 & k_F\left(1+\tfrac{c_2}{c_1}\right) & 0\end{bmatrix}\in\mathbb{R}^{3\times3}.$$

The characteristic polynomial of $\widehat{\boldsymbol{A}}_5$ is given by

$$\chi_{\widehat{\boldsymbol{A}}_5}(s)=s^3+\underbrace{\left(\frac{d_S}{\Theta_2}\left(1+\frac{c_2}{c_1}\right)+\frac{\nu_2}{\Theta_2}\right)}_{=:m_2}s^2+\underbrace{\frac{c_S+k_Fd_S}{\Theta_2}\left(1+\frac{c_2}{c_1}\right)}_{=:m_1}s+\underbrace{k_F\frac{c_S}{\Theta_2}\left(1+\frac{c_2}{c_1}\right)}_{=:m_0}.$$

For c_1, c_2 and k_F as in (5.35) the coefficients m_0, m_1 and m_2 are positive and

$$m_2\,m_1-m_0\overset{(5.35)}{>}\frac{c_S}{\Theta_2}\left(1+\frac{c_2}{c_1}\right)\left[\frac{d_S}{\Theta_2}\left(1+\frac{c_2}{c_1}\right)-k_F\right]\overset{(5.35)}{>}0,$$

hence $\chi_{\widehat{\boldsymbol{A}}_5}$ is Hurwitz [77, Theorem 3.4.71, p. 339] and $\operatorname{spec}(\widehat{\boldsymbol{A}}_5)\subset\mathbb{C}_{<0}$. Now the same argumentation as in Step 2 of the proof of Proposition 5.11 shows that property ($\mathcal{S}_2$-sp$_2$) is satisfied. This completes Step 2. Combining Step 1 and Step 2 completes the proof of Proposition 5.13. □

Clearly, affiliation of augmented 2MS (1.26), (1.27), (5.36) (without saturation) to system class $\mathcal{S}_2$ implies applicability of the high-gain adaptive controllers (3.46), (4.67), (3.46)+(5.3) and (4.67)+(5.3) for position control (see Theorem 3.13, Theorem 4.13 and Corollary 5.2, respectively). Moreover, if funnel controller (4.67) is applied to 2MS (1.26), (1.27), (5.36), then Theorem 4.15 allows to account for actuator saturation as in (1.26) (see Fig. 5.3(b)). Hence high-gain adaptive position control of the augmented 2MS (1.26), (1.27), (5.36) is feasible.

To allow for load position tracking of reference $\phi_{2,\mathrm{ref}}(\cdot)\in\mathcal{W}^{2,\infty}(\mathbb{R}_{\geq0};\mathbb{R})$, due to the augmented

output in (5.36), the use of the augmented reference

$$\forall t \geq 0\colon \qquad y_{\mathrm{ref}}(t) \;:=\; (c_1 + c_2)\,\phi_{2,\mathrm{ref}}(t), \qquad \phi_{2,\mathrm{ref}}(\cdot) \in \mathcal{W}^{2,\infty}(\mathbb{R}_{\geq 0}; \mathbb{R}), \tag{5.40}$$

is necessary and so the augmented error is given by

$$\begin{aligned} \forall t \geq 0\colon \qquad e(t) \;&=\; y_{\mathrm{ref}}(t) - y(t) \\ &\overset{(5.36)}{=}\; y_{\mathrm{ref}}(t) - \left(\frac{c_1}{g_r}\phi_1(t) + c_2\phi_2(t) + c_1 x_F(t)\right) \\ &=\; y_{\mathrm{ref}}(t) - \left(c_1\left(\frac{1}{g_r}\phi_1(t) - \phi_2(t)\right) + (c_1 + c_2)\phi_2(t) + c_1 x_F(t)\right) \\ &\overset{(5.14),(5.40)}{=}\; (c_1 + c_2)\big(\phi_{2,\mathrm{ref}}(t) - \phi_2(t)\big) - c_1\big(\phi_S(t) + x_F(t)\big). \end{aligned} \tag{5.41}$$

The following corollary states the observations above more precisely.

Corollary 5.14 (High-gain adaptive position control of augmented 2MS)**.**
Consider the 2MS (1.26), (1.27) with filter and augmented output as in (5.36) and suppose that actuator saturation is negligible, i.e. $\hat{u}_A \to \infty$ in (1.26), and that c_1 and c_2 satisfy (5.35). Let $\phi_{2,\mathrm{ref}}(\cdot) \in \mathcal{W}^{2,\infty}(\mathbb{R}_{\geq 0}; \mathbb{R})$, $\lambda > 0$, $\phi_S(t)$ as in (5.14), $e(t)$ as in (5.41) and $(\psi_0(\cdot), \psi_1(\cdot)) \in \mathcal{B}_2$ such that $|e(0)| < \psi_0(0)$ and $|\dot{e}(0)| < \psi_1(0)$.

(i) (a) Application of adaptive λ-tracking controller (3.46) and funnel controller (4.67) with derivative feedback for position control of augmented 2MS (1.26), (1.27), (5.36) is admissible and for both closed-loop systems the following holds:

$$\forall\, t \geq 0\colon \qquad \phi_{2,\mathrm{ref}}(t) - \phi_2(t) = \frac{1}{c_1 + c_2}\Big(e(t) + c_1\big(\phi_S(t) + x_F(t)\big)\Big). \tag{5.42}$$

(b) If steady state is reached, i.e. $\lim_{t\to\infty} \frac{d}{dt}\,(\boldsymbol{x}(t)^\top,\, x_F(t)) = \mathbf{0}_5^\top$, then

$$\limsup_{t\to\infty} |\phi_{2,\mathrm{ref}}(t) - \phi_2(t)| \leq \frac{\lambda}{c_1 + c_2} \quad \text{and} \quad \limsup_{t\to\infty} |\phi_{2,\mathrm{ref}}(t) - \phi_2(t)| \leq \frac{\limsup_{t\to\infty} \psi_0(t)}{c_1 + c_2},$$

respectively.

(ii) (a) Application of the controller combinations (3.46)+(5.3) and (4.67)+(5.3) with proportional-integral internal model (5.3) for position control of augmented 2MS (1.26), (1.27), (5.36) is admissible. Moreover for $q_1 > 0$, $\dot{x}_I(t)$ as in (5.3), $k(t)$ as in (3.46) and $k_0(t)$, $k_1(t)$ as in (4.67), the following holds

$$\forall\, t \geq 0\colon \quad \phi_{2,\mathrm{ref}}(t) - \phi_2(t) = \frac{1}{c_1 + c_2}\left(\frac{\dot{x}_I(t)}{k(t)^2} - \frac{q_1}{k(t)}\dot{e}(t) + c_1\big(\phi_S(t) + x_F(t)\big)\right) \tag{5.43}$$

for closed-loop system (1.26), (1.27), (5.36), (3.46)+(5.3) and the following holds

$$\forall\, t \geq 0\colon \quad \phi_{2,\mathrm{ref}}(t) - \phi_2(t) = \frac{1}{c_1 + c_2}\left(\frac{\dot{x}_I(t)}{k_0(t)^2} - \frac{k_1(t)}{k_0(t)}\dot{e}(t) + c_1\big(\phi_S(t) + x_F(t)\big)\right) \tag{5.44}$$

for closed-loop system (1.26), (1.27), (5.36), (4.67)+(5.3).

(b) If steady state is reached, i.e. $\lim_{t\to\infty} \frac{d}{dt}\,(\boldsymbol{x}(t)^\top,\, x_F(t),\, x_I(t)) = \mathbf{0}_6^\top$, *and* $\lim_{t\to\infty} \dot{\phi}_{2,\mathrm{ref}}(t) = 0$, *then for both closed-loop systems the augmented error and the load position error vanishes asymptotically, i.e.* $\lim_{t\to\infty} e(t) = 0$ *and* $\lim_{t\to\infty} \phi_{2,\mathrm{ref}}(t) - \phi_2(t) = 0$, *respectively.*

Proof of Corollary 5.14.
Assertion (i)(a) follows from Proposition 5.13 combined with Theorem 3.13 and Theorem 4.13. Moreover, (5.42) directly follows from (5.41). Next Assertion (i)(b) is shown. Clearly,

$$\lim_{t\to\infty} \dot{x}_F(t) = 0 \quad \overset{(5.36)}{\Longrightarrow} \quad \lim_{t\to\infty} (x_F(t) + \phi_S(t)) = 0 = \limsup_{t\to\infty} |x_F(t) + \phi_S(t)|. \tag{5.45}$$

Hence, Assertion (i)(b) directly follows from (5.42), (5.45) and Assertion (iv) of Theorem 3.13 and Assertion (iii) of Theorem 4.13, respectively.
Assertion (ii)(a) follows from Proposition 5.13 combined with Corollary 5.2, where (5.43) and (5.44) are obtained by inserting (3.46) and (4.67)—with $u(t)$ replaced by $v(t)$ and with $e(t)$ as in (5.41)—into (5.3) and solving for $\phi_{2,\mathrm{ref}}(t) - \phi_2(t)$, respectively. In view of (5.40), the presuppositions in Assertion (ii)(b) imply $\lim_{t\to\infty} \dot{y}_{\mathrm{ref}}(t) = 0$ and $\lim_{t\to\infty} \dot{e}(t) = \lim_{t\to\infty} \big(\dot{y}_{\mathrm{ref}}(t) - \boldsymbol{c}^\top \dot{\boldsymbol{x}}(t)\big) = 0$. Hence Assertion (ii)(b) directly follows from $\lim_{t\to\infty} \frac{\mathrm{d}}{\mathrm{d}t}\,(\boldsymbol{x}(t)^\top,\, x_F(t),\, x_I(t)) = \mathbf{0}_6^\top$, Assertion (iii) of Corollary 5.2, (5.45), (5.43) and (5.44), respectively. This completes the proof of Corollary 5.14. □

From (5.42) it follows that funnel controller (4.67) cannot in general assure that load position error $\phi_{2,\mathrm{ref}}(\cdot) - \phi_2(\cdot)$ evolves within the prescribed region. However, usually $\phi_S(\cdot) + x_F(\cdot)$ in (5.42) is small, e.g. at the laboratory setup the sum's magnitude does not exceed 10^{-2} [rad]. Hence, for small $c_1/(c_1+c_2)$, it is to be expected that $\phi_{2,\mathrm{ref}}(t) - \phi_2(t) \approx e(t)/(c_1+c_2)$ for all $t \geq 0$.

Although it was not possible to prove that active damping of shaft oscillations is achieved by the use of the augmented output and the high-pass filter as in (5.36), the measurement results in Section 5.2.3.3 show that damping is feasible by adequate design of feedback coefficients c_1 and c_2.

Remark 5.15 (Design parameters c_1, c_2 and k_F)**.**
If $0 < d_{S,\min} \leq d_S$ *and* $\Theta_{2,\max} \geq \Theta_2 > 0$ *and lower bound* $d_{S,\min}$ *and upper bound* $\Theta_{2,\max}$ *are known, then it is easy to see that*

$$0 < k_F < \frac{d_{S,\min}}{\Theta_{2,\max}} \left(1 + \frac{c_2}{c_1}\right) \tag{5.46}$$

satisfies (5.35)*. Besides the constraints imposed by the presuppositions in* (5.35)*, the constants* c_1*,* c_2 *and* k_F *in* (5.36) *are free design parameters and directly affect (load) position control performance. Measurements at the laboratory setup* ($g_r = 1$) *indicate following rule of thumb: for* $c_1 \ll |c_2|$ *the system response is* badly *damped, best damped responses are obtained for* $c_1 \approx c_2$ *(e.g.* $c_1 = c_2 = 1$*). Cut-off frequency* k_F *should not be chosen too small to avoid "slow filter dynamics" which yields a deceleration of the system response (in particular, the smaller* k_F *the longer it takes to reach steady state).*

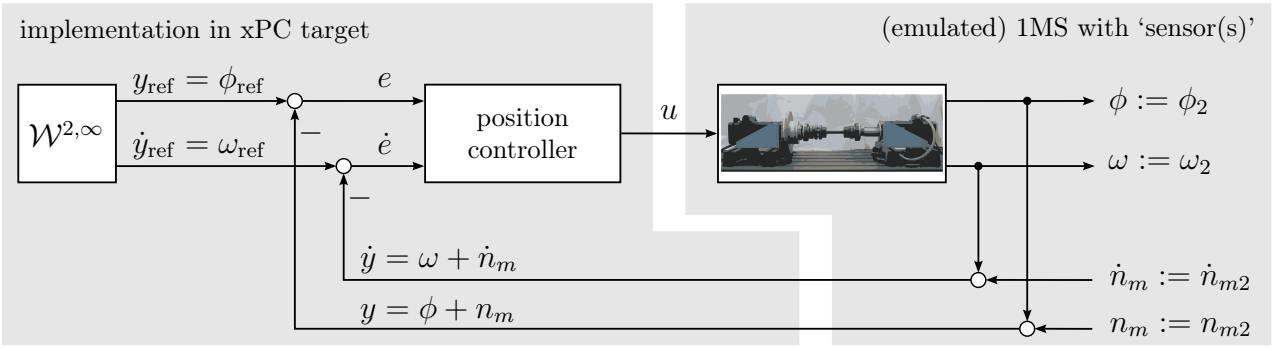

Figure 5.12: *Block diagram of implementation at laboratory setup for position control of 1MS.*

5.2.3.3 Measurements

In the previous two sections, it has been shown that, from a theoretical point of view, high-gain adaptive position control of (the models of) 1MS (1.24), (1.25) and 2MS (1.26), (1.27) is admissible. It remains to show that, in "real world", high-gain adaptive position control of stiff and flexible industrial servo-systems is feasible. Therefore, similar to the speed control experiments, three position control (PC) experiments are carried out at the laboratory setup (see Section 5.2.1). The experiments will illustrate that:

- adaptive λ-tracking controller (3.46) and funnel controller (4.67) with derivative feedback in combination with proportional-integral internal model (5.3) can compete with standard PID position control of stiff servo-systems (1MS);
- high-gain adaptive position control with active damping of shaft oscillations of flexible servo-systems (2MS) is feasible and
- position funnel control of 1MS and 2MS with constrained actuator may perform even if feasibility condition (4.107) does *not* hold.

Experiment PC1 — position control of 1MS:
Five controllers are applied for position control of the emulated 1MS (see Fig. 5.4(a)). The PID controller (1.28) with feedforward control is implemented as benchmark controller (the industrial standard). The remaining four controllers are the adaptive λ-tracking controller (3.46), the funnel controller (4.67) and the high-gain adaptive controller combinations (3.46)+(5.3) and (4.67)+(5.3) with proportional-integral internal model (5.3).

So Experiment PC1 comprises five runs at the laboratory setup: one for each controller. Each run takes 50 [s]. Control task is position set-point tracking without load (i.e. the interval [0, 5] [s]) and position reference tracking under varying load (i.e. the overall interval [0, 50] [s]). Reference $y_{\text{ref}}(\cdot) = \phi_{\text{ref}}(\cdot) \in \mathcal{W}^{2,\infty}(\mathbb{R}_{\geq 0}; \mathbb{R})$ and load torque $m_L(\cdot) \in \mathcal{L}^\infty(\mathbb{R}_{\geq 0}; \mathbb{R})$ are shown in Fig. 5.14 (see top and bottom, respectively). Implementation in xPC target is illustrated in Fig. 5.12 for measured position and speed signals (with index $_m$) deteriorated by measurement errors subsumed in $n_m(\cdot)$ and $\dot{n}_m(\cdot)$, respectively. For each run, one of the five controllers above is implemented as 'position controller' in Fig. 5.12.

To guarantee identical conditions for each run, the following constraints are imposed (similar to Experiment SC1):

(i) the available drive torque of the laboratory setup must not be exceeded, i.e. $|u(t)| \leq \hat{u}_A = 22$ [Nm] for all $t \geq 0$,

(ii) fastest initial acceleration is desired, i.e. $u(0) = \hat{u}_A = 22$ [Nm], and

(iii) for set-point tracking (without load), maximum rise time, maximum settling time and maximum overshoot must be assured. More precisely, the following must be fulfilled:

$$t^r_{\mathrm{ref},0.8} = 1.0\,[\mathrm{s}]\,, \quad t^s_{\mathrm{ref},0.1} = 2.0\,[\mathrm{s}] \quad \text{and} \quad \Delta^{os}_{\mathrm{ref}} = 0.5\,[\%] \quad \text{for} \quad \hat{y}_{\mathrm{ref}} = \pi\,[\mathrm{rad}]\,. \tag{5.47}$$

Since large overshoots may cause deficient workpieces, in many industrial applications—such as position control of machine tools or milling machines—overshoots are to be avoided (see e.g. [166, p. 250]). The motion control objectives in (5.47) account for such a demand.

To achieve small overshoots, the PID controller (1.28) is equipped with (decelerating) feedforward control[2] (see [51, 123] and u_F in Tab. 5.4), whereas the high-gain adaptive controllers are tuned according to Remark 3.14 and the observations in Section 4.4.2.3. Therefore a lower bound $\underline{\gamma_0}$ on the high-frequency gain $\gamma_0 = k_A/(g_r\Theta)$ is needed for implementation (see Tab. 5.4).

Remark 5.16. *If lower bound $\underline{\gamma_0}$ is not known a priori, then appropriate choices for constant q_1 in (3.46) and gain scaling function $\varsigma_1(\cdot)$ in (4.67) may be found by trial and error. Clearly, this will increase implementation effort in the sense that several attempts are needed to obtain satisfactory results, but obviates the need of rough system knowledge.*

For design of PID controller (1.28), adaptive λ-tracking controller (3.46) and adaptive λ-tracking controller combination (3.46)+(5.3) with internal model, several implementation attempts are necessary to meet the specifications in (5.47). In contrast, funnel controller (4.67) and funnel controller combination (4.67)+(5.3) with internal model are easier to implement. By adequate boundary design, maximum rise and settling time are guaranteed right away. Since speed measurement is very noisy (recall the problems during speed control experiments in Section 5.2.2.3), as a precaution the asymptotic accuracy of "speed funnel boundary" $\psi_1(\cdot)$ is chosen (extra) large with $\lambda_1 = 10\,[\mathrm{rad/s}]$. A complete list of the implementation data is given in Tab. 5.4. The following color and line style assignment is used for the different controllers (control laws are restated to ease readability):

——— (1.28), i.e. PID controller with feedforward control (to suppress overshoots):

$$u(t) = k_P\, e(t) + k_I \int_0^t e(\tau)\,\mathrm{d}\tau \; + k_D\, \dot{e}(t) + u_F(t);$$

- - - - - - (3.46), i.e. adaptive λ-tracking controller with derivative feedback:

$$u(t) = k(t)^2 e(t) + q_1 k(t)\dot{e}(t) \;\text{ where }\; \dot{k}(t) = q_2 \exp\big(-q_3 q_4 k(t)\big)\, d_\lambda\left(\left\|\begin{pmatrix} e(t) \\ \frac{\dot{e}(t)}{k(t)} \end{pmatrix}\right\|\right)^{q_4},\; k(0) = k_0;$$

[2] Another common approach, to avoid overshoots for PID position control, is to smooth the reference signal by a first order filter (see e.g. [166, p. 81 f.]). However then, set-point tracking of an initial reference step—as required for Experiment PC1—is not possible.

(4.67), i.e. funnel controller with derivative feedback:

$$u(t) = k_0(t)^2 e(t) + k_0(t)k_1(t)\dot{e}(t) \quad \text{where} \quad k_i(t) = \frac{\varsigma_i(t)}{\psi_i(t) - |e^{(i)}(t)|},\ i \in \{0,1\};$$

(3.46)+(5.3), i.e. adaptive λ-tracking controller with internal model ($k_P = 1$):

$$u(t) = k(t)^2 e(t) + q_1 k(t)\dot{e}(t) + k_I \int_0^t \big(k(\tau)^2 e(\tau) + q_1 k(\tau)\dot{e}(\tau)\big)\,\mathrm{d}\tau$$
$$\text{where} \quad \dot{k}(t) = q_2 \exp\big(-q_3 q_4 k(t)\big)\, d_\lambda\big(\,\|(e(t),\, \dot{e}(t)/k(t))\|\,\big)^{q_4}, \quad k(0) = k_0;$$

(4.67)+(5.3), i.e. funnel controller with internal model ($k_P = 1$):

$$u(t) = k_0(t)^2 e(t) + k_0(t)k_1(t)\dot{e}(t) + k_I \int_0^t \big(k_0(\tau)^2 e(\tau) + k_0(\tau)k_1(\tau)\dot{e}(\tau)\big)\,\mathrm{d}\tau$$
$$\text{where} \quad k_i(t) = \frac{\varsigma_i(t)}{\psi_i(t) - |e^{(i)}(t)|},\ i \in \{0,1\}.$$

Control performance of all controllers is compared. Therefore, for set-point tracking, rise time $t^r_{y(\cdot),0.8}$, settling time $t^s_{y(\cdot),0.1}$ and overshoot $\Delta^{os}_{y(\cdot)}$ are analyzed and, for reference tracking, the ITAE criterion as in (3.82) (with $t_{end} = 50$ [s]) is evaluated. The evaluation results are summarized in Tab. 5.5. Measurement results are depicted in Fig. 5.13(a) for set-point tracking and in Fig. 5.14 for reference tracking. To allow for a direct comparison of the controller gains of (1.28), (3.46), (4.67), (3.46)+(5.3) and (4.67)+(5.3), the "proportional gains" k_P, $k(\cdot)^2$ and $k_0(\cdot)^2$ and the "derivative gains" k_D, $q_1\, k(\cdot)$ and $k_0(\cdot)\, k_1(\cdot)$ are plotted in Fig. 5.14, respectively.

Discussion of the measurement results for set-point tracking (see Fig. 5.13(a)):
Clearly, all five controllers accomplish the control objectives in (5.47) (see Tab. 5.5). Moreover, their control performance is almost identical (see Tab. 5.5). Adaptive λ-tracking controller (3.46) and funnel controller (4.67) show no overshoot but do not achieve steady state accuracy. The controllers with integral control action, i.e. (1.28), (3.46)+(5.3) and (4.67)+(5.3), exhibit very small (almost negligible) overshoots and achieve steady state accuracy for set-point tracking. The funnel controllers and, by chance, also the other controllers assure error evolution within the performance funnel.

Discussion of the measurement results for reference tracking (see Fig. 5.14):
Adaptive λ-tracking controller (3.46) and funnel controller (4.67) yield noticeable contouring errors and so large ITAE values. Since funnel controller (4.67) assures error evolution within the prescribed region, its ITAE performance is better than that of adaptive λ-tracking controller (3.46), but many times worse than the ITAE performance of PID controller (1.28) and of controller combinations (3.46)+(5.3) and (4.67)+(5.3) with internal model (see Tab. 5.5). All three controllers with integral control action achieve asymptotic disturbance rejection. Nevertheless, the ITAE value of PID controller (1.28) is almost three times larger than that of funnel controller combination (4.67)+(5.3). Similar to the

controller/system	Experiment PC1 (1MS)	Experiment PC2 (2MS)
assumed bounds	$\underline{\gamma_0} = \gamma_0/3 \left[\frac{1}{\mathrm{kg\,m^2}}\right]$ where $\gamma_0 = \frac{k_A}{g_r \Theta} = 2.92 \left[\frac{1}{\mathrm{kg\,m^2}}\right]$	$\underline{\gamma_0} = \gamma_0/3$ where $\gamma_0 \overset{(5.39)}{=} 6.02 \left[\frac{1}{\mathrm{kg\,m^2}}\right]$, $d_{S,\min} = d_S/5$, $\Theta_{2,\max} = 3\Theta_2$
reference	$\hat{y}_{\mathrm{ref}} = \pi$ [rad], for $y_{\mathrm{ref}}(\cdot)$ see top of Fig. 5.14 or 5.16, resp. $\|y_{\mathrm{ref}}\|_\infty = 5\pi$ [rad], $\|\dot{y}_{\mathrm{ref}}\|_\infty = \pi/2 \left[\frac{\mathrm{rad}}{\mathrm{s}}\right]$ and $\|\ddot{y}_{\mathrm{ref}}\|_\infty = 15.72 \left[\frac{\mathrm{rad}}{\mathrm{s^2}}\right]$	
load torque	for $m_L(\cdot)$ see bottom of Fig. 5.14 or 5.16, $\|m_L\|_\infty = 10$ [Nm]	
augmented output & filter as in (5.36)	—	$c_1 = c_2 = 1$ [1], $k_F = 0.01$ [rad/s]
initial error	$e(0) = \pi$ [rad]	$e(0) = (c_1 + c_2)\hat{y}_{\mathrm{ref}} = 2\pi$ [rad]
PID controller as in (1.28)	$k_P = 11 \left[\frac{\mathrm{Nms}}{\mathrm{rad}}\right]$, $k_I = 7 \left[\frac{\mathrm{Nm}}{\mathrm{rad}}\right]$ $k_D = 4 \left[\frac{\mathrm{Nms^2}}{\mathrm{rad}}\right]$, $u_F = -12.6$ [Nm]	—
λ-tracking controller as in (3.46)	$q_1 = 2/\sqrt{\underline{\gamma_0}}$ [1], $q_2 = 2$ [1], $q_3 = 0.1$ [1], $q_4 = 2$ [1], $\lambda = 0.09\pi$ [rad], $k_0 = \sqrt{\frac{\hat{u}_A}{e(0)}} = 2.65 \left[\frac{\mathrm{Nms}}{\mathrm{rad}}\right]$	$k_0 = \sqrt{\frac{\hat{u}_A}{e(0)}} = 1.87 \left[\frac{\mathrm{Nms}}{\mathrm{rad}}\right]$
funnel controller as in (4.67)	$(\psi_0(\cdot), \psi_1(\cdot))$ as in (4.64) where $\Lambda_0 = 2e(0)$, $\lambda_0 = \lambda$, $\lambda_1 = 10 \left[\frac{\mathrm{rad}}{\mathrm{s}}\right]$, $T_E = 0.35$ [s]	$T_E = 0.28$ [s]
gain scaling	$\varsigma_0(t) = \sqrt{\frac{\hat{u}_A}{e(0)}} \frac{(\Lambda_0 - e(0))}{\Lambda_0} \psi_0(t)$ and $\varsigma_1(t) = \frac{2}{\sqrt{\underline{\gamma_0}}} \psi_1(t)$	
internal model as in (5.3)	$k_P = 1$ [1], $k_I = 5 \left[\frac{1}{\mathrm{s}}\right]$	$k_P = 1$ [1], $k_I = 3 \left[\frac{1}{\mathrm{s}}\right]$

Table 5.4: *Implementation data of Experiment PC1 (position control of 1MS) and Experiment PC2 (position control of 2MS) (centered values hold for both experiments, resp.)*

experiment	controller	$t^r_{y(\cdot),0.8}$ [s]	$t^s_{y(\cdot),0.1}$ [s]	$\Delta^{os}_{y(\cdot)}$ [%]	ITAE [rad s]
PC1 (1MS)	(1.28)	0.85	1.19	0.02	60.7
	(3.46)	0.89	1.22	0.00	405.3
	(4.67)	0.82	1.17	0.00	261.2
	(3.46)+(5.3)	0.86	1.21	0.01	6.5
	(4.67)+(5.3)	0.83	1.19	0.01	21.8
PC2 (2MS)	(3.46)	0.76	1.01	0.00	281.1
	(4.67)	0.65	0.88	0.00	148.5
	(3.46)+(5.3)	0.71	0.98	0.01	12.2
	(4.67)+(5.3)	0.65	0.89	0.01	27.3

Table 5.5: *Controller performance for Experiment PC1 (position control of 1MS) and Experiment PC2 (position control of 2MS).*

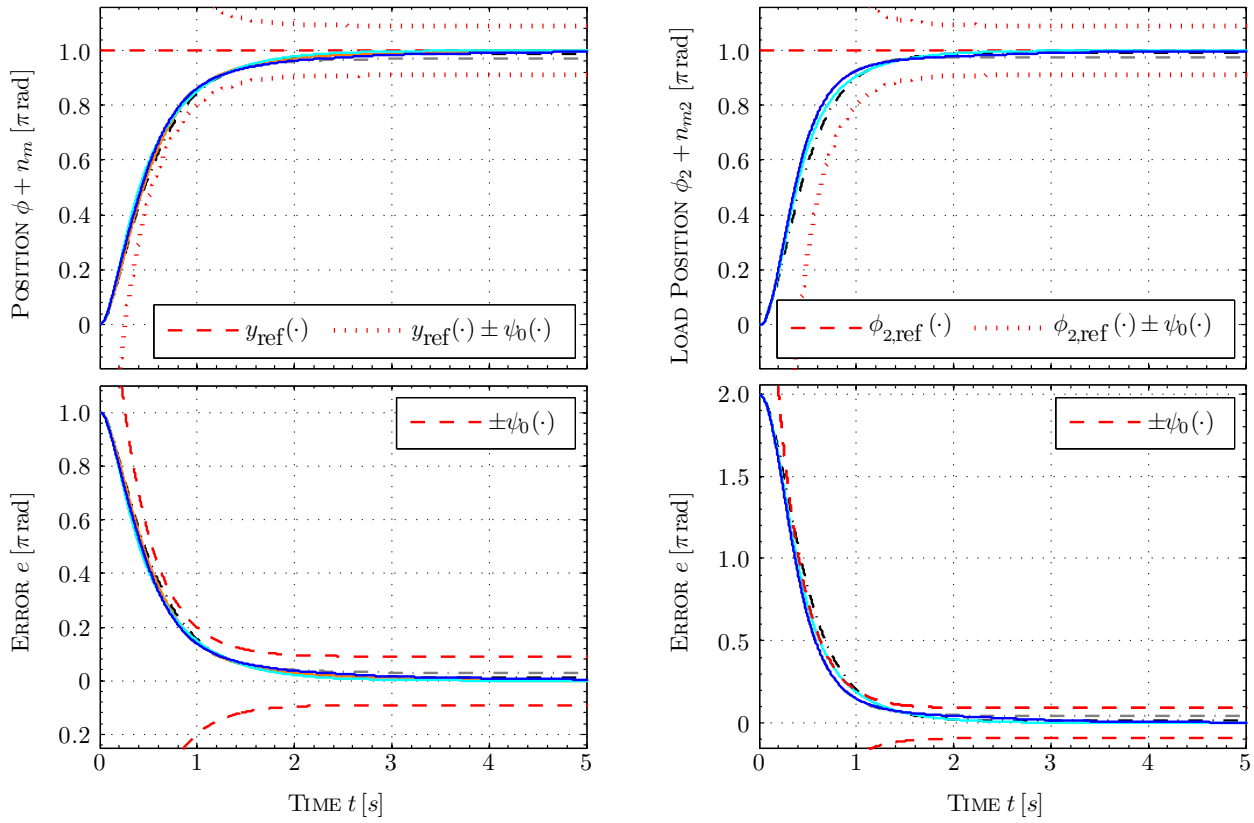

(a) *Experiment PC1 (1MS)*
top: measured position $\phi(\cdot) + n_m(\cdot)$*;*
bottom: position error $e(\cdot)$

(b) *Experiment PC2 (2MS)*
top: measured load position $\phi_2(\cdot) + n_{m2}(\cdot)$*;*
bottom: (augmented) error $e(\cdot)$

Figure 5.13: *Measurement results of Experiments PC1 & PC2: set-point tracking position control of 1MS (left) and 2MS (right) for different controllers (see p. 216):* ——(1.28) *(only for 1MS),* ·-·-·(3.46), ·····(4.67), ——(3.46)+(5.3), ——(4.67)+(5.3) *with parametrization as in Tab. 5.4.*

speed control experiments, adaptive λ-tracking controller combination ——(3.46)+(5.3) shows the best ITAE performance. Noise sensitivity (i.e. noise amplification) of all four high-gain adaptive controllers is acceptable. Especially, for funnel controller ·····(4.67) *without* internal model, noise amplification is temporarily noticeable due to the largest proportional gain (i.e. $\max_{t\in[0,\,50]} k_0(t)^2 \approx 55\,[\text{Nm/rad}]$) and the largest derivative gain (i.e. $\max_{t\in[0,\,50]} k_0(t)k_1(t) \approx 17\,[\text{Nms/rad}]$). Clearly, due to monotone gain adaption, the λ-tracking controllers ·-·-·(3.46) and ——(3.46)+(5.3) yield large proportional and derivative gains at the end of the experiment. Since, for adaptive λ-tracking controller combination ——(3.46)+(5.3), the λ-strip is reached after $\approx 2\,[\text{s}]$ and not left again, gain adaption stops and proportional gain $k(\cdot)^2$ and derivative gain $q_1 k(\cdot)$ of ——(3.46)+(5.3) remain constant on $[2,\,50]\,[\text{s}]$. Note that, for most of the time, proportional gain $k_0(\cdot)^2$ and derivative gain $k_0(\cdot)k_1(\cdot)$ of funnel controller combination ——(4.67)+(5.3) is even smaller than proportional gain k_P and derivative gain k_D of PID controller ——(1.28), respectively. The generated control actions are very similar and mainly differ in noise amplification.

Remark 5.17. *Similar to the speed control experiment SC1, the PID controller could be imple-*

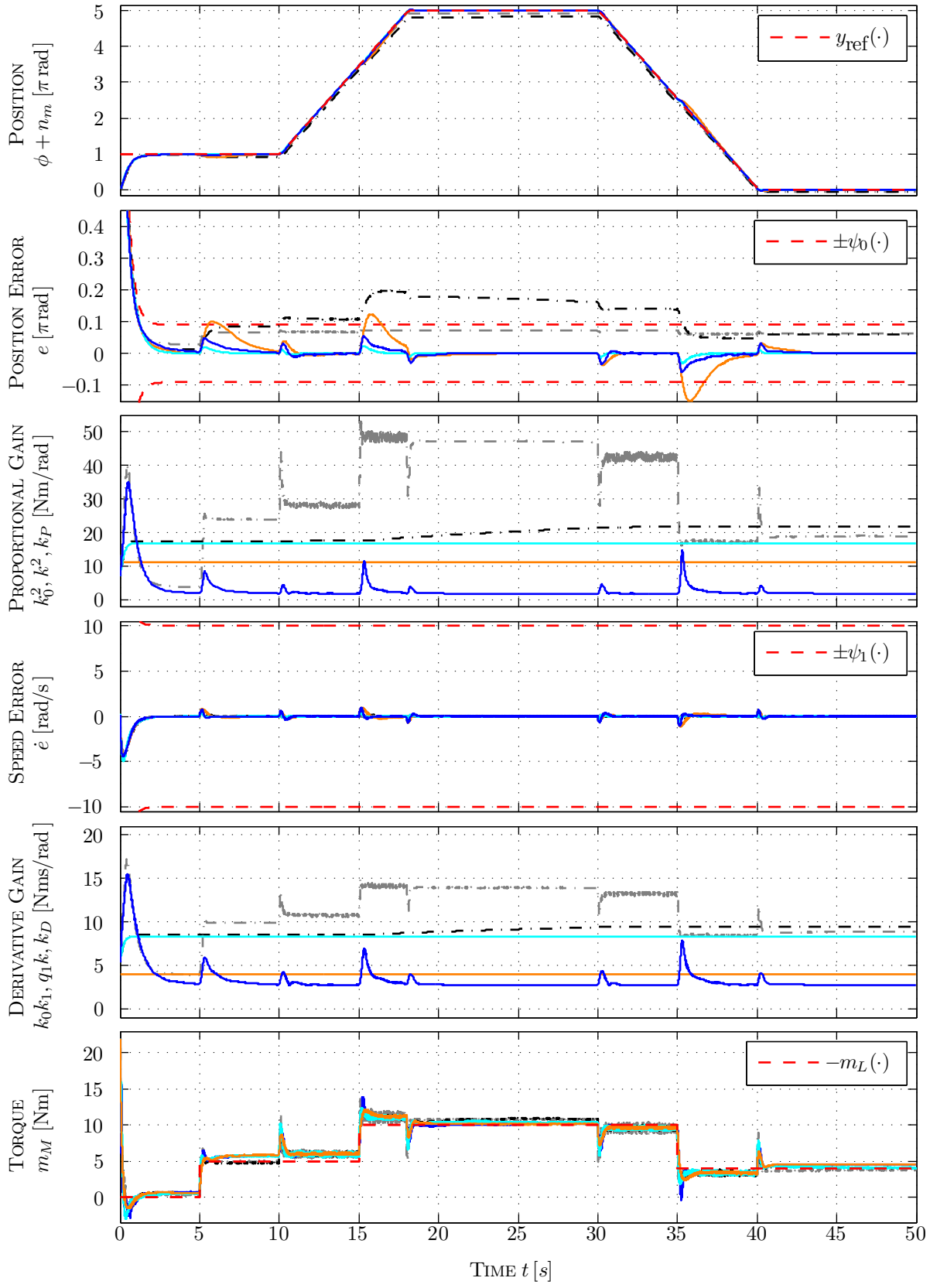

Figure 5.14: *Measurement results of Experiment PC1 (position control of 1MS) for different controllers (see p. 216):* —(1.28), -·-·-(3.46), ·····(4.67), —(3.46)+(5.3), —(4.67)+(5.3) *with parametrization as in Tab. 5.4 (from top to bottom: measured position $\phi(\cdot) + n_m(\cdot)$, position error $e(\cdot)$, proportional gain k_P, $k(\cdot)^2$ & $k_0(\cdot)^2$, error derivative $\dot{e}(\cdot)$, derivative gain k_D, $q_1 k(\cdot)$ & $k_0(\cdot)k_1(\cdot)$ and drive torque $m_M(\cdot) = \mathrm{sat}_{\hat{u}_A}\big(u(\cdot) + u_A(\cdot)\big)$).*

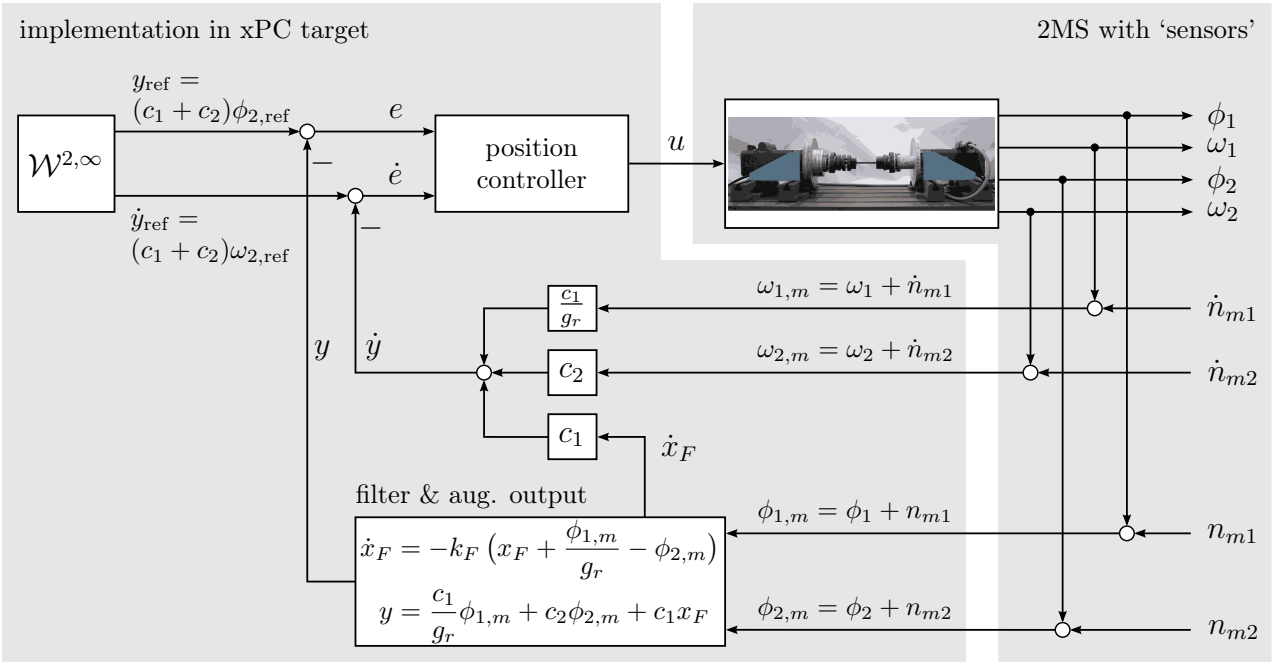

Figure 5.15: *Block diagram of implementation at laboratory setup for position control of 2MS.*

mented with larger gains to accelerate the closed-loop system response and to achieve a better control performance, but then the controller runs into actuator saturation which necessitates anti-wind up strategies. Again the comparison tries to highlight the drawbacks of classical PID controller design with constant gains: varying and unknown disturbances may unexpectedly deteriorate control performance (e.g. customer specifications may not be accomplished under load).

Experiment PC2 — position control of 2MS:
Experiment PC2 is similar to Experiment PC1. Now the high-gain adaptive controllers (3.46), (4.67), (3.46)+(5.3) and (4.67)+(5.3) are implemented at the laboratory setup for position control of an flexible servo-system (see Fig. 5.4(b)). Since P(I)D control is "inadequate" for flexible servo-systems (see [174, p. 225]), a comparison with a PID controller is omitted. So Experiment PC2 consists of four runs à 50 [s]. Control task is load position tracking of reference $\phi_{2,\text{ref}}(\cdot) \in \mathcal{W}^{2,\infty}(\mathbb{R}_{\geq 0}; \mathbb{R})$ under varying load disturbance $m_L(\cdot) \in \mathcal{L}^{\infty}(\mathbb{R}_{\geq 0}; \mathbb{R})$. Reference and load signals are the same as in Experiment PC1 (see top and bottom of Fig. 5.16, respectively). Moreover, each controller of Experiment PC2 is designed under the identical constraints (i)-(iii) as in Experiment PC1.

In Section 5.2.2.2 it has been shown that an augmented output is necessary to allow for high-gain adaptive position control of flexible servo-systems. Moreover, to achieve steady state accuracy, dynamic feedback is required and so, for this experiment, the high-gain adaptive controllers ·····(3.46), ·····(4.67), ——(3.46)+(5.3) and ——(4.67)+(5.3) are implemented in conjunction with the augmented output and the filter as in (5.36). Color and line style assignment is identical to Experiment PC1 (see p. 216). Real-time implementation is illustrated in Fig. 5.15. Filter and augmented output are shown for measured signals (with index $_m$). Position and speed on motor and load side are deteriorated by measurement errors $n_{m1}(\cdot)$ & $\dot{n}_{m1}(\cdot)$ and $n_{m2}(\cdot)$ & $\dot{n}_{m2}(\cdot)$, respectively. For each run, one of the four high-gain adaptive controllers is implemented as 'position controller' in Fig. 5.15. Design parameters are collected in Tab. 5.4.

Fig. 5.13(b) and Fig. 5.16 show the measurement results for set-point tracking (i.e. the interval [0, 5] [s]) and for reference tracking under changing load (i.e. the complete interval [0, 50] [s]). Note that, for filter design, a lower bound $d_{S,\min}$ on damping coefficient d_S and an upper bound $\Theta_{2,\max}$ on load inertia Θ_2 must be known a priori. The assumed bounds are rough (see Tab. 5.4) and yield relative errors of 80% and 200%, respectively. For these bounds and feedback coefficients $c_1 = c_2 = 1$, the upper bound as in (5.35) on the cut-off frequency k_F is given by $d_{S,\min}/\Theta_{2,\max}\,(1 + c_2/c_1) = 0.1$. Clearly the choice $k_F = 0.01$ [rad/s] satisfies the presupposition in (5.35).

Similar to Experiment PC1, for each run, rise time $t^r_{y(\cdot),0.8}$, settling time $t^s_{y(\cdot),0.1}$ and overshoot $\Delta^{os}_{y(\cdot)}$ are used to rate set-point tracking control performance. Overall control performance of each run is evaluated by the ITAE criterion (where $e(\tau)$ in (3.82) is replaced by load position error $\phi_{2,\mathrm{ref}}(\tau) - \phi_2(\tau)$). Tab. 5.5 lists the evaluation results.

Discussion of the measurement results for set-point tracking (see Fig. 5.13(b)):
First note that each of the four controllers can fulfill the control objectives in (5.47) and each closed-loop system response is well damped. Concerning rise time, settling time and overshoot all high-gain adaptive controllers show comparable results (see Tab. 5.5). Funnel controller ·····(4.67) and funnel controller with internal model ——(4.67)+(5.3) yield the fastest transient responses (see Tab. 5.5). Conform to the Assertions of Corollary 5.14, only the high-gain adaptive controllers with internal model, i.e. ——(3.46)+(5.3) and ——(4.67)+(5.3), achieve steady state accuracy in augmented error $e(\cdot)$ *and* load position error $\phi_{2,\mathrm{ref}}(\cdot) - \phi_2(\cdot)$.

Discussion of the measurement results for reference tracking (see Fig. 5.16):
The measurement results are almost identical to Experiment PC1, since all controllers in conjunction with augmented output and filter assure a well damped closed-loop system response. Adaptive λ-tracking controller ·····(3.46) gives large contouring errors yielding the largest ITAE value. Clearly, the funnel controllers ·····(4.67) and ——(4.67)+(5.3) achieve tracking with prescribed transient behavior, i.e. the augmented error (5.41) evolves within the performance funnel. By chance, also adaptive λ-tracking controller with internal model ——(3.46)+(5.3) yields an error evolution within the prescribed region. Again, its ITAE performance is the best in this study (see Tab. 5.5). Noise sensitivity of all four high-gain adaptive controllers is acceptable. Funnel controller ·····(4.67) yields the most noticeable noise amplification.

Experiment PC3 — saturated funnel controller for position control of 1MS & 2MS:
For Experiment PC3, the runs of Experiment PC1 & PC2 with funnel controller (4.67) are repeated. However now, instead of (4.67), the saturated funnel controller (4.104) (with $u_F(\cdot) = 0$), i.e.

$$\begin{aligned} u(t) &= \mathrm{sat}_{\hat{u}}\left(k_0(t)^2 e(t) + k_0(t)k_1(t)\dot{e}(t)\right) \quad \text{where for } i \in \{0,1\}\text{:} \\ k_i(t) &= \frac{\varsigma_i(t)}{\psi_i(t) - |e^{(i)}(t)|} \quad \text{and} \quad \varsigma_i(\cdot),\ \psi_i(\cdot) \text{ as in Tab. 5.4,} \end{aligned}$$

is implemented for position control of 1MS and 2MS (see implementation in Fig. 5.12 and Fig. 5.15). Each run is carried out under the same conditions as specified in Experiment PC1 & PC2, e.g. constraints (i)-(iii), reference, disturbance and boundary design (see Tab. 5.4) are identical. For both runs, saturation level $\hat{u}$ of funnel controller (4.104) is reduced stepwise (by

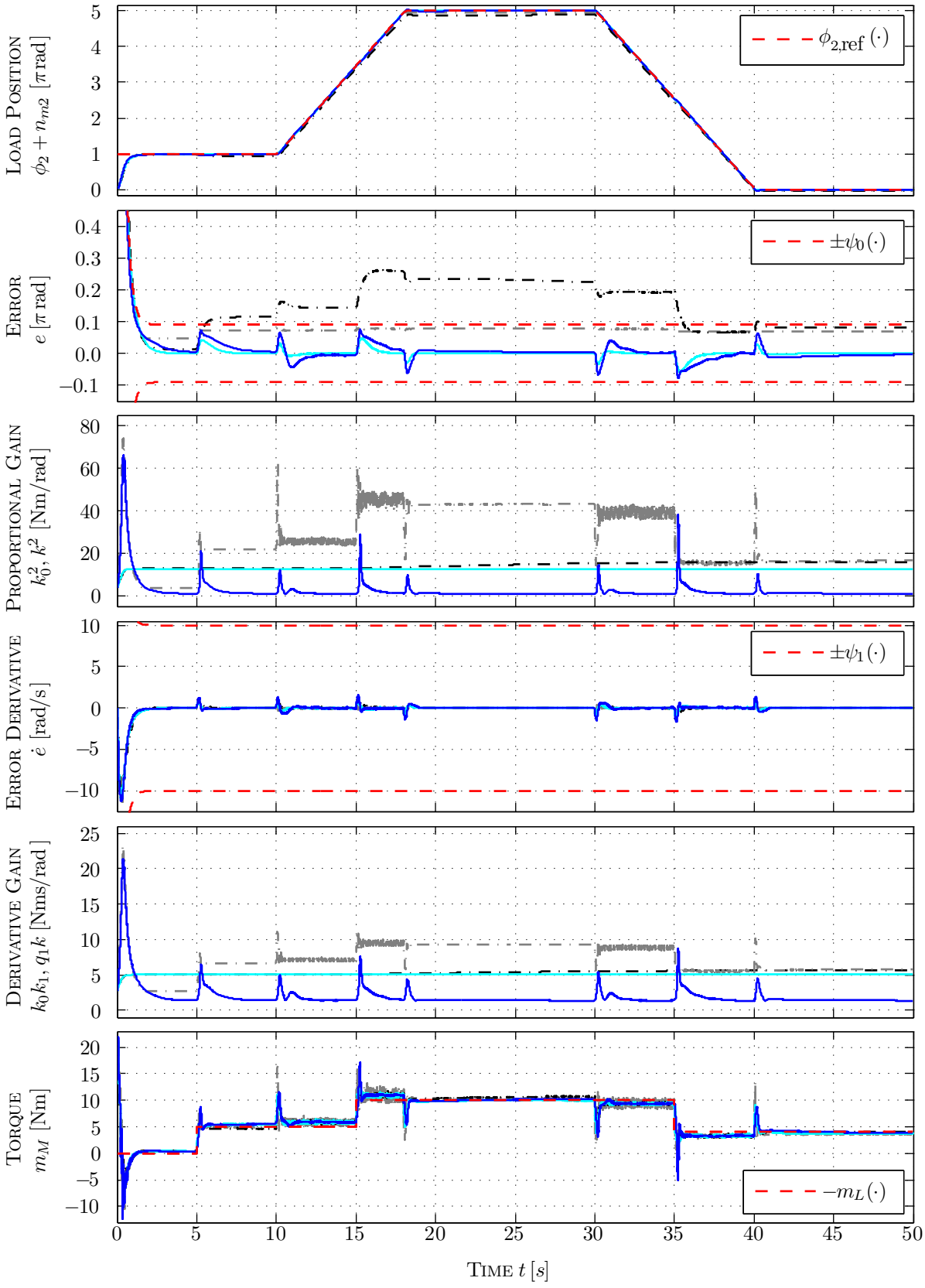

Figure 5.16: *Measurement results of Experiment PC2 (position control of 2MS) for different controllers (see p. 216):* ·-·-·(3.46), ·····(4.67), ——(3.46)+(5.3), ——(4.67)+(5.3) *with parametrization as in Tab. 5.2 (from top to bottom: measured load position* $\phi_2(\cdot)+n_{m2}(\cdot)$*, (augmented) error* $e(\cdot)$*, proportional gain* $k(\cdot)^2$ *&* $k_0(\cdot)^2$*, (augmented) error derivative* $\dot{e}(\cdot)$*, derivative gain* $q_1 k(\cdot)$ *&* $k_0(\cdot)k_1(\cdot)$ *and drive torque* $m_M(\cdot) = \mathrm{sat}_{\hat{u}_A}\big(u(\cdot) + u_A(\cdot)\big)$*).*

0.5 [Nm] at a time) until position control fails for 1MS and 2MS. So, for the circumstances of this experiment, a necessary (minimum) drive torque level $\hat{u}$ is obtained for 1MS and 2MS, which assures tracking with prescribed transient accuracy in the presence of control saturation. In contrast, evaluation of feasibility condition (4.107) yields a sufficient lower bound u_{feas} for 1MS and 2MS. The goal of this experiment is to show that funnel control in the presence of actuator saturation is applicable for position control of 1MS and 2MS, even if feasibility condition (4.107) is violated.

The measurement results are depicted in Fig. 5.17 for 1MS and 2MS. Note that, within the first two seconds, the augmented error $e(\cdot)$ of the 2MS is so close to the boundary $\psi_0(\cdot)$ such that proportional gain $k_0(\cdot)^2$ and derivative gain $k_0(\cdot)k_1(\cdot)$ attain their maximal values $\max_{t\in[0,\,2]} k_0(t)^2 = 1.56 \cdot 10^6$ [Nms/rad] and $\max_{t\in[0,\,2]} k_0(t)k_1(t) = 4.20 \cdot 10^3$ [Nm/rad], respectively. In Fig. 5.17(b), these peaks are not shown to allow for a quantitative comparison with the measurement results of the 1MS. Clearly, the measurement results prove feasibility of position funnel control of 1MS and 2MS with saturated actuator. For the settings of Experiment PC3, the following necessary (minimum) saturation levels are determined: $\hat{u} = 11.5$ [Nm] for 1MS and $\hat{u} = 13.0$ [Nm] for 2MS. Now feasibility condition (4.107) is evaluated for 1MS (1.24), (1.25) and for augmented 2MS (1.26), (1.27), (5.36) (with filter). For simplicity, it is assumed that both plants are exactly known. Hence the data in Tab. 5.1 is available to the control designer. Furthermore, the parameters of funnel design and gain scaling in Tab. 5.4 yield the following (rounded) values:

$$\text{for 1MS:}\quad \|\psi_0\|_\infty = 2\pi,\ \|\dot{\psi}_0\|_\infty = 17.13,\ \|\psi_1\|_\infty = 27.13,\ \|\dot{\psi}_1\|_\infty = 48.89,\ \varsigma_0 = 0.37,\ \text{etc.}$$

$$\text{for 2MS:}\quad \|\psi_0\|_\infty = 4\pi,\ \|\dot{\psi}_0\|_\infty = 43.87,\ \|\psi_1\|_\infty = 53.87,\ \|\dot{\psi}_1\|_\infty = 156.63,\ \varsigma_0 = 0.26,\ \text{etc.}$$

Then, collecting the data above and the data in Tables 5.1 & 5.4 (reference, disturbance, etc.) allows to compute M as in (4.78) and, for $\delta = \lambda_1 = 10$ [rad/s], to evaluate $\hat{u}_S$ in (4.105) and L as in (4.106). Combining altogether gives the following (rounded) values[3]:

$$\text{for 1MS:}\quad M = 64.5\ \left[1/\text{s}^2\right],\quad \hat{u}_S = 3.89 \cdot 10^4\ \left[1/\text{s}^2\right],\ L = 2.65 \cdot 10^7\ \left[1/\text{s}^2\right]\quad \text{and}$$
$$\gamma_0 = 2.92\ \left[1/\text{kg m}^2\right] \implies \boxed{u_{\text{feas}} = 9.08 \cdot 10^6\ [\text{Nm}]\quad \text{whereas}\quad \hat{u} = 11.5\ [\text{Nm}]\,!}$$

$$\text{for 2MS:}\quad M = 1.10 \cdot 10^{13}\ \left[1/\text{s}^2\right],\quad \hat{u}_S = 1.02 \cdot 10^7\ \left[1/\text{s}^2\right],\quad L = 1.84 \cdot 10^{12}\ \left[1/\text{s}^2\right]\quad \text{and}$$
$$\gamma_0 = 6.02\ \left[1/\text{kg m}^2\right] \implies \boxed{u_{\text{feas}} = 2.14 \cdot 10^{12}\ [\text{Nm}]\quad \text{whereas}\quad \hat{u} = 13\ [\text{Nm}]\,!}$$

The computed values of feasibility number u_{feas} for 1MS and 2MS are both extremely huge and unrealistic and by far exceed the actually required torque $\hat{u} = 11.5$ [Nm] for 1MS and $\hat{u} = 13.0$ [Nm] for 2MS. This is mainly due to L as in (4.106), where e.g. the term $(\|\psi_1\|_\infty + \|\dot{\psi}_0\|_\infty)^4$ yields $\approx 3.84 \cdot 10^6$ for the 1MS and $\approx 91.27 \cdot 10^6$ for the 2MS. For the 2MS, the rough bound $M_{\boldsymbol{z}}$ as in (4.77) on the zero dynamics degrades M and so usefulness of the feasibility condition even more. To conclude, similar to speed control experiment SC3, also for position control, feasibility condition (4.107) is mainly of theoretical interest. For implementation more realistic feasibility

[3] To compute M for the feasibility check, the augmented 2MS (1.26), (1.27), (5.36) must be transformed into BIF (see proof of Proposition 5.13) such that $|\hat{a}_1|$, $\|\hat{\boldsymbol{a}}_2\|$, etc. are available for evaluation of $M_{\dot{V}}$ as in (4.76) and $M_{\boldsymbol{z}}$ as in (4.77). The details are omitted.

numbers are desirable. This far, the available theory cannot serve this need. Nevertheless, the presented measurement results underpin applicability of funnel controller (4.67) for position control of 1MS and 2MS even in the presence of actuator saturation.

5.3 Position funnel control of rigid revolute joint robotic manipulators

As a "side product" of the theoretical development of Theorem 4.13, a first result for funnel control with derivative feedback in robotics has been found. In this section, it will be shown that the (SISO) funnel controller (4.67) may be extended to the MIMO case and then applied for position control of rigid revolute joint robotic manipulators if the inertia matrix is known. For illustration the proposed MIMO funnel controller is implemented for position control of a planar (elbow-like) two degree-of-freedom (DOF) robotic manipulator and simulation results are shown.

In the following let $n \in \mathbb{N}$ and consider a n-DOF robotic manipulator, given by the functional differential equation (see e.g. [112, p. 77], there without dynamic friction term)

$$\begin{aligned} \boldsymbol{M}(\boldsymbol{y}(t))\ddot{\boldsymbol{y}}(t) + \big(\boldsymbol{C}(\boldsymbol{y}(t), \dot{\boldsymbol{y}}(t)) + \boldsymbol{C}_V\big)\dot{\boldsymbol{y}}(t) + (\boldsymbol{\mathfrak{F}}\dot{\boldsymbol{y}})(t) + \boldsymbol{g}(\boldsymbol{y}(t)) + \boldsymbol{d}(t) = \boldsymbol{u}(t), \\ \big(\boldsymbol{y}(0), \quad \dot{\boldsymbol{y}}(0)\big) = \big(\boldsymbol{y}^0, \quad \boldsymbol{y}^1\big) \in \mathbb{R}^{2n}, \end{aligned} \tag{5.48}$$

where $\boldsymbol{y}(t)$ in $[\text{rad}]^n$ and $\dot{\boldsymbol{y}}(t)$ in $[\text{rad/s}]^n$ represent position and speed (vector) at time $t \geq 0$, respectively. $\boldsymbol{M}(\cdot) \in \mathcal{C}(\mathbb{R}^n; \mathbb{R}^{n\times n})$ is the position dependent inertia matrix. $\boldsymbol{C}(\cdot,\cdot) \in \mathcal{C}(\mathbb{R}^n \times \mathbb{R}^n; \mathbb{R}^{n\times n})$ is the position and speed dependent centrifugal and Coriolis force matrix. $\boldsymbol{C}_V := \operatorname{diag}\{\nu_1, \ldots, \nu_n\} \in \mathbb{R}^{n\times n}$ with $\nu_1, \ldots, \nu_n > 0$ represents the viscous friction matrix and $\boldsymbol{\mathfrak{F}}\colon \mathcal{C}(\mathbb{R}_{\geq 0}; \mathbb{R}^n) \to \mathcal{L}^\infty(\mathbb{R}_{\geq 0}; \mathbb{R}^n)$ with $\boldsymbol{\mathfrak{F}} := (\mathfrak{F}_1, \ldots, \mathfrak{F}_n)^\top$ and $\mathfrak{F}_1, \ldots, \mathfrak{F}_n$ as in (1.22) models dynamic friction. Similar to 1MS and 2MS, it is assumed that friction may be split into unbounded viscous part $\boldsymbol{C}_V\dot{\boldsymbol{y}}$ and bounded nonlinear and dynamic part $\boldsymbol{\mathfrak{F}}\dot{\boldsymbol{y}}$ modeled by the simplified LuGre friction operator. $\boldsymbol{d}(\cdot) \in \mathcal{L}^\infty(\mathbb{R}_{\geq 0}; \mathbb{R}^n)$ represents an exogenous disturbance and $\boldsymbol{g}(\cdot) \in \mathcal{C}(\mathbb{R}^n; \mathbb{R}^n)$ is the position dependent gravity vector. The robot is actuated by joint torque vector $\boldsymbol{u}$ $[\text{Nm}]^n$ (control input). For simplicity, elasticity in the joints (or the links), torque generation in the actuator and actuator saturation are neglected. The following assumptions are imposed on the model (5.48):

(A_1) the inertia matrix is uniformly bounded from above and below (see e.g. [63]), i.e.

$$\exists\, \bar{c}_{\boldsymbol{M}}, \underline{c}_{\boldsymbol{M}} > 0\ \forall\, \boldsymbol{y} \in \mathbb{R}^n : \qquad 0 < \underline{c}_{\boldsymbol{M}} \boldsymbol{I}_n \leq \boldsymbol{M}(\boldsymbol{y}) = \boldsymbol{M}(\boldsymbol{y})^\top \leq \bar{c}_{\boldsymbol{M}} \boldsymbol{I}_n;$$

(A_2) the centrifugal and Coriolis force matrix is upper bounded (see e.g. [112, Sections 4.2]) as follows

$$\exists\, c_{\boldsymbol{C}} > 0\ \forall\, \boldsymbol{y}, \boldsymbol{v}, \boldsymbol{w} \in \mathbb{R}^n : \qquad \|\boldsymbol{C}(\boldsymbol{y}, \boldsymbol{v})\boldsymbol{w}\| \leq c_{\boldsymbol{C}} \|\boldsymbol{v}\| \|\boldsymbol{w}\|;$$

(A_3) the gravity vector is uniformly bounded (see e.g. [112, Sections 4.3]), i.e.

$$\exists\, c_{\boldsymbol{g}} > 0\ \forall\, \boldsymbol{y} \in \mathbb{R}^n : \qquad \|\boldsymbol{g}(\boldsymbol{y})\| \leq c_{\boldsymbol{g}};$$

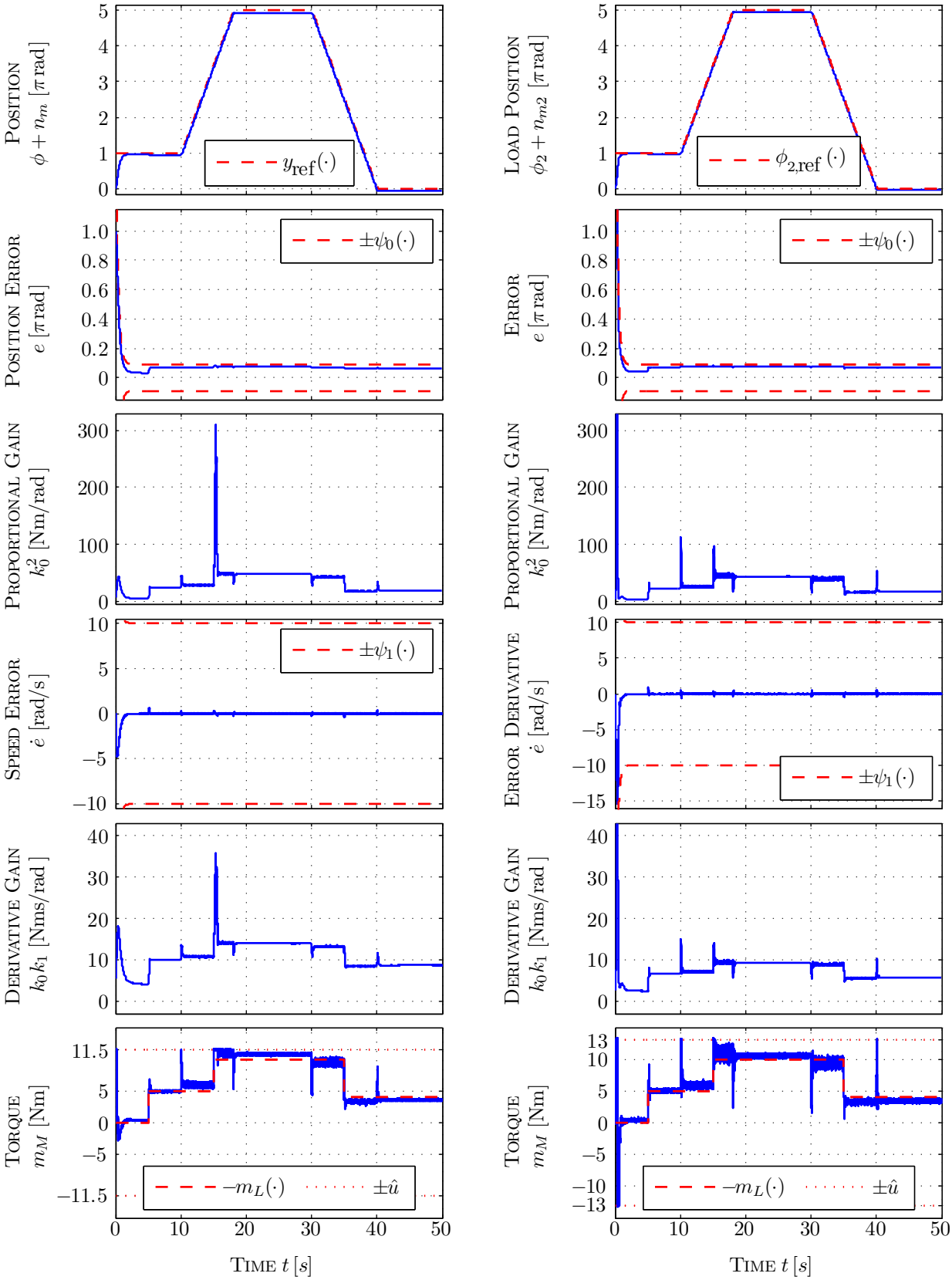

(a) *one-mass system (1MS):* $\hat{u} = 11.5$ [Nm] (b) *two-mass system (2MS):* $\hat{u} = 13$ [Nm].

Figure 5.17: *Measurement results of Experiment PC3: saturated funnel controller* (4.104) *for position control of 1MS (——left) and 2MS (——right).*

(A_4) the friction operator is element of class $\mathcal{T}$ and globally bounded, i.e.

$$\mathfrak{F} \in \mathcal{T} \text{ and } M_{\mathfrak{F}} := \sup\{\|(\mathfrak{F}\boldsymbol{\xi})(t)\| \mid t \geq 0,\ \boldsymbol{\xi}(\cdot) \in \mathcal{C}(\mathbb{R}_{\geq 0}, \mathbb{R}^n)\} < \infty;$$

(A_5) the exogenous disturbance is uniformly bounded, i.e. $\boldsymbol{d}(\cdot) \in \mathcal{L}^\infty(\mathbb{R}_{\geq 0}; \mathbb{R}^n)$ and

(A_6) feedback of position $\boldsymbol{y}(\cdot)$ and speed $\dot{\boldsymbol{y}}(\cdot)$ is admissible.

Assumptions (A_1)-(A_3) are standard properties of rigid robotic manipulators with exclusively revolute joints (see e.g. [112, Sections 4.1-4.3]). Assumptions (A_4)-(A_6) are similar to system properties ($\mathcal{S}_2$-sp$_3$)-($\mathcal{S}_2$-sp$_5$) and realistic for mechatronic systems.

Funnel control in robotics is introduced in [71]. Although a robot of form (5.48) has (strict vector) relative degree two, a MIMO funnel controller for relative degree one systems (see [99]) is applied. The (vector) relative degree is reduced to one by introducing the auxiliary output

$$\forall t \geq 0\colon\ \widehat{\boldsymbol{y}}(t) := \boldsymbol{K}_P \boldsymbol{y}(t) + \boldsymbol{K}_D \dot{\boldsymbol{y}}(t) \text{ where } 0 < \boldsymbol{K}_P = \boldsymbol{K}_P^\top \in \mathbb{R}^{n\times n},\ 0 < \boldsymbol{K}_D = \boldsymbol{K}_D^\top \in \mathbb{R}^{n\times n}.$$

Control objective is reference tracking of position reference $\boldsymbol{y}_{\mathrm{ref}}(\cdot) \in \mathcal{W}^{2,\infty}(\mathbb{R}_{\geq 0}; \mathbb{R}^n)$. In [71] it is shown that, for auxiliary reference $\widehat{\boldsymbol{y}}_{\mathrm{ref}}(\cdot) := \boldsymbol{K}_P \boldsymbol{y}_{\mathrm{ref}}(\cdot) + \boldsymbol{K}_D \dot{\boldsymbol{y}}_{\mathrm{ref}}(\cdot)$, auxiliary error $\widehat{\boldsymbol{y}}_{\mathrm{ref}}(\cdot) - \widehat{\boldsymbol{y}}(\cdot)$ evolves within a prescribed (MIMO) performance funnel. However, the drawback of this approach is that

$$\text{actual position error } \boldsymbol{e}(\cdot) := \boldsymbol{y}_{\mathrm{ref}}(\cdot) - \boldsymbol{y}(\cdot) \text{ or actual speed error } \dot{\boldsymbol{e}}(\cdot) := \dot{\boldsymbol{y}}_{\mathrm{ref}}(\cdot) - \dot{\boldsymbol{y}}(\cdot)$$

may leave the prescribed region. Therefore an extension of (SISO) funnel controller (4.67) with derivative feedback to the robot model (5.48) is desirable to achieve tracking with prescribed transient accuracy for position error $\boldsymbol{e}(\cdot)$ and speed error $\dot{\boldsymbol{e}}(\cdot)$, respectively. More precisely, for $(\boldsymbol{\psi}_0(\cdot), \boldsymbol{\psi}_1(\cdot)) \in \mathcal{B}_2^n$, introduce the (MIMO) performance funnel

$$\mathcal{F}_{(\boldsymbol{\psi}_0,\boldsymbol{\psi}_1)} := \{(t, \boldsymbol{\xi}, \boldsymbol{\eta}) \in \mathbb{R}_{\geq 0} \times \mathbb{R}^n \times \mathbb{R}^n \mid \forall\, i \in \{1, \ldots, n\}\colon\ |\xi_i| < \psi_{0,i}(t) \wedge |\eta_i| < \psi_{1,i}(t)\} \tag{5.49}$$

and find a (MIMO) funnel controller which assures that position and speed error evolve within the prescribed performance funnel, i.e. $(t, \boldsymbol{e}(t), \dot{\boldsymbol{e}}(t)) \in \mathcal{F}_{(\boldsymbol{\psi}_0,\boldsymbol{\psi}_1)}$ for all $t \geq 0$. If inertia matrix $\boldsymbol{M}(\cdot)$ is known, then the result directly follows from a straightforward extension of Theorem 4.13 to the MIMO case.

Theorem 5.18 (Funnel control with derivative feedback of rigid revolute joint robotic manipulators)**.** *Let $n \in \mathbb{N}$ and consider a n-th DOF rigid revolute joint robotic manipulator of form (5.48) which satisfies assumptions (A_1)-(A_6). Then, for arbitrary position reference $\boldsymbol{y}_{\mathrm{ref}}(\cdot) \in \mathcal{W}^{2,\infty}(\mathbb{R}_{\geq 0}, \mathbb{R}^n)$, funnel boundary $(\boldsymbol{\psi}_0(\cdot), \boldsymbol{\psi}_1(\cdot)) \in \mathcal{B}_2^n$, gain scaling $\boldsymbol{\varsigma}_0(\cdot), \boldsymbol{\varsigma}_1(\cdot) \in \mathcal{B}_1^n$ and initial value $(\boldsymbol{y}^0, \boldsymbol{y}^1) \in \mathbb{R}^{2n}$ satisfying*

$$\forall\, i \in \{1, \ldots, n\}\colon \qquad |y_{\mathrm{ref,i}}(0) - y_i^0| < \psi_{0,i}(0) \qquad \text{and} \qquad |\dot{y}_{\mathrm{ref,i}}(0) - y_i^1| < \psi_{1,i}(0), \tag{5.50}$$

the MIMO funnel controller

$$\left.\begin{aligned} &\boldsymbol{u}(t) = \boldsymbol{M}(\boldsymbol{y}(t))\Big(\boldsymbol{K}_0(t)^2\boldsymbol{e}(t) + \boldsymbol{K}_0(t)\boldsymbol{K}_1(t)\dot{\boldsymbol{e}}(t)\Big) \quad \text{where} \quad \boldsymbol{e}(t) = \boldsymbol{y}_{\mathrm{ref}}(t) - \boldsymbol{y}(t),\\ &\boldsymbol{K}_0(t) = \operatorname{diag}\big\{k_{0,1}(t), \ldots, k_{0,n}(t)\big\}, \quad \boldsymbol{K}_1(t) = \operatorname{diag}\big\{k_{1,1}(t), \ldots, k_{1,n}(t)\big\} \quad \text{and}\\ &\forall\, i \in \{1, \ldots, n\}\colon \quad k_{0,i}(t) = \frac{\varsigma_{0,i}(t)}{\psi_{0,i}(t) - |e_i(t)|} \quad \text{and} \quad k_{1,i}(t) = \frac{\varsigma_{1,i}(t)}{\psi_{1,i}(t) - |\dot{e}_i(t)|} \end{aligned}\right\} \tag{5.51}$$

applied to (5.48) *yields a closed-loop initial-value problem with the properties:*

(i) there exists a solution $(\boldsymbol{y}, \dot{\boldsymbol{y}}) : [0, T) \to \mathbb{R}^{2n}$ *which can be maximally extended and* $T \in (0, \infty]$*;*

(ii) the solution $(\boldsymbol{y}(\cdot), \dot{\boldsymbol{y}}(\cdot))$ *does not have finite escape time, i.e.* $T = \infty$*;*

(iii) the signals $\boldsymbol{e}(\cdot)$ *and* $\dot{\boldsymbol{e}}(\cdot)$ *are uniformly bounded, i.e.*

$$\forall\, i \in \{1, \ldots, n\}\ \exists \varepsilon_{0,i}, \varepsilon_{1,i} > 0\ \forall\, t \geq 0 : \quad \psi_{0,i}(t) - |e_i(t)| \geq \varepsilon_{0,i} \quad \text{and} \quad \psi_{1,i}(t) - |\dot{e}_i(t)| \geq \varepsilon_{1,i};$$

(iv) control action and control gain matrices are uniformly bounded, i.e. $\boldsymbol{u}(\cdot) \in \mathcal{L}^\infty(\mathbb{R}_{\geq 0}; \mathbb{R}^n)$ *and* $\boldsymbol{K}_0(\cdot)$, $\boldsymbol{K}_1(\cdot) \in \mathcal{L}^\infty(\mathbb{R}_{\geq 0}; \mathbb{R}^{n\times n})$.

This far, exact knowledge of inertia matrix $\boldsymbol{M}(\cdot)$ is essential for the proof of Theorem 5.18. Only then the basic idea of the proof of Theorem 4.13 can be reused and allows to extend the (SISO) funnel controller (4.67) with derivative feedback to the MIMO case. Including inertia matrix $\boldsymbol{M}(\cdot)$ into the controller as in (5.51) yields a decoupled mechanical system, in the sense that actual error acceleration $\ddot{e}_i(t)$ of joint i is solely affected by

$$k_{0,i}(t)^2 e_i(t) + k_{0,i}(t)\, k_{1,i}(t) \dot{e}_i(t), \qquad i \in \{1, \ldots, n\},$$

which corresponds to SISO controller (4.67) (applied to each joint i). It was not possible to extend the result to unknown or roughly known inertia matrices.

Proof of Theorem 5.18.

Step 1: Some preliminaries.
It is easy to see, that (A_1) is equivalent to

$$\exists \underline{\gamma_0}, \overline{\gamma_0} > 0\ \forall\, \boldsymbol{y} \in \mathbb{R}^n : \quad \underline{\gamma_0}\boldsymbol{I}_n \leq \boldsymbol{\Gamma}_0(\boldsymbol{y}) := \boldsymbol{M}^{-1}(\boldsymbol{y}) = \boldsymbol{\Gamma}_0(\boldsymbol{y})^\top \leq \overline{\gamma_0}\boldsymbol{I}_n. \tag{5.52}$$

Write system (5.48) as

$$\frac{\mathrm{d}}{\mathrm{d}t}\begin{pmatrix}\boldsymbol{y}(t)\\ \dot{\boldsymbol{y}}(t)\end{pmatrix} = \begin{pmatrix} \dot{\boldsymbol{y}}(t) \\ -\boldsymbol{\Gamma}_0(\boldsymbol{y}(t))\Big[\big(\boldsymbol{C}(\boldsymbol{y}(t), \dot{\boldsymbol{y}}(t)) + \boldsymbol{C}_V\big)\dot{\boldsymbol{y}}(t) + (\mathfrak{F}\dot{\boldsymbol{y}})(t) \\ \qquad + \boldsymbol{g}(\boldsymbol{y}(t)) + \boldsymbol{d}(t)\Big] \end{pmatrix} + \begin{pmatrix}\boldsymbol{0}\\ \boldsymbol{\Gamma}_0(\boldsymbol{y}(t))\end{pmatrix}\boldsymbol{u}(t)$$

and, for error $\boldsymbol{e}(t) = \boldsymbol{y}_{\mathrm{ref}}(t) - \boldsymbol{y}(t)$, as

$$\left.\begin{aligned}\tfrac{\mathrm{d}}{\mathrm{d}t}\begin{pmatrix}\boldsymbol{e}(t)\\ \dot{\boldsymbol{e}}(t)\end{pmatrix} = &\begin{pmatrix}\dot{\boldsymbol{e}}(t)\\ \boldsymbol{\Gamma}_0(\boldsymbol{y}_{\mathrm{ref}}(t)-\boldsymbol{e}(t))\Big[\big(\boldsymbol{C}(\boldsymbol{y}_{\mathrm{ref}}(t)-\boldsymbol{e}(t),\,\dot{\boldsymbol{y}}_{\mathrm{ref}}(t)-\dot{\boldsymbol{e}}(t))+\boldsymbol{C}_V\big)(\dot{\boldsymbol{y}}_{\mathrm{ref}}(t)-\dot{\boldsymbol{e}}(t))\\ +(\mathfrak{F}(\dot{\boldsymbol{y}}_{\mathrm{ref}}-\boldsymbol{e}))(t)+\boldsymbol{g}(\boldsymbol{y}_{\mathrm{ref}}(t)-\boldsymbol{e}(t))+\boldsymbol{d}(t)\Big]\end{pmatrix}\\ &+\begin{pmatrix}\boldsymbol{0}\\ \ddot{\boldsymbol{y}}_{\mathrm{ref}}(t)\end{pmatrix}-\begin{pmatrix}\boldsymbol{0}\\ \boldsymbol{\Gamma}_0(\boldsymbol{y}_{\mathrm{ref}}(t)-\boldsymbol{e}(t))\end{pmatrix}\boldsymbol{u}(t), \qquad \begin{pmatrix}\boldsymbol{e}(0)\\ \dot{\boldsymbol{e}}(0)\end{pmatrix} = \begin{pmatrix}\boldsymbol{y}_{\mathrm{ref}}(0)-\boldsymbol{y}^0\\ \dot{\boldsymbol{y}}_{\mathrm{ref}}(0)-\boldsymbol{y}^1\end{pmatrix}.\end{aligned}\right\} \tag{5.53}$$

For the following define the constants

$$\begin{aligned}&\forall\, i\in\{1,\dots,n\}\colon \quad \varsigma_{0,i} := \inf_{t\geq 0}\varsigma_{0,i}(t) \quad \text{and} \quad \varsigma_{1,i} := \inf_{t\geq 0}\varsigma_{1,i}(t),\\ &\forall\, i\in\{1,\dots,n\}\colon \quad \lambda_{0,i} := \inf_{t\geq 0}\psi_{0,i}(t) \quad \text{and} \quad \lambda_{1,i} := \inf_{t\geq 0}\psi_{1,i}(t).\end{aligned} \tag{5.54}$$

Step 2: It is shown that Assertion (i) holds true, i.e. existence of a maximally extended solution. It suffices to consider system (5.48) in the form (5.53). For $\mathcal{F}_{(\psi_0,\psi_1)}$ as in (5.49) define the non-empty and open set

$$\mathcal{D} := \left\{(\tau,\boldsymbol{\mu},\boldsymbol{\xi})\in\mathbb{R}\times\mathbb{R}^n\times\mathbb{R}^n \;\middle|\; (|\tau|,\boldsymbol{\mu},\boldsymbol{\xi})\in\mathcal{F}_{(\psi_0,\psi_1)}\right\}, \tag{5.55}$$

the function

$$\boldsymbol{f}\colon \mathbb{R}_{\geq 0}\times\mathcal{D}\times\mathbb{R}^n\to\mathbb{R}\times\mathbb{R}^{2n},$$

$$(t,(\tau,\boldsymbol{\mu},\boldsymbol{\xi}),\boldsymbol{w})\mapsto\begin{pmatrix}1\\ \boldsymbol{\xi}\\ \boldsymbol{\Gamma}_0(\boldsymbol{y}_{\mathrm{ref}}(t)-\boldsymbol{\mu})\Big[\big(\boldsymbol{C}(\boldsymbol{y}_{\mathrm{ref}}(t)-\boldsymbol{\mu},\,\dot{\boldsymbol{y}}_{\mathrm{ref}}(t)-\boldsymbol{\xi})+\boldsymbol{C}_V\big)(\dot{\boldsymbol{y}}_{\mathrm{ref}}(t)-\boldsymbol{\xi})\\ +\boldsymbol{w}+\boldsymbol{g}(\boldsymbol{y}_{\mathrm{ref}}(t)-\boldsymbol{\mu})+\boldsymbol{d}(t)\Big]+\ddot{\boldsymbol{y}}_{\mathrm{ref}}(t)\\ -\operatorname{diag}\left\{\frac{\varsigma_{0,1}(t)}{\psi_{0,1}(|\tau|)-|\mu_1|},\dots,\frac{\varsigma_{0,n}(t)}{\psi_{0,n}(|\tau|)-|\mu_n|}\right\}^2\boldsymbol{\mu}\\ -\operatorname{diag}\left\{\frac{\varsigma_{0,1}(t)\varsigma_{1,1}(t)}{(\psi_{0,1}(|\tau|)-|\mu_1|)(\psi_{1,1}(|\tau|)-|\xi_1|)},\dots,\frac{\varsigma_{0,n}(t)\varsigma_{1,n}(t)}{(\psi_{0,n}(|\tau|)-|\mu_n|)(\psi_{1,n}(|\tau|)-|\xi_n|)}\right\}\boldsymbol{\xi}\end{pmatrix}$$

and the operator

$$\hat{\mathfrak{T}}\colon\mathcal{C}(\mathbb{R}_{\geq 0};\mathbb{R}\times\mathbb{R}^{2n})\to\mathcal{L}^\infty_{\mathrm{loc}}(\mathbb{R}_{\geq 0};\mathbb{R}^n), \qquad (\hat{\mathfrak{T}}(\tau,\boldsymbol{\mu},\boldsymbol{\xi}))(t) := (\mathfrak{F}\boldsymbol{\xi})(t).$$

Then, for artifact $\tau\colon\mathbb{R}\to\mathbb{R},\ t\mapsto t$ and extended state variable $\hat{\boldsymbol{x}} := (\tau,(\boldsymbol{e},\dot{\boldsymbol{e}}))$, the initial-value problem (5.53), (5.51) may be expressed in standard form

$$\frac{\mathrm{d}}{\mathrm{d}t}\hat{\boldsymbol{x}}(t) = \boldsymbol{f}(t,\hat{\boldsymbol{x}}(t),(\hat{\mathfrak{T}}\hat{\boldsymbol{x}})(t)), \qquad \hat{\boldsymbol{x}}(0) = \begin{pmatrix}0\\ \boldsymbol{y}_{\mathrm{ref}}(0)-\boldsymbol{y}^0\\ \dot{\boldsymbol{y}}_{\mathrm{ref}}(0)-\boldsymbol{y}^1\end{pmatrix}\in\mathbb{R}^{2n+1}. \tag{5.56}$$

Choose a compact set $\mathfrak{C}\subset\mathcal{D}\times\mathbb{R}^n$ and observe that the following holds

$$\begin{aligned}&\exists\, M_{\mathfrak{C}}>0\ \forall\,((\tau,\boldsymbol{\mu},\boldsymbol{\xi}),\boldsymbol{w})\in\mathfrak{C}\colon \quad \|((\tau,\boldsymbol{\mu},\boldsymbol{\xi}),\boldsymbol{w})\|\leq M_{\mathfrak{C}}\\ &\exists\, m_{\mathfrak{C}}>0\ \forall\,((\tau,\boldsymbol{\mu},\boldsymbol{\xi}),\boldsymbol{w})\in\mathfrak{C}\colon \quad \min_{i\in\{1,\dots,n\}}\{\psi_{0,i}(|\tau|)-|\mu_i|,\ \psi_{1,i}(|\tau|)-|\xi_i|\}\geq m_{\mathfrak{C}}.\end{aligned} \tag{5.57}$$

Then, for $\boldsymbol{d}(\cdot) \in \mathcal{L}^\infty(\mathbb{R}_{\geq 0}; \mathbb{R}^n)$, $\boldsymbol{y}_{\text{ref}}(\cdot) \in \mathcal{W}^{2,\infty}(\mathbb{R}_{\geq 0}; \mathbb{R}^n)$ and $\boldsymbol{\varsigma}_0(\cdot), \boldsymbol{\varsigma}_1(\cdot) \in \mathcal{W}^{1,\infty}(\mathbb{R}_{\geq 0}, \mathbb{R}^n_{>0})$, note that the function $\boldsymbol{f}(\cdot,\cdot,\cdot)$ has the following properties: (i) $\boldsymbol{f}(t,\cdot,\cdot)$ is continuous for each fixed $t \geq 0$, (ii) for each fixed $((\tau,\boldsymbol{\mu},\boldsymbol{\xi}),\boldsymbol{w}) \in \mathcal{D}\times\mathbb{R}^n$ the function $\boldsymbol{f}(\cdot,(\tau,\boldsymbol{\mu},\boldsymbol{\xi}),\boldsymbol{w})$ is measurable and (iii) for almost all $t \geq 0$ and for all $((\tau,\boldsymbol{\mu},\boldsymbol{\xi}),\boldsymbol{w}) \in \mathfrak{C}$ the following holds

$$\begin{aligned}\|\boldsymbol{f}(t,(\tau,\boldsymbol{\mu},\boldsymbol{\xi}),\boldsymbol{w})\| \overset{(A_1)-(A_5),\ (5.57)}{\leq}\ & 1 + M_{\mathfrak{C}} + \overline{\gamma_0}\Big[c_{\boldsymbol{C}}(\|\dot{\boldsymbol{y}}_{\text{ref}}(t)\| + M_{\mathfrak{C}})^2 + \\ & \max\{\nu_1,\dots,\nu_n\}(\|\dot{\boldsymbol{y}}_{\text{ref}}(t)\| + M_{\mathfrak{C}}) + M_{\mathfrak{C}} + c_{\boldsymbol{g}} + \|\boldsymbol{d}(t)\|\Big] \\ & \|\ddot{\boldsymbol{y}}_{\text{ref}}(t)\| + \|\boldsymbol{\varsigma}_0(t)\|\left(\|\boldsymbol{\varsigma}_0(t)\| + \|\boldsymbol{\varsigma}_1(t)\|\right)\frac{M_{\mathfrak{C}}}{m_{\mathfrak{C}}^2} =: l_{\mathfrak{C}}(t)\end{aligned}$$

where $l_{\mathfrak{C}}(\cdot) \in \mathcal{L}^\infty(\mathbb{R}_{\geq 0};\mathbb{R}_{\geq 0}) \subset \mathcal{L}^1_{\text{loc}}(\mathbb{R}_{\geq 0},\mathbb{R}_{\geq 0})$. Hence $\boldsymbol{f}(\cdot,\cdot,\cdot)$ is a Carathéodory function (see Definition 3.1) and invoking Theorem 3.2 yields existence of a solution $\hat{\boldsymbol{x}} : [0,T) \to \mathbb{R}\times\mathbb{R}^{2n}$ of the initial-value problem (5.56) with $\hat{\boldsymbol{x}}([0,T)) \in \mathcal{D}$, $T \in (0,\infty]$. Each solution can be extended to a maximal solution. Moreover $\boldsymbol{f}(\cdot,\cdot,\cdot)$ is essentially bounded and so, if $T < \infty$, then for any compact $\tilde{\mathfrak{C}} \subset \mathcal{D}$, there exists $\tilde{t} \in [0,T)$ such that $\hat{\boldsymbol{x}}(\tilde{t}) \notin \tilde{\mathfrak{C}}$. In the following, let $\hat{\boldsymbol{x}} := (\tau,\boldsymbol{e},\dot{\boldsymbol{e}})\colon [0,T) \to \mathbb{R}\times\mathbb{R}^n\times\mathbb{R}^n$ be a fixed and maximally extended solution of the initial-value problem (5.56). Note that $(\boldsymbol{e},\dot{\boldsymbol{e}}) : [0,T) \to \mathbb{R}^n\times\mathbb{R}^n$ solves the closed-loop initial-value problem (5.53), (5.51) for almost all $t \in [0,T)$. This shows Assertion (i) and completes Step 2.

Step 3: Some technical inequalities are introduced.
In view of Step 1, $\boldsymbol{e}(\cdot)$ and $\dot{\boldsymbol{e}}(\cdot)$ are continuous on $[0,T)$ and evolve within the funnel $\mathcal{F}_{(\psi_0,\psi_1)}$. Hence and due to the properties of $\mathcal{B}_2$ (see p. 153), it follows that

$$\forall\, i \in \{1,\dots,n\}\ \forall\, t \in [0,T): \quad |e_i(t)| < \psi_{0,i}(t) \leq \|\psi_{0,i}\|_\infty \ \text{ and } \ |\dot{e}_i(t)| < \psi_{1,i}(t) \leq \|\psi_{1,i}\|_\infty$$

or

$$\forall\, t \in [0,T): \qquad \|\boldsymbol{e}(t)\| < \|\boldsymbol{\psi}_0\|_\infty \qquad \text{and} \qquad \|\dot{\boldsymbol{e}}(t)\| < \|\boldsymbol{\psi}_1\|_\infty. \tag{5.58}$$

Define

$$\begin{aligned}\widehat{\boldsymbol{d}}\colon\ \mathbb{R}_{\geq 0}\times\mathbb{R}^n\times\mathbb{R}^n\times\mathbb{R}^n \ &\to\ \mathbb{R}^n; \\ (t,\boldsymbol{\mu},\boldsymbol{\xi},\boldsymbol{w}) \ &\mapsto\ \boldsymbol{\Gamma}_0(\boldsymbol{y}_{\text{ref}}(t)-\boldsymbol{\mu})\Big[\big(\boldsymbol{C}(\boldsymbol{y}_{\text{ref}}(t)-\boldsymbol{\mu},\,\dot{\boldsymbol{y}}_{\text{ref}}(t)-\boldsymbol{\xi}) + \boldsymbol{C}_V\big)(\dot{\boldsymbol{y}}_{\text{ref}}(t)-\boldsymbol{\xi}) \\ &\qquad + \boldsymbol{w} + \boldsymbol{g}(\boldsymbol{y}_{\text{ref}}(t)-\boldsymbol{\mu}) + \boldsymbol{d}(t)\Big] + \ddot{\boldsymbol{y}}_{\text{ref}}(t) =: \widehat{\boldsymbol{d}}(t,\boldsymbol{\mu},\boldsymbol{\xi},\boldsymbol{w})\end{aligned}$$

and the constant

$$\begin{aligned}M \ :=\ & \overline{\gamma_0}\Big[c_{\boldsymbol{C}}\left(\|\dot{\boldsymbol{y}}_{\text{ref}}\|_\infty + \|\boldsymbol{\psi}_1\|_\infty\right)^2 + \max\{\nu_1,\dots,\nu_n\}\left(\|\dot{\boldsymbol{y}}_{\text{ref}}\|_\infty + \|\boldsymbol{\psi}_1\|_\infty\right) \\ & + M_{\mathfrak{F}} + c_{\boldsymbol{g}} + \|\boldsymbol{d}\|_\infty\Big] + \|\ddot{\boldsymbol{y}}_{\text{ref}}\|_\infty.\end{aligned} \tag{5.59}$$

Invoking assumptions (A_2), (A_3), (A_4) and (A_5) yields for almost all $t \in [0,T)$

$$\begin{aligned}\left\|\widehat{\boldsymbol{d}}\big(t,\boldsymbol{e}(t),\dot{\boldsymbol{e}}(t),(\boldsymbol{\mathfrak{F}}(\boldsymbol{y}_{\mathrm{ref}}-\boldsymbol{e}))(t)\big)\right\| &\overset{(5.52)}{\leq} \overline{\gamma_0}\Big[c_{\boldsymbol{C}}\left\|\dot{\boldsymbol{y}}_{\mathrm{ref}}(t)-\dot{\boldsymbol{e}}(t)\right\|^2 + M_{\boldsymbol{\mathfrak{F}}} + c_{\boldsymbol{g}} + \|\boldsymbol{d}\|_\infty \\ &\qquad + \max\{\nu_1,\dots,\nu_n\}\left\|\dot{\boldsymbol{y}}_{\mathrm{ref}}(t)-\dot{\boldsymbol{e}}(t)\right\|\Big] + \|\ddot{\boldsymbol{y}}_{\mathrm{ref}}\|_\infty \\ &\overset{(5.58),(5.59)}{\leq} M,\end{aligned}$$

hence the following holds

$$\forall\, i \in \{1,\dots,n\} \text{ for a.a. } t\in[0,T): \qquad |\widehat{d}_i\big(t,\boldsymbol{e}(t),\dot{\boldsymbol{e}}(t),(\boldsymbol{\mathfrak{F}}(\boldsymbol{y}_{\mathrm{ref}}-\boldsymbol{e}))(t)\big)| \leq M. \tag{5.60}$$

Inserting (5.51) into (5.53) and invoking (5.60) yields

$$\begin{aligned}&\forall\, i \in \{1,\dots,n\}\ \forall\, t\in[0,T):\\ &-M - k_{0,i}(t)^2\, e_i(t) - k_{0,i}(t)\, k_{1,i}(t)\, \dot{e}_i(t) \leq \ddot{e}_i(t) \leq M - k_{0,i}(t)^2\, e_i(t) - k_{0,i}(t)\, k_{1,i}(t)\, \dot{e}_i(t).\end{aligned} \tag{5.61}$$

Step 4: For all $i \in \{1,\dots,n\}$ it is shown that $|e_i(\cdot)|$ is uniformly bounded away from the boundary $\psi_{0,i}(\cdot)$; more precisely for positive

$$\begin{aligned}\varepsilon_{0,i} \leq \min\Bigg\{&\tfrac{\lambda_{0,i}}{4}, \tfrac{\psi_{0,i}(0)-|e_i(0)|}{2}, \frac{\frac{1}{2}\delta_i \underline{\varsigma}_{0,i}\lambda_{0,i}}{2\|\varsigma_{1,i}\|_\infty\|\psi_{1,i}\|_\infty + \sqrt{4\|\varsigma_{1,i}\|_\infty^2\|\psi_{1,i}\|_\infty^2 + 2\delta_i^2\lambda_{0,i}(M+\|\dot{\psi}_{1,i}\|_\infty)}},\\ &\frac{\frac{1}{2}\delta_i \underline{\varsigma}_{0,i}^2\lambda_{0,i}}{2\underline{\varsigma}_{0,i}\|\varsigma_{1,i}\|_\infty\|\psi_{1,i}\|_\infty + \delta_i\big(\|\psi_{1,i}\|_\infty+\|\dot{\psi}_{0,i}\|_\infty\big)^2 + \sqrt{\big(2\underline{\varsigma}_{0,i}\|\varsigma_{1,i}\|_\infty\|\psi_{1,i}\|_\infty + \delta_i(\|\psi_{1,i}\|_\infty+\|\dot{\psi}_{0,i}\|_\infty)^2\big)^2 + 2\delta_i^2\underline{\varsigma}_{0,i}^2\lambda_{0,i}M}}\Bigg\},\end{aligned} \tag{5.62}$$

with $\lambda_{0,i}$, $\lambda_{1,i}$, $\underline{\varsigma}_{0,i}$ and $\underline{\varsigma}_{1,i}$ as in (5.54), $\delta_i = \delta$ as in (4.61) and M as in (5.59), it holds that $\psi_{0,i}(t) - |e_i(t)| \geq \varepsilon_{0,i}$ for all $i \in \{1,\dots,n\}$ and all $t \in [0,T)$.

Choose $i \in \{1,\dots,n\}$ arbitrarily and note that for $\varepsilon_{0,i}$ as in (5.62) the Steps 3a-e in the proof of Theorem 4.13 (see p. 159ff.) go through without changes (using $\gamma_0 = 1$). Hence the claim of Step 4 holds true.

Step 5: For all $i \in \{1,\dots,n\}$ it is shown that $|\dot{e}_i(\cdot)|$ is uniformly bounded away from the boundary $\psi_{1,i}(\cdot)$; more precisely for positive

$$\varepsilon_{1,i} \leq \min\left\{\frac{\lambda_{1,i}}{2},\ \psi_{1,i}(0) - |\dot{e}_i(0)|,\ \frac{\frac{1}{2}\underline{\varsigma}_{0,i}\underline{\varsigma}_{1,i}\lambda_{1,i}\varepsilon_{0,i}^2}{\|\psi_{0,i}\|_\infty(M+\|\dot{\psi}_{1,i}\|_\infty)\varepsilon_{0,i}^2 + \|\varsigma_{0,i}\|_\infty^2\|\psi_{0,i}\|_\infty^2}\right\}, \tag{5.63}$$

with M as in (5.59) and $\varepsilon_{0,i}$ as in (5.62), it holds that $\psi_{1,i}(t) - |\dot{e}_i(t)| \geq \varepsilon_{1,i}$ for all $i \in \{1,\dots,n\}$ and all $t \in [0,T)$.

Again choose $i \in \{1,\dots,n\}$ arbitrarily and observe that identical arguments as in Step 4 of the proof of Theorem 4.13 (see p. 163ff. and set $\gamma_0 = 1$) show the claim of Step 5.

Step 6: It is shown that Assertions (ii)-(iv) hold true.
For M as in (5.59), $\varepsilon_{0,i}$ as in (5.62) and $\varepsilon_{1,i}$ as in (5.63), $i \in \{1, \dots, n\}$ define

$$\widetilde{\mathfrak{C}} := \left\{ (t, \boldsymbol{\mu}, \boldsymbol{\xi}) \in [0,T] \times \mathbb{R}^{2n} \;\middle|\; \forall\, i \in \{0, \dots, n\} : \; |\mu_i| \leq \psi_{0,i}(t) - \varepsilon_{0,i} \;\wedge\; |\xi_i| \leq \psi_{1,i}(t) - \varepsilon_{1,i} \right\}$$

Let $\mathcal{D}$ be as in Step 2. If $T < \infty$ then $\widetilde{\mathfrak{C}} \subset \mathcal{D}$ and contains the whole graph of the solution $t \mapsto (\boldsymbol{e}(t), \dot{\boldsymbol{e}}(t))$, which contradicts maximality of the solution. Hence $T = \infty$. Assertion (iii) follows from Step 4 and Step 5. Moreover, Step 4 and Step 5 with boundedness of $\boldsymbol{\varsigma}_0(\cdot)$ and $\boldsymbol{\varsigma}_1(\cdot)$ on $\mathbb{R}_{\geq 0}$ imply that $\boldsymbol{K}_0(\cdot)$ and $\boldsymbol{K}_1(\cdot)$ are uniformly bounded on $\mathbb{R}_{\geq 0}$, respectively. Then, from (5.58), (A_1) and (5.51), it follows that $\boldsymbol{u}(\cdot)$ is uniformly bounded on $\mathbb{R}_{\geq 0}$, hence Assertion (iv) is shown. This completes the proof. □

Simulation

For illustration, the MIMO funnel controller (5.51) with derivative feedback is applied to the planar two DOF rigid revolute joint robotic manipulator depicted in Fig. 5.18.

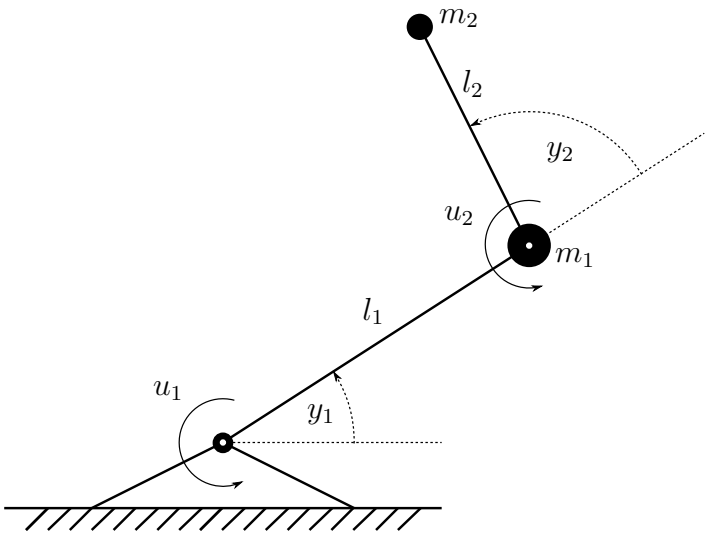

Figure 5.18: *Planar two DOF rigid revolute joint robotic manipulator.*

The planar (elbow-like) robot has two revolute joints actuated by u_1 and u_2 [Nm], respectively. The links are assumed massless and have length l_1 and l_2 [m]. Point masses m_1 and m_2 [kg] are attached to their distal ends, respectively. Control objective is position control of joint angles y_1 and y_2 [rad] with prescribed transient accuracy. The mathematical model of this robot is given by (see e.g. [174, p. 259ff.])

$$\boldsymbol{M}(\boldsymbol{y}(t))\,\ddot{\boldsymbol{y}}(t) + \boldsymbol{C}(\boldsymbol{y}(t), \dot{\boldsymbol{y}}(t))\,\dot{\boldsymbol{y}}(t) + \boldsymbol{g}(\boldsymbol{y}(t)) = \boldsymbol{u}(t), \qquad \big(\boldsymbol{y}(0), \;\; \dot{\boldsymbol{y}}(0)\big) = \big(\boldsymbol{0}, \;\; \boldsymbol{0}\big) \in \mathbb{R}^4 \quad (5.64)$$

	data/parametrization
Matlab solver	`ode45 (Dormand-Prince)` with variable step size (max. 10^{-3} [s])
robot (5.64)	$m_1 = m_2 = 1$ [kg], $l_1 = l_2 = 1$ [m], $g = 9.81$ [m/s^2], $(\boldsymbol{y}(0), \dot{\boldsymbol{y}}(0)) = (\boldsymbol{0}, \boldsymbol{0})$ $\left[\text{rad}, \frac{\text{rad}}{\text{s}}\right]^2$
reference	$(y_{\text{ref},1}(\cdot), y_{\text{ref},2}(\cdot))$ as in top of Fig. 5.19
initial error	$\boldsymbol{e}(0) = (\pi/2, -\pi/4)^\top$ [rad]^2
(MIMO) funnel controller (5.51)	$\boldsymbol{M}(\boldsymbol{y})$ as in (5.65), $(\psi_{0,i}(\cdot), \dot{\psi}_{0,i}(\cdot))$, $i \in \{1,2\}$ as in (4.64) with $(\Lambda_{0,1}, \Lambda_{0,2}) = 5\,\boldsymbol{e}(0)$ [rad]^2, $(\lambda_{0,1}, \lambda_{0,2}) = (\pi/18, \pi/18)$ [rad]^2, $(T_{E,1}, T_{E,2}) = (1.32, 1.63)$ [s]^2, $(\lambda_{1,1}, \lambda_{1,2}) = (\pi, \pi)$ [rad/s]^2, $\boldsymbol{\varsigma}_0(\cdot) = (\psi_{0,1}(\cdot), \psi_{0,2}(\cdot))$, $\boldsymbol{\varsigma}_1(\cdot) = 10\,(\psi_{1,1}(\cdot), \psi_{1,2}(\cdot))$

Table 5.6: *Robot, simulation and controller parameters for simulation.*

with inertia matrix

$$\boldsymbol{M}\colon \mathbb{R}^2 \to \mathbb{R}^{2\times 2},$$
$$\boldsymbol{y} \mapsto \boldsymbol{M}(\boldsymbol{y}) := \begin{bmatrix} m_1 l_1^2 + m_2\,(l_1^2 + l_2^2 + 2 l_1 l_2 \cos(y_2)), & m_2(l_2^2 + l_1 l_2 \cos(y_2)) \\ m_2(l_2^2 + l_1 l_2 \cos(y_2)), & m_2 l_2^2 \end{bmatrix}, \tag{5.65}$$

centrifugal and Coriolis force matrix

$$\boldsymbol{C}\colon \mathbb{R}^2 \times \mathbb{R}^2 \to \mathbb{R}^{2\times 2}, \quad (\boldsymbol{y}, \boldsymbol{v}) \mapsto \boldsymbol{C}(\boldsymbol{y}, \boldsymbol{v}) = \begin{bmatrix} -2 m_2 l_1 l_2 \sin(y_2) v_1, & -m_2 l_1 l_2 \sin(y_2) v_2 \\ -m_2 l_1 l_2 \sin(y_2) v_1, & 0 \end{bmatrix}$$

and gravity vector

$$\boldsymbol{g}\colon \mathbb{R}^2 \to \mathbb{R}^2, \quad \boldsymbol{y} \mapsto \boldsymbol{g}(\boldsymbol{y}) := g \begin{pmatrix} m_1 l_1 \cos(y_1) + m_2(l_1 \cos(y_1) + l_2 \cos(y_1 + y_2)) \\ m_2 l_2 \cos(y_1 + y_2) \end{pmatrix}$$

where $g = 9.81\,[\text{kg}\,\text{m}^2]$ is the (rounded) gravity constant. For simplicity, friction, gears, disturbances and measurement errors (e.g. noise) are neglected. The simulation is performed in Matlab/Simulink. Robot, simulation and controller parameters are collected in Tab. 5.6.

The simulation results for closed-loop system (5.64), (5.51) are shown in Fig. 5.19. The funnel controller (5.51) achieves tracking with prescribed transient accuracy for joint positions $y_1(\cdot)$ & $y_2(\cdot)$ and joint velocities $\dot{y}_1(\cdot)$ & $\dot{y}_2(\cdot)$, respectively. Both joint position errors $e_1(\cdot)$ & $e_2(\cdot)$ and both joint velocity errors $\dot{e}_1(\cdot)$ & $\dot{e}_2(\cdot)$ evolve within the performance funnel. Since gears are not considered in the simulation, the generated motor torques $u_1(\cdot)$ & $u_2(\cdot)$ are seemingly large. In "real world" gears (with ratios $\gg 10$) yield a torque reduction on motor side.

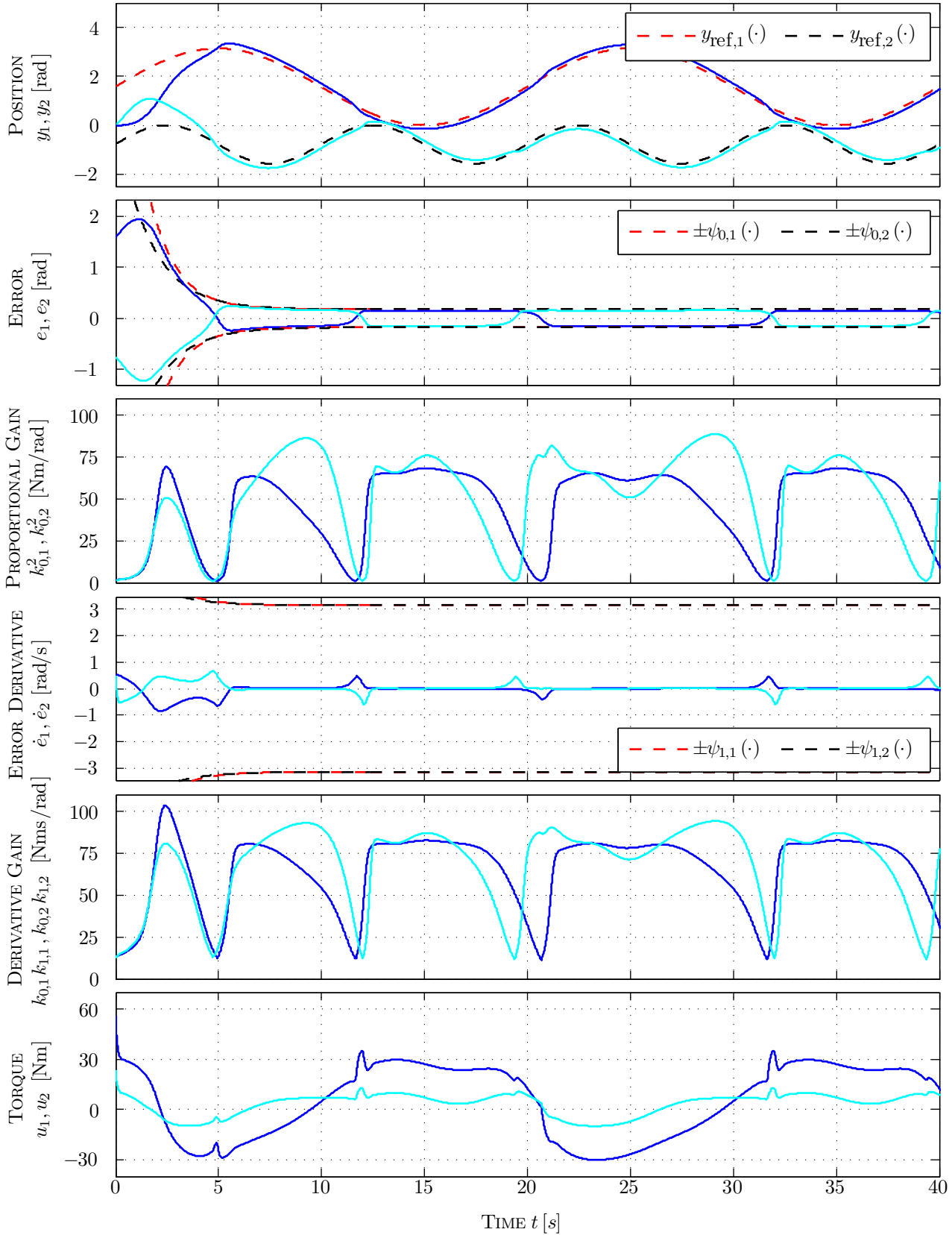

Figure 5.19: *Simulation results for closed-loop system* (5.64), (5.51): —*joint* $i = 1$ *and* —*joint* $i = 2$ *(from top to bottom: position* $y_1(\cdot)$ *&* $y_2(\cdot)$*, position error* $e_1(\cdot)$ *&* $e_2(\cdot)$*, proportional gain* $k_{0,1}(\cdot)^2$ *&* $k_{0,2}(\cdot)^2$*, speed error* $\dot{e}_1(\cdot)$ *&* $\dot{e}_2(\cdot)$*, derivative gain* $k_{0,1}(\cdot)k_{1,1}(\cdot)$ *&* $k_{0,2}(\cdot)k_{1,2}(\cdot)$ *and torque* $u_1(\cdot)$ *&* $u_2(\cdot)$*).*

Chapter 6

Conclusion and outlook

High-gain adaptive control and its possible applications in mechatronics—i.e. speed and position control—have been discussed. More precisely, starting with "classical" high-gain adaptive control for linear time-invariant (LTI) single-input single-output (SISO) systems, adaptive λ-tracking control and funnel control have been revisited and developed, in a general framework, for SISO systems with

(i) relative degree one (for speed control) *or* relative degree two (for position control),

(ii) known sign of the high-frequency gain,

(iii) bounded disturbances and state-dependent, functional perturbations and

(iv) stable zero-dynamics (the unperturbed system is minimum-phase).

Moreover, it is assumed that (v) the systems with relative degree one allow for feedback of the regulated output (the variable to be controlled is measured and hence available for feedback), whereas the systems with relative degree two allow for feedback of the regulated output *and* its derivative. In particular for position control, derivative feedback is justified. The presented high-gain adaptive controllers are "simple" (in the sense of non-complex and of low order). Especially for the relative degree two case, since the developed high-gain adaptive controllers incorporate derivative feedback, they are (much) simpler than the available high-gain adaptive controllers in literature.

For controller implementation, only the "structural system properties" (i)-(v) must be satisfied. Therefore, the presented adaptive λ-tracking controllers and funnel controllers are inherently robust (e.g. to parameter uncertainties not affecting the "system properties") and, consequently, attractive for industrial application. Moreover, due to their non-complex structure and since design parameters have distinct and easy to understand influence on the closed-loop control performance, the controllers are easy to implement (in any process automation software providing standard building blocks for e.g. integration, summation, multiplication, etc.) and easy to tune. Furthermore,

- the adaptive λ-tracking controllers guarantee *tracking with prescribed asymptotic accuracy* (see Theorem 3.3 for the relative degree one case and Theorem 3.13 for the relative degree two case), i.e. for prescribed $\lambda > 0$ the tracking error (the difference between reference signal and measured output) approaches the interval $[-\lambda, \lambda]$ asymptotically;

- the funnel controllers assure *tracking with prescribed transient accuracy* (see Theorem 4.4 for the relative degree one case and Theorem 4.13 for the relative degree two case), i.e. the absolute value of the tracking error is bounded by a prescribed positive (possibly non-increasing) function of time (i.e. the funnel boundary). Moreover, the funnel controllers are feasible in the presence of (actuator) saturation, if a feasibility condition is satisfied (see Theorem 4.7 for the relative degree one case and Theorem 4.15 for the relative degree two case);

- in conjunction with a proportional-integral internal model (similar to a PI controller), the "proportional" and "memoryless" (i.e. without integral control action) high-gain adaptive controllers achieve steady state accuracy (i.e. the tracking error vanishes asymptotically) if steady state is reached (see Corollary 5.2).

Concerning application, the developed adaptive λ-tracking controllers and funnel controllers have been proposed for speed and position control of industrial servo-systems. In addition, as a "side product" of the development of funnel control with derivative feedback for systems with relative degree two, a first result for position funnel control of rigid revolute joint robotic manipulators (with known inertia matrix) has been established (see Theorem 5.18). The considered mechatronic systems are subject to unknown (but bounded) disturbances (e.g. load torques, measurement noise, etc.) and nonlinear friction (on motor and load side). Friction is modeled by unbounded viscous friction and by a bounded, causal friction operator (covering dynamic friction effects such as presliding displacement or frictional memory) motivated by the well known LuGre friction model. To allow for application of the high-gain adaptive controllers in "real world", the mechatronic systems must "solely" satisfy "system properties" (i)-(v). System identification or parameter estimation is not required. For the considered mechatronic systems, it has been shown that "system properties" (i)-(v) hold under mild presuppositions and if actuator saturation is negligible (see Propositions 5.5, 5.6, 5.10 and 5.11). The "system properties" may be checked by invoking rough system knowledge only (using upper or lower bounds on system parameters). In the majority of cases, already the signs of the system parameters (such as inertia or gear ratio, etc.) are sufficient for an affirmative verification. By physical means, these signs either are known to the control designer or can be determined easily.

The proposed adaptive λ-tracking controllers and funnel controllers have been implemented at the laboratory setup for speed and position control of a stiff one-mass system (1MS) and a flexible two-mass system (2MS). For speed and position funnel control with saturation, the feasibility conditions yield (very) conservative and unrealistic bounds on the required drive torque. Nevertheless, as measurement results show, application is reasonable even if the feasibility condition is violated. To allow for steady state accuracy, the high-gain adaptive controllers have also been implemented in conjunction with a proportional-integral internal model. In particular for speed and position control of the 1MS, the measurement results confirm that the adaptive λ-tracking controllers and the funnel controllers (without and with internal model) guarantee speed and position tracking with prescribed asymptotic accuracy and with prescribed transient accuracy, respectively. High-gain adaptive speed control and high-gain adaptive position control of the flexible 2MS are slightly more involved. Besides reference tracking and disturbance rejection, the controllers must also assure damping of shaft oscillations. Therefore, the high-gain adaptive controllers are supplemented by dynamic feedback (i.e. a high-pass filter for angle of twist) which allows to suppress oscillations. Moreover, to assure the "structural system prop-

erties" (i)-(v) and so applicability of the adaptive controllers, an augmented output (i.e. a linear combination of motor *and* load quantities) must be introduced (see Proposition 5.7 for speed control and Proposition 5.13 for position control). As a consequence, the adaptive λ-tracking controllers and the funnel controllers "solely" achieve tracking with prescribed asymptotic accuracy and with prescribed transient accuracy for the *augmented* output, respectively. Hence, load speed or load position does not necessarily evolve within the prescribed region. This is only assured if steady state is attained.

The experimental results at the laboratory setup verify that the control performance of the high-gain adaptive controllers *with* internal model can keep up with the control performance of PI and PID controllers (without anti-windup), respectively, for speed and position control of stiff servo-systems. Especially the funnel controllers allow to include costumer specifications—such as maximum rise time, maximum settling time and maximum overshoot—into controller design by adequate "shaping" of the funnel boundary. Hence implementation effort is reduced. Also for flexible servo-systems, the experimental results underpin industrial applicability of the high-gain adaptive controllers for speed and position control. Active damping of shaft oscillations is feasible by adequate feedback and filter design.

Due to a dynamic and monotone gain adaption, the adaptive λ-tracking controllers generate non-decreasing controller gains and, at first sight, seem to be inadequate for real implementation in contrast to the funnel controllers which, due to a time-varying gain adaption (inversely proportional to the distance between funnel boundary and absolute value of the error), also allow for gain decrease. In fact, measurement results show that adaptive λ-tracking speed and position control is reasonable and may even yield better control performance than funnel control. From a practical point of view, in order to avoid permanently too large gains, gain adaption of the adaptive λ-tracking controllers may be stopped as soon as control performance (evaluated by e.g. the ITAE criterion) is satisfactory. The presented measurement results also show that speed funnel control under load *without* proportional-integral internal model may fail, if boundary design is too demanding and speed measurement is too noisy. Due to (temporarily) too large gains and limited sampling rate in the real-time system, noise sensitivity (amplification) may be too high to keep the tracking error within the prescribed region. As a consequence, funnel control should preferably be implemented *with* (proportional-integral) internal model.

To summarize: it has been shown that high-gain adaptive speed control and high-gain adaptive position control of mechatronics systems are admissible and, in conjunction with an internal model, achieve a very acceptable control performance. Consequently, high-gain adaptive motion control may be considered as a simple, robust and promising alternative to standard motion control in industry. However, some issues are still to be examined. Future research should include the following:

- consideration of gear backlash and gear dynamics (as starting point see e.g. [139]);
- improvement of the feasibility condition(s) for funnel control with saturation (e.g. evaluation of time-varying feasibility condition(s), as starting point see [121]);
- derivation of feasibility condition(s) for adaptive λ-tracking control with saturation (as starting point see e.g. [61, 100]);

- analysis of the effect(s) of windup caused by high-gain adaptive controllers with proportional-integral internal model applied to systems with (actuator) saturation (as starting point see e.g. [166, Section 5.6]);
- extension of position funnel control to rigid revolute joint robotic manipulators *without* known inertia matrix and, eventually, to flexible revolute joint robotic manipulators (as starting point see e.g. [152]) and
- theoretical analysis of discrete time implementation of high-gain adaptive controllers on sampled data systems (as starting point see e.g. [97]).

Appendix

A Abbreviations

Abbreviation	Meaning
1MS	one-mass system (servo-drive with stiff coupling)
2MS	two-mass system (servo-drive with elastic coupling)
AC	alternating current
BIF	Byrnes-Isidori form
CCF	controllable canonical form
DC	direct current
DOF	degrees of freedom
DTC	direct torque control (of induction motors)
FOC	field oriented control (of induction motors)
IM	induction motor (or machine)
ITAE	integral time(-weighted) absolute error criterion with value $x_{ITAE}(t_0, T) := \int_{t_0}^{T} \tau \cdot \lvert e(\tau) \rvert \, \mathrm{d}\tau \,, \quad 0 \leq t_0 \leq T,\ e(\cdot) \in \mathcal{L}^{\infty}(\mathbb{R}_{\geq 0}; \mathbb{R})$
LTI	linear time-invariant (system)
MIMO	multiple-input multiple-output (system)
MPDTC	model predictive direct torque control (of induction motors)
ODE	ordinary differential equation
PMSM	permanent magnetic synchronous motor (or machine)
PWM	pulse width modulation
RMS	root mean square (quadratic mean) of signal $x(\cdot) \in \mathcal{L}^{\infty}(\mathbb{R}_{\geq 0}; \mathbb{R})$ $x_{RMS}(t_0, T) := \sqrt{\frac{1}{T} \int_{t_0}^{t_0+T} x(\tau)^2 \, \mathrm{d}\tau} \,, \qquad 0 \leq t_0 \leq T$
SISO	single-input single-output (system)

B Two simple operators of class $\mathcal{T}$

Two examples of operator class $\mathcal{T}$ are presented and operator properties (op_1)-(op_3) are checked.

Example B.1 ("Static nonlinearity").
In the simplest case the operator class $\mathcal{T}$ may describe any (possibly nonlinear) locally Lipschitz continuous function $\boldsymbol{g}(\cdot)\colon \mathbb{R}^n \to \mathbb{R}^m$, $n, m \in \mathbb{N}$. Note that due to the locally Lipschitz condition, the following holds: for any compact $\mathfrak{C}_g \subset \mathbb{R}^n$ there exists $L_g \geq 0$ such that $\|\boldsymbol{g}(\boldsymbol{v}) - \boldsymbol{g}(\boldsymbol{w})\| \leq L_g \, \|\boldsymbol{v} - \boldsymbol{w}\|$ for all $\boldsymbol{v}, \boldsymbol{w} \in \mathfrak{C}_g$. Now define the operator

$$\mathfrak{T}_{SN}\colon \ \mathcal{C}(\mathbb{R}_{\geq 0}; \mathbb{R}^n) \to \mathcal{L}^\infty_{\mathrm{loc}}(\mathbb{R}_{\geq 0}; \mathbb{R}^m), \qquad \boldsymbol{x}(\cdot) \mapsto (\mathfrak{T}_{SN}\boldsymbol{x})(\cdot) := \boldsymbol{g}(\boldsymbol{x}(\cdot)).$$

It is shown that $\mathfrak{T}_{SN}$ is element of operator class $\mathcal{T}$: It is easy to see that properties (op_1) and $(op_3)(a)$ trivially hold. Next, choose $\delta > 0$ and $\boldsymbol{x}(\cdot) \in \mathcal{C}(\mathbb{R}_{\geq 0}; \mathbb{R}^n)$ with $\sup_{t \geq 0} \|\boldsymbol{x}(t)\| < \delta$, then $\|(\mathfrak{T}_{SN}\boldsymbol{x})(t)\| = \|\boldsymbol{g}(\boldsymbol{x}(t))\| < \sup_{\boldsymbol{w} \in \mathbb{B}_\delta(\boldsymbol{0})} \|\boldsymbol{g}(\boldsymbol{w})\| =: \Delta < \infty$ for all $t \geq 0$. Hence property (op_2) also holds. Now, for any $t \geq 0$, fix $\boldsymbol{\beta}(\cdot) \in \mathcal{C}([0, t]; \mathbb{R}^n)$ and $\tau, \delta > 0$ arbitrarily and define $M := \max_{s \in [0,\, t]} \|\boldsymbol{\beta}(s)\| + \delta$. Then, for all $\boldsymbol{x}_1(\cdot), \boldsymbol{x}_2(\cdot) \in \mathcal{C}(\mathbb{R}_{\geq 0}; \mathbb{R}^n)$ with $\boldsymbol{x}_1(\cdot)|_{[0,t]} = \boldsymbol{x}_2(\cdot)|_{[0,t]} = \boldsymbol{\beta}(\cdot)$ and $\boldsymbol{x}_1(s), \boldsymbol{x}_2(s) \in \mathbb{B}_\delta(\boldsymbol{\beta}(t))$ for all $s \in [t, t + \tau]$, the following holds $\boldsymbol{x}_1(s), \boldsymbol{x}_2(s) \in \overline{\mathbb{B}}_M(\boldsymbol{0}) \subset \mathbb{R}^n$ for all $s \in [t, t + \tau]$. Note that $\overline{\mathbb{B}}_M(\boldsymbol{0})$ is compact and therefore there exists $L_{\overline{\mathbb{B}}_M} > 0$ such that $\|(\mathfrak{T}_{SN}\boldsymbol{x}_1)(s) - (\mathfrak{T}_{SN}\boldsymbol{x}_2)(s)\| \leq L_{\overline{\mathbb{B}}_M} \, \|\boldsymbol{x}_1(s) - \boldsymbol{x}_2(s)\|$ for all $s \in [t, t + \tau]$, which shows property $(op_3)(b)$. Hence, $\mathfrak{T}_{SN} \in \mathcal{T}$.

Example B.2 (Linear time-invariant single-input single-output systems).
For $n \in \mathbb{N}$ consider the linear dynamical system given by

$$\begin{array}{rcll} \dot{\boldsymbol{x}}(t) & = & \boldsymbol{A}\boldsymbol{x}(t) + \boldsymbol{b}\, u(t), & \boldsymbol{x}(0) = \boldsymbol{x}^0 \in \mathbb{R}^n, \ (\boldsymbol{A}, \boldsymbol{b}, \boldsymbol{c}, d) \in \mathbb{R}^{n \times n} \times \mathbb{R}^n \times \mathbb{R}^n \times \mathbb{R} \\ y(t) & = & \boldsymbol{c}^\top \boldsymbol{x}(t) + d\, u(t), & u(\cdot) \in \mathcal{C}(\mathbb{R}_{\geq 0}; \mathbb{R}), \ \mathrm{spec}(\boldsymbol{A}) \subset \mathbb{C}_{<0}. \end{array} \tag{B.1}$$

Variation-of-Constants yields

$$\forall\, t \geq 0\colon \qquad \boldsymbol{x}(t) = \exp(\boldsymbol{A}t)\boldsymbol{x}^0 + \int_0^t \exp(\boldsymbol{A}(t - \tau))\, \boldsymbol{b}\, u(\tau)\, \mathrm{d}\tau$$

and $\mathrm{spec}(\boldsymbol{A}) \subset \mathbb{C}_{<0}$ implies that there exist $\lambda_{\boldsymbol{A}} > 0$ and $M_{\boldsymbol{A}} \geq 1$ (see e.g. [77, Lemma 3.3.19, p. 263]), such that

$$\forall\, t \geq 0\colon \qquad \|\exp(\boldsymbol{A}t)\| \leq M_{\boldsymbol{A}} \exp(-\lambda_{\boldsymbol{A}} t). \tag{B.2}$$

Define the operator

$$\mathfrak{T}_L\colon \mathcal{C}(\mathbb{R}_{\geq 0}; \mathbb{R}) \to \mathcal{L}^\infty_{\mathrm{loc}}(\mathbb{R}_{\geq 0}; \mathbb{R}^n), \quad (\mathfrak{T}_L u)(t) := \boldsymbol{c}^\top \int_0^t \exp(\boldsymbol{A}(t - \tau))\, \boldsymbol{b}\, u(\tau)\, \mathrm{d}\tau \ + d\, u(t).$$

Note that the operator $\mathfrak{T}_L$ is linear and taking norms and invoking (B.2) yields

$$\forall\, t \geq 0\colon \quad \|(\mathfrak{T}_L u)(t)\| \leq M_{\boldsymbol{A}} \ \|\boldsymbol{c}\| \ \|\boldsymbol{b}\| \int_0^t \exp(-\lambda_{\boldsymbol{A}}(t - \tau))|u(\tau)|\, \mathrm{d}\tau \ + |d| \, |u(t)|. \tag{B.3}$$

It is shown that $\mathfrak{T}_L \in \mathcal{T}$. Set $h = 0$. It is easy to see that Properties (op_1) and $(op_3)(a)$ hold. Furthermore, for all $u(\cdot) \in \mathcal{C}(\mathbb{R}_{\geq 0}; \mathbb{R})$ with $|u(\cdot)| < \delta$ on $\mathbb{R}_{\geq 0}$, the following holds $\|(\mathfrak{T}_L u)(t)\| \leq$

$(M_{\boldsymbol{A}}\,\|\boldsymbol{c}\|\,\|\boldsymbol{b}\|\,/\lambda_{\boldsymbol{A}}+|d|)\,\delta =: \Delta$ *for all* $t \geq 0$ *and hence Property* (op_2) *also holds. Now for* $\tau > 0$ *and* $u_1(\cdot), u_2(\cdot) \in \mathcal{C}(\mathbb{R}_{\geq 0};\mathbb{R})$ *with* $u_1(\cdot) = u_2(\cdot)$ *on* $[0,t]$*, one obtains*

$$\begin{aligned}
&\sup_{s\in[t,\,t+\tau]} \|(\mathfrak{T}_L u_1)(s) - (\mathfrak{T}_L u_2)(s)\| \\
&\qquad \leq \|\boldsymbol{c}\| \sup_{s\in[t,\,t+\tau]} \Big\| \exp(\boldsymbol{A}s)\Big(\int_0^t \exp(-\boldsymbol{A}\alpha)\,\boldsymbol{b}\,\underbrace{(u_1(\alpha)-u_2(\alpha))}_{=0 \text{ on } [0,t]}\,\mathrm{d}\alpha \\
&\qquad\quad + \int_t^s \exp(-\boldsymbol{A}\alpha)\,\boldsymbol{b}\,(u_1(\alpha)-u_2(\alpha))\,\mathrm{d}\alpha\Big)\Big\| + |d| \sup_{s\in[t,\,t+\tau]} |u_1(s)-u_2(s)| \\
&\qquad\qquad \leq \underbrace{\max\left\{\frac{M_{\boldsymbol{A}}}{\lambda_{\boldsymbol{A}}}\,\|\boldsymbol{c}\|\,\|\boldsymbol{b}\|\,,|d|\right\}}_{=:c_0} \sup_{s\in[t,\,t+\tau]} |u_1(s)-u_2(s)|,
\end{aligned}$$

which shows that Property $(op_3)(b)$ *is also satisfied. Hence* $\mathfrak{T}_L$ *is of class* $\mathcal{T}$ *and systems of the form* (B.1) *may be expressed in the compact form*

$$y(t) = \boldsymbol{c}^\top \exp(\boldsymbol{A}t)\boldsymbol{x}^0 + (\mathfrak{T}_L u)(t), \qquad \begin{array}{l}(\boldsymbol{A},\boldsymbol{c}) \in \mathbb{R}^{n\times n}\times\mathbb{R}^n,\ \mathrm{spec}(\boldsymbol{A}) \subset \mathbb{C}_{<0},\ \boldsymbol{x}_0 \in \mathbb{R}^n,\\ h = 0,\ \mathfrak{T}_L \in \mathcal{T} \text{ and } u(\cdot) \in \mathcal{C}(\mathbb{R}_{\geq 0};\mathbb{R}).\end{array}$$

C Root locus center of LTI SISO systems in state space

For the following let a LTI SISO system be given by the ODE

$$\begin{array}{rcll} \dot{\boldsymbol{x}}(t) & = & \boldsymbol{A}\,\boldsymbol{x}(t) + \boldsymbol{b}\,u(t), & \tilde{n} \in \mathbb{N},\ \boldsymbol{x}(0) = \boldsymbol{x}_0 \in \mathbb{R}^{\tilde{n}}, \\ y(t) & = & \boldsymbol{c}^\top \boldsymbol{x}(t) & (\boldsymbol{A}, \boldsymbol{b}, \boldsymbol{c}) \in \mathbb{R}^{\tilde{n}\times\tilde{n}} \times \mathbb{R}^{\tilde{n}} \times \mathbb{R}^{\tilde{n}} \end{array} \tag{C.4}$$

or by the transfer function (with coprime numerator and denominator)

$$F(s) = \frac{y(s)}{u(s)} = \gamma_0 \frac{c_0 + c_1 s + \cdots + c_{m-1} s^{m-1} + s^m}{a_0 + a_1 s + \cdots + a_{n-1} s^{n-1} + s^n}\ , \qquad \begin{array}{l} n,\ m \in \mathbb{N},\ n > m,\ \gamma_0 \neq 0 \\ c_0, \ldots, c_{m-1} \in \mathbb{R}, \\ a_0, \ldots, a_{n-1} \in \mathbb{R}. \end{array} \tag{C.5}$$

Definition C.3 (Root locus center of LTI SISO systems in state space)**.**
Consider a system of form (C.4) *with known relative degree* $1 \leq r \leq \tilde{n}$*. Then*

$$\Xi(\boldsymbol{A}, \boldsymbol{b}, \boldsymbol{c}) := \frac{1}{r} \frac{\boldsymbol{c}^\top \boldsymbol{A}^r \boldsymbol{b}}{\boldsymbol{c}^\top \boldsymbol{A}^{r-1} \boldsymbol{b}} \tag{C.6}$$

is called the root locus center of (C.4)*.*

The root locus center of a transfer function (C.5) and the root locus center of its minimal realization (C.4) are related.

Lemma C.4. *Denote the root locus center of* (C.4) *and* (C.5) *by* Ξ_{SS} *and* Ξ_{TF}*, respectively. If* (C.4) *is a minimal realization of* (C.5)*, then* $\Xi_{SS} = \Xi_{TF}$*.*

Proof of Lemma C.4.
Denote the relative degree of (C.5) by $r = n - m > 0$. From Lemma 2.2 it follows that relative degree of (minimal) realization (C.4) and transfer function (C.5) are equal. Since (C.4) is a minimal realization of (C.5), $(\boldsymbol{A}, \boldsymbol{b})$ is controllable and $\tilde{n} = n$. Hence, there exists $\boldsymbol{T} \colon \mathbb{R}^n \to \mathbb{R}^n$, $\boldsymbol{x} \mapsto \boldsymbol{x}_C := \boldsymbol{T}\boldsymbol{x}$ which converts (C.4) into controllable canonical form (see [24, p. 822-823])

$$\begin{array}{rcll} \dot{\boldsymbol{x}}_C(t) & = & \boldsymbol{A}_C\,\boldsymbol{x}_C(t) + \boldsymbol{b}_C\,u(t), & \boldsymbol{x}_C(0) = \boldsymbol{T}\boldsymbol{x}_0 \in \mathbb{R}^n, \\ y(t) & = & \boldsymbol{c}_C^\top \boldsymbol{x}_C(t) & \end{array}$$

where

$$\boldsymbol{A}_C = \boldsymbol{T}\boldsymbol{A}\boldsymbol{T}^{-1} = \begin{bmatrix} 0 & 1 & 0 & \ldots & 0 \\ \vdots & \ddots & \ddots & \ddots & \vdots \\ \vdots & & \ddots & \ddots & 0 \\ 0 & \ldots & \ldots & 0 & 1 \\ -\alpha_0 & -\alpha_1 & \ldots & -\alpha_{n-2} & -\alpha_{n-1} \end{bmatrix} \in \mathbb{R}^{n\times n}, \qquad \boldsymbol{b}_C = \boldsymbol{T}\boldsymbol{b} = \begin{pmatrix} 0 \\ \vdots \\ 0 \\ 1 \end{pmatrix} \in \mathbb{R}^n$$

$$\text{and} \quad \boldsymbol{c}_C^\top = \boldsymbol{c}^\top \boldsymbol{T}^{-1} = \begin{pmatrix} \beta_0, & \ldots, & \beta_{n-1} \end{pmatrix} \in \mathbb{R}^n. \tag{C.7}$$

Moreover, by comparing coefficients of numerator and denominator in

$$F(s) = \boldsymbol{c}^\top (s\,\boldsymbol{I}_n - \boldsymbol{A})^{-1} \boldsymbol{b} = \boldsymbol{c}_C^\top (s\,\boldsymbol{I}_n - \boldsymbol{A}_C)^{-1} \boldsymbol{b}_C = \frac{\beta_0 + \beta_1\, s + \cdots + \beta_{n-1}\, s^{n-1}}{\alpha_0 + \alpha_1\, s + \cdots + \alpha_{n-1}\, s^{n-1} + s^n}$$

it follows that

$$\begin{aligned} &\forall\, i \in \{0,\dots,n-1\}\colon \quad \alpha_i = a_i, \quad \forall\, i \in \{0,\dots,m-1\}\colon \quad \beta_i = \gamma_0\, c_i, \\ &\beta_m = \gamma_0 \quad \text{and} \quad \forall j \in \{m+1,\dots,n-1\}\colon \quad \beta_j = 0. \end{aligned} \tag{C.8}$$

In view of (C.7), (C.8) and $r = n - m$, the following hold

$$\forall\, i \in \{0,\dots,r-1\}\colon \quad \boldsymbol{c}_C^\top \boldsymbol{A}_C^i = (\boldsymbol{0}_i^\top, \underbrace{\beta_0, \dots, \beta_{m-1}}_{\in \mathbb{R}^{1\times m}}, \underbrace{\beta_m, 0, \dots, 0}_{\in \mathbb{R}^{1\times (r-i)}}) \in \mathbb{R}^{1\times n} \tag{C.9}$$

and

$$\boldsymbol{A}_C \boldsymbol{b}_C = \begin{pmatrix} \boldsymbol{0}_{n-2}^\top, & 1, & -\alpha_{n-1} \end{pmatrix}^\top \in \mathbb{R}^n. \tag{C.10}$$

Hence

$$\begin{aligned} \boldsymbol{c}^\top \boldsymbol{A}^r \boldsymbol{b} &\overset{(2.11)}{=} \boldsymbol{c}_C^\top \boldsymbol{A}_C^r \boldsymbol{b}_C = \boldsymbol{c}_C^\top \boldsymbol{A}_C^{r-1} \boldsymbol{A}_C \boldsymbol{b}_C = \\ &\overset{(C.9)(C.10)}{=} \begin{pmatrix} \boldsymbol{0}_{r-1}^\top, & \underbrace{\beta_0, \dots, \beta_{m-1}}_{\in \mathbb{R}^m}, & \beta_m \end{pmatrix} \begin{pmatrix} \boldsymbol{0}_{n-2} \\ 1 \\ -\alpha_{n-1} \end{pmatrix} = \beta_{m-1} - \beta_m \alpha_{n-1} \overset{(C.8)}{=} \gamma_0 (c_{m-1} - a_{n-1}) \end{aligned}$$

and

$$\begin{aligned} \boldsymbol{c}^\top \boldsymbol{A}^{r-1} \boldsymbol{b} &\overset{(2.11)}{=} \boldsymbol{c}_C^\top \boldsymbol{A}_C^{r-1} \boldsymbol{b}_C = \boldsymbol{c}_C^\top \boldsymbol{A}_C^{r-2} \boldsymbol{A}_C \boldsymbol{b}_C \\ &\overset{(C.9)(C.10)}{=} \begin{pmatrix} \boldsymbol{0}_{r-2}^\top, & \underbrace{\beta_0, \dots, \beta_{m-1}}_{\in \mathbb{R}^m}, & \beta_m, & 0 \end{pmatrix} \begin{pmatrix} \boldsymbol{0}_{n-2} \\ 1 \\ -\alpha_{n-1} \end{pmatrix} \overset{(C.8)}{=} \gamma_0. \end{aligned}$$

Combining the results above, recalling $r = n - m$ and evaluating (C.6) yields

$$\Xi_{SS} = \frac{1}{r} \frac{\boldsymbol{c}^\top \boldsymbol{A}^r \boldsymbol{b}}{\boldsymbol{c}^\top \boldsymbol{A}^{r-1} \boldsymbol{b}} = \frac{1}{n-m} (c_{m-1} - a_{n-1}) = \Xi_{TF},$$

which completes the proof. □

D Technical data of laboratory setup

The electrical block diagram of the laboratory setup is depicted in Fig. D.1. The three-phase mains-operated power supply with alternating current (AC) is rectified by a converter and balanced by an intermediate circuit capacitor for each permanent magnetic synchronous machine (PMSM). The intermediate circuits of both machines are connected in parallel. The intermediate circuit voltage u_0 (DC link) allows for pulse width modulation (PWM) in each power inverter. The machines are fed by variable currents (with appropriate frequency and amplitude) required for torque generation. In regenerative mode (braking) the stored kinetic energy of the setup is fed back to the intermediate circuit. If necessary, excessive energy is dissipated in the braking module (resistor) to avoid over-voltages in the DC link. Technical data of the laboratory setup is collected in Tab. D.2.

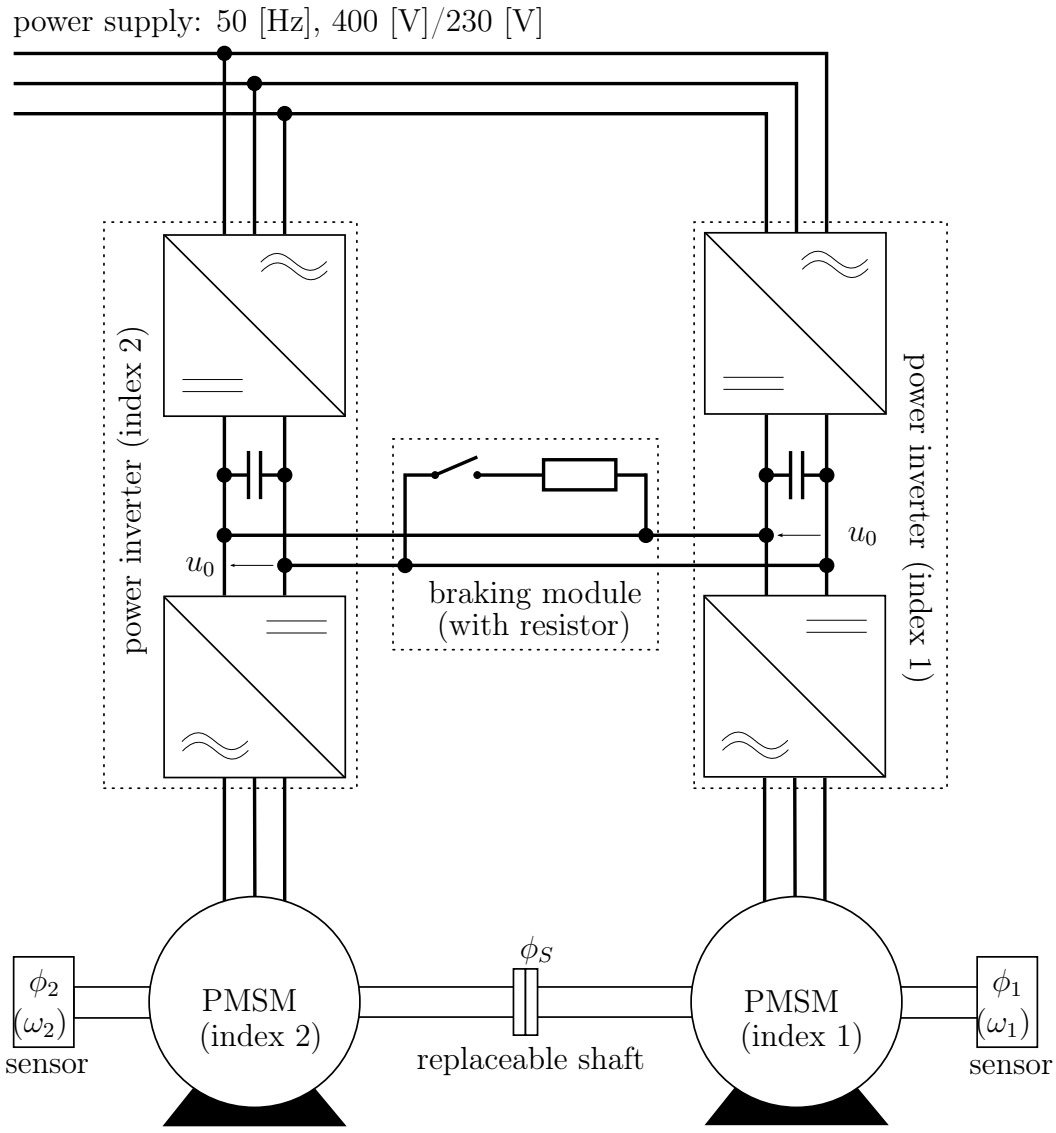

Figure D.1: *Electrical block diagram of laboratory setup.*

Description	Symbol & Value	Dimension
Machines: *SIEMENS "Brushless Servomotor" 1FT6086-8AC71-1CD3*		
Nominal speed	$n_N = 2000\ \left[\frac{1}{\text{min}}\right]$, $\omega_N = 209.44\ \left[\frac{\text{rad}}{\text{s}}\right]$	$\left[\frac{1}{\text{min}}\right] = \frac{60}{2\pi}\ \left[\frac{\text{rad}}{\text{s}}\right]$
Nominal torque	$m_N = 22.0$	[Nm]
Nominal current	$i_N = 10.9$	[A]
Nominal motor power	$P_N = 4.8$	[kW] $= 10^3$ [W]
Rotor inertia	$\Theta_{Rotor} = 6.65 \cdot 10^{-3}$	[kg m^2]
Inverters: *SIEMENS Simovert MasterDrive SC 6SE7022-6EC30*		
Mains voltage (3-phase, AC)	$u_{AC}^{RMS} = 380 \ldots 460\ (\pm 15\%)$	[V]
Voltage link (DC)	$u_0 = 510 \ldots 620\ (\pm 15\%)$	[V]
Output voltage (3-phase AC)	$u_{out}^{RMS} = 0 \ldots 0.86 \cdot u_{AC}^{RMS}$	[V]
Mains frequency	$f_n = 50/60\ (\pm 15\%)$	[Hz] $= \left[\frac{1}{\text{s}}\right]$
Output frequency	$f_{out} = 0 \ldots 600$	[Hz] $= \left[\frac{1}{\text{s}}\right]$
Pulse frequency	$f_p = 5 \ldots 7,5$	[kHz] $= 10^3$ [Hz]
Output nominal current	$i_N^{RMS} = 25.5$	[A]
Base load current	$i_{BL}^{RMS} = 23.2$	[A]
Short-time current	$i_{max}^{RMS} = 40.8$	[A]
Dissipation loss	$P_{loss} = 0.43$ (at 5 [Hz])	[kW] $= 10^3$ [W]
Efficiency factor	$\eta = 96 \ldots 98\%$	[1]
Encoders: *HEIDENHAIN RON 3350 Sinusoidal 2048*		
Lines (per revolution)	$l_r = 2048$	[1]
Interpolation	12 bit ($2^{12} = 4096$)	–
Sinusoidal output voltage	$u_{pp} = 1$	[V]
Different inertia wheels		
Small inertia wheel	$\Theta_{sw} = 8.93 \cdot 10^{-5}$	[kg m^2]
Medium inertia wheel	$\Theta_{mw} = 1.3 \cdot 10^{-3}$	[kg m^2]
Large inertia wheel	$\Theta_{lw} = 77.2 \cdot 10^{-3}$	[kg m^2]
Drive 1 axle inertia	$\Theta_{ai1} = 2.4 \cdot 10^{-3}$	[kg m^2]
Drive 2 axle inertia	$\Theta_{ai2} = 9.1 \cdot 10^{-3}$	[kg m^2]

Table D.2: *Technical data of machines, inverters, encoders and inertia wheels.*

Bibliography

[1] M. Aberger and M. Otter. Modeling friction in Modelica with the Lund-Grenoble friction model. In *Proceedings of the 2nd International Modelica Conference*, pages 285–294, Oberpfaffenhofen, Germany, 2002.

[2] F. Allgöwer, J. Ashman, and A. Ilchmann. High-gain adaptive λ-tracking for nonlinear systems. *Automatica*, 33(5):881–888, 1997.

[3] F. Altpeter. *Friction Modeling, Identification and Compensation*. Dissertation, École Polytechnique Fédérale de Lausanne, Switzerland, 1999.

[4] H. Amann and J. Escher. *Analysis I*. Birkhäuser Verlag, Basel Boston Stuttgart, 1998.

[5] H. Amann and J. Escher. *Analysis II*. Birkhäuser Verlag, Basel Boston Stuttgart, 1999.

[6] H. Amann and J. Escher. *Analysis III*. Birkhäuser Verlag, Basel Boston Stuttgart, 2001.

[7] B. Angerer, C. Hintz, and D. Schröder. Online identification of a nonlinear mechatronic system. *Control Engineering Practice*, 12(11):1465–1478, 2004.

[8] B. Armstrong-Helouvry. Stick-slip arising from Stribeck friction. In *Proceedings of the IEEE International Conference on Robotics and Automation*, volume 2, pages 1377–1382, Cincinnati, Ohio, USA, 1990.

[9] B. Armstrong-Hélouvry. *Control of Machines with Friction*. Kuwer Academic Publishers, Boston, 1991.

[10] B. Armstrong-Hélouvry, P. Dupont, and C. C. De Wit. A survey of models, analysis tools and compensation methods for the control of machines with friction. *Automatica*, 30(7): 1083–1138, 1994.

[11] J. M. Aseltine and C. Sarture. A survey of adaptive control systems. *IRE Transactions on Automatic Control*, 6(1):102–108, 1958.

[12] K. J. Åström. Theory and applications of adaptive control – a survey. *Automatica*, 19 (5):471–486, 1983.

[13] K. J. Åström. Adaptive control around 1960. *IEEE Control Systems Magazine*, 16(3): 44–49, 1996.

[14] K. J. Åström and B. Wittenmark. On self tuning regulators. *Automatica*, 9(2):185–199, 1973.

[15] K. J. Åström and B. Wittenmark. *Adaptive Control*. Addison-Wesley Publishing Company, Inc., Boston, 2nd edition, 1995.

[16] K. J. Åström and B. Wittenmark. *Adaptive Control*. Dover Publications Inc., Mineola, New York, 2nd (revised and corrected) edition, 2008.

[17] D. M. Auslander. What is mechatronics? *IEEE/ASME Transactions on Mechatronics*, 1(1):5–9, 1996.

[18] D. Bainov and P. Simeonov. *Integral Inequalities and Applications*, volume 57 of *Mathematics and Its Applications (East European Series)*. Kluwer Academic Publishers, Boston, 1992.

[19] N. Barabanov and R. Ortega. Necessary and sufficient conditions for passivity of the LuGre friction model. *IEEE Transaction on Automatic Control*, 45(4):830–832, 2000.

[20] C. Behn. Adaptive λ-tracking-control for relative degree two systems with application to bio-inspired sensors. *Nonlinear Dynamics*, 50(4):817–828, 2007.

[21] S. Bennett. *A History of Control Engineering 1800-1930*. Peter Peregrinus Ltd., London, 1979.

[22] S. Bennett. *A History of Control Engineering 1930-1955*. Number 47 in IEE Control Engineering Series. Peter Peregrinus Ltd., Stevenage, United Kingdom, 1st edition, 1993.

[23] G. Berman and R. Stanton. The asymptotes of the root locus. *SIAM Review*, 5(3): 209–218, 1963.

[24] D. S. Bernstein. *Matrix Mathematics — Theory, Facts, and Formulas with Application to Linear System Theory*. Princeton University Press, Princeton and Oxford, 2nd edition, 2009.

[25] H. S. Black. Stabilized feedback amplifiers. *Bell System Technical Journal*, 13(1):1–18, 1934.

[26] H. W. Bode. Relations between attenuation and phase in feedback amplifier design. *Bell System Technical Journal*, 19(3):421–454, 1940.

[27] S. Bolognani, A. Venturato, and M. Zigliotto. Theoretical and experimental comparison of speed controllers for elastic two-mass-systems. In *Proceedings of the 31th Annual IEEE Power Electronics Specialists Conference*, volume 3, pages 1087–1092, 2000.

[28] B. Bona and M. Indri. Friction compensation in robotics: An overview. In *Proceedings of the 44th IEEE Conference on Decision and Control and the European Control Conference*, pages 4360–4367, Sevilla, Spain, 2005.

[29] D. Bradley. What is mechatronics and why teach it? *International Journal of Electrical Engineering Education*, 41(4):275–291, 2004.

[30] G. Brandenburg and W. Papiernik. Feedforward and feedback strategies applying the principle of input balancing for minimal tracking errors in CNC machine tools. In *Proceedings of 4th International Workshop on Advanced Motion Control*, volume 2, pages 612–618, 1996.

[31] G. Brandenburg and U. Schäfer. Influence and adaptive compensation of simultaneously acting backlash and Coulomb friction in elastic two-mass systems of robots and machine tools. In *Proceedings of the IEEE International Conference on Control and Applications*, pages 407–410, 1989.

[32] G. Brandenburg and U. Schäfer. Influence and compensation of Coulomb friction in industrial pointing and tracking systems. In *Conference Record of the IEEE Industry Applications Society Annual Meeting*, volume 2, pages 1407–1413, 1991.

[33] E. Bullinger. *Adaptive λ-Tracking for Systems with Higher Relative Degree*. Dissertation, Eidgenössische Technische Hochschule (ETH), Zürich, Switzerland, 2000. Diss. ETH No. 13858.

[34] E. Bullinger and F. Allgöwer. Adaptive λ-tracking for nonlinear higher relative degree systems. *Automatica*, 41:1191–1200, 2005.

[35] E. Bullinger, C. Frei, T. Sieber, A. Glattfelder, F. Allgöwer, and A. Zbinden. Adaptive λ-tracking in anesthesia. In E. Carson and E. Salzsieder, editors, *Proceedings of the 4th IFAC Symposium Modelling and Control in Biomedical Systems*, pages 181–186, Oxford, United Kingdom, 2000.

[36] C. I. Byrnes and A. Isidori. A frequency domain philosophy for nonlinear systems, with applications to stabilization and to adaptive control. In *Proceedings of the 23rd IEEE Conference on Decision and Control*, pages 1569–1573, Las Vegas, USA, 1984.

[37] C. I. Byrnes and J. C. Willems. Adaptive stabilization of multivariable linear systems. In *Proceedings of the 23rd Conference on Decision and Control*, pages 1574–1577, Las Vegas, USA, 1984.

[38] J. Cabrera and K. Furuta. Improving the robustness of Nussbaum-type regulators by the use of σ-modification — local results. *Systems & Control Letters*, 12(5):412–429, 1989.

[39] C. Canudas de Wit, H. Olsson, K. Åström, and P. Lischinsky. A new model for control of systems with friction. *IEEE Transactions on Automtic Control*, 40(3):419–425, 1995.

[40] R. Comerford. Mecha...what? *IEEE Spectrum*, 31(8):46–49, 1993.

[41] C. A. d. Coulomb. *Théorie des machines simples, en ayant égard au frottement de leurs parties et à la roideur des cordages*. Paris, nouvelle edition, 1821.

[42] L. Da Vinci. *The Notebooks of Leonardo Da Vinci*, volume 2. Dover Publications, Inc., New York, 1980.

[43] P. Dahl. Measurement of solid friction parameters of ball bearings. In *Proceedings of the 6th Annual Symposium on Incremental Motion, Control Systems and Devices*, pages 49–59, Urbana-Campanga, Illinois, 1977.

[44] R. Dahl. A solid friction model. Technical Report TOR-0158(3107-18-1), Aerospace Corporation, El Segundo, California, 1968.

[45] L. De-Peng. Parameter identification for LuGre friction model using genetic algorithms. In *Proceedings of the 5th International Conference on Machine Learning and Cybernetics*, pages 3419–3422, 2006.

[46] C. A. Desoer and M. Vidyasagar. *Feedback Systems — Input–Output Properties*. Classics in Applied Mathematics. Society for Industrial and Applied Mathematics, Philadelphia, 2009.

[47] R. Drenick and R. Shahbender. Adaptive servomechanisms. *Transactions of the American Institute of Electrical Engineers*, 76:286–297, 1957.

[48] B. Drury. *The Control Techniques, Drives and Controls Handbook*, volume 57 of *IET Power and Energy Series*. The Institution of Engineering and Technology, Stevenage, United Kingdom, 2nd edition, 2009.

[49] P. Dupont, V. Hayward, B. Armstrong, and F. Almperter. Single state elastoplastic friction models. *IEEE Transactions on Automatic Control*, 47(5):787–792, 2002.

[50] P. E. Dupont. Avoiding stick-slip through PD control. *IEEE Transactions on Automatic Control*, 39(4):1094–1097, 1994.

[51] G. Ellis and R. D. Lorenz. Comparison of motion control loops for industrial applications. In *Conference Record of the IEEE Industry Applications Conference and 34th Industrial Application Society Annual Meeting*, volume 4, pages 2599–2605, 1999.

[52] G. W. Evans. Bringing root locus to the classroom. *IEEE Control Systems Magazine*, 24 (6):74–81, 2004.

[53] W. Evans. *Control-System Dynamics*. McGraw-Hill Book Company, Inc., New York, 1954.

[54] W. R. Evans. Graphical analysis of control systems. *Transactions of the American Institute of Electrical Engineers*, 67(1):547–551, 1948.

[55] W. R. Evans. Control system synthesis by root locus method. *Transactions of the American Institute of Electrical Engineers*, 69(1):66–69, 1950.

[56] P. Ferreira. The servomechanism problem and the method of state-space in the frequency domain. *International Journal of Control*, 23(2):245–255, 1976.

[57] G. Ferretti, G. Magnani, and P. Rocco. Single and multistate integral friction models. *IEEE Transactions on Automatic Control*, 49(12):2292–2297, 2004.

[58] O. Föllinger. *Regelungstechnik (8. Auflage)*. Hüthig Buch Verlag, Heidelberg, 1994.

[59] M. French, A. Ilchmann, and E. P. Ryan. Robustness in the graph topology of a common adaptive controller. *SIAM Journal of Control and Optimization*, 45(5):1736–1757, 2006.

[60] P. Georgieva and A. Ilchmann. Adaptive λ-tracking control of activated sludge processes. *International Journal of Control*, 74(12):1247–1259, 2001.

[61] P. Georgieva, A. Ilchmann, and M.-F. Eirig. Modelling and adaptive control aerobic of continuous stirred tank reactors. *European Journal of Control*, 7:476–491, 2001.

[62] T. Geyer, G. Papafotiou, and M. Morari. Model predictive direct torque control – Part I: Concept, algorithm, and analysis. *IEEE Transaction on Industrial Electronics*, 56(6): 1894–1905, 2009.

[63] F. Ghorbel, B. Srinivasan, and M. W. Spong. On the positive definiteness and uniform boundedness of the inertia matrix of robot manipulators. In *Proceedings of the 32nd IEEE Conference on Decision and Control*, pages 1103–1108, San Antonio, USA, 1993.

[64] C. Hackl. Stabilitätsuntersuchungen adaptiver Regelungskonzepte für mechatronische Systeme. Diplomarbeit, Lehrstuhl für Elektrische Antriebssysteme, Technische Universität München, 2004.

[65] C. M. Hackl. High-gain adaptive position control. *accepted for publication in "International Journal of Control" (preprint available at the author)*, 2011.

[66] C. M. Hackl and B. Mair. Smoothing the tension - optimal web tension control with a dSPACE prototyping system. *dSPACE Magazine*, 2:40–45, 2008.

[67] C. M. Hackl and D. Schröder. Extension of high-gain controllable systems for improved accuracy. In *Proceedings of the IEEE International Conference on Control Applications*, pages 2231–2236, Munich, Germany, 2006.

[68] C. M. Hackl and D. Schröder. Funnel-control with online foresight. In *Proceedings of the 26th IASTED International Conference MODELLING, IDENTIFICATION AND CONTROL*, pages 171–176, Innsbruck, Austria, 2007.

[69] C. M. Hackl, Y. Ji, and D. Schröder. Enhanced funnel-control with improved performance. In *Proceedings of the 15th Mediterranean Conference on Control and Automation*, pages Paper T01–016, Athens, Greek, 2007.

[70] C. M. Hackl, C. Endisch, and D. Schröder. Error reference control of nonlinear two-mass flexible servo systems. In *Proceedings of the 16th Mediterranean Conference on Control and Automation*, pages 1047–1053, Ajaccio, France, 2008.

[71] C. M. Hackl, C. Endisch, and D. Schröder. Contributions to non-identifier based adaptive control in mechatronics. *Robotics and Autonomous Systems, Elsevier*, 57(10):996–1005, 2009.

[72] C. M. Hackl, N. Hopfe, A. Ilchmann, M. Mueller, and S. Trenn. Funnel control for systems with relative degree two. *submitted to SIAM Journal on Control and Optimization (preprint available at the author)*, 2010.

[73] E. Hairer and G. Wanner. *Solving Ordinary Differential Equations II: Stiff and Differential–Algebraic Problems.* Springer Series in Computational Mathematics. Springer-Verlag, Berlin, 2nd revised edition, 2004.

[74] R. Hecker, G. Flores, Q. Xie, and R. Haran. Servocontrol of machine-tools: A review. *Latin American Applied Research*, 38(1):85–94, 2008.

[75] U. Helmke and D. Prätzel-Wolters. Stability and robustness properties of universal adaptive controllers for first order linear systems. *International Journal of Control*, 48:1153–1182, 1988.

[76] J. Hewitt. Mechatronics — the contributions of advanced control. In *Proceedings of the 2nd Conference on Mechatronics and Robotics*, Duisburg/Moers, Germany, 1993.

[77] D. Hinrichsen and A. Pritchard. *Mathematical Systems Theory I — Modelling, State Space Analysis, Stability and Robustness*. Number 48 in Texts in Applied Mathematics. Springer-Verlag, Berlin, 2005.

[78] C. Hintz. *Identifikation nichtlinearer mechatronischer Systeme mit strukturierten rekurrenten Netzen*. Dissertation, Institute for Electrical Drive Systems, Technische Universität München (TUM), Germany, 2003.

[79] M. Hirata and M. Tomizuka. Short track seeking of hard disk drives under multirate control—computationally efficient approach based on initial value compensation. *IEEE/ASME Journal of Mechatronics*, 10(5):535–545, 2005.

[80] J. Hoagg and D. Bernstein. Direct adaptive dynamic compensation for minimum phase systems with unknown relative degree. *IEEE Transactions on Automatic Control*, 52(4): 610–621, 2007.

[81] N. Hopfe. *Feedback Control: Systems with Higher Unknown Relative Degree, Input Constraints and Positivity*. Dissertation, Technical University of Ilmenau, Germany, 2010.

[82] N. Hopfe, A. Ilchmann, and E. P. Ryan. Funnel control with saturation: Linear MIMO systems. *IEEE Transactions on Automatic Control*, 55(2):532–538, 2010.

[83] N. Hopfe, A. Ilchmann, and E. P. Ryan. Funnel control with saturation: Nonlinear SISO systems. *IEEE Transactions on Automatic Control*, 55(9):2177–2182, 2010.

[84] T.-R. Hsu. Mechatronics — An overview. *IEEE Transaction on Components, Packaging and Manufacturing Technology*, 20(1):4–7, 1997. (Part C).

[85] A. Ilchmann. Non-identifier-based adaptive control of dynamical systems: A survey. *IMA Journal of Mathematical Control & Information*, 8:321–366, 1991.

[86] A. Ilchmann. *Non-Identifier-Based High-Gain Adaptive Control*, volume 189 of *Lecture notes in control and information sciences*. Springer-Verlag, London, 1993.

[87] A. Ilchmann. Adaptive λ-tracking for polynomial minimum phase systems. *Dynamics and Stability of Systems*, 13(4):341–371, 1998.

[88] A. Ilchmann and A. Isidori. Adaptive dynamic output feedback stabilization of nonlinear systems. *Asian Journal of Control*, 4(3):246–254, 2002.

[89] A. Ilchmann and M. Mueller. Robustness of λ-tracking in the gap metric. *SIAM Journal of Control and Optimization*, 5(5):2724–2744, 2008.

[90] A. Ilchmann and M. Mueller. Robustness of funnel control in the gap metric. *SIAM Journal of Control and Optimization*, 47(5):2724–2744, 2009.

[91] A. Ilchmann and D. Owens. Treshold switching functions in high-gain adaptive control. *IMA Journal of Mathematical Control & Information*, 8:409–429, 1991.

[92] A. Ilchmann and M. Pahl. Adaptive multivariable pH regulation of a biogas tower reactor. *European Journal of Control*, 4:116–131, 1998.

[93] A. Ilchmann and E. Ryan. High-gain control without identification: A survey. *GAMM-Mitteilungen*, 31(1):115–125, 2008.

[94] A. Ilchmann and E. P. Ryan. Asymptotic tracking with prescribed transient behaviour for linear systems. *International Journal of Control*, 79(8):910–917, 2006.

[95] A. Ilchmann and R. Ryan. Universal λ-tracking for nonlinearly-perturbed systems in the presence of noise. *Automatica*, 30(2):337–346, 1994.

[96] A. Ilchmann and H. Schuster. PI-funnel control for two mass systems. *IEEE Transactions on Automatic Control*, 54(4):918–923, 2009.

[97] A. Ilchmann and S. Townley. Adaptive sampling control of high-gain stabilizable systems. *IEEE Transactions on Automatic Control*, 44(10):1961–1965, 1999.

[98] A. Ilchmann and S. Trenn. Input constrained funnel control with applications to chemical reactor models. *Systems & Control Letters*, 53(5):361–375, 2004.

[99] A. Ilchmann, E. P. Ryan, and C. J. Sangwin. Tracking with prescribed transient behaviour. *ESAIM: Control, Optimisation and Calculus of Variations*, 7:471–493, 2002.

[100] A. Ilchmann, M. Thuto, and S. Townley. Input constrained adaptive tracking with applications to exothermic checmical reaction models. *SIAM Journal of Control and Optimization*, 43(1):154–173, 2004.

[101] A. Ilchmann, E. P. Ryan, and S. Trenn. Tracking control: Performance funnels and prescribed transient behaviour. *Systems & Control Letters*, 54:655–670, 2005.

[102] A. Ilchmann, E. Ryan, and P. Townsend. Tracking control with prescribed transient behaviour for systems of known relative degree. *Systems & Control Letters*, 55:396–406, 2006.

[103] A. Ilchmann, E. Ryan, and P. Townsend. Tracking with prescribed transient behaviour for nonlinear systems of known relative degree. *SIAM Journal on Control and Optimization*, 46(1):210–230, 2007.

[104] A. Ilchmann, H. Logemann, and P. R. Eugene. Tracking with prescribed transient performance for hysteretic systems. *SIAM Journal of Control and Optimization*, 48(7): 4731–4752, 2010.

[105] P. Ioannou and P. Kokotovic. Instability analysis and improvement of robustness of adaptive control. *Automatica*, 20(5):583–594, 1984.

[106] P. Ioannou and J. Sun. *Robust Adaptive Control*. Prentice Hall International Inc., Upper Saddle River, New Jersey, 1996. (out of print in 2003, electronic copy at: `http://www-rcf.usc.edu/~ioannou/Robust_Adaptive_Control.htm`).

[107] A. Isidori. *Nonlinear Control Systems*. Springer-Verlag, London, 3rd edition, 1995.

[108] O. Jacobs. A review of self-adjusting systems in automatic control. *International Journal of Electronics*, 10(4):311–322, 1961.

[109] R. E. Kalman. A new approach to linear filtering and prediction problems. *Transaction of the American Society of Mechanical Engineering (Journal of Basic Engineering)*, 82 (Series D)(1):35–45, 1960.

[110] R. E. Kalman. Contributions to the theory of optimal control. *Boletin de la Sociedad Matematica Mexicana*, 5:102–119, 1960.

[111] R. E. Kalman. Mathematical description of linear dynamical systems. *SIAM Journal on Control*, 1(2):152–192, 1963.

[112] R. Kelly, V. S. Davila, and A. Loría. *Control of Robot Manipulators in Joint Space*. Springer-Verlag, London, 2005.

[113] H. Khalil. Universal integral controllers for minimum–phase nonlinear systems. *IEEE Transactions on Automatic Control*, 45(3):490–494, 2000.

[114] H. Khalil and A. Saberi. Adaptive stabilization of a class of nonlinear systems using high-gain feedback. *IEEE Transactions on Automatic Control*, 32(11):1031–1035, 1987.

[115] H. K. Khalil. *Nonlinear Systems*. Prentice-Hall Internation Inc., Upper Saddle River, New Jersey, 3nd edition, 2002.

[116] H. W. Knobloch and F. Kappel. *Gewöhnliche Differentialgleichungen*. Mathematische Leitfäden. Teubner Verlag, Stuttgart, 1974.

[117] A. Krall. An extension and proof of the root-locus method. *Journal of the Society for Industrial and Applied Mathematics*, 4(9):644–653, 1961.

[118] A. Krall. The root locus method: A survey. *SIAM Review*, 12(1):64–72, 1970.

[119] N. Kyura and H. Oho. Mechatronics — An industrial perspective. *IEEE/ASME Transactions on Mechtronics*, 1(1):10–15, 1996.

[120] W. Levine, editor. *The Control Handbook*. CRC Press LLC (with IEEE Press), Boca Raton, Florida, 1st edition, 1996.

[121] D. Liberzon and S. Trenn. The bang-bang funnel controller. In *Proceedings of the 49th IEEE Conference on Decision and Control*, pages 690–695, Atlanta, USA, 2010.

[122] H. Logemann and B. Mårtensson. Adaptive stabilization of infinite-dimensional systems. *IEEE Transactions on Automatic Control*, 37(12):1869–1883, 1992.

[123] R. Lorenz, T. Lipo, and D. Novotny. Motion control with induction motors. *Proceedings of the IEEE*, 82(8):1215–1240, 1994.

[124] J. Lunze. *Regelungstechnik 1 - Systemtheoretische Grundlagen, Analyse und Entwurf einschleifiger Regelungen (4. erweiterte und überarbeitete Auflage).* Springer-Verlag, Berlin, 2004.

[125] A. M. Lyapunov. *The General Problem of the Stability of Motion (In Russian).* Dissertation, V.N. Karazin Kharkiv National University, 1892. "Problème Géneral de la Stabilité de Mouvement" in Annales de la Faculté des Sciences de l'Université de Toulouse, Vol. 9 (1907), pp. 203-474, reprinted in Princeton University Press (1949).

[126] A. M. Lyapunov. *Stability of Motion*, volume 30 of *Mathematics in Science and Engineering.* Academic Press, New York, London, 1966.

[127] A. M. Lyapunov. *The General Problem of the Stability of Motion.* Taylor & Francis Ltd., London, Washington D.C., 1992.

[128] J. M. Maciejowski. The changing face and role of CASCD. In *Proceedings of the IEEE Conference on Computer Aided Control Systems Design*, pages 1–7, Munich, Germany, 2006.

[129] I. Mareels. A simple selftuning controller for stably invertible systems. *Systems & Control Letters*, 4(1):5–16, 1984.

[130] I. Mareels, S. Van Gils, J. Polderman, and A. Ilchmann. Asymptotic dynamics in adaptive gain control. In P. Frank, editor, *Advances in Control, Highlights of ECC '99*, pages 29–63. Spinger-Verlag, London, 1999.

[131] J. C. Maxwell. On governors. *Proceedings of the Royal Society of London*, pages 270–283, 1868.

[132] O. Mayr. *Zur Frühgeschichte der technischen Regelungen.* Oldenbourg Verlag, München, Wien, 1969.

[133] I. McCausland. Adaption in feedback control systems. *Journal of the Franklin Institute*, 268(3):143–147, 1959.

[134] D. E. Miller and E. J. Davison. An adaptive controller which provides an arbitrarily good transient and steady-state response. *IEEE Transactions on Automatic Control*, 36 (1):68–81, 1991.

[135] D. E. Miller and E. J. Davison. An adaptive tracking problem. *International Journal of Adaptive Control and Signal Processing*, 6(1):45–63, 1992.

[136] A. Morin. New friction experiments carried out at Metz in 1831-1833 (in french). *Proceedings of the French Royal Academy of Sciencies*, 4:1–128, 591–696, 1833.

[137] A. S. Morse. Recent problems in parameter adaptive control. In I. D. Landau, editor, *Outils et Modèles Mathématiques pour l'Automatique, l'Analyse de Systèmes et le Traitment du Signal*, volume 3, pages 733–740. Éditions du Centre National de la Recherche Scientifique, Paris, 1983.

[138] K. Narendra and A. Annaswamy. *Stable Adaptive Systems*. Prentice-Hall Internation Inc., Upper Saddle River, New Jersey, 1989.

[139] H. Nevzat Özgöven and D. Houser. Mathematical models used in gear dynamics — A review. *Journal of Sound and Vibration*, 121(3):383–411, 1988.

[140] M. Nordin and P.-O. Gutman. Controlling mechanical systems with backlash — A survey. *Automatica*, 38:1633–1649, 2002.

[141] R. Nussbaum. Some remarks on the conjecture in parameter adaptive ccontrol. *Systems & Control Letters*, 3(5):243–246, 1983.

[142] H. Nyquist. Regeneration theory. *Bell System Technical Journal*, 11(1):126–147, 1932.

[143] K. Ohnishi, M. Shibata, and T. Murakami. Motion control for advanced mechatronics. *IEEE/ASME Transactions on Mechatronics*, 1(1):56–67, 1996.

[144] B. Øksendal. *Stochastic Differential Equations*. Springer-Verlag, 6th edition, 2003.

[145] H. Olsson. *Control Systems with Friction*. Dissertation, Department of Automatic Control, Faculty of Engineering, Lund University, Sweden, 1996.

[146] H. Olsson and K. J. Åström. Friction generated limit cycles. *IEEE Transaction on Control Systems Technology*, 9(4):629–636, 2001.

[147] H. Olsson, K. Åström, C. Canudas de Wit, M. Gäfert, and P. Lischinsky. Friction models and friction compensation. *European Journal of Control*, 4(3):176–195, 1998.

[148] G. Papafotiou, J. Kley, K. G. Papadopoulos, P. Bohren, and M. Morari. Model predictive direct torque control – Part II: Implementation and experimental evaluation. *IEEE Transaction on Industrial Electronics*, 56(6):1906–1915, 2009.

[149] M.-H. Park and K.-S. Kim. Chattering reduction in the position control of induction motor using the sliding mode. *IEEE Transactions on Power Electronics*, 6(3):317–325, 1991.

[150] Z. Qu. *Robust Control of Nonlinear Uncertain Systems*. Wiles Series in Nonlinear Science. John Wiley & Sons, Inc., New York, 1998.

[151] M. Rau. *Nichtlineare modellbasierte prädiktive Regelung auf Basis lernfähiger Zustandsraummodelle*. Dissertation, Institute for Electrical Drive Systems, Technische Universität München (TUM), Germany, 2003.

[152] M. Readman. *Flexible Joint Robots*. Mechatronics Series. CRC Press, Inc., London Tokyo, 1994.

[153] O. Reynolds. On the theory of lubrication and its application to Mr. Beauchamp tower's experiments, including an experimental determination of the viscosity of olive oil. *Philosophical Transactions of the Royal Society of London*, 177:157–234, 1886.

[154] E. J. Routh. *A Treatise on the Stability of a Given State of Motion: Particularly Steady Motion*. MaxMillian and Co., London, 1877.

[155] E. P. Ryan. Universal $W^{1,\infty}$-tracking for a class of nonlinear systems. *Systems & Control Letters*, 18(3):201–210, 1992.

[156] E. P. Ryan. A nonlinear universal servomechanism. *IEEE Transactions on Automatic Control*, 39(4):753–761, 1994.

[157] R. P. Ryan and C. J. Sangwin. Controlled functional differential equations and adaptive stabilization. *International Journal of Control*, 74:77–90, 2001.

[158] R. P. Ryan and C. J. Sangwin. Controlled functional differential equations and adaptive tracking. *Systems & Control Letters*, 47(5):365–374, 2002.

[159] S. Sankaanarayanan and F. Khorrami. Model independent friction compensation. In *Proceedings of the IEEE American Control Conference*, pages 463–467, Philadelphia, Pennsylvania, USA, 1998.

[160] D. Schröder. *Elektrische Antriebe — Grundlagen (2. Auflage)*. Springer-Verlag, Berlin, 2000.

[161] D. Schröder. *Intelligent Observer and Control Design for Nonlinear Systems*. Springer-Verlag, Berlin, 2000.

[162] D. Schröder. *Elektrische Antriebe — Regelung von Antriebssystemen (2. Auflage)*. Springer-Verlag, Berlin, 2001.

[163] D. Schröder. *Leistungselektronische Bauelemente (2. Auflage)*. Springer-Verlag, Berlin, 2006.

[164] D. Schröder. *Elektrische Antriebe — Grundlagen (3.,erw. Auflage)*. Springer-Verlag, 2007.

[165] D. Schröder. *Leistungselektronische Schaltungen - Funktion, Auslegung und Anwendung (2. Auflage)*. Springer-Verlag, Berlin, 2008.

[166] D. Schröder. *Elektrische Antriebe - Regelung von Antriebssystemen (3., bearb. Auflage)*. Springer-Verlag, Berlin, 2009.

[167] D. Schröder. *Intelligente Verfahren: Identifikation und Regelung nichtlinearer Systeme*. Springer-Verlag, Berlin, 2010.

[168] D. Schröder, H. Schuster, and C. Westermaier. Mechatronics — Advanced computational intelligence. In *Proceedings of the 7th International Conference on Power Electronics and Drive Systems*, pages 994 – 1001, 2007.

[169] H. Schuster. *Hochverstärkungsbasierte Regelung nichtlinearer Antriebssysteme*. Dissertation, Institute for Electrical Drive Systems, Technische Universität München (TUM), Germany, 2009.

[170] H. Schuster, C. Westermaier, and D. Schröder. High-gain control of systems with arbitrary relative degree: Speed control for a two mass flexible servo system. In *Proceedings of the 8th IEEE International Conference on Intelligent Engineering Systems*, pages 486–491, Cluj-Napoca, Romania, 2004.

[171] H. A. Simon. Dynamic programming under uncertainty with quadratic criterion function. *Econometrica, Journal of the Econometric Society*, 24(1):73–81, 1956.

[172] E. D. Sontag. *Mathematical Control Theory — Deterministic Finite Dimensional Systems*. Springer-Verlag, Berlin, 2nd edition, 1998.

[173] E. D. Sontag. Adaption and regulation with signal detection implies internal model. *Systems & Control Letters*, 50(2):119–126, 2003.

[174] M. W. Spong, S. Hutchinson, and M. Vidyasagar. *Robot Modeling and Control*. John Wiley & Sons, Inc., New York, 2006.

[175] M. Steinbuch and M. Norg. Advanced motion control: An industrial perspective. *European Journal of Control*, 4:278–293, 294–297, 1998.

[176] R. Stribeck. Kugellager für beliebige Belastungen. *Zeitschrift des Vereines deutscher Ingenieure*, 45(3,4):73–96, 118–125, 1901.

[177] R. Stribeck. Die wesentlichen Eigenschaften der Gleit- und Rollenlager. *Zeitschrift des Vereines deutscher Ingenieure*, 46(37,38,39):1341–1348, 1432–1438, 1463–1470, 1902.

[178] J. Swevers, F. Al-Bender, C. G. Ganseman, and T. Prajogo. An integrated friction model structure with improved presliding behavior for accurate friction compensation. *IEEE Transaction on Automatic Control*, 45(4):675–686, 2000.

[179] H. Taghirad and P. Bélanger. An experimental study on modelling and identification of harmonic drive systems. In *Proceedings of the 35th IEEE Conference on Decision and Control*, pages 4725–4730, 1996.

[180] M. Tomizuka. Mechatronics: From the 20th to 21st century. *Control Engineering Practice*, 10:877–886, 2002.

[181] T. D. Tuttle and W. P. Seering. A nonlinear model of a harmonic drive gear transmission. *IEEE Transactions on Robotics and Automation*, 12(3):368–374, 1996.

[182] Z. Wenjing. Parameter identification of LuGre friction model in servo system based on improved particle swarm optimization algorithm. In *Proceedings of Chines Control Conference*, pages 135–139, Zhangjiajie, Hunan, China, 2007.

[183] A. Whiteley. Fundamental principles of automated regulators and servo mechanisms. *Journal of the Institution of Electrical Engineers — Part IIA: Automatic Regulators and Servo Mechanisms*, 94(1):5–19, 1947.

[184] A. Whiteley. Servo mechanisms — a review of progress. *Proceedings of the IEE — Part I: General*, 98(113):289–297, 1951.

[185] N. Wiener. *Cybernetics: or Control and Communication in the Animal and the Machine*. John Wiley & Sons Inc., New York, 1948.

[186] J. Wikander, M. Törngren, and M. Hanson. The science and education of mechatronics engineering. *IEEE Robotics & Automation Magazine*, 8(2):20–26, 2001.

[187] J. C. Willems and C. I. Byrnes. Global adaptive stabilization in the absence of information on the sign of the high frequency gain. *in: Analysis and Optimization of Systems (Lecture Notes in Control and Information Sciences), Springer Berlin, Heidelberg*, 62(2):49–57, 1984.

[188] B. Wittenmark. A survey of adaptive control applications. In *Proceedings of the IEEE Industry Applications Society Workshop on Dynamic Modeling Control Applications for Industry*, Vancouver, Canada, 1997.

[189] W. M. Wonham. *Linear Multivariable Control: A Geometric Approach*. Number 10 in Applications of Mathematics. Springer-Verlag, Berlin, 3rd edition, 1985.

[190] X. Ye. Universal λ-tracking for nonlinearly-perturbed systems without restrictions on the relative degree. *Automatica*, 35(1):109–119, 1999.